Mixed Isogeometric Methods for Hodge–Laplace Problems induced by Second-Order Hilbert Complexes

Vom Fachbereich Mathematik der Rheinland-Pfälzischen Technischen Universität Kaiserslautern-Landau zur Verleihung des akademischen Grades

Doktor der Naturwissenschaften
(Doctor rerum naturalium, Dr. rer. nat.)
genehmigte

DISSERTATION

von

Jeremias Nathanael Arf

Gutachter: Prof. Dr. Bernd Simeon
Asst.-Prof. Dr. Deepesh Toshniwal

Datum der Disputation: 23.02.2024

DE-386

Acknowledgements

Completing a thesis over the years requires support and assistance from various sources, making it possible to reach the finish line of this academic marathon. I extend my heartfelt gratitude to those who have been instrumental in this journey.

First and foremost, I would like to express my profound gratitude to my thesis supervisor, Prof. Dr. Bernd Simeon who helped me with his expertise and experience several times over the years. But he has been more than just an advisor in matters related to mathematical themes. Prof. Dr. Bernd Simeon not only provided constant encouragement when things did not go as planned but also instilled courage and facilitated connections with other researchers. His trust in allowing me significant autonomy in selecting the specific focus of my thesis is something for which I am truly grateful. Secondly, I am very thankful to Asst.-Prof. Dr. Deepesh Toshniwal for accepting the role as the second referee for this thesis.

Further, I extend my thanks to my colleagues and friends Rozan Rosandi, Max Aehle and Henry Jäger from the RPTU Kaiserslautern. Their willingness to engage in discussions about my work and their assistance with various questions and challenges have been invaluable. Their collaboration has significantly enriched my research journey.

A special acknowledgment goes to my project partner, Mathias Reichle (RWTH Aachen University). I appreciate his patience in accepting short-notice schedule changes and consider him one of the most important contacts during my doctoral studies.

Lastly, I would like to express my gratitude to Prof. Dr. Annalisa Buffa and her research group at EPFL (Lausanne). Their warm hospitality and mentorship during the two weeks were invaluable. The numerous discussions provided me with important insights and fresh perspectives. I extend my thanks to Dr. Espen Sande and Dr. Rafael Vázquez for their genuine interest in my work and for presenting new possibilities.

To all mentioned above and to those who have supported me on this academic journey, I extend my heartfelt thanks. Your guidance has been instrumental in shaping the outcome of my thesis, and I am truly grateful for the privilege of having such dedicated mentors and collaborators.

Abstract

Partial differential equations (PDEs) play a crucial role in mathematics and physics to describe numerous physical processes. In numerical computations within the scope of PDE problems, the transition from classical to weak solutions is often meaningful. The latter may not precisely satisfy the original PDE, but they fulfill a weak variational formulation, which, in turn, is suitable for the discretization concept of *Finite Elements* (FE). A central concept in this context is the *well-posed problem*. A class of PDE problems for which not only well-posedness statements but also suitable weak formulations are known are the so-called *abstract Hodge–Laplace* problems. These can be derived from Hilbert complexes and constitute a central aspect of the Finite Element Exterior Calculus (FEEC).

This thesis addresses the discretization of *mixed formulations* of Hodge-Laplace problems, focusing on two key aspects. Firstly, we utilize *Isogeometric Analysis* (IGA) as a specific paradigm for discretization, combining geometric representations with *Non-Uniform Rational B-Splines* (NURBS) and Finite Element discretizations. Secondly, we primarily concentrate on mixed formulations exhibiting a saddle-point structure and generated from *Hilbert complexes* with *second-order derivative* operators. We go beyond the well-known case of the classical *de Rham complex*, considering complexes such as the Hessian or elasticity complex. The BGG (Bernstein–Gelfand–Gelfand) method is employed to define and examine these second-order complexes.

The main results include proofs of discrete well-posedness and *a priori* error estimates for two different discretization approaches. One approach demonstrates, through the introduction of a Lagrange multiplier, how the so-called *isogeometric discrete differential forms* can be reused. A second method addresses the question of how standard NURBS basis functions, through a modification of the mixed formulation, can also lead to convergent procedures. Numerical tests and examples, conducted using *MATLAB* and the open-source software *GeoPDEs*, illustrate the theoretical findings. Our primary application extends to linear elasticity theory, extensively discussing mixed methods with and without strong symmetry of the stress tensor.

The work demonstrates the potential of IGA in numerical computations, particularly in the challenging scenario of second-order Hilbert complexes. It also provides insights into how IGA and FEEC can be meaningfully combined, even for non-de Rham complexes.

Zusammenfassung

Partielle Differentialgleichungen (PDEs) spielen eine entscheidende Rolle in Mathematik und Physik, um zahlreiche physikalische Prozesse zu beschreiben. Bei numerischen Berechnungen im Rahmen von PDE-Problemen ist oft der Übergang von klassischen zu schwachen Lösungen sinnvoll. Letztere erfüllen möglicherweise nicht genau die ursprüngliche PDE, jedoch erfüllen sie eine schwache Variationsformulierung, die sich wiederum für das Diskretisierungskonzept der *Finiten Elemente* (FE) eignet. Ein zentraler Begriff in diesem Kontext ist das *wohlgestellte Problem*. Eine Klasse von PDE-Problemen, für die nicht nur Wohlgestelltheitsaussagen, sondern auch passende schwache Formulierungen bekannt sind, sind die sogenannten *abstrakten Hodge–Laplace Probleme*. Diese können aus Hilbertkomplexen abgeleitet werden und stellen einen zentralen Aspekt des Finite Element Exterior Calculus (FEEC) dar.

Die vorliegende Arbeit setzt hier an und beschäftigt sich mit der Diskretisierung von *gemischten Formulierungen* von Hodge–Laplace-Problemen. Dabei liegt der Fokus auf zwei Punkten: Zum einen nutzen wir die *Isogeometrische Analyse* (IGA) als spezifisches Paradigma für die Diskretisierung, indem Geometriedarstellungen mit *Nicht-Uniforme Rationale B-Splines* (NURBS) und Finite-Elemente-Diskretisierungen kombiniert werden. Zum anderen konzentrieren wir uns hauptsächlich auf solche gemischten Formulierungen, die eine Sattelpunktstruktur aufweisen und aus *Hilbertkomplexen* mit Ableitungsoperatoren *zweiter Ordnung* generiert werden. Insbesondere gehen wir über den bekannten Fall der klassischen *de Rham-Kette* hinaus und betrachten beispielsweise den *Hessian- oder Elastizitätskomplex*. Zur Definition und Untersuchung der Komplexe zweiter Ordnung nutzen wir das Bernstein–Gelfand–Gelfand-Verfahren (BGG).

Die Hauptergebnisse umfassen Beweise für diskrete Wohlgestelltheit und a-priori-Fehlerabschätzungen von zwei verschiedenen Diskretisierungsansätzen. Ein Ansatz zeigt durch die Einführung eines Lagrange-Multiplikators, wie die sogenannten *isogeometrischen diskreten Differentialformen* wiederverwendet werden können. Eine zweite Methode geht der Frage nach, wie standardmäßige NURBS-Basisfunktionen durch eine Modifikation der gemischten Formulierung ebenfalls zu konvergierenden Verfahren führen können. Numerische Tests und Beispiele, durchgeführt mit *MATLAB* und der Open-Source-Software *GeoPDEs*, veranschaulichen die theoretischen Ergebnisse. Unsere Hauptanwendung erstreckt sich auf die lineare Elastizitätstheorie, wobei gemischte Methoden mit und ohne starke Symmetrie des Spannungstensors ausführlich diskutiert werden.

Die Arbeit demonstriert das Potential von IGA bei numerischen Berechnungen im Rahmen des anspruchsvollen Falls von Hilbertkomplexen zweiter Ordnung. Zudem zeigt sie Zugänge auf, wie IGA und FEEC auch für nicht-de-Rham-Komplexe sinnvoll zu kombinieren sind.

Contents

1 Introduction

Partial differential equations (PDEs) play a central role in mathematics and physics, as many physical processes can be described by suitable PDE equations. For various linear equations, existence and approximation approaches of (local) solutions are known. However, it has proven meaningful to depart from the restrictive concept of strong or classical solutions and turn to weak solutions instead. Weak solutions may not exactly satisfy the original PDE, but they are solutions of a so-called weak formulation, which, in the case of existence, is also satisfied by the strong solution. The concept of well-posed problems plays a crucial role in this context. This means, simplistically put, that given appropriate boundary and initial conditions, a unique solution to the PDE will be obtained. Additionally, small changes in the input data, i.e. the boundary and initial values, should result in only small changes in the solutions within a limited time interval. A form of continuous dependence on the input data is sought. Because, given the inherent inaccuracies in computer calculations involving real numbers, developing a numerical method for an ill-posed problem is futile.

A class of PDEs for which not only well-posedness is shown but also suitable weak formulations can be provided are the so-called abstract *Hodge–Laplace problem*s. These time-independent PDEs can be interpreted as a generalization of the well-known Poisson equation, but they go far beyond that. In fact, the definition of the Hodge–Laplace operator and its variational formulations can be traced back to Hilbert complexes. Such complexes consist of chains of Hilbert spaces interconnected by differential operators, such that the composition of two adjacent operators in the complex yields the zero operator. By choosing the Hilbert spaces in the complex, many different PDEs can be generated. The *Finite Element Exterior Calculus* (FEEC) [11, 5] established by Arnold, Winther and Falk explains the theoretical foundations and constructions of strong and weak formulations of Hodge–Laplace problems, and also develops criteria for applying Finite Element Methods (FEMs) in the discrete case in a well-posed manner. A pivotal tool within FEEC are the - we call it - structure-preserving discretizations of the Hilbert complexes. This means one uses finite-dimensional subcomplexes of the continuous chains, where the former preserve the key features, like exactness or the validity of the Poincaré inequality.

This elegant and abstract concept serves as the starting point for this present work. The goal is to utilize a specific paradigm or a specific type of FEMs for the discretization of the Hodge–Laplace problem, namely *Isogeometric Analysis* (IGA) [49, 31, 17]. A trigger behind introducing IGA was to combine geometry representations using Non-Uniform Rational B-splines (NURBS) with Finite Element discretizations, which now also rely on NURBS. That is why the first and seminal IGA paper by Hughes et al. was entitled "*Isogeometric analysis: CAD, Finite Elements, NURBS, exact geometry and mesh refinement*". The idea of connecting FEEC and IGA is not new and was demonstrated, at the latest, by Buffa et al. in [27] with the introduction of *isogeometric discrete differential forms* in 2011 based on B-splines. However, these results apply only to the classical de Rham complexes, meaning only first-order differential operators are involved. When Hilbert complexes with higher derivatives are to be discretized, such as the elasticity complex in continuum mechanics (see e.g. [4, 10, 6, 59]), this is not always directly achievable. This is where the present work comes in, addressing the discretization of Hodge–Laplace equations generated from second-order Hilbert complexes, meaning Hilbert complexes with appearing differential operators of second order. In doing so, approaches from IGA are used, i.e. B-splines and NURBS-based function spaces, as well as mixed weak formulations provided by FEEC. Pivotal for our investigations is the Bernstein–Gelfand–Gelfand (BGG) construction (compare [12]) procedure which can be utilized to generate from two linked Hilbert complexes a new output complex. The latter technique not only gives us new chains, but it helps to understand important properties like the dimension of the cohomology spaces or

exactness for the output chains. Besides, the BGG algorithm is also appropriate for finding suitable spline spaces for various second-order complexes, including the *Hessian*, *elasticity* and *divdiv* complexes. In this context the product structure of B-splines is crucial as well as their smoothness can be utilized to handle the arising derivatives. But, these considerations still operate in the cubical reference domain of B-splines, which has limited utility for applications. Because, in IGA the reference domain is typically deformed into the desired computational domain through a NURBS parametrization, and the actual Finite Element (FE) spaces are defined through some push-forward operation from the parametric spaces. Unfortunately, in this transition from parametric to physical domain via the parameterization function, important properties of the spline complexes are lost in general, even up to the loss of the Hilbert complex structure.
In other words, aside from the special case of de Rham complexes, it is quite challenging to align the design steps of FEEC with IGA. But even if one resolves the focus on IGA and turns to classical FEEC on simplicial meshes, dealing with other than de Rham chains can often be difficult and laborious to discretize. Therefore, an approach has been pursued in [10, 42], for example in the context of elasticity complexes, which involves introducing additional Lagrange multipliers to bring somewhat mixed formulations back to the case of the de Rham complexes. This is because a direct discretization of the elasticity sequence based on the FEEC paradigm leads to complicated non-trivial FE spaces; compare [6, 4].

Aim of this work is to demonstrate how IGA can be meaningfully utilized in approximating Hodge–Laplace problems, stemming from second-order complexes, in particular not induced from de Rham sequences. We primarily focus on a specific class of Hilbert complexes derived through the BGG procedure for Alt^l-valued forms, where the latter can be seen as an extension of the well-known differential forms. This class explained and discussed in [12] encompasses chains in arbitrary dimensions, including the previously mentioned Hessian, elasticity, or divdiv complexes. Even with this restriction to specific chains, it remains unclear and non-trivial to find suitable NURBS or spline spaces for discretizations for parameterized geometries. As mentioned before, a structure-preserving transition between the parametric domain and the physical domain is generally not known.

To mitigate this issue, the main part of the work considers a specific case of Hodge–Laplace equations leading to weak formulations in the form of *saddle-point problems*; cf. [20, §4 in Chapter 3]. In this context, conditions for the well-posedness of the discretization are established. Two approaches are pursued: firstly, how the aforementioned isogeometric discrete differential forms can be reused is discussed, and secondly, standard NURBS basis functions are also allowed, and provided certain conditions they still lead to well-posed discretizations. For both approaches, quasi-optimal error estimates can be shown, meaning that the error in the respective choice of FE spaces is minimal, apart from a multiplicative constant. Particularly, the case of the mixed formulation with Lagrange multiplier proves to be challenging and requires the application of the *macroelement method* (see [23]) to show discrete well-posedness. What is remarkable is that, while we no longer explicitly require structure-preserving discretizations of the underlying complexes, this concept emerges in both approaches. In one case, we directly employ structure-preserving discretizations of the de Rham sequence, and in another, we rely on the existence of suitable, also structure-preserving spline complexes in cubical domains in a central proof. So, we are harnessing and accommodating the principles of FEEC, effectively integrating ideas and insights from both, FEEC and IGA.

These largely theoretical considerations are also illustrated in the work through numerical tests and examples. The main application lies in linear elasticity theory, where mixed methods with and without strong symmetry of the stress tensor are introduced, convergence is proved, and error computations are performed to support the theoretical statements. The numerical examples also

include so-called IGA multi-patch geometries described by multiple local parameterizations, as well as mixed-type boundary conditions. As a concluding point and in terms of a perspective, we discuss whether the existing restriction to specific Hodge–Laplace problems can be extended or relaxed. This is particularly interesting because for many standard FEMs, the regularity requirements associated with higher derivatives are often difficult to meet. And, at least in a single-patch geometry, smoothness of NURBS can easily be varied.

The main assertion and motivation of the work can be summarized as follows: Since it is relatively straightforward to define high-regularity NURBS within a single IGA reference domain, it is natural to extend the existing isogeometric discrete differential forms to higher-order complexes. However, using IGA in the context of second-order complexes is not a simple extension of the already known constructions for de Rham chains. Nevertheless, for certain Hodge–Laplace equations, B-splines and NURBS-based spaces can be sensibly employed, and it is possible to demonstrate convergence and well-posedness. Despite the limitations, the considerations are usable for a whole class of saddle-point systems and particularly applicable in the context of linear elasticity theory.

Before turning to a structuring of the thesis, it should be emphasized that the content of the thesis did not emerge in a vacuum but is built upon and utilizes existing knowledge in the literature. This is explicitly acknowledged at various points throughout the text. While previously mentioned, it is worth highlighting three key references in this context: [5, 27, 12]. These are the primary sources, and we frequently refer back to them. Additionally, we want to mention the thesis [62], which, although not directly incorporated, inspired us along with [10] to explore discretization with Lagrange multipliers. For the theory of mixed methods and saddle point problems, upon which we base our discretization schemes, we recommend the works [26, 24]. Concerning the mathematical foundations of functional analysis, PDEs, and Finite Elements, our primary references include [2, 69, 41] and [20].

Certainly, there are numerous publications addressing the theory of Hilbert complexes and their applications. In the field of IGA, for instance, the de Rham sequence is especially suitable for flow problems ([31, Chapter 4],[29]) and numerical computations within electromagnetism; see [31, Chapter 3], [28]. Recently we find papers that focus on extending the idea of isogeometric discrete differential forms to wider settings, application areas, respectively. For instance in [67, 40], the authors face the connection of hierarchical B-splines with the de Rham structure. This ansatz allows for local refinements of the mesh structures, an important aspect in the development of efficient approximation schemes. And in [30] it is shown how spline complexes can be used for multi-patch geometries. Additionally, in [71] multi-degree and polar spline complexes are introduced to cover the case of disk-like domains. A similar direction is taken in [57], where isogeometric discretizations in toroidal domains are considered. While many numerical approaches in the context of differential forms operate within the classical FEEC setting of simplicial complexes, our thesis will also turn to and follow the concept of isogeometric discretizations later. Therefore, we refer to [5] and the references therein for more information on discretizations on simplicial meshes. Further, to gain an overview of existing literature, particularly recent publications in the field of Hilbert complexes, we recommend the report [48]. This report not only touches upon various current research directions, but also provides a whole bunch of relevant publications. Moreover, it should be noted that Hilbert complexes beyond de Rham, such as the Hessian, elasticity and divdiv complexes, and their discretization, have received increased attention in the last years ([19, 35, 34, 47, 59, 60]). Numerous works on this topic have emerged lately, where in this context, the previously mentioned BGG construction ([12]) has proven to be helpful for the understanding of the underlying structure. However, even in relatively simple geometry, conforming Finite Elements often yield non-trivial basis functions,

discrete spaces, respectively. The challenge is particularly pronounced in the case of curved mesh elements, as encountered in IGA. Thus as we address in our thesis the question of how to integrate second-order Hilbert complexes with IGA, more precisely, how to leverage chains beyond the de Rham complex for mixed discretization methods, we face a topic that is currently under intensive discussion in the literature.

As the last point of the introduction let us now clarify the underlying structure of the text. The organization of the thesis is outlined as follows:

- Section 2: We start with introducing several mathematical notions and present some well-known results from the field of functional analysis that we will repeatedly use. Therefore, we commence with a concise preparatory section. Readers familiar with the field of functional analysis and variational formulations may choose to skip this section.

- Section 3: We continue by explaining the fundamental concepts in the realm of FEEC, particularly the so-called mixed weak formulations and their structure-preserving discretization. So, the central points from the important references [5, 11], which are crucial for understanding, are presented.

- Section 4: Then, we proceed by introducing possibilities how to generate new complexes, where we mainly face the BGG construction, a method by Arnold and Hu ([12]) suitable for building second-order Hilbert complexes. Here, we will also define a special type of the BGG procedure involving Alt^l-valued forms and leading to classical second-order complexes, such as the elasticity or Hessian complex. Within the same section, we also demonstrate a general approach for reformulating mixed weak formulations with additional Lagrange multipliers which will assist us later in developing a second discretization scheme. This yields for example the mixed weak formulation with weakly imposed symmetry within linear elasticity.

- Section 5: Moving on to the next part, Section 5, we then delve into general and abstract considerations on how to discretize specific saddle-point problems defined by Hilbert complexes. In other words, we establish various conditions that should lead us to well-posed discretizations. In proving the main results, we will directly or indirectly employ the concept of structure-preserving discretizations. It should also be noted here that this fifth section is once again to be considered as a preparatory chapter, as we will later apply the observations from this part to concrete IGA discretizations.

- Section 6: In the sixth section, which serves as an intermediary section, we take a detour to the fundamentals of IGA and mention important known estimates. In particular, we define B-splines and derive from them isogeometric Finite Element spaces. Additionally, we focus on various projections onto B-spline spaces, which prove to be useful at different points in the thesis. With this knowledge of IGA, we can become more concrete starting from Section 7.

- Section 7: We address specific second-order complexes from Alt^l-valued forms and the corresponding discretization utilizing B-splines. We clarify why it is feasible to find suitable FE spaces in cubic-shaped domains without difficulties, leading to spline complexes. We further define the isogeometric discrete differential forms, which determine a proper discretization for the de Rham complex also in the possibly deformed physical domain. Basis for this section are the references [19] and [27].

- Section 8: Subsequently, in Section 8 we utilize such structure-preserving discretizations in the parametric domain and the de Rham complex discretizations to make statements regarding non-trivial geometries as well, meaning parametrized computational domains involving curved boundary and shapes. We provide well-posedness results and error estimates for two distinct approaches, namely with and without a Lagrange multiplier, across a whole class of problems. However, as indicated earlier, we will confine ourselves to mixed weak formulations with a saddle-point structure. Nevertheless, this chapter can be regarded as the centerpiece of the thesis, as it presents the most important proofs and main results.

- Section 9: A resulting special case for the systems faced in Section 8 are mixed-weak formulations for the equations of linear elasticity. The latter serves as our primary application example and is extensively treated in Section 9, with again two different discretization methods. They cover the classical Hellinger-Reissner mixed system, a stress-displacement formulation, and the variant of it with weakly imposed symmetry. Throughout, we illustrate and validate our theoretical investigations with a series of numerical tests.

- Section 10: In the last part, Section 10, we briefly explore the question of whether we can discretize further problems that do not exhibit a saddle-point structure. Again, we present several numerical tests to support our conjectures and comment on possible directions for further generalizations. And finally we end the thesis with a conclusion, in which we draw an overall summary once again.

Finally, before we come to the first section it should also be noted here that all numerical tests and calculations were performed using MATLAB and the open-source software package GeoPDEs; [53, 37, 73]. Additionally, all the illustrations were generated using the mentioned software together with the LaTeX package *TikZ*.

2 Mathematical Preliminaries

A central element within the text are Hilbert spaces. We take advantage of structures coming along with their defining properties and we relate them by considering linear operators. In other words, some introductory words regarding functional analysis seem reasonable. This should be the guideline for this chapter. First, we will mention a few important definitions and statements related to linear operators on Hilbert spaces. Then, we will briefly address the concept of weak derivatives and Sobolev spaces. And at the end of the first chapter, we will focus on so-called variational formulations. Beforehand we want to emphasize our very limited perspective, since we concentrate only on specific aspects that point out to be useful later. The subsequent brief explanations are mainly to clarify notation and do not constitute a profound introduction. All the definitions and results of this part are well-known and can be found in different textbooks. Basis of the formulations and explanations below are the books [5, 2, 20, 1, 38], but we also recommend [41, 69] for more details. As a final point, we would like to mention that in the following, fundamental mathematical concepts especially in the field of topology are assumed to be known, i.e. for example terms like *closure* and *completeness* as well as the notions of vector and Banach spaces will not be explicitly explained.

2.1 Hilbert spaces and (unbounded) operators

In the following we only look at $\mathbb{R}$-Hilbert spaces, meaning Banach spaces over the field $\mathbb{R}$ that are endowed with an inner product structure. To be more precise, we have a pair $(W, \langle\cdot,\cdot\rangle_W)$ composed of a vector space W and the inner product $\langle\cdot,\cdot\rangle_W \colon W \times W \to \mathbb{R}$ which defines a norm $\|w\|_W \coloneqq \sqrt{\langle w, w\rangle_W}$ that in turn yields a complete metric space $(W, \|\cdot\|_W)$. Given the inner product, we can introduce the orthogonal complement of a subspace $V \subset W$ which is the closed linear space

$$V^{\perp_W} \coloneqq \{w \in W \mid \langle w, v\rangle_W = 0,\ \forall v \in V\}.$$

Writing $\overline{V}$ for the closure of V in W one has the decomposition

$$W = \overline{V} \perp V^{\perp_W},$$

where $\perp$ stands for the orthogonal direct sum[1]; compare Lemma 2.6. If the inner product is clear from the context we sometimes write just $V^\perp$ and $\langle\cdot,\cdot\rangle$ for the inner product. Additionally we should note the useful *Cauchy–Schwarz inequality* that reads

$$|\langle v, w\rangle| \leq \|v\|_W \|w\|_W, \quad \forall v,\, w \in W.$$

In the last line and in the following $|\cdot|$ stands for the Euclidean norm in $\mathbb{R}^n$, $n \in \mathbb{N}$. We call a linear operator $T \colon X \to Y$ between two Banach spaces X and Y with associated norms $\|\cdot\|_X$ and $\|\cdot\|_Y$ bounded if $\|Tv\|_Y \leq C\|v\|_X$, $\forall v \in X$ for a constant $C > 0$. The smallest possible C in the last inequality is called the operator norm of T. For the set of bounded linear operators from X to Y we use the abbreviation $\mathcal{L}(X, Y)$. The dual space of a Hilbert or Banach space X is denoted just by X', i.e.

$$X' \coloneqq \{T \colon X \to \mathbb{R} \mid T \text{ linear and bounded}\}.$$

Latter space X' is in fact again a Banach space, where the corresponding operator norm reads

$$\|T\|_{X'} \coloneqq \sup_{x \in X, \|x\|_X = 1} |Tx|,\ T \in X'.$$

[1] $Z = X \perp Y$ (X, Y, Z subspaces of Hilbert space $(W, \langle\cdot,\cdot\rangle)$) : $\iff \forall z \in Z,\ \exists_1 y \in Y, \exists_1 x \in X$ s.t. $z = x + y,\ \langle x, y\rangle = 0$.

In view of weak derivatives we allow also for unbounded operators $T\colon X \to Y$. Then the actual domain space $\mathrm{Dom}(T) \subset X$ has to be provided and it is reasonable to write $(T, \mathrm{Dom}(T))$ instead of just T. Further, the range and kernel of such a linear operator T is abbreviated with $\mathcal{R}(T, \mathrm{Dom}(T)) \coloneqq \{Tv \mid v \in \mathrm{Dom}(T)\}$, $\mathcal{N}(T, \mathrm{Dom}(T)) \coloneqq \{v \in \mathrm{Dom}(T) \mid Tv = 0\}$. In the case $\mathrm{Dom}(T) = X$ we just write $\mathcal{R}(T)$, $\mathcal{N}(T)$. Frequently, one can assume dense domain spaces, particularly when dealing with standard differential operators such as the *gradient* or *divergence* operator, which later appear in the de Rham complex.
For densely defined operators between Hilbert spaces the adjoints can be introduced.

Assumption 2.1. *In the following, let U, W denote Hilbert spaces and X, Y Banach spaces.*

Definition 2.1 (Adjoint operator, cf. [75, Section 4.4])**.** *Let $T\colon \mathrm{Dom}(T) \subset U \to W$ be a densely defined linear operator.*
Set $\mathrm{Dom}(T^*) \coloneqq \{w \in W \mid \exists C > 0 \text{ s.t. } |\langle Tv, w\rangle_W| \leq C \|v\|_U, \forall v \in \mathrm{Dom}(T)\}$. Then there is a unique operator $T^*\colon \mathrm{Dom}(T^*) \subset W \to U$ s.t.

$$\langle Tv, w\rangle_W = \langle v, T^*w\rangle_U, \quad \forall v \in \mathrm{Dom}(T),\, w \in \mathrm{Dom}(T^*),$$

which is called the adjoint of $(T, \mathrm{Dom}(T))$.

We have titled the last block as a definition; however, strictly speaking, the introduction of adjoint operators is connected to a statement that needs to be proven. To establish the well-definedness of the adjoint operator T^* the Riesz representation theorem can be employed, which we briefly mention here.

Lemma 2.1 (**Riesz representation theorem**, see e.g. [2, Section 4.1])**.** *We obtain with*

$$J\colon W \to W' \,,\ w \mapsto \Big(v \mapsto \langle v, w\rangle_W\Big)$$

an isometric isomorphism between Banach spaces.

One observes that in the special case $T \in \mathcal{L}(U, W)$ we get by the Cauchy–Schwarz inequality that $T^* \in \mathcal{L}(W, U)$.
The class of densely defined unbounded operators is still quite large and often more structure is required. A useful and important subset is that of *closed operators*.

Definition 2.2 (**Closed operators**)**.** *An operator $T\colon \mathrm{Dom}(T) \subset U \to W$ is said to be* closed *if for sequences $(v_m)_{m\in\mathbb{N}} \subset \mathrm{Dom}(T)$ with $v_m \xrightarrow{U} v \in U$ and $Tv_m \xrightarrow{W} w$ it is $v \in \mathrm{Dom}(T)$ as well as $Tv = w$.*[2]

The notation of closed operators can be seen as the generalization of bounded operators, since for the case $\mathrm{Dom}(T) = U$ the last definition is equivalent to the continuity condition; compare [75, Theorem 5.2.]. Closed operators allow us to interpret the domain space as Hilbert space itself. Namely, the *graph inner product*

$$\langle v, w\rangle_{\mathrm{Dom}(T)} \coloneqq \langle v, w\rangle_U + \langle Tv, Tw\rangle_W, \quad v,\ w \in \mathrm{Dom}(T)$$

makes $\mathrm{Dom}(T)$ to a Hilbert space iff the underlying operator is closed. This aspect becomes crucial if one looks at the domain complexes of Hilbert complexes in FEEC; see Section 3.
An interesting connection between the closedness property and the previously defined adjoint operators is given in the next lemma.

[2] If a sequence $(x_m)_{m\in\mathbb{N}} \subset X$, $(X, \|\cdot\|_X)$ Banach space, converges to $x \in X$ w.r.t. $\|\cdot\|_X$, then we write $x_m \xrightarrow{X} x$.

Lemma 2.2 (**Adjoint of closed densely defined operator**, see Propositions 3.3, 3.4 and Theorem 3.5 in [5])**.** *In case of a closed densely defined operator* $T\colon \mathrm{Dom}(T) \subset U \to W$ *the adjoint* $T^*\colon \mathrm{Dom}(T^*) \subset W \to U$ *is also closed and densely defined. Moreover, then we have* $(T^*)^* = T$ *and* $\mathcal{R}(T, \mathrm{Dom}(T))^\perp = \mathcal{N}(T^*, \mathrm{Dom}(T^*))$.

It is important to mention again here that a closed operator does not necessarily have a closed range. However, if the closed range property holds, it also applies to the adjoint.

Lemma 2.3 (**Closed range theorem**, see Theorem 3.7 in [5])**.** *Let the assumptions of the last lemma be valid. In this case we have a closed range of* T *if and only if the range of the adjoint is closed.*

Attempting to provide a profound introduction to the extensive topic of Hilbert spaces and linear operators within a few pages is bound to fail. It is, therefore, advisable to refer to the available textbooks like [2, 70, 41, 1]. Nevertheless, we would like to briefly outline the following statements here, as they will be used multiple times later and will be generally helpful for understanding the explanations in the upcoming chapters.

Further useful statements

Lemma 2.4 (**Bounded inverse theorem**,[2, Theorem 5.8])**.** *For a bijective operator* $T \in \mathcal{L}(X, Y)$ *it holds* $T^{-1} \in \mathcal{L}(Y, X)$.

Corollary 2.1. *Let* $T\colon U \to W$ *be a bounded linear operator between Hilbert spaces with closed range* $\mathcal{R}(T) \subset W$*. We have then the property*

$$\forall w \in \mathcal{R}(T),\ \exists v \in U,\quad \text{s.t. } Tv = w \quad \text{and} \quad \|v\|_U \leq C \|w\|_W ,$$

where $C > 0$ *does not dependent on* w*. In particular, the mapping* $T\colon U \to \mathcal{R}(T)$ *has a bounded right-inverse.*

Proof. We look at the restricted operator $T_|\colon \mathcal{N}(T)^\perp \to \mathcal{R}(T)\ ,\ v \mapsto Tv$, which is obviously a bijective and bounded mapping between Hilbert spaces. Hence, due to Lemma 2.4 the inverse $T_|^{-1}$ is bounded and $TT_|^{-1}w = w$ on $\mathcal{R}(T)$. □

Lemma 2.5 (**Bounded right-inverse**, compare [24, Theorem 0.1])**.** *Let* $T\colon U \to W$ *be a bounded linear mapping w.r.t the norms* $\|\cdot\|_U$, $\|\cdot\|_W$ *induced by the inner products. Further assume*

$$\inf_{0\neq w\in W} \sup_{0\neq v\in U} \frac{\langle Tv, w\rangle_W}{\|v\|_U \ \|w\|_W} \geq C_\dagger > 0.$$

Then there is for all $w \in W$ *an element* $v \in U$ *s.t.* $Tv = w$ *and* $\|v\|_U \leq \frac{1}{C_\dagger} \|w\|_W$.

Proof. We follow the proof steps of [7, Lemma 2].
The adjoint $T^*\colon W \to U$ exists and satisfies

$$C_\dagger \|w\|_W \leq \sup_{0\neq v\in U} \frac{\langle Tv, w\rangle_W}{\|v\|_U} = \sup_{0\neq v\in U} \frac{\langle v, T^*w\rangle_U}{\|v\|_U} = \|T^*w\|_U , \quad \forall w \in W.$$

Thus we have injectivity of T^* and the left-inverse of T^* is bounded with operator norm $\leq 1/C_\dagger$. This implies the surjectivity of T and the operator norm of the right-inverse $T^\dagger$ of T is bounded by $1/C_\dagger$. □

Lemma 2.6 (**Orthogonal projection**, see Theorem 2.2 in [2]). *For every closed subspace V of a Hilbert space W there exists a unique bounded mapping $\mathcal{P}_V \colon W \to V$ which satisfies*

$$\langle \mathcal{P}_V w - w, v \rangle_W = 0, \quad \forall v \in V,\, w \in W.$$

$\mathcal{P}_V$ is called the orthogonal projection onto V and clearly $\mathcal{P}_V w - w \in V^\perp$.

Definition 2.3 (**Moore-Penrose inverse**). *Let us suppose $T \in \mathcal{L}(U, W)$ to have a closed range in W. As in the proof of Corollary 2.1 we see that the restriction $T_| \colon \mathcal{N}(T)^\perp \to \mathcal{R}(T)$ of T has a bounded inverse mapping $T_|^{-1}$. Then we set for $w \in W$*

$$T^\dagger w := T_|^{-1} w_2, \quad \text{where} \quad w = w_1 + w_2,\ w_1 \in \mathcal{R}(T)^\perp,\ w_2 \in \mathcal{R}(T).$$

We call the implied mapping $T^\dagger \colon W \to U$ the Moore-Penrose *inverse of T. It it is easy to check that $T^\dagger$ fulfills the properties*

$$T^\dagger \in \mathcal{L}(W, U), \qquad T^\dagger T = \mathcal{P}_{\mathcal{N}(T)^\perp}, \qquad T T^\dagger = \mathcal{P}_{\mathcal{R}(T)}. \tag{2.1.1}$$

Standard example and starting point for various different space definitions in the field of Sobolev spaces is the space $L^2(\Omega)$ of square integrable functions on a suitable domain $\Omega \subset \mathbb{R}^n$, $n \in \mathbb{N}$ in the Euclidean space. For our purposes it is enough to assume bounded Lipschitz domains Ω that guarantee boundary values and boundary integrals for the spaces we address later. Furthermore, the class of Lipschitz domains are helpful for extending Sobolev spaces.

Definition 2.4 (**Lipschitz domain**). *A bounded domain $\Omega \subset \mathbb{R}^n$, $n \in \mathbb{N}_{\geq 2}$ is a Lipschitz domain, if there are finitely many open sets $U_i \subset \mathbb{R}^n$ s.t. $\partial\Omega \subset \bigcup_i U_i$ and that the boundary segments $\Gamma_i := U_i \cap \partial\Omega$ can be expressed as a part of the graph of a Lipschitz continuous function $\phi_i \colon \mathbb{R}^{n-1} \to \mathbb{R}$. The latter might require a rigid body motion of the coordinate axis. Furthermore, we assume for each index i, after a possible renaming of the coordinate axis, that $\{(x, x_n) \in \mathbb{R}^{n-1} \times \mathbb{R} \mid \phi_i(x) > x_n\} \cap U_i = \Omega \cap U_i$.*

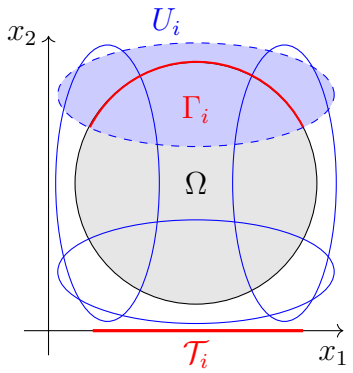

Figure 1: Obviously, an open disk defines a Lipschitz domain Ω.

Assumption 2.2 (Domains). *Here and in the rest of the whole text Ω always stands for a Lipschitz domain.*

Definition 2.5 (**The space $L^2(\Omega)$**). *On the set*

$$\mathcal{L}^2(\Omega) := \left\{ v \colon \Omega \to \mathbb{R} \;\middle|\; v \text{ Lebesgue measurable}, \int_\Omega |v|^2 \, dx < \infty \right\}$$

we can introduce the equivalence relation

$$f \sim g \text{ in } \mathcal{L}^2(\Omega) \;:\Leftrightarrow\; \text{Lebesgue measure of } \{x \in \Omega \mid f(x) \neq g(x)\} \text{ is zero,}$$

where we consider the integrals always in the sense of Lebesgue integration theory; see [2, Chapter 1]. Then the quotient vector space

$$L^2(\Omega) \coloneqq \mathcal{L}^2(\Omega)/\sim$$

can be endowed with the inner product $\langle v, w\rangle_{L^2(\Omega)} \coloneqq \int_\Omega v\, w\, dx$ *which yields a Hilbert space and we write* $\|\cdot\|_{L^2(\Omega)}$ *for the norm induced by* $\langle\cdot,\cdot\rangle_{L^2(\Omega)}$.
Though, $L^2(\Omega)$ *is a quotient space, we stipulate to identify for* $f \in L^2(\Omega)$ *always* f *with one representative. This means in calculations we can think of classical functions.*
If the domain is clear from the context we write in the following sometimes just $\|\cdot\| = \|\cdot\|_{L^2(\Omega)}$ *and* $\langle\cdot,\cdot\rangle$ *for the* L^2 *inner product.*

Before facing the notion of weak derivatives, let us highlight here a crucial density result for functions in $L^2(\Omega)$.

Lemma 2.7 (**Density of smooth functions**, [2, 2.14])**.** *Every mapping in* $L^2(\Omega)$ *can be approximated utilizing test functions, i.e.*

$$L^2(\Omega) = \overline{C_c^\infty(\Omega)}^{\|\cdot\|_{L^2(\Omega)}}.$$

Here, $\overline{X}^{\|\cdot\|}$ *denotes the closure of* X *w.r.t.* $\|\cdot\|$ *and* $C_c^\infty(\Omega)$ *is the set of infinitely differentiable functions with compact support in* Ω.

2.2 Weak derivatives and Sobolev spaces

Within the theory of PDEs, especially the numerical investigation of PDE problems, it becomes apparent that the classical notion of derivatives is often inconvenient. The concept of weak derivatives, or even more general, distributional derivatives is more appropriate. Also for the class of Sobolev spaces the notion of weak derivatives is underlying. For this reason we clarify what we actually mean by a weak derivative.
First of all, for $\alpha = (\alpha_1, \dots, \alpha_n) \in \mathbb{N}_0^n$ let us introduce the multi-index notation $\partial^\alpha \coloneqq \partial^{\alpha_1,\alpha_2,\dots,\alpha_n} \coloneqq \partial_1^{\alpha_1} \dots \partial_n^{\alpha_n}$, where $\partial_i^{\alpha_i}$ is the classical α_i-th partial derivative w.r.t. the i-th coordinate. And naturally, we write below just ∂_i for ∂_i^1. Obviously, ∂^α determines a densely defined operator $\partial^\alpha \colon C_c^\infty(\Omega) \subset L^2(\Omega) \to L^2(\Omega)$, due to Lemma 2.7. We can look at the adjoint $(\partial^\alpha)^*$ of $(\partial^\alpha, C_c^\infty(\Omega))$ for which it is $C_c^\infty(\Omega) \subset \mathrm{Dom}((\partial^\alpha)^*)$, by the rules of partial integration. Consequently, the next definition makes sense.

Definition 2.6 (**Weak derivatives**)**.** *Let* $\alpha \in \mathbb{N}_0^n$. *An element* $v \in L^2(\Omega)$ *has a weak derivative* $\partial^\alpha v$ *if there is a* $w \in L^2(\Omega)$ *s.t.*

$$\langle w, \phi\rangle = \langle v, (\partial^\alpha)^* \phi\rangle, \quad \forall \phi \in C_c^\infty(\Omega).$$

We set $\partial^\alpha v \coloneqq w$.

For sufficiently regular ϕ, namely $\phi \in C^{|\alpha|_1}(\overline{\Omega})$, $|\alpha|_1 \coloneqq \alpha_1 + \dots + \alpha_n$, the weak and strong derivatives coincide.[3] Further, by a density argument it is easy to see that weak derivatives are always unique. Based on this, one defines the scalar Sobolev spaces $H^k(\Omega)$ without boundary conditions.

[3] $C^k(U)$, $k \in \mathbb{N}_0$, stands for the space of k-times continuously differentiable functions on U.

Definition 2.7 (**Sobolev spaces**). *For $k \in \mathbb{N}_0$ one sets*

$$H^k(\Omega) \coloneqq \{w \in L^2(\Omega) \mid \partial^\alpha w \in L^2(\Omega) \text{ exists in a weak sense, } \forall \alpha \in \mathbb{N}_0^n \text{ with } |\alpha|_1 \leq k\}.$$

In particular $H^0(\Omega) = L^2(\Omega)$.

The different $H^k(\Omega)$, endowed with the inner products

$$\langle v, w\rangle_{H^k(\Omega)} \coloneqq \sum_{|\alpha|_1 \leq k} \langle \partial^\alpha v, \partial^\alpha w\rangle \quad \text{and norms} \quad \|v\|^2_{H^k(\Omega)} \coloneqq \sum_{|\alpha|_1 \leq k} \|\partial^\alpha v\|^2,$$

are Hilbert spaces; for more details we refer to the explanation in [2, Section 1.25]. Regarding the spaces $H^k(\Omega)$ there is a useful density result related to smooth mappings. It reads

$$H^k(\Omega) = \overline{C^\infty(\overline{\Omega})}^{\|\cdot\|_{H^k(\Omega)}} \quad , \tag{2.2.1}$$

which for example follows directly from [2, Lemma A6.7]. Above $C^\infty(\overline{\Omega})$ stands for the space of smooth functions with continuously extendable derivatives to the closure $\overline{\Omega}$. Such relations (2.2.1) are especially important because they allow classical rules of differentiation to be extended to the concept of weak differentiation. Namely we have e.g. the product rule $\partial_i(v\,w) = (\partial_i v)w + v\,\partial_i w$ for $v, w \in H^k(\Omega), k \geq 1$ which ensures $v\,w \in H^k(\Omega)$. And having a C^1-diffeomorphism $\mathbf{F}$ from one Lipschitz domain $\widehat{\Omega} \subset \mathbb{R}^n$ to second one $\Omega \subset \mathbb{R}^n$ one can prove

$$v \in H^1(\Omega) \Longrightarrow v \circ \mathbf{F} \in H^1(\widehat{\Omega})$$

as well as the chain rule formula

$$\hat{\partial}_i(v \circ \mathbf{F}) = \textstyle\sum_{j=1}^n (\partial_j v \circ \mathbf{F}) \cdot J_{ji}.$$

Above J_{ji} are the entries of the Jacobian matrix field $\mathbf{J} = D\mathbf{F}$ of $\mathbf{F}$. We further added a *hat* $\hat{}$ to emphasize the differentiation w.r.t. the new coordinates.
Another point we would like to mention is the possibility to extend Sobolev spaces. For this purpose let use define

$$H^k(\mathbb{R}^n) \coloneqq \{v\colon \mathbb{R}^n \to \mathbb{R} \mid v \in H^k(B_r(0)), \forall r > 0 \text{ and } r \mapsto \|v\|_{H^k(B_r(0))} \text{ is bounded}\}$$

and norms

$$\|v\|_{H^k(\mathbb{R}^n)} \coloneqq \lim_{r\to\infty} \|v\|_{H^k(B_r(0))}.$$

Above $B_r(0)$ stands for the open Euclidean r-neighborhood of the origin. The last auxiliary definitions are exploited in the next extension result.

Lemma 2.8 (**Stein extension operator**, see [68, Theorem 5 on page 181]). *Let $\Omega \subset \mathbb{R}^n$ be a Lipschitz domain. Further let $k \in \mathbb{N}_0$. Then there exists an* extension operator $\mathcal{E}$ *of the form*

$$\mathcal{E}\colon H^k(\Omega) \to H^k(\mathbb{R}^n),$$

meaning $\mathcal{E}v = v$ on Ω, s.t. $\|\mathcal{E}v\|_{H^i(\mathbb{R}^n)} \leq C_{\mathcal{E}} \|v\|_{H^i(\Omega)}, \forall v \in H^k(\Omega)$, for $i = 0, \ldots, k$ and a proper constant $C_{\mathcal{E}}$.

The restriction to Lipschitz domains is not only important for the last lemma but is also needed to define the outward normal vector $\mathbf{n}$ to the boundary $\partial\Omega$ and to establish the notion of boundary values. As demonstrated in [2, A6.5], such a normal vector $\mathbf{n}$ does indeed exist, and its components are elements of the boundary Lebesgue space $L^2(\partial\Omega)$. Moreover, the trace theorem

holds for $H^1(\Omega)$, which provides the existence of a unique bounded operator $\gamma\colon H^1(\Omega) \to L^2(\partial\Omega)$ with

$$\gamma(\phi) = \phi_{|\partial\Omega}, \quad \forall \phi \in H^1(\Omega) \cap C^0(\bar{\Omega}) \qquad \text{(see [2, A6.6])}.$$

For a precise definition of L^2 spaces on the domain boundary, i.e. $L^2(\partial\Omega)$, we again refer to [2, A6.5]. The trace operator allows us to restrict H^1 functions to the boundary, where we write $u(x)$ instead of $\gamma(u)(x)$ for $x \in \partial\Omega$. By utilizing the trace theorem (see [69, Theorem 2.21]) and the outer unit normal $\mathbf{n}$, it becomes possible to formulate the fundamental integration by parts equation, which will be repeatedly used in later chapters. Specifically, it can be expressed as follows: For $u,\, v \in H^1(\Omega)$ the relation

$$\langle \partial_i u, v\rangle = -\langle u, \partial_i v\rangle + \int_{\partial\Omega} uv\, n_i\, ds \qquad \text{(see [2, A6.8])} \tag{2.2.2}$$

holds, where above n_i is the i-th component of the outer unit normal vector $\mathbf{n}$ to the boundary $\partial\Omega$ and $\int_{\partial\Omega} \cdot\, ds$ denotes the usual boundary integral.

A generalization of the spaces $H^k(\Omega)$ to the vector-valued or matrix-valued setting is straightforward using a component-wise point of view. This corresponds to a tensor product construction and we write then $H^k(\Omega) \otimes \mathbb{R}^n$ for vector-valued functions. More general for a finite-dimensional $\mathbb{R}$-Hilbert space $\mathbb{E}$ we can consider $\mathbb{E}$-valued Sobolev spaces $H^k(\Omega) \otimes \mathbb{E}$, where we refer to [75, Section 3.4] for a detailed definition of product Hilbert spaces. Let $e_1, \dots, e_d$ be an orthonormal basis of $\mathbb{E}$. Then we can uniquely express each $v \in H^k(\Omega) \otimes \mathbb{E}$ through a sum of the form $v = \sum_{i=1}^d v_i\, e_i,\ v_i \in H^k(\Omega)$ determined by

$$v\colon \Omega \to \mathbb{E}\ ,\ v(x) \coloneqq \textstyle\sum_{i=1}^d v_i(x)\, e_i.$$

In other words we interpret $H^k(\Omega) \otimes \mathbb{E}$ as the space of $\mathbb{E}$-valued fields with coefficient functions in $H^k(\Omega)$. The inner products generalize naturally in the sense

$$\langle v, w\rangle_{H^k(\Omega)\otimes\mathbb{E}} \coloneqq \textstyle\sum_{i=1}^d \langle v_i, w_i\rangle_{H^k(\Omega)}, \quad \text{if } \ v = \sum_{i=1}^d v_i\, e_i,\ w = \sum_{i=1}^d w_i\, e_i,$$

which leads again to Hilbert spaces. In the situation $k = 0$ we will again drop the indices and write $\langle v, w\rangle_{H^0(\Omega)\otimes\mathbb{E}} = \langle v, w\rangle$ and for the corresponding L^2 norm $\|\cdot\|$. Further, if the underlying space and domain is clear, we use the notation $\|v\|_{H^k} = \|v\|_{H^k(\Omega)\otimes\mathbb{E}}$ for the norm induced by the mentioned inner product on $H^k(\Omega) \otimes \mathbb{E}$. To emphasize the actual domain we also write sometimes $\|v\|_{H^k(\Omega)} = \|v\|_{H^k(\Omega)\otimes\mathbb{E}}$.

Having two spaces $L^2(\Omega)\otimes\mathbb{E},\ L^2(\Omega)\otimes\tilde{\mathbb{E}}$ with underlying bases $\{e_1, \dots, e_d\} \subset \mathbb{E},\ \{\tilde{e}_1, \dots, \tilde{e}_m\} \subset \tilde{\mathbb{E}}$, we can define differential operators of the form

$$\mathcal{D} \coloneqq \textstyle\sum_{i=1,j=1}^{d,m}\ c_{ij}\, \partial^{\alpha^{i,j}} \otimes \tilde{e}_j, \quad c_{ij} \in \mathbb{R},\ \alpha^{i,j} \in \mathbb{N}_0^n,$$

defined through

$$\mathcal{D}v \coloneqq \textstyle\sum_{i=1,j=1}^{d,m}\ c_{ij}\, (\partial^{\alpha^{i,j}} v_i)\ \tilde{e}_j, \quad \text{where} \quad v \coloneqq \sum_{i=1}^d v_i\, e_i, \tag{2.2.3}$$

for regular v_i. Then this $\mathcal{D}$ is a densely defined operator $\mathcal{D}\colon L^2(\Omega) \otimes \mathbb{E} \to L^2(\Omega) \otimes \tilde{\mathbb{E}}$ as we can choose $C_c^\infty(\Omega) \otimes \mathbb{E}$ as domain space. And the density of the latter in $L^2(\Omega) \otimes \mathbb{E}$ is clear. We say the operator has order

$$\operatorname{ord}(\mathcal{D}) = l, \quad \text{if} \quad \max_{i,j}\{|\alpha^{i,j}|_1 \mid c_{ij} \neq 0\} = l.$$

Again it is clear that for the above definitions, the adjoint $\mathcal{D}^* = (\mathcal{D}, C_c^\infty(\Omega) \otimes \mathbb{E})^*$ exists and $C_c^\infty(\Omega) \otimes \tilde{\mathbb{E}} \subset \operatorname{Dom}(\mathcal{D}^*)$. Thus one can use an analogous formula like in Definition 2.6 to define

the differential operator $\mathcal{D}$ in a weak sense. For $v \in L^2(\Omega) \otimes \mathbb{E}$ we say $\mathcal{D}v = w \in L^2(\Omega) \otimes \tilde{\mathbb{E}}$ in a weak sense, if

$$\langle w, \phi \rangle = \langle v, \mathcal{D}^* \phi \rangle, \quad \forall \phi \in C_c^\infty(\Omega) \otimes \tilde{\mathbb{E}}.$$

So one can consider the space

$$W(\Omega, \mathcal{D}, \mathbb{E}) \coloneqq \{v \in L^2(\Omega) \otimes \mathbb{E} \mid \mathcal{D}v \in L^2(\Omega) \otimes \tilde{\mathbb{E}}\},$$

where here $\mathcal{D}$ is again meant in a weak manner.

Lemma 2.9. *The space $W(\Omega, \mathcal{D}, \mathbb{E})$ is a Hilbert space endowed with the graph inner product $\langle \cdot, \cdot \rangle_{H(\mathcal{D})} = \langle \cdot, \cdot \rangle + \langle \mathcal{D}\cdot, \mathcal{D}\cdot \rangle$ related to $\mathcal{D}$.*

Proof. It is enough to check the closedness of $\mathcal{D}$: $W(\Omega, \mathcal{D}, \mathbb{E}) \subset L^2(\Omega) \otimes \mathbb{E} \to L^2(\Omega) \otimes \tilde{\mathbb{E}}$. Therefore assume $W(\Omega, \mathcal{D}, \mathbb{E}) \ni v_m \xrightarrow{L^2} v, \;\; \mathcal{D}v_m \xrightarrow{L^2} w$. One observes

$$\langle w, \phi \rangle = \lim_{m \to \infty} \langle \mathcal{D}v_m, \phi \rangle = \lim_{m \to \infty} \langle v_m, \mathcal{D}^* \phi \rangle = \langle v, \mathcal{D}^* \phi \rangle, \quad \forall \phi \in C_c^\infty(\Omega) \otimes \tilde{\mathbb{E}},$$

and sees $w = \mathcal{D}v$. □

With the abbreviation $\|\cdot\|^2_{H(\mathcal{D})} \coloneqq \|\cdot\|^2 + \|\mathcal{D}\cdot\|^2$ for the graph norm and due to the obvious fact $C^\infty(\overline{\Omega}) \otimes \mathbb{E} \subset W(\Omega, \mathcal{D}, \mathbb{E})$ we can look at the closure

$$H(\Omega, \mathcal{D}, \mathbb{E}) \coloneqq \overline{C^\infty(\overline{\Omega}) \otimes \mathbb{E}}^{\|\cdot\|_{H(\mathcal{D})}}, \tag{2.2.4}$$

which gives us again a Hilbert space. Latter construction guarantees the possibility to approximate every element by means of smooth functions. Using (2.2.1) there is no problem to see

$$H^l(\Omega) \otimes \mathbb{E} \subset H(\Omega, \mathcal{D}, \mathbb{E}), \quad \text{with } \operatorname{ord}(\mathcal{D}) = l.$$

In view of the literature on Sobolev spaces (see e.g. [1, 38]) we gave above in fact only the definition for a special class of Sobolev spaces. They will be convenient for weak PDE formulations later. Nevertheless, e.g. also spaces with negative exponent $H^{-k}(\Omega)$, $k \in \mathbb{N}_{>0}$ will appear and therefore a brief explanation comes next. Firstly, we need to introduce the Sobolev spaces with zero boundary values $H_0^k(\Omega)$. They are defined as the closure of the space of compactly supported test functions w.r.t. to the $\|\cdot\|_{H^k(\Omega)}$ norm. More precisely,

$$H_0^k(\Omega) \coloneqq \overline{C_c^\infty(\Omega)}^{\|\cdot\|_{H^k(\Omega)}}.$$

This construction makes also sense if we face more involved spaces. In other words, we can consider the next spaces with generalized zero boundary conditions

$$H_0(\Omega, \mathcal{D}, \mathbb{E}) \coloneqq \overline{C_c^\infty(\Omega) \otimes \mathbb{E}}^{\|\cdot\|_{H(\mathcal{D})}} \;. \tag{2.2.5}$$

Let $\mathcal{D}^*$ be the adjoint differential operator to $\mathcal{D}$ obtained through a successive application of integration by parts. Then, it is easy to check the relation

$$H_0(\Omega, \mathcal{D}^*, \tilde{\mathbb{E}}) \subset \operatorname{Dom}\Big((\mathcal{D}, H(\Omega, \mathcal{D}, \mathbb{E}))^*\Big). \tag{2.2.6}$$

Now one defines

$$H^{-k}(\Omega) \coloneqq \Big(H_0^k(\Omega)\Big)',$$

as the dual space of the Sobolev space with zero boundary values. The norm $\|\cdot\|_{H^{-k}(\Omega)}$ is then the associated operator norm. One observes that Lemma 2.1 implies a Hilbert space structure

on the duals of Hilbert spaces. Namely, having v', w' in the dual space W' of a Hilbert space W we get a suitable inner product through $\langle v', w' \rangle_{W'} \coloneqq \langle J^{-1}v', J^{-1}w' \rangle_W$, where $J\colon W \to W'$ is the Riesz isomorphism. It is therefore justified to later speak of $H^{-k}(\Omega)$ as Hilbert spaces.
There is no issue to consider also spaces of the form $H^z(\Omega) \otimes \mathbb{E}$ with $z \in \mathbb{Z}$. An element $v = \sum_{i=1}^d v_i' \, e_i \in H^{-k}(\Omega) \otimes \mathbb{E}$, i.e. $v_i' \in H^{-k}(\Omega)$, can be seen as a mapping which acts on $H_0^k(\Omega)$ per definition as

$$v(w) \coloneqq \textstyle\sum_{i=1}^d v_i'(w) \, e_i, \quad \forall w \in H_0^k(\Omega).$$

Note, we assume the e_i to form an orthonormal basis of $\mathbb{E}$. Hence we can interpret the range $\mathcal{R}(v)$ as a subspace of $\mathbb{E}$. Such spaces $H^{-k}(\Omega)$ and differential operators like $\mathcal{D}$ from (2.2.3) motivate the generalization of the weak derivative notion even more. More precisely, one can look at derivatives in a distributional sense. A distribution on Ω is a linear functional $T\colon C_c^\infty(\Omega) \to \mathbb{R}$ that satisfies: $\forall K \subset \Omega,\ K$ compact in $\mathbb{R}^n,\ \exists N_K,\ C_K \in \mathbb{N}$ s.t.

$$|T(\phi)| \leq C_K \sup\{|\partial^\alpha \phi(x)| \mid x \in K,\, |\alpha|_1 \leq N_K\},\ \forall \phi \in C_c^\infty(\overset{\circ}{K}). \quad \text{(compare [2, 3.15])}$$

We use the notation $\overset{\circ}{K}$ to denote the interior of K. Consequently, every $f \in H^z(\Omega),\ z \in \mathbb{Z}$ defines a distribution, where for $z \geq 0$ we might identify f with the distribution T_f determined through

$$T_f(\phi) \coloneqq \langle f, \phi \rangle, \quad \forall \phi \in C_c^\infty(\Omega).$$

The partial derivative ∂^α of a distribution T is defined by

$$\partial^\alpha T(\phi) \coloneqq (-1)^{|\alpha|_1} T(\partial^\alpha \phi),$$

meaning we get a new distribution. A simple calculation involving integration by parts shows for $f \in L^2(\Omega)$ with existing weak derivative $\partial^\alpha f \in L^2(\Omega)$ that we get the equation

$$\partial^\alpha T_f = T_{\partial^\alpha f}$$

and we can identify the weak derivative with the distributional concept. Now, using the distributional derivative idea, it is possible to generalize an operator $\mathcal{D}$ of the form (2.2.3) to the case with $v_i \in H^{-k}(\Omega),\ k \in \mathbb{N}$. If l is the order of differential operator $\mathcal{D}$, we get

$$\mathcal{D}\colon H^{-k}(\Omega) \otimes \mathbb{E} \to H^{-k-l}(\Omega) \otimes \tilde{\mathbb{E}} \tag{2.2.7}$$

in the sense of distributions. To be more precise we set for $v' = \sum_{i=1}^d v_i' \, e_i \in H^{-k}(\Omega) \otimes \mathbb{E}$ just

$$\mathcal{D}v'(\phi) \coloneqq \textstyle\sum_{i=1,j=1}^{d,m} c_{ij} \left[\partial^{\alpha^{i,j}} v_i'\right](\phi) \tilde{e}_j \in \tilde{\mathbb{E}}, \quad \forall \phi \in C_c^\infty(\Omega),$$

with $\left[\partial^{\alpha^{i,j}} v_i'\right](\phi) \in \mathbb{R}$ denoting the action of the distribution $\partial^{\alpha^{i,j}} v_i'$ on ϕ. Further let us denote with $|\cdot|$ a norm in the space $\mathbb{E}$, $\tilde{\mathbb{E}}$, respectively. Then we can estimate

$$\begin{aligned} |\mathcal{D}v'(\phi)| &= \left| \textstyle\sum_{i,j} c_{ij} \left[\partial^{\alpha^{i,j}} v_i'\right](\phi) \tilde{e}_j \right| \leq \textstyle\sum_{i,j} \left| c_{ij} \left[v_i'\right](\partial^{\alpha^{i,j}} \phi) \tilde{e}_j \right| \\ &\leq C \textstyle\sum_{i,j} \|v_i'\|_{H^{-k}(\Omega)} \left\| \partial^{\alpha^{i,j}} \phi \right\|_{H^k(\Omega)} \leq C_v' \, \|\phi\|_{H^{k+l}(\Omega)}, \end{aligned}$$

where the constant C_v' depends not on ϕ. Now by construction we have density of $C_c^\infty(\Omega)$ in $H_0^{k+l}(\Omega)$. Due to that there is a unique extension of $\mathcal{D}v'$ to the whole $H_0^{k+l}(\Omega)$ such that we have boundedness w.r.t. $\|\cdot\|_{H^{k+l}(\Omega)}$; see e.g. [70, Lemma 6.5.1]. Thus, $\mathcal{D}v'$ can be interpreted as an element in $H^{-k-l}(\Omega) \otimes \tilde{\mathbb{E}}$. This makes the line (2.2.7) clearer. Before we go on let us refer to the book [50] here for a profound introduction to the topic of distributions.

Sobolev functions and weak derivative operators are the natural ingredients for PDE variational formulations. The latter will be briefly discussed in the next section.

2.3 Variational formulations and well-posedness

As already indicated, it is reasonable to interpret an equation like $\mathcal{D}v = f$ with an operator of the form (2.2.3) no longer in its strong form when introducing Finite Element discretizations of PDEs. Instead, it is more appropriate to consider the differentials in a weak sense and to consider so-called *weak formulations* of the PDEs. To derive the latter one starts in general by multiplying the equation $\mathcal{D}u = f$ with test functions meaning

$$\langle \mathcal{D}u, v\rangle = \langle f, v\rangle, \quad \forall v \in L^2(\Omega) \otimes \tilde{\mathbb{E}}. \tag{2.3.1}$$

This shows the feasibility to interpret the both sides of a PDE as elements in the corresponding dual space. However, in concrete applications, appropriate boundary and initial conditions also play a role. Then with possible additional regularity conditions regarding the solution u and the source function f together with integration by parts, equations of the form (2.3.1) are typically transformed into modified equations $\mathcal{B}(u, v) = \mathcal{F}(v),\ \forall v \in W$ involving some bilinear $\mathcal{B}$ form on a proper Hilbert space $U \times W$. This transformation of a PDE into an equation of this form leads to the mentioned weak formulation or variational formulation. An element that satisfies the weak formulation is naturally referred to as a weak solution. The transition from the actual PDE problem to equations involving test functions must naturally occur consistently. This means that if there exists a smooth and therefore strong solution to the PDE problem, it must also satisfy the new weak formulation.
The modified formulation then serves as the starting point for the numerical analysis within the framework of the FEM. Namely, the fundamental idea is to no longer seeking for u and choosing v in the continuous spaces U and W, but rather from finite-dimensional subspaces. The specific choice of the bilinear form $\mathcal{B}$ and discrete spaces that make sense for providing a good approximation of the original PDE obviously depends on the problem itself and is generally difficult to answer. This is because establishing of $\mathcal{B}$ and selecting the spaces W, U is indeed a central aspect of the theory of Finite Elements. For a detailed introduction and explanation of the connection between FEM and weak formulations of PDEs, we recommend the book by Braess [20]. However, we will refrain from delving further into this and proceed with useful definitions and results in the field of variational formulations.

Definition 2.8 (**Abstract variational formulation**). *Given two Hilbert spaces U and W, a bilinear form $\mathcal{B}\colon U \times W \to \mathbb{R}$ as well as a functional $\mathcal{F}\colon W \to \mathbb{R}$, we define the abstract variational problem:*

Find all $u \in U$ s.t.

$$\mathcal{B}(u, v) = \mathcal{F}(v), \quad \forall v \in W. \tag{2.3.2}$$

Such weak formulations allow for relaxing the restrictive regularity requirements of the original PDE and open the door to an elegant and abstract solution theory based on functional analysis; see [20, Chapter 2]. Clearly, a variational problem as defined above might have several solutions or even no solution. Nevertheless, in order to conduct meaningful analysis and subsequently address discretizations, restrictions must be made. More precisely, one generally deals with well-posed problems:

Definition 2.9 (**Well-posed variational problem**). *We call the variational problem from Definition 2.8* well-posed *if the next two conditions are fulfilled:*

- *For every bounded functional $\mathcal{F} \in W'$, there exists a unique solution $u \in U$ of* (2.3.2).
- *The solution u depends continuously on $\mathcal{F}$ in the sense*

$$\|u\|_U \leq C \|\mathcal{F}\|_{W'}, \quad C = \text{const}.$$

In the following we assume continuous bilinear forms, i.e. we suppose the relation

$$\mathcal{B}(v,w) \leq C_{\mathcal{B}} \|v\|_U \|w\|_W , \quad \forall v \in U,\, w \in W,$$

for some constant $C_{\mathcal{B}} > 0$. Given a continuous bilinear form a more elegant way of describing a well-posed variational problem reads as follows:

$$\text{"well-posedness"} \quad \Longleftrightarrow \quad \mathfrak{B}\colon U \to W' \ ,\ v \mapsto (w \mapsto \mathcal{B}(v,w)) \text{ has a bounded inverse.}$$

In view of Lemma 2.4 this means we have well-posedness if and only if $\mathfrak{B}$ is bijective. A classical result from [56] gives us two conditions implying well-posedness.

Lemma 2.10 (**Generalized Lax-Milgram theorem**; cf. [56, Theorem 3.1])**.** *Assume the bilinear $\mathcal{B}\colon U \times W \to \mathbb{R}$ to be continuous. Let $\mathcal{B}$ satisfy*

- $\inf\limits_{v\in U} \sup\limits_{0\neq w\in W} \mathcal{B}(v,w) \geq C \|v\|_U \|w\|_W$,
- $\inf\limits_{w\in W} \sup\limits_{0\neq v\in U} \mathcal{B}(v,w) \geq C \|v\|_U \|w\|_W$.

Then the abstract variational problem induced by $\mathcal{B}$ is well-posed.

We remark here that such formulations can be also considered if we look at bilinear and linear forms on reflexive Banach spaces $X,\ Y$ instead of the Hilbert spaces $U,\ W$. Analogous inf-sup conditions still give well-posedness; see e.g. Theorem 2.1 in [46]. In fact all these statements regarding the well-posedness can be seen as generalizations of the well-known Lax-Milgram theorem ([2, Theorem 4.2]) which in turn is based on the Riesz representation theorem (Lemma 2.1).

The seek for weak solutions of PDEs usually reduces to the study of variational problems on specific Sobolev spaces. But, although the inf-sup relations yield a concise pointer for reasonable weak formulations, they are not trivial to proof in general, especially if we proceed to finite-dimensional approximation spaces. And the latter is crucial in the design of numerical methods. Then a reformulated well-posedness condition in case of the class of saddle-point problems might be helpful.

Definition 2.10 (**Saddle-point problem**)**.** *Here saddle-point problem means that we have Hilbert spaces $U^1,\ U^2$ and continuous bilinear forms*

$$\mathfrak{a}\colon U^1 \times U^1 \to \mathbb{R}, \qquad \mathfrak{b}\colon U^1 \times U^2 \to \mathbb{R}$$

such that the bilinear form $\mathcal{B}$ has the special structure

$$\mathcal{B}\Big((\sigma,u),(\tau,v)\Big) \coloneqq \mathfrak{a}(\sigma,\tau) - \mathfrak{b}(\tau,u) + \mathfrak{b}(\sigma,v). \tag{2.3.3}$$

Hence, for $\mathcal{F} \in (U^1 \times U^2)'$ we search now for an element $(\sigma,u) \in U^1 \times U^2$ satisfying

$$\mathfrak{a}(\sigma,\tau) - \mathfrak{b}(\tau,u) + \mathfrak{b}(\sigma,v) = \mathcal{F}((\tau,v)), \quad \forall (\tau,v) \in U^1 \times U^2.$$

Equivalently, one can place the problem: For $\mathfrak{g} \in (U^1)'$, $\mathfrak{f} \in (U^2)'$ find $(\sigma,u) \in U^1 \times U^2$ such that

$$\mathfrak{a}(\sigma,\tau) - \mathfrak{b}(\tau,u) = \mathfrak{g}(\tau), \quad \forall \tau \in U^1, \tag{2.3.4}$$
$$\mathfrak{b}(\sigma,v) = \mathfrak{f}(v), \quad \forall v \in U^2 \ . \tag{2.3.5}$$

It is possible to adapt the well-posedness condition when dealing with saddle-point problems. From the standard theory on these kind of systems (see [24]) we get the next lemma, which is e.g. presented in [46]. The only change is our restriction to Hilbert spaces, the natural setting for the Hilbert complexes appearing later.

Lemma 2.11 (**Saddle-point conditions**, see [46, Corollary 2.1])**.** *Let U^1, U^2 be Hilbert spaces endowed with continuous bilinear forms $\mathfrak{a}\colon U^1 \times U^1 \to \mathbb{R}$ and $\mathfrak{b}\colon U^1 \times U^2 \to \mathbb{R}$. Then we have the equivalence of the next three statements:*

1. (Well-posedness) *For every $\mathfrak{g} \in (U^1)'$, $\mathfrak{f} \in (U^2)'$ there is a unique pair $(\sigma, u) \in U^1 \times U^2$ satisfying equations* (2.3.4)-(2.3.5)*. For this solution it is $\|\sigma\|_{U^1} + \|u\|_{U^2} \leq C\Big(\|\mathfrak{g}\|_{(U^1)'} + \|\mathfrak{f}\|_{(U^2)'} \Big)$ for a proper constant $C > 0$.*

2. (Inf-sup condition) *Set $Z \coloneqq \{\tau \in U^1 \mid \mathfrak{b}(\tau, v) = 0,\ \forall v \in U^2\}$. We have the relations*

$$\sup_{0 \neq \tau \in Z} \mathfrak{a}(\sigma, \tau) \geq \tilde{C}\, \|\sigma\|_{U^1}\ \|\tau\|_{U^1}\,,\ \forall \sigma \in Z \qquad \text{and} \qquad \sup_{\sigma \in Z} \mathfrak{a}(\sigma, \tau) > 0 \quad \forall \tau \in Z \backslash \{0\}. \tag{2.3.6}$$

   for a suitable constant $\tilde{C} > 0$. Further, it holds

$$\inf_{v \in U^2} \sup_{0 \neq \tau \in U^1} \mathfrak{b}(\tau, v) \geq \tilde{C}\, \|\tau\|_{U^1}\ \ \|v\|_{U^2}\ . \tag{2.3.7}$$

3. (Coercivity) *It exists a constant $\tilde{C} > 0$ such that the underlying bilinear form $\mathcal{B}$ given by* (2.3.3) *fulfills the inequalities*

$$\inf_{(\sigma,u) \in U^1 \times U^2}\ \sup_{(0,0) \neq (\tau,v) \in U^1 \times U^2} \mathcal{B}\Big((\sigma, u), (\tau, v)\Big) \geq \tilde{C}\Big(\|\sigma\|_{U^1} + \|u\|_{U^2} \Big) \Big(\|\tau\|_{U^1} + \|v\|_{U^2} \Big),$$

   and

$$\sup_{(\sigma,u) \in U^1 \times U^2} \mathcal{B}\Big((\sigma, u), (\tau, v)\Big) > 0$$

   for all $(\tau, v) \in U^1 \times U^2 \backslash \{(0, 0)\}$.

Applying the last lemma we directly see the next auxiliary result.

Corollary 2.2. *Let the assumptions of the last lemma apply. If the variational problem induced by $\mathfrak{a}(\cdot, \cdot)$ on $Z \times Z$ is well-posed and if it holds* (2.3.7) *for $\mathfrak{b}(\cdot, \cdot)$, then the corresponding composed saddle-point problem* (2.3.4)-(2.3.5) *is well-posed.*

Before we continue, we would like to point out Chapter 3 in [20], where the topic of saddle-point problems is discussed in detail and is therefore recommended for further reading.

The previous statements seem to be more directed towards the continuous case. However, the concept of well-posedness can be meaningfully applied not only to discretizations but also to derive error bounds for specific Finite Element (FE) spaces. Therefore, we now assume that we have a family of discrete subspaces $(U_h)_h$, $(W_h)_h$ i.e. $U_h \subset U\,, W_h \subset W$, and we consider the next finite-dimensional version of problem (2.3.2): Find all $u_h \in U_h$ s.t.

$$\mathcal{B}(u_h, v_h) = \mathcal{F}(v_h), \quad \forall v_h \in W_h. \tag{2.3.8}$$

As usual, we assume that $h \in \mathbb{R}_{>0}$, and the smaller the value of h, the larger the trial spaces become. In other words, in the language of the FEM, h simply corresponds to the mesh size of the underlying mesh.

Definition 2.11 (**Well-posed discretization**). *Let $(U_h)_h$ and $(W_h)_h$ be two families of finite-dimensional spaces with $U_h \subset U\,, W_h \subset W$. Further let $\mathcal{B}$ be a bilinear form defining a well-posed variational formulation in the sense of Definition 2.9. We call the discretization* (2.3.8) well-posed *if*

- $\lim\limits_{h\to 0} \inf\limits_{v_h \in X_h} \|w - v_h\|_X = 0, \quad \forall w \in X,\ X \in \{U, W\}$,
- $\inf\limits_{v_h \in U_h} \sup\limits_{0 \neq w_h \in W_h} \mathcal{B}(v_h, w_h) \geq C_{IS} \|v_h\|_U \|w_h\|_W \qquad$ *and*
$$\inf_{w_h \in W_h} \sup_{0 \neq v_h \in U_h} \mathcal{B}(v_h, w_h) \geq C_{IS} \|v_h\|_U \|w_h\|_W,$$
where C_{IS} does not depend on h.

Obviously, we have the existence of a unique discrete solution u_h if the assumptions of the last definition are valid. Further, the first point in the last definition should emphasize that the discrete spaces must converge to the continuous pendants in order to be able to calculate meaningful approximations.
Having a well-posed discretization, one can derive a quasi-optimal statement relatively easily. The latter is an important standard result that we will use multiple times throughout the text, so let us briefly explain it here.

Lemma 2.12 (**Quasi-optimal approximation**). *Given finite-dimensional spaces $(U_h)_h$ and $(W_h)_h$ defining a well-posed discretization of a well-posed weak formulation* (2.3.2). *Then for the error between exact (u) and discrete (u_h) solution it holds the estimate*

$$\|u - u_h\|_U \leq C_{QO} \inf_{v_h \in U_h} \|v_h - u\|_U\,, \quad 0 < C_{QO} = \text{const.}$$

Proof. Let $v_h \in U_h \backslash \{u_h\}$ be arbitrary but fixed. The inf-sup condition from Definition 2.11 guarantees a $0 \neq w_h \in W_h$ s.t.

$$\|v_h - u_h\|_U \leq \frac{\mathcal{B}(v_h - u_h, w_h)}{C_{IS} \|w_h\|_W} = \frac{\mathcal{B}(v_h - u, w_h)}{C_{IS} \|w_h\|_W} \leq \frac{C_{\mathcal{B}}}{C_{IS}} \|v_h - u\|_U\,,$$

for constants C_{IS}, $C_{\mathcal{B}}$. One notes the exploited continuity of $\mathcal{B}$ and the fact $\mathcal{B}(u - u_h, w_h) = 0,\ \forall w_h \in W_h$. Hence the triangle inequality yields

$$\|u - u_h\|_U \leq \|u - v_h\|_U + \|v_h - u_h\|_U \leq \left(1 + \frac{C_{\mathcal{B}}}{C_{IS}}\right) \|u - v_h\|_U\,.$$

The arbitrariness of v_h finishes the proof. □

Based on the last lemma, we see convergence for well-posed discretizations to the exact (weak) solution and up to a constant factor we obtain the smallest possible deviations.

With our above brief explanations of various mathematical concepts, we have familiarized ourselves with the key terms needed to delve deeper into the field of Hilbert complexes. The latter will be examined in the next section, where we look at their connection to PDEs and variational formulations.

3 Hilbert Complexes and the Abstract Hodge–Laplace Problem

Now we turn to the notion of Hilbert complexes the basic framework within the text as well as basis of the Finite Element Exterior Calculus (FEEC) theory developed by Arnold, Falk and Winther [11]. While this notion is often connected to differential forms and exterior derivatives, the concept is quite general and applies to various chains of operators including high-order differential operators. Latter aspect becomes useful if PDE problems are considered arising from non-standard Hodge–Laplace operators. For example, the biharmonic problem appearing in the Kirchhoff plate theory can be derived from the so-called divdiv complex; cf. [60]. Another application in the context of second-order Hilbert complexes would be the Hessian complex which is used to study the linearized Einstein equations in General Relativity; see [62]. The built-in generality of the underlying theoretical constructions is a major advantage of FEEC and leads to elegant proofs and results. Moreover, the abstract point of view might also be beneficial in understanding the essence of the design steps.
The following results and notations can be found in the original works ([5, 11, 9]) by the mentioned authors Arnold, Falk and Winther. We want to collect here the most important parts, at least the ones useful for the investigations in the subsequent chapters. We orient ourselves towards the notation in the mentioned literature and begin with abstract formulations. Doing so, we address the Hodge–Laplace problem and its weak formulation. After that, we present the example of the de Rham complex. It is something like a standard model in the context of Hilbert complexes and is related to several applications. Furthermore, in view of the *complexes from complexes* approach ([12]) we will exploit properties of the de Rham sequence also for second-order complexes. Thus, providing some details concerning de Rham sequence is useful.

3.1 Finite Hilbert complexes

First of all we give a precise definition, what is actually meant by a *Hilbert complex*.

Definition 3.1 (Hilbert complex). *Let $(W^k)_{k\in\mathbb{Z}}$ be a sequence of Hilbert spaces and let there for each k be closed and densely defined operators $d^k\colon W^k \to W^{k+1}$ such that the domain spaces $V^k \coloneqq \mathrm{Dom}(d^k) \subset W^k$ form a Hilbert space endowed with the graph inner product. If for all k the property $\mathcal{R}(d^k, V^k) \subset \mathcal{N}(d^{k+1}, V^{k+1})$ is fulfilled, then the spaces together with the operators form a Hilbert complex which we denote by (W°, d°).*

Since we have by definition $d^k V^k \subset V^{k+1}$ the domain spaces V^k together with the graph inner products $\langle\cdot,\cdot\rangle_{V^k} \coloneqq \langle\cdot,\cdot\rangle_{W^k} + \langle d^k\cdot, d^k\cdot\rangle_{W^{k+1}}$ yield again a Hilbert complex, the so-called associated *domain complex* which is abbreviated with (V°, d°). When talking about domain complexes we should always clarify what are the underlying Hilbert complexes, the inner products, respectively. In other words, it is not sufficient to only specify the domain spaces, but (W°, d°) should be clear from the context. However, for calculations involving the operators d^k or the discretizations later, the V^k become central and have to be known in the specific application case. To increase readability, we will make some common simplifications regarding notation. Specifically, we will omit the indices k for inner products and norms and simply write for $v,\, w \in V^k$ just $\langle v, w\rangle_V \coloneqq \langle v, w\rangle_{V^k},\ \|v\|_V^2 \coloneqq \langle v, v\rangle_{V^k}$ as well as $\langle v, w\rangle = \langle v, w\rangle_{W^k},\ \|v\|^2 \coloneqq \langle v, v\rangle_{W^k}$ for $v,\, w \in W^k$.
Although in the previous definition an infinite sequence appears, one often considers finite Hilbert complexes, meaning there are two indices $z_1, z_2 \in \mathbb{Z}$ s.t. $W^k = 0,\ d^k = 0$ for all $k \in \mathbb{Z}\backslash[z_1, z_2]$.
A complex is said to be bounded if all the d^k are bounded operators. Obviously, the domain complex always yields a *bounded complex*, where the graph norms are underlying. Moreover,

one speaks of a *closed complex* when all the operators d^k have closed ranges $\mathcal{R}(d^k, V^k)$ in W^{k+1}. Further basic terms for complexes are summarized in the next definition.

Definition 3.2 (**Cocycles, coboundaries and cohomology spaces**). *Let a Hilbert complex (W°, d°) with domain complex (V°, d°) be given:*

- *We write for the kernel $\mathfrak{Z}^k \coloneqq \mathcal{N}(d^k, V^k)$, also known as the k-th cocycle.*
- *The range $\mathcal{R}(d^{k-1}, V^{k-1})$ is abbreviated with $\mathfrak{B}^k$ and is called k-th coboundary.*
- *We define the k-th* cohomology space $\mathcal{H}^k$ *as the quotient space*

$$\mathcal{H}^k \coloneqq \mathfrak{Z}^k / \mathfrak{B}^k.$$

We say the complex is exact at level k *if $\mathcal{H}^k = \{0\}$, meaning $\mathcal{R}(d^{k-1}, V^{k-1}) = \mathcal{N}(d^k, V^k)$.*

Assumption 3.1. *In the following all the considered Hilbert complexes are assumed to be closed.*

In view of Lemma 2.2, the (d^k, V^k) have closed and densely defined adjoints

$$d^*_{k+1} \coloneqq (d^k)^* \colon W^{k+1} \to W^k.$$

For the domain of the adjoint d^*_{k+1} we write V^*_{k+1}. Choosing arbitrary elements $v \in V^{k-1}$ and $w \in V^*_{k+1}$ one obtains

$$0 = \langle w, 0 \rangle = \langle w, d^k d^{k-1} v \rangle = \langle d^*_{k+1} w, d^{k-1} v \rangle.$$

This implies that $d^*_{k+1} w \in V^*_k$ and it has to be $d^*_k d^*_{k+1} w = 0$. Thus, it is natural to give the next definition.

Definition 3.3 (**Dual complex**). *Except for a decreasing of the indices, the adjoints and the Hilbert spaces W^k define a Hilbert complex. It is denoted by $(W^\circ, d^*_\circ)$ and called the* dual complex *to (W°, d°).*

An application of the closed range theorem (see Lemma 2.3) guarantees a closed dual complex if d^k have closed ranges. Thinking of differential operators for the d^k it becomes clear that the d^k and d^*_k can not have the same domains in general, since for integration by parts formulas boundary integral terms have to be taken into account; see (2.2.2). In other words, at least one of the domains V^k or V^*_k are often endowed with specific boundary conditions and thus in the domain complex associated to the dual complex usually different type of spaces appear compared to the V^k.

Given a closed Hilbert complex, it is possible to write down the space W^k and V^k as a decompositon involving kernels and ranges. The latter is called the *Hodge decomposition* and is an important part within the scope of complexes. In view of Assumption 3.1, both $\mathfrak{B}^k$ and $\mathfrak{Z}^k$ are closed subspaces of W^k, hence Hilbert spaces. In particular the space

$$\mathfrak{H}^k \coloneqq \mathfrak{Z}^k \cap (\mathfrak{B}^k)^\perp \tag{3.1.1}$$

is closed and well-defined. If nothing else is explicitly mentioned, we mean always with $X^\perp$ the orthogonal complement in the spaces W^k, i.e. using the W^k inner product. Elements in the space $\mathfrak{H}^k$ are called *harmonic forms*. Furthermore, since $\mathfrak{B}^k \subset \mathfrak{Z}^k$ it is clear that

$$\mathfrak{Z}^k = \mathfrak{Z}^k \cap \mathfrak{B}^k \perp \mathfrak{Z}^k \cap (\mathfrak{B}^k)^\perp = \mathfrak{B}^k \perp \mathfrak{Z}^k \cap (\mathfrak{B}^k)^\perp = \mathfrak{B}^k \perp \mathfrak{H}^k,$$

where the orthogonal sum is valid for both the W^k and V^k inner product.

Lemma 3.1 (**Hodge decomposition**, see [5, Section 4.2.2.]). *One has the decomposition*

$$W^k = \mathfrak{Z}^k \perp (\mathfrak{Z}^k)^\perp = \mathfrak{B}^k \perp \mathfrak{H}^k \perp (\mathfrak{Z}^k)^\perp$$

One notes $d^k \circ d^{k-1} = 0$ and the closed range of d^k also with respect to the graph norm $\|\cdot\|_V$. Because of this, it is possible to consider a similar orthogonal decomposition with respect to $\langle\cdot,\cdot\rangle_V$. In fact, one gets

$$V^k = \mathfrak{B}^k \perp \mathfrak{H}^k \perp (\mathfrak{Z}^k)^{\perp_V},$$

where one notes $(\mathfrak{Z}^k)^{\perp_V} \coloneqq (\mathfrak{Z}^k)^{\perp_{V^k}} = (\mathfrak{Z}^k)^\perp \cap V^k$ and that the orthogonality is w.r.t. to $\langle\cdot,\cdot\rangle_W$ as well as $\langle\cdot,\cdot\rangle_V$.

Remark 3.1. In the papers concerning Hodge theory or FEEC (see [11, 5]) one often finds more general results, e.g. a Hodge decomposition is also available in non-closed Hilbert complexes. Nevertheless, other key features require the closedness, like the famous *Poincaré inequality* shown below. Due the last point and the closed range property for the standard differential operators we will use later, we suppose closed ranges $\mathcal{R}(d^k, V^k) \subset W^{k+1}$.

In view of the last decomposition we see that $d^k\colon (\mathfrak{Z}^k)^{\perp_V} \to \mathfrak{B}^k$ is a V-bounded and bijective mapping between Hilbert spaces, hence Lemma 2.4 gives us

Lemma 3.2 (**Poincaré inequality**, [5, Theorem 4.6]). *It holds*

$$\|v\|_V \leq C_P \left\|d^k v\right\|, \quad \forall v \in (\mathfrak{Z}^k)^{\perp_V},$$

where $\|\cdot\|$ is the W-norm and $C_P > 0$ is referred to as Poincaré constant.
When it comes to the Hodge–Laplace problem and related calculations a fundamental relation between the cohomology spaces and the harmonic forms is pivotal. In fact, they are isomorphic, meaning

$$\mathfrak{H}^k \cong \mathcal{H}^k.$$

Basically, this relation is a consequence of the defining equation (3.1.1). An element $w \in \mathfrak{H}^k$ is identified with the equivalence class $[w] \in \mathcal{H}^k$ by the canonical projection $\pi\colon \mathfrak{H}^k \to \mathcal{H}^k$, $w \to [w]$. Indeed the identification leads to a bijective mapping. First of all let $[w] = 0$ as a class with $w \in \mathfrak{H}^k$. But then we have $w \in \mathfrak{B}^k \cap (\mathfrak{B}^k)^\perp = 0$. On the other hand let $[\tilde{w}] \in \mathcal{H}^k$ arbitrary. Obviously, $\tilde{w} = w \perp v$, where $w \in (\mathfrak{B}^k)^\perp$, $v \in \mathfrak{B}^k$. Hence $[\tilde{w}] = [w]$ and $w \in \mathfrak{H}^k$ which implies surjectivity.

3.2 The abstract Hodge–Laplacian

In this section we are again given a closed Hilbert complex (W°, d°) with associated domain complex (V°, d°). With the basic definitions from the previous section we are ready to introduce the fundamental problem in the context of FEEC, the Hodge–Laplace equation. First define formally the operator

$$T^k_{\mathrm{HL}} \coloneqq d^*_{k+1} \circ d^k + d^{k-1} \circ d^*_k \tag{3.2.1}$$

that is called in [5] the *abstract Hodge Laplacian*. The natural domain is

$$\mathrm{Dom}(T^k_{\mathrm{HL}}) \coloneqq \{v \in V^k \cap V^*_k \mid d^k v \in V^*_{k+1} \text{ and } d^*_k v \in V^{k-1}\},$$

which gives us a well-defined mapping $T^k_{\mathrm{HL}}\colon \mathrm{Dom}(T^k_{\mathrm{HL}}) \to W^k$. It is easy seen that in general T^k_{HL} might not be invertible. Namely, adding a harmonic form $p \in \mathfrak{H}^k$ to a $v \in \mathrm{Dom}(T^k_{\mathrm{HL}})$ we

obtain $T^k_{\mathrm{HL}}(v+w) = T^k_{\mathrm{HL}}w$. One observes Lemma 2.2 which ensures $\mathfrak{H}^k \subset \mathrm{Dom}(T^k_{\mathrm{HL}})$. But, with the short calculation

$$\langle T^k_{\mathrm{HL}}v, w\rangle = \langle d^k v, d^k w\rangle + \langle d^*_k v, d^*_k w\rangle = 0 + 0, \quad \forall v \in \mathrm{Dom}(T^k_{\mathrm{HL}}),\ \forall w \in \mathfrak{H}^k\ , \tag{3.2.2}$$

one has

$$T^k_{\mathrm{HL}} \colon \mathrm{Dom}(T^k_{\mathrm{HL}}) \cap (\mathfrak{H}^k)^\perp \to W^k \cap (\mathfrak{H}^k)^\perp. \tag{3.2.3}$$

A central and interesting result is the invertibility of the last mapping. Even more, we have in some sense a continuous inverse; see [5, Theorem 4.8]. Before we come to an explanation and the proof idea used by Arnold et al., we give another useful definition.

Definition 3.4 (**Hodge–Laplace problem**). *The k-th level (abstract) Hodge–Laplace problem reads:*

For $f \in W^k \cap (\mathfrak{H}^k)^\perp$ find an $u \in \mathrm{Dom}(T^k_{\mathrm{HL}}) \cap (\mathfrak{H}^k)^\perp$ s.t.

$$T^k_{\mathrm{HL}}u = f. \tag{3.2.4}$$

At a first glance, the solvability of (3.2.4) seems to be an issue. Already, the operator T^k_{HL} itself has a complicated domain in general and its domain might lead to non-standard linear spaces. If, for example, the d^k are differential operators, one must be prepared for the fact that they may lead to spaces that do not correspond to the well-understood Sobolev spaces of the form $H^k(\Omega)$. This, in turn, can make it difficult to find or implement suitable spaces for discretization. However, to show the existence of a suitable solution to equation, Arnold presents in [5, Section 4.4.1] an elegant approach by introducing an equivalent weak formulation. This offers at least two major advantages. On the one hand, the proof concerning invertibility of the operator T^k_{HL} becomes clearer and uses the classical theory on variational problems, cf. Section 2.3. On the other hand, the consideration of the so-called mixed weak form paves the way for establishing dicretization methods.
So let us define the mentioned weak formulation first.

Definition 3.5 (**Mixed weak formulation of the Hodge–Laplace problem**, see [5, Section 4.4.1]). *Given $f \in W^k \cap (\mathfrak{H}^k)^\perp$ one seeks $(\sigma, u, p) \in V^{k-1} \times V^k \times \mathfrak{H}^k$ with*

$$\langle \sigma, \tau\rangle - \langle u, d^{k-1}\tau\rangle = 0, \qquad \forall \tau \in V^{k-1}, \tag{3.2.5}$$

$$\langle d^{k-1}\sigma, v\rangle + \langle d^k u, d^k v\rangle + \langle p, v\rangle = \langle f, v\rangle, \quad \forall v \in V^k, \tag{3.2.6}$$

$$\langle u, q\rangle = 0, \qquad \forall q \in \mathfrak{H}^k\ . \tag{3.2.7}$$

The procedure outlined in [5] can be divided in two main steps. First one shows the equivalence of latter mixed weak form an the original Hodge–Laplace problem. Afterwards, in a second step the well-posedness of (3.2.5) (3.2.7) in the sense of Definition 2.9. Due to importance and relevance of the mentioned steps, also in view of understanding, and for reasons of completeness we sketch the underlying proofs similar to the ones in literature. However, we use a slightly different wording and notation.

Lemma 3.3 (**Feasibility of the mixed weak formulation**, compare Theorem 4.7 in [5]). *If $u \in \mathrm{Dom}(T^k_{\mathrm{HL}})$ is a solution to (3.2.4), then $(d^*_k u, u, 0)$ is a solution to (3.2.5)-(3.2.7). Conversely, if (σ, u, p) is solution of the latter, then it follows $u \in \mathrm{Dom}(T^k_{\mathrm{HL}})$ and (3.2.4) holds.*

Proof. We show both directions separately.
" $\Rightarrow$ ": Let u solve the abstract Hodge–Laplace problem. Hence (3.2.7) is fulfilled and $u \in V^*_k$, $d^k u \in V^*_{k+1}$. We can set $\sigma := d^*_k u \in V^{k-1}$ which gives the validity of (3.2.5). And setting

$p = 0$ we get equation (3.2.6).
" $\Leftarrow$ ": Let (σ, u, p) fulfill (3.2.5)-(3.2.7). Since $V^{k-1} \subset W^{k-1}$ is dense, one has $u \in V_k^*$, $\sigma = d_k^* u \in V^{k-1}$ by the first equation of the system. Analogously, the second line (3.2.6) implies $d^k u \in V_{k+1}^*$ as well as $T_{\mathrm{HL}}^k u = f - p$. Clearly, $u \in \mathrm{Dom}(T_{\mathrm{HL}}^k)$. Using an arbitrary element $v \in \mathfrak{H}^k$ in the mentioned line one obtains $\langle p, v\rangle = 0$. Thus $p = 0$, meaning $T_{\mathrm{HL}}^k u = f$. □

Lemma 3.4 (**Well-posedness of the mixed weak formulation**, see [5, Theorem 4.8])**.** *The underlying variational problem of the mixed weak system is well-posed. More precisely, for every* $(\mathfrak{g}, \mathfrak{f}, \mathfrak{h}) \in (V^{k-1})' \times (V^k)' \times (W^k)'$ *there is a unique solution* $(\sigma, u, p) \in V^{k-1} \times V^k \times \mathfrak{H}^k$ *of the weak formulation* (2.3.2)*, with*

$$\mathcal{B}\Big((\sigma, u, p), (\tau, v, q)\Big) \coloneqq \langle \sigma, \tau\rangle - \langle u, d^{k-1}\tau\rangle - \langle d^{k-1}\sigma, v\rangle - \langle d^k u, d^k v\rangle - \langle p, v\rangle - \langle u, q\rangle$$

and $\mathcal{F}\Big((\tau, v, q)\Big) = \mathfrak{g}(\tau) + \mathfrak{f}(v) + \mathfrak{h}(q)$*. Further one obtains the estimate*

$$\|u\|_V + \|\sigma\|_V + \|p\| \leq C\Big(\|\mathfrak{g}\|_{V'} + \|\mathfrak{f}\|_{V'} + \|\mathfrak{h}\|_{W'} \Big) .$$

Remark 3.2. We interpret here $\mathfrak{H}^k$ as a closed subspace of W^k and hence endowed with the norm $\|\cdot\| = \|\cdot\|_W$.

Proof. We sketch the proof idea of Theorem 4.9 in [5] and we refer to it for more details.
In reference to Section 2.3 it is enough to show the inf-sup conditions of Lemma 2.10 for $\mathcal{B}$ to prove the statement. First we fix an element $(\sigma, u, p) \in V^{k-1} \times V^k \times \mathfrak{H}^k$. One exploits the Hodge decomposition, meaning one can write $u = u_{\mathfrak{B}} + u_{\mathfrak{H}} + u_\perp$, $u_{\mathfrak{B}} \in \mathfrak{B}^k$, $u_{\mathfrak{H}} \in \mathfrak{H}^k$, $u_\perp \in (\mathfrak{Z}^k)^\perp \cap V^k$. An application of the Poincaré inequality (cf. Lemma 3.2) twice yields a constant $C_P > 0$ and a $\rho \in (\mathfrak{Z}^k)^{\perp_V}$ s.t.

$$d^{k-1}\rho = u_{\mathfrak{B}}, \qquad \|\rho\|_V \leq C_P \|u_{\mathfrak{B}^k}\| , \qquad \|u_\perp\|_V \leq C_P \|du_\perp\| = C_P \|du\| .$$

Using the latter, then the choice

$$\tau \coloneqq \sigma - \frac{1}{C_P^2}\rho, \qquad v \coloneqq -u - d^{k-1}\sigma - p, \qquad q \coloneqq -p + u_{\mathfrak{H}}$$

leads to the estimates $\mathcal{B}\Big((\sigma, u, p), (\tau, v, q)\Big) \geq C_\eta\Big(\|u\|_V^2 + \|\sigma\|_V^2 + \|p\|^2 \Big)$ and $\|v\|_V + \|\tau\|_V + \|q\| \leq C_\eta\Big(\|u\|_V + \|\sigma\|_V + \|p\| \Big)$ with a $C_\eta > 0$ not depending on (σ, u, p), (τ, v, q). Note, here $\mathcal{B}$ is symmetric which finishes the proof. □

Remark 3.3. In order to get a symmetric bilinear form, one multiplies in fact (3.2.6) and (3.2.7) by -1 to define $\mathcal{B}$ in the last lemma. Obviously, this does not change the well-posedness property.

3.3 The (Sobolev) de Rham complex

Up to now we concentrated on a very abstract setting suitable for more insight. Let us move on to something more concrete as we consider differential forms and exterior derivatives. This in turn will be specified even more leading to the classical de Rham chain in $2D$ and $3D$ using vector proxies. We need to begin with some definitions from the field of exterior calculus, e.g. multilinear *k-forms* or the *wedge product*. We restrict us only to very few aspects in order to explain the concept behind the de Rham chain on a Lipschitz domain. For instance, we omit a description of the general case for Riemannian manifolds which is possible but not needed for our purposes.
It should be noted again that we are presenting well-known results here, which can be found in references [11, 5], but also in [39] and are more extensively discussed there.

3.3.1 A little exterior calculus and the de Rham complex on differential forms

Definition 3.6 (K**-forms**). *Let U be a linear space of dimension n and let $k \in \mathbb{N},\ k \leq n$. A k-form is a $\mathbb{R}$-multilinear mapping of the form $\omega\colon \underbrace{U \times \cdots \times U}_{k-\text{times}} \to \mathbb{R}$.*

Further, a k-form ω is called alternating *if it holds:*

$$\omega(u_1, \ldots, u_i, \ldots, u_j, \ldots, u_k) = 0, \quad \text{if } u_i = u_j, \quad \text{and} \quad i \neq j \quad ,$$

meaning ω vanishes if two entries coincide. This implies the change $\omega \mapsto -\omega$ if we swap exactly two entries.
The space of alternating k-forms on U is denoted by $\mathrm{Alt}^k(U)$. Formally we set $\mathrm{Alt}^k(U) = 0$ if $k > n$ and $\mathrm{Alt}^0(U) = \mathbb{R}$.

An easy example for a given U would be the space of 1-forms, linear functionals, respectively. If $e_1, \ldots, e_n$ is a basis of U we can introduce the canonical dual basis $dx^i\colon U \to \mathbb{R}$ with $dx^i(e_j) = \delta_{ij}$.[4] Obviously, the dx^i form a basis of $\mathrm{Alt}^1(U)$. Moreover, all the possible k-forms can be constructed from the dx^i by means of the *exterior* or *wedge product* $\wedge$. Given a k- and an l-form ω and η on U one defines

$$\omega \wedge \eta(u_1, \ldots, u_{k+l}) \coloneqq \sum_{\sigma_<} \mathrm{sgn}(\sigma)\omega(u_{\sigma_1}, \ldots, u_{\sigma_k})\, \eta(u_{\sigma_{k+1}}, \ldots, u_{\sigma_{k+l}}),$$

where $\mathrm{sgn}(\sigma)$ is the sign of the permutation $\sigma = (\sigma_1, \ldots, \sigma_{k+l})$ of $(1, 2, \ldots, k+l)$. Further, the index $\sigma_<$ means that we only sum over all permutations σ satisfying $\sigma_1 < \cdots < \sigma_k$ as well as $\sigma_{k+1} < \cdots < \sigma_{k+l}$.
It can be checked that this wedge-product indeed gives us an element in $\mathrm{Alt}^{k+l}(U)$. Moreover it satisfies the property

$$\omega \wedge \eta = (-1)^{kl} \eta \wedge \omega.$$

And an iterative application makes it possible to obtain k-forms $dx^{\sigma_1} \wedge \cdots \wedge dx^{\sigma_k}$ using the basic 1-forms. Even more, every k-form ω in $\mathrm{Alt}^k(U)$ can be uniquely represented as

$$\omega = \sum_{\sigma \in \Sigma_<(k,n)} c_\sigma\ dx^{\sigma_1} \wedge \cdots \wedge dx^{\sigma_k}, \tag{3.3.1}$$

with

$$\Sigma_<(k, n) \coloneqq \{\sigma = (\sigma_i)_i \in \mathbb{N}^k \mid 1 \leq \sigma_1 < \cdots < \sigma_k \leq n\}.$$

For a proof we see [39, Proposition 1]. We simply refer to the $c_\sigma \in \mathbb{R}$ from above as *coefficients* of ω. A closer look at the last equation shows us that the dimension of $\mathrm{Alt}^k(U)$ is $n|k \coloneqq \binom{n}{k}$, i.e. equal to a binomial coefficient. In particular we can naturally identify the k-forms with their coefficients as elements in $\mathbb{R}^{n|k}$. In the following we assume that we have fixed an ordering of the terms in (3.3.1) which justifies the usage of a vector $\mathbf{c}_\omega = (c_1, \ldots, c_{n|k})^{\mathrm{T}} \in \mathbb{R}^{n|k}$ to represent a ω, where c_j corresponds to the j-th term in the sum.[5] We call then $\mathbf{c}_\omega$ the *coefficient vector* related to Ω. Exploiting the representation (3.3.1) it is possible to equip $\mathrm{Alt}^k(U)$ with an inner product structure, which turns it to a Hilbert space. Namely, for two basis k-forms $\omega = dx^{\sigma_1} \wedge \cdots \wedge dx^{\sigma_k},\ \eta = dx^{s_1} \wedge \cdots \wedge dx^{s_k}$ with $\sigma, s \in \Sigma_<(k, n)$ one sets

$$\langle \omega, \eta \rangle \coloneqq \begin{cases} 1, & \text{if } \sigma_i = s_i,\ \forall i \\ 0, & \text{else .} \end{cases}$$

[4] $\delta_{ij} \in \{0, 1\}$ stands for the Kronecker delta; it is $\delta_{ij} = 1$ iff $i = j$.
[5] w^{T} denotes the transpose of a vector or matrix w.

Bilinearity determines then the complete inner product.
The standard example and the only case we will consider in the following is $U = \mathbb{R}^n$ for which we assume the dx^i to be the dual basis corresponding to the canonical basis of the Euclidean space.

In order to move again towards the field of Hilbert complexes, we introduce the notion of differential forms on a Lipschitz domain Ω.

Definition 3.7 (**Differential forms**). *In our setting, a differential k-form on $\Omega \subset \mathbb{R}^n$ is just a mapping*

$$\omega \colon \Omega \to \mathrm{Alt}^k(\mathbb{R}^n).$$

Hence, in (3.3.1) *we then obtain coefficient functions $c_\sigma = c_\sigma(x)$ with $c_\sigma(x)$ corresponding to $\omega_x \coloneqq \omega(x)$, $x \in \Omega$. And, trivially, the coefficient vector $\mathbf{c}_\omega$ becomes a vector field on Ω.*
The set of differential k-forms with coefficients $c_\sigma \in L^2(\Omega)$ is denoted with $L^2\Lambda^k(\Omega)$. If the coefficients are elements of some Sobolev space $H^q(\Omega)$ we write $H^q\Lambda^k(\Omega)$, and in case of smooth coefficients in $C_c^\infty(\Omega)$ we write analogously $C_c^\infty\Lambda^k(\Omega)$.

The Hilbert space structure on $L^2(\Omega) \otimes \mathbb{R}^{n|k}$ yields that $L^2\Lambda^k(\Omega)$ is a Hilbert space, too. For two k-forms $\omega,\ \eta \in L^2\Lambda^k(\Omega)$ we just set

$$\langle \omega, \eta \rangle_{L^2\Lambda^k(\Omega)} \coloneqq \langle \mathbf{c}_\omega, \mathbf{c}_\eta \rangle_{L^2(\Omega)}\ ,$$

where $\mathbf{c}_\omega$ and $\mathbf{c}_\eta$ denote the coefficient vector fields of ω and η. Completely analogous, one can define a H^l-inner product on the space $H^l\Lambda^k(\Omega)$. For the induced norms we will write again just $\|\omega\|_{L^2(\Omega)}$, and $\|\omega\|_{H^k(\Omega)}$ for a smooth enough k-form ω.
It should be pointed out here that with the preceding remarks, it becomes clear that we can interpret the spaces $H^q\Lambda^k(\Omega)$ as a product space of two Hilbert spaces, namely $H^q(\Omega) \otimes \mathrm{Alt}^k(\mathbb{R}^n)$.

Next we utilize the representation (3.3.1) to define the exterior derivative operator.

Definition 3.8 (**Exterior derivative**). *Suppose $\omega \in L^2\Lambda^k(\Omega)$ of the form* (3.3.1) *with coefficients $c_\sigma \in L^2(\Omega)$. We define the exterior derivative as the densely defined linear operator $\mathrm{d}^k \colon L^2\Lambda^k(\Omega) \to L^2\Lambda^{k+1}(\Omega)$ determined by*

$$\mathrm{d}^k\omega \coloneqq \sum_{\sigma \in \Sigma_<(k,n)} \sum_{i=1}^{n} (\partial_i c_\sigma)\, dx^i \wedge dx^{\sigma_1} \wedge \cdots \wedge dx^{\sigma_k}.$$

The domain of d^k is denoted with $H\Lambda^k(\Omega)$ with

$$H\Lambda^k(\Omega) \coloneqq \{\omega \in L^2\Lambda^k(\Omega) \mid \mathrm{d}^k\omega \in L^2\Lambda^{k+1}(\Omega)\},$$

where derivatives are meant in a weak sense; see the subsequent explanations.

The operator is indeed densely defined since it is straightforward to see that the k-forms with smooth coefficients are dense in $L^2\Lambda^k(\Omega)$. We can introduce the notion of a weak derivative $\mathrm{d}^k\omega = \eta \in L^2\Lambda^{k+1}(\Omega)$ in a similar manner like the one on standard Sobolev spaces, namely it has to hold

$$\langle \eta, \phi \rangle_{L^2\Lambda^{k+1}(\Omega)} = \langle \omega, \delta\phi \rangle_{L^2\Lambda^k(\Omega)}, \quad \forall \phi \in C_c^\infty\Lambda^k(\Omega)\ ,$$

where $\delta \colon L^2\Lambda^{k+1}(\Omega) \to L^2\Lambda^k(\Omega)$ is the existent adjoint of the exterior derivative, meaning $(\mathrm{d}^k, C_c^\infty\Lambda^k(\Omega))^*$. It is obvious that $C_c^\infty\Lambda^{k+1}(\Omega) \subset \mathrm{Dom}(\delta)$. But, since we have a connection between $L^2\Lambda^k(\Omega)$ and $L^2(\Omega) \otimes \mathbb{R}^{n|k}$ via the coefficients of the forms, the derivatives here can be reduced to classical weak derivatives in the sense of Sobolev spaces.

The exterior derivative is appropriate to define Hilbert complexes as the next lemma implies.

Lemma 3.5 (**The L^2 de Rham complex**; compare [5, Section 6.2.6])**.** *The exterior derivative operators* d^k *are closed densely defined with domains* $H\Lambda^k(\Omega)$ *and closed ranges* $\mathcal{R}(\mathrm{d}^k, H\Lambda^k(\Omega)) \subset L^2\Lambda^{k+1}(\Omega)$*. Besides, it is* $\mathrm{d}^k H\Lambda^k(\Omega) \subset H\Lambda^{k+1}(\Omega)$ *and it holds*

$$\mathrm{d}^{k+1} \circ \mathrm{d}^k = 0 \ .$$

In other words the chain

$$0 \longrightarrow L^2\Lambda^0(\Omega) \xrightarrow{\mathrm{d}^0} L^2\Lambda^1(\Omega) \xrightarrow{\mathrm{d}^1} \quad \cdots \quad \xrightarrow{\mathrm{d}^{n-1}} L^2\Lambda^n(\Omega) \longrightarrow 0$$

determines a closed Hilbert complex with associated domain complex

$$0 \longrightarrow H\Lambda^0(\Omega) \xrightarrow{\mathrm{d}^0} H\Lambda^1(\Omega) \xrightarrow{\mathrm{d}^1} \quad \cdots \quad \xrightarrow{\mathrm{d}^{n-1}} H\Lambda^n(\Omega) \longrightarrow 0.$$

In the next lemma we use the term *starlike* domain $\Omega \subset \mathbb{R}^n$ from [36], which is in our case a Lipschitz domain for which we can find an open Ball $B \subset \mathbb{R}^n$ s.t. for every $x \in \Omega$ the convex hull of $\{x\} \cup B$ is a subset of Ω.

Lemma 3.6 (**Exactness on starlike domains**, see [36, Theorem 1.1 and Proposition 4.1])**.** *Let the domain* $\Omega \subset \mathbb{R}^n$ *be starlike. Then the de Rham complex is exact at each level except for* $k = 0$*. More precisely, for* $k > 0$ *one has*

$$\mathcal{N}(\mathrm{d}^k, H\Lambda^k(\Omega)) = \mathcal{R}(\mathrm{d}^{k-1}, H\Lambda^{k-1}(\Omega)).$$

Even more, it can be shown that we indeed have $\mathcal{N}(\mathrm{d}^k, H\Lambda^k(\Omega)) = \mathcal{R}(\mathrm{d}^{k-1}, H^1\Lambda^{k-1}(\Omega))$.

Remark 3.4. The theory regarding the de Rham sequence is actually valid in a more general framework of smooth manifolds; compare e.g. [5, Section 6.2.6] or [51, Chapter 17]. A well-known and deep result is the fact that the dimension of the cohomology spaces is a topological invariant; see [51, Corollary 17.12]. Thus if we consider a domain diffeomorphic to a starlike domain, we still get the exactness of the L^2 de Rham sequence from above. The latter can also be seen utilizing the *pullback* operation under a smooth map (see Definition 3.9, [5, Section 6.2.1] for more details). Because, this pullback commutes with the exterior derivative (cf. (3.3.4)) and thus implies exactness of the de Rham complex in one domain Ω if it is exact in a domain diffeomorphic to Ω. Furthermore, the second equation in the last lemma remains also valid after a diffeomorphic deformation of the domain.

In a arbitrary Lipschitz domain we also see by the results from [36], especially Theorem 4.9. therein, we always have finite-dimensional cohomology spaces. Even though we do not have exactness of the de Rham complex at level $k > 0$ in general Lipschitz domains, it turns out that we get this property always at level n. The latter follows by [36, Remark 4.10]. This means that in this case, more complicated topologies would not be a problem, which is advantageous for numerical considerations.

Lemma 3.7 (**Exactness at level** n, [36, Remark 4.10])**.** *For every* $\eta \in L^2\Lambda^n(\Omega)$ *there exists a* $\omega \in H^1\Lambda^{n-1}(\Omega)$ *s.t.*

$$\mathrm{d}^{n-1}\omega = \eta.$$

A further point that should be mentioned here and is also useful for proofs is the density of $C^\infty\Lambda^k(\overline{\Omega})$ in $H\Lambda^k(\Omega)$.[6] As mentioned in [11, page 323], this can be proven using a classical smoothing argument; cf. [41, Section 5.3].

Let us insert here the useful definition of the *pullback* operation on differential forms. This pullback makes it possible to relate de Rham sequences on different domains, which turns out to be central point in the context of discrete differential forms; cf. [27].

Definition 3.9 (**Pullback of a differential form**). *Let $\mathbf{F}\colon \widehat{\Omega} \to \Omega$ be a C^1-diffeomorphism between two Lipschitz domains in $\mathbb{R}^n$ with Jacobian matrix $\mathbf{J} = \mathbf{J}(\hat{x})$. Then for $k > 0$ one defines the pullback $\mathcal{Y}^k_{\mathbf{F}}\colon L^2\Lambda^k(\Omega) \to L^2\Lambda^k(\widehat{\Omega})$, $\omega \mapsto \eta$, determined through*

$$\eta_{\hat{x}}\colon \mathbb{R}^n \times \cdots \times \mathbb{R}^n \to \mathbb{R} \ , \ (v_1, \ldots, v_k) \mapsto \omega_{\mathbf{F}(\hat{x})}(\mathbf{J}v_1, \ldots, \mathbf{J}v_k), \quad \forall \hat{x} \in \widehat{\Omega}.$$

For the case $k = 0$ for which we make the identification $L^2\Lambda^0(\Omega) = L^2(\Omega)$ we further introduce

$$\mathcal{Y}^0_{\mathbf{F}}\omega = \omega \circ \mathbf{F}, \quad \forall \omega \in L^2(\Omega).$$

This pullback operation satisfies several properties and is discussed in most textbooks related to exterior calculus and differential forms; we refer to [72, §17] for details on the pullbacks in a more general framework involving manifolds. Before we explain the connection of the $\mathcal{Y}^k_{\mathbf{F}}$ with the de Rham complex we insert here

Lemma 3.8. *Let the assumptions from the last definition hold and let $l \in \mathbb{N}_0$, where we assume the mapping $\mathbf{F}$ to be C^{l+1}-smooth on the closure $\overline{\widehat{\Omega}}$. Then we have for $k = 0, \ldots, n$ the following properties:*

- *It is*
$$\mathcal{Y}^k_{\mathbf{F}}\Big(H^l\Lambda^k(\Omega)\Big) \subset H^l\Lambda^k(\widehat{\Omega})$$
and there is a constant C s.t.
$$\Big\|\mathcal{Y}^k_{\mathbf{F}}\omega\Big\|_{H^l(\widehat{\Omega})} \leq C \left\|\omega\right\|_{H^l(\Omega)}, \quad \forall \omega \in H^l\Lambda^k(\Omega). \tag{3.3.2}$$

- *If $l \geq 1$, then we have*
$$\mathcal{Y}^k_{\mathbf{F}}\Big(H^1_0\Lambda^k(\Omega)\Big) \subset H^1_0\Lambda^k(\widehat{\Omega}), \tag{3.3.3}$$
where $H^1_0\Lambda^k(U)$ is the space of differential forms on U with coefficients in $H^1_0(U)$.

- *The pullback is compatible with the exterior derivative, meaning*
$$\hat{\mathrm{d}}^k\mathcal{Y}^k_{\mathbf{F}}\omega = \mathcal{Y}^{k+1}_{\mathbf{F}}\mathrm{d}^k\omega, \quad \forall \omega \in H\Lambda^k(\Omega), \tag{3.3.4}$$
where we added a hat *on the left side to emphasize that the exterioir derivative is meant w.r.t. to the coordinates $\hat{x}$ in $\widehat{\Omega}$, i.e. $\mathbf{F}(\hat{x}) = x$.*

Proof. The last point above concerning the commutativity property is a fundamental result in exterior calculus for a smooth differential k-form ω; see e.g. [51, Proposition 14.23]. A density argument yields the validity of (3.3.4) for every $\omega \in H\Lambda^k(\Omega)$. The rest of the points can be shown without difficulty and a proof sketch is given in Appendix 11.1. □

[6] Again $C^\infty\Lambda^k(\overline{\Omega})$ means that the smooth coefficients of the k-form can be extended continuously to the boundary.

With property (3.3.4), one can now recognize the connection between the pullback operation and the de Rham complex. Because, for $\omega \in H\Lambda^k(\Omega)$, we have $\mathcal{Y}_{\mathbf{F}}^k\omega \in H\Lambda^k(\widehat{\Omega})$. This means that the pullbacks transform the de Rham complex in Ω to its counterpart in $\widehat{\Omega}$ and preserve the complex structure. Therefore, it is possible to switch from one de Rham chain to another. More precisely, we obtain the commutative diagram:

$$\begin{array}{ccccccc} \cdots & & H\Lambda^k(\Omega) & \xrightarrow{\mathrm{d}^k} & H\Lambda^{k+1}(\Omega) & & \cdots \\ & & \mathcal{Y}_{\mathbf{F}}^k\downarrow & & \mathcal{Y}_{\mathbf{F}}^{k+1}\downarrow & & \\ \cdots & & H\Lambda^k(\widehat{\Omega}) & \xrightarrow{\hat{\mathrm{d}}^k} & H\Lambda^{k+1}(\widehat{\Omega}) & & \cdots \quad . \end{array}$$

This particular property of the pullback is of central importance in the definition of isogeometric discrete differential forms; see Section 7.3. If we have a good, namely structure-preserving discretization of the de Rham complex in the domain Ω, then the pullbacks of the discrete chain automatically provide us with a structure-preserving discretization of the complex in $\widehat{\Omega}$. The reverse direction is, of course, also possible by simply replacing $\mathbf{F}$ with $\mathbf{F}^{-1}$.

After we showed in some sense the classical de Rham complex as a L^2 Hilbert complex, we briefly address now de Rham sequences with different inner products and Hilbert spaces underlying. We will call them *Sobolev de Rham complexes*. Although the latter are not directly utilized in numerical computations later, they are central for the *complexes from complexes* approach by Arnold and Hu (see [12]), a concept we will exploit later.
On the basis of the last considerations we can introduce an analogous de Rham chain on Ω, but with underlying Hilbert spaces of the form $H^{z_k}\Lambda^k(\Omega)$, $z_k \in \mathbb{Z}$ instead of $L^2\Lambda^k(\Omega)$. Basically, if we have $z_k = q - k$ with $q \in \mathbb{N}_{\geq n}$ one directly sees that we get a bounded Hilbert complex

$$0 \longrightarrow H^q\Lambda^0(\Omega) \xrightarrow{\mathrm{d}^0} H^{q-1}\Lambda^1(\Omega) \xrightarrow{\mathrm{d}^1} \cdots \xrightarrow{\mathrm{d}^{n-1}} H^{q-n}\Lambda^n(\Omega) \longrightarrow 0,$$

since the exterior derivatives are differential operators of order 1. Interpreting the d^k in the distributional sense allows us to consider the chain even in the case where $\gamma < n$. More precisely, the exterior derivative extends to a bounded mapping

$$\mathrm{d}^k \colon H^z\Lambda^k(\Omega) \to H^{z-1}\Lambda^{k+1}(\Omega), \quad z \in \mathbb{Z}.$$

Lemma 3.9 (**Sobolev de Rham complex**). *As a result, we obtain with the pairs* $(H^{q-\circ}\Lambda^\circ(\Omega), \mathrm{d}^\circ)$ *for each* $q \in \mathbb{Z}$ *a bounded Hilbert complex. This complex is referred to as a Sobolev de Rham complex.*

Sequences of this nature, and even more general ones, are subjects of the papers [36, 12]. In [12] we see the appropriateness of the sequences $(H^{q-\circ}\Lambda^0(\Omega), \mathrm{d}^\circ)$ for the construction of new and higher order complexes. Regarding the latter, we will give more details in the Section 4.2 below. But still, we want to mention here useful outcomes of [36] and [12].
On one hand it should be remarked that the Sobolev de Rham sequences have finite-dimensional cohomology spaces. A complex with this property is also called *Fredholm* and due to [5, Theorem 3.8] it is a closed Hilbert complex. Furthermore, a smooth element in the kernel d^k can be expressed as image of another smooth element, at least in starlike domains.

Lemma 3.10 (**Exactness of the Sobolev de Rham complex**, [36, Proposition 4.1 and Theorem 4.9]). *Let* $\Omega \subset \mathbb{R}^n$ *be a starlike domain. For* $k > 0$, $q \in \mathbb{Z}$ *and* $\eta \in H^q\Lambda^k(\Omega)$ *with* $\mathrm{d}^k\eta = 0$, *there exits a* $\omega \in H^{q+1}\Lambda^{k-1}(\Omega)$ *s.t.*

$$\mathrm{d}^{k-1}\omega = \eta.$$

Besides for every Lipschitz domain $\Omega \subset \mathbb{R}^n$, it is

$$H^q\Lambda^n(\Omega) = \mathcal{R}(\mathrm{d}^{n-1}, H^{q+1}\Lambda^{n-1}(\Omega)),\ \forall q \in \mathbb{Z}.$$

Lemma 3.11 (**Bounded regular potential**, compare [36, Proposition 4.1])**.** *Given a $q \in \mathbb{Z}$. Assume $\eta \in L^2\Lambda^k(\Omega)$ s.t. $\eta \in \mathcal{R}(\mathrm{d}^{k-1}, H^{q+1}\Lambda^{k-1}(\Omega))$.*
Then there is a $\omega \in H^{q+1}\Lambda^{k-1}(\Omega)$ with

$$\mathrm{d}^{k-1}\omega = \eta, \quad \|\omega\|_{H^{q+1}(\Omega)} \leq C \|\eta\|_{H^q(\Omega)},$$

where C does not depend on η.

Remark 3.5. If some Lipschitz domain is given by a smooth and invertible deformation of a starlike domain. Then Lemma 3.10 is still applicable. Namely, using the pullback operation Definition 3.9 together with [36, Proposition 4.1] one obtains the statement for the deformed domain.

3.3.2 Proxy complex

Actually, there are different possibilities to identify k-forms with vectors in $\mathbb{R}^{n|k}$. As already mentioned, the coefficient vector $\mathbf{c}_\omega$ of a k-form ω relates it to a vector in the Euclidean space, where we assume $\mathbf{c}_\omega$ to be a column vector. But obviously, given an invertible matrix $A_k \in \mathbb{R}^{(n|k)\times(n|k)}$, we might also use $\tilde{\mathbf{c}}_\omega \coloneqq A_k\mathbf{c}_\omega$ for identification. To give us some leeway when transitioning between differential forms and classical Sobolev functions, we want to introduce the concept of a *proxy map*. The latter is actually just a tool to be able to express various statements more compactly and with a certain generality as we proceed.

Definition 3.10 (**Proxy map**)**.** *Let $k \in \{0, \dots, n\}$ and let $A_k \in \mathbb{R}^{(n|k)\times(n|k)}$ be an invertible matrix. We call a mapping of the form*

$$\mathcal{J}_k \colon \mathrm{Alt}^k(\mathbb{R}^n) \to \mathbb{R}^{n|k}\ ,\ \omega \mapsto A_k\mathbf{c}_\omega \tag{3.3.5}$$

a proxy map.
This $\mathcal{J}_k$ trivially induces for each set $U \subset \mathbb{R}^n$ the identification

$$\mathcal{J}_k \colon L^2\Lambda^k(U) \to L^2(U) \otimes \mathbb{R}^{n|k}\ ,\ \omega \mapsto \Big(x \mapsto A_k\mathbf{c}_\omega(x)\Big), \tag{3.3.6}$$

mapping a k-form ω with coefficient vector field $\mathbf{c}_\omega = (c_1, \dots, c_{n|k})^{\mathrm{T}}$ to the vector-field $A_k\mathbf{c}_\omega(\cdot)$. In the case of differential forms, we use the same notation $\mathcal{J}_k$ and also refer to them as proxy maps.

Depending on the maps $\mathcal{J}_k$ we obtain densely defined operators on the space $L^2(\Omega)$ by setting

$$\mathcal{D}^k \colon L^2(\Omega) \otimes \mathbb{R}^{n|k} \to L^2(\Omega) \otimes \mathbb{R}^{n|k+1}\ ,\ u \mapsto \mathcal{J}_{k+1}\mathrm{d}^k\mathcal{J}_k^{-1}u, \tag{3.3.7}$$

where we use above and in the following the abbreviation

$$n|k \pm z \coloneqq n|(k \pm z) \coloneqq \binom{n}{k \pm z}$$

for $z \in \mathbb{Z}$.
By the definition of the $\mathcal{J}_k$, we obtain operators $\mathcal{D}^k$ of the form (2.2.3). Thus, they are also

closed and we obtain the Hilbert space $H(\Omega, \mathcal{D}^k, \mathbb{R}^{n|k})$; see (2.2.4). We also have $\mathcal{D}^{k+1} \circ \mathcal{D}^k = 0$. Namely, if $v \in C^\infty(\overline{\Omega}) \otimes \mathbb{R}^{n|k}$ it is

$$\mathcal{D}^{k+1}\mathcal{D}^k v = \mathcal{J}_{k+2}\mathrm{d}^{k+1}\mathcal{J}_{k+1}^{-1}\mathcal{J}_{k+1}\mathrm{d}^k\mathcal{J}_k^{-1}v = \mathcal{J}_{k+2}\,0\,\mathcal{J}_k^{-1}v = 0.$$

Applying a density argument shows then $\mathcal{D}^{k+1} \circ \mathcal{D}^k = 0$ on $H(\Omega, \mathcal{D}^k, \mathbb{R}^{n|k})$.
Furthermore, one obtains indeed a closed operator

$$\mathcal{D}^k \colon H(\Omega, \mathcal{D}^k, \mathbb{R}^{n|k}) \to H(\Omega, \mathcal{D}^{k+1}, \mathbb{R}^{n|k+1}),$$

because: Given a $w \in H(\Omega, \mathcal{D}^k, \mathbb{R}^{n|k})$ there is a sequence $(w_m)_m \subset C^\infty(\overline{\Omega}) \otimes \mathbb{R}^{n|k}$ s.t. $\|w_m - w\|_{H(\mathcal{D})} \overset{m\to\infty}{\longrightarrow} 0$. Thus $\mathcal{D}^k w_m \in C^\infty(\overline{\Omega}) \otimes \mathbb{R}^{n|k+1}$ with

$$\left\|\mathcal{D}^k w_m - \mathcal{D}^k w\right\|_{H(\mathcal{D})} = \left\|\mathcal{D}^k w_m - \mathcal{D}^k w\right\| \overset{m\to\infty}{\longrightarrow} 0.$$

This means we have a smooth approximating sequence and $\mathcal{D}^k w \in H(\Omega, \mathcal{D}^{k+1}, \mathbb{R}^{n|k+1})$.

Hence, analogously to the statement in Lemma 3.5 the chain

$$0 \longrightarrow L^2(\Omega) \xrightarrow{\mathcal{D}^0} L^2(\Omega) \otimes \mathbb{R}^n \xrightarrow{\mathcal{D}^1} \quad \cdots \quad \xrightarrow{\mathcal{D}^{n-1}} L^2(\Omega) \longrightarrow 0$$

is a Hilbert complex with domain complex

$$0 \longrightarrow H(\Omega, \mathcal{D}^0, \mathbb{R}^1) \xrightarrow{\mathcal{D}^0} H(\Omega, \mathcal{D}^1, \mathbb{R}^n) \xrightarrow{\mathcal{D}^1} \cdots \xrightarrow{\mathcal{D}^{n-1}} H(\Omega, \mathcal{D}^n, \mathbb{R}^1) \longrightarrow 0.$$

Even more, we get a closed complex.

Lemma 3.12 (**Proxy complex**). *The tuples $(L^2(\Omega) \otimes \mathbb{R}^{n|\circ}, \mathcal{D}^\circ)$ determine a closed L^2 Hilbert complex, meaning the L^2 inner product structure is underlying. If $\Omega \subset \mathbb{R}^n$ is starlike then it holds*

$$\mathcal{N}(\mathcal{D}^k, H(\Omega, \mathcal{D}^k, \mathbb{R}^{n|k})) = \mathcal{R}(\mathcal{D}^{k-1}, H^1(\Omega) \otimes \mathbb{R}^{n|k-1}),\ \forall k > 0.$$

Proof. The first part of the assertion is clear by Lemma 3.5 and the definition of the $\mathcal{D}^k$.
The only thing we show is the direction "$\subset$" of the equation.
Choosing an element $w \in \mathcal{N}(\mathcal{D}^k, H(\Omega, \mathcal{D}^k, \mathbb{R}^{n|k}))$, we get with $\tilde{w} = \mathcal{J}_k^{-1}w$ an element $\tilde{w} \in \mathcal{N}(\mathrm{d}^k, H\Lambda^k(\Omega))$. Thus, applying Lemma 3.6, there is $\tilde{v} \in \mathcal{R}(\mathrm{d}^{k-1}, H^1\Lambda^{k-1}(\Omega))$ with $\mathrm{d}^{k-1}\tilde{v} = \tilde{w}$. But then $\mathcal{D}^{k-1}\mathcal{J}_{k-1}\tilde{v} = w$. And clearly, $\mathcal{J}_{k-1}\tilde{v} \in H^1(\Omega) \otimes \mathbb{R}^{n|k-1}$. □

A direct consequence of Lemma 3.7 is

Corollary 3.1. *For every $w \in L^2(\Omega)$, there is a $v \in H^1(\Omega) \otimes \mathbb{R}^n$ with $\mathcal{D}^{n-1}v = w$.*

One observes that actually $\mathcal{J}_k$ maps bijectively from $H\Lambda^k(\Omega)$ to $H(\Omega, \mathcal{D}^k, \mathbb{R}^{n|k})$. Because, by definition of the $\mathcal{D}^k$ it is straightforward to see that $\mathcal{D}^k(\mathcal{J}_k\omega) = \mathcal{J}_{k+1}\mathrm{d}^k\omega$, if $\omega \in H\Lambda^k(\Omega)$ and $\mathrm{d}^k(\mathcal{J}_k^{-1}v) = \mathcal{J}_{k+1}^{-1}\mathcal{D}^k v$, if $v \in H(\Omega, \mathcal{D}^k, \mathbb{R}^{n|k})$. Thus, we have the next commuting diagram structure.

$$\begin{array}{ccc} H\Lambda^k(\Omega) & \xrightarrow{\mathrm{d}^k} & H\Lambda^{k+1}(\Omega) \\ \mathcal{J}_k\downarrow & & \mathcal{J}_{k+1}\downarrow \\ H(\Omega, \mathcal{D}^k, \mathbb{R}^{n|k}) & \xrightarrow{\mathcal{D}^k} & H(\Omega, \mathcal{D}^{k+1}, \mathbb{R}^{n|k+1}) \end{array}$$

At the end of Section 3.3.1, we briefly discussed the Sobolev de Rham complex. This means that we departed from the L^2 Hilbert space structure and considered the exterior derivative as a distributional derivative on spaces of the form $H^z\Lambda^k(\Omega),\ z \in \mathbb{Z}$. Naturally, in a completely analogous manner, we can also view the operators $\mathcal{D}^k$ as distributional derivatives in the sense of

$$\mathcal{D}^k \colon H^z(\Omega) \otimes \mathbb{R}^{n|k} \to H^{z-1}(\Omega) \otimes \mathbb{R}^{n|k+1}, \quad z \in \mathbb{Z}.$$

Hence for $q \in \mathbb{Z}$ this results again in a bounded Hilbert complex $\Big(H^{q-\circ}(\Omega) \otimes \mathbb{R}^{n|\circ}, \mathcal{D}^\circ\Big)$, i.e. we have the chain

$$0 \longrightarrow H^q(\Omega) \otimes \mathbb{R} \xrightarrow{\mathcal{D}^0} H^{q-1}(\Omega) \otimes \mathbb{R}^n \xrightarrow{\mathcal{D}^1} \quad \cdots \quad \xrightarrow{\mathcal{D}^{n-1}} H^{q-n}(\Omega) \otimes \mathbb{R} \longrightarrow 0.$$

It is clear that, due to our special type of proxy maps (3.3.5) and the definition (3.3.7), the statements of the Lemmata 3.10, 3.11 also apply analogously to the complex $\Big(H^{q-\circ}(\Omega) \otimes \mathbb{R}^{n|\circ}, \mathcal{D}^\circ\Big)$.

Something we have somewhat neglected are the dual complexes, which play a role in the formulation of the Hodge–Laplace problems. To derive the dual domain spaces, one approach, for instance in [5], involves introducing a generalization of the trace operator for differential forms; for more detailed information, we refer to [5, Section 6.2.6]. However, it turns out that, in the end, one obtains a relatively elegant description for the dual domains.

Lemma 3.13 (**Dual de Rham complex**, cf. [5, Theorem 6.5]). *Let (δ_k, V_k^*) denote the adjoint of $(\mathrm{d}^{k-1}, H\Lambda^{k-1}(\Omega))$, i.e. $V_k^* = \mathrm{Dom}(\delta_k)$. Then it is*

$$V_k^* = \overline{C_c^\infty \Lambda^k(\Omega)}^{\|\cdot\|_{H(\delta)}},$$

where we write for the norm coming from the respective graph inner product of the adjoint δ just $\|\cdot\|_{H(\delta)}$. One notes, that δ is indeed a closed densely defined operator due to Lemma 2.2.

Before we illustrate de Rham complexes for $\Omega \subset \mathbb{R}^3$ and $\Omega \subset \mathbb{R}^2$, considering specific choices of $\mathcal{J}_k$ we want to give some remarks concerning the pullback in the context of proxy maps. We assume again $\mathbf{F} \colon \widehat{\Omega} \to \Omega$ to be a diffeomorphism between two Lipschitz domains. Besides let $\mathcal{J}_k \colon \mathrm{Alt}^k \to \mathbb{R}^{n|k}$ be a proxy map which induces bijections $\mathcal{J}_k \colon L^2\Lambda^k(\Omega) \to L^2(\Omega) \otimes \mathbb{R}^{n|k}$, $\mathcal{J}_k \colon L^2\Lambda^k(\widehat{\Omega}) \to L^2(\widehat{\Omega}) \otimes \mathbb{R}^{n|k}$ by a point-wise identification; see Definition 3.9.[7] For $\omega \in L^2\Lambda^k(\Omega)$ let us consider the pullback form $\eta = \mathcal{Y}_{\mathbf{F}}^k \omega \in L^2\Lambda^k(\widehat{\Omega})$. Then, clearly we get for each $x = \mathbf{F}(\hat{x})$ a matrix $\mathbf{M}(\hat{x}) \in \mathbb{R}^{(n|k)\times(n|k)}$ such that

$$\mathcal{J}_k \eta_{\hat{x}} = \mathbf{M}(\hat{x}) \Big[\mathcal{J}_k \omega_{\mathbf{F}(\hat{x})}\Big] \in \mathbb{R}^{n|k},$$

where on the right-hand side we have a matrix-vector multiplication. Hence, in fact the pullback can be described by a suitable matrix field $\mathbf{M} \colon \widehat{\Omega} \to \mathbb{R}^{(n|k)\times(n|k)}$. The entries of this field depend by definition of the pullback only on the parametrization and its first derivatives. In other words, in case of a smooth parametrization such a representation matrix $\mathbf{M}$ varies smoothly on $\widehat{\Omega}$. To be more precise, we have

Lemma 3.14 (**The pullback in the context proxy fields**). *Let $k \in \{0, \dots, n\}$ and $\mathcal{J}_k \colon L^2\Lambda^k(U) \to L^2(U) \otimes \mathbb{R}^{n|k},\ \forall U \subset \mathbb{R}^n$ be a proxy map in the sense of Definition 3.10. Further let $\mathbf{F} \colon \widehat{\Omega} \to \Omega$ be a diffeomorphism between domains in $\mathbb{R}^n$ which is C^{l+1}-smooth, i.e. $l+1$-times continuously differentiable, for some $l \in \mathbb{N}_0$. Then there exists a matrix field $\mathbf{M} \colon \widehat{\Omega} \to \mathbb{R}^{(n|k)\times(n|k)}$ s.t.*

$$\mathcal{J}_k \mathcal{Y}_{\mathbf{F}}^k \omega = \mathbf{M}\Big[(\mathcal{J}_k \omega) \circ \mathbf{F}\Big],$$

[7] We use the abbreviation $\mathrm{Alt}^k = \mathrm{Alt}^k(\mathbb{R}^n)$

where the entries of $\mathbf{M}$ *only depend on the first derivatives of* $\mathbf{F}$ *and are thus* C^l*-regular. On the right-hand side above we have point-wise the classical matrix-vector multiplication, i.e. as a result a vector-field with* $(n|k)$ *components.*
If the inverse $\mathbf{F}^{-1}$ *exists and is* C^{l+1}*-smooth, then we have due to* $\left(\mathcal{Y}^k_{\mathbf{F}}\right)^{-1} = \mathcal{Y}^k_{\mathbf{F}^{-1}}$ *the invertibility of the matrices* $\mathbf{M}(\hat{x})$ *and analogously*

$$\mathcal{J}_k\mathcal{Y}^k_{\mathbf{F}^{-1}}\hat{\omega} = \left(\mathbf{M}^{-1}(\mathbf{F}^{-1}\cdot)\right)\left[(\mathcal{J}_k\hat{\omega})\circ\mathbf{F}^{-1}\right].$$

In the last line $\mathbf{M}^{-1}(\mathbf{F}^{-1}\cdot)$ *denotes matrix field* $x \mapsto \mathbf{M}^{-1}(\mathbf{F}^{-1}(x))$*, where the latter is the inverse matrix of* $\mathbf{M}(\mathbf{F}^{-1}(x))$*.*

Proof. The first part of assertion follows directly by the special change of coefficients for differential forms induced by the pullback. This coefficient change is shown in Appendix 11.1; see Lemma 11.1. The second part is already answered by the mentioned fact $\left(\mathcal{Y}^k_{\mathbf{F}}\right)^{-1} = \mathcal{Y}^k_{\mathbf{F}^{-1}}$. □

Example 3.1 (Proxy de Rham chain for $\Omega \subset \mathbb{R}^3$)**.** *Let us choose the proxy maps determined through:*

- $\mathcal{J}_0(c) \coloneqq c$,
- $\mathcal{J}_1(c_1\,dx^1 + c_2\,dx^2 + c_3\,dx^3) \coloneqq (c_1, c_2, c_3)^{\mathrm{T}}$,
- $\mathcal{J}_2(c_1\,dx^1\wedge dx^2 + c_2\,dx^1\wedge dx^3 + c_3\,dx^2\wedge dx^3) \coloneqq (c_3, -c_2, c_1)^{\mathrm{T}}$,
- $\mathcal{J}_3(c\,dx^1\wedge dx^2\wedge dx^3) \coloneqq c$.

Applying the exterior derivatives and using the ansatz (3.3.7)*, we obtain the standard de Rham domain complex in* $3D$ *which has the form*

$$0 \longrightarrow H^1(\Omega) \xrightarrow{\nabla} H(\Omega, \nabla\times, \mathbb{R}^3) \xrightarrow{\nabla\times} H(\Omega, \nabla\cdot, \mathbb{R}^3) \xrightarrow{\nabla\cdot} L^2(\Omega) \longrightarrow 0 \tag{3.3.8}$$

with underlying L^2 *inner product. In this context,* ∇*,* $\nabla\times$*,* $\nabla\cdot$ *represent the classical gradient, curl and divergence operators in* $3D$*. We remark here the obvious relation* $H(\Omega, \nabla, \mathbb{R}) = H^1(\Omega)$ *which justifies the first non-trivial space. In view of Lemma 3.13 together with the definitions* (2.2.5)*,* (3.3.7) *and with integration by parts there is no difficulty to see that the dual domain complex has the structure*

$$0 \longleftarrow L^2(\Omega) \xleftarrow{-\nabla\cdot} H_0(\Omega, \nabla\cdot, \mathbb{R}^3) \xleftarrow{\nabla\times} H_0(\Omega, \nabla\times, \mathbb{R}^3) \xleftarrow{-\nabla} H^1_0(\Omega) \longleftarrow 0.$$

Example 3.2 (Proxy de Rham chain for $\Omega \subset \mathbb{R}^2$)**.** *Next we can also define proxy maps for the planar case. More precisely, we set*

- $\mathcal{J}_0(c) \coloneqq c$,
- $\mathcal{J}_1(c_1\,dx^1 + c_2\,dx^2) \coloneqq (c_2, -c_1)^{\mathrm{T}}$,
- $\mathcal{J}_2(c\,dx^1\wedge dx^2) \coloneqq c$.

At this, the exterior derivatives on $L^2\Lambda^k(\Omega)$ *imply the operators* $\mathcal{D}^0 = \operatorname{curl}$, $\operatorname{curl}(v) \coloneqq (\partial_2 v, -\partial_1 v)^{\mathrm{T}}$ *and* $\mathcal{D}^1$ *is the usual divergence. Consequently, we have the chain*

$$0 \longrightarrow H^1(\Omega) \xrightarrow{\operatorname{curl}} H(\Omega, \nabla\cdot, \mathbb{R}^2) \xrightarrow{\nabla\cdot} L^2(\Omega) \longrightarrow 0. \tag{3.3.9}$$

And since obviously for $v \in H^1(\Omega)$, $(w_1, w_2)^{\mathrm{T}} \in H_0^1(\Omega)\otimes\mathbb{R}^2$ *it is* $\langle \operatorname{curl}(v), w\rangle = \langle v, -\partial_2 w_1 + \partial_1 w_2\rangle$ *we have the dual chain*

$$0 \longleftarrow L^2(\Omega) \xleftarrow{\operatorname{curl}^*} H_0(\Omega, \operatorname{curl}^*, \mathbb{R}^2) \xleftarrow{-\nabla} H_0^1(\Omega) \longleftarrow 0,$$

with $\operatorname{curl}^*(w_1, w_2) = \partial_1 w_2 - \partial_2 w_1$.

Before finishing this chapter on Hilbert complexes, we want to emphasize once again that many of the results presented remain valid in more general contexts. For example, one can consider Sobolev spaces with real exponents or define differential forms on Riemannian manifolds instead of just Lipschitz domains. And the statements related to bounded potentials are generalizable utilizing the existence of a uniform set of cohomology representatives; see also [12, Theorem 2 and Theorem 5]. However, we have chosen to focus only on the versions that we will actually need later for the discretizations. For more information on exterior calculus also on manifolds we refer to [39, 5, 51, 72].

3.4 Structure-preserving discretization of Hilbert complexes

The sections above deal with basic aspects from the field of Hilbert complexes. But the original aim is the design of numerical methods for the Hodge–Laplace problem using the underlying structure, the underlying complex, respectively. Basically, this was a major trigger for studying Hilbert complexes in the context of numerical analysis. That is why the seminal paper [11] by Arnold, Falk and Winther is titled with "*Finite Element Exterior Calculus: From Hodge Theory to Numerical Stability*" which suggests the motivation. Remarkably, the FEEC theory yields abstract sufficient conditions for obtaining good, namely well-posed discretizations (see Definition 2.11), of the Hodge–Laplace problems associated to a closed Hilbert complex. Admittedly, a fundamental requirement would be the well-posedness of the continuous problem that has to be approximated. Otherwise, numerical calculations are not really meaningful. Fortunately, we focus on the Hodge–Laplace problem and well-posedness is guaranteed; see Lemma 3.4.

Let in the following (V°, d°) denote the domain complex of a closed Hilbert complex (W°, d°). Further we continue to use here the notation from Section 3.1.
In view of the results of FEEC, especially [5, 11], we see a guideline how to choose a family of finite-dimensional spaces $V_h^j \subset V^j$ such that discretized versions of the mixed weak form (3.2.5)-(3.2.7) lead to a well-posed discretization of the continuous pendant; cf. Definition 2.11. We state and explain here the needed conditions derived in [5], where we restrict ourselves to the case of trivial cohomology spaces.

Assumption 3.2 (**Trivial cohomology**). *In what follows we have the requirement* $\mathfrak{H}^k = \{0\}$, *i.e. the corresponding complex is exact at level* k.

The last restriction is reasonable since later on, we essentially only consider de Rham complexes or sequences derived from them and they are exact, except of the first level e.g. for smoothly deformed starlike domains. By applying Lemmata 3.6 and 3.7, one will find that exactness is indeed present for our applications. Simultaneously, $\mathfrak{H}^k = \{0\}$ brings about a simplification of the mixed formulation from Definition 3.5.

Basic idea for the choice of the V_h^j is to preserve the structure of the complex, i.e. we want to obtain a discrete complex (V_h°, d°). Then, we can carry over, re-use respectively, the results and proofs from the Hilbert complex framework in the discrete setting. The hope is that this simplifies the proofs and allows general statements. In particular, in this section it is not important how the V_h^j are defined exactly. We only focus on the main conditions they should fulfill. As outlined in [5] the next three properties have to be considered, where the first one is standing to reason and does not need further explanations.

Convergence property

We assume a convergence of the V_h^j to the V^j. To be more precise, let us suppose

$$\lim_{h\to 0} \inf_{v_h \in V_h^j} \|v - v_h\|_V = 0, \quad \forall v \in V^j,\ \forall j.$$

Subcomplex property

The V_h^j satisfy the subcomplex property if $V_h^j \subset V^j$ and $d^j V_h^j \subset V_h^{j+1}$ for all j. In other terms, (V_h°, d°) determine Hilbert complexes.

Finally, one requires a proper connection between the continuous and discrete complex via compatible projections, so-called *bounded cochain projections*.

Bounded cochain projection property

We assume uniformly W^j-bounded projections $\Pi_h^j \colon V^j \to V_h^j$ with the compatibility relation $d^j \circ \Pi_h^j = \Pi_h^{j+1} \circ d^j$ for all j. This means we have a commuting diagram

$$\begin{array}{ccccccc}
\cdots & V^{k-1} & \xrightarrow{d^{k-1}} & V^k & \xrightarrow{d^k} & V^{k+1} & \cdots \\
& \Pi_h^{k-1}\downarrow & & \Pi_h^k\downarrow & & \Pi_h^{k+1}\downarrow & \\
\cdots & V_h^{k-1} & \xrightarrow{d^{k-1}} & V_h^k & \xrightarrow{d^k} & V_h^{k+1} & \cdots
\end{array}$$

and the continuity constants of the projections have to be independent of h.

Definition 3.11 (**Structure-preserving discretization**). *We call a family of discrete spaces $(V_h^\circ)_h$ satisfying the three above properties a* structure-preserving discretization *of the Hilbert complex (V°, d°).*

For such finite-dimensional complexes (V_h°, d°) we can introduce completely analogous to Definition 3.2 cocycles, coboundaries etc. We indicate them with a h, i.e. we write $\mathfrak{Z}_h^k$, $\mathfrak{H}_h^k$ and so forth. Certainly, one can also establish a Hodge decomposition for the V_h^k.

Next we explain why the three mentioned properties indeed lead to a well-posed discretization. Beforehand we put an auxiliary lemma.

Lemma 3.15 (**Discrete Poincaré inequality**, [5, Theorem 5.3]). *Given a structure-preserving discretization V_h° of (V°, d°). Then*

$$\|v_h\|_V \le \tilde{C}_P \left\| d^j v_h \right\|, \quad \forall v_h \in (\mathfrak{Z}_h^j)^{\perp_{V_h}},\ \forall j\ ,$$

where $(\mathfrak{Z}_h^j)^{\perp_{V_h}} := \{w \in V_h^j \mid \langle w, v\rangle_V = 0,\ \forall v \in \mathfrak{Z}_h^j\}$.
Above, $\tilde{C}_P > 0$ might depend on j, but is independent of h, v_h.

Proof. Using the cochain projections and the subcomplex property this can be derived from the continuous Poincaré inequality; for more details see the proof of [5, Theorem 5.3]. □

Hence, a crucial aspect in the context of closed Hilbert complexes and the Hodge–Laplace problems, namely the Poincaré inequality, is valid for (V_h°, d°). Another point is the exactness, which is preserved for structure-preserving methods. Otherwise, the discrete mixed weak formulation would have a different form from the continuous one, which would contradict the term "structure-preserving discretization". Indeed, if one has $\mathfrak{H}^k = \{0\}$ and $d^k v_h = 0$ for $v_h \in V_h^k$, then there is a $w \in V^{k-1}$ s.t. $d^{k-1}w = v_h$. Setting $w_h \coloneqq \Pi_h^{k-1} w$ gives us directly

$$d^{k-1} w_h = \Pi_h^k d^{k-1} w = \Pi_h^k v_h = v_h.$$

Consequently we can conclude $\mathfrak{H}_h^k = \{0\}$. This makes the next lemma clearer.

Lemma 3.16 (**Discretized mixed weak formulation**; see [5, Theorem 5.4 and Theorem 5.5])**.** *Let $(V_h^\circ)_h$ be a structure-preserving discretization of (V°, d°) and let $\mathfrak{H}^k = \{0\}$. Given a $f \in W^k$, the mixed weak formulation* (3.2.5)-(3.2.7) *reduces to the problem: Find $(\sigma, u) \in V^{k-1} \times V^k$ with*

$$\begin{aligned} \langle \sigma, \tau \rangle \quad &- \langle u, d^{k-1}\tau \rangle = 0, \qquad \forall \tau \in V^{k-1}, \\ \langle d^{k-1}\sigma, v \rangle \; &+ \langle d^k u, d^k v \rangle = \langle f, v \rangle, \quad \forall v \in V^k. \end{aligned}$$

The discretized version seeks $(\sigma_h, u_h) \in V_h^{k-1} \times V_h^k$ with

$$\langle \sigma_h, \tau_h \rangle \quad - \langle u_h, d^{k-1}\tau_h \rangle = 0, \qquad \forall \tau_h \in V_h^{k-1}, \tag{3.4.1}$$

$$\langle d^{k-1}\sigma_h, v_h \rangle + \langle d^k u_h, d^k v_h \rangle = \langle f, v_h \rangle, \quad \forall v_h \in V_h^k. \tag{3.4.2}$$

The latter is a well-posed discretization of the continuous problem in the sense of Definition 2.11 and the (σ_h, u_h) converge to the exact solution (σ, u) in a quasi-optimal manner. In particular, we have the estimate

$$\|\sigma - \sigma_h\|_V + \|u - u_h\|_V \leq C_{conv} \left(\inf_{(\tau, v) \in V_h^{k-1} \times V_h^k} \|\sigma - \tau\|_V + \|u - v\|_V \right),$$

for a proper constant C_{conv}.

Proof. In principle one can repeat the proof for the continuous case; cf. [5, Theorem 4.9]. The only steps which seem to imply h-dependent "constants" are the applications of the Poincaré inequality. But Lemma 3.15 shows that this is not an issue. □

With Section 3, we have now familiarized ourselves with the most important terms and concepts in the field of FEEC for the further part of the thesis. Most of the discussion above took place at a relatively abstract level, and we only became more concrete in the case of the de Rham complex and the definition of the exterior derivative, a special first-order differential operator.

However, for our thesis plan, we intend to explore Hodge–Laplace problems and their discretizations that arise from Hilbert complexes involving second-order differential operators. It is still not clear what these latter complexes look like or what specific type of complexes we want to consider. We aim to resolve these uncertainties in the next section, where we will address the question of how to construct new complexes under certain conditions from existing Hilbert complexes. Because one of these methods, the BGG construction, is not only suitable for generating higher-order complexes but is also used to define the class of second-order complexes, which will serve as the foundation for the development of numerical methods in Sections 8 and 9.

4 Construction of New Complexes

This section is dedicated to two methods on how we can construct from given Hilbert complexes new complexes. The first one is in some sense standard and is based on exploitation of cochain maps and the second one is the *complexes from complexes* ansatz from Arnold and Hu ([12]). The latter uses the so-called *BGG* (Bernstein-Gelfand-Gelfand) construction and makes it possible to obtain higher-order complexes. Both approaches are useful for considerations regarding IGA discretizations and second-order complexes below. On the one hand, we utilize later the pullback operation which acts as a cochain map between de Rham sequences to define the isogeometric discrete differential forms. On the other hand, the BGG construction guides us in Section 4.2.3 to a special class of second-order complexes that are used to introduce and discretize specific saddle-point problems in the main part of the work.

4.1 New complexes via cochain maps

We begin with a simple, but still important way to map one Hilbert complex structure to a second one, namely using cochain maps.

Lemma 4.1 (**Bounded cochain maps**). *Let (W°, d°) be a closed Hilbert complex with domain complex (V°, d°). Additionally, we assume Hilbert spaces $\widehat{W}^i$ together with linear, bounded and bijective mappings $\mathcal{Y}^i \colon W^i \to \widehat{W}^i$. Further, let us set $\widehat{V}^i \coloneqq \mathcal{Y}^i(V^i)$ and define*

$$\hat{d}^j \colon \widehat{V}^j \to \widehat{W}^{j+1} \ , \ \hat{v} \mapsto \mathcal{Y}^{j+1} d^j \left(\mathcal{Y}^j\right)^{-1} \hat{v}.$$

Then $(\widehat{W}^\circ, \hat{d}^\circ)$ defines a closed Hilbert complex with domain complex $(\widehat{V}^\circ, \hat{d}^\circ)$.
Furthermore, if (V°, d°) is exact at level k so is $(\widehat{V}^\circ, \hat{d}^\circ)$. We call the mappings $\mathcal{Y}^\circ$ a bounded cochain map *from (W°, d°) to $(\widehat{W}^\circ, \hat{d}^\circ)$.*

Proof. The proof is straightforward. We only show the closed range property. Let $\hat{d}^j \hat{v}_m \xrightarrow{\widehat{W}} \hat{w} \in \widehat{W}^{j+1}$. Then $d^j \left(\mathcal{Y}^j\right)^{-1} \hat{v}_m = \left(\mathcal{Y}^{j+1}\right)^{-1} \hat{d}^j \hat{v}_m \xrightarrow{W} \left(\mathcal{Y}^{j+1}\right)^{-1} \hat{w}$ which implies an $\hat{u} \in \widehat{V}^j$ such that $d^j \left(\mathcal{Y}^j\right)^{-1} \hat{u} = \left(\mathcal{Y}^{j+1}\right)^{-1} \hat{w}$ and thus $\hat{d}^j \hat{u} = \hat{w}$. □

One observes that by construction we have $\hat{d}^j \circ \mathcal{Y}^j = \mathcal{Y}^{j+1} \circ d^j$ and this commutativity yields the boundedness of the $\mathcal{Y}^j$ w.r.t. the graph norms.

We have applied a method akin to that presented in the previous lemma within Section 3.3.2 to establish the proxy complex. And, in the end, the transition from the de Rham complex in Ω to the one in $\widehat{\Omega}$ in Section 3.3.1 also aligns with this approach, where the pullback operation correspond to the cochain map. In this context one notes the relation $\hat{\mathrm{d}}^k \circ \mathcal{Y}^k_{\mathbf{F}} = \mathcal{Y}^{k+1}_{\mathbf{F}} \circ \mathrm{d}^k$ for the exterior derivatives. Hence, we have already utilized the possibility to modify or transform Hilbert complexes using bijective operators.

Helpful in the context of discretizations is the following obvious auxiliary result, which states that cochain maps $\mathcal{Y}^\circ$ are compatible with structure-preserving discretizations.

Lemma 4.2. *If $(V_h^\circ)_h$ is a structure-preserving discretization of (V°, d°) and $\mathcal{Y}^\circ$ a bounded cochain map from (W°, d°) to $(\widehat{W}^\circ, \hat{d}^\circ)$ in the sense of Lemma 4.1.*
Then the spaces $\widehat{V}_h^i \coloneqq \mathcal{Y}^i(V_h^i)$ define a structure-preserving discretization of $(\widehat{V}^\circ, \hat{d}^\circ)$.

Proof. The subcomplex property is obviously fulfilled by assumption. Also the convergence property is clear due to the continuity of the $\mathcal{Y}^j$ w.r.t. the graph norms related to the operators

d^j, $\hat{d}^j$. The natural candidates for the cochain projections are $\widehat{\Pi}_h^j \coloneqq \mathcal{Y}^j \circ \Pi_h^j \circ \left(\mathcal{Y}^j\right)^{-1}$. A simple calculation shows us indeed $\hat{d}^j \circ \widehat{\Pi}_h^j = \widehat{\Pi}_h^{j+1} \circ \hat{d}^j$. And clearly we have boundedness of the projections. □

The connection between the different spaces and the projections $\widehat{\Pi}_h^j$ introduced in the proof of the last lemma can be well illustrated in the following commutative diagram

$$\begin{array}{ccccccc}
\cdots & V^{k-1} & \xrightarrow{d^{k-1}} & V^k & \xrightarrow{d^k} & V^{k+1} & \cdots \\
& \mathcal{Y}^{k-1}\downarrow & & \mathcal{Y}^k\downarrow & & \mathcal{Y}^{k+1}\downarrow & \\
\cdots & \widehat{V}^{k-1} & \xrightarrow{\hat{d}^{k-1}} & \widehat{V}^k & \xrightarrow{\hat{d}^k} & \widehat{V}^{k+1} & \cdots \\
& \widehat{\Pi}_h^{k-1}\downarrow & & \widehat{\Pi}_h^k\downarrow & & \widehat{\Pi}_h^{k+1}\downarrow & \\
\cdots & \widehat{V}_h^{k-1} & \xrightarrow{\hat{d}^{k-1}} & \widehat{V}_h^k & \xrightarrow{\hat{d}^k} & \widehat{V}_h^{k+1} & \cdots\ .
\end{array}$$

Even though this transition from one complex to another using the $\mathcal{Y}^\circ$ is quite obvious, it is crucial in the definition of isogeometric discrete differential forms; see [27]. The ansatz to define the latter is outlined in Section 7.3 and can be summarized as follows: First, suitable spaces are defined for the discretization of the complex in a simple reference domain, e.g., a cube. Then, cochain maps are used to obtain a discretization in the actual computational domain. As already mentioned and in view of Lemma 3.8, we see the suitability of the pullback operation to go from the reference to the computational domain in case of the general de Rham sequence. Besides, there is no problem to relate the proxy complexes in different domains using the pullback. In fact, proper cochain maps $\mathcal{Y}^\circ$ for the proxy de Rham sequences in $2D$ (3.3.9) and $3D$ (3.3.8) are well-known. Below we will list them without proofs.

Example 4.1 (Piola mappings for the de Rham complex)**.** *Let $\mathbf{F}\colon \widehat{\overline{\Omega}} \to \overline{\Omega}$ be a C^1-diffeomorphism between two Lipschitz domains in $\mathbb{R}^n$ and $D\mathbf{F} = \mathbf{J} = (J_{ij})_{i,j}$ the corresponding Jacobian. Then the mappings*

$$\begin{aligned}
\mathcal{Y}_3^0(\phi) &\coloneqq \phi \circ \mathbf{F}, && \phi \in L^2(\Omega)\ , \\
\mathcal{Y}_3^1(v) &\coloneqq \mathbf{J}^{\mathrm{T}}(v \circ \mathbf{F}), && v \in L^2(\Omega) \otimes \mathbb{R}^3\ , \\
\mathcal{Y}_3^2(v) &\coloneqq \det(\mathbf{J})\mathbf{J}^{-1}(v \circ \mathbf{F}), && v \in L^2(\Omega) \otimes \mathbb{R}^3\ , \\
\mathcal{Y}_3^3(\phi) &\coloneqq \det(\mathbf{J})(\phi \circ \mathbf{F}), && \phi \in L^2(\Omega)\ ,
\end{aligned}$$

for $\Omega \subset \mathbb{R}^3$, and

$$\begin{aligned}
\mathcal{Y}_2^0(\phi) &\coloneqq \phi \circ \mathbf{F}, && \phi \in L^2(\Omega)\ , \\
\mathcal{Y}_2^1(v) &\coloneqq \det(\mathbf{J})\mathbf{J}^{-1}(v \circ \mathbf{F}), && v \in L^2(\Omega) \otimes \mathbb{R}^2\ , \\
\mathcal{Y}_2^2(\phi) &\coloneqq \det(\mathbf{J})(\phi \circ \mathbf{F}), && \phi \in L^2(\Omega)\ ,
\end{aligned}$$

in $2D$, respectively, define bounded cochain projections from (3.3.8) *and* (3.3.9) *to the chains in the parametric domain $\widehat{\Omega}$. In other words, one obtains the commuting diagrams*

$$\begin{array}{ccccccccccc}
0 & \longrightarrow & H^1(\Omega) & \xrightarrow{\nabla} & H(\Omega, \nabla\times, \mathbb{R}^3) & \xrightarrow{\nabla\times} & H(\Omega, \nabla\cdot, \mathbb{R}^3) & \xrightarrow{\nabla\cdot} & L^2(\Omega) & \longrightarrow & 0 \\
& & \mathcal{Y}_3^0\downarrow & & \mathcal{Y}_3^1\downarrow & & \mathcal{Y}_3^2\downarrow & & \mathcal{Y}_3^3\downarrow & & \\
0 & \longrightarrow & H^1(\widehat{\Omega}) & \xrightarrow{\widehat{\nabla}} & H(\widehat{\Omega}, \widehat{\nabla}\times, \mathbb{R}^3) & \xrightarrow{\widehat{\nabla}\times} & H(\widehat{\Omega}, \widehat{\nabla}\cdot, \mathbb{R}^3) & \xrightarrow{\widehat{\nabla}\cdot} & L^2(\widehat{\Omega}) & \longrightarrow & 0
\end{array}$$

and

$$\begin{array}{ccccccccc} 0 & \longrightarrow & H^1(\Omega) & \xrightarrow{\operatorname{curl}} & H(\Omega,\nabla\cdot,\mathbb{R}^2) & \xrightarrow{\nabla\cdot} & L^2(\Omega) & \longrightarrow & 0 \\ & & \mathcal{Y}_2^0\downarrow & & \mathcal{Y}_2^1\downarrow & & \mathcal{Y}_2^2\downarrow & & \\ 0 & \longrightarrow & H^1(\widehat{\Omega}) & \xrightarrow{\widehat{\operatorname{curl}}} & H(\widehat{\Omega},\widehat{\nabla}\cdot,\mathbb{R}^2) & \xrightarrow{\widehat{\nabla}\cdot} & L^2(\widehat{\Omega}) & \longrightarrow & 0\ . \end{array}$$

Above the hat *indicate that we need to consider the differential operators in the bottom complexes w.r.t. the new coordinates ζ_i determined by $\mathbf{F}(\zeta_1,\dots,\zeta_n)=(x_1,\dots,x_n)$. The commutativity relations of the mappings can be shown by a simple application of the chain rule. We omit here details.*

After these brief remarks on a first method to modify complexes, we turn to the second approach, which is important for our work: generating new complexes with the BGG construction. The latter in rough terms, creates a new output complex by two input complexes including linking maps.

4.2 The BGG construction

In this part we present the ansatz *complexes from complexes* by Arnold and Hu based on the Bernstein-Gelfand-Gelfand (BGG) procedure; see [12].We start our explanations of the concept in an abstract fashion. Afterwards in the second subsection we move on to a bit more concrete setting involving Sobolev spaces. In the last subsection, we finally get even more concrete and introduce a special class of BGG constructions and underlying L^2 Hilbert complexes. Moreover, to define this class the already discussed de Rham sequences again come into play.

4.2.1 The abstract formulation

The approach of Arnold and Hu is useful to derive and study the different second-order complexes considered later. Also, to establish a special approximation method in the context of second-order complexes, we utilize in Section 8 the structure behind BGG. This in turn can be exploited in the context of linear elasticity; see Section 9.
We start with the assumption that we have given two bounded Hilbert chains (V°,d°), $(\bar V^\circ,\bar d^\circ)$, which we sometimes refer to as *input complexes*. Here, for the inner product we write just $\langle\cdot,\cdot\rangle_V$, $\langle\cdot,\cdot\rangle_{\bar V}$ and $\|\cdot\|_V$, $\|\cdot\|_{\bar V}$ for the induced norms, i.e. again we omit an index for reasons of readability. Further, we assume both complexes to be finite in the sense that there is an index $n\in\mathbb{N}_{>0}$ with $\bar d^n=0,\ d^n=0$ and we suppose $d^z=0,\ \bar d^z=0,\ \forall z<0$. In particular we might set $V^i=0,\ \bar V^i=0$ for $i\notin\{0,1,\dots,n-1\}$. Now we connect the mentioned two complexes by proper linking maps S^i, namely we require:

$$\begin{aligned} &S^i\colon V^i\to\bar V^{i+1} \text{ is bounded with closed range and}\\ &\qquad \bar d^{i+1}\circ S^i=-S^{i+1}\circ d^i,\ \forall i\ . \quad \text{(anti-commutativity)} \end{aligned} \tag{4.2.1}$$

Besides, we have to assume the existence of an index $J\in\{0,1,\dots,n-1\}$ s.t.

$$S^i \text{ is } \begin{cases} \text{injective,} & \text{if } i<J,\\ \text{bijective,} & \text{if } i=J,\\ \text{surjective,} & \text{if } i>J, \end{cases} \tag{4.2.2}$$

where for $i<0$ and $i\geq n$ we set S^i just to the zero map. Consequently, we end up with two coupled complexes as indicated in Figure 2 below. Following the steps and results by Arnold

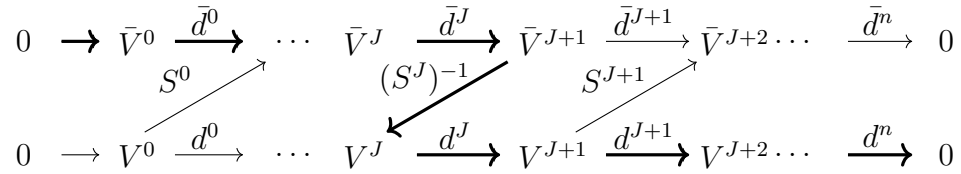

Figure 2: As shown in [12] we can built from the coupled complexes a new complex, provided suitable linking maps.

and Hu ([12]) it is possible to define a new combined complex form the top and bottom line in the mentioned figure.

Definition 4.1 (**BGG output complex**). *To be more precise, it can be shown that the spaces*

$$\mathscr{V}^i \coloneqq \begin{cases} \bar{V}^i \cap \mathcal{R}(S^{i-1})^{\perp_{\bar{V}}}, & 0 \le i \le J, \\ V^i \cap \mathcal{N}(S^i), & J < i \le n \end{cases} \tag{4.2.3}$$

and operators

$$\mathscr{D}^i \coloneqq \begin{cases} \mathcal{P}_{\mathcal{R}(S)^\perp} \bar{d}^i, & i < J, \\ d^J (S^J)^{-1} \bar{d}^J, & i = J, \\ d^i, & i > J, \end{cases} \tag{4.2.4}$$

define another bounded Hilbert complex $(\mathscr{V}^\circ, \mathscr{D}^\circ)$*, the so-called* output complex.

Above we write $\mathcal{R}$ and $\mathcal{N}$ for the range and kernel of the different mappings and $\mathcal{P}_X$ stands for the orthogonal projection onto the respective spaces X, where $\mathcal{P}_{\mathcal{R}(S)^\perp \bar{v}} \coloneqq \mathcal{P}_{\mathcal{R}(S^i)^{\perp_{\bar{V}}} \bar{v}}$.

Lemma 4.3 (**BGG output complex**; compare [12, Theorem 6]). *The spaces* $\mathscr{V}^\circ$ *together with the operators* $\mathscr{D}^\circ$ *define a bounded Hilbert complex.*

Proof. Indeed, we see directly the boundedness of $\mathscr{D}^i$ and if $i \ge J$ we get obviously $\mathscr{D}^{i+1} \circ \mathscr{D}^i = 0$. Further for $v \in \mathscr{V}^i$, $i > J$ we have $S^{i+1}\mathscr{D}^i v = S^{i+1} d^i v = -\bar{d}^{i+1} S^i v = 0$. Thus, $\mathscr{D}^i v \in \mathscr{V}^{i+1}$. In the situation $i = J$ and $v \in \mathscr{V}^i$ we have $S^{J+1}\mathscr{D}^J v = S^{J+1} d^J (S^J)^{-1} \bar{d}^J v = -\bar{d}^{J+1} S^J (S^J)^{-1} \bar{d}^J v = 0$ which implies $\mathscr{D}^J v \in \mathscr{V}^{J+1}$.

Let now $v \in \mathscr{V}^i$ with $i < J - 1$. Note

$$0 = \mathcal{P}_{\mathcal{R}(S)^\perp} \bar{d}^{i+1} \bar{d}^i v = \mathcal{P}_{\mathcal{R}(S)^\perp} \bar{d}^{i+1} (\mathcal{P}_{\mathcal{R}(S)^\perp} + \mathcal{P}_{\mathcal{R}(S)}) \bar{d}^i v,$$

where $\mathcal{P}_{\mathcal{R}(S)} \bar{v} \coloneqq \mathcal{P}_{\mathcal{R}(S^i)} \bar{v}$ for $\bar{v} \in \bar{V}^{i+1}$ denotes the $\bar{V}$-orthogonal projection. Let $w \in V^i$ s.t. $S^i w = \mathcal{P}_{\mathcal{R}(S)} \bar{d}^i v$. Using (4.2.1) we see

$$\mathcal{P}_{\mathcal{R}(S)^\perp} \bar{d}^{i+1} \mathcal{P}_{\mathcal{R}(S)} \bar{d}^i v = -\mathcal{P}_{\mathcal{R}(S)^\perp} S^{i+1} d^i w = 0.$$

This shows us $\mathscr{D}^{i+1}\mathscr{D}^i v = 0$ and by definition of $\mathscr{D}^i$ we also see $\mathscr{D}^i v \in \bar{V}^{i+1} \cap \mathcal{R}(S^i)^{\perp_{\bar{V}}}$ for $i < J - 1$.

Finally we look at the case $i = J - 1$ and $v \in \mathscr{V}^{J-1}$. Analogously to before set $S^{J-1} w = \mathcal{P}_{\mathcal{R}(S)} \bar{d}^{J-1} v$ and see

$$d^J (S^J)^{-1} \bar{d}^J \mathcal{P}_{\mathcal{R}(S)} \bar{d}^{J-1} v = d^J (S^J)^{-1} \bar{d}^J S^{J-1} w = -d^J \bar{d}^{J-1} w = 0.$$

Hence $0 = d^J (S^J)^{-1} \bar{d}^J \bar{d}^{J-1} v = d^J (S^J)^{-1} \bar{d}^J \mathcal{P}_{\mathcal{R}(S)^\perp} \bar{d}^{J-1} v = \mathscr{D}^J \mathscr{D}^{J-1} v$. The trivial relation $\mathscr{D}^{J-1} v \in \mathscr{V}^J$ finishes the proof. □

Checking the proofs and the setting in [12] one sees a slightly different definition of the involved spaces. In the latter publication they concentrate on Hilbert spaces $V^i,\ \bar{V}^i$ which are the product of Hilbert spaces times a finite-dimensional inner product spaces, meaning $V^i = U^i \otimes \mathbb{E},\ \bar{V}^i = \bar{U}^i \otimes \bar{\mathbb{E}}^i$, together with the restriction $U^i = \bar{U}^{i+1}$ is made. In this setting the S^i linking maps reduce to operators $s^i \colon \mathbb{E}^i \to \bar{\mathbb{E}}^{i+1}$, i.e. $S^i = \mathrm{id} \otimes s^i$, like taking the trace or the symmetric part of matrix. Nevertheless, the output complex construction from Definition is in principle the same as in [12, Section 3], is taken from the latter, respectively. Namely, suppose $V^i = U^i \otimes \mathbb{E}^i,\ \bar{V}^i = \bar{U}^i \otimes \bar{\mathbb{E}}^i,\ U^i = \bar{U}^{i+1}$ and $s^i \colon \mathbb{E}^i \to \bar{\mathbb{E}}^{i+1},\ S^i = \mathrm{id} \otimes s^i$. Then we have $\bar{U}^i \otimes \mathcal{R}(s^{i-1}) = \bar{V}^i \cap \mathcal{R}(S^{i-1}),\ U^i \otimes \mathcal{N}(s^i) = V^i \cap \mathcal{N}(S^i)$ and $\mathrm{id} \otimes \mathcal{P}_{\mathcal{R}(s^i)^\perp} = \mathcal{P}_{\mathcal{R}(S^i)^{\perp_{\bar{V}}}}$.

All the lemmata showing the complex structure of $(\mathscr{V}^\circ, \mathscr{D}^\circ)$ in [12] and also an estimate for the cohomology spaces (see next lemma) can be proven effectively in the same way. The only thing one has to adapt is the Moore-Penrose inverse t^i of the operators s^{i-1}; see (29) in [12]. Because for our modified setting, we do not have directly these Moore-Penrose inverse as defined in latter paper. However, it is enough to replace in the proofs of Arnold and Hu the $T^i := \mathrm{id} \otimes t^i$ (see (29) and page 1752 in [12]) by the generalized Moore-Penrose inverse of S^i which is well-defined by the closed ranges of the S^i; see Lemma 2.3. Here it is worth to emphasize that the equations $t^i s^{i-1} = \mathcal{P}_{\mathcal{N}(s^{i-1})^\perp},\ s^{i-1}t^i = \mathcal{P}_{\mathcal{R}(s^{i-1})}$ for the Moore-Penrose inverse t^i from line (29) in [12] are in direct alignment with those presented in (2.1.1).
Thus, if we change the T^i from [12] to $(S^i)^\dagger$ in the sense of Lemma 2.3 one can use the proof steps of Lemma 1 - Lemma 6 from latter article still for our setting. Thus we obtain the next Lemma which estimates the dimension of the cohomolgy spaces $\mathscr{H}^\circ$ of $(\mathscr{V}^\circ, \mathscr{D}^\circ)$.

Lemma 4.4 (**Cohomology of the output complex**, [12, Theorem 6])**.** *Let $\mathcal{H}^i$ and $\bar{\mathcal{H}}^i$ denote the i-th level cohomology space of (V°, d°), $(\bar{V}^\circ, \bar{d}^\circ)$, respectively. Then one can estimate the dimension of the i-th cohomology space $\mathscr{H}^i$ of the output complex via the formula*

$$\dim \mathscr{H}^i(\mathscr{V}^\circ, \mathscr{D}^\circ) \leq \dim \mathcal{H}^i(V^\circ, d^\circ) + \dim \bar{\mathcal{H}}^i(\bar{V}^\circ, \bar{d}^\circ).$$

So if we have the exactness at level k of both, the top and bottom complex in Figure 2, we also obtain the exactness at level k of the output complex.

Before we go on let us point out that it is no problem to combine the two methods from Section 4.1 and Section 4.2 to get new complexes. This means, provided suitable bijective mappings between Hilbert spaces for the top and bottom complex in Figure 2 we can still combine the modified input chains. Namely, let $\mathcal{Y}^\circ,\ \bar{\mathcal{Y}}^\circ$ be bounded cochain maps from (V°, d°) to $(\widehat{V}^\circ, \hat{d}^\circ)$, $(\bar{V}^\circ, \bar{d}^\circ)$ to $(\hat{\bar{V}}^\circ, \hat{\bar{d}}^\circ)$, respectively. Then to apply the BGG approach and to built a new output complex from the new input chains $(\hat{\bar{V}}^\circ, \hat{\bar{d}}^\circ)$ and $(\widehat{V}^\circ, \hat{d}^\circ)$ we need to adapt the linking maps. Because, $S^i \widehat{V}^i$ might not be defined and we might not get a subspace of $\hat{\bar{V}}^{i+1} := \bar{\mathcal{Y}}^{i+1}\big(\bar{V}^{i+1}\big)$. With an easy modification of the S^i we get new proper linking $\hat{S}^i$ maps:

$$\hat{S}^i \colon \widehat{V}^i \to \hat{\bar{V}}^{i+1}\ ,\ \hat{S}^i := \bar{\mathcal{Y}}^{i+1} \circ S^i \circ \big(\mathcal{Y}^i\big)^{-1}. \tag{4.2.5}$$

Then S^i is injective iff $\hat{S}^i$ is injective. And S^i is surjective iff $\hat{S}^i$ is surjective. And also easy to see is the next auxiliary result.

Lemma 4.5. *If the differential operators $d^i,\ \bar{d}^i$ and the S^i satisfy the anti-commutativity property* (4.2.1) *so do the modified linking maps $\hat{S}^i$ and the operators $\hat{\bar{d}}^i$.*

Proof. We drop here the composition symbol " $\circ$ ".

$$\begin{aligned}\hat{\bar{d}}^{i+1}\hat{S}^i &= \hat{\bar{d}}^{i+1}\bar{\mathcal{Y}}^{i+1}S^i\big(\mathcal{Y}^i\big)^{-1} = \bar{\mathcal{Y}}^{i+2}\bar{d}^{i+1}S^i\big(\mathcal{Y}^i\big)^{-1}\\ &= -\bar{\mathcal{Y}}^{i+2}S^{i+1}\bar{d}^i\big(\mathcal{Y}^i\big)^{-1} = -\bar{\mathcal{Y}}^{i+2}S^{i+1}\big(\mathcal{Y}^{i+1}\big)^{-1}\hat{\bar{d}}^i = -\hat{S}^{i+1}\hat{\bar{d}}^i.\end{aligned}$$

□

Consequently, it is justified to repeat the BGG construction to get a modified output complex $(\widehat{\mathscr{V}}^\circ, \widehat{\mathscr{D}}^\circ)$ utilizing the $\widehat{V}^i$, $\hat{\bar{V}}^i$ and the $\hat{S}^i$; see Figure 3. In particular, the corresponding definitions (4.2.3), (4.2.4) have to be adapted accordingly. Hence, by changing the linking maps we obtain in general completely different operators $\widehat{\mathscr{D}}$.

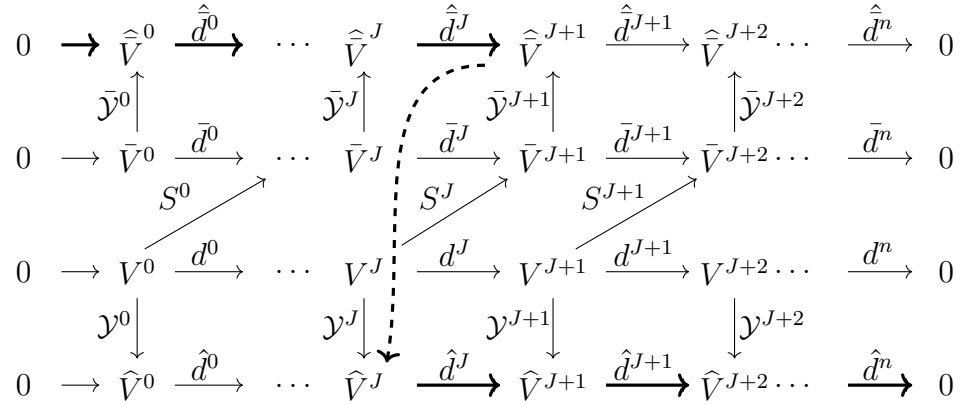

Figure 3: If we have bounded cochain maps for the top and bottom complexes, it is possible to combine the modified input chains by a change $S^i \to \hat{S}^i$ of the linking maps.

Now that we have introduced the BGG construction in an abstract manner, we aim to explore a specific case of it where we once again find ourselves in the context of Sobolev spaces. The objective is to establish Hilbert complexes with underlying L^2 inner products, which will in turn prove to be relevant for the numerical methods in the later stages of the work.

4.2.2 L^2 output complexes

Now we come back to Sobolev spaces on some Lipschitz domain Ω. Basically, we turn towards the kind of complexes also considered in [12]. But here we focus on the underlying L^2 Hilbert complexes and their domain complexes. The L^2 inner product structure is especially suitable when it comes to associated Hodge–Laplace problems and their discretization. On the one hand, standard FE methods and software often deal with L^2 spaces. More specifically, common FE implementations are based on and utilize the L^2 Hilbert space structure. On the other hand we will need only low regularity requirements for the test space definitions as well as for the source terms. This is an important point if the computational domain has a complicated shape or if in applications non-smooth load functions appear.
Again we combine two complexes like in the previous section, but now with a specific type of spaces. To be more precise according to the notation from Section 4.2.1 we assume input complexes

$$V^i = H^{q_{i+1}}(\Omega) \otimes \mathbb{E}^i, \quad \bar{V}^i = H^{q_i}(\Omega) \otimes \bar{\mathbb{E}}^i, \tag{4.2.6}$$

where $\mathbb{E}^i$ and $\bar{\mathbb{E}}^i$ denote finite-dimensional inner product spaces and $q_j \in \mathbb{Z}$. Note, in the definition of V^i an exponent q_{i+1} appears, whereas on the right for $\bar{V}^i$ we use q_i. As in Section 4.2.1 we make the restriction $V^i = \bar{V}^i = 0$, $\mathbb{E}^i = \bar{\mathbb{E}}^i = \{0\}$, respectively, for indices $i \notin \{0, \dots, n\}$. Additionally, we require differential operators

$$d^j \colon V^j \to V^{j+1}, \quad \bar{d}^j \colon \bar{V}^j \to \bar{V}^{j+1}, \quad \forall j, \tag{4.2.7}$$

of the form (2.2.3) s.t. (V°, d°), $(\bar{V}^\circ, \bar{d}^\circ)$ define bounded Hilbert complexes. And according to the previous section we make the restriction $d^i = 0$, $\bar{d}^i = 0$ for $i \notin \{0, \dots, n-1\}$.

Besides we have the next underlying assumptions, which further clarify the setting.

Assumption 4.1. *For every $i \in \mathbb{Z}$ and a fixed $J \in \{0, \dots, n-1\}$ we require:*

- *We have a linking map $S^i \colon L^2(\Omega) \otimes \mathbb{E}^i \to L^2(\Omega) \otimes \bar{\mathbb{E}}^{i+1}$, where $S^i = \mathrm{id} \otimes s^i$ and $s^i \colon \mathbb{E}^i \to \bar{\mathbb{E}}^{i+1}$ is $\begin{cases} \text{injective}, & \text{if } i \leq J, \\ \text{surjective}, & \text{if } i \geq J. \end{cases}$*
- *It is $\bar{d}^{i+1} \circ S^i = -S^{i+1} \circ d^i$ on $H(\Omega, d^i, \mathbb{E}^i)$.*
- *The Sobolev space indices correspond to the orders of the differential operators, i.e. $q_{i+1} - q_i = \mathrm{ord}(d^{i-1})$, $q_{i+1} - q_i = \mathrm{ord}(\bar{d}^i)$ and it is $d^{i+1} \circ d^i = 0$, $\bar{d}^{i+1} \circ \bar{d}^i = 0$.*

For the sake of readability we write in the following several times $H^z\mathbb{W} \coloneqq H^z(\Omega) \otimes \mathbb{W}$ for a inner product space $\mathbb{W}$. In particular, for the current setting we have the diagram structure:

$$\begin{array}{ccccccccccccc}
0 & \longrightarrow & H^{q_0}\bar{\mathbb{E}}^0 & \xrightarrow{\bar{d}^0} & \cdots & H^{q_J}\bar{\mathbb{E}}^J & \xrightarrow{\bar{d}^J} & H^{q_{J+1}}\bar{\mathbb{E}}^{J+1} & \xrightarrow{\bar{d}^{J+1}} & H^{q_{J+2}}\bar{\mathbb{E}}^{J+2} & \cdots & \xrightarrow{\bar{d}^n} & 0 \\
 & & & \nearrow_{S^0} & & & \swarrow_{(S^J)^{-1}} & & \nearrow_{S^{J+1}} & & & & \\
0 & \longrightarrow & H^{q_1}\mathbb{E}^0 & \xrightarrow{d^0} & \cdots & H^{q_{J+1}}\mathbb{E}^J & \xrightarrow{d^J} & H^{q_{J+2}}\mathbb{E}^{J+1} & \xrightarrow{d^{J+1}} & H^{q_{J+3}}\mathbb{E}^{J+2} & \cdots & \xrightarrow{d^n} & 0
\end{array}$$

Figure 4: Here we combine two complexes involving Sobolev spaces $H^z(\Omega)$. The idea is to obtain L^2 based Hilbert complexes as the previously introduced de Rham complex.

With the choice in line 4.2.6 and the last point of Assumption 4.1 we see that it is enough to specify the first exponent q_0 and then the rest of the q_i are determined by the orders of the differential operators. In other words having

$$q_0 = q \quad \text{we obtain successively} \quad q_i = q_{i-1} - \mathrm{ord}(\bar{d}^i),\ i = 1, 2, \dots \ . \tag{4.2.8}$$

In the following, we want to assume that we can choose this first exponent q_0 arbitrarily in $\mathbb{Z}$, meaning we are now considering a whole family of complexes.

Assumption 4.2. *For each $q_0 = q \in \mathbb{Z}$ the spaces* (4.2.6) *together with the operators* (4.2.7) *define bounded Hilbert complexes, meaning the top and bottom sequences in Figure 4 define bounded Hilbert complexes.*

Here it should be pointed out that we have already encountered a family of Sobolev Hilbert complexes, namely the Sobolev de Rham complexes in Section 3.3.1. To express it more clearly, if we set $\mathbb{E}^i = \mathrm{Alt}^i$, $\bar{\mathbb{E}}^i = \mathrm{Alt}^i$ and chose for d^i and $\bar{d}^i$ in (4.2.7) the exterior derivatives, we would have bounded Hilbert complexes in Figure 4 as long as $q_j - q_{j+1} = 1$, $\forall j$. Later in a subsequent section, we will also explain why we can find suitable linking maps for de Rham type complexes.

Before we address again a BGG type construction, we insert here a remark that should clarify, what we mean by exactness in the context of a complexes family.

Remark 4.1 (Regarding exactness). If we demand exactness at a certain level k and do not specify the exponents q_i, we require

$$\mathcal{R}(\bar{d}^{k-1}, H^{q+\bar{l}}\bar{\mathbb{E}}^{k-1}) = \mathcal{N}(\bar{d}^k, H^q\bar{\mathbb{E}}^k) \quad \text{and} \quad \mathcal{R}(d^{k-1}, H^{q+l}\mathbb{E}^{k-1}) = \mathcal{N}(d^k, H^q\mathbb{E}^k),\ \forall q \in \mathbb{N}_0,$$

where $\bar{l} = \mathrm{ord}(\bar{d}^{k-1})$ and $l = \mathrm{ord}(d^{k-1})$. The latter is especially fulfilled if we use Sobolev de Rham sequences as top and bottom chains; see Lemma 3.10.

With regard to linking maps, it is worth noting that, based on Assumption 4.1, bounded mappings $S^i\colon H^z(\Omega)\otimes\mathbb{E}^i\to H^z(\Omega)\otimes\bar{\mathbb{E}}^{i+1}$ are clearly obtained independently of z. Hence, utilizing the aforementioned assumption and the choice (4.2.6)-(4.2.7), we can once again apply the BGG construction, but now with a focus on the L^2 inner product.
For this purpose, let us introduce the auxiliary abbreviations

$$\mathbb{W}^i\coloneqq\begin{cases}\bar{\mathbb{E}}^i, & i\leq J,\\ \mathbb{E}^i, & i>J.\end{cases}$$

Having this in mind we come to the next

Definition 4.2. *We introduce the spaces $\mathcal{W}^i\coloneqq L^2(\Omega)\otimes\mathbb{W}^i$ and analogously to [12], to Section 4.2, respectively, we define the operators*

$$\mathscr{D}^i\colon\mathcal{W}^i\to\mathcal{W}^{i+1},\quad\text{with}\quad\mathscr{D}^i\coloneqq\begin{cases}\mathcal{P}_{\mathcal{R}(S)^{\perp_{L^2}}}\bar{d}^i, & i<J,\\ d^J(S^J)^{-1}\bar{d}^J, & i=J,\\ d^i, & i>J.\end{cases}\tag{4.2.9}$$

We interpret the differential operators $\mathscr{D}^i$ in a weak sense, which are obviously densely defined. Moreover, exploiting the special linking maps $S^i=\mathrm{id}\otimes s^i$, we can find linear mappings $r^i\colon\bar{\mathbb{E}}^i\to\bar{\mathbb{E}}^i$ such that $\mathcal{P}_{\mathcal{R}(S^{i-1})^{\perp_{L^2}}}=\mathrm{id}\otimes r^i$. Thus, the operators $\mathscr{D}^i$ can be re-written in the form (2.2.3) and they determine closed operators.

Corollary 4.1. *The differential operators $\mathscr{D}^i\colon\mathcal{W}^i\to\mathcal{W}^{i+1}$ are closed and densely defined.*

Proof. One notes Lemma 2.9 and Section 2.2. □

This means, the spaces

$$\mathscr{U}^i\coloneqq H(\Omega,\mathscr{D}^i,\mathbb{W}^i)\tag{4.2.10}$$

define Hilbert spaces endowed with the graph inner product and the norm

$$\|v\|^2_{H(\mathscr{D})}\coloneqq\|v\|^2_{\mathscr{U}}\coloneqq\|v\|^2+\left\|\mathscr{D}^iv\right\|^2,\ \forall v\in\mathscr{U}^i.\tag{4.2.11}$$

Next we change the underlying spaces $\mathcal{W}^i$ according to the BGG construction to obtain later a Hilbert complex whose cohomology is related to the cohomology of the input sequences. Namely, we set

$$\mathscr{W}^i\coloneqq\begin{cases}\mathcal{W}^i\cap\mathcal{R}(S^{i-1})^{\perp_{L^2}}, & \text{for } i\leq J\\ \mathcal{W}^i\cap\mathcal{N}(S^i), & \text{for } i>J.\end{cases}\tag{4.2.12}$$

Lemma 4.6 (BGG L^2 output complex). *If we restrict the mappings $\mathscr{D}^i$ from Definition 4.2 to the spaces in $\mathscr{W}^i$ then we get closed and densely defined operators*

$$\mathscr{D}^i\colon\mathscr{W}^i\to\mathscr{W}^{i+1}\ ,$$

with domains

$$\mathscr{V}^i\coloneqq H(\Omega,\mathscr{D}^i,\mathbb{V}^i),\ \text{where}\quad\mathbb{V}^i\coloneqq\begin{cases}\mathbb{W}^i\cap\mathcal{R}(s^{i-1})^{\perp}, & \text{for } i\leq J,\\ \mathbb{W}^i\cap\mathcal{N}(s^i), & \text{for } i>J\ .\end{cases}\tag{4.2.13}$$

Further we have the property $\mathscr{D}^{i+1}\mathscr{D}^iv=0$ for all $v\in\mathscr{V}^i$ and it is $\mathscr{D}^i\mathscr{V}^i\subset\mathscr{V}^{i+1}$.
Consequently, $(\mathscr{D}^\circ,\mathscr{V}^\circ)$ is indeed the domain complex to the Hilbert complex $(\mathscr{D}^\circ,\mathscr{W}^\circ)$, where for the latter we have the L^2 inner product structure underlying.

Proof. The second part related to the property $\mathscr{D}^{i+1} \circ \mathscr{D}^i = 0$ can be seen by a density argument similarly to the case of the proxy de Rham complex in Section 3.3.
For the first part of the assertion we show in view of Corollary 4.1 for reasons of completeness only the relation $\mathscr{D}^i \mathscr{V}^i \subset \mathscr{W}^{i+1}$.
Note, the $\mathscr{W}^i \subset \mathcal{W}^i$ are closed subspaces. First assume $i < J$. Then we see directly $\mathscr{D}^i v \in \mathscr{W}^{i+1}$ for smooth $v \in \mathscr{U}^i$ and thus $\mathscr{D}^i \mathscr{V}^i \subset \mathscr{W}^{i+1}$. Now let $i = J$. Choose a sequence of smooth v_m converging to a $v \in \mathscr{V}^J$ and $\phi \in C_c^\infty(\Omega) \otimes \bar{\mathbb{E}}^{J+1}$. One has the chain

$$\langle S^{J+1} \mathscr{D}^J v, \phi \rangle = \lim_{m \to \infty} \langle S^{J+1} d^J (S^J)^{-1} \bar{d}^J v_m, \phi \rangle = - \lim_{m \to \infty} \langle \bar{d}^{J+1} \bar{d}^J v_m, \phi \rangle = 0.$$

Thus we also get a closed and densely defined operator $\mathscr{D}^J \colon \mathscr{W}^J \to \mathscr{W}^{J+1}$. Finally let $i > J$ and $v \in \mathscr{V}^i$. For an approximating sequence of smooth functions $(v_m)_m \subset C^\infty(\overline{\Omega}) \otimes \mathbb{V}^i, v_m \xrightarrow{\mathscr{V}} v$ one sees

$$\langle S^{i+1} \mathscr{D}^i v, \phi \rangle = \lim_{m \to \infty} \langle S^{i+1} d^i v_m, \phi \rangle = - \lim_{m \to \infty} \langle \bar{d}^{i+1} S^i v_m, \phi \rangle = 0,$$

for all $\phi \in C_c^\infty(\Omega) \otimes \bar{\mathbb{E}}^{i+2}$. This implies $\mathscr{D}^i \mathscr{V}^i \subset \mathscr{W}^{i+1}$ for $i > J$. □

We refer to the complex $(\mathscr{D}^\circ, \mathscr{W}^\circ)$ of the last lemma as the L^2 *output complex* to emphasize the inner product structure. Although this complex $(\mathscr{D}^\circ, \mathscr{W}^\circ)$ is not directly the same as the one we would obtain by doing directly the BGG construction in the sense of Definition 4.1 with the spaces (4.2.6), we still can exploit Lemma 4.4 to make a statement regarding exactness.

Lemma 4.7 (**Exactness of L^2 output complex**). *Let the top and bottom complex in Figure 4 be exact at level k, in the sense of Remark 4.1.*
Then it holds

$$\mathcal{R}(\mathscr{D}^{k-1}, \mathscr{V}^{k-1}) = \mathcal{N}(\mathscr{D}^k, \mathscr{V}^k). \tag{4.2.14}$$

Consequently $\mathscr{D}^{k-1}$ has closed range. Furthermore, it holds

$$\mathcal{R}(\mathscr{D}^{k-1}, H^{q+l_{k-1}} \mathbb{V}^{k-1}) = \mathcal{N}(\mathscr{D}^k, H^q \mathbb{V}^k), \quad \forall q \in \mathbb{N}_0, \tag{4.2.15}$$

with l_{k-1} denoting the order of the differential operator $\mathscr{D}^{k-1}$.

Proof. We only show equation (4.2.14), since the rest of the assertion follows directly by Lemma 4.4.
Let us consider an element $w \in \mathscr{V}^k$ s.t. $\mathscr{D}^k w = 0$. By assumption together with Lemma 4.4 we have a trivial cohomology space in the sense that we find for w an element $v \in H^{l_{k-1}} \mathbb{V}^{k-1}$ such that $\mathscr{D}^{k-1} w = v$. Since obviously $H^{l_{k-1}} \mathbb{V}^{k-1} \subset \mathscr{V}^{k-1}$, we get $v \in \mathcal{R}(\mathscr{D}^{k-1}, \mathscr{V}^{k-1}), \mathcal{N}(\mathscr{D}^k, \mathscr{V}^k) \subset \mathcal{R}(\mathscr{D}^{k-1}, \mathscr{V}^{k-1})$, respectively. The other direction "$\supset$" is clear from Lemma 4.6 above and we get $\mathcal{N}(\mathscr{D}^k, \mathscr{V}^k) = \mathcal{R}(\mathscr{D}^{k-1}, \mathscr{V}^{k-1})$. □

If we have exactness one obtains in the same manner like in Lemma 3.11 the existence of bounded regular potentials. More precisely, it holds:

Corollary 4.2. *Let the equation in line* (4.2.15) *be fulfilled for a $q \in \mathbb{N}_0$. Then there is a constant $C > 0$ s.t. for every $v \in \mathscr{V}^k \cap H^q \mathbb{V}^k$ with $\mathscr{D}^k v = 0$ we find a $w \in H^{q+l_{k-1}} \mathbb{V}^{k-1}$ satisfying*

$$\mathscr{D}^{k-1} w = v, \quad \|w\|_{H^{q+l_{k-1}}(\Omega)} \leq C \|v\|_{H^q(\Omega)}.$$

In the next section we finally consider a special class of BGG constructions utilizing de Rham sequences which lead to standard second order Hilbert complexes like the Hessian, divdiv or elasticity complex.

4.2.3 Second-order complexes from Alt^l-valued forms

After considering these abstract deliberations, one may naturally wonder whether there are concrete instances of Hilbert complexes that align with the framework outlined in the preceding sections. The affirmative response to this question can also be found in the publication by Arnold et al. [12], where the authors present evidence of suitable spaces $\mathbb{E}^i$ and $\bar{\mathbb{E}}^i$, along with linking maps S^i, for an entire class of illustrative examples. Their work establishes the feasibility of BGG coupling of two sequences akin to de Rham complexes, thereby yielding a second-order complex applicable in arbitrary dimensions. The aim of this section is to briefly present this example class from [12] involving Alt^l-valued forms.
To explain the underlying ansatz, we need to introduce a tensor product notion on k-forms. Namely, given a basis k-form $\omega = dx^{\sigma_1} \wedge \cdots \wedge dx^{\sigma_k}$ and a basis l-form $\eta = dx^{s_1} \wedge \cdots \wedge dx^{s_l}$ on $\mathbb{R}^n$ then the tenor product $\omega \otimes \eta$ is defined as the multi-linear map

$$\omega \otimes \eta \colon \mathbb{R}^n \times \cdots \times \mathbb{R}^n \to \mathbb{R} \ , \ (v_1, \dots, v_{l+k}) \mapsto \omega(v_1, \dots, v_k)\, \eta(v_{k+1}, \dots, v_{k+l}).$$

By linearity, the tensor product between arbitrary k- and l-forms is clear. We write $\mathrm{Alt}^{k,l} \coloneqq \mathrm{Alt}^k \otimes \mathrm{Alt}^l$, $\mathrm{Alt}^i \coloneqq \mathrm{Alt}^i(\mathbb{R}^n)$, for the space of elements of the form $\omega \otimes \eta$, $\omega \in \mathrm{Alt}^k$, $\eta \in \mathrm{Alt}^l$. Thus, it is clear that the set

$$\Big\{ (dx^{\sigma_1} \wedge \cdots \wedge dx^{\sigma_k}) \otimes (dx^{s_1} \wedge \cdots \wedge dx^{s_l}) \;\Big|\; \sigma \in \Sigma_<(k,n),\ s \in \Sigma_<(l,n) \Big\} \tag{4.2.16}$$

yields a basis for $\mathrm{Alt}^{k,l}$. It is worth mentioning here that we can also interpret $\mathrm{Alt}^{k,l}$ as the space of Alt^l*-valued* k*-forms*.
Next, let us define for $k \in \{0, \dots, n-1\},\ J \in \{1, \dots, n\}$ the linear mapping

$$s^{k,J} \colon \mathrm{Alt}^{k,J} \to \mathrm{Alt}^{k+1,J-1} \ ,$$

determined by its action on basis forms, namely

$$\begin{aligned} s^{k,J}\Big((dx^{\sigma_1} \wedge \cdots \wedge dx^{\sigma_k}) \otimes (dx^{s_1} \wedge \cdots \wedge dx^{s_J}) \Big) \coloneqq \\ \sum_{l=1}^{J} (-1)^{l-1} (dx^{s_l} \wedge dx^{\sigma_1} \wedge \cdots \wedge dx^{\sigma_k}) \otimes (dx^{s_1} \wedge \cdots \wedge \cancel{dx^{s_l}} \wedge \cdots \wedge dx^{s_J}), \end{aligned}$$

which corresponds to [12, (72)]. The crossed-out term in the above definition is omitted, so that one indeed has a $J-1$-form on the right-hand side. For these maps it can be shown

Lemma 4.8 ([12, Lemma 2])**.** *Let $k \in \{0, \dots, n-1\},\ J \in \{1, \dots, n\}$. If $0 \leq k \leq J-1$ then the mapping $s^{k,J}$ is injective, whereas we have surjectivity for $J-1 \leq k \leq n-1$, which also implies the bijectivity of $s^{J-1,J}$.*

So, the last lemma provides an initial indication that these $s^{k,J}$ might be candidates for coupling of complexes in the sense of Section 4.2.2. Because, by a tensoring we have directly $S^{k,J} = \mathrm{id} \otimes s^{k,J} \colon H^q(\Omega) \otimes \mathrm{Alt}^{k,J} \to H^q(\Omega) \otimes \mathrm{Alt}^{k+1,J-1}$ and the injectivity/surjectivity properties of $s^{k,l}$ are trivially valid for $S^{k,J}$. Here $\Omega \subset \mathbb{R}^n$ is again a Lipschitz domain.
But in view of the BGG construction we additionally require a proper Hilbert complex structure on such spaces $H^q(\Omega) \otimes \mathrm{Alt}^{k,l}$. The latter is obtained by the following natural extension of the classical exterior derivative:

$$\begin{aligned} \mathrm{d}^k \colon H^1(\Omega) \otimes \mathrm{Alt}^{k,l} &\to L^2(\Omega) \otimes \mathrm{Alt}^{k+1,l} \ , \\ c_{\sigma,s}(dx^{\sigma_1} \wedge \cdots \wedge dx^{\sigma_k}) \otimes (dx^{s_1} \wedge \cdots \wedge dx^{s_l}) &\mapsto \\ \sum_{i=1}^{n} \partial_i c_{\sigma,s} (dx^i \wedge dx^{\sigma_1} \wedge \cdots \wedge dx^{\sigma_k}) &\otimes (dx^{s_1} \wedge \cdots \wedge dx^{s_l}), \end{aligned} \tag{4.2.17}$$

where we assume $c_{\sigma,s} \in H^1(\Omega)$ to be the coefficient function and the general case is again obtained by linearity. It is clear, and is also handled as such in [12], that in the sense of distributional differentiation, we indeed have

$$\mathrm{d}^k \colon H^q(\Omega) \otimes \mathrm{Alt}^{k,l} \to H^{q-1}(\Omega) \otimes \mathrm{Alt}^{k+1,l},\ q \in \mathbb{Z}.$$

Further, it should also be noted that in (4.2.17), we can simply regard d^k as a j-fold copy of the classical exterior derivative, since the operator leaves the last term $(dx^{s_1} \wedge \cdots \wedge dx^{s_l})$ untouched. For this reason, we also use the same notation d^k as for the original exterior derivative. Properties of the classical de Rham sequence (cf. Lemma 3.9, Lemma 3.10) are directly transferred to the new setting (4.2.17).

Corollary 4.3. *Let $\Omega \subset \mathbb{R}^n$ be a Lipschitz domain and $l \in \{0, \dots, n\}$. We obtain with $(H^{q-\circ}(\Omega) \otimes \mathrm{Alt}^{\circ,l}, \mathrm{d}^\circ)$ bounded Hilbert complexes for each $q \in \mathbb{Z}$. In case of starlike domains we further have $\mathcal{R}(\mathrm{d}^{k-1}, H^{q+1}(\Omega) \otimes \mathrm{Alt}^{k-1,l}) = \mathcal{N}(\mathrm{d}^k, H^q(\Omega) \otimes \mathrm{Alt}^{k,l})$, if $0 < k \leq n$.*
Moreover, in any Lipschitz domain we have $\mathcal{R}(\mathrm{d}^{n-1}, H^{q+1}(\Omega) \otimes \mathrm{Alt}^{n-1,l}) = H^q(\Omega) \otimes \mathrm{Alt}^{n,l}$.

Besides we can consider analogously to the original de Rham complex the underlying L^2 complex with associated domain complex, i.e. utilizing the spaces

$$\begin{aligned} L^2\Lambda^{k,l}(\Omega) &\coloneqq L^2(\Omega) \otimes \mathrm{Alt}^{k,l}, \\ H\Lambda^{k,l}(\Omega) &\coloneqq \left\{ \omega \in L^2\Lambda^{k,l}(\Omega) \;\middle|\; \mathrm{d}^k\omega \in L^2\Lambda^{k+1,l}(\Omega) \right\}, \end{aligned}$$

we obtain for each $l \in \{0, \dots, n\}$ a Hilbert complex $(L^2\Lambda^{\circ,l}(\Omega), \mathrm{d}^\circ)$ with associated domain complex $(H\Lambda^{\circ,l}(\Omega), \mathrm{d}^\circ)$.

Remark 4.2 (Extending the sequences). Even though it has not been explicitly stated until now, we always extend the de Rham sequences to the left and right with zeros, meaning $\mathrm{d}^k = 0$ for $k \notin \{0, \dots, n-1\}$. Accordingly, we expand the definition of $s^{k,J}$ for indices $k \notin \{0, \dots, n-1\}$ as follows:

$$\begin{aligned} s^{k,J} &\colon \{0\} \to \{0\}, && \text{if } k < -1, \\ s^{-1,J} &\colon \{0\} \to H^q(\Omega) \otimes \mathrm{Alt}^{0,J-1}, \\ s^{n,J} &\colon H^q(\Omega) \otimes \mathrm{Alt}^{n,J} \to \{0\}, \\ s^{k,J} &\colon \{0\} \to \{0\}, && \text{if } k > n. \end{aligned}$$

With this convention, definitions and statements can be expressed more concisely.

After these technical definitions, the connection to the BGG construction is revealed with the next result, again from [12].

Lemma 4.9 (**Output complex from Alt^l-valued forms,** cf. [12, Lemma 2] and [12, Section 4.2])**.** *Let $k \in \{0, \dots, n-1\}$, $J \in \{1, \dots, n\}$ and let $\Omega \subset \mathbb{R}^n$ be a Lipschitz domain.*
For $S^{k,J} \coloneqq \mathrm{id} \otimes s^{k,J} \colon L^2(\Omega) \otimes \mathrm{Alt}^{k,J} \to L^2(\Omega) \otimes \mathrm{Alt}^{k+1,J-1}$ we have the anti-commutativity relation

$$\mathrm{d}^{k+1} \circ S^{k,J} = -S^{k+1,J} \circ \mathrm{d}^k$$

on $H\Lambda^{k,J}(\Omega)$, in the sense of distributions, respectively.
Hence, we can apply the BGG construction from Section 4.2.2 with $\bar{\mathbb{E}}^i = \mathrm{Alt}^{i,J-1}$, $\mathbb{E}^i = \mathrm{Alt}^{i,J}$ and $S^i = S^{i,J}$. As a result, we obtain a L^2 Hilbert complex $(L^2(\Omega) \otimes \mathbb{A}_n^{\circ,J}, \mathscr{D}_n^{\circ,J})$ with associated domain complex $(\mathscr{V}_n^{\circ,J}, \mathscr{D}_n^{\circ,J})$, where

$$\mathbb{A}_n^{i,J} \coloneqq \begin{cases} \mathcal{R}(s^{i-1,J})^\perp, & \text{if } i \leq J-1, \\ \mathcal{N}(s^{i,J}), & \text{if } i \geq J, \end{cases} \tag{4.2.18}$$

$$\mathscr{V}_n^{i,J} \coloneqq H(\Omega, \mathscr{D}_n^{i,J}, \mathbb{A}_n^{i,J}), \tag{4.2.19}$$

and the operators $\mathscr{D}_n^{i,J}$ are determined according to the general construction given Definition 4.2. One further notes Remark 4.2.

Exploiting the well-known properties of the de Rham sequence (compare Corollary 4.3) and Lemma 4.7 we directly get the next

Corollary 4.4. *Let Ω be a starlike Lipschitz domain. Then, the output complex $(\mathscr{V}_n^{\circ,J}, \mathscr{D}_n^{\circ,J})$ is exact at level $k \geq 1$ with*

$$\mathcal{R}(\mathscr{D}_n^{k-1,J}, H^{q+l}(\Omega) \otimes \mathbb{A}_n^{k-1,J}) = \mathcal{N}(\mathscr{D}_n^{k,J}, H^q(\Omega) \otimes \mathbb{A}_n^{k,J}), \quad q \in \mathbb{Z}, \quad l = \operatorname{ord}(\mathscr{D}_n^{k-1,J}).$$

Furthermore we have the equation

$$\mathcal{R}(\mathscr{D}_n^{n-1,J}, H^l(\Omega) \otimes \mathbb{A}_n^{n-1,J}) = L^2(\Omega) \otimes \mathbb{A}_n^{n,J}, \quad l = \operatorname{ord}(\mathscr{D}_n^{n-1,J}),$$

for each Lipschitz domain Ω.

It may be somewhat confusing here that, in the coupling just mentioned, the spaces $\mathrm{Alt}^{k,l}$ appear, which in turn represent tensor products of spaces of mappings. However, one can trace this setting back to the situation with $\mathbb{E}^i = \mathbb{R}^{(n|J)\times(n|i)}$, $\bar{\mathbb{E}}^i = \mathbb{R}^{(n|J-1)\times(n|i)}$ by a proper identification $\mathrm{Alt}^{k,l} \cong \mathbb{R}^{(n|l)\times(n|k)}$. To be more precise, let us proceed as follows here. First, let us have proxy maps $\mathcal{J}_k \colon \mathrm{Alt}^k \to \mathbb{R}^{n|k}$, $0 \leq k \leq n$ in the sense of Definition (3.10), which associate a vector to a k-form. Furthermore, we number the basis elements in $\{dx^{s_1} \wedge \cdots \wedge dx^{s_l} \mid s \in \Sigma_<(l,n)\} \subset \mathrm{Alt}^l$. Now, let $dx^{s_1} \wedge \cdots \wedge dx^{s_l}$ be the i-th element in the ordered basis of Alt^l. Then, we make the association

$$(dx^{\sigma_1} \wedge \cdots \wedge dx^{\sigma_k}) \otimes (dx^{s_1} \wedge \cdots \wedge dx^{s_l}) \in \mathrm{Alt}^{k,l} \longleftrightarrow E \in \mathbb{R}^{(n|l)\times(n|k)}$$

with E being the matrix whose i-th row is equal to the vector $\mathcal{J}_k\big(dx^{\sigma_1} \wedge \cdots \wedge dx^{\sigma_k}\big)$ and that contains only zeros elsewhere. This approach with all possible basis elements in (4.2.16) determines how we want to relate $\mathrm{Alt}^{k,l}$ to $\mathbb{R}^{(n|l)\times(n|k)}$. We will again simply write $\mathcal{J}_k$ for the resulting proxy map on $\mathrm{Alt}^{k,l}$ and if $\omega \in L^2(\Omega) \otimes \mathrm{Alt}^{k,l}$, then $\mathcal{J}_k\omega$ stands for the element $L^2(\Omega) \otimes \mathbb{R}^{(n|l)\times(n|k)}$ obtained by a point-wise identification. Thus we get proxy maps of the form

$$\mathcal{J}_k \colon L^2(\Omega) \otimes \mathrm{Alt}^{k,l} \to L^2(\Omega) \otimes \mathbb{R}^{(n|l)\times(n|k)}. \tag{4.2.20}$$

Definition 4.3 (**Proxy map for $\mathrm{Alt}^{k,l}$**)**.** *We call the mappings* (4.2.20) *obtained by the above explained identification procedure again just proxy maps.*

The underlying row-wise ansatz has the effect that (4.2.17) reduces to a differential operator $\tilde{\mathcal{D}}^k \colon H^q(\Omega) \otimes \mathbb{R}^{(n|l)\times(n|k)} \to H^{q-1}(\Omega) \otimes \mathbb{R}^{(n|l)\times(n|k+1)}$, which simply corresponds to a row-wise application of the proxy operator $\mathcal{D}^k \coloneqq \mathcal{J}_{k+1} \circ \mathrm{d}^k \circ \mathcal{J}_k^{-1}$ from (3.3.7).

Remark 4.3. We can relate to the de Rham complex $(H\Lambda^\circ(\Omega), \mathrm{d}^\circ)$ the proxy complex $(H(\Omega, \mathcal{D}^\circ, \mathbb{R}^{n|\circ}), \mathcal{D}^\circ)$; see Section 3.3.2. Obviously, the analogous is possible if we have the extended chain $(H\Lambda^{\circ,l}(\Omega), \mathrm{d}^\circ)$ to which we can associate the extended proxy complex $\big(H(\Omega, \mathcal{D}^\circ, \mathbb{R}^{(n|l)\times(n|\circ)}), \mathcal{D}^\circ\big)$, where $\mathcal{D}^\circ$ is just acting row-wise.

Then modifying the linking maps according to

$$s^{k,J} \mapsto \tilde{s}^{k,J} \coloneqq \mathcal{J}_{k+1} \circ s^{k,J} \circ \mathcal{J}_k^{-1} \quad \text{and} \quad S^{k,J} \mapsto \tilde{S}^{k,J} \coloneqq \mathcal{J}_{k+1} \circ S^{k,J} \circ \mathcal{J}_k^{-1}, \tag{4.2.21}$$

we can indeed trace the BGG construction back to the case $\mathbb{E}^i = \mathbb{R}^{(n|J)\times(n|i)}$, $\bar{\mathbb{E}}^i = \mathbb{R}^{(n|J-1)\times(n|i)}$ and $S^i = \tilde{S}^{i,J}$.

Definition 4.4 (**Proxy output complex**). *Consequently, utilizing the proxy maps and applying the BGG construction we obtain some proxy L^2 output complex on the spaces*

$$L^2(\Omega)\otimes\mathbb{V}_n^{i,J},\quad \mathbb{V}_n^{i,J}\coloneqq\begin{cases}\mathcal{R}(\tilde{s}^{i-1,J})^{\perp}\subset\mathbb{R}^{(n|J-1)\times(n|i)}, & \text{if } 0\leq i\leq J-1,\\ \mathcal{N}(\tilde{s}^{i,J})\subset\mathbb{R}^{(n|J)\times(n|i)}, & \text{if } J\leq i\leq n,\end{cases}\tag{4.2.22}$$

which we want to denote as $(L^2(\Omega)\otimes\mathbb{V}_n^{\circ,J},\mathfrak{D}_n^{\circ,J})$. Again we extend the space definitions for indices $i\notin\{0,\dots,n\}$ though a zero extension, i.e. for this case we set $\mathbb{V}_n^{i,J}\coloneqq\{0\}$, $\mathfrak{D}_n^{i,J}\coloneqq 0$. The domain complex is then given accordingly by

$$(\mathfrak{V}_n^{\circ,J},\mathfrak{D}_n^{\circ,J})\coloneqq\Big(H(\Omega,\mathfrak{D}_n^{\circ,J},\mathbb{V}_n^{\circ,J}),\mathfrak{D}_n^{\circ,J}\Big).\tag{4.2.23}$$

We call $(\mathfrak{V}_n^{\circ,J},\mathfrak{D}_n^{\circ,J})$ the proxy output complex.

Finally, before we delve into specific examples, we would like to relate the various introduced spaces and operators once more through the following commutative diagram:

$$\begin{array}{ccccccccc}
\cdots & H^q\mathbb{R}^{(n|J-1)\times(n|k)} & \xrightarrow{\mathcal{D}^k} & H^{q-1}\mathbb{R}^{(n|J-1)\times(n|k+1)} & \xrightarrow{\mathcal{D}^{k+1}} & H^{q-2}\mathbb{R}^{(n|J-1)\times(n|k+2)} & \cdots & & \\
 & \uparrow{\scriptstyle\mathcal{J}_k} & & \uparrow{\scriptstyle\mathcal{J}_{k+1}} & & \uparrow{\scriptstyle\mathcal{J}_{k+2}} & & & \\
\cdots & H^q\mathrm{Alt}^{k,J-1} & \xrightarrow{\mathrm{d}^k} & H^{q-1}\mathrm{Alt}^{k+1,J-1} & \xrightarrow{\mathrm{d}^{k+1}} & H^{q-2}\mathrm{Alt}^{k+2,J-1} & \cdots & & \\
 & {\scriptstyle S^{k-1,J}}\nearrow & & {\scriptstyle -S^{k,J}}\nearrow & & {\scriptstyle S^{k+1,J}}\nearrow & & & \\
\cdots & H^q\mathrm{Alt}^{k-1,J} & \xrightarrow{\mathrm{d}^{k-1}} & H^{q-1}\mathrm{Alt}^{k,J} & \xrightarrow{\mathrm{d}^k} & H^{q-2}\mathrm{Alt}^{k+1,J} & \cdots & & \\
 & \downarrow{\scriptstyle\mathcal{J}_{k-1}} & & \downarrow{\scriptstyle\mathcal{J}_k} & & \downarrow{\scriptstyle\mathcal{J}_{k+1}} & & & \\
\cdots & H^q\mathbb{R}^{(n|J)\times(n|k-1)} & \xrightarrow{\mathcal{D}^{k-1}} & H^{q-1}\mathbb{R}^{(n|J)\times(n|k)} & \xrightarrow{\mathcal{D}^k} & H^{q-2}\mathbb{R}^{(n|J)\times(n|k+1)} & \cdots & & .
\end{array}\tag{4.2.24}$$

From the diagram, it also becomes clear how one can transit from Hilbert complexes on Alt^l-valued forms to those on matrix fields.
There is no doubt that a similar statement as in Corollary 4.4 is also true if we move to the proxy complex, and for reasons of completeness let us state

Corollary 4.5. *Let Ω be a starlike Lipschitz domain. Then, the proxy output complex $(\mathfrak{V}_n^{\circ,J},\mathfrak{D}_n^{\circ,J})$ is exact at level $k\geq 1$. Furthermore we have the equation*

$$\mathcal{R}(\mathfrak{D}_n^{n-1,J},H^l(\Omega)\otimes\mathbb{V}_n^{n-1,J})=L^2(\Omega)\otimes\mathbb{V}_n^{n,J},\quad l=\mathrm{ord}(\mathfrak{D}_n^{n-1,J}),$$

for each Lipschitz domain Ω.

Now we turn to examples, which fit to the case of Sobolev de Rham complexes. Strictly speaking, the diagrams presented below are just special cases of a general construction shown before. We focus on such complexes, which will also play a role later in the context of numerical examples. Furthermore, we directly present the proxy de Rham chains and thus proxy output complexes. And doing so, we utilize the proxy maps $\mathcal{J}_k$ determined through Example 3.1 ($3D$) and Example 3.2 ($2D$). It should be pointed out that in the subsequent diagrams we insert the L^2 spaces emphasizing the inner product structure and thus the differential operators should be seen as densely defined mappings.

Example 4.2 (Chains in $2D$). *In two dimensions there are two possibilities to obtain a proxy output complex $(\mathfrak{V}_n^{\circ,J},\mathfrak{D}_n^{\circ,J})$, namely for $J=1$ and $J=2$. With the ansatz* (4.2.21) *for the*

linking maps one can assemble the double diagram (4.2.25) *which is a slightly different version of [12, (54)]. Here it is*

$$\operatorname{mskew}(\phi) := \begin{bmatrix} 0 & \phi \\ -\phi & 0 \end{bmatrix}, \qquad 2\operatorname{sskew} \begin{bmatrix} M_{11} & M_{12} \\ M_{21} & M_{22} \end{bmatrix} := M_{21} - M_{12}$$

and for this example we write $\mathbb{M} := \mathbb{R}^{2\times 2}$.

$$\begin{array}{ccccccccc} 0 & \longrightarrow & L^2(\Omega) & \xrightarrow{\operatorname{curl}} & L^2(\Omega)\otimes\mathbb{R}^2 & \xrightarrow{\nabla\cdot} & L^2(\Omega) & \longrightarrow & 0 \\ & & & \nearrow_{\mathrm{id}} & & \nearrow_{-2\mathrm{sskew}} & & & \\ 0 & \longrightarrow & L^2(\Omega)\otimes\mathbb{R}^2 & \xrightarrow{\operatorname{curl}} & L^2(\Omega)\otimes\mathbb{M} & \xrightarrow{\nabla\cdot} & L^2(\Omega)\otimes\mathbb{R}^2 & \longrightarrow & 0 \\ & & & \nearrow_{-\mathrm{mskew}} & & \nearrow_{\mathrm{id}} & & & \\ 0 & \longrightarrow & L^2(\Omega) & \xrightarrow{\operatorname{curl}} & L^2(\Omega)\otimes\mathbb{R}^2 & \xrightarrow{\nabla\cdot} & L^2(\Omega) & \longrightarrow & 0\,. \end{array} \tag{4.2.25}$$

Above, in the second row the differential operators act row-wise. The highlighted linking maps in red are the bijective ones, whereas the green and blue linking maps are injective, surjective, respectively. The domain complex induced by the BGG coupling of the first two rows from (4.2.25) *yields the* elasticity complex *in* $2D$*, namely*

$$0 \longrightarrow H^2(\Omega) \xrightarrow{\operatorname{curl}^2} H(\Omega, \nabla\cdot, \mathbb{S}) \xrightarrow{\nabla\cdot} L^2(\Omega)\otimes\mathbb{R}^2 \longrightarrow 0, \tag{4.2.26}$$

with $\mathbb{S}$ *denoting the space of symmetric matrices. As the name suggests, one can (and we will later) exploit this chain to handle the problem of plane linear elasticity, where the last two levels are identified with the stress and displacement field. The* curl^2 *operator is in fact the so-called airy stress operator from continuum mechanics. By the Nečas inequality ([55, Lemma 2.2]) we see* $H^2(\Omega) = H(\Omega, \operatorname{curl}^2, \mathbb{R})$*, which explains the appearing of* $H^2(\Omega)$ *in the elasticity complex. Another domain complex is obtained by the combination of the last two rows in diagram 4.2.25. More precisely, we get the* $2D$ divdiv complex

$$0 \longrightarrow H^1(\Omega)\otimes\mathbb{R}^2 \xrightarrow{\operatorname{symcurl}} H(\Omega, \nabla\cdot\nabla\cdot, \mathbb{S}) \xrightarrow{\nabla\cdot\nabla\cdot} L^2(\Omega) \longrightarrow 0, \tag{4.2.27}$$

with

$$2\operatorname{symcurl}\big((v_1, v_2)^{\mathrm{T}}\big) := \begin{bmatrix} \operatorname{curl}(v_1) \\ \operatorname{curl}(v_2) \end{bmatrix} + \begin{bmatrix} \operatorname{curl}(v_1) \\ \operatorname{curl}(v_2) \end{bmatrix}^{\mathrm{T}}.$$

In view of the Korn inequality, see [16, Theorem 2], we have used above $H(\Omega, \operatorname{symcurl}, \mathbb{R}^2) = H^1(\Omega)\otimes\mathbb{R}^2$*; because it is*

$$\big\|\operatorname{symcurl}\big((v_1, v_2)^{\mathrm{T}}\big)\big\|_{L^2(\Omega)} = \big\|\operatorname{sym}\nabla\big((v_2, -v_1)^{\mathrm{T}}\big)\big\|_{L^2(\Omega)}.$$

Similarily, one can derive the proxy output complexes $(\mathfrak{V}_n^{\circ,J}, \mathfrak{D}_n^{\circ,J})$ for $\Omega \subset \mathbb{R}^3$, i.e. $n = 3$.

Example 4.3 (Chains in $3D$)**.** *First let us define*

$$\operatorname{mskew}\begin{bmatrix} v_1 \\ v_2 \\ v_3 \end{bmatrix} := \begin{bmatrix} 0 & -v_3 & v_2 \\ v_3 & 0 & -v_1 \\ -v_2 & v_1 & 0 \end{bmatrix}, \quad \operatorname{skew} M := \frac{1}{2}(M - M^{\mathrm{T}}), \quad \operatorname{vskew} := \operatorname{mskew}^{-1} \circ \operatorname{skew}$$

and

$$\iota(\phi) \coloneqq \begin{bmatrix} \phi & & 0 \\ & \phi & \\ 0 & & \phi \end{bmatrix}, \qquad \mathcal{S}M = M^{\mathrm{T}} - \mathrm{tr}(M)\mathrm{I}.^{8}$$

Then, using the BGG construction in [12] they established for the three-dimensional setting the diagram

$$\begin{array}{ccccccccccc}
0 & \longrightarrow & L^2(\Omega) & \xrightarrow{\nabla} & L^2(\Omega)\otimes\mathbb{R}^3 & \xrightarrow{\nabla\times} & L^2(\Omega)\otimes\mathbb{R}^3 & \xrightarrow{\nabla\cdot} & L^2(\Omega) & \longrightarrow & 0 \\
 & & & \nearrow_{\mathrm{id}} & & \nearrow_{\mathrm{2vskew}} & & \nearrow_{\mathrm{tr}} & & & \\
0 & \longrightarrow & L^2(\Omega)\otimes\mathbb{R}^3 & \xrightarrow{\nabla} & L^2(\Omega)\otimes\mathbb{M} & \xrightarrow{\nabla\times} & L^2(\Omega)\otimes\mathbb{M} & \xrightarrow{\nabla\cdot} & L^2(\Omega)\otimes\mathbb{R}^3 & \longrightarrow & 0 \\
 & & & \nearrow_{-\mathrm{mskew}} & & \nearrow_{\mathcal{S}} & & \nearrow_{\mathrm{2vskew}} & & & \\
0 & \longrightarrow & L^2(\Omega)\otimes\mathbb{R}^3 & \xrightarrow{\nabla} & L^2(\Omega)\otimes\mathbb{M} & \xrightarrow{\nabla\times} & L^2(\Omega)\otimes\mathbb{M} & \xrightarrow{\nabla\cdot} & L^2(\Omega)\otimes\mathbb{R}^3 & \longrightarrow & 0 \\
 & & & \nearrow_{\iota} & & \nearrow_{-\mathrm{mskew}} & & \nearrow_{\mathrm{id}} & & & \\
0 & \longrightarrow & L^2(\Omega) & \xrightarrow{\nabla} & L^2(\Omega)\otimes\mathbb{R}^3 & \xrightarrow{\nabla\times} & L^2(\Omega)\otimes\mathbb{R}^3 & \xrightarrow{\nabla\cdot} & L^2(\Omega) & \longrightarrow & 0\,,
\end{array} \tag{4.2.28}$$

with $\mathbb{M} \coloneqq \mathbb{R}^{n\times n}$. *Again, in the second and third row of the last diagram the different differential operators act row-wise. It is relatively easy to determine that* $\mathcal{S}$ *is bijective with* $\mathcal{S}^{-1}M = M^{\mathrm{T}} - \frac{1}{2}\mathrm{tr}(M)\mathrm{I}$. *Additionally, we once again have the surjectivity of the blue and the injectivity of the green linking maps in diagram* (4.2.28). *By BGG coupling of the first two, the second two and the last two rows of diagram* (4.2.28)*, this leads us to the Hessian, elasticity and divdiv complexes in* $3D$.

The Hessian complex *reads*

$$0 \longrightarrow H^2(\Omega) \xrightarrow{\nabla^2} H(\Omega,\nabla\times,\mathbb{S}) \xrightarrow{\nabla\times} H(\Omega,\nabla\cdot,\mathbb{T}) \xrightarrow{\nabla\cdot} L^2(\Omega)\otimes\mathbb{R}^3 \longrightarrow 0, \tag{4.2.29}$$

where $\mathbb{S}$ *and* $\mathbb{T}$ *denote the spaces of symmetric and trace-free* 3×3 *matrices. Here we used the fact* $H^2(\Omega) = H(\Omega,\nabla^2,\mathbb{R})$*; compare [55, Lemma 2.2].*

The $3D$ elasticity complex *is given by*

$$0 \longrightarrow H^1(\Omega)\otimes\mathbb{R}^3 \xrightarrow{\mathrm{sym}\nabla} H(\Omega,\mathrm{inc},\mathbb{S}) \xrightarrow{\mathrm{inc}} H(\Omega,\nabla\cdot,\mathbb{S}) \xrightarrow{\nabla\cdot} L^2(\Omega)\otimes\mathbb{R}^3 \longrightarrow 0, \tag{4.2.30}$$

with $\mathrm{inc} = \nabla\times\circ\mathcal{S}^{-1}\circ\nabla\times$. *We note here that the Korn inequality [16, Theorem 2] justifies the first non-zero entry in the chain, because* $H(\Omega,\mathrm{sym}\nabla,\mathbb{R}^3) = H^1(\Omega)\otimes\mathbb{R}^3$*, where* $\mathrm{sym}\nabla$ *is the symmetric gradient.*

And finally, for the combination of the last two rows in (4.2.28) *we get the* divdiv complex*:*

$$0 \longrightarrow H^1(\Omega)\otimes\mathbb{R}^3 \xrightarrow{\mathrm{dev}\nabla} H(\Omega,\mathrm{sym}\nabla\times,\mathbb{T}) \xrightarrow{\mathrm{sym}\nabla\times} H(\Omega,\nabla\cdot\nabla\cdot,\mathbb{S}) \xrightarrow{\nabla\cdot\nabla\cdot} L^2(\Omega) \longrightarrow 0, \tag{4.2.31}$$

where $\mathrm{dev}\nabla v = \nabla v - \frac{1}{3}\mathrm{tr}(\nabla v)\mathrm{I}$ *is the deviatoric gradient and* $\mathrm{sym}\nabla\times M \coloneqq \frac{1}{2}\big(\nabla\times M + (\nabla\times M)^{\mathrm{T}}\big)$. *Interestingly, an application of [60, Lemma 3.2] gives us directly* $H(\Omega,\mathrm{dev}\nabla,\mathbb{R}^3) = H^1(\Omega)\otimes\mathbb{R}^3$ *which justifies the space* $H^1(\Omega)\otimes\mathbb{R}^3$ *in the divdiv chain.*

[8] $\mathrm{tr}(M)$ stands for the trace of the matrix M and I denotes the identity matrix.

An important property of all the sequences above follows directly from Lemma 3.10 and Lemma 4.7,namely:

Corollary 4.6. *If the domain Ω is a starlike domain. Then all the chains* (4.2.26),(4.2.27),(4.2.29)-(4.2.31) *are exact except at the first level. Further in every chain the last differential operator is a surjection onto the respective L^2 spaces.*

We have now become acquainted with a method that generates a new L^2 output complex from two de Rham complexes on Alt^l-valued forms. As special cases, we obtain e.g. the chains in Examples 4.2, 4.3 above. Due to the BGG construction and the corresponding choice of operators (4.2.9), we got second-order complexes, meaning second-order differential operators. In (4.2.29), for example, this would be the Hessian operator ∇^2 or in (4.2.31), the double divergence $\nabla\cdot\nabla\cdot$. In fact with Lemma 4.9, we have introduced an entire class of second-order complexes in arbitrary dimensions, namely the pairs $(\mathscr{V}_n^{\circ,J}, \mathscr{D}_n^{\circ,J})$, $(\mathfrak{V}_n^{\circ,J}, \mathfrak{D}_n^{\circ,J})$, respectively. Chains like these form the basis for the establishment and examination of numerical methods in Sections 8 and 9. There, we will primarily focus on the discretization of the Hodge–Laplace problems of level n induced by $(\mathscr{V}_n^{\circ,J}, \mathscr{D}_n^{\circ,J})$. We will present and consider two approximation methods, both of them will involve the connection to the BGG construction and the de Rham complexes.

One approach follows the idea of incorporating the conditions in (4.2.12) related to the linking maps through suitable additional variables. In the next section, we will explain in a somewhat more abstract context what we mean by additional variables and how we can modify mixed weak formulations for the Hodge–Laplace problem by adding appropriate variables. In this phase, we will not perform discretizations yet and will remain in a continuous setting. Nevertheless, in the context of numerical analysis later, we will refer back to and make use of the forthcoming explanations.

4.2.4 Mixed formulation with Lagrange multiplier

In this section we show the feasibility of mixed weak forms for the Hodge–Laplace problem with Lagrange multipliers in the context of the L^2 complexes arising from a coupling of complexes. Here we suppose the assumptions and follow the framework explained in Section 4.2.2. In particular, we utilize the notation from this part.
The construction of the output complex utilizing the linking maps leads to subspaces of kernels $\mathcal{N}(S^i)$ or of the orthogonal complements $\mathcal{R}(S^i)^{\perp_{L^2}}$; see (4.2.12). But if we want to choose proper discrete spaces in order to approximate the underlying Hodge–Laplace problem, then such constraints in the definition might become problematic or not easy to be fulfilled. Here we show the possibility to set up equivalent mixed weak forms on the spaces $\mathscr{U}^i$ defined in (4.2.10) instead of the $\mathscr{V}^i$ from Lemma 4.6. We hope that a reduction to the former is beneficial for numerical considerations. Indeed we will use this re-formulation ansatz for a special discretization method in Section 8.3 and it will also be exploited within the field of linear elasticity later. It guides us for example to the *Hellinger-Reissner formulation with weakly imposed symmetry* also part of the paper [10]. Doing so, we exploit the mentioned approach only for a special sub-class of problems later. Nevertheless, for reasons of completeness we show applicability of the Lagrange multiplier idea in more general situations. The concept of incorporating constraints in an optimization problem or a variational formulation using auxiliary variables, known as Lagrange multipliers, is well-established; see e.g. [20, §4, Chapter 3]. However, the following explanations can also be understood without a detailed knowledge of this concept.

Assumption 4.3. *We are in the setting of Section 4.2.2, i.e. we import the notation and all assumptions from that part, meaning e.g. $(\mathscr{V}^\circ, \mathscr{D}^\circ)$ denotes the BGG L^2 output complex*

introduced in Lemma 4.6. Besides, here the underlying bottom and top complexes in Figure 4 are exact at level k in the sense of Remark 4.1. Consequently the corresponding output domain complex $(\mathscr{V}^\circ, \mathscr{D}^\circ)$ is exact at some fixed level k; cf. Lemma 4.7.

Hence, in view of Definition 3.5 and Lemma 3.4 we obtain for the level k Hodge–Laplace problem the next well-posed variational problem:

Definition 4.5 (**Output mixed weak formulation**)**.** For $f \in \mathscr{W}^k$ find $(\sigma, u) \in \mathscr{V}^{k-1} \times \mathscr{V}^k$ s.t.

$$\langle \sigma, \tau \rangle \qquad - \langle u, \mathscr{D}^{k-1}\tau \rangle \; = 0, \qquad \forall \tau \in \mathscr{V}^{k-1}, \tag{4.2.32}$$

$$\langle \mathscr{D}^{k-1}\sigma, v \rangle + \langle \mathscr{D}^k u, \mathscr{D}^k v \rangle = \langle f, v \rangle, \quad \forall v \in \mathscr{V}^k. \tag{4.2.33}$$

Below, the notation $\langle \cdot, \cdot \rangle$, $\|\cdot\|$ means always the L^2 inner products and norms related to the respective $L^2(\Omega) \otimes \mathbb{E}^i$, $L^2(\Omega) \otimes \bar{\mathbb{E}}^i$ spaces. Moreover, we denote with $X^\perp$ the orthogonal complement w.r.t. the L^2 inner product and write $\|\cdot\|_{\mathscr{U}}$ for the graph norm on $\mathscr{U}^i$; cf. (4.2.11). As already mentioned the basic idea is now to enforce the subspace conditions for the elements in $\mathscr{V}^i$, coming from the linking maps S^i, weakly; see (4.2.12). The aim is to set up a new mixed weak formulation for the Hodge–Laplace problem, utilizing the spaces $\mathscr{U}^i$ given in (4.2.10) instead of the $\mathscr{V}^i$. In preparation for this purpose we prepend two lemmata. In the explanations below, J denotes the index from Assumption 4.1 and we write in proofs $A \prec B$, if expression A is smaller than B up to some constant C, where C does not depend on appearing specific space elements.

Lemma 4.10. *Let $i < J$. The inf-sup relation*

$$\inf_{0 \neq \mu \in L^2(\Omega) \otimes \mathbb{E}^i} \; \sup_{0 \neq \tau \in \mathscr{U}^{i+1}} \frac{\langle \tau, S^i \mu \rangle}{\|\tau\|_{\mathscr{U}} \, \|\mu\|} > 0$$

is valid.

Proof. We fix some $0 \neq \mu \in L^2(\Omega) \otimes \mathbb{E}^i$. There is a sequence of smooth mappings $(\mu_m)_m \subset C_c^\infty(\Omega) \otimes \mathbb{E}^i$ which converges in the L^2 sense to μ. Hence $\tau_m := S^i \mu_m \in \mathscr{U}^{i+1}$. For $i < J-1$ it is $\mathscr{D}^{i+1} S^i \mu_m = \mathcal{P}_{\mathcal{R}(S^{i+1})^\perp} \bar{d}^{i+1} S^i \mu_m = -\mathcal{P}_{\mathcal{R}(S^{i+1})^\perp} S^{i+1} d^i \mu_m = 0$ and further, if $i = J-1$, one has

$$\mathscr{D}^J S^{J-1} \mu_m = d^J (S^J)^{-1} \bar{d}^J S^{J-1} \mu_m = -d^J (S^J)^{-1} S^J d^{J-1} \mu_m = 0 \; .$$

This implies

$$\|\tau_m - \tau_l\|_{\mathscr{U}}^2 = \|\tau_m - \tau_l\|^2 \leq C_S \, \|\mu_m - \mu_l\|^2 \longrightarrow 0, \text{ for } m, l \to \infty \;\; \text{and it is} \;\; \|\tau_m\|_{\mathscr{U}} = \|\tau_m\| \, ,$$

for some S^i-dependent constant C_S. The completeness of the space $\mathscr{U}^{i+1}$ yields a $\tau \in \mathscr{U}^{i+1}$ with $\tau_m \xrightarrow{\mathscr{U}} \tau$. Due to the injectivity of s^i we have $|s^i e| \geq C|e|$, $\forall e \in \mathbb{E}^i$ which implies $\|S^i \mu_m\| \geq C \, \|\mu_m\|$ for a proper constant C.[9] Consequently, we get

$$\frac{\langle \tau, S^i \mu \rangle}{\|\tau\|_{\mathscr{U}} \, \|\mu\|} \xleftarrow[m \to \infty]{} \frac{\langle \tau_m, S^i \mu_m \rangle}{\|\tau_m\|_{\mathscr{U}} \, \|\mu_m\|} \geq \frac{\|S^i \mu_m\|^2}{\|S^i \mu_m\| \, \|\mu_m\|} \geq C > 0 \; ,$$

where C does not depend on μ. □

[9] Here $|\cdot|$ is an abbreviation for norms in $\mathbb{E}^i$ and $\bar{\mathbb{E}}^{i+1}$.

The second auxiliary lemma also deals with an inf-sup inequality. For the following we use the notation $\|\cdot\|_{\bar{U}}$, $\langle\cdot,\cdot\rangle_{\bar{U}}$ for the graph norm and inner product for the spaces

$$\bar{U}^i \coloneqq H(\Omega, \bar{d}^i, \bar{\mathbb{E}}^i); \quad \text{see in Figure 4.}$$

Further using 4.2.9 and (4.2.10) one notes $\mathscr{U}^i = H(\Omega, d^i, \mathbb{E}^i)$ as well as $S^i v \in \bar{U}^{i+1}$, $\forall v \in \mathscr{U}^i$ for $i > J$, since $\bar{d}^{i+1} S^i v = -S^{i+1} d^i v$. Finally we remark that we use the abbreviation

$$\bar{l}_j \coloneqq \mathrm{ord}(\bar{d}^j)$$

at different places of this section.

Lemma 4.11. *Let $i > J$. We assume that the underlying top complex $(H^{q_\circ}\bar{\mathbb{E}}^\circ, \bar{d}^\circ)$ be exact at level $i+1$ and $i+2$ in the sense $\mathcal{R}(\bar{d}^{m-1}, H^{\bar{l}_{m-1}}\bar{\mathbb{E}}^{m-1}) = \mathcal{N}(\bar{d}^m, \bar{U}^m)$, for $m \in \{i+1, i+2\}$; see Figure 4. Then the inequality*

$$\inf_{0\neq\mu\in\bar{U}^{i+1}} \sup_{0\neq\tau\in\mathscr{U}^i} \frac{\langle S^i\tau, \mu\rangle_{\bar{U}}}{\|\tau\|_{\mathscr{U}} \|\mu\|_{\bar{U}}} > 0$$

holds.

Proof. We follow the proof idea of Theorem 3 in [12]. Fix some non-vanishing $\mu \in \bar{U}^{i+1}$. By assumption together with Corollary 2.1 we can choose an $u \in H^{\bar{l}_{i+1}}\bar{\mathbb{E}}^{i+1}$ s.t. $\bar{d}^{i+1}u = \bar{d}^{i+1}\mu$ and $\|u\|_{H^{\bar{l}_{i+1}}} \prec \left\|\bar{d}^{i+1}\mu\right\|$, since $\bar{d}^{i+1}\colon H^{\bar{l}_{i+1}}\bar{\mathbb{E}}^{i+1} \to \mathcal{R}(\bar{d}^{i+1}, H^{\bar{l}_{i+1}}\bar{\mathbb{E}}^{i+1})$ is a bounded map between Hilbert spaces. By the assumed exactness we find a $y \in H^{\bar{l}_i}\bar{\mathbb{E}}^i$ with $\bar{d}^i y = \mu - u$. Again in view of Corollary 2.1 we can assume $\|y\|_{H^{\bar{l}_i}} \prec \|\mu - u\|$. Since S^i defines a bounded and surjective mapping from $H^{\bar{l}_{i+1}}\mathbb{E}^i$ to $H^{\bar{l}_{i+1}}\bar{\mathbb{E}}^{i+1}$, we can choose a $\eta \in H^{\bar{l}_{i+1}}\mathbb{E}^i$ s.t. $S^i\eta = u$, $\|\eta\|_{H^{\bar{l}_{i+1}}} \prec \|u\|_{H^{\bar{l}_{i+1}}}$; see Corollary 2.1.
In an analogous manner we find $\kappa \in H^{\bar{l}_i}\mathbb{E}^{i-1}$ with $S^{i-1}\kappa = y$, $\|\kappa\|_{H^{\bar{l}_i}} \prec \|y\|_{H^{\bar{l}_i}}$. Now set

$$\tau \coloneqq -d^{i-1}\kappa + \eta \in \mathscr{U}^i. \tag{4.2.34}$$

It holds $S^i\tau = \bar{d}^i S^{i-1}\kappa + S^i\eta = \bar{d}^i y + u = \mu$. Furthermore we have the chain

$$\begin{aligned}\|\tau\|_{\mathscr{U}} &\leq \left\|d^{i-1}\kappa\right\| + \|\eta\|_{\mathscr{U}} \prec \|y\|_{H^{\bar{l}_i}} + \|u\|_{H^{\bar{l}_{i+1}}} \\ &\prec \|\mu - u\| + \left\|\bar{d}^{i+1}\mu\right\| \prec \|\mu\| + \|u\| + \left\|\bar{d}^{i+1}\mu\right\| \prec \|\mu\|_{\bar{U}}.\end{aligned}$$

In other words, plugging the chosen μ and τ from (4.2.34) into the fraction in the assertion we get something greater than a positive constant C, which in turn does not depend on the chosen μ. □

Next we face the reformulation of (4.2.32)-(4.2.33) with weakly enforced kernel and range conditions in the defining equation (4.2.12). For this purpose, additional variables, Lagrange multipliers respectively, need to be introduced. These lead to extra equations and columns compared to the original mixed weak system. We distinguish three cases $k \leq J$, $k = J+1$ and $k > J+1$.

Case $k \leq J$:

Firstly, let $k \leq J$ and consider the modified problem: *Find* $(\sigma, u, \lambda_1, \lambda_2) \in \mathscr{U}^{k-1} \times \mathscr{U}^k \times L^2(\Omega) \otimes \mathbb{E}^{k-2} \times L^2(\Omega) \otimes \mathbb{E}^{k-1}$ *s.t.*

$$\begin{aligned}
&\langle \sigma, \tau \rangle - \langle u, \mathscr{D}^{k-1}\tau \rangle + \langle S^{k-2}\lambda_1, \tau \rangle = 0, && \forall \tau \in \mathscr{U}^{k-1}, && (4.2.35)\\
&\langle \mathscr{D}^{k-1}\sigma, v \rangle + \langle \mathscr{D}^k u, \mathscr{D}^k v \rangle + \langle S^{k-1}\lambda_2, v \rangle = \langle f, v \rangle, && \forall v \in \mathscr{U}^k, && (4.2.36)\\
&\langle \sigma, S^{k-2}\mu_1 \rangle = 0, && \forall \mu_1 \in L^2(\Omega) \otimes \mathbb{E}^{k-2}, && (4.2.37)\\
&\langle u, S^{k-1}\mu_2 \rangle = 0, && \forall \mu_2 \in L^2(\Omega) \otimes \mathbb{E}^{k-1}, && (4.2.38)
\end{aligned}$$

for some $f \in \mathscr{W}^k$. Latter mixed weak form omits the spaces $\mathscr{V}^i$ but still yields the solution to (4.2.32)-(4.2.33).

Lemma 4.12. *The system* (4.2.35)-(4.2.38) *is well-posed and the solution* $(\sigma, u, \lambda_1, \lambda_2)$ *gives the solution* (σ, u) *to the original problem* (4.2.32)-(4.2.33) *for* $k \leq J$.

Proof. First with (4.2.10) and (4.2.13) we observe that

$$\begin{aligned}
Z &\coloneqq \Big\{ (\tau, v) \in \mathscr{U}^{k-1} \times \mathscr{U}^k \mid \langle \tau, S^{k-2}\mu_1 \rangle + \langle v, S^{k-1}\mu_2 \rangle = 0,\\
&\qquad \forall (\mu_1, \mu_2) \in L^2(\Omega) \otimes \mathbb{E}^{k-2} \times L^2(\Omega) \otimes \mathbb{E}^{k-1} \Big\}\\
&= \mathscr{V}^{k-1} \times \mathscr{V}^k.
\end{aligned}$$

Besides, we set

$$\mathfrak{a}((\sigma, u), (\tau, v)) \coloneqq \langle \sigma, \tau \rangle - \langle u, \mathscr{D}^{k-1}\tau \rangle - \langle \mathscr{D}^{k-1}\sigma, v \rangle - \langle \mathscr{D}^k u, \mathscr{D}^k v \rangle,$$

for $(\sigma, u),\ (\tau, v) \in \mathscr{U}^{k-1} \times \mathscr{U}^k$. The well-posedness of the original mixed weak form (4.2.32)-(4.2.33) yields the inf-sup property (2.3.6) for $\mathfrak{a}$ on $Z \times Z$; compare Lemma 2.10. Besides, using Lemma 4.10 we find for $0 \neq \mu_i \in L^2(\Omega) \otimes \mathbb{E}^{k-3+i},\ i \in \{1, 2\}$ elements $(\tau, v) \in \mathscr{U}^{k-1} \times \mathscr{U}^k$ satisfying

$$\langle \tau, S^{k-2}\mu_1 \rangle + \langle v, S^{k-1}\mu_2 \rangle \geq \|\mu_1\|^2 + \|\mu_2\|^2, \quad \|\tau\|_{\mathscr{U}} + \|v\|_{\mathscr{U}} \prec \|\mu_1\| + \|\mu_2\|.$$

But this shows us the validity of the inf-sup property (2.3.7) for the bilinear form

$$\mathfrak{b}((\tau, v), (\mu_1, \mu_2)) \coloneqq \langle \tau, S^{k-2}\mu_1 \rangle + \langle v, S^{k-1}\mu_2 \rangle,$$

with $U^1 = \mathscr{U}^{k-1} \times \mathscr{U}^k,\ U^2 = (L^2(\Omega) \otimes \mathbb{E}^{k-2}) \times (L^2(\Omega) \otimes \mathbb{E}^{k-1})$. Hence in view of Corollary 2.2 we established the well-posedness. And clearly the solution $(\sigma, u, \lambda_1, \lambda_2)$ to (4.2.35)-(4.2.38) yields the solution (σ, u) of (4.2.32)-(4.2.33). This finishes the proof. □

Case $k = J + 1$:

Next we switch to the situation $k = J + 1$ and look at the problem: *Find* $(\sigma, u, \lambda_1, \lambda_2) \in \mathscr{U}^J \times \mathscr{U}^{J+1} \times L^2(\Omega) \otimes \mathbb{E}^{J-1} \times \bar{U}^{J+2}$ *s.t.*

$$\begin{aligned}
&\langle \sigma, \tau \rangle - \langle u, \mathscr{D}^J\tau \rangle + \langle S^{J-1}\lambda_1, \tau \rangle = 0, && \forall \tau \in \mathscr{U}^J, && (4.2.39)\\
&\langle \mathscr{D}^J\sigma, v \rangle + \langle d^{J+1}u, d^{J+1}v \rangle + \langle \lambda_2, S^{J+1}v \rangle_{\bar{U}} = \langle f, v \rangle, && \forall v \in \mathscr{U}^{J+1}, && (4.2.40)\\
&\langle \sigma, S^{J-1}\mu_1 \rangle = 0, && \forall \mu_1 \in L^2(\Omega) \otimes \mathbb{E}^{J-1}, && (4.2.41)\\
&\langle S^{J+1}u, \mu_2 \rangle_{\bar{U}} = 0, && \forall \mu_2 \in \bar{U}^{J+2}, && (4.2.42)
\end{aligned}$$

provided a $f \in \mathscr{W}^{J+1}$.

Lemma 4.13. *We assume* $\mathcal{R}(\bar{d}^{m-1}, H^{\bar{l}_{m-1}}\bar{\mathbb{E}}^{m-1}) = \mathcal{N}(\bar{d}^m, \bar{U}^m)$, for $m \in \{J+2, J+3\}$. *Then System* (4.2.39) -(4.2.42) *is well-posed and yields the solution* (σ, u) *to* (4.2.32)-(4.2.33) *for* $k = J+1$.

Proof. The proof uses a similar argumentation as the one for the previous lemma. Again using (4.2.10) and (4.2.13) we can conclude that

$$Z \coloneqq \Big\{(\tau, v) \in \mathscr{U}^J \times \mathscr{U}^{J+1} \mid \langle \tau, S^{J-1}\mu_1\rangle + \langle S^{J+1}v, \mu_2\rangle_{\bar{U}} = 0, \\ \forall (\mu_1, \mu_2) \in L^2(\Omega) \otimes \mathbb{E}^{J-1} \times \bar{U}^{J+2}\Big\}$$

is equal to $\mathscr{V}^J \times \mathscr{V}^{J+1}$. By the well-posedness of the original mixed weak form (4.2.32) - (4.2.33) and due to Corollary 2.2, it is enough to check the related inf-sup condition (2.3.7) for

$$\mathfrak{b}((\tau, v), (\mu_1, \mu_2)) \coloneqq \langle \tau, S^{J-1}\mu_1\rangle + \langle S^{J+1}v, \mu_2\rangle_{\bar{U}},$$

where the underlying spaces are $U^1 = \mathscr{U}^J \times \mathscr{U}^{J+1}$ and $U^2 = L^2(\Omega) \otimes \mathbb{E}^{J-1} \times \bar{U}^{J+2}$. Applying both, Lemma 4.10 and Lemma 4.11 one obtains for $\mu_1 \in L^2(\Omega) \otimes \mathbb{E}^{J-1}$, $\mu_2 \in \bar{U}^{J+2}$ elements $(\tau, v) \in \mathscr{U}^J \times \mathscr{U}^{J+1}$ satisfying

$$\langle \tau, S^{J-1}\mu_1\rangle + \langle S^{J+1}v, \mu_2\rangle_{\bar{U}} \geq \|\mu_1\|^2 + \|\mu_2\|_{\bar{U}}^2, \quad \|\tau\|_{\mathscr{U}} + \|v\|_{\mathscr{U}} \prec \|\mu_1\| + \|\mu_2\|_{\bar{U}}.$$

Consequently, the needed inf-sup property for $\mathfrak{b}$ is fulfilled. The fact that the new formulation with Lagrange multipliers gives us the solution of the original problem is clear. □

Case $k > J+1$:

And for the third case, meaning $k > J+1$ one might consider the reformulation:
Given $f \in \mathscr{W}^k$, *we seek for* $(\sigma, u, \lambda_1, \lambda_2) \in \mathscr{U}^{k-1} \times \mathscr{U}^k \times \bar{U}^k \times \bar{U}^{k+1}$ *with*

$$\begin{aligned}
&\langle \sigma, \tau\rangle && - \langle u, d^{k-1}\tau\rangle + \langle \lambda_1, S^{k-1}\tau\rangle_{\bar{U}} && = 0, && \forall \tau \in \mathscr{U}^{k-1}, && (4.2.43)\\
&\langle d^{k-1}\sigma, v\rangle && + \langle d^k u, d^k v\rangle && + \langle \lambda_2, S^k v\rangle_{\bar{U}} = \langle f, v\rangle, && \forall v \in \mathscr{U}^k, && (4.2.44)\\
&\langle S^{k-1}\sigma, \mu_1\rangle_{\bar{U}} && && = 0, && \forall \mu_1 \in \bar{U}^k, && (4.2.45)\\
& && \langle S^k u, \mu_2\rangle_{\bar{U}} && = 0, && \forall \mu_2 \in \bar{U}^{k+1}. && (4.2.46)
\end{aligned}$$

Again one can assure oneself that the mixed formulation involving the $\mathscr{U}^i$ makes sense.

Lemma 4.14. *Let* $k > J+1$ *and for the top complex in Figure 4 we require the property* $\mathcal{R}(\bar{d}^{m-1}, H^{\bar{l}_{m-1}}\bar{\mathbb{E}}^{m-1}) = \mathcal{N}(\bar{d}^m, \bar{U}^m)$, for $m \in \{k, k+1, k+2\}$. *Then we obtain a well-posed problem* (4.2.43)-(4.2.46) *which yields the solution* (σ, u) *of problem* (4.2.32)-(4.2.33).

Proof. The proof is very similar and analogous to the one of Lemma 4.13 and applies basically Lemma 4.11. That is why we omit here details. □

Remark 4.4. For $k > 0$ the technical assumptions in the different lemmata above are satisfied if the row complexes in Figure 4 are vector-valued de Rham complexes on starlike domains, due to Lemma 3.10. Thus, e.g. for the chains (4.2.29) -(4.2.31) and the L^2 output complexes from Lemma 4.9 we might apply the procedure involving Lagrange multipliers.

With admittedly somewhat involved new formulations, our intention was merely to highlight a potentially useful observation. Namely, as long as the input complexes are exact, it is possible to incorporate the conditions coming from the S^i in (4.2.12) through auxiliary variables in a weak form. In doing so, these new formulations lead to the solution to the original mixed weak form, even though the spaces $\mathscr{V}^i$ no longer appear explicitly. It is, however, entirely clear that the introduction of new variables also brings about the issue of an increasing number of degrees of freedom when dealing with discretizations. Nevertheless, there are examples where the utilization of Lagrange multipliers might make it easier to find suitable FE spaces. This has already been demonstrated, for example, in [10] in the context of linear elasticity, where the symmetry condition is imposed weakly. And we will follow this path involving Lagrange multipliers in Section 8.3.

Now we have reached the point at which we have introduced the second-order complexes $(\mathscr{V}_n^{\circ,J}, \mathscr{D}_n^{\circ,J})$ relevant to us in the numerical part, and have also explained how to transform the mixed weak formulation into a modified version through additional variables. With this, we have actually defined everything we need to finally focus on discretizations in the context of such output complexes. Before we turn to isogeometric analysis, which we will later use as a fundamental basis for the concrete definition of FE spaces, we will precede with a chapter in which we present generally useful and more general auxiliary results and observations regarding discretizations of mixed weak formulations of the form (4.2.32)-(4.2.33). In the next section, statements will be shown that we will then reuse in a concrete context of the section. However, for the sake of completeness, we will also consider and deal with statements that are not directly used in the mentioned section but still appear noteworthy to us.

5 Regarding the Discretization of the Output Complex

In this section, we would like to address aspects concerning the discretization of the output complexes $(\mathscr{V}^\circ, \mathscr{D}^\circ)$ from Lemma 4.6 defined on some Lipschitz domain $\Omega \subset \mathbb{R}^n$. More precisely, here we have Assumption 4.3 underlying and we face the discretization of (4.2.32)-(4.2.33). In doing so, as already mentioned at the end of the previous chapter, we make relatively general statements and observations, which have two underlying motivations. Firstly, we want to become familiar with the problem and difficulties of discretization and foster a better understanding of it. Secondly, we aim to demonstrate technical auxiliary results that we can later refer to in Section 8 . So, at least in part, one can consider the following discussions as a preparatory chapter for later ones.

Actually, everything seems to have been clarified in this regard through the abstract FEEC theory; see Section 3. The ideal approach would be to employ a structure-preserving discretization for the complex $(\mathscr{V}^\circ, \mathscr{D}^\circ)$ in order to solve the mixed weak formulation in the finite-dimensional setting. However, that is where the challenge lies. When going from the classical de Rham chain to different type of Hilbert complexes, constructing such spaces that are suitable according to the FEEC theory is not straightforward. This is particularly true for the second-order complexes $(\mathscr{V}_n^{\circ,J}, \mathscr{D}_n^{\circ,J})$ introduced through Lemma 4.9. Especially when considering non-trivial domains with curved boundaries, the form of structure-preserving discretizations is an open question. Nevertheless, our goal remains to apply IGA in the context of second-order complexes. In order to do this, we need to relax conditions and may not always satisfy all three properties from Section 3.4 simultaneously. This seems to be a problematic step, as we should expect not to achieve well-posedness. With the explanations in this section, however, we aim to establish various conditions that still guide us to well-posed discretizations and will turn out later to be useful for isogeometric methods.

These explanations can be broadly divided into two parts. First, let us explore how well-posedness can be achieved if we use conforming FE spaces but ignore the subcomplex property. In this context, we will introduce an equivalent but modified weak formulation. Afterwards, we will pursue the approach of utilizing the Lagrange multiplier formulation from Section 4.2.4, focusing on the case of saddle-point systems meaning the case where $k = n$. Latter approach will also lead us back to FEEC, in the sense that structure-preserving discretizations will once again play a role.

5.1 Considerations for the case of trivial cohomology

Here we have an abstract point of view and assume the existence of families of discrete spaces $\mathscr{V}_h^{k-1} \subset \mathscr{V}^{k-1}$, $\mathscr{V}_\theta^k \subset \mathscr{V}^k$, where k is a fixed index; cf. Assumption 4.3. In this context, we use two distinct indices, h and θ, to emphasize that the spaces can be defined entirely differently. We call θ and h the mesh sizes of the spaces and they might differ. This notation is convenient, as we will see in later examples, making mesh refinements for the individual spaces more distinguishable. However, as before, we maintain the natural and intuitive assumption:

$$\lim_{h\to 0} \inf_{\tau_h \in \mathscr{V}_h^{k-1}} \|\tau - \tau_h\|_{\mathscr{V}} = 0, \quad \forall \tau \in \mathscr{V}^{k-1}, \qquad \lim_{\theta\to 0} \inf_{v_\theta \in \mathscr{V}_\theta^{k}} \|v - v_\theta\|_{\mathscr{V}} = 0, \quad \forall v \in \mathscr{V}^{k},$$

with $\|\cdot\|_{\mathscr{V}}^2 \coloneqq \|\cdot\|^2 + \|\mathscr{D}^i \cdot\|^2$ denoting the respective graph norms. And as always, $\|\cdot\|$ stands for L^2-based norms on the respective spaces of the form $L^2(\Omega) \otimes \mathbb{W}$. For the order of the output

differential operators $\mathscr{D}^i$ we write again $l_i \coloneqq \mathrm{ord}(\mathscr{D}^i)$.
Regarding the different mesh sizes, it is important to clarify and explain the following:

Assumption 5.1 (Regarding the different mesh sizes)**.** *When we talk about discretizations using $\mathscr{V}_h^{k-1}$, $\mathscr{V}_\theta^k$, we mean that we are actually dealing with tuples of finite-dimensional spaces $(\mathscr{V}_h^{k-1}, \mathscr{V}_\theta^k)$, i.e. for each space $\mathscr{V}_\theta^k$ there is an associated space $\mathscr{V}_h^{k-1}$. Thus, while we allow distinct meshes for $\mathscr{V}_h^{k-1}$ and $\mathscr{V}_\theta^k$, we still require that a reduction in θ also implies a reduction in h. In other words, the mesh sizes may be different, but they are coupled, and if we talk about families of discrete spaces consider them as a family in θ and determine h through a mapping $h = h(\theta)$. This means strictly speaking, we have to write in the following everywhere $\mathscr{V}_{h(\theta)}^{k-1}$, instead of $\mathscr{V}_h^{k-1}$. However, below we often find it more convenient and easier to write down the expressions, when we simply refer to two indices, θ and h, while keeping the coupling in mind. In particular we abbreviate below*

$$(\mathscr{V}_h^{k-1},\ \mathscr{V}_\theta^k)_\theta \coloneqq (\mathscr{V}_{h(\theta)}^{k-1},\ \mathscr{V}_\theta^k)_\theta.$$

Next we introduce the discrete version of problem (4.2.32)-(4.2.33), namely: *For $f \in \mathscr{W}^k$ find $(\sigma_h, u_\theta) \in \mathscr{V}_h^{k-1} \times \mathscr{V}_\theta^k$ s.t.*

$$\langle \sigma_h, \tau_h \rangle \qquad - \langle u_\theta, \mathscr{D}^{k-1}\tau_h \rangle \ = 0, \qquad \forall \tau_h \in \mathscr{V}_h^{k-1}, \tag{5.1.1}$$

$$\langle \mathscr{D}^{k-1}\sigma_h, v_\theta \rangle + \langle \mathscr{D}^k u_\theta, \mathscr{D}^k v_\theta \rangle = \langle f, v_\theta \rangle, \quad \forall v_\theta \in \mathscr{V}_\theta^k. \tag{5.1.2}$$

From the theory we know what should be satisfied in order to have a reasonable discrete scheme, namely we need inf-sup stability; compare Definition 2.11 and Lemma 2.12. This means we want to have

$$\inf_{(0,0)\neq(\tau_h,v_\theta)\in\mathscr{V}_h^{k-1}\times\mathscr{V}_\theta^k} \sup_{(0,0)\neq(\sigma_h,u_\theta)\in\mathscr{V}_h^{k-1}\times\mathscr{V}_\theta^k} \frac{\mathcal{B}\Big((\sigma_h,u_\theta),(\tau_h,v_\theta)\Big)}{\|(\sigma_h,u_\theta)\|_{\mathcal{B}}\,\|(\tau_h,v_\theta)\|_{\mathcal{B}}} \geq C_{IS} > 0, \tag{5.1.3}$$

with

$$\mathcal{B}\Big((\sigma,u),(\tau,v)\Big) \coloneqq \langle \sigma,\tau\rangle - \langle u, \mathscr{D}^{k-1}\tau\rangle - \langle \mathscr{D}^{k-1}\sigma, v\rangle - \langle \mathscr{D}^k u, \mathscr{D}^k v\rangle,$$
$$\|(\sigma,u)\|_{\mathcal{B}}^2 \coloneqq \|\sigma\|_{\mathscr{V}}^2 + \|u\|_{\mathscr{V}}^2,$$

and C_{IS} independent from mesh refinement. If we would have structure-preserving discretizations we would get automatically a well-posed scheme, due to Lemma 3.16. However, the output spaces $\mathscr{V}^i$ and their connection to the linking maps S^i coming from the BGG construction (see Lemma 4.6) are sometimes difficult to handle and, as already mentioned, for chains with higher order differential operators the construction of such structure-preserving discretization is not trivial or even not known in general. For reasons of completeness, we start by giving first a criterion which leads at least to the invertibility of the discrete systems. For this purpose, we need the next

Assumption 5.2 (Discrete spaces)**.** *In view of Lemma 4.6, let us assume for the discrete spaces the following:*

- $\mathscr{V}_h^{k-1} \subset \mathscr{V}^{k-1}$ *and* $\mathscr{V}_\theta^k \subset \mathscr{V}^k$.
- *There is a projection $\Pi_h^{k-1}\colon \mathscr{V}^{k-1} \to \mathscr{V}_h^{k-1}$ s.t.*

$$\Big\|\mathscr{D}^{k-1}\Pi_h^{k-1}\tau - \mathscr{D}^{k-1}\tau\Big\| \leq C_1 h\,\|\tau\|_{H^{l_{k-1}+1}},\ \forall \tau \in H^{l_{k-1}+1}(\Omega)\otimes\mathbb{V}^{k-1},$$
$$\Big\|\Pi_h^{k-1}\tau\Big\|_{\mathscr{V}} \leq C_1\,\|\tau\|_{H^{l_{k-1}}},\ \forall \tau \in H^{l_{k-1}}(\Omega)\otimes\mathbb{V}^{k-1},$$

for a constant C_1 independent of h. Note, $l_{k-1} \coloneqq \mathrm{ord}(\mathscr{D}^{k-1})$.

- *It is* $\mathscr{V}_\theta^k \subset H^1(\Omega) \otimes \mathbb{V}^k$. *Further, there is constant* C_2 *independent of* θ *with*

$$\|v_\theta\|_{H^1} \leq \frac{C_2}{\theta} \|v_\theta\|, \ \forall v_\theta \in \mathscr{V}_\theta^k.$$

Lemma 5.1. *Let the Assumptions 4.3 and 5.2 hold. Then, there is a positive constant* c_R *s.t. if the mesh sizes fulfill* $h \leq c_R\theta$ *we have the invertibility of the discrete system* (5.1.1)-(5.1.2). *Consequently, after a suitable mesh refinement related to the discrete space* $\mathscr{V}_h^{k-1}$ *we have a unique discrete solution.*

Proof. Let us look at the system (5.1.1)-(5.1.2) with $f = 0$. Then it follows directly $\sigma_h = 0$, $\mathscr{D}^k u_\theta = 0$ just by setting $\tau_h = \sigma_h$ and $v_\theta = u_\theta$. By assumption we know $u_\theta \in H^1\mathbb{V}^k$. Hence, because of the exactness at level k for our setting, we find a $\tau \in H^{l_{k-1}+1}\mathbb{V}^{k-1}$ s.t. $\mathscr{D}^{k-1}\tau = u_\theta$ and $\|\tau\|_{H^{l_{k-1}+1}} \leq C \|u_\theta\|_{H^1}$ for a proper C; see Corollary 4.2 or [12, Theorem 2]. In particular due to the first line (5.1.1) one has the estimate

$$\begin{aligned}
0 = \langle u_\theta, \mathscr{D}^{k-1}\Pi_h^{k-1}\tau\rangle &= \|u_\theta\|^2 + \langle u_\theta, \mathscr{D}^{k-1}\Pi_h^{k-1}\tau - \mathscr{D}^{k-1}\tau\rangle \\
&\geq \|u_\theta\|^2 - \|u_\theta\| \left\|\mathscr{D}^{k-1}\Pi_h^{k-1}\tau - \mathscr{D}^{k-1}\tau\right\| \\
&\geq \|u_\theta\|^2 - C_1 h \|u_\theta\| \|\tau\|_{H^{l_{k-1}+1}} \geq \|u_\theta\|^2 - C_1 C h \|u_\theta\| \|u_\theta\|_{H^1} \\
&\geq \|u_\theta\|^2 - C_1 C_2 C \frac{h}{\theta} \|u_\theta\|^2 .
\end{aligned}$$

One notes the application of the Cauchy–Schwarz inequality and Assumption 5.2. Hence if $C_1 C_2 C \frac{h}{\theta} < 1$, we get also $u_\theta = 0$ and consequently the invertibility of the whole system. □

The conditions we have imposed on the spaces $\mathscr{V}_h^{k-1}$, $\mathscr{V}_\theta^k$ may seem difficult. However, when applying classical estimates from IGA theory, it becomes apparent that such inequalities and conditions are satisfied for standard IGA spaces; see Section 6. In other words, without significant effort, it can be shown using the Lemma 5.1 that various mixed weak formulations of the Hodge–Laplace problems for the complexes $(\mathscr{V}^\circ, \mathscr{D}^\circ)$ from Alt^l-valued forms, along with IGA discretizations, yield unique solutions. With the aforementioned lemma in mind, it is natural to choose the space $\mathscr{V}_h^{k-1}$ to be sufficiently large compared to $\mathscr{V}_\theta^k$. However, this does not necessarily result in well-posedness of the discretization scheme, as in (5.1.3) the infimum is also taken over elements in $\mathscr{V}_h^{k-1}$. To establish a somewhat more manageable well-posedness condition, we will therefore introduce an equivalent but modified mixed weak form. This change in the variational formulation is inspired by the method of *augmented Lagrangian functions* from [52].

Definition 5.1 (**Modified weak formulation**). *Given a* $f \in \mathscr{W}^k$ *one seeks for* $(\sigma, u) \in \mathscr{V}^{k-1} \times \mathscr{V}^k$ *with*

$$\begin{aligned}
\langle \sigma, \tau\rangle_{\mathscr{V}} \quad - \langle u, \mathscr{D}^{k-1}\tau\rangle &= \langle f, \mathscr{D}^{k-1}\tau\rangle, \ \forall \tau \in \mathscr{V}^{k-1}, && (5.1.4)\\
\langle \mathscr{D}^{k-1}\sigma, v\rangle + \langle \mathscr{D}^k u, \mathscr{D}^k v\rangle &= \langle f, v\rangle, \qquad \forall v \in \mathscr{V}^k, && (5.1.5)
\end{aligned}$$

where $\langle \cdot, \cdot\rangle_{\mathscr{V}} = \langle \cdot, \cdot\rangle + \langle \mathscr{D}^{k-1}\cdot, \mathscr{D}^{k-1}\cdot\rangle$ *denotes the graph inner product.*

The new formulation is indeed equivalent to the one in Definition 4.5. Because, if on the one hand (σ, u) solves the modified system we get by (5.1.5):

$$\langle \mathscr{D}^{k-1}\sigma, \mathscr{D}^{k-1}\tau\rangle = \langle \mathscr{D}^{k-1}\sigma, \mathscr{D}^{k-1}\tau\rangle + \langle \mathscr{D}^k u, \mathscr{D}^k \mathscr{D}^{k-1}\tau\rangle = \langle f, \mathscr{D}^{k-1}\tau\rangle, \quad \forall \tau \in \mathscr{V}^{k-1}. \qquad (5.1.6)$$

Using this we get with (5.1.4) directly (4.2.32). On the other hand, let (σ, u) be the solution to (4.2.32)-(4.2.33), then (4.2.32) together with (5.1.6) shows the validity of the modified system.

More generally, we have the following. Namely, let us change the right-hand sides of the modified system (5.1.4) and (5.1.5) to some arbitrary $\mathfrak{g} \in (\mathscr{V}^{k-1})'$ and $\mathfrak{f} \in (\mathscr{V}^k)'$ in the dual spaces. Then one sees with an analogous argument as above that there is a unique solution (σ, u) which satisfies the original system (4.2.32)-(4.2.33) with right-hand sides $\tilde{\mathfrak{g}} = \mathfrak{g} - \mathfrak{f}(\mathscr{D}^{k-1}\cdot)$ and $\tilde{\mathfrak{f}} = \mathfrak{f}$. In the last sentence $\mathfrak{f}(\mathscr{D}^{k-1}\cdot)$ denotes the linear form $\tau \mapsto \mathfrak{f}(\mathscr{D}^{k-1}\tau)$. By the well-posedness of the original mixed weak form we have

$$\|u\|_{\mathscr{V}} + \|\sigma\|_{\mathscr{V}} \leq C\Big(\|\tilde{\mathfrak{g}}\|_{\mathscr{V}'} + \big\|\tilde{\mathfrak{f}}\big\|_{\mathscr{V}'} \Big) \leq C\Big(\|\mathfrak{g}\|_{\mathscr{V}'} + 2\,\|\mathfrak{f}\|_{\mathscr{V}'} \Big),$$

since $|\mathfrak{f}(\mathscr{D}^{k-1}\tau)| \leq \tilde{C} \left\|\mathscr{D}^{k-1}\tau\right\|_{\mathscr{V}} \leq \tilde{C}\,\|\tau\|_{\mathscr{V}}$, for proper constants C, $\tilde{C}$. By this observation, we can conclude the well-posedness also for the new formulation from Definition 5.1.

After having justified why it is possible to consider the modified system as well, we now aim to establish a first auxiliary statement concerning well-posedness.

Lemma 5.2. *Assume*

$$\forall u_\theta \in \mathscr{V}_\theta^k,\ \exists \eta_h \in \mathscr{V}_h^{k-1}\ \ s.t.\ \ |\langle \mathscr{D}^{k-1}\eta_h - \mathcal{P}_{\mathcal{N}(\mathscr{D}^k)} u_\theta, u_\theta\rangle| \leq c_\Pi \|u_\theta\|^2 \ \text{ and } \ \|\eta_h\|_{\mathscr{V}} \leq C_\Pi \left\|\mathcal{P}_{\mathcal{N}(\mathscr{D}^k)} u_\theta\right\|,$$

where $0 < c_\Pi < \frac{1}{2}$, $0 < C_\Pi$ are constants independent of h and θ and $\mathcal{P}_{\mathcal{N}(\mathscr{D}^k)}$ is the $\mathscr{V}$-orthogonal projection onto the kernel $\mathcal{N}(\mathscr{D}^k, \mathscr{V}^k)$. Then the related discretization of the system from Definition 5.1 is well-posed.[10]

Proof. We follow the proof steps of Arnold from [5, Theorem 4.9], but with alterations at different places.
By multiplying the second line (5.1.5) by -1 we see immediately that it is allowed to consider the symmetric and bounded bilinear form

$$\tilde{\mathcal{B}}\Big((\sigma, u), (\tau, v)\Big) \coloneqq \langle \sigma, \tau\rangle_{\mathscr{V}} - \langle u, \mathscr{D}^{k-1}\tau\rangle - \langle \mathscr{D}^{k-1}\sigma, v\rangle - \langle \mathscr{D}^k u, \mathscr{D}^k v\rangle$$

to check well-posedness. To be more precise, we show for $\tilde{\mathcal{B}}$ the discrete inf-sup stability; cf. Definition 2.11. For this purpose fix some arbitrary $(\sigma_h, u_\theta) \in \mathscr{V}_h^{k-1} \times \mathscr{V}_\theta^k$. In view of the Hodge decomposition (Lemma 3.1) we can assume $u_\theta = u_{\mathfrak{B}} + u_{\mathfrak{B}}^\perp$ with $\langle u_{\mathfrak{B}}, u_{\mathfrak{B}}^\perp\rangle = 0$ and $u_{\mathfrak{B}} = \mathcal{P}_{\mathcal{N}(\mathscr{D}^k)} u_\theta$. Next we set

$$\tau_h \coloneqq \sigma_h - \frac{1}{C_\Pi^2}\eta_h \in \mathscr{V}_h^{k-1}, \qquad v_\theta \coloneqq -u_\theta \in \mathscr{V}_\theta^k\ ,$$

where η_h is chosen such that it satisfies the two inequalities in the assertion. Inserting this choice into the formula for $\tilde{\mathcal{B}}$, we obtain

$$\tilde{\mathcal{B}}\Big((\sigma_h, u_\theta), (\tau_h, v_\theta)\Big) = \|\sigma_h\|_{\mathscr{V}}^2 + \left\|\mathscr{D}^k u_\theta\right\|^2 - \frac{1}{C_\Pi^2}\langle \sigma_h, \eta_h\rangle_{\mathscr{V}} + \frac{1}{C_\Pi^2}\langle u_\theta, \mathscr{D}^{k-1}\eta_h\rangle. \tag{5.1.7}$$

Then, analogous to the proof of Theorem 4.9 in [5], we estimate the second last term of (5.1.7) utilizing the Cauchy–Schwarz inequality together with the algebraic-geometric mean inequality. More precisely,

$$|\langle \sigma_h, \eta_h\rangle_{\mathscr{V}}| \leq \frac{C_\Pi^2}{2}\|\sigma_h\|_{\mathscr{V}}^2 + \frac{1}{2C_\Pi^2}\|\eta_h\|_{\mathscr{V}}^2 \leq \frac{C_\Pi^2}{2}\|\sigma_h\|_{\mathscr{V}}^2 + \frac{1}{2}\|u_{\mathfrak{B}}\|^2. \tag{5.1.8}$$

[10] $\mathscr{V}$-orthogonal means orthogonality w.r.t. the graph inner product $\langle\cdot,\cdot\rangle_{\mathscr{V}} = \langle\cdot,\cdot\rangle + \langle\mathscr{D}^k\cdot, \mathscr{D}^k\cdot\rangle$.

Moreover for the last term in (5.1.7) one has the inequality

$$\langle u_\theta, \mathscr{D}^{k-1}\eta_h\rangle = \langle u_{\mathfrak{B}}, u_{\mathfrak{B}}\rangle + \langle u_\theta, \mathscr{D}^{k-1}\eta_h - u_{\mathfrak{B}}\rangle \tag{5.1.9}$$

and by assumption

$$|\langle u_\theta, \mathscr{D}^{k-1}\eta_h - u_{\mathfrak{B}}\rangle| \leq c_\Pi \left\|u_\theta\right\|^2 \ . \tag{5.1.10}$$

By the Poincaré inequality (Lemma 3.2), applied to the continuous complex, one can estimate

$$\left\|\mathscr{D}^k u_\theta\right\|^2 \geq \frac{1}{C_P^2}\left\|u_{\mathfrak{B}}^\perp\right\|^2 . \tag{5.1.11}$$

W.l.o.g. we can suppose $C_\Pi \geq C_P$. Otherwise we can just set $C_\Pi \coloneqq C_P$ and redo the previous proof steps. Thus we can combine the lines (5.1.8)-(5.1.11) to see

$$\begin{aligned}
\tilde{\mathcal{B}}\Big((\sigma_h, u_\theta), (\tau_h, v_\theta)\Big) &\geq \Big(1-\frac{1}{2}\Big)\left\|\sigma_h\right\|_{\mathscr{V}}^2 + \frac{1}{C_\Pi^2}\Big(1-\frac{1}{2}\Big)\left\|u_{\mathfrak{B}}\right\|^2 + \left\|\mathscr{D}^k u_\theta\right\|^2 - \frac{c_\Pi}{C_\Pi^2}\left\|u_\theta\right\|^2 \\
&\geq \frac{1}{2}\left\|\sigma_h\right\|_{\mathscr{V}}^2 + \frac{1}{2C_\Pi^2}\left\|u_{\mathfrak{B}}\right\|^2 + \frac{1}{2}\left\|\mathscr{D}^k u_\theta\right\|^2 + \frac{1}{2C_\Pi^2}\left\|u_{\mathfrak{B}}^\perp\right\|^2 - \frac{c_\Pi}{C_\Pi^2}\left\|u_\theta\right\|^2 \\
&\geq \frac{1}{2}\left\|\sigma_h\right\|_{\mathscr{V}}^2 + \frac{1}{2}\left\|\mathscr{D}^k u_\theta\right\|^2 + \Big(\frac{1}{2C_\Pi^2} - \frac{c_\Pi}{C_\Pi^2}\Big)\left\|u_{\mathfrak{B}}\right\|^2 + \Big(\frac{1}{2C_\Pi^2} - \frac{c_\Pi}{C_\Pi^2}\Big)\left\|u_{\mathfrak{B}}^\perp\right\|^2 .
\end{aligned}$$

One notes $\left\|u_\theta\right\|^2 = \left\|u_{\mathfrak{B}}\right\|^2 + \left\|u_{\mathfrak{B}}^\perp\right\|^2$. Setting $C = \min\{\frac{1}{2},\ \frac{1}{2C_\Pi^2} - \frac{c_\Pi}{C_\Pi^2}\} > 0$ we get

$$\tilde{\mathcal{B}}\Big((\sigma_h, u_\theta), (\tau_h, v_\theta)\Big) \geq C\Big(\left\|\sigma_h\right\|_{\mathscr{V}}^2 + \left\|u_h\right\|_{\mathscr{V}}^2\Big). \tag{5.1.12}$$

Moreover, one easily sees $\left\|\tau_h\right\|_{\mathscr{V}} \leq \left\|\sigma_h\right\|_{\mathscr{V}} + \frac{1}{C_\Pi}\left\|u_{\mathfrak{B}}\right\| \leq \left\|\sigma_h\right\|_{\mathscr{V}} + \frac{1}{C_\Pi}\left\|u_\theta\right\|$ and $\left\|v_\theta\right\|_{\mathscr{V}} = \left\|u_\theta\right\|_{\mathscr{V}}$. The last norm estimates, (5.1.12) and the arbitrariness of (σ_h, u_θ) imply the inf-sup property (5.1.3) with $\mathcal{B}$ replaced by $\tilde{\mathcal{B}}$. This finishes the proof. □

The assumptions required in the previous Lemma 5.2 may appear complex and not immediately evident. In fact, these are satisfied when a special inf-sup condition is met, as the next lemma demonstrates.

Lemma 5.3. *Let $\mathcal{P}_{\mathcal{N}(\mathscr{D}^k)}$ denote the $\mathscr{V}$-orthogonal projection onto the kernel $\mathcal{N}(\mathscr{D}^k, \mathscr{V}^k)$. If we have a family of discrete spaces $(\mathscr{V}_h^{k-1},\ \mathscr{V}_\theta^k)_\theta$ in the sense of Assumption 5.1, such that*

$$\inf_{v_\theta \in \mathscr{V}_\theta^k,\ \mathcal{P}_{\mathcal{N}(\mathscr{D}^k)} v_\theta \neq 0} \ \sup_{0 \neq \tau_h \in \mathscr{V}_h^{k-1}} \frac{\langle \mathscr{D}^{k-1}\tau_h, \mathcal{P}_{\mathcal{N}(\mathscr{D}^k)} v_\theta\rangle}{\left\|\tau_h\right\|_{\mathscr{V}} \left\|\mathcal{P}_{\mathcal{N}(\mathscr{D}^k)} v_\theta\right\|} \geq C_{IS} > 0 \ , \tag{5.1.13}$$

with C_{IS} not depending on θ, then the corresponding discretization of the mixed weak form (5.1.4)-(5.1.5) *is well-posed.*

Proof. We define the finite-dimensional linear space $\mathscr{R}_\theta \coloneqq \mathcal{P}_{\mathcal{N}(\mathscr{D}^k)}\mathscr{V}_\theta^k \subset L^2(\Omega)\otimes\mathbb{V}^k$. And we write $\mathcal{P}_{\mathscr{R}} \colon L^2(\Omega)\otimes\mathbb{V}^k \to \mathscr{R}_\theta$ for the L^2-orthogonal projection onto that space. Furthermore,

$$T \colon \mathscr{V}_h^{k-1} \to \mathscr{R}_\theta \ , \ w \mapsto \mathcal{P}_{\mathscr{R}}\mathscr{D}^{k-1}w$$

is a bounded linear map in the sense $\left\|Tw\right\| \leq C\left\|w\right\|_{\mathscr{V}}$. In particular, due to the assumed inf-sup condition we can apply Lemma 2.5 to see for each $\mathcal{P}_{\mathcal{N}(\mathscr{D}^k)}u_\theta \in \mathscr{R}_\theta$ the existence of a $\tau_h \in \mathscr{V}_h^{k-1}$ with

$$\left\|\tau_h\right\|_{\mathscr{V}} \leq \frac{1}{C_{IS}}\left\|\mathcal{P}_{\mathcal{N}(\mathscr{D}^k)}u_\theta\right\|, \qquad \mathcal{P}_{\mathscr{R}}\mathscr{D}^{k-1}\tau_h = \mathcal{P}_{\mathcal{N}(\mathscr{D}^k)}u_\theta. \tag{5.1.14}$$

Let $u_\theta = u_{\mathfrak{B}} + u_{\mathfrak{B}}^{\perp}$ with $u_{\mathfrak{B}} = \mathcal{P}_{\mathcal{N}(\mathscr{D}^k)} u_\theta,\ u_{\mathfrak{B}}^{\perp} \in \mathcal{N}(\mathscr{D}^k, \mathscr{V}^k)^{\perp_{\mathscr{V}}}$. Hence, we obtain

$$\begin{aligned}\langle \mathscr{D}^{k-1}\tau_h - \mathcal{P}_{\mathcal{N}(\mathscr{D}^k)} u_\theta, u_\theta\rangle &= \langle \mathscr{D}^{k-1}\tau_h, u_{\mathfrak{B}}\rangle - \langle u_{\mathfrak{B}}, u_{\mathfrak{B}}\rangle \\ &= \langle \mathcal{P}_{\mathscr{R}} \mathscr{D}^{k-1}\tau_h, u_{\mathfrak{B}}\rangle - \langle u_{\mathfrak{B}}, u_{\mathfrak{B}}\rangle = 0. \end{aligned} \tag{5.1.15}$$

Combining (5.1.14) and (5.1.15) the assertion follows directly by Lemma 5.2. □

Remark 5.1. The inf-sup condition occurring in the last lemma is valid in the continuous setting because of the Poincaré inequality; see Lemma 3.2. Hence, this condition is in some sense natural and we can set for the non-discretized spaces just $C_{IS} = 1/C_P$, where C_P is the underyling Poincaré constant related to $\mathscr{D}^{k-1}$. Indeed, assuming the Poincaré inequality we find for each $v \in \mathscr{V}^k$ a $\rho \in \mathcal{N}(\mathscr{D}^{k-1}, \mathscr{V}^{k-1})^{\perp_{\mathscr{V}}}$ with $\mathscr{D}^{k-1}\rho = \mathcal{P}_{\mathcal{N}(\mathscr{D}^k)} v,\quad \|\rho\|_{\mathscr{V}} \leq C_P \left\|\mathcal{P}_{\mathcal{N}(\mathscr{D}^k)} v\right\|$. Hence, inserting this special ρ into the expression from (5.1.13) we see directly the possibility to set indeed $C_{IS} = 1/C_P$ for the continuous case.

The inf-sup condition of the Lemma 5.3 is particularly interesting because it provides a direction on how to modify the discrete spaces in order to increase the chance of achieving well-posedness. In equation (5.1.13), the infimum is taken only over elements in $\mathcal{P}_{\mathcal{N}(\mathscr{D}^k)}\mathscr{V}_\theta^k$, and the supremum is taken over elements in $\mathscr{V}_h^{k-1}$. This suggests that by considering a sufficiently large space $\mathscr{V}_h^{k-1}$ compared to $\mathscr{V}_\theta^k$, the inf-sup condition might be satisfied. In other words, mesh refinements for the σ space, meaning for the$\mathscr{V}_h^{k-1}$, appear to stabilize the modified weak system. This line of thought also aligns with the Lemma 5.1, which requires sufficiently small fractions $\frac{h}{\theta}$. Later, we will revisit this point regarding inf-sup stability for the modified system in Section 10.1. In the next section, we will delve into the important special case of $k = n$ in Definition 5.1, leading us to a saddle-point structure for which more precise statements are available.

5.2 Restriction to saddle-point systems

Next we show special conditions how to achieve well-posedness for the situation $k = n$. This means in alignment with the BGG construction in Lemma 4.6 we assume here $\mathscr{D}^k = \mathscr{D}^n = 0$ in (5.1.4)-(5.1.5). Besides we suppose Assumption 4.3 and that the output complex fulfills

Assumption 5.3.

$$\mathcal{R}(\mathscr{D}^{n-1}, H^l(U) \otimes \mathbb{V}^{n-1}) = L^2(U) \otimes \mathbb{V}^n, \quad l \coloneqq \operatorname{ord}(\mathscr{D}^{n-1}), \tag{5.2.1}$$

on each bounded Lipschitz domain U.

Then the modified continuous mixed weak form given in Definition 5.1 for the Hodge–Laplace problem reduces to:

Find $(\sigma, u) \in \mathscr{V}^{n-1} \times \mathscr{V}^n$ *s.t.*

$$\begin{aligned} \langle \sigma, \tau\rangle_{\mathscr{V}} \quad -\langle u, \mathscr{D}^{n-1}\tau\rangle &= \langle f, \mathscr{D}^{n-1}\tau\rangle, \quad \forall \tau \in \mathscr{V}^{n-1}, && (5.2.2)\\ \langle \mathscr{D}^{n-1}\sigma, v\rangle \qquad\quad &= \langle f, v\rangle, \qquad \forall v \in \mathscr{V}^n, && (5.2.3)\end{aligned}$$

with its discrete pendant: *Find* $(\sigma_h, u_\theta) \in \mathscr{V}_h^{n-1} \times \mathscr{V}_\theta^n$ *s.t.*

$$\begin{aligned} \langle \sigma_h, \tau_h\rangle_{\mathscr{V}} \quad -\langle u_\theta, \mathscr{D}^{n-1}\tau_h\rangle &= \langle f, \mathscr{D}^{n-1}\tau_h\rangle, \quad \forall \tau_h \in \mathscr{V}_h^{n-1}, && (5.2.4)\\ \langle \mathscr{D}^{n-1}\sigma_h, v_\theta\rangle \qquad\quad &= \langle f, v_\theta\rangle, \qquad \forall v_\theta \in \mathscr{V}_\theta^n. && (5.2.5)\end{aligned}$$

In our discussions in Section 4.2.2, the assumption was always $d^n = 0$, $\bar{d}^n = 0$, which explains why indeed $\mathscr{D}^n = 0$. Hence, we obtain the nice property $\mathcal{P}_{\mathcal{N}(\mathscr{D}^n)} = \mathrm{id}$ and in this situation the inf-sup condition from Lemma 5.3 simplifies to

$$\inf_{0\neq v_\theta \in \mathscr{V}_\theta^n} \sup_{0\neq \tau_h \in \mathscr{V}_h^{n-1}} \frac{\langle \mathscr{D}^{n-1}\tau_h, v_\theta\rangle}{\|\tau_h\|_{\mathscr{V}} \|v_\theta\|} \geq C_{IS} > 0. \tag{5.2.6}$$

In view of the trivial coercivity relation $\mathfrak{a}(\tau,\tau) := \langle \tau,\tau\rangle_{\mathscr{V}} = \|\tau\|_{\mathscr{V}}^2$ the latter line obviously corresponds to the classical inf-sup condition for saddle-point problems; see Lemma 2.11 . So we can interpret (5.1.13) as a generalized version of the inf-sup condition for non-saddle-point problems induced by the Hodge–Laplace problem.
Similar to Lemma 5.2, we see immediately the following

Corollary 5.1. *Let $(\mathscr{V}_h^{n-1},\ \mathscr{V}_\theta^n)_\theta$ be a family of discrete spaces in the sense of Assumption 5.1. Assume the existence of constants $0 < c_\Pi < 1,\ 0 < C_\Pi$ not depending on θ s.t. we find for each $v_\theta \in \mathscr{V}_\theta^n$ a $\tau_h \in \mathscr{V}_h^{n-1}$ with*

$$\left\|\mathscr{D}^{n-1}\tau_h - v_\theta\right\| \leq c_\Pi \|v_\theta\| \quad \text{and} \quad \|\tau_h\|_{\mathscr{V}} \leq C_\Pi \|v_\theta\|.$$

Then the discretization (5.2.4)-(5.2.5) *of the saddle-point system is well-posed.*

Proof. We get directly (5.2.6), which finishes the proof, due to Lemma 5.3. □

The conditions of Corollary 5.1 are easy to write down, but so far it is not clear how we can actually satisfy them in concrete cases. Moreover, for a given output complex and FE spaces, it is not immediately apparent whether we can apply the aforementioned corollary. Therefore, it is reasonable to demand some additional structure for the discrete spaces, so that we can arrive at conditions that are easier to fulfill. We aim to do this in the following.

The idea now is as follows. While it is true that for the second-order complexes $(\mathscr{V}_n^{\circ,J}, \mathscr{D}_n^{\circ,J})$ from Section 4.2.3, no structure-preserving IGA method is known for arbitrary domains Ω, there are indeed such methods for very simple geometries. Specifically, as long as Ω has a cubic shape, it is relatively easy to derive structure-preserving discretizations for various second-order complexes. We will delve into this point further in Section 7. Therefore, it is reasonable to leverage these known results for other Lipschitz domains as well. This is precisely what we aim to demonstrate with the next lemma. Namely, the existence of suitable structure-preserving discretizations on cubical domains yields well-posed discretizations for the saddle-point problem (5.2.2)-(5.2.3) on deformed domains. In doing so, we need to consider not only the original complex of the computational domain Ω but also the analogous complex $(\tilde{\mathscr{V}}^\circ, \mathscr{D}^\circ)$ on an auxiliary domain $K \supset \Omega$. In particular, in addition to $(\mathscr{V}_h^{n-1}, \mathscr{V}_\theta^n)$, we have spaces $\tilde{\mathscr{V}}_\rho^i$ that discretize the auxiliary complex $(\tilde{\mathscr{V}}^\circ, \mathscr{D}^\circ)$. How exactly these additional spaces can be used for our original saddle-point problem is illustrated by the following lemma.

Lemma 5.4. *The points from Assumptions 5.2 and 5.3 apply for the case $k = n$ and let $l = \mathrm{ord}(\mathscr{D}^{n-1})$. Besides, we have the following additional requirements and assumptions:*
Let $\Omega \subset K$, K bounded Lipschitz domain, such that there is a structure-preserving discretization $(\tilde{\mathscr{V}}_\rho^\circ)_\rho$, $\rho = \frac{1}{m},\ m \in \mathbb{N}_{>0}$ of the output complex $(\tilde{\mathscr{V}}^\circ, \mathscr{D}^\circ)$ on the auxiliary domain K; see Definition 3.11. We require $\tilde{\mathscr{V}}_\rho^{n-1} \subset H^{l+1}(K) \otimes \mathbb{V}^{n-1},\ \tilde{\mathscr{V}}_\rho^n \subset H^1(K) \otimes \mathbb{V}^n$ and further the associated bounded cochain projections $\tilde{\Pi}_\rho^i \colon \tilde{\mathscr{V}}^i \to \tilde{\mathscr{V}}_\rho^i$ should satisfy

- $\left\|\tilde{\Pi}_\rho^{n-1} w\right\|_{H^s(K)} \leq \tilde{C}_1 \|w\|_{H^s(K)},\ \forall w \in H^s(K) \otimes \mathbb{V}^{n-1},\ 0 \leq s \leq l+1$,

- $\left\|\tilde{\Pi}_\rho^n w - w\right\|_{H^s(K)} \leq \tilde{C}_1 \rho^{j-s} \|w\|_{H^j(K)}\,,\ \forall w \in H^j(K) \otimes \mathbb{V}^n,\ 0 \leq s \leq j \leq 1\ .$
  Moreover there is a constant $\tilde{C}_2$ *with*
- $\|w_\rho\|_{H^{l+1}(K)} \leq \tilde{C}_2 \rho^{-1} \|w_\rho\|_{H^l(K)}\,,\ \forall w_\rho \in \tilde{\mathscr{V}}_\rho^{n-1}\ ,$
- $\|w_\rho\|_{H^1(K)} \leq \tilde{C}_2 \rho^{-1} \|w_\rho\|_{L^2(K)}\,,\ \forall w_\rho \in \tilde{\mathscr{V}}_\rho^{n}\ .$

Let $(\mathscr{V}_h^{n-1},\ \mathscr{V}_\theta^n)_\theta$ *be a family of discrete spaces in the sense of Assumption 5.1. Then, there is a constant* $c_R > 0$ *s.t. if* $h = h(\theta) \leq c_R\,\theta$*, we obtain a well-posed discretization of* (5.2.2)-(5.2.3)*.*

Proof. The basic idea is to apply at the end Corollary 5.1.
We start by choosing some $v_\theta \in \mathscr{V}_\theta^n$. By the Stein extension theorem (see Lemma 2.8) we find a $\tilde{v} \in H^1(K) \otimes \mathbb{V}^n$ s.t.

$$\tilde{v} = v_\theta \text{ on } \Omega \quad \text{and} \quad \|\tilde{v}\|_{H^i(K)} \leq C_{\mathcal{E}} \|v_\theta\|_{H^i(\Omega)}\,,\ i = 0,\, 1. \tag{5.2.7}$$

Set now $\tilde{v}_\rho \coloneqq \tilde{\Pi}_\rho^n \tilde{v} \in H^1(K) \otimes \mathbb{V}^n$. By the exactness of the output complex (see (5.2.1)) we find a $\tilde{\tau} \in H^l(K) \otimes \mathbb{V}^{n-1}$ with

$$\|\tilde{\tau}\|_{H^l(K)} \leq \tilde{C}_B \|\tilde{v}_\rho\|_{L^2(K)}\,, \quad \mathscr{D}^{n-1}\tilde{\tau} = \tilde{v}_\rho, \tag{5.2.8}$$

for a suitable constant $\tilde{C}_B$; cf. Corollary 4.2. Hence, by the structure-preserving discretization on K we have for $\tilde{\tau}_\rho \coloneqq \tilde{\Pi}_\rho^{n-1}\tilde{\tau}$ directly

$$\mathscr{D}^{n-1}\tilde{\tau}_\rho = \mathscr{D}^{n-1}\tilde{\Pi}_\rho^{n-1}\tilde{\tau} = \tilde{\Pi}_\rho^n \mathscr{D}^{n-1}\tilde{\tau} = \tilde{v}_\rho, \quad \|\tilde{\tau}_\rho\|_{H^l(K)} \leq \tilde{C}_1 \|\tilde{\tau}\|_{H^l(K)} \leq \tilde{C}_1\tilde{C}_B \|\tilde{v}_\rho\|_{L^2(K)}\,, \tag{5.2.9}$$

where the last inequalities are due to assumption and (5.2.8). Further we define

$$\tau_h \coloneqq \Pi_h^{n-1}\tilde{\tau}_{\rho,|}\ \ ,$$

where $\tilde{\tau}_{\rho,|} \in H^{l+1}(\Omega) \otimes \mathbb{V}^{n-1}$ is the restriction of $\tilde{\tau}_\rho$ to Ω and Π_h^{n-1} is the projection from Assumption 5.2 (Note: $k = n$). Then, with the different definitions we can go ahead with some estimates.

$$\left\|\tilde{\Pi}_\rho^n \tilde{v} - \tilde{v}\right\|_{L^2(K)} \leq \tilde{C}_1 \rho \|\tilde{v}\|_{H^1(K)} \leq \tilde{C}_1 C_{\mathcal{E}} \rho \|v_\theta\|_{H^1(\Omega)} \leq \tilde{C}_1 C_{\mathcal{E}} C_2 \frac{\rho}{\theta} \|v_\theta\|_{L^2(\Omega)}\,. \tag{5.2.10}$$

In the last line we utilized (5.2.7) and Assumption 5.2. Next we see

$$\begin{aligned}
\left\|\mathscr{D}^{n-1}\tau_h - v_\theta\right\|_{L^2(\Omega)} &\leq \left\|\mathscr{D}^{n-1}\tau_h - \mathscr{D}^{n-1}\tilde{\tau}_\rho\right\|_{L^2(\Omega)} + \left\|\mathscr{D}^{n-1}\tilde{\tau}_\rho - v_\theta\right\|_{L^2(\Omega)} \\
&= \left\|\mathscr{D}^{n-1}\tau_h - \mathscr{D}^{n-1}\tilde{\tau}_\rho\right\|_{L^2(\Omega)} + \|\tilde{v}_\rho - v_\theta\|_{L^2(\Omega)} \\
&\overset{(5.2.7)}{\leq} C_1 h \|\tilde{\tau}_\rho\|_{H^{l+1}(\Omega)} + \left\|\tilde{\Pi}_\rho^n \tilde{v} - \tilde{v}\right\|_{L^2(\Omega)} \qquad \text{(see Assumption 5.2)} \\
&\leq C_1 \tilde{C}_2 \frac{h}{\rho} \|\tilde{\tau}_\rho\|_{H^l(K)} + \tilde{C}_1 C_{\mathcal{E}} C_2 \frac{\rho}{\theta} \|v_\theta\|_{L^2(\Omega)} \\
&\overset{(5.2.9)}{\leq} C_1 \tilde{C}_2 \tilde{C}_1 \tilde{C}_B \frac{h}{\rho} \|\tilde{v}_\rho\|_{L^2(K)} + \tilde{C}_1 C_{\mathcal{E}} C_2 \frac{\rho}{\theta} \|v_\theta\|_{L^2(\Omega)} \\
&\overset{(5.2.7)}{\leq} C_1 \tilde{C}_2 \tilde{C}_1 \tilde{C}_B C_{\mathcal{E}} \frac{h}{\rho} \|v_\theta\|_{L^2(\Omega)} + \tilde{C}_1 C_{\mathcal{E}} C_2 \frac{\rho}{\theta} \|v_\theta\|_{L^2(\Omega)}\,.
\end{aligned}$$

For the second inequality sign one notes $\mathscr{D}^{n-1}\tilde{\tau}_\rho = \tilde{v}_\rho$ and for the fourth one we applied (5.2.10). Consequently, there are constants c_1, c_2 independent of mesh sizes with

$$\left\|\mathscr{D}^{n-1}\tau_h - v_\theta\right\|_{L^2(\Omega)} \leq \left(c_1\frac{h}{\rho} + c_2\frac{\rho}{\theta}\right)\|v_\theta\|_{L^2(\Omega)} =: C_{Res}\,\|v_\theta\|_{L^2(\Omega)}\,. \tag{5.2.11}$$

The idea is now to show that there is a $c_R > 0$ such that the condition $h \leq c_R\theta$ implies a ρ s.t. $\left(c_1\frac{h}{\rho} + c_2\frac{\rho}{\theta}\right) = C_{Res} \leq \frac{4}{5}$. Let now $h \leq c_R\theta$ for some $c_R > 0$. In more detail, let us consider the two conditions

$$c_1\frac{h}{\rho} \overset{!}{\leq} \frac{2}{5}, \quad c_2\frac{\rho}{\theta} \overset{!}{\leq} \frac{2}{5}.$$

Hence,

$$\frac{5c_1}{2}\,h \leq \rho \leq \frac{2}{5c_2}\theta, \qquad \frac{5c_1\,c_R}{2}\theta \leq \rho \leq \frac{2}{5c_2}\theta \text{ , respectively.}$$

Inserting our assumption $\rho = \frac{1}{m}$ one gets the conditions

$$\frac{5c_2}{2\theta} \leq m \leq \frac{2}{5c_1c_R\theta} \quad \text{and} \quad m \in \mathbb{N}.$$

In other words, if the last conditions for m are satisfied, we can set $C_{Res} \leq \frac{4}{5}$, provided $h \leq c_R\theta$. In fact, we can choose always such an m since $\frac{1}{\theta}\left(\frac{2}{5c_1c_R} - \frac{5c_2}{2}\right) > 1$ for c_R small enough. Noting that a mesh refinement means a decreasing of θ we indeed get a constant c_R.
Furthermore, we obtain for the norm of τ_h the next inequality chain:

$$\begin{aligned}
\|\tau_h\|_{\mathscr{V}} &\leq C_1\,\|\tilde{\tau}_\rho\|_{H^l(\Omega)} \qquad \text{(see Assumption 5.2)}\\
&\overset{(5.2.9)}{\leq} C_1\tilde{C}_1\tilde{C}_B\,\|\tilde{v}_\rho\|_{L^2(K)}\\
&\leq C_1\tilde{C}_1\tilde{C}_B(1+\tilde{C}_1)\,\|\tilde{v}\|_{L^2(K)}\\
&\overset{(5.2.7)}{\leq} C_1\tilde{C}_1\tilde{C}_B(1+\tilde{C}_1)C_{\mathcal{E}}\,\|v_\theta\|_{L^2(\Omega)}\,.
\end{aligned} \tag{5.2.12}$$

So we have now demonstrated two things. On the one hand, we have seen that it is possible to choose $C_{Res} < 1$ in (5.2.11). And on the other hand, we have the norm estimate (5.2.12). Further, all the different constants appearing above do not depend on the mesh sizes or specific space elements. This means that when we apply Corollary 5.1 now, we directly obtain the claim. □

By exploiting the structure-preserving discretizations on K, we now obtain a practical condition $h \overset{!}{\leq} c_R\theta$, with an appropriate constant c_R, to see the well-posedness of the discretization. Although a series of constants appear in the actual proof, giving the impression that this c_R must be chosen very small, later numerical tests show that only very moderate and in some cases no additional mesh refinements, i.e. $h = \theta$, are necessary to observe stable convergence behavior. This raises the hope that c_R is often larger than what the pessimistic estimates in the proof might indicate.

Remark 5.2. To simplify the proof of Lemma 5.4 we made the assumption that the mesh sizes for the auxiliary spaces are of the form $\rho = \frac{1}{m}$. Certainly, other mesh sizes are still possible and lead to analgous results. For example, there is no issue to have $\rho = \frac{c}{m}$, $m \in \mathbb{N}_{>0}$ for a constant c in the proof. The only thing that might change is the constant c_R that relates h and θ.

5.3 Discretization approach utilizing Lagrange multiplier

Within last section, we have now established different well-posedness criteria for a modified variational problem (see Definition 5.1) coming from the Hodge–Laplace problem. One drawback of the above elaborations is the departure from the concept of a structure-preserving discretization in the sense of FEEC. For example, we did not care about the subcomplex property and for sure we have in general $\mathscr{D}^{n-1}\mathscr{V}_h^{n-1} \nsubseteq \mathscr{V}_\theta^n$. This is already clear by the mentioned possible choice of different meshes for the σ and u variable. However, in constructing complexes using the BGG procedure in Section 4.2.2, it shows that for a linking map $S^J \neq S^{n-1}$ a different discretization approach is appropriate. In such a case, the suitability of the Lagrange multiplier method from Section 4.2.4 becomes apparent, as it allows us to reintroduce the concept of a structure-preserving complex discretization. We would like to briefly explain this approach in the following. However, we also want to emphasize that this ansatz has already been demonstrated and utilized in other works, such as [10, 7, 42]. Nevertheless, in this context, we aim to present a somewhat modified and more abstract version.

Here, for the second discretization ansatz we are still in the framework of Section 4.2.2. But to clarify our setting once more, let us summarize additional key assumptions for the upcoming explanations.

Assumption 5.4.

- *We require Assumption 4.3 for the situation $k = n$. In particular we also take the points from Assumption 4.1 for granted.*
- *The differential operators d^i, $\bar{d}^i$ from (4.2.7) define closed L^2 Hilbert complexes $(\bar{W}^\circ, \bar{d}^\circ)$ and (W°, d°), where*
$$\bar{W}^i \coloneqq L^2(\Omega) \otimes \bar{\mathbb{E}}^i, \quad W^i \coloneqq L^2(\Omega) \otimes \mathbb{E}^i.$$
Then the associated domain complexes are denoted with $(\bar{U}^\circ, \bar{d}^\circ)$ and (U°, d°), meaning
$$\bar{U}^i \coloneqq H(\Omega, \bar{d}^i, \bar{\mathbb{E}}^i), \quad U^i \coloneqq H(\Omega, d^i, \mathbb{E}^i).$$
Thus, we require
$$\mathcal{R}(d^{n-1}, H^l(\Omega) \otimes \mathbb{E}^{n-1}) = U^n = L^2(\Omega) \otimes \mathbb{E}^n, \quad l \coloneqq \operatorname{ord}(d^{n-1}). \tag{5.3.1}$$
- *The index J appearing in the BGG construction (see Definition 4.2) fulfills the condition $J < n-1$, i.e. in view of the notation from Section 4.2.2, line (4.2.10) and Lemma 4.6, respectively, it is $\mathscr{U}^i = U^i, \mathscr{D}^i = d^i$ for $i = n-1$ and $i = n$.*

One notes that the linking maps $S^i \colon L^2(\Omega) \otimes \mathbb{E}^i \to L^2(\Omega) \otimes \bar{\mathbb{E}}^{i+1}$ from Assumption 4.1 satisfy $\bar{d}^{i+1} \circ S^i = -S^{i+1} \circ d^i$ on $H(\Omega, d^i, \mathbb{E}^i)$. Thus, we directly have $S^i \colon U^i \to \bar{U}^{i+1}$. Consequently, with the above mentioned points and remarks we obtain the diagram structure

$$\begin{array}{ccccccccc}
\cdots & \bar{U}^{n-2} & \xrightarrow{\bar{d}^{n-2}} & \bar{U}^{n-1} & \xrightarrow{\bar{d}^{n-1}} & \bar{U}^n & \longrightarrow & 0 \\
 & & \nearrow_{S^{n-2}} & & \nearrow_{S^{n-1}} & & & \\
\cdots & U^{n-2} & \xrightarrow{d^{n-2}} & U^{n-1} & \xrightarrow{d^{n-1}} & U^n & \longrightarrow & 0.
\end{array}$$

Now let us use this connection of the different spaces to discretize the mixed weak formulation of the Hodge–Laplace problem ((4.2.32)-(4.2.33)) of level $k = n$.

In Section 4.2.4 we saw the feasibility of the Lagrange multiplier formulations for the mixed weak Hodge–Laplace formulation. One notes that for the special setting clarified through Assumption 5.4 we have $n = k > J + 1$. Thus, in view of (4.2.43)-(4.2.46) we see that one can consider instead of (4.2.32)-(4.2.33) the new problem: *Find* $(\sigma, u, \kappa) \in U^{n-1} \times U^n \times \bar{U}^n$ *s.t.*

$$\begin{aligned}
\langle \sigma, \tau \rangle \qquad - \langle u, d^{n-1}\tau \rangle + \langle \kappa, S^{n-1}\tau \rangle &= 0, \qquad \forall \tau \in U^{n-1}, && (5.3.2)\\
\langle d^{n-1}\sigma, v \rangle \qquad\qquad\qquad\quad &= \langle f, v \rangle, \quad \forall v \in U^n, && (5.3.3)\\
\langle S^{n-1}\sigma, \eta \rangle \qquad\qquad\qquad\quad &= 0, \qquad \forall \eta \in \bar{U}^n, && (5.3.4)
\end{aligned}$$

given a $f \in U^n$. One observes that for our setting here $U^{n-1} = \mathscr{U}^{n-1}$, $U^n = \mathscr{U}^n$ and $\bar{U}^{n+1} = \{0\}$, which yields only one multiplier κ in contrast to the system (4.2.43)-(4.2.46).
Since $\mathscr{D}^{n-1} = d^{n-1}$ and due to the appearing spaces U^{n-1}, U^n in the system with Lagrange multiplier the idea is to exploit structure-preserving discretizations for (U°, d°). Attaining the latter is often easier in applications when compared to directly discretizing the BGG output complex. Then one can prove another well-posedness statement.

Lemma 5.5. *Let Assumption 5.4 hold and suppose that suitable spaces $(U_h^j)_h \subset U^j$ define a structure-preserving discretization of the bottom domain complex (U°, d°); cf. Definition 3.11. Further let $\bar{U}_h^n \subset \bar{U}^n$ s.t. the inf-sup condition*

$$\inf_{0 \neq \eta_h \in \bar{U}_h^n} \sup_{0 \neq \tau_h \in U_h^{n-2}} \frac{\langle \bar{d}^{n-1} S^{n-2} \tau_h, \eta_h \rangle}{\|\tau_h\|_U \, \|\eta_h\|} \geq C_{IS} > 0 \tag{5.3.5}$$

is valid, where C_{IS} does not depend on h and $\|\tau\|_U^2 \coloneqq \|\tau\|^2 + \|d^{n-2}\tau\|^2$.
Then the discrete system with multiplier, i.e. the problem to seek for $(\sigma_h, u_h, \kappa_h) \in U_h^{n-1} \times U_h^n \times \bar{U}_h^n$ s.t.

$$\begin{aligned}
\langle \sigma_h, \tau_h \rangle \qquad - \langle u_h, d^{n-1}\tau_h \rangle + \langle \kappa_h, S^{n-1}\tau_h \rangle &= 0, \qquad \forall \tau_h \in U_h^{n-1}, && (5.3.6)\\
\langle d^{n-1}\sigma_h, v_h \rangle \qquad\qquad\qquad\quad &= \langle f, v_h \rangle, \quad \forall v_h \in U_h^n, && (5.3.7)\\
\langle S^{n-1}\sigma_h, \eta_h \rangle \qquad\qquad\qquad\quad &= 0, \qquad \forall \eta_h \in \bar{U}_h^n, && (5.3.8)
\end{aligned}$$

determines a well-posed discretization; see Definition 2.11.

Proof. The proof is inspired by the proof steps in [42, Theorem 9.1].
At different places below we will write for the reason of readability $A \prec B$, if expression A is smaller than B up to some constant C, where C does not depend on appearing specific space elements. Further, we use the abbreviation $\|\cdot\|_U$ for the graph norms related to the d^i, U^i, respectively.
First we set

$$Z \coloneqq \left\{ \tau_h \in U_h^{n-1} \;\middle|\; \langle v_h, d^{n-1}\tau_h \rangle + \langle \eta_h, S^{n-1}\tau_h \rangle = 0, \ \forall (v_h, \eta_h) \in U_h^n \times \bar{U}_h^n \right\}$$

and $\mathfrak{a}(\sigma, \tau) \coloneqq \langle \sigma, \tau \rangle$. By the subcomplex property, meaning $d^{n-1}U_h^{n-1} \subset U_h^n$, we see that

$$\mathfrak{a}(\sigma_h, \sigma_h) = \|\sigma_h\|_U^2, \quad \forall \, \sigma_h \in Z. \tag{5.3.9}$$

Fix some arbitrary $(u_h, \kappa_h) \in U_h^n \times \bar{U}_h^n$ and set $l \coloneqq \operatorname{ord}(d^{n-1})$.
By the exactness assumption (5.3.1) at level n we find due to Corollary 2.1 a $\nu \in H^l(\Omega) \otimes \mathbb{E}^{n-1}$ that satisfies

$$d^{n-1}\nu = u_h \quad \text{and} \quad \|\nu\|_{H^l} \prec \|u_h\| \,.$$

This implies

$$d^{n-1}\nu_h = u_h, \quad \|\nu_h\|_U \prec \|u_h\|\,, \tag{5.3.10}$$

if $\nu_h \coloneqq \Pi_h^{n-1}\nu$ with Π_h^j denoting the L^2-bounded cochain projections onto (U_h°, d°).
Let $\bar{P}_h^n\colon L^2(\Omega)\otimes\bar{\mathbb{E}}^n \to \bar{U}_h^n$ denote the L^2-orthogonal projection onto the space $\bar{U}_h^n$.
Consequently, $\langle \bar{d}^{n-1}S^{n-2}\tau, \eta_h\rangle = \langle \bar{P}_h^n\bar{d}^{n-1}S^{n-2}\tau, \eta_h\rangle$, $\forall \eta_h \in \bar{U}_h^n$, $\tau \in U^{n-2}$. Hence, because of the inf-sup inequality (5.3.5) from the assertion and applying Lemma 2.5 we see that

$$\bar{P}_h^n\bar{d}^{n-1}S^{n-2}\colon U_h^{n-2} \to \bar{U}_h^n \quad \text{(compare Figure 5)}$$

has a bounded right-inverse, where the operator norm bound for the right-inverse does not depend on h. More precisely, it is possible to choose a $w_h \in U_h^{n-2}$ s.t.

$$\bar{P}_h^n\bar{d}^{n-1}S^{n-2}w_h = \bar{P}_h^nS^{n-1}\nu_h - \kappa_h \quad \text{and} \quad \|w_h\|_U \prec \left\|\bar{P}_h^nS^{n-1}\nu_h - \kappa_h\right\|.$$

Set $\tau_h \coloneqq d^{n-2}w_h + \nu_h \in U_h^{n-1}$. Then, on the one hand, it follows $d^{n-1}\tau_h = d^{n-1}\nu_h = u_h$ and

$$\begin{aligned}\langle S^{n-1}\tau_h, \kappa_h\rangle &= \langle -\bar{d}^{n-1}S^{n-2}w_h + S^{n-1}\nu_h, \kappa_h\rangle = \langle -\bar{P}_h^n\bar{d}^{n-1}S^{n-2}w_h + \bar{P}_h^nS^{n-1}\nu_h, \kappa_h\rangle\\ &= \langle \kappa_h - \bar{P}_h^nS^{n-1}\nu_h + \bar{P}_h^nS^{n-1}\nu_h, \kappa_h\rangle = \|\kappa_h\|^2\,.\end{aligned} \tag{5.3.11}$$

One notes $\bar{d}^{n-1}S^{n-2}w_h = -S^{n-1}d^{n-2}w_h$. And on the other hand, we can estimate

$$\begin{aligned}\|\tau_h\|_U &\le \left\|d^{n-2}w_h\right\| + \|\nu_h\| + \left\|d^{n-1}\nu_h\right\|\\ &\prec \left\|S^{n-1}\nu_h - \kappa_h\right\| + \|u_h\| \prec \|\kappa_h\| + \|u_h\|\,.\end{aligned} \tag{5.3.12}$$

The last estimates (5.3.10)-(5.3.12) yield

$$\begin{gathered}\|\kappa_h\|^2 + \|u_h\|^2 = \langle d^{n-1}\tau_h, u_h\rangle + \langle S^{n-1}\tau_h, \kappa_h\rangle\\ \|\tau_h\|_U \prec \|\kappa_h\| + \|u_h\|\,.\end{gathered}$$

The arbitrariness of the tuple (u_h, κ_h) leads to the inf-sup relation

$$\inf_{(0,0)\neq(v_h,\eta_h)\in U_h^n\times\bar{U}_h^n}\ \sup_{0\neq\sigma_h\in U_h^{n-2}} \frac{\langle d^{n-1}\sigma_h, v_h\rangle + \langle S^{n-1}\sigma_h, \eta_h\rangle}{\|\sigma_h\|_U\,(\|\eta_h\| + \|v_h\|)} \ge C > 0\,. \tag{5.3.13}$$

This and (5.3.9) finish the proof, due to Lemma 2.11.

□

For the sake of clarity and a better understanding, in the next figure, we have displayed all the relevant spaces and projections appearing in the proof of the previous lemma for this second approach involving the Lagrange multiplier.

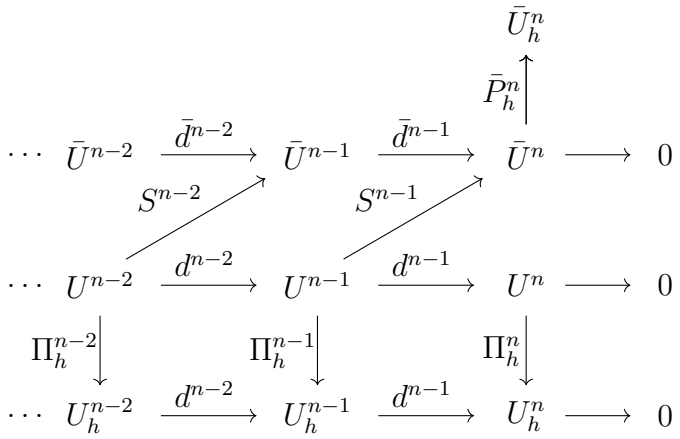

Figure 5: If $k = n$ and $J < n - 1$ one can use structure-preserving discretizations of the bottom chain to state a well-posedness condition for the Lagrange multiplier formulation. In this situation we only need U_h^{n-1}, U_h^n, $\bar{U}_h^n$ for disretization, whereas U_h^{n-2} is an auxiliary space relevant for the mentioned condition.

For the specific Hodge–Laplace problem implied by the output complex at level n, we see here that knowledge of a discretization of the input complexes might be helpful. This raises the question: Why not always discretize the input complexes in a structure-preserving manner during the BGG construction procedure to create Finite Element spaces for the actual output complex $(\mathscr{V}^\circ, \mathscr{D}^\circ)$? Although this approach initially sounds promising, it becomes evident that generally the discretization of the input chains is not compatible with the linking maps. By the previously introduced notation and the properties of S^i we have e.g. $S^i \colon U^i \to \bar{U}^{i+1}$. Such relations often do not hold if we go to the discrete setting and use structure-preserving discretizations $U_h^j \subset U^j$, $\bar{U}_h^j \subset \bar{U}^j$. This is why the BGG construction from Section 4.2 is an important tool for generating and studying new Hilbert chains. However, in general, it does not directly address the question of how to find proper discretizations of the generated sequences.

We want to conclude the investigation regarding the discretization of the complex $(\mathscr{V}^\circ, \mathscr{D}^\circ)$ within the more abstract setting for now and finally take a step towards concrete numerical methods and applications. Specifically, we will now turn to the theory of isogeometric analysis and briefly outline the key ideas and fundamental concepts of this numerical paradigm. This will lay the groundwork, or rather, define the FE spaces that we will also use to develop discretization schemes. The plan and long-term objective is to apply both Lemmata 5.4 and 5.5 in the context of the complexes $(\mathscr{V}_n^{\circ,J}, \mathscr{D}_n^{\circ,J})$ from Alt^l-valued forms (defined though Lemma 4.9) exploiting results and ideas of isogeometric analysis.

6 Isogeometric Analysis

The objective of this section is to summarize main aspects within the field of Isogeometric Analysis (IGA) and to state some expedient results for the considerations later in the text. Fundamental idea behind IGA is to use the same function spaces for representing or parameterizing the computational domain as well as for defining the actual FE spaces. Typically, B-splines or NURBS are used for this purpose, bridging the capabilities of Computer-Aided Design (CAD) with classical FE theory. In addition to providing greater flexibility in representing geometries, this approach also allows for easier manipulation of the regularity of the basis functions. The development of the underlying numerical paradigm was triggered by Hughes et al. in 2005 through the seminal paper [49].
Certainly, the subsequent remarks and statements should not be seen as an exhaustive introduction into this wide field and we refer interested readers to the publications [61] or [31, 17] on this subject to get more detailed information. Below we divide the explanations roughly into three parts. We start with the definition of B-splines and NURBS which are the elementary function classes for isogeometric methods. Thereafter we show how one can define isogeometric discrete functions spaces utilizing the mentioned B-splines. And as a last point we look at properties of the introduced objects. In particular we concentrate on projections onto the finite-dimensional spline spaces and related approximation properties. Here, our main references are [31, 49] as well as [17, 27] and we orient ourselves towards the results and notions of them.

6.1 B-splines and NURBS

Our starting point are some very basic definitions that however are necessary to understand the important properties of isogeometric function spaces, e.g. the possibility to regulate the function smoothness.

6.1.1 Univariate case

As done quite often in books and papers dealing with B-splines and NURBS we begin with definitions in the one-dimensional case. Because, the definition of the multivariate splines will be obtained from the $1D$ case by a tensor product argument.

An non-decreasing sequence of real numbers

$$\Xi \coloneqq \{\xi_1 \leq \xi_2 \leq \cdots \leq \xi_{\mathfrak{n}+p+1}\} \tag{6.1.1}$$

for some $p \in \mathbb{N}$ is named a *knot vector*. If the multiplicity of the first and last knots ξ_1 and $\xi_{\mathfrak{n}+p+1}$ is $p+1$, which means $\xi_1 = \xi_2 = \cdots = \xi_{p+1}$ and $\xi_{\mathfrak{n}+1} = \xi_{\mathfrak{n}+2} = \cdots = \xi_{\mathfrak{n}+p+1}$, then the knot vector is referred to as *p-open*. Further, we write m_j for the multiplicity of the j-th knot, i.e. it is

$$\{\underbrace{\xi_1, \ldots, \xi_1}_{m_1 \text{ times}}, \underbrace{\xi_2, \ldots, \xi_2}_{m_2 \text{ times}}, \ \cdots\}.$$

Definition 6.1 (**B-splines**). *The B-spline functions $\widehat{B}_{i,p}$ of degree p corresponding to a given p-open knot vector $\Xi = \{\xi_1 \leq \xi_2 \leq \cdots \leq \xi_{\mathfrak{n}+p+1}\}$ is defined recursively by the* Cox–DeBoor formula*:*

$$\widehat{B}_{i,0}(\zeta) \coloneqq \begin{cases} 1, & \text{if } \zeta \in [\xi_i, \xi_{i+1}), \\ 0, & \text{else,} \end{cases} \tag{6.1.2}$$

and if $p \in \mathbb{N}_{\geq 1}$ we set

$$\widehat{B}_{i,p}(\zeta) \coloneqq \frac{\zeta - \xi_i}{\xi_{i+p} - \xi_i} \widehat{B}_{i,p-1}(\zeta) + \frac{\xi_{i+p+1} - \zeta}{\xi_{i+p+1} - \xi_{i+1}} \widehat{B}_{i+1,p-1}(\zeta). \tag{6.1.3}$$

In the last line we use the convention $0/0 \coloneqq 0$ *to obtain well-definedness.*

In view of the previous definition we obtain $\mathfrak{n}$ splines $\widehat{B}_{1,p}, \dots, \widehat{B}_{\mathfrak{n},p}$ for degree p if the knot vector has the form (6.1.1).

Assumption 6.1. *If we consider B-splines of degree* p *then we require the underlying knot vector to be* p*-open and that the multiplicity of each knot is bounded by* $p+1$*. Further, w.l.o.g. we assume the first and last knot to be* 0*,* 1*, respectively.*

Due to the recursive definition we get several properties for B-spline functions. The most important ones, at least for our purposes, are listed in the subsequent lemma.

Lemma 6.1 (**Properties of the B-splines**)**.**

- *B-splines are piecewise smooth. To be more precise,* $\widehat{B}_{i,p}$ *restricted to each open interval* (ξ_j, ξ_{j+1}) *is a polynomial of degree* p*. The support of the spline* $\widehat{B}_{i,p}$ *is a subset of the interval* $[\xi_i, \xi_{i+p+1}]$*.*
- *If the multiplicities of all inner knots* m_j *fulfill* $1 \leq m_j \leq m \leq p$ *then one has* $\widehat{B}_{i,p} \in C^{p-m}((\xi_1, \xi_{\mathfrak{n}+p+1}))$*. Further, if the multiplicity at a knot* ξ_j *fulfills* $m(\xi_j) = p+1$*, then there exist B-splines which are discontinuous at* ξ_j*; cf. Figure 7 (b).*
- *The B-spline functions* $\widehat{B}_{1,p}, \dots, \widehat{B}_{\mathfrak{n},p}$ *are linearly independent and form a partition of unity, this means* $\sum_i \widehat{B}_{i,p} = 1$*.*
- *For* $p \geq 1$ *and in the interior of each open knot interval we can compute the derivative* $\partial_\zeta \widehat{B}_{i,p}$ *via the formula*

$$\partial_\zeta \widehat{B}_{i,p}(\zeta) = \frac{p}{\xi_{i+p} - \xi_i} \widehat{B}_{i,p-1}(\zeta) - \frac{p}{\xi_{i+p+1} - \xi_{i+1}} \widehat{B}_{i+1,p-1}(\zeta) \tag{6.1.4}$$

  with $\widehat{B}_{1,p-1}(\zeta) \coloneqq \widehat{B}_{\mathfrak{n}+1,p-1}(\zeta) \coloneqq 0$*. Consequently, derivatives of B-splines yield again B-splines and the differentiation can be implemented efficiently.*

Proof. Follows by induction utilizing the Cox–DeBoor formula and the remarks in [31, Section 2.1.1]. □

As an example, we display in Figure 6 the six B-spline functions of degree $p = 2$ and their first derivatives corresponding to the knot vector $\Xi = \{0, 0, 0, 0.25, 0.5, 0.75, 1, 1, 1\}$.

Next we define NURBS (**N**on-**u**niform **r**ational **B**-**s**plines) with the help of B-splines and so-called weights $w_1, \dots, w_{\mathfrak{n}} \in \mathbb{R}_{>0}$.[11] That is done by the following formula.

Definition 6.2 (**NURBS**)**.** *For given knot vector* Ξ *of the form* (6.1.1) *and positive weights* $w_1, \dots, w_{\mathfrak{n}}$ *we define the NURBS basis functions*

$$\widehat{N}_{i,p}(\zeta) \coloneqq \frac{w_i \, \widehat{B}_{i,p}(\zeta)}{\sum_{j=1}^{\mathfrak{n}} w_j \, \widehat{B}_{j,p}(\zeta)}, \qquad \text{for } i = 1, \dots, \mathfrak{n}. \tag{6.1.5}$$

[11] $\mathbb{R}_{>0}$ denotes the set of positive real numbers.

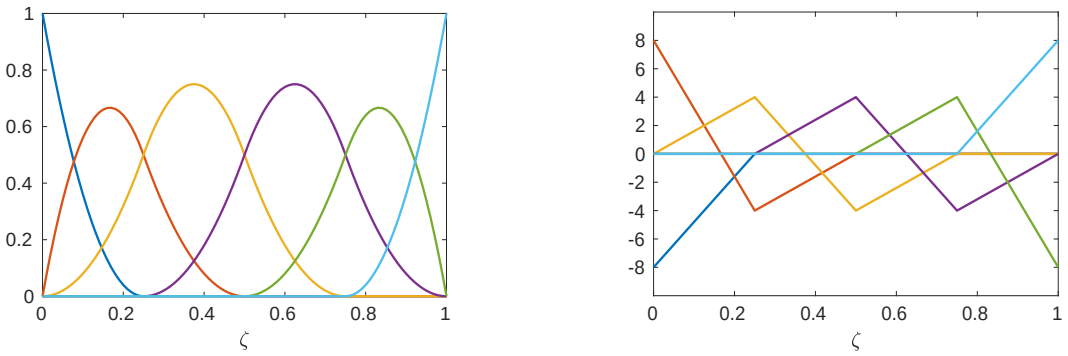

(a) Quadratic B-spline functions

(b) Corresponding first derivatives

Figure 6: Due to the multiplicity $m = 1$ of the interior knots we obtain C^1-regular B-splines $\widehat{B}_{i,p}$ on the left. The corresponding first derivatives $\partial_\zeta \widehat{B}_{i,p}$ are shown on the right.

To show the influence of the w_i we display in Figure 7 (a) the quadratic NURBS obtained by the B-splines from Figure 6 (a) together with a vector of weights $\mathbf{w} = (1, 4, 2, 1, 3, 1)$. Obviously, NURBS can be interpreted as generalized B-splines since the choice $w_1 = 1, \dots, w_{\mathfrak{n}} = 1$ yields the usual B-splines. Without difficulties, similar properties as in Lemma 6.1 can be proven for NURBS, too. This means the piecewise smoothness holds and one sees $\widehat{N}_{i,p} \in C^{p-m}((\xi_1, \xi_{\mathfrak{n}+p+1}))$ if m bounds the multiplicity of the inner knots. Furthermore, the functions $\widehat{N}_{1,p}, \dots, \widehat{N}_{\mathfrak{n},p}$ remain linearly independent. The space spanned by the NURBS determined by the knot vector Ξ, the weights $w_1, \dots, w_{\mathfrak{n}}$ and the degree p is denoted as

$$\widehat{N}(\Xi, p, W) \coloneqq \operatorname{span}\{\widehat{N}_{1,p}, \dots, \widehat{N}_{\mathfrak{n},p}\},$$

where $W(\zeta) \coloneqq \sum_{j=1}^{\mathfrak{n}} w_j \, \widehat{B}_{j,p}(\zeta)$ is called *weight function*. Using NURBS we can parameterize curves. Namely, provided *control points* $\mathbf{C}_1, \dots, \mathbf{C}_{\mathfrak{n}} \in \mathbb{R}^n$ we get with

$$F(\zeta) = \sum_{i=1}^{\mathfrak{n}} \widehat{N}_{i,p}(\zeta) \, \mathbf{C}_i,$$

a curve which starts in $\mathbf{C}_1$ and ends at $\mathbf{C}_{\mathfrak{n}}$. The idea of using NURBS for the description of geometric objects or for parametrization is fundamental. Admittedly, the one-dimensional case with its curves is quite limiting, but an analogous combination of NURBS and control points is also carried out in the multi-dimensional case later on. However, before that, we would like to explain two ways to refine a given NURBS space. In other words, we are looking for ways to obtain a new space $\widehat{N}(\tilde{\Xi}, \tilde{p}, W) \supset \widehat{N}(\Xi, p, W)$ from $\widehat{N}(\Xi, p, W)$. In doing so, we aim to maintain regularity at the internal knot points, and the weight function W should also remain unchanged. The latter is important for NURBS parametrizations in order to modify the NURBS spaces without changing the geometry.

- **h-refinement:** On the one hand, it is possible to successively insert additional knots $\tilde{\xi}_1, \dots, \tilde{\xi}_k$ so that a new knot vector $\tilde{\Xi} \supset \Xi$ is obtained. The polynomial degree remains fixed in this process, i.e. $\tilde{p} = p$. The knot insertion will later correspond to a step of mesh refinement in isogeometric methods. The procedure for inserting a single knot $\tilde{\xi}_1$ can be condensed in three steps:
  - Find j such that $\xi_j \leq \tilde{\xi}_1 \leq \xi_{j+1}$.

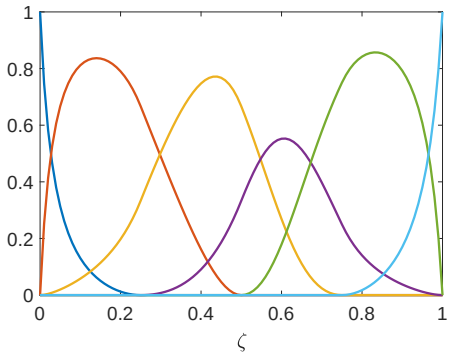

(a) Quadratic NURBS

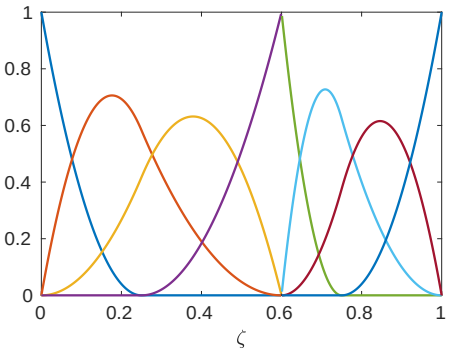

(b) B-splines with discontinuity

Figure 7: On the left we see the deformed B-splines from Figure 6 (a) due to a non-trivial weight function. On the right we see B-splines with a discontinuity at 0.6 because of the knot vector $\{0,0,0,0.25,0.6,0.6,0.6,0.75,1,1,1\}$ and $p=2$.

– Set

$$\alpha_i = \begin{cases} 1, \text{ for } i \leq j-p \\ \frac{\tilde{\xi}_1 - \xi_i}{\xi_{i+p+1}-\xi_i}, \text{ for } i = j-p+1,\dots,j \\ 0, \text{ for } i > j\ . \end{cases}$$

– Define a new vector of weights

$$(\tilde{w}_1,\dots,\tilde{w}_{\mathfrak{n}+1}) \coloneqq (w_1,\dots,w_{j-p},w^a_{j-p+1},\dots,w^a_j,w_j,\dots,w_{\mathfrak{n}}),$$

with $w^a_i = \alpha_i w_i + (1-\alpha_{i+1})w_{i+1}$ for $i = j-p+1,\dots,j$.
Then the new basis functions are determined by the new knots and weights $\tilde{w}_i$.

- **p-refinement:** On the other hand one can increase the polynomial degree $p \to p+1$ while maintaining the regularity of the basis functions. Therefore, we also obtain a new knot vector $\tilde{\Xi}$ to ensure the correct regularity at the inner knots. More specifically, if we initially have s distinct knots, applying a p refinement algorithm that preserves regularity results in an addition of s extra knots.We refrain from providing an explicit description of a degree elevation procedure here and refer to [61] for further information.

In the both latter refinement cases we have $\widehat{N}(\Xi,p,W) \subset \widehat{N}(\tilde{\Xi},\tilde{p},W)$.
It should be noted the existence of another refinement strategy, namely the **k-refinement** which is a combination of degree elevation and knot insertion step. First one elevates the degree and then one inserts new knots in such a way that the regularity at the new knots is maximal. However, for our purposes it is enough to know the degree elevation and the knot insertion procedure. That is why we do not give details on k-refinement here.

As a last point for this subsection, we want to introduce an abbreviation for special NURBS spaces. In case of a constant weight function W and if all internal knots have multiplicity $m = p-r,\ r \in \{-1,0,\dots,p-1\}$, we write for the space $\widehat{N}(\Xi,p,W)$ just

$$S^r_p \coloneqq \operatorname{span}\{\widehat{B}_{1,p},\dots,\widehat{B}_{\mathfrak{n},p}\}. \tag{6.1.6}$$

In other words, S^r_p denotes always a space of B-splines with degree p and global regularity r, i.e. $S^r_p \subset C^r((0,1))$. Clearly, the S^r_p still depend on the actual knot values, but often for explanations the exact knots are not directly needed. More important is the *mesh size* of the subdivisions induced by the knot distribution. More details on that in the after next section.

6.1.2 Multivariate case

Multivariate B-splines are defined utilizing univariate splines following a tensorization argument. Unfortunately, this comes along with a somewhat more elaborate notation. Again we write n for the number of spatial dimensions. Then we define the polynomial degree vector $\mathbf{p} \coloneqq (p_1, \dots, p_n)$ and for each spatial dimension a p_l-open knot vector $\Xi_l = \{\xi_1^l, \dots, \xi_{\mathfrak{n}_l+p_l+1}^l\}$, $l = 1, \dots, n$. Besides we write $\boldsymbol{\Xi} \coloneqq \Xi_1 \times \Xi_2 \times \cdots \times \Xi_n$. Using the multi-index set

$$\mathbf{I} \coloneqq \{(i_1, \dots, i_n) \mid 1 \leq i_l \leq \mathfrak{n}_l,\ l = 1, \dots, n\}$$

and the already defined univariate spline basis functions, we introduce multivariate B-spline basis through:

Definition 6.3 (**Multivariate B-splines**).

$$\widehat{B}_{\mathbf{i},\mathbf{p}}(\boldsymbol{\zeta}) \coloneqq \prod_{l=1}^{n} \widehat{B}_{i_l,p_l}(\zeta_l), \qquad \forall\, \mathbf{i} \in \mathbf{I}, \tag{6.1.7}$$

where $\boldsymbol{\zeta} = (\zeta_1, \dots, \zeta_n) \in \mathbb{R}^n$. This leads us to an obvious definition for multivariate NURBS. We only need to change the weights set to $\{w_\mathbf{i} \mid \mathbf{i} \in \mathbf{I},\ 0 < w_\mathbf{i}\}$ and use

Definition 6.4 (**Multivariate NURBS**).

$$\widehat{N}_{\mathbf{i},\mathbf{p}}(\boldsymbol{\zeta}) \coloneqq \frac{w_\mathbf{i}\, \widehat{B}_{\mathbf{i},\mathbf{p}}(\boldsymbol{\zeta})}{\sum_{\mathbf{j}\in\mathbf{I}} w_\mathbf{j}\, \widehat{B}_{\mathbf{j},\mathbf{p}}(\boldsymbol{\zeta})}, \qquad \forall\, \mathbf{i} \in \mathbf{I}. \tag{6.1.8}$$

The set $\widehat{\Omega} \coloneqq (\xi_1^1, \xi_{\mathfrak{n}_1+p_1+1}^1) \times \cdots \times (\xi_1^n, \xi_{\mathfrak{n}_n+p_n+1}^n)$ is referred to as the *parametric domain*. The regularity properties of multivariate splines stem from the characteristics of univariate B-splines and NURBS. For instance, $\widehat{N}_{\mathbf{i},\mathbf{p}}$ exhibits piecewise smoothness within $\widehat{\Omega}$, and $\widehat{N}_{\mathbf{i},\mathbf{p}} \in C^{p-m}(\widehat{\Omega})$ if the polynomial degrees satisfy $1 \leq p \leq p_i$ and all multiplicities of the internal knots of each knot vector Ξ_l are bounded by m. Additionally, we denote $\widehat{N}(\boldsymbol{\Xi}, \mathbf{p}, W)$ as the space spanned by the NURBS functions $\widehat{N}_{\mathbf{i},\mathbf{p}}$ within $\widehat{\Omega}$. Here, W represents the weight function in the denominator of (6.1.8).

Moreover, analogous refinement strategies to those in one dimension are also applicable to $\widehat{N}(\boldsymbol{\Xi}, \mathbf{p}, W)$, namely knot insertion and degree elevation. These strategies are just employed for each coordinate direction separately.

The generalization of NURBS curves to the case of multivariate splines leads to NURBS surfaces, NURBS volumes etc. and are defined in the subsequent chapter.

6.2 Mesh structure and discrete function spaces

The extension to multi-dimensions gives us the possibility to parametrize various geometries in different dimensions. For example if we choose a set of control points $\{\mathbf{C}_\mathbf{i} \mid \mathbf{i} \in \mathbf{I}\}$ in $\mathbb{R}^m$ then we obtain with

$$\mathbf{F} \colon \widehat{\Omega} \to \mathbb{R}^m\ ,\ \boldsymbol{\zeta} \mapsto \mathbf{F}(\boldsymbol{\zeta}) \coloneqq \sum_{\mathbf{i}\in\mathbf{I}} \widehat{N}_{\mathbf{i},\mathbf{p}}(\boldsymbol{\zeta})\, \mathbf{C}_\mathbf{i}, \tag{6.2.1}$$

the parametrization of a manifold in $\mathbb{R}^m$.

As already mentioned, we assume after some rescaling w.l.o.g. that the knot vectors satisfy $\xi_1^l = 0$ and $\xi_{\mathfrak{n}_l+p_l+1} = 1$ for $l = 1, \dots, n$. For this reason the parametric domain has the form $\widehat{\Omega} = (0, 1)^n$, i.e. it is the interior of an n-dimensional unit hypercube.

To apply isogeometric methods for approximating weak solutions of PDEs, such as the abstract Hodge–Laplacian, one follows a procedure similar to the standard FE approach. Firstly, a partition of the computational domain $\Omega \subset \mathbb{R}^n$ is needed to create a mesh. Secondly, discrete spaces must be defined that correspond to this mesh. However, while classical FE methods often approximate curved geometries using triangles or more general polyhedra, the isogeometric analysis approach allows for accurate representations for various shapes, e.g. conic sections as demonstrated in [18]. The fundamental concept of IGA, as implied by its name, is to utilize B-splines and NURBS for both describing the computational domain Ω and defining the discrete function spaces. This implies that, given a knot vector $\boldsymbol{\Xi}^0$ and polynomial degree p, the domain Ω can be represented as a mapping of the form (6.2.1), meaning $\Omega = \mathbf{F}(\widehat{\Omega})$, with appropriately chosen control points. Specifically, we assume that it holds $\mathbf{F} \in (\widehat{N}(\boldsymbol{\Xi}^0, \mathbf{p}^0, W))^n$.

Subsequently, we will consider two types of meshes associated with a refinement $\widehat{N}(\boldsymbol{\Xi}, \mathbf{p}, W) \supset \widehat{N}(\boldsymbol{\Xi}^0, \mathbf{p}^0, W)$. The so-called *Bézier* mesh $\widehat{M}$ in the parametric domain $\widehat{\Omega}$ is determined by the knots in $\boldsymbol{\Xi}$ as follows:

Let $\boldsymbol{\Psi} = \{\psi_1^1, \dots, \psi_{L_1}^1\} \times \cdots \times \{\psi_1^n, \dots, \psi_{L_n}^n\}$ be the knot vector $\boldsymbol{\Xi}$ without knot repetitions.
Then $\widehat{M} \coloneqq \{K_{\mathbf{j}} \coloneqq (\psi_{j_1}^1, \psi_{j_1+1}^1) \times \cdots \times (\psi_{j_n}^n, \psi_{j_n+1}^n) \mid \mathbf{j} = (j_1, \dots, j_n), \text{ with } 1 \leq j_i < L_i\}$
determines the *parametric mesh*.

And the second mesh $\mathcal{M}$ in the domain Ω often termed *physical mesh* is just given by the image of the mesh $\widehat{M}$.

$$\mathcal{M} \coloneqq \{\mathcal{K} \subset \Omega \mid \mathcal{K} = \mathbf{F}(K_{\mathbf{j}}),\ K_{\mathbf{j}} \in \widehat{M}\}.$$

For a mesh $\mathcal{M}$ one defines the global mesh size $h \coloneqq \max\{h_{\mathcal{K}} \mid \mathcal{K} \in \mathcal{M}\}$, where for $\mathcal{K} \in \mathcal{M}$ the diameter $h_{\mathcal{K}} \coloneqq \operatorname{diam}(\mathcal{K})$ is the *element size*. A physical mesh with mesh size h is denoted in the following with $\mathcal{M}_h$.

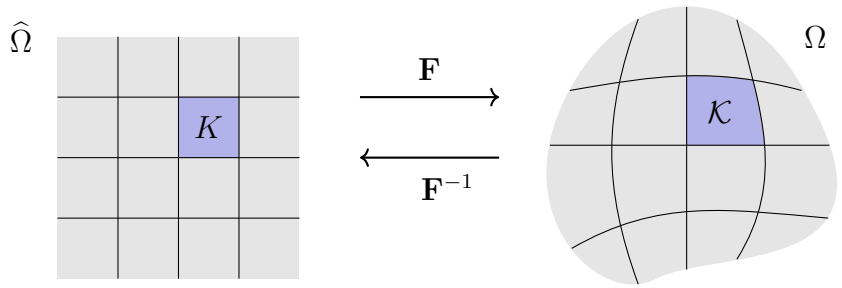

Figure 8: Mesh in the physical domain is obtained from mesh in the parametric domain.

In order to exploit approximation results and to obtain appropriate functions in the physical domain when using isogeometric methods, we have to require additional properties for the mesh. Further, there are also some restrictions on $\mathbf{F}$. The different assumptions are summarized in the next definition.

Definition 6.5 (**Regular mesh and parametrization**).
We will call a family of countably infinite meshes $\left(\mathcal{M}_h\right)_h$, $h > 0$, $h \to 0$, *defined utilizing the parametrization* $\mathbf{F}$ *regular, if we have:*

- ***Regular parametrization:*** $\mathbf{F}$ *is globally Lipschitz continuous with Lipschitz continuous inverse* $\mathbf{F}^{-1}$. *Besides,* $\mathbf{F}$ *restricted to the closure of one element* $K = \mathbf{F}^{-1}(\mathcal{K}) \in \widehat{M}$ *is*

smooth with smooth inverse, i.e. $\mathbf{F}_{|\overline{K}}$, $\mathbf{F}_{|\overline{\mathcal{K}}}^{-1}$ *are* C^∞*-regular. Here,* $\widehat{M}$ *stands for the non-refined mesh, i.e. the parametric mesh with maximal mesh size* h*.*

- ***Quasi-uniform mesh:*** *Further there exists a constant* c_u *independent from the mesh size such that* $h_{\mathcal{K}} \leq h \leq c_u\, h_{\mathcal{K}}$ *for all* $\mathcal{K} \in \mathcal{M}_h$*.*
- ***Shape-regular mesh:*** *We can choose a* $c_s > 0$ *independent of the mesh size* h *and element sizes* $h_{\mathcal{K}}$ *s.t.* $h_{\mathcal{K}} \leq c_s|\mathcal{K}|$, $\forall \mathcal{K} \in \mathcal{M}_h$*, where* $|\mathcal{K}|$ *denotes the volume of element* $\mathcal{K}$ *in* $\mathbb{R}^n$*.*

Assumption 6.2. *From now on we assume all meshes and parametrizations to fulfill the regularity properties from above. And when we are talking about a regular mesh* $\mathcal{M}_h$ *alone, we simply mean that there exists a family of regular meshes, as defined above, to which* $\mathcal{M}_h$ *belongs.*

Remark 6.1 (Regarding mesh sizes). To enhance reproducibility and simplify the explanation of the examples, we will consistently use in the different examples later meshes generated through uniform parametric Bézier meshes. Additionally, in all following numerical tests the term "mesh size ρ" refers to the situation where the corresponding Bézier mesh consists of ρ^{-n} many elements. This implies that we have $1/\rho$ subdivisions in each coordinate direction. Since we consistently employ smooth parametrizations, this new concept of mesh size is equivalent to the previously introduced one, ensuring that the mesh sizes are of the same order as the original mesh sizes.

Having such a regular mesh we can introduce the IGA basis functions corresponding to the mesh.

Definition 6.6 (**Isogeometric discrete function spaces**)**.**
Let $\widehat{N}(\boldsymbol{\Xi}, \mathbf{p}, W) \supset \widehat{N}(\boldsymbol{\Xi}^0, \mathbf{p}^0, W)$ *be a refinement of the NURBS space which defines the geometry* Ω *and let the refinement define a regular mesh* $\mathcal{M}_h$ *with mesh size* h*.*
Then we define two types of discrete spaces. On the one hand we consider

$$U_{h,\mathbf{p}} \coloneqq \{u_h = \hat{u}_h \circ \mathbf{F}^{-1} \mid \hat{u}_h \in \widehat{U}_{h,\mathbf{p}}\}, \quad \text{where } \widehat{U}_{h,\mathbf{p}} \coloneqq \widehat{N}(\boldsymbol{\Xi}, \mathbf{p}, W).$$

This means for latter definition we follow the isoparametric paradigm meaning we use the same NURBS for geometry description and the spaces. But sometimes, especially if one considers discrete Hilbert chains, it is convenient to focus on the push-forwards of B-splines. Hence, on the other hand, we set

$$V_{h,\mathbf{p}} \coloneqq \{v_h = \hat{v}_h \circ \mathbf{F}^{-1} \mid \hat{v}_h \in \widehat{V}_{h,\mathbf{p}}\}, \quad \text{where } \widehat{V}_{h,\mathbf{p}} \coloneqq \widehat{N}(\boldsymbol{\Xi}, \mathbf{p}, 1),$$

i.e. the parametric basis functions have a constant weight function $W = 1$*.*

Sometimes, we will simply refer to spaces from the last definition as IG spaces. Further, in view of (6.1.7) and the abbreviation (6.1.6), we write for special spaces of the form $\widehat{N}(\boldsymbol{\Xi}, \mathbf{p}, 1)$ just $S^{r_1,\dots,r_2}_{p_1,\dots,p_n}$ or $S^{\mathbf{r}}_{\mathbf{p}}$ for proper $\mathbf{p} = (p_1, \dots, p_n)$, $\mathbf{r} = (r_1, \dots, r_n)$. To be more precise, we define

$$S^{\mathbf{r}}_{\mathbf{p}} \coloneqq S^{r_1,\dots,r_2}_{p_1,\dots,p_n} \coloneqq S^{r_1}_{p_1} \otimes \ \dots \ \otimes S^{r_n}_{p_n}. \tag{6.2.2}$$

Consequently, for reasons of readability, we drop the mesh size h or the knot vector in the notation. Such spaces $V_{h,\mathbf{p}}$ and also the $U_{h,\mathbf{p}}$ will be used later to get approximate solutions to different PDE problems and they take on the role of Finite Element spaces in the context of the numerical methods.
Finally we want to remark that the spaces $V_{h,\mathbf{p}}$ and $U_{h,\mathbf{p}}$ are spanned by the basis functions

$$N_{\mathbf{i},\mathbf{p}} \coloneqq \widehat{N}_{\mathbf{i},\mathbf{p}} \circ \mathbf{F}^{-1}, \quad \mathbf{i} \in \mathbf{I}, \tag{6.2.3}$$

$$B_{\mathbf{i},\mathbf{p}} \coloneqq \widehat{B}_{\mathbf{i},\mathbf{p}} \circ \mathbf{F}^{-1}, \quad \mathbf{i} \in \mathbf{I}, \tag{6.2.4}$$

respectively. Note, above $\widehat{N}_{\mathbf{i},\mathbf{p}}$, $\widehat{B}_{\mathbf{i},\mathbf{p}}$ stand for the basis functions in the parametric domain.

Up to know we had the point of view that the parametrization has the form $\mathbf{F}\colon (0,1)^n \to \mathbb{R}^n$ meaning we have a so-called single patch parametrization. In applications frequently domains have to be considered which can not be parameterized accurately by means of a single patch. To achieve more flexibility one decomposes Ω into several simpler shapes and defines IG spaces for each patch separately. In other words, in multi-patch framework one has

$$\overline{\Omega} = \cup_{k=1}^{m} \overline{\Omega}_k, \qquad \mathbf{F}_{|\Omega_k} \coloneqq \mathbf{F}_k \colon (0,1)^n \to \Omega_k \ , \ \boldsymbol{\zeta} \mapsto \textstyle\sum_{\mathbf{i}\in\mathbf{I}^{(k)}} \widehat{N}^{(k)}_{\mathbf{i},\mathbf{p}}(\boldsymbol{\zeta})\, \mathbf{C}^{(k)}_{\mathbf{i}},$$

where the index k should indicate that the NURBS and the control points might depend on the specific patch. This means each patch is determined by some suitable NURBS parametrization. The multi-patch IG spaces are then defined patch-wise together with suitable coupling conditions between the patches. These conditions depend on the wanted global regularity. If we consider later for numerical examples multi-patch geometries, then for reasons of simplification we restrict ourselves to the case of conforming multi-patch discretizations, i.e. the next assumption is underlying.

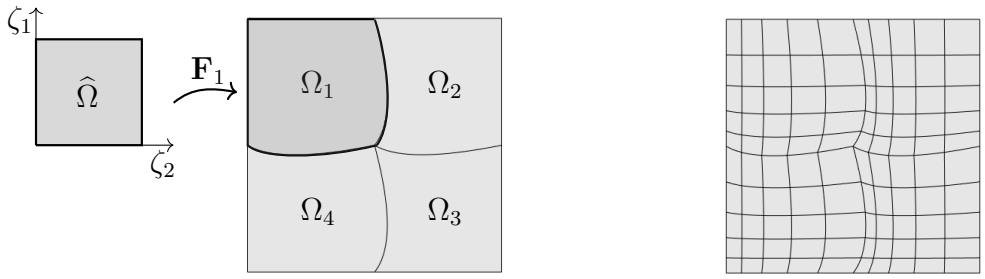

(a) A 4-patch geometry

(b) A related conforming mesh.

Figure 9: In order to consider complicated computational domains, in IGA a multi-patch ansatz is possible (left). We require conforming meshes, meaning, the mesh structures defined by the different patches fit at the interfaces (right).

Assumption 6.3 (Conforming multi-patch geometries; cf. [32, Assumption 3.3])**.**

- *Each of the parametrizations $\mathbf{F}_k$ are regular in the sense of Definition 6.5.*
- *Either $\Gamma_{i,j} \coloneqq \overline{\Omega}_i \cap \overline{\Omega}_j$, $\forall i,j$ is empty or the image of a vertex, a full edge, or a full face for both related parametric domains.*
- *The control points and mesh structure induced by the patches at an interface coincide, meaning we have a well-defined global mesh.*

With the assumption of conforming multi-patch geometries it is easy to define globally continuous IG spaces. For more details on IGA in the context of multi-patch geometries, we refer to [32].

After we clarified the type of spaces we use, it is natural to have a closer look on the properties of isogeometric spaces, especially with regard to approximation estimates. Because these estimates are crucial to check the feasibility of specific choices and suggest convergence rates in numerical applications.

6.3 Projections onto IG spaces

6.3.1 Results in the physical domain

In order to state approximation estimates it is helpful to introduce projections onto the single-patch spaces $V_{h,\mathbf{p}}$ and $U_{h,\mathbf{p}}$. Here, in this chapter we restrict ourselves sometimes just to the statements and will drop the proofs. Nevertheless, we will give references at different places for interested readers.
We directly start with the central approximation property of the discrete IGA spaces. The goal is to approximate functions u in various Sobolev norms $\|\cdot\|_{H^s(\Omega)}$ using functions from discrete IGA spaces. The key observation is that the smoother the function u, the more accurate the approximation becomes. Following lemma condenses this.

Lemma 6.2 (**IGA approximation estimates**). *Let $V_{h,\mathbf{p}}$ and $U_{h,\mathbf{p}}$, $\mathbf{p} = (p_1, \dots, p_n)$ be the discrete IG spaces on Ω, where the underlying mesh is regular with mesh size h and let l, $s \in \mathbb{N}$ such that the polynomial degrees p_i fulfill $0 \leq s \leq l \leq p+1$, $p \coloneqq \min_i\{p_i\}$. Then there exist projection operators*

$$\Pi_h^U \colon L^2(\Omega) \to U_{h,\mathbf{p}}, \qquad\qquad \Pi_h^V \colon L^2(\Omega) \to V_{h,\mathbf{p}},$$

such that

$$\left\|u - \Pi_h^U u\right\|_{H^s(\Omega)} \leq C_\Pi\, h^{l-s}\, \|u\|_{H^l(\Omega)} \quad \text{and} \quad \left\|u - \Pi_h^V u\right\|_{H^s(\Omega)} \leq C_\Pi\, h^{l-s}\, \|u\|_{H^l(\Omega)},$$

for all $u \in H^l(\Omega)$, provided that $V_{h,\mathbf{p}} \subset H^s(\Omega)$, $U_{h,\mathbf{p}} \subset H^s(\Omega)$. Thereby C_Π can be chosen independently from the mesh size h and the mapping u.

Proof. For the first estimate, see Corollary 2 on page 129 in [31] or [17, Theorem 3.1]. For the estimate involving Π_h^V we refer to [27, Remark 5.1]. □

Up to now we focused on scalar NURBS functions. It becomes apparent that for a lot of problems vector-valued mappings are necessary. In fact one might define discretizations for spaces of the form $L^2(\Omega) \otimes \mathbb{E}$ with $\mathbb{E}$ being a suitable finite-dimensional space, just by a component-wise generalization. It is straightforward to derive similar estimates for such a vector-valued case.

Remark 6.2 (Vector-valued projection operators). Let $\{e_1, \dots, e_k\}$ denoting an orthonormal basis of some $\mathbb{R}$-Hilbert space $\mathbb{E}$, then we can define

$$V_{h,\mathbf{p}}^{\mathbb{E}} \coloneqq \operatorname{span}\Big\{(x \mapsto u_i(x) e_i) \in L^2(\Omega) \otimes \mathbb{E} \;\Big|\; u_i \in V_{h,\mathbf{p}},\ i = 1, \dots, k\Big\}.$$

And then for an element $u_i\, e_i \in L^2(\Omega) \otimes \mathbb{E}$ we set

$$\Pi_h^{V,\mathbb{E}} u \coloneqq \left(\Pi_h^V u_i\right) e_i,$$

which defines the projection by linearity. The approximation properties from Lemma 6.2 are still true for the vector-valued case, since for $u = \sum_{i=1}^k u_i\, e_i \in H^l(\Omega) \otimes \mathbb{E}$ it is

$$\left\|u - \Pi_h^{V,\mathbb{E}} u\right\|_{H^s(\Omega)}^2 = \sum_{i=1}^k \left\|u_i - \Pi_h^V u_i\right\|_{H^s(\Omega)}^2 \leq C_\Pi^2\, h^{2(l-s)} \sum_{i=1}^k \|u_i\|_{H^l(\Omega)}^2 = C_\Pi^2\, h^{2(l-s)}\, \|u\|_{H^l(\Omega)}^2.$$

Clearly, we can substitute the B-spline space $V_{h,\mathbf{p}}$ with $U_{h,\mathbf{p}}$ without encountering any challenges. Furthermore, it is evident that we can employ distinct IG spaces for different components.

Subsequent inverse inequalities provide other valuable estimates for IGA discretizations.

Lemma 6.3 (**Inverse inequalities**). *Let $v_h \in V_{h,\mathbf{p}} \cap H^s(\Omega)$ or $v_h \in U_{h,\mathbf{p}} \cap H^s(\Omega)$. Then the estimate*

$$\|v_h\|_{H^s(\Omega)} \leq C_{inv}\, h^{l-s}\, \|v_h\|_{H^l(\Omega)}\,, \quad \text{for } \; 0 \leq l \leq s \tag{6.3.1}$$

holds. The constant C_{inv} is independent of h and v_h if we have a family of regular meshes. But it might depend on the parametrization $\mathbf{F}$, the parameters s, l and on $\mathbf{p}$.

Proof. The estimate follows directly by Theorem 4.2 in [17] and the regular mesh assumption; see Definition 6.5. □

In case of B-spline spaces of the form $S^{\mathbf{r}}_{\mathbf{p}} = S^{r_1,\dots,r_n}_{p_1,\dots,p_n}$ the mentioned NURBS projections can be chosen in such a way that they are compatible with derivatives and such that they respect the product structure of the multivariate B-splines. More details on this point in the next section.

6.3.2 Derivative-compatible projections onto B-spline spaces

In this section we follow the approach and the results of Buffa et al. ([27]). In particular we follow the idea to introduce spline projections which commute with derivative operators. To explain the relevant parts for our purposes, we first go back to the parametric $1D$ situation, i.e. we deal with the spaces S^r_p defined above; cf. (6.1.6). If we consider spline spaces in the following, we always assume that they belong to a regular mesh structure with a mesh size of h.

Definition 6.7 (**Compatible projections**). *We define different projections onto univariate spline spaces, where they are inspired by the approach from paper [27]. We just generalize the projections to the case of higher derivatives. These projection operators are the basis of the projections in the multivariate case which commute with differential operators.*
First, for $-1 \leq r \leq p-1$ define

$$\widehat{\Pi}^0_{p,r} \colon L^2((0,1)) \to S^r_p \;,\; v \mapsto \sum_{i=1}^{\mathfrak{n}} \lambda^p_i(v)\; \widehat{B}_{i,p},$$

where $\lambda^p_i(\cdot)$ stand for the dual basis vectors for the B-spline basis $\{\widehat{B}_{1,p}, \dots, \widehat{B}_{\mathfrak{n},p}\}$ of S^r_p from [65, Theorem 6.60]. This means the $\lambda^p_i(\cdot)$ fulfill $\lambda^p_i(\widehat{B}_{j,p}) = \delta_{ij}$.
We mention here that the latter projection $\widehat{\Pi}^0_{p,r}$ corresponds to (3.6) in [27]. *Next, for $l \in \mathbb{N}_{\geq 1}$ and $l-1 \leq r \leq p-1$ we introduce recursively*

$$\widehat{\Pi}^l_{p,r} \colon L^2((0,1)) \to S^{r-l}_{p-l} \;,\; v \mapsto \partial_\zeta \left(\widehat{\Pi}^{l-1}_{p,r} \int_0^\zeta v(\tau)\; d\tau \right), \tag{6.3.2}$$

where the derivative is meant in a weak sense. For $l = 1$ we obtain the projection (3.9) in [27].

Before we come to some statements regarding the introduced projections, we bring us the well-definedness of the $\widehat{\Pi}^l_{p,r}$ to mind. Namely, assuming $l = 1,\ 0 \leq r \leq p-1$ we get $\widehat{\Pi}^{l-1}_{p,r} w \in S^r_p \subset H^1(\Omega) = H^l(\Omega)$ for $w \in L^2((0,1))$. In fact, applying [20, 5.2, Chapter 2] we have $S^r_p \subset H^{r+1}((0,1))$ if $-1 \leq r \leq p-1$. Thus the derivative operator ∂_ζ in (6.3.2) makes sense. Furthermore, in view of the formula (6.1.4) one sees directly $\partial_\zeta S^r_p \subset S^{r-1}_{p-1}$. Even more, it is easy to check that indeed $\partial_\zeta S^r_p = S^{r-1}_{p-1}$. Hence, the definition of $\widehat{\Pi}^1_{p,r}$ is clear. And using an inductive argument one has the well-definedness for every $\widehat{\Pi}^l_{p,r}$.
Let now $\{\psi_1 < \dots < \psi_L\}$ be the knot vector without knot repetitions of the underlying spline space, which defines a subdivision of the interval $(0,1)$. Then, for each element $I = (\psi_j, \psi_{j+1})$ we can find an i with $(\psi_j, \psi_{j+1}) = (\xi_i, \xi_{i+1})$ and in this case we write $\tilde{I}_p \coloneqq (\xi_{i-p}, \xi_{i+p+1})$ for the so-called *support extension* of I. In the next lemma these auxiliary intervals $\tilde{I}_p$ appear.

Lemma 6.4 (**Projection properties - univariate case**). *Let $I = (\psi_j, \psi_{j+1})$ be some element of the mesh induced by the underlying knots. Then, the above univariate projections satisfy the following properties, where we have the assumption $-1 \leq r \leq p-1$.*

$$\widehat{\Pi}^0_{p,r} s = s \qquad \forall s \in S^r_p, \tag{6.3.3}$$

$$|\widehat{\Pi}^0_{p,r} v|_{H^m(I)} \leq C\ |v|_{H^m(\tilde{I}_p)} \qquad \forall v \in H^m((0,1)),\ 0 \leq m \leq p+1, \tag{6.3.4}$$

for some constant C independent of mesh refinement. Above $|\cdot|_{H^k}$ stands for the classical Sobolev seminorm.[12]
And if it is $0 \leq l-1 \leq r \leq p-1$, we further have

$$\widehat{\Pi}^l_{p,r} s = s \qquad \forall s \in S^{r-l}_{p-l}, \tag{6.3.5}$$

$$\partial_\zeta \widehat{\Pi}^{l-1}_{p,r} \partial^{l-1}_\zeta v = \widehat{\Pi}^l_{p,r} \partial^l_\zeta v \qquad \forall v \in H^l((0,1)), \tag{6.3.6}$$

$$|\widehat{\Pi}^l_{p,r} v|_{H^m(I)} \leq C\ |v|_{H^m(\tilde{I}_p)} \qquad \forall v \in H^m((0,1)),\ 0 \leq m \leq p+1-l. \tag{6.3.7}$$

Proof. The first two statements correspond to the properties (3.7)-(3.8) in [27] if we keep the regular mesh assumption in mind. Also the other points in the assertion for $l = 1$ are obtained by (3.10)-(3.12) in latter reference. For reasons of completeness we show (6.3.5)-(6.3.7) for the case $l > 1$ utilizing a proof by induction. This means we assume the validity of the different points for some $l \geq 1$ and we have the requirement $l \leq r \leq p-1$.
Firstly, we have by definition

$$\widehat{\Pi}^{l+1}_{p,r} s = \partial_\zeta \Bigg(\widehat{\Pi}^l_{p,r} \underbrace{\int_0^\zeta s(\tau)\ d\tau}_{\in S^{r-l}_{p-l}} \Bigg) = \partial_\zeta \Bigg(\int_0^\zeta s(\tau)\ \ d\tau \Bigg) = s, \quad \forall s \in S^{r-l-1}_{p-l-1}.$$

Further, for $v \in H^{l+1}((0,1)), \quad 1 \leq l \leq r \leq p-1$ we write in view of the spline preserving property

$$\widehat{\Pi}^{l+1}_{p,r} \partial^{l+1}_\zeta v = \partial_\zeta \Bigg(\widehat{\Pi}^l_{p,r} \int_0^\zeta \partial^{l+1}_\zeta v(\tau)\ d\tau \Bigg) = \partial_\zeta \widehat{\Pi}^l_{p,r} \Big(\partial^l_\zeta v + a \Big) = \partial_\zeta \widehat{\Pi}^l_{p,r} \partial^l_\zeta v, \tag{6.3.8}$$

with $a \in \mathbb{R}$ being a proper integration constant. The last point can be proven using the fact that if $v \in H^m((0,1)),\ 0 \leq m \leq p-l$ then $w(\zeta) \coloneqq \int_0^\zeta v(\tau) d\tau \in H^{m+1}((0,1))$. Then it is

$$|\widehat{\Pi}^{l+1}_{p,r} v|_{H^m(I)} \leq |\widehat{\Pi}^l_{p,r} w|_{H^{m+1}(I)} \leq C\, |w|_{H^{m+1}(\tilde{I}_p)} = C\, |v|_{H^m(\tilde{I}_p)}.$$

The second inequality sign in the last line comes from the induction hypothesis. We note that we used the proof ansatz from [27, Lemma 3.2] above. □

For the multivariate case we define projections exploiting a tensor product construction, meaning one respects the product structure of the multivariate B-splines. More precisely, given vectors $\mathbf{p} = (l_i)_i$, $\mathbf{r} = (l_i)_i$, $\mathbf{l} = (l_i)_i$ in $\mathbb{Z}^n$ with $-1 \leq l_i - 1 \leq r_i \leq p_i - 1$ we set

$$\widehat{\Pi}^{\mathbf{l}}_{\mathbf{p},\mathbf{r}} \colon L^2(\widehat{\Omega}) \to S^{\mathbf{r}-\mathbf{l}}_{\mathbf{p}-\mathbf{l}} = S^{r_1-l_1,\ldots,r_n-l_n}_{p_1-l_1,\ldots,p_n-l_n}\ ,\ v \mapsto (\widehat{\Pi}^{l_1}_{p_1,r_1} \otimes\ \ldots\ \otimes \widehat{\Pi}^{l_n}_{p_n,r_n}) v, \tag{6.3.9}$$

where $\widehat{\Omega} = (0,1)^n$. Like explained in [27, Section 4.1] one can regard such tensor product mappings as a composition of the different $1D$ projection operators. In more detail, let $v \in L^2(\widehat{\Omega})$

[12] $|v|^2_{H^k} \coloneqq |v|^2_{H^k(\Omega)} \coloneqq \sum_{|\alpha|=k} \|\partial^\alpha v\|^2_{L^2(\Omega)}$.

be a smooth mapping, meaning for $i \in \{1, \dots, n\}$ and $\zeta_k \in (0,1), \forall k$ we can define the univariate mappings

$$v[\zeta_1, \dots, \zeta_{i-1}, \zeta_{i+1}, \dots, \zeta_n] \colon (0,1) \to \mathbb{R} \ , \ \tau \mapsto v(\zeta_1, \dots, \zeta_{i-1}, \tau, \zeta_{i+1}, \dots, \zeta_n).$$

This means we only vary the i-th input parameter. Consequently, we can consider $\widehat{\Pi}^{l_i}_{p_i,r_i} v[\zeta_1, \dots, \zeta_{i-1}, \zeta_{i+1}, \dots, \zeta_n]$. Since the result depends on the ζ_k it again can be interpreted as a mapping in $L^2(\widehat{\Omega})$, namely $\bar{v}^{l_i,\otimes} \colon (\zeta_1, \dots, \zeta_{i-1}, \tau, \zeta_{i+1}, \dots, \zeta_n) \mapsto \left(\widehat{\Pi}^{l_i}_{p_i,r_i} v[\zeta_1, \dots, \zeta_{i-1}, \zeta_{i+1}, \dots, \zeta_n]\right)(\tau)$. Hence, it makes sense to introduce

$$\widehat{\Pi}^{l_i,\otimes}_{p_i,r_i} v \coloneqq \bar{v}^{l_i,\otimes}.$$

With this consideration one gets

$$\widehat{\Pi}^{\mathbf{l}}_{\mathbf{p},\mathbf{r}} v = \left(\widehat{\Pi}^{l_1,\otimes}_{p_1,r_1} \circ \dots \circ \widehat{\Pi}^{l_n,\otimes}_{p_n,r_n}\right) v.$$

A density argument extends the last projection to the whole L^2 space. The product construction directly implies similar properties for the multivariate projections as those for $\widehat{\Pi}^{l}_{p,r}$. In the style of Lemma 4.1 and Lemma 4.2 of [27] we summarize them below.

Lemma 6.5 (L^2**-stability and spline preservation**). *Let $K \in \widehat{M}$ be an element of the Bézier mesh and $-1 \leq l_i - 1 \leq r_i \leq p_i - 1$. The projection $\widehat{\Pi}^{\mathbf{l}}_{\mathbf{p},\mathbf{r}}$ is continuous in the sense*

$$\left\| \widehat{\Pi}^{\mathbf{l}}_{\mathbf{p},\mathbf{r}} v \right\|_{L^2(K)} \leq C \left\| v \right\|_{L^2(\tilde{K})}, \quad \forall v \in L^2(\widehat{\Omega}),$$

for a suitable constant C. Above $\tilde{K}$ denotes the extended support of the mesh element K. This means if $K = (\psi^1_{i_1}, \psi^1_{i_1+1}) \times \dots \times (\psi^n_{i_n}, \psi^n_{i_n+1})$, we find indices j_l with $K = (\xi^1_{j_1}, \xi^1_{j_1+1}) \times \dots \times (\xi^n_{j_n}, \xi^n_{j_n+1})$ for suitable knots. Then we set

$$\tilde{K} \coloneqq (\xi^1_{j_1-p_1}, \xi^1_{j_1+p_1+1}) \times \dots \times (\xi^n_{j_n-p_n}, \xi^n_{j_n+p_n+1}).$$

Further if $s \in S^{\mathbf{r}-\mathbf{l}}_{\mathbf{p}-\mathbf{l}} \coloneqq S^{r_1-l_1,\dots,r_n-l_n}_{p_1-l_1,\dots,p_n-l_n}$ it holds

$$\widehat{\Pi}^{\mathbf{l}}_{\mathbf{p},\mathbf{r}} s = s.$$

Hence, we have indeed a projection.

Proof. The statement follows by the regular mesh assumption, the product structure of the multivariate projections and the properties of the univariate spline projections; see Lemma 6.4. □

Lemma 6.6 (**Compatibility with derivatives**). *Assume $-1 \leq l_i - 1 \leq r_i \leq p_i - 1$, $k \in \{1, \dots, n\}$ with $p_k - l_k \geq 1$, $r_k - l_k \geq 0$ and let $v \in L^2(\widehat{\Omega})$, such that the (weak) partial derivative w.r.t. the k-th coordinate $\partial_{\zeta_k} v \in L^2(\widehat{\Omega})$ exists in the sense $v \in H(\widehat{\Omega}, \partial_{\zeta_k}, \mathbb{R})$; cf. (2.2.4). In this case we have*

$$\partial_{\zeta_k} \widehat{\Pi}^{\mathbf{l}}_{\mathbf{p},\mathbf{r}} v = \widehat{\Pi}^{\mathbf{l}+\mathbf{e}_k}_{\mathbf{p},\mathbf{r}} \partial_{\zeta_k} v,$$

where $\mathbf{e}_k \in \mathbb{N}^n$ is the k-th canonical basis vector.

Proof. We show the proof only for $n = 2$ and $k = 2$. The other situations can be proven completely analogous, just with a more cumbersome notation.
By a density argument, we can choose a sequence $(v_m)_m \subset C^\infty([0,1]^n)$ s.t. $\partial_{\zeta_2} v_m \xrightarrow{L^2} \partial_{\zeta_2} v$ and $v_m \xrightarrow{L^2} v$.

The smoothness of the v_m, the product structure of the projection and the commutativity relation for the derivatives in Lemma 6.4 yield

$$\begin{aligned}\partial_{\zeta_2}\widehat{\Pi}^{\mathbf{l}}_{\mathbf{p},\mathbf{r}}v_m &= \partial_{\zeta_2}\big(\widehat{\Pi}^{l_1}_{p_1,r_1}\otimes\widehat{\Pi}^{l_2}_{p_2,r_2}\big)v_m = \big(\widehat{\Pi}^{l_1}_{p_1,r_1}\otimes\partial_{\zeta_2}\widehat{\Pi}^{l_2}_{p_2,r_2}\big)v_m\\ &= \big(\widehat{\Pi}^{l_1}_{p_1,r_1}\otimes\widehat{\Pi}^{l_2+1}_{p_2,r_2}\partial_{\zeta_2}\big)v_m = \widehat{\Pi}^{\mathbf{l}+\mathbf{e}_2}_{\mathbf{p},\mathbf{r}}\partial_{\zeta_2}v_m. \end{aligned} \tag{6.3.10}$$

This means, because of the L^2 continuity of the projections, $\partial_{\zeta_2}\widehat{\Pi}^{\mathbf{l}}_{\mathbf{p},\mathbf{r}}v_m$ converges for $m\to\infty$ to some spline τ. Assume now $\tau\neq\partial_{\zeta_2}\widehat{\Pi}^{\mathbf{l}}_{\mathbf{p},\mathbf{r}}v$. Then, by the piecewise smoothness of the splines we find a non-empty open set $U\subset(0,1)^2$ s.t. w.l.o.g. $\tau-\partial_{\zeta_2}\widehat{\Pi}^{\mathbf{l}}_{\mathbf{p},\mathbf{r}}v>0$ in U. Next, choose a non-negative $\phi\in C^\infty_c(U)$ with $\phi>0$ on a non-empty open set $B\subset U$. Such a choice is indeed possible, cf. [2, U1.3]. Taking the limit $m\to\infty$ on both sides of the next equation

$$\langle\partial_{\zeta_2}\widehat{\Pi}^{\mathbf{l}}_{\mathbf{p},\mathbf{r}}v_m-\partial_{\zeta_2}\widehat{\Pi}^{\mathbf{l}}_{\mathbf{p},\mathbf{r}}v,\phi\rangle=-\langle\widehat{\Pi}^{\mathbf{l}}_{\mathbf{p},\mathbf{r}}v_m-\widehat{\Pi}^{\mathbf{l}}_{\mathbf{p},\mathbf{r}}v,\partial_{\zeta_2}\phi\rangle$$

gives for the left-hand side just $\langle\tau-\partial_{\zeta_2}\widehat{\Pi}^{\mathbf{l}}_{\mathbf{p},\mathbf{r}}v,\phi\rangle\neq0$. On the right-hand side we get by the continuity of the projections 0. In particular we have a contradiction which implies $\tau=\partial_{\zeta_2}\widehat{\Pi}^{\mathbf{l}}_{\mathbf{p},\mathbf{r}}v$. Thus, taking the limit $m\to\infty$ in (6.3.10) finishes the proof. □

As already mentioned, the spline spaces as well as the corresponding projections can be generalized easily to product spaces of the form $L^2(\Omega)\otimes\mathbb{E}$ appearing in Section 2.2, where $\mathbb{E}$ is a finite-dimensional Hilbert space. One just uses a component-wise approach, coefficient-wise, respectively, analogously to Remark 6.2.

Next we show an approximation result for the introduced projections of the type $\widehat{\Pi}^{\mathbf{l}}_{\mathbf{p},\mathbf{r}}$.

Lemma 6.7 (**Approximation estimate**). *Let $\widehat{\Pi}^{\mathbf{l}}_{\mathbf{p},\mathbf{r}}$ be the projection onto $S^{\mathbf{r}-\mathbf{l}}_{\mathbf{p}-\mathbf{l}}=:S^{s_1,\dots,s_n}_{q_1,\dots,q_n}$, i.e. $q_i=p_i-l_i$, $s_i=r_i-l_i$. And let $0\le q\le q_i$ and $-1\le s\le s_i\le q_i-1$ for q, $s\in\mathbb{Z}$ and all i. Furthermore, we assume the corresponding Bézier mesh $\widehat{M}_h$ of the spline space to be regular with mesh size h.*
Then there exists a constant $\widehat{C}_\Pi>0$ independent of mesh refinement s.t.

$$\left\|v-\widehat{\Pi}^{\mathbf{l}}_{\mathbf{p},\mathbf{r}}v\right\|_{H^k(\widehat{\Omega})}\le\widehat{C}_\Pi h^{m-k}\left\|v\right\|_{H^m(\widehat{\Omega})},\quad\text{if } 0\le k\le m\le q+1,\ k\le s+1, \tag{6.3.11}$$

and provided that $v\in H^m(\widehat{\Omega})$.

Proof. We follow the proof steps from Lemma 5.1 in [27].
Note, by assumption we have $\widehat{\Pi}^{\mathbf{l}}_{\mathbf{p},\mathbf{r}}v\in H^k(\widehat{\Omega})$. By [17, Lemma 3.4] we see the existence of spline $s\in S^{q-1,\dots,q-1}_{q,\dots,q}\subset S^{s_1,\dots,s_n}_{q_1,\dots,q_n}$ s.t.

$$\left\|v-s\right\|_{H^{\tilde{k}}(\widehat{\Omega})}\le Ch^{\tilde{m}-\tilde{k}}\left\|v\right\|_{H^{\tilde{m}}(\widehat{\Omega})},\quad\text{for }\ 0\le\tilde{k}\le\tilde{m}\le q+1. \tag{6.3.12}$$

Above C does not depend on h. By the spline preserving property of the projection (see Lemma 6.5) and the triangle inequality we get the next line

$$\left\|v-\widehat{\Pi}^{\mathbf{l}}_{\mathbf{p},\mathbf{r}}v\right\|_{H^k(\widehat{\Omega})}\le\left\|\widehat{\Pi}^{\mathbf{l}}_{\mathbf{p},\mathbf{r}}(v-s)\right\|_{H^k(\widehat{\Omega})}+\left\|v-s\right\|_{H^k(\widehat{\Omega})}. \tag{6.3.13}$$

Since the B-splines are piecewise polynomials we can apply a standard inverse estimate, which yields

$$\left\|\widehat{\Pi}^{\mathbf{l}}_{\mathbf{p},\mathbf{r}}(v-s)\right\|_{H^k(\widehat{\Omega})}\le C\frac{1}{h^k}\left\|\widehat{\Pi}^{\mathbf{l}}_{\mathbf{p},\mathbf{r}}(v-s)\right\|_{L^2(\widehat{\Omega})}\le C_\Pi C\frac{1}{h^k}\left\|v-s\right\|_{L^2(\widehat{\Omega})}, \tag{6.3.14}$$

for some constant $C>0$. One observes the L^2-stability of the projection which yields some additional constant C_Π. Now inserting (6.3.14) into (6.3.13) we obtain the wanted estimate due to (6.3.12). □

Now we have learned various properties of NURBS and B-splines, and we have also introduced corresponding projections. In other words, we finally have the tools ready to address the discretization of Hilbert complexes. The investigation and development of numerical methods using the IGA theory will accompany us from the next chapter until the end of the work.

7 Spline Complexes and Isogeometric Discrete Differential Forms

In this section we want to demonstrate how the B-splines introduced in the last part can be utilized to set up structure-preserving discretizations for several Hilbert complexes in $\widehat{\Omega} = (0,1)^n$. The cube domain enables us to exploit the product structure of the spaces $S^{\mathbf{r}}_{\mathbf{p}}$. Doing so, we first focus on the de Rham sequence, but in the second subsection we explain also the feasibility of B-splines to discretize the second-order complexes induced by the coupling of Alt^l-valued forms; see Section 4.2.3. For example, we show the possibility to construct finite-dimensional versions of the diagrams in Figures 4.2.25 and 4.2.28.
Certainly, it is clear that the restriction to the domain $(0,1)^n$ questions the applicability of the observations within the framework of numerical methods. It is indeed shown that at least for the de Rham sequence, the transition to other geometries is possible, with the help of the pullback operation. We then obtain the so-called *isogeometric discrete differential forms* which will be introduced in the third subsection below. However, it is easily apparent that this pullback operation is not directly applicable in the case of second-order complexes. In other words, the later defined second-order spline complexes cannot be readily extended to non-trivial domains. Nevertheless, restricting to case of cubical domains will lead us to results that are still useful for the considerations of different saddle-point problems also in deformed computational domains. The latter is explained and will become clear in Section 8, in which we will reuse the considerations that will follow now within the framework of mixed weak formulations for Hodge–Laplace problems. More specifically, we want to establish the prerequisites now to be able to later apply the auxiliary results from above Section 5 in the context of isogeometric FE spaces.

Before we delve into discrete spline spaces, we would like to note in advance that this chapter is built upon existing results in the literature. Regarding the de Rham complexes, we follow the work of Buffa et al. [27], while the constructions in the realm of second-order spline complexes align with the approach and results of [19]. This will be highlighted at various points by providing the corresponding references. However, it is worth mentioning that we employ our own notation, and in contrast to the three-dimensional setting in [27], we will introduce isogeometric differential forms in arbitrary dimensions.

To begin with, let us clarify some points concerning notation. Namely, if we have in the following some differential operator of the form $\mathcal{D}\colon H(\Omega,\mathcal{D},\mathbb{E}) \to L^2(\Omega)\otimes\tilde{\mathbb{E}}$ with $\mathbb{E}$, $\tilde{\mathbb{E}}$ finite-dimensional spaces and $\mathcal{D}$ as in (2.2.3), we use for $s \in \mathbb{N}$ the abbreviations $H^s(\Omega,\mathcal{D},\mathbb{E}) \coloneqq H(\Omega,\mathcal{D},\mathbb{E}) \cap \{v \in H^s(\Omega)\otimes\mathbb{E} \mid \mathcal{D}v \in H^s(\Omega)\otimes\tilde{\mathbb{E}}\}$ and

$$\begin{aligned}\|\cdot\|^2_{H^s(\mathcal{D})} &\coloneqq \|\cdot\|^2_{H^s(\Omega)} + \|\mathcal{D}\cdot\|^2_{H^s(\Omega)}\,,\\ \|\cdot\|^2_{H(\mathcal{D})} &\coloneqq \|\cdot\|^2_{L^2(\Omega)} + \|\mathcal{D}\cdot\|^2_{L^2(\Omega)}\,.\end{aligned}$$

And, to emphasize that we are considering derivatives with respect to the parametric coordinates in $\widehat{\Omega}$, we use the hat symbol "$\widehat{\cdot}$" above the differential operators, meaning for example $\widehat{\mathrm{curl}}$ instead curl. Additionally, when dealing with the exterior derivative on the parametric domain, we use the notation $\hat{\mathrm{d}}^j$ as opposed to the original d^j. Furthermore, for the spline spaces below within one chain or diagram we have a single regular mesh underlying, which implies in this context $S^{r_1,\dots,r_n}_{p_1,\dots,p_n} \subset S^{s_1,\dots,s_n}_{q_1,\dots,q_n}$ as long as $r_i \geq s_i$, $q_i \geq p_i$, $\forall i$. And as a last point, we remark that appearing vectors and matrices with spline spaces as entries should be an abbreviation for spaces of vector- or matrix valued mappings with entries in the respective spline spaces.

7.1 De Rham spline sequence

Prior to the facing of second-order complexes discretizations on the parametric domain $\widehat{\Omega}$, we first make sure how the classical de Rham sequence can be approximated utilizing B-splines. Actually, also discrete versions of the second-order output complexes like shown in Examples 4.2 and 4.3 on a cubical domain can be constructed utilizing the de Rham sequences, since they are derived exploiting the *complexes from complexes* idea from [12]. So it makes sense to go first a step back and check how suitable B-splines for the de Rham sequences, especially (3.3.8) and (3.3.9), look like. Fortunately, the problem in $3D$ is addressed and analyzed in detail by Buffa et al. in [27] by the introduction of isgeometric discrete differential forms. Since in the latter reference a tensor product construction is exploited like in [8] the procedure is generalizable to arbitrary dimensions. For the subsequent definitions of the spaces, we use again the language of differential forms in order to explain the spline complexes in a systematic manner. For more details concerning the related notions and notation we refer to Section 3.3.1

Let again $\widehat{\Omega} = (0,1)^n$ be assumed. In this section we make use of the fact that one can describe an element in $\omega \in L^2\Lambda^k(\widehat{\Omega})$ through its coefficients and its representation $\omega = \sum_{\sigma\in\Sigma_<(k,n)} c_\sigma \, dx^{\sigma_1} \wedge \cdots \wedge dx^{\sigma_k}$. So, let us consider the left ending of the de Rham sequence (see Lemma 3.5), namely the space $H\Lambda^0(\widehat{\Omega})$. We might discretize the latter simply through some spline space

$$Q^{\mathbf{r}}_{\mathbf{p}}\Lambda^0 \coloneqq S^{\mathbf{r}}_{\mathbf{p}} = S^{r_1,\dots,r_n}_{p_1,\dots,p_n},$$

assuming once again that $p_i > r_i \geq 0$, $\forall i$. This allows the application of the exterior derivative in a weak sense, which for an element $\omega \in Q^{\mathbf{r}}_{\mathbf{p}}\Lambda^0$ results in $\hat{\mathrm{d}}^0\omega = \sum_{i=1}^n \hat{\partial}_i\omega \, dx^i$ by definition. The last equation gives rise to a space of suitable spline differential 1-forms, namely we set

$$Q^{\mathbf{r}}_{\mathbf{p}}\Lambda^1 \coloneqq \mathrm{span}\Big\{ \textstyle\sum_{i=1}^n c_i \, dx^i \;\Big|\; c_i \in S^{\mathbf{r}-\mathbf{e}_i}_{\mathbf{p}-\mathbf{e}_i} \Big\},$$

with $\mathbf{e}_i$ denoting the i-th canonical basis vector. Because, then we trivially get $\hat{\mathrm{d}}^0 Q^{\mathbf{r}}_{\mathbf{p}}\Lambda^0 \subset Q^{\mathbf{r}}_{\mathbf{p}}\Lambda^1$. Inductively, one can now determine the remaining appropriate spline spaces for a discretization of the de Rham sequence using the definition of the exterior derivative. One then sees that a successive approach gives spaces

$$Q^{\mathbf{r}}_{\mathbf{p}}\Lambda^k \coloneqq \left\{ \sum_{\sigma\in\Sigma_<(k,n)} c_\sigma \; dx^{\sigma_1} \wedge \cdots \wedge dx^{\sigma_k} \;\middle|\; c_\sigma \in S^{\mathbf{r}-\mathbf{e}_\sigma}_{\mathbf{p}-\mathbf{e}_\sigma} \right\}, \quad k = 1,\dots,n, \tag{7.1.1}$$

where

$$\mathbb{N}^n \ni \mathbf{e}_\sigma, \; (\mathbf{e}_\sigma)_i = \begin{cases} 1, \text{ if } i \in \{\sigma_1,\dots,\sigma_k\}, \\ 0, \text{ else.} \end{cases} \tag{7.1.2}$$

The latter can also be seen by the tensor product approach from [8].

Indeed, let $\omega \in Q^{\mathbf{r}}_{\mathbf{p}}\Lambda^k$. By the definition of the exterior derivative and the properties of the wedge product one has

$$\hat{\mathrm{d}}^k\omega = \sum_{\sigma\in\Sigma_<(k,n)} \sum_{\substack{i=1 \\ i\notin\{\sigma_1,\dots,\sigma_k\}}}^{n} \hat{\partial}_i c_\sigma \, dx^i \wedge dx^{\sigma_1} \wedge \cdots \wedge dx^{\sigma_k}, \tag{7.1.3}$$

with $c_\sigma \in S^{\mathbf{r}-\mathbf{e}_\sigma}_{\mathbf{p}-\mathbf{e}_\sigma}$. Obviously, for $i \in \{1,\dots,n\}\backslash\{\sigma_1,\dots,\sigma_k\}$ there are unique increasing numbers $1 \leq s_1 < \cdots < s_{k+1} \leq n$ s.t. $\{i\} \cup \{\sigma_1,\dots,\sigma_k\} = \{s_1,\dots,s_{k+1}\}$ and then $\hat{\partial}_i c_\sigma \in S^{\mathbf{r}-\mathbf{e}_s}_{\mathbf{p}-\mathbf{e}_s}$. Consequently,

$$\hat{\mathrm{d}}^k\omega \in \left\{ \sum_{s\in\Sigma_<(k+1,n)} c_s \, dx^{s_1} \wedge \cdots \wedge dx^{s_{k+1}} \;\middle|\; c_s \in S^{\mathbf{r}-\mathbf{e}_s}_{\mathbf{p}-\mathbf{e}_s} \right\} = Q^{\mathbf{r}}_{\mathbf{p}}\Lambda^{k+1}.$$

Hence, by the remarks from above it is clear, that the spaces in (7.1.1), $(Q^{\mathbf{r}}_{\mathbf{p}}\Lambda^\circ, \hat{\mathrm{d}}^\circ)$, respectively, determine a discrete Hilbert complex. One notes that if $p_i > r_i \geq 0$, the piecewise smoothness of the splines imply directly $Q^{\mathbf{r}}_{\mathbf{p}}\Lambda^k \subset H\Lambda^k(\widehat{\Omega})$ and we get a discrete subcomplex of the L^2 de Rham domain complex $(H\Lambda^\circ(\widehat{\Omega}), \hat{\mathrm{d}}^\circ)$ from Lemma 3.5. The next step is to realize that these spline differential forms determine a structure-preserving discretization of the continuous complex, at least in case of underlying regular meshes. To see this, we need to show the existence of L^2-bounded cochain projections. It becomes apparent, the special projections $\widehat{\Pi}^{\mathbf{l}}_{\mathbf{p},\mathbf{r}}$ from Section 6.3.2 are suitable for defining these cochain projections. To be more precise, we introduce

$$\begin{aligned}\widehat{\Pi}^{k,\Lambda}_{h,n}\colon L^2\Lambda^k(\widehat{\Omega}) &\to Q^{\mathbf{r}}_{\mathbf{p}}\Lambda^k\,,\\ \sum_{\sigma\in\Sigma_<(k,n)} c_\sigma\, dx^{\sigma_1}\wedge\cdots\wedge dx^{\sigma_k} &\mapsto \sum_{\sigma\in\Sigma_<(k,n)} \left(\widehat{\Pi}^{\mathbf{e}_\sigma}_{\mathbf{p},\mathbf{r}} c_\sigma\right) dx^{\sigma_1}\wedge\cdots\wedge dx^{\sigma_k}.\end{aligned}$$

The mesh size index h is added to emphasize the dependence on the mesh structure, which we require to be regular. In other words, $\widehat{\Pi}^{k,\Lambda}_{h,n}$ means, we project onto a spline space with mesh size h. Further one notes that with Lemma 6.5 we get $\widehat{\Pi}^{\mathbf{e}_\sigma}_{\mathbf{p},\mathbf{r}}\colon L^2(\widehat{\Omega}) \to S^{\mathbf{r}-\mathbf{e}_\sigma}_{\mathbf{p}-\mathbf{e}_\sigma}$ and we have L^2 stability. Consequently, the above definition indeed gives us a well-defined projection. The next lemma demonstrates the feasibility of these projections.

Lemma 7.1. *The mappings $\widehat{\Pi}^{\circ,\Lambda}_{h,n}$ define L^2-bounded cochain projections from the de Rham chain $(H\Lambda^\circ(\widehat{\Omega}), \hat{\mathrm{d}}^\circ)$ onto the complex $(Q^{\mathbf{r}}_{\mathbf{p}}\Lambda^\circ, \hat{\mathrm{d}}^\circ)$, which means we have*

$$\hat{\mathrm{d}}^k \circ \widehat{\Pi}^{k,\Lambda}_{h,n} = \widehat{\Pi}^{k+1,\Lambda}_{h,n} \circ \hat{\mathrm{d}}^k$$

on $H\Lambda^k(\widehat{\Omega})$.

Proof. Two things are clear by Lemma 6.5 and the definition of the $\widehat{\Pi}^{k,\Lambda}_{h,n}$. They are projections onto the spaces $Q^{\mathbf{r}}_{\mathbf{p}}\Lambda^k$ and they are L^2-bounded where the boundedness does not depend on the mesh size, provided a family of regular meshes. Thus, the only thing to check is the commutativity relation involving the exterior derivative. But also the latter is relative easy to see, namely for smooth $v \in L^2(\widehat{\Omega})$ and choice $\sigma \in \Sigma_<(k,n)$ we obtain utilizing Lemma 6.6 directly

$$\hat{\partial}_i \widehat{\Pi}^{\mathbf{e}_\sigma}_{\mathbf{p},\mathbf{r}} v = \widehat{\Pi}^{\mathbf{e}_\sigma+\mathbf{e}_i}_{\mathbf{p},\mathbf{r}} \hat{\partial}_i v = \widehat{\Pi}^{\mathbf{e}_s}_{\mathbf{p},\mathbf{r}} \hat{\partial}_i v, \quad \text{if } i \notin \{\sigma_1,\dots,\sigma_k\},$$

where $1 \leq s_1 < \cdots < s_{k+1} \leq n$ s.t. $\{i\} \cup \{\sigma_1,\dots,\sigma_k\} = \{s_1,\dots,s_{k+1}\}$. Thus, for a smooth differential k-form ω we see by (7.1.3) that

$$\hat{\mathrm{d}}^k \widehat{\Pi}^{k,\Lambda}_{h,n}\omega = \widehat{\Pi}^{k+1,\Lambda}_{h,n}\hat{\mathrm{d}}^k\omega.$$

The general statement follows by a density argument. □

Moreover, these projections satisfy classical approximation estimates as the next lemma shows.

Lemma 7.2. *Let $0 \leq k < n$ and $\mathbf{p} = (p_i)_i, \mathbf{r} = (r_i)_i \in \mathbb{N}^n$ s.t. $p_i > r_i \geq 0$ and set $p = \min_i\{p_i\}$, $r = \min_i\{r_i\}$. Further let a family of regular meshes be given. Then for the projections $\widehat{\Pi}^{k,\Lambda}_{h,n}$ related to the meshes, degrees $\mathbf{p}$ and regularities $\mathbf{r}$, we obtain the estimates*

$$\left\|\omega - \widehat{\Pi}^{k,\Lambda}_{h,n}\omega\right\|_{H^s(\hat{\mathrm{d}}^k)} \leq C_{\widehat{\Pi}} h^{l-s} \left\|\omega\right\|_{H^l(\hat{\mathrm{d}}^k)}, \qquad \forall \omega \in H^l(\widehat{\Omega}, \hat{\mathrm{d}}^k, \mathrm{Alt}^k), \qquad 0 \leq s \leq l \leq p,\ s \leq r,$$

with $C_{\widehat{\Pi}}$ independent of h. Besides, it is

$$\left\|\omega - \widehat{\Pi}^{k,\Lambda}_{h,n}\omega\right\|_{H^s} \leq C_{\widehat{\Pi}} h^{l-s} \left\|\omega\right\|_{H^l}, \qquad \forall \omega \in H^l\Lambda^k(\widehat{\Omega}), \qquad 0 \leq s \leq l \leq \tilde{p},\ s \leq r,$$

with abbreviation $\tilde{p} = p$ for $k > 0$ and $\tilde{p} = p+1$ for $k = 0$.

Proof. We begin with the second inequality. For $\omega \in H^l\Lambda^k(\widehat{\Omega})$ with representation $\omega = \sum_{\sigma\in\Sigma_<(k,n)} c_\sigma \, dx^{\sigma_1} \wedge \cdots \wedge dx^{\sigma_k}$, i.e. coefficients $c_\sigma \in H^l(\widehat{\Omega})$, it is $\widehat{\Pi}^{k,\Lambda}_{h,n}\omega \in H^s\Lambda^k(\widehat{\Omega})$ and

$$\left\|\omega - \widehat{\Pi}^{k,\Lambda}_{h,n}\omega\right\|_{H^s} \leq \sum_{\sigma\in\Sigma_<(k,n)} \left\|c_\sigma - \widehat{\Pi}^{\mathbf{e}_\sigma}_{\mathbf{p},\mathbf{r}} c_\sigma\right\|_{H^s} \leq \sum_{\sigma\in\Sigma_<(k,n)} Ch^{l-s} \left\|c_\sigma\right\|_{H^l} \leq \tilde{C}h^{l-s} \left\|\omega\right\|_{H^l}, \quad (7.1.4)$$

for proper constants C, $\tilde{C}$, due to Lemma 6.7. Here we remark that for the special case $k = 0$ it is $H^s\Lambda^0(\widehat{\Omega}) = H^s(\widehat{\Omega})$ and $\widehat{\Pi}^{k,\Lambda}_{h,n} = \widehat{\Pi}^{(0,\dots,0)}_{\mathbf{p},\mathbf{r}}$ which explains the possibility of $s = p + 1$.

Next we show the first estimate in the assertion. Therefore let $\omega \in H^l(\widehat{\Omega}, \hat{\mathrm{d}}^k, \mathrm{Alt}^k)$. By the choice of parameter $s \leq r \leq r_i$ and because of Lemma 7.1 we get beside $\widehat{\Pi}^{k,\Lambda}_{h,n}\omega \in H^s\Lambda^k(\widehat{\Omega})$ also $\hat{\mathrm{d}}^k\widehat{\Pi}^{k,\Lambda}_{h,n}\omega \in H^s\Lambda^{k+1}(\widehat{\Omega})$. Then, we see the wanted estimate by applying the already shown one (7.1.4), namely

$$\begin{aligned}
\left\|\omega - \widehat{\Pi}^{k,\Lambda}_{h,n}\omega\right\|^2_{H^s(\hat{\mathrm{d}}^k)} &= \left\|\omega - \widehat{\Pi}^{k,\Lambda}_{h,n}\omega\right\|^2_{H^s} + \left\|\hat{\mathrm{d}}^k\omega - \hat{\mathrm{d}}^k\widehat{\Pi}^{k,\Lambda}_{h,n}\omega\right\|^2_{H^s} \\
&= \left\|\omega - \widehat{\Pi}^{k,\Lambda}_{h,n}\omega\right\|^2_{H^s} + \left\|\hat{\mathrm{d}}^k\omega - \widehat{\Pi}^{k+1,\Lambda}_{h,n}\hat{\mathrm{d}}^k\omega\right\|^2_{H^s} \\
&\leq C\Big(h^{2(l-s)} \left\|\omega\right\|^2_{H^l} + h^{2(l-s)} \left\|\hat{\mathrm{d}}^k\omega\right\|^2_{H^l}\Big) \\
&= Ch^{2(l-s)} \left\|\omega\right\|^2_{H^l(\hat{\mathrm{d}}^k)}.
\end{aligned}$$

□

Of course, one can also return from differential forms back to classical functions and Sobolev spaces, by identifying the coefficients of the k-forms using proxy maps $\mathcal{J}_k$ with elements in $L^2(\widehat{\Omega}) \otimes \mathbb{R}^{n|k}$; see Section 3.3.2 and Definition 3.3.2. The resulting proxy Hilbert complex $(\widehat{\mathcal{D}}^\circ, H(\widehat{\Omega}, \widehat{\mathcal{D}}^\circ, \mathbb{R}^{n|\circ}))$, generated by operators of the form $\widehat{\mathcal{D}}^k = \mathcal{J}_{k+1} \circ \hat{\mathrm{d}}^k \circ \mathcal{J}_k^{-1}$, can also be discretized in a structure-preserving manner using B-splines. We simply take

$$\widehat{V}^k_{h,n} \coloneqq \mathcal{J}_k\Big(Q^{\mathbf{r}}_{\mathbf{p}}\Lambda^k\Big), \quad k = 0, \dots, , n, \quad (7.1.5)$$

as the discretization spaces. The corresponding projections are then given through

$$\widehat{\Pi}^k_{h,n} \coloneqq \mathcal{J}_k \circ \widehat{\Pi}^{k,\Lambda}_{h,n} \circ \mathcal{J}_k^{-1},$$

which ensures

$$\widehat{\mathcal{D}}^k \circ \widehat{\Pi}^k_{h,n} = \mathcal{J}_{k+1} \circ \hat{\mathrm{d}}^k \circ \mathcal{J}_k^{-1} \circ \mathcal{J}_k \circ \widehat{\Pi}^{k,\Lambda}_{h,n} \circ \mathcal{J}_k^{-1} = \mathcal{J}_{k+1} \circ \widehat{\Pi}^{k+1,\Lambda}_{h,n} \circ \hat{\mathrm{d}}^k \circ \mathcal{J}_k^{-1} = \widehat{\Pi}^{k+1}_{h,n} \circ \widehat{\mathcal{D}}^k$$

on $H(\widehat{\Omega}, \widehat{\mathcal{D}}^k, \mathbb{R}^{n|k})$. From the two Lemmata 7.1, 7.2 and the definition of $\widehat{\mathcal{D}}^k$, the next result follows directly.

Corollary 7.1. *Let the $\mathcal{J}_k \colon L^2\Lambda^k(\Omega) \to L^2(\Omega) \otimes \mathbb{R}^{n|k}$ be proxy maps as defined in* (3.3.6) *and $\widehat{\mathcal{D}}^k = \mathcal{J}_{k+1} \circ \hat{\mathrm{d}}^k \circ \mathcal{J}_k^{-1}$; see* (3.3.7)*. For a family of regular meshes, the spaces $\widehat{V}^k_{h,n}$ define a structure-preserving discretization of the proxy complex $\Big(H(\widehat{\Omega}, \widehat{\mathcal{D}}^\circ, \mathbb{R}^{n|\circ}), \widehat{\mathcal{D}}^\circ\Big)$. Moreover, if the assumptions and notation of the previous lemma apply, then it is*

$$\begin{aligned}
\left\|v - \widehat{\Pi}^k_{h,n}v\right\|_{H^s(\widehat{\mathcal{D}}^k)} &\leq C_{\widehat{\Pi}}h^{l-s} \left\|v\right\|_{H^l(\widehat{\mathcal{D}}^k)}, \qquad \forall v \in H^l(\widehat{\Omega}, \widehat{\mathcal{D}}^k, \mathbb{R}^{n|k}), \qquad 0 \leq s \leq l \leq p,\ s \leq r, \\
\left\|v - \widehat{\Pi}^k_{h,n}v\right\|_{H^s} &\leq C_{\widehat{\Pi}}h^{l-s} \left\|v\right\|_{H^l}, \qquad \forall v \in H^l(\widehat{\Omega}) \otimes \mathbb{R}^{n|k}, \qquad 0 \leq s \leq l \leq \tilde{p},\ s \leq r,
\end{aligned}$$

for a proper constant $C_{\widehat{\Pi}}$.

Now that we have established the construction of de Rham sequences using B-splines, our primary focus shifts to second-order complexes. In the upcoming section, we will elucidate how splines can be employed within the framework of the BGG construction.

7.2 Second-order spline complexes

The aim for this section is to explain the existence of B-spline discretizations of the second-order complexes derived by the coupling of two de Rham sequences with the procedure from Section 4.2.3. Therefore, please refer to this section for notation-related matters, as we will be reusing the spaces and notation introduced from there. Once more we restrict ourselves to complexes in the reference cube $\Omega = \widehat{\Omega} = (0,1)^n$ and we add a *hat*, meaning we write e.g. $\widehat{\mathscr{D}}_n^{k,J}$, $\widehat{\mathscr{V}}_n^{k,J}$ instead of $\mathscr{D}_n^{k,J}$, $\mathscr{V}_n^{k,J}$, where the latter operators and spaces are defined through Lemma 4.9. For the special setting of a cubical domain a general construction of discrete Alt^l-valued forms that fit to the BGG procedure from the mentioned Section 4.2.3 is outlined in [19]. In the following let us briefly discuss the relevant spaces and projections established in the latter paper. Again we first start with a abstract notation involving differential forms, subspaces of $L^2(\widehat{\Omega}) \otimes \mathrm{Alt}^{k,l}$, respectively, to highlight the underlying structure. Nevertheless at the end of the section we explain why the results directly transfer to cases where we deal with proxy complexes and classical matrix- or vector-fields.

7.2.1 General construction for complexes from Alt^l-valued forms

Analogously to the approach for the de Rham complex we introduce subspaces of $L^2(\widehat{\Omega}) \otimes \mathrm{Alt}^{k,l}$ by utilizing B-spline coefficient functions. But, whereas in case of the de Rham sequence the convenient spline spaces are easily implied by the definition of the exterior derivative and the property $\hat{\partial}_i S^{\mathbf{r}}_{\mathbf{p}} = S^{\mathbf{r}-\mathbf{e}_i}_{\mathbf{p}-\mathbf{e}_i}$, the situation is more complicated for the output complexes $(\widehat{\mathscr{V}}_n^{\circ,J}, \widehat{\mathscr{D}}_n^{\circ,J})$. Because, now the new differential operators depend on the appearing linking maps $S^{k,l}$ and might be more complicated to handle. That is why we describe and define the important spaces and projections, but we refer to [19] for more details and proofs.

Firstly, let the components of the degree and regularity vectors $\mathbf{p} = (p_i)_i \in \mathbb{N}^n$ and $\mathbf{r} = (r_i)_i \in \mathbb{N}^n$ fulfill this time $p_i > r_i > 0$ and let us use again the notation $\mathbf{e}_\tau \in \mathbb{N}_0^n$ for the characteristic vector of an element $\tau \in \Sigma_<(k,n)$; compare (7.1.2).
Then, for $k, l \in \{0, \dots, n\}$ we start with the definition

$$\begin{aligned}\mathscr{Q}^{\mathbf{r}}_{\mathbf{p}}\Lambda^{k,l} &= \left\{ \sum_{\sigma\in\Sigma_<(k,n)} \sum_{s\in\Sigma_<(l,n)} c_{\sigma,s}(dx^{\sigma_1}\wedge\cdots\wedge dx^{\sigma_k})\otimes(dx^{s_1}\wedge\cdots\wedge dx^{s_l}) \,\middle|\, c_{\sigma,s} \in S^{\mathbf{r}-\mathbf{e}_\sigma-\mathbf{e}_s}_{\mathbf{p}-\mathbf{e}_\sigma-\mathbf{e}_s} \right\} \\ &\subset L^2\Lambda^{k,l}(\widehat{\Omega}). \end{aligned} \tag{7.2.1}$$

One notes our restriction $p_i > r_i > 0$. Consequently, the entries of the vector $\mathbf{p} - \mathbf{e}_\sigma - \mathbf{e}_s$ are greater or equal to zero and similarly the entries of $\mathbf{r} - \mathbf{e}_\sigma - \mathbf{e}_s$ are greater or equal to -1. In particular these spaces $\mathscr{Q}^{\mathbf{r}}_{\mathbf{p}}\Lambda^{k,l}$ above are well-defined.
By the definition (4.2.17) of the exterior product in the context of these $\mathrm{Alt}^{k,l}$-forms and the observations from Section 7.1 we see for an element $\omega = c_{\sigma,s}(dx^{\sigma_1}\wedge\cdots\wedge dx^{\sigma_k})\otimes(dx^{s_1}\wedge\cdots\wedge dx^{s_l}) \in \mathscr{Q}^{\mathbf{r}}_{\mathbf{p}}\Lambda^{k,l}$, i.e. $c_{\sigma,s} \in S^{\mathbf{r}-\mathbf{e}_\sigma-\mathbf{e}_s}_{\mathbf{p}-\mathbf{e}_\sigma-\mathbf{e}_s}$, that

$$\begin{aligned}\hat{\mathrm{d}}^k\omega &= \sum_{\substack{i=1\\ i\notin\{\sigma_1,\dots,\sigma_k\}}}^{n} \hat{\partial}_i c_{\sigma,s}(dx^i\wedge dx^{\sigma_1}\wedge\cdots\wedge dx^{\sigma_k})\otimes(dx^{s_1}\wedge\cdots\wedge dx^{s_l}) \\ &= \sum_{\substack{i=1\\ i\notin\{\sigma_1,\dots,\sigma_k\}}}^{n} (-1)^{j_i}\Big(\hat{\partial}_i c_{\sigma,s}\Big)(dx^{\eta^{(i)}_1}\wedge\cdots\wedge dx^{\eta^{(i)}_{k+1}})\otimes(dx^{s_1}\wedge\cdots\wedge dx^{s_l}),\end{aligned}$$

where above $\eta^{(i)} \in \Sigma_<(k+1,n)$ is the unique element s.t. $\{i\}\cup\{\sigma_1,\dots,\sigma_k\} = \{\eta^{(i)}_1,\dots,\eta^{(i)}_{k+1}\}$ and j_i are suitable numbers in $\{0,1\}$. For an $i \notin \{\sigma_1,\dots,\sigma_k\}$ we have $\hat{\partial}_i c_{\sigma,s} \in S^{\mathbf{r}-\mathbf{e}_\sigma-\mathbf{e}_s-\mathbf{e}_i}_{\mathbf{p}-\mathbf{e}_\sigma-\mathbf{e}_s-\mathbf{e}_i}$,

which gives with $\tau \coloneqq \eta^{(i)}$ directly $\hat{\partial}_i c_{\sigma,s} \in S^{\mathbf{r}-\mathbf{e}_\tau-\mathbf{e}_s}_{\mathbf{p}-\mathbf{e}_\tau-\mathbf{e}_s}$. Again $\hat{\mathrm{d}}^k$ stands for the exterior derivative in the reference cube $(0,1)^n$. Thus we indeed see $\hat{\mathrm{d}}^k\,\omega \in \mathscr{Q}^{\mathbf{r}}_{\mathbf{p}}\Lambda^{k+1,l}$ and linearity implies

$$\hat{\mathrm{d}}^k\,\mathscr{Q}^{\mathbf{r}}_{\mathbf{p}}\Lambda^{k,l} \subset \mathscr{Q}^{\mathbf{r}}_{\mathbf{p}}\Lambda^{k+1,l}.$$

So the $\mathscr{Q}^{\mathbf{r}}_{\mathbf{p}}\Lambda^{k,l}$ seem to be candidates for a discretization of the output complexes $(\widehat{\mathscr{V}}^{\circ,J}_n, \widehat{\mathscr{D}}^{\circ,J}_n)$. But actually, it becomes quickly clear that it is not enough to have discrete versions of the input chains, namely the $(H\Lambda^{\circ,l}(\widehat{\Omega}), \hat{\mathrm{d}}^\circ)$. Since, we also need to take the linking maps $s^{k,l}$ or $S^{k,l}$ into account, which are central to the BGG construction of the output complexes. In [19, Section 2.3], it is shown that we indeed obtain a diagram of the form

$$\begin{array}{ccccccccc}
\cdots & & \mathscr{Q}^{\mathbf{r}}_{\mathbf{p}}\Lambda^{k,J-1} & \xrightarrow{\hat{\mathrm{d}}^k} & \mathscr{Q}^{\mathbf{r}}_{\mathbf{p}}\Lambda^{k+1,J-1} & \xrightarrow{\hat{\mathrm{d}}^{k+1}} & \mathscr{Q}^{\mathbf{r}}_{\mathbf{p}}\Lambda^{k+2,J-1} & & \cdots \\
& S^{k-1,J}\nearrow & & S^{k,J}\nearrow & & S^{k+1,J}\nearrow & & & \\
\cdots & \mathscr{Q}^{\mathbf{r}}_{\mathbf{p}}\Lambda^{k-1,J} & \xrightarrow{\hat{\mathrm{d}}^{k-1}} & \mathscr{Q}^{\mathbf{r}}_{\mathbf{p}}\Lambda^{k,J} & \xrightarrow{\hat{\mathrm{d}}^k} & \mathscr{Q}^{\mathbf{r}}_{\mathbf{p}}\Lambda^{k+1,J} & \cdots & , &
\end{array} \tag{7.2.2}$$

where the anti-commutativity property $\hat{\mathrm{d}}^{l+1} \circ S^{l,J} = -S^{l+1,J} \circ \hat{\mathrm{d}}^l$ is satisfied. Furthermore, the simple structure $S^{k,l} = \mathrm{id} \otimes s^{k,l}$ of the linking maps implies that the injectivity/surjectivity properties of $s^{k,l}$ given in Lemma 4.8 also remain analogously valid in the case of the above diagram; see [19, Remark 3].

Remark 7.1 (Notation in [19]). When checking the results from [19] to which we referred to, there might arise some confusion at first glance. Namely, if one looks e.g. at equation (23) in the mentioned paper, there appear spaces of the form $\mathrm{Alt}^{i_1,j_1} \otimes \cdots \otimes \mathrm{Alt}^{i_n,j_n}$, where in this situation $\mathrm{Alt}^{i_l,j_l} = \mathrm{Alt}^{i_l}(\mathbb{R}) \otimes \mathrm{Alt}^{j_l}(\mathbb{R})$. As implied by [19, Lemma 1], however, we have for $\sigma \in \Sigma_<(k,n)$, $s \in \Sigma_<(l,n)$ the identification

$$(dx^{\sigma_1} \wedge \cdots \wedge dx^{\sigma_k}) \otimes (dx^{s_1} \wedge \cdots \wedge dx^{s_l}) \longleftrightarrow \mathrm{Alt}^{i_1,j_1} \otimes \cdots \otimes \mathrm{Alt}^{i_n,j_n},\ i_m = (\mathbf{e}_\sigma)_m,\ j_m = (\mathbf{e}_s)_m,\ \forall m.$$

In other words, in (7.2.1) we simply use a slightly different representation of the spaces compared to [19]. A similar adaptation of notation is used below in the definition of the various projections.

Corollary 7.2 (**Discrete output complex**). *So, by applying the BGG construction as in Lemma 4.9 now to diagram* (7.2.2)*, we actually obtain subcomplexes of the continuous pendants* $(\widehat{\mathscr{V}}^{\circ,J}_n, \widehat{\mathscr{D}}^{\circ,J}_n)$*. We will write for the resulting discrete complexes simply* $(\widehat{\mathscr{V}}^{\circ,J}_{h,n}, \widehat{\mathscr{D}}^{\circ,J}_n)$*, although it is clear that there is a dependence on the underlying meshes as well as on the vectors* $\mathbf{p}$, $\mathbf{r}$.

Naturally, the question arises as to whether these $\widehat{\mathscr{V}}^{\circ,J}_{h,n}$ also represent a structure-preserving discretization, allowing us to construct bounded cochain projections from $\widehat{\mathscr{V}}^{\circ,J}_n$ onto $\widehat{\mathscr{V}}^{\circ,J}_{h,n}$ once again. Before we clarify this question, we make a naive attempt inspired by the projections in the case of the de Rham sequence. More precisely, we set

$$\begin{aligned}
&\widehat{\Pi}^{k,l,\Lambda}_{h,n} \colon L^2(\widehat{\Omega}) \otimes \mathrm{Alt}^{k,l} \to \mathscr{Q}^{\mathbf{r}}_{\mathbf{p}}\Lambda^{k,l}\ , \\
&\quad \sum_{\sigma\in\Sigma_<(k,n)} \sum_{s\in\Sigma_<(l,n)} c_{\sigma,s}(dx^{\sigma_1} \wedge \cdots \wedge dx^{\sigma_k}) \otimes (dx^{s_1} \wedge \cdots \wedge dx^{s_l}) \mapsto \\
&\qquad \sum_{\sigma\in\Sigma_<(k,n)} \sum_{s\in\Sigma_<(l,n)} \Big(\widehat{\Pi}^{\mathbf{e}_\sigma+\mathbf{e}_s}_{\mathbf{p},\mathbf{r}} c_{\sigma,s}\Big)(dx^{\sigma_1} \wedge \cdots \wedge dx^{\sigma_k}) \otimes (dx^{s_1} \wedge \cdots \wedge dx^{s_l}).
\end{aligned} \tag{7.2.3}$$

Through this definition, two things are automatically fulfilled. Firstly, they are projections onto the $\mathscr{Q}^{\mathbf{r}}_{\mathbf{p}}\Lambda^{k,l}$. And secondly, these mappings are L^2-bounded, as follows from the Lemma

6.5. Demonstrating compatibility with the operators $\widehat{\mathscr{D}}_n^{\circ,J}$ and the linking maps $S^{l,J}$ is more challenging to see, but follows from the results in [19]. For this purpose, let us define for $i = 1, \dots, n$ the projections

$$\pi_i^{k,l} \colon L^2((0,1)) \to L^2((0,1)) \ , \ \pi_i^{k,l} \coloneqq \begin{cases} \widehat{\Pi}^0_{p_i,r_i}, \ \text{if } k=0,\, l=0, \\ \widehat{\Pi}^1_{p_i,r_i}, \ \text{if } k=1,\, l=0, \\ \widehat{\Pi}^1_{p_i,r_i}, \ \text{if } k=0,\, l=1, \\ \widehat{\Pi}^2_{p_i,r_i}, \ \text{if } k=1,\, l=1, \end{cases} \tag{7.2.4}$$

utilizing notation from Definition 6.7 and with p_i, r_i denoting the entries of the degree and regularity vectors. Due to Definition 1 and Section 3.1 in [19] suitable bounded cochains projections for the output complex are obtained by

$$\begin{aligned} &\tilde{\Pi}^{k,l}_{h,n} \colon L^2(\widehat{\Omega}) \otimes \mathrm{Alt}^{k,l} \to \mathscr{Q}^{\mathbf{r}}_{\mathbf{p}} \Lambda^{k,l} \ , \\ &\sum_{\sigma \in \Sigma_<(k,n)} \sum_{s \in \Sigma_<(l,n)} c_{\sigma,s} (dx^{\sigma_1} \wedge \cdots \wedge dx^{\sigma_k}) \otimes (dx^{s_1} \wedge \cdots \wedge dx^{s_l}) \mapsto \\ &\qquad \sum_{\sigma \in \Sigma_<(k,n)} \sum_{s \in \Sigma_<(l,n)} \Big(\pi^{\sigma,s} c_{\sigma,s}\Big) (dx^{\sigma_1} \wedge \cdots \wedge dx^{\sigma_k}) \otimes (dx^{s_1} \wedge \cdots \wedge dx^{s_l}), \end{aligned}$$

where

$$\pi^{\sigma,s} \coloneqq \pi_1^{i_1,j_1} \otimes \cdots \otimes \pi_n^{i_n,j_n}, \ i_l = (\mathbf{e}_\sigma)_l, \ j_l = (\mathbf{e}_s)_l, \ \forall l. \tag{7.2.5}$$

What we mean by *suitable* in this context is clarified by the next lemma. But before stating this lemma we go back to the definition (7.2.4) of the auxiliary projections and see for the last line directly $\pi_l^{i_l,j_l} = \widehat{\Pi}^{i_l+j_l}_{p_i,r_i}$.
Consequently, utilizing our definition (6.3.9), then (7.2.5) yields

$$\pi^{\sigma,s} = \widehat{\Pi}^{\mathbf{e}_\sigma + \mathbf{e}_s}_{\mathbf{p},\mathbf{r}}. \tag{7.2.6}$$

That is, the projections introduced in (7.2.3) above coincide with those derived through the tensor product approach in [19].

Therefore, we can summarize the following because of Theorem 2, Theorem 3, and the Section 3.1 in [19]:

Lemma 7.3 (**Spline output complexes**, see [19, Theorem 2, Theorem 3])**.** *Applying the BGG construction to diagram* (7.2.2)*, we obtain as result a subcomplex* $(\widehat{\mathscr{V}}^{\circ,J}_{h,n}, \widehat{\mathscr{D}}^{\circ,J}_n)$ *of the continuous output complex* $(\widehat{\mathscr{V}}^{\circ,J}_n, \widehat{\mathscr{D}}^{\circ,J}_n)$ *from Section 4.2.3, where here* $J \in \{1, \dots, n\}$*. Moreover the projections* $\widehat{\Pi}^{k,l,\Lambda}_{h,n}$ *determine in fact* L^2*-bounded cochain projections onto the discrete sequence. In more detail, with*

$$\mathscr{P}^{k,J,\Lambda}_{h,n} \coloneqq \begin{cases} \widehat{\Pi}^{k,J-1,\Lambda}_{h,n}, \ \text{if } k \le J-1, \\ \widehat{\Pi}^{k,J,\Lambda}_{h,n}, \ \text{if } k \ge J \end{cases} \tag{7.2.7}$$

and the notation from Lemma 4.9, it is

$$\begin{aligned} \mathscr{P}^{\circ,J,\Lambda}_{h,n} &\colon L^2(\widehat{\Omega}) \otimes \mathbb{A}^{k,J}_n \to \widehat{\mathscr{V}}^{k,J}_{h,n}, \\ \mathscr{P}^{k+1,J,\Lambda}_{h,n} \circ \widehat{\mathscr{D}}^{k,J}_n &= \widehat{\mathscr{D}}^{k,J}_n \circ \mathscr{P}^{k,J,\Lambda}_{h,n}, \quad \text{on } \widehat{\mathscr{V}}^{k,J}_n, \text{ and} \\ \left\| \widehat{\Pi}^{k,l,\Lambda}_{h,n} \omega \right\|_{L^2} &\le C_{\widehat{\Pi}} \left\| \omega \right\|_{L^2}, \qquad \text{on } L^2\Lambda^{k,l}(\widehat{\Omega}), \end{aligned}$$

for some positive constant $C_{\widehat{\Pi}}$*. Thus,* $(\widehat{\mathscr{V}}^{\circ,J}_{h,n}, \widehat{\mathscr{D}}^{\circ,J}_n)$ *represents a structure-preserving discretization of* $(\widehat{\mathscr{V}}^{\circ,J}_n, \widehat{\mathscr{D}}^{\circ,J}_n)$*.*

Proof. This is a direct consequence of the Lemmata 2–4 from [19] and the remarked equivalence between the projections discussed on the mentioned reference and the ones we defined in (7.2.3); see (7.2.6). □

In view of the previous lemma and the properties related to projections of the form $\widehat{\Pi}^{\mathbf{l}}_{\mathbf{p},\mathbf{r}}$ (Lemma 6.7) one can proof completely analogously to the situation of a de Rham sequence, see Lemma 7.2, the next approximation estimates.

Lemma 7.4. *Let us assume to have a family of regular meshes on $\widehat{\Omega}$ and let us consider the corresponding spaces $\widehat{\mathscr{V}}^{\circ,J}_{h,n}$ from Lemma 7.3 forming a discrete output complex. Further we assume for the underling degree and regularity vector $\mathbf{p} = (p_i)_i, \mathbf{r} = (r_i)_i \in \mathbb{N}^n$ that $p_i > r_i \geq 1$ and we set $p = \min_i\{p_i\},\ r = \min_i\{r_i\}$. Then there exists a constant $C_{\widehat{\Pi}}$ independent of mesh size h with*

$$\left\|\omega - \mathscr{P}^{k,J,\Lambda}_{h,n}\omega\right\|_{H(\widehat{\mathscr{D}})} \leq C_{\widehat{\Pi}} h^l \left\|\omega\right\|_{H^l(\widehat{\mathscr{D}})}, \qquad \forall \omega \in H^l(\widehat{\Omega}, \widehat{\mathscr{D}}^{k,J}_n, \mathbb{A}^{k,J}_n), \qquad 0 \leq l \leq p-1.$$

Moreover, one has the inclusions $\widehat{\mathscr{V}}^{k,J}_{h,n} \subset H^{r-1}(\widehat{\Omega}) \otimes \mathbb{A}^{k,J}_n$ and the additional error estimate

$$\left\|\omega - \mathscr{P}^{k,J,\Lambda}_{h,n}\omega\right\|_{H^t} \leq C_{\widehat{\Pi}} h^{l-t} \left\|\omega\right\|_{H^l}, \qquad \forall \omega \in H^l(\widehat{\Omega}) \otimes \mathbb{A}^{k,J}_n, \qquad 0 \leq t \leq l \leq p-1,\ t \leq r-1.$$

Certainly, all the above estimates are fulfilled for every $k \in \{0, \dots, n\}$.

Proof. In principle we use the same steps as in the proof of Lemma 7.2, but now with the restriction $p_i > r_i > 0$. For example, we obtain for $\omega \in H^t(\widehat{\Omega}) \otimes \mathbb{A}^{k,l}_n$ with (7.2.3) and Lemma 6.7 directly

$$\begin{aligned}\left\|\omega - \widehat{\Pi}^{k,l,\Lambda}_{h,n}\omega\right\|_{L^2} &\leq \sum_{\sigma\in\Sigma_<(k,n)} \sum_{s\in\Sigma_<(l,n)} \left\|c_{\sigma,s} - \widehat{\Pi}^{\mathbf{e}_\sigma+\mathbf{e}_s}_{\mathbf{p},\mathbf{r}} c_{\sigma,s}\right\|_{L^2} \leq C \sum_{\sigma\in\Sigma_<(k,n)} \sum_{s\in\Sigma_<(l,n)} h^t \left\|c_{\sigma,s}\right\|_{H^t} \\ &\leq \tilde{C} h^t \left\|\omega\right\|_{H^t}, \quad 0 \leq t \leq p-1,\end{aligned}$$

where ω is represented w.r.t. the standard basis (4.2.16). And this gives the first inequality in the assertion due to abbreviation (7.2.7) and Lemma 7.3, the commutativity property of the projections, respectively. The mentioned inclusions are clear by the definition of r and the additional estimates are again a straightforward application of Lemma 6.7. □

Since all the $\widehat{\mathscr{V}}^{\circ,J}_{h,n}$ are built by standard spline spaces, we can directly conclude from Lemma 6.3 the next inverse estimates.

Corollary 7.3 (**Inverse estimates**)**.** *Let the assumptions of the previous Lemma 7.4 hold. Then there is a constant C_{inv} s.t.*

$$\left\|\omega_h\right\|_{H^s} \leq C_{inv} h^{l-s} \left\|\omega_h\right\|_{H^l}, \qquad \forall \omega_h \in \widehat{\mathscr{V}}^{k,J}_{h,n}, \qquad 0 \leq l \leq s \leq r-1,$$

with C_{inv} independent from h.

As outlined in Section 4.2.3 (see Definition 4.3), we can reduce the situation of coupled Alt^k-valued forms to the situation of matrix- or vector-valued mappings. The only things we need are proxy maps $\mathcal{J}_k$ on Alt^k-forms and the resulting proxy output complex was denoted with $(\mathfrak{V}^{\circ,J}_n, \mathfrak{D}^{\circ,J}_n)$. For more details on the exact identification approach, we refer to the mentioned section. So, there is no problem to analogously identify elements in the spaces $\mathscr{Q}^{\mathbf{r}}_{\mathbf{p}}\Lambda^{k,J}$, $\mathscr{Q}^{\mathbf{r}}_{\mathbf{p}}\Lambda^{k,J-1}$ with matrix-valued mappings. To be more precise, we consider the proxy spaces

$$\widehat{V}^{k,l}_{h,n} \coloneqq \mathcal{J}_k(\mathscr{Q}^{\mathbf{r}}_{\mathbf{p}}\Lambda^{k,l}), \quad l \in \{J-1, J\}. \tag{7.2.8}$$

Just as in the continuous case (see Section 4.2.3), where the proxy maps yield a proxy output complex, applying the BGG construction to the setting in diagram (7.2.9) results in a discrete proxy output complex. We will denote the latter as $(\widehat{\mathfrak{V}}_{h,n}^{\circ,J}, \widehat{\mathfrak{D}}_n^{\circ,J})$. It should also be mentioned here that when transitioning from de Rham involving differential forms to proxy complexes in Section 4.2.3, we have replaced the exterior derivative d^k with operators of the form $\mathcal{D}^k := \mathcal{J}_{k+1} \circ \mathrm{d}^k \circ \mathcal{J}_k^{-1}$. Now, if we add a *hat*, meaning we write $\widehat{\mathcal{D}}^k$, highlighting our current restriction to the reference domain, we obtain in the case of proxy complexes a following diagram analogous to (7.2.2):

$$\begin{array}{ccccccccccc} \dots & & \widehat{V}_{h,n}^{k,J-1} & & \xrightarrow{\widehat{\mathcal{D}}^k} & & \widehat{V}_{h,n}^{k+1,J-1} & \xrightarrow{\widehat{\mathcal{D}}^{k+1}} & \widehat{V}_{h,n}^{k+2,J-1} & & \dots \\ & \tilde{S}^{k-1,J} \nearrow & & & & \tilde{S}^{k,J} \nearrow & & & & \tilde{S}^{k+1,J} \nearrow & \\ \dots & & \widehat{V}_{h,n}^{k-1,J} & \xrightarrow{\widehat{\mathcal{D}}^{k-1}} & & \widehat{V}_{h,n}^{k,J} & \xrightarrow{\widehat{\mathcal{D}}^{k}} & & \widehat{V}_{h,n}^{k+1,J} & \dots & . \end{array} \tag{7.2.9}$$

In this process, the new linking maps $\tilde{S}^{l,J}$ result from the original ones by setting $\tilde{S}^{l,J} = \mathcal{J}_{l+1} \circ S^{l,J} \circ \mathcal{J}_l^{-1}$.

Since we are not altering the underlying structures but only switching between the spaces $L^2(\widehat{\Omega}) \otimes \mathrm{Alt}^{k,l}$ and $L^2(\widehat{\Omega}) \otimes \mathbb{R}^{(n|l)\times(n|k)}$ using the $\mathcal{J}_k$, it is clear that the same results as in Lemma 7.3 and Lemma 7.4 also apply to the discrete proxy output complex. For the sake of completeness, we would like to briefly summarize them here once again.

Corollary 7.4. *The discrete complexes $(\widehat{\mathfrak{V}}_{h,n}^{\circ,J}, \widehat{\mathfrak{D}}_n^{\circ,J})$, given by a BGG construction applied to the proxy complexes, meaning diagram (7.2.9), determine a structure-preserving discretization of the continuous proxy output complex $(\widehat{\mathfrak{V}}_n^{\circ,J}, \widehat{\mathfrak{D}}_n^{\circ,J})$ on $\widehat{\Omega}$, provided a family of regular meshes. L^2-bounded cochain projections are given by*

$$\mathscr{P}_{h,n}^{k,J} := \mathcal{J}_k \circ \mathscr{P}_{h,n}^{k,J,\Lambda} \circ \mathcal{J}_k^{-1}, \tag{7.2.10}$$

with proxy maps $\mathcal{J}_k \colon L^2(\Omega) \otimes \mathrm{Alt}^{k,l} \to L^2(\Omega) \otimes \mathbb{R}^{(n|l)\times(n|k)}$; compare the explanations before Definition 4.3.
The estimates from Lemma 7.4 hold in an analogous manner also for $\mathscr{P}_{h,n}^{k,J}$, hence e.g. it is

$$\left\| v - \mathscr{P}_{h,n}^{k,J} v \right\|_{H(\widehat{\mathfrak{D}})} \leq C_{\widehat{\Pi}} h^l \left\| v \right\|_{H^l(\widehat{\mathfrak{D}})}, \qquad \forall v \in H^l(\widehat{\Omega}, \widehat{\mathfrak{D}}_n^{k,J}, \mathbb{V}_n^{k,J}), \qquad 0 \leq l \leq p-1,$$

where we refer to (4.2.22) for a definition of the $\mathbb{V}_n^{\circ,J}$.

7.2.2 Complexes in $2D$

Here we want to be more specific and use the general definitions from the last subsection in a concrete setting. More precisely, similarly to the discussions in [19] we present a finite-dimensional approximation of the diagram (4.2.25) given in Example 4.2. It should be noted that the last diagram has been created with the help of proper proxy maps $\mathcal{J}_k$ defined in Example 3.1 ($3D$) and Example 3.2 ($2D$). But, as we explained how to incorporate such proxy mappings in the BGG framework, the below concentration on specific vector- or matrix valued mappings is justified; compare (7.2.8). To simplify the analysis, we will assume that the underlying spaces in (7.2.1) have degree and regularity vectors in the form of $\mathbf{p} = (p, p)$ and $\mathbf{r} = (r, r)$, with $p > r > 0$. If we now map the resulting spaces $\mathscr{Q}_{\mathbf{p}}^{\mathbf{r}} \Lambda^{k,l}$ back to those in $L^2(\widehat{\Omega}) \otimes \mathbb{R}^{(n|l)\times(n|k)}$, in the sense of (7.2.8), then the following diagram structure is obtained:

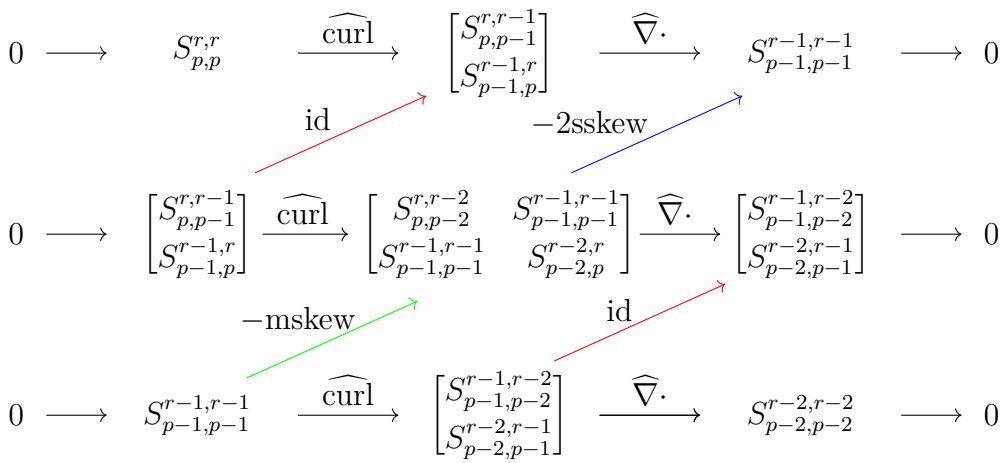

Figure 10: Each row represents a discrete de Rham sequence, where the blue (green) linking map is surjective (injective) between the discrete spaces.

One verifies easily that the spaces in Figure 10 fit, i.e. that the individual rows represent bounded Hilbert complexes and the linking maps satisfy the surjectivity and injectivity conditions from (4.2.2) and similarly to (4.2.25). In other words, the coupling of consecutive rows provides discrete versions of the elasticity and divdiv complexes in $2D$ on $\widehat{\Omega}$; compare Example 4.2. However, we require more than just subcomplexes, rather, we aim for structure-preserving discretizations. This necessitates bounded cochain projections from the continuous chains to the corresponding spline spaces, whereby the operator norm of the projections must not depend on the mesh size. In other words, we must also provide projections onto the spaces in Figure 10. But we already know in the general case, which projections are suitable, namely the one from (7.2.3), (7.2.10), respectively. To provide an overview, we would like to summarize the relevant projections in a further diagram. In Figure 11, we repeat the diagram from Figure 10, but at the respective places, we incorporate the associated projections, not the spline spaces, where we use the abbreviation $\widehat{\Pi}^{l_1,l_2} := \widehat{\Pi}^{\mathbf{l}}_{\mathbf{p},\mathbf{r}}$, $\mathbf{l} = (l_1, l_2)$, for a better readability.

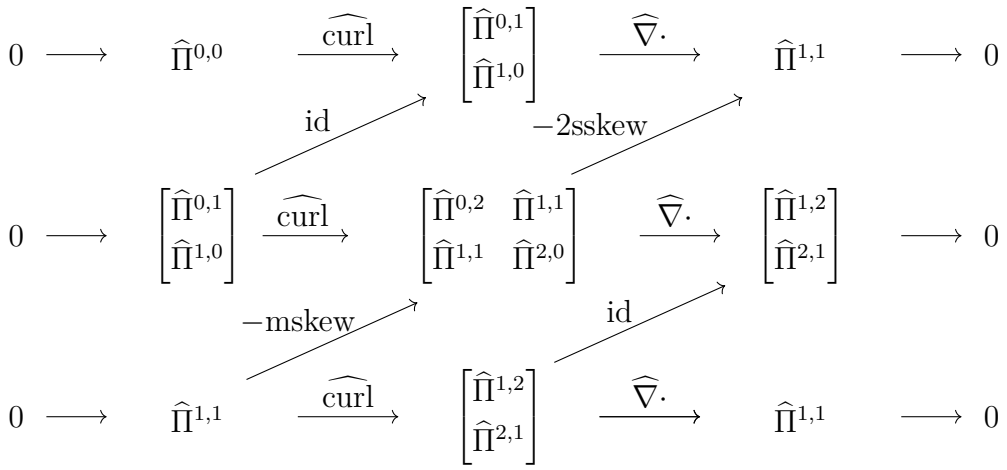

Figure 11: In this diagram we summarize the projections onto the related spaces in the previous Figure 10 which in fact determine the cochain projections onto the respective output complexes.

We have a possible discretization of the general BGG construction in $2D$, as discussed in Section 4.2.3. Consequently, it is also evident how we obtain finite-dimensional versions of

elasticity and divdiv complexes; see (4.2.26). and (4.2.27). We only need to combine the first or last two rows in Figure 10, following the BGG construction principles. One gets:

Corollary 7.5 (**Discrete elasticity complex**-$2D$)**.** *The spaces*

$$\widehat{\mathfrak{V}}^{0,1}_{h,2} \coloneqq S^{r,r}_{p,p}, \qquad \widehat{\mathfrak{V}}^{1,1}_{h,2} \coloneqq \begin{bmatrix} S^{r,r-2}_{p,p-2} & S^{r-1,r-1}_{p-1,p-1} \\ S^{r-1,r-1}_{p-1,p-1} & S^{r-2,r}_{p-2,p} \end{bmatrix} \cap L^2(\widehat{\Omega}) \otimes \mathbb{S}, \qquad \widehat{\mathfrak{V}}^{2,1}_{h,2} \coloneqq \begin{bmatrix} S^{r-1,r-2}_{p-1,p-2} \\ S^{r-2,r-1}_{p-2,p-1} \end{bmatrix}$$

determine a structure-preserving discretization of the elasticity complex on $(0,1)^2$*; see* (4.2.26)*. Thus we especially have the discrete complex*

$$0 \longrightarrow \widehat{\mathfrak{V}}^{0,1}_{h,2} \xrightarrow{\widehat{\operatorname{curl}}^2} \widehat{\mathfrak{V}}^{1,1}_{h,2} \xrightarrow{\widehat{\nabla}\cdot} \widehat{\mathfrak{V}}^{2,1}_{h,2} \longrightarrow 0. \tag{7.2.11}$$

Corollary 7.6 (**Discrete divdiv complex**-$2D$)**.** *The spaces*

$$\widehat{\mathfrak{V}}^{0,2}_{h,2} \coloneqq \begin{bmatrix} S^{r,r-1}_{p,p-1} \\ S^{r-1,r}_{p-1,p} \end{bmatrix}, \qquad \widehat{\mathfrak{V}}^{1,2}_{h,2} \coloneqq \begin{bmatrix} S^{r,r-2}_{p,p-2} & S^{r-1,r-1}_{p-1,p-1} \\ S^{r-1,r-1}_{p-1,p-1} & S^{r-2,r}_{p-2,p} \end{bmatrix} \cap L^2(\widehat{\Omega}) \otimes \mathbb{S}, \qquad \widehat{\mathfrak{V}}^{2,2}_{h,2} \coloneqq S^{r-2,r-2}_{p-2,p-2}$$

determine a structure-preserving discretization of the divdiv complex on $(0,1)^2$*; see* (4.2.27)*. We have the Hilbert complex*

$$0 \longrightarrow \widehat{\mathfrak{V}}^{0,2}_{h,2} \xrightarrow{\widehat{\operatorname{symcurl}}} \widehat{\mathfrak{V}}^{1,2}_{h,2} \xrightarrow{\widehat{\nabla}\cdot\widehat{\nabla}\cdot} \widehat{\mathfrak{V}}^{2,2}_{h,2} \longrightarrow 0. \tag{7.2.12}$$

In the simple reference area, i.e., $(0,1)^2$, the exactness of the complexes from the previous corollaries holds for levels $k > 0$. We will exploit this in the following two examples.

Example 7.1 (Elasticity complex: Hodge–Laplace problem of level $k = 1$)**.** *We now intend to demonstrate how one can utilize the spline spaces to approximately solve a Hodge–Laplace problem on* $\widehat{\Omega}$ *induced by the elasticity complex* (4.2.26)*. In particular, we aim to illustrate through a numerical test that we can achieve the convergence behavior suggested by the theory. In view of Definition 4.5 and the notation from Section 4.2.2 we consider the continuous complex* $(\mathscr{V}^\circ, \mathscr{D}^\circ)$ *with differential operators* $\mathscr{D}^0 \coloneqq \widehat{\operatorname{curl}}^2$ *,* $\mathscr{D}^1 \coloneqq \widehat{\nabla}\cdot$ *and spaces* $\mathscr{V}^0 \coloneqq H^2(\widehat{\Omega})$*,* $\mathscr{V}^1 \coloneqq H(\widehat{\Omega}, \widehat{\nabla}\cdot, \mathbb{S})$*,* $\mathscr{V}^2 \coloneqq L^2(\widehat{\Omega}) \otimes \mathbb{R}^2$*. Using integration by parts one gets the adjoint differential operators* $\mathscr{D}_2^* = -\operatorname{sym}\widehat{\nabla}\colon L^2(\widehat{\Omega})\otimes\mathbb{R}^2 \to L^2(\widehat{\Omega})\otimes\mathbb{S}$ *and* $\mathscr{D}_1^* = (\widehat{\operatorname{curl}}^2)^*\colon L^2(\widehat{\Omega})\otimes\mathbb{S} \to L^2(\widehat{\Omega})$ *which are related to suitable boundary conditions. The Hodge–Laplace equation of level* $k = 1$ *has the form*

$$T^1_{\mathrm{HL}} u \coloneqq \Big(\widehat{\operatorname{curl}}^2(\widehat{\operatorname{curl}}^2)^* - \operatorname{sym}\widehat{\nabla}\widehat{\nabla}\cdot\Big)u = f, \quad u \in H(\widehat{\Omega}, \widehat{\nabla}\cdot, \mathbb{S}),\ f \in L^2(\widehat{\Omega})\otimes\mathbb{S}, \quad \text{cf. Section 3.2.} \tag{7.2.13}$$

Actually, one searches for $u \in \operatorname{Dom}(T^1_{\mathrm{HL}}) \coloneqq \Big\{H(\widehat{\Omega}, \widehat{\nabla}\cdot, \mathbb{S}) \cap \mathscr{V}_1^* \;\Big|\; \widehat{\nabla}\cdot u \in \mathscr{V}_2^* \text{ and } (\widehat{\operatorname{curl}}^2)^* u \in H^2(\widehat{\Omega})\Big\}$*, where the* $\mathscr{V}_i^* \coloneqq \operatorname{Dom}\Big((\mathscr{D}^{i-1}, \mathscr{V}^{i-1})^*\Big)$ *denote the domains of the adjoints. Using Corollary 7.5, the associated discrete mixed weak form is then given by:* Find $(\sigma_h, u_h) \in \widehat{\mathfrak{V}}^{0,1}_{h,2} \times \widehat{\mathfrak{V}}^{1,1}_{h,2}$ with

$$\langle \sigma_h, \tau_h\rangle \qquad - \langle u_h, \widehat{\operatorname{curl}}^2 \tau_h\rangle \quad = 0, \qquad \forall \tau_h \in \widehat{\mathfrak{V}}^{0,1}_{h,2}, \tag{7.2.14}$$

$$\langle \widehat{\operatorname{curl}}^2 \sigma_h, v_h\rangle + \langle \widehat{\nabla}\cdot u_h, \widehat{\nabla}\cdot v_h\rangle = \langle f, v_h\rangle, \quad \forall v_h \in \widehat{\mathfrak{V}}^{1,1}_{h,2}. \tag{7.2.15}$$

We now choose the right-hand side f such that the exact solution of equation (7.2.13) *is given by*

$$u = \begin{bmatrix} 2w & w \\ w & -2w \end{bmatrix}, \quad w(\zeta_1, \zeta_2) \coloneqq \sin(\pi\zeta_1)^2 \sin(\pi\zeta_2)^2.$$

There is no doubt that $u \in \mathrm{Dom}(T^1_{\mathrm{HL}})$, and our choice fits with the abstract Hodge–Laplace problem. Considering the discretization (7.2.14)-(7.2.15) *and the smooth manufactured solution, we should expect an error decrease of $\mathcal{O}(h^{p-1})$ for polynomial degree p, where the errors are measured through $\|\sigma - \sigma_h\|_{H^2}$ and $\|u - u_h\|_{H(\widehat{\nabla}\cdot)}$.*[13] *Note Lemma 3.16 and Corollary 7.4 for this matter. The computed errors between the exact and approximated solution are summarized in Figure 12 for polynomial degrees $p = 2, \dots, 5$ and regularities $r = p - 1$. In the plots, by "mesh size h", we mean that the corresponding Bézier mesh consists of $1/h^2$ identical squares; see Remark 6.1. Indeed, in Figure 12, we observe the expected stable convergence behavior, and the test numerically supports the statements of Corollary 7.4.*

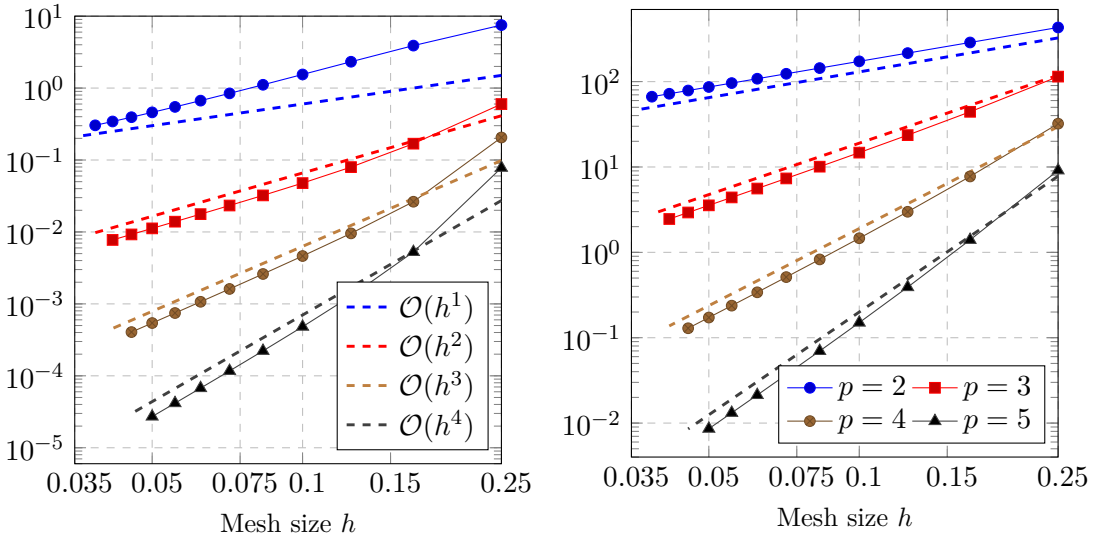

(a) $\|u - u_h\|_{H(\widehat{\nabla}\cdot)}$ (b) $\|\sigma - \sigma_h\|_{H^2}$

Figure 12: We see the error decay for the mixed weak formulation and the spaces $\widehat{\mathfrak{V}}^{i,1}_{h,2}$, where the regularity is chosen as $r = p - 1$. The observed convergence rates fit to theoretically expected ones.

Of course, we can also utilize Corollary 7.5 for another Hodge–Laplace problem by going to the next level $k = 2$. This then leads us to a saddle-point problem, which appears in a modified form again in the application example of linear elasticity; see Section 9.2 which explains the frequently used term "elasticity complex".

Example 7.2 (Elasticity complex: Hodge–Laplace problem of level $k = 2$)**.** *We look at a test case analogous to Example 7.1. But this time we have the equation*

$$T^2_{\mathrm{HL}} u \coloneqq -\widehat{\nabla} \cdot \mathrm{sym}\widehat{\nabla} u = f, \quad u,\, f \in L^2(\widehat{\Omega}) \otimes \mathbb{R}^2. \tag{7.2.16}$$

since for the 2D elasticity complex $\mathscr{D}^1 = \widehat{\nabla}\cdot$ and $\mathscr{D}^2 = 0$. Thus we seek for $u \in \left\{ H^1_0(\Omega) \otimes \mathbb{R}^2 \;\middle|\; \mathrm{sym}\widehat{\nabla} u \in H(\widehat{\Omega}, \widehat{\nabla}\cdot, \mathbb{S}) \right\}$ where the zero boundary conditions ensure the validity of the related

[13] We use the standard Big-$\mathcal{O}$-Notation; $\|v - v_h\| \in \mathcal{O}(h^p) :\iff \|v - v_h\| \leq Ch^p$ for $h \to 0$.

mixed weak form. The discretized version of the latter reads: Find $(\sigma_h, u_h) \in \widehat{\mathfrak{V}}^{1,1}_{h,2} \times \widehat{\mathfrak{V}}^{2,1}_{h,2}$ with

$$\langle \sigma_h, \tau_h \rangle \quad -\langle u_h, \widehat{\nabla} \cdot \tau_h \rangle = 0, \qquad \forall \tau_h \in \widehat{\mathfrak{V}}^{1,1}_{h,2}, \tag{7.2.17}$$

$$\langle \widehat{\nabla} \cdot \sigma_h, v_h \rangle \qquad\qquad = \langle f, v_h \rangle, \quad \forall v_h \in \widehat{\mathfrak{V}}^{2,1}_{h,2}, \tag{7.2.18}$$

where one observes the definitions in Corollary 7.6. If we select f such that the exact solution is

$$\boxed{u = (w, -w)^{\mathrm{T}}, \quad w(\zeta_1, \zeta_2) := \sin(\pi\zeta_1)\sin(\pi\zeta_2)},$$

we should observe for our well-posed discretization analogous convergence rates $\|u - u_h\| + \|\sigma - \sigma_h\|_{H(\widehat{\nabla}\cdot)} \in \mathcal{O}(h^{p-1})$ ($\|\cdot\| = \|\cdot\|_{L^2}$) as for the first Example 7.1. This is confirmed by Figure 13 which shows a very stable decay behavior, although we increase regularity in the sense $r = p - 1$.

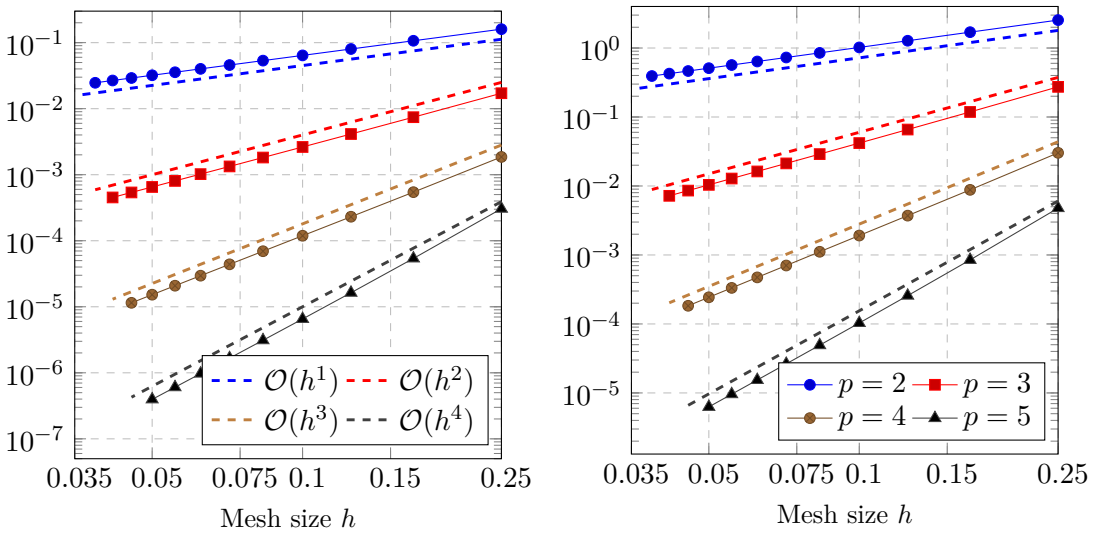

(a) $\|u - u_h\|$ (b) $\|\sigma - \sigma_h\|_{H(\widehat{\nabla}\cdot)}$

Figure 13: Convergence plots for the manufactured solution and discretization (7.2.17)-(7.2.18). These plots demonstrate the feasibility of the spaces $\widehat{\mathfrak{V}}^{1,1}_{h,2}$, $\widehat{\mathfrak{V}}^{2,1}_{h,2}$.

The examples have once again clarified how, in $2D$ and in the case of a square domain, we can discretize the second-order complexes implied by the coupling in the previous section in a structure-preserving manner. There is no doubt about the possibility of discretizing the diagram (4.2.28) in $3D$ using spline spaces as well, in such a way that we also obtain suitable finite-dimensional counterparts for the three second-order complexes mentioned earlier in (4.2.29)-(4.2.31). For the sake of completeness, we would like to summarize the most important spaces and the corresponding diagrams in three dimensions in the next section.

7.2.3 Complexes in $3D$

The idea here in the three-dimensional case $n = 3$ is entirely the same as in the previous chapter, this means we use the general construction outlined in Section 7.2.1 together with the proxy maps to establish a discrete version of (4.2.28) from Example 4.3. Again we make the assumption of $p_i = p,\ r_i = r,\ \forall i$ for the components of degree and regularity vectors $\mathbf{p}$, $\mathbf{r}$. As a result one obtains the diagram in Figure 14, in which each row is a vector-valued spline de Rham sequence. The injectivity of the green, the surjectivity of the blue as well as the bijectivity of the red linking maps in the mentioned figure can be checked easily. The relevant projections are further given

in Figure 15, with an analogous notation simplification as in $2D$, i.e. $\widehat{\Pi}^{l_1,l_2,l_3} \coloneqq \widehat{\Pi}^{\mathbf{l}}_{\mathbf{p},\mathbf{r}}$, $\mathbf{l} = (l_i)_i$. Then we can apply the BGG construction in the discrete setting for consecutive rows in Figs. 14 to get a discrete Hessian, elasticity and divdiv complex in $3D$. Note, the latter chains are also introduced in Example 4.3. Exploiting the observations from Section 7.2.1, especially Corollary 7.4, we directly obtain the next three corollaries:

Corollary 7.7 (**Discrete Hessian complex**-$3D$)**.** *The spaces*

$$\widehat{\mathfrak{V}}^{0,1}_{h,3} \coloneqq S^{r,r,r}_{p,p,p}, \qquad \widehat{\mathfrak{V}}^{1,1}_{h,3} \coloneqq \begin{bmatrix} S^{r-2,r,r}_{p-2,p,p} & S^{r-1,r-1,r}_{p-1,p-1,p} & S^{r-1,r,r-1}_{p-1,p,p-1} \\ & S^{r,r-2,r}_{p,p-2,p} & S^{r,r-1,r-1}_{p,p-1,p-1} \\ \text{sym} & & S^{r,r,r-2}_{p,p,p-2} \end{bmatrix} \cap L^2(\widehat{\Omega}) \otimes \mathbb{S},$$

$$\widehat{\mathfrak{V}}^{2,1}_{h,3} \coloneqq \begin{bmatrix} S^{r-1,r-1,r-1}_{p-1,p-1,p-1} & S^{r-2,r,r-1}_{p-2,p,p-1} & S^{r-2,r-1,r}_{p-2,p-1,p} \\ S^{r,r-2,r-1}_{p,p-2,p-1} & S^{r-1,r-1,r-1}_{p-1,p-1,p-1} & S^{r-1,r-2,r}_{p-1,p-2,p} \\ S^{r,r-1,r-2}_{p,p-1,p-2} & S^{r-1,r,r-2}_{p-1,p,p-2} & S^{r-1,r-1,r-1}_{p-1,p-1,p-1} \end{bmatrix} \cap L^2(\widehat{\Omega}) \otimes \mathbb{T}, \qquad \widehat{\mathfrak{V}}^{3,1}_{h,3} \coloneqq \begin{bmatrix} S^{r-2,r-1,r-1}_{p-2,p-1,p-1} \\ S^{r-1,r-2,r-1}_{p-1,p-2,p-1} \\ S^{r-1,r-1,r-2}_{p-1,p-1,p-2} \end{bmatrix}$$

determine a structure-preserving discretization of the Hessian complex on $(0,1)^3$*; see* (4.2.29)*. We have the Hilbert complex*

$$0 \longrightarrow \widehat{\mathfrak{V}}^{0,1}_{h,3} \xrightarrow{\widehat{\nabla}^2} \widehat{\mathfrak{V}}^{1,1}_{h,3} \xrightarrow{\widehat{\nabla}\times} \widehat{\mathfrak{V}}^{2,1}_{h,3} \xrightarrow{\widehat{\nabla}\cdot} \widehat{\mathfrak{V}}^{3,1}_{h,3} \longrightarrow 0.$$

Corollary 7.8 (**Discrete elasticity complex**-$3D$)**.** *The spaces*

$$\widehat{\mathfrak{V}}^{0,2}_{h,3} \coloneqq \begin{bmatrix} S^{r-1,r,r}_{p-1,p,p} \\ S^{r,r-1,r}_{p,p-1,p} \\ S^{r,r,r-1}_{p,p,p-1} \end{bmatrix}, \qquad \widehat{\mathfrak{V}}^{1,2}_{h,3} \coloneqq \begin{bmatrix} S^{r-2,r,r}_{p-2,p,p} & S^{r-1,r-1,r}_{p-1,p-1,p} & S^{r-1,r,r-1}_{p-1,p,p-1} \\ & S^{r,r-2,r}_{p,p-2,p} & S^{r,r-1,r-1}_{p,p-1,p-1} \\ \text{sym} & & S^{r,r,r-2}_{p,p,p-2} \end{bmatrix} \cap L^2(\widehat{\Omega}) \otimes \mathbb{S}$$

$$\widehat{\mathfrak{V}}^{2,2}_{h,3} \coloneqq \begin{bmatrix} S^{r,r-2,r-2}_{p,p-2,p-2} & S^{r-1,r-1,r-2}_{p-1,p-1,p-2} & S^{r-1,r-2,r-1}_{p-1,p-2,p-1} \\ & S^{r-2,r,r-2}_{p-2,p,p-2} & S^{r-2,r-1,r-1}_{p-2,p-1,p-1} \\ \text{sym} & & S^{r-2,r-2,r}_{p-2,p-2,p} \end{bmatrix} \cap L^2(\widehat{\Omega}) \otimes \mathbb{S}, \qquad \widehat{\mathfrak{V}}^{3,2}_{h,3} \coloneqq \begin{bmatrix} S^{r-1,r-2,r-2}_{p-1,p-2,p-2} \\ S^{r-2,r-1,r-2}_{p-2,p-1,p-2} \\ S^{r-2,r-2,r-1}_{p-2,p-2,p-1} \end{bmatrix}$$

determine a structure-preserving discretization of the elasticity complex on $(0,1)^3$*; see* (4.2.30)*. We have the Hilbert complex*

$$0 \longrightarrow \widehat{\mathfrak{V}}^{0,2}_{h,3} \xrightarrow{\operatorname{sym}\widehat{\nabla}} \widehat{\mathfrak{V}}^{1,2}_{h,3} \xrightarrow{\widehat{\operatorname{inc}}} \widehat{\mathfrak{V}}^{2,2}_{h,3} \xrightarrow{\widehat{\nabla}\cdot} \widehat{\mathfrak{V}}^{3,2}_{h,3} \longrightarrow 0.$$

Corollary 7.9 (**Discrete divdiv complex**-$3D$)**.** *The spaces*

$$\widehat{\mathfrak{V}}^{0,3}_{h,3} \coloneqq \begin{bmatrix} S^{r,r-1,r-1}_{p,p-1,p-1} \\ S^{r-1,r,r-1}_{p-1,p,p-1} \\ S^{r-1,r-1,r}_{p-1,p-1,p} \end{bmatrix}, \qquad \widehat{\mathfrak{V}}^{1,3}_{h,3} \coloneqq \begin{bmatrix} S^{r-1,r-1,r-1}_{p-1,p-1,p-1} & S^{r,r-2,r-1}_{p,p-2,p-1} & S^{r,r-1,r-2}_{p,p-1,p-2} \\ S^{r-2,r,r-1}_{p-2,p,p-1} & S^{r-1,r-1,r-1}_{p-1,p-1,p-1} & S^{r-1,r,r-2}_{p-1,p,p-2} \\ S^{r-2,r-1,r}_{p-2,p-1,p} & S^{r-1,r-2,r}_{p-1,p-2,p} & S^{r-1,r-1,r-1}_{p-1,p-1,p-1} \end{bmatrix} \cap L^2(\widehat{\Omega}) \otimes \mathbb{T}$$

$$\widehat{\mathfrak{V}}^{2,3}_{h,3} \coloneqq \begin{bmatrix} S^{r,r-2,r-2}_{p,p-2,p-2} & S^{r-1,r-1,r-2}_{p-1,p-1,p-2} & S^{r-1,r-2,r-1}_{p-1,p-2,p-1} \\ & S^{r-2,r,r-2}_{p-2,p,p-2} & S^{r-2,r-1,r-1}_{p-2,p-1,p-1} \\ \text{sym} & & S^{r-2,r-2,r}_{p-2,p-2,p} \end{bmatrix} \cap L^2(\widehat{\Omega}) \otimes \mathbb{S}, \qquad \widehat{\mathfrak{V}}^{3,3}_{h,3} \coloneqq S^{r-2,r-2,r-2}_{p-2,p-2,p-2}$$

determine a structure-preserving discretization of the divdiv complex on $(0,1)^3$*; see* (4.2.31)*. We have the Hilbert complex*

$$0 \longrightarrow \widehat{\mathfrak{V}}^{0,3}_{h,3} \xrightarrow{\operatorname{dev}\widehat{\nabla}} \widehat{\mathfrak{V}}^{1,3}_{h,3} \xrightarrow{\operatorname{sym}\widehat{\nabla}\times} \widehat{\mathfrak{V}}^{2,3}_{h,3} \xrightarrow{\widehat{\nabla}\cdot\widehat{\nabla}\cdot} \widehat{\mathfrak{V}}^{3,3}_{h,3} \longrightarrow 0.$$

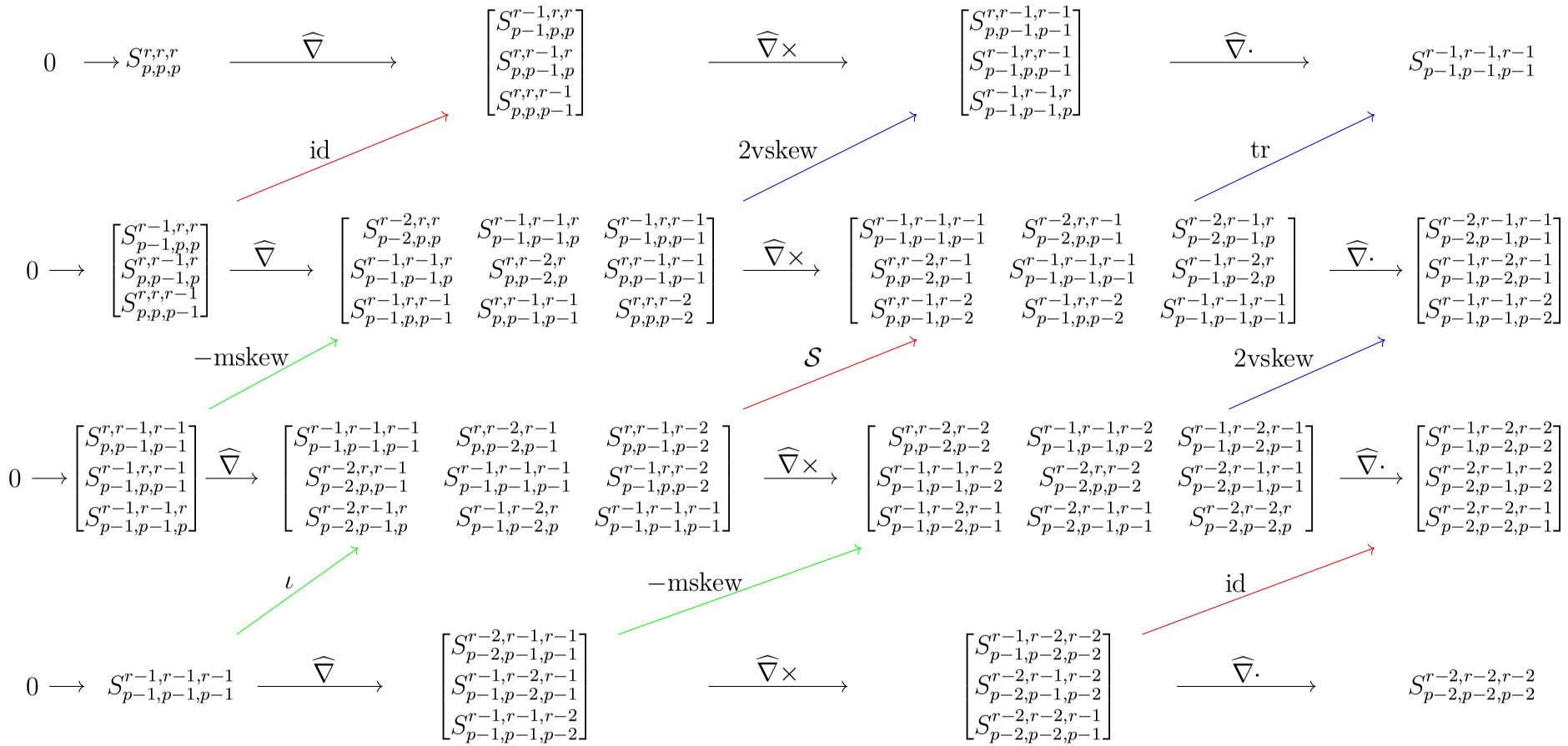

Figure 14: Here we see a discretized version of diagram (4.2.28) in the parametric domain. The blue (green) linking maps are surjective (injective) and the red ones are bijective.

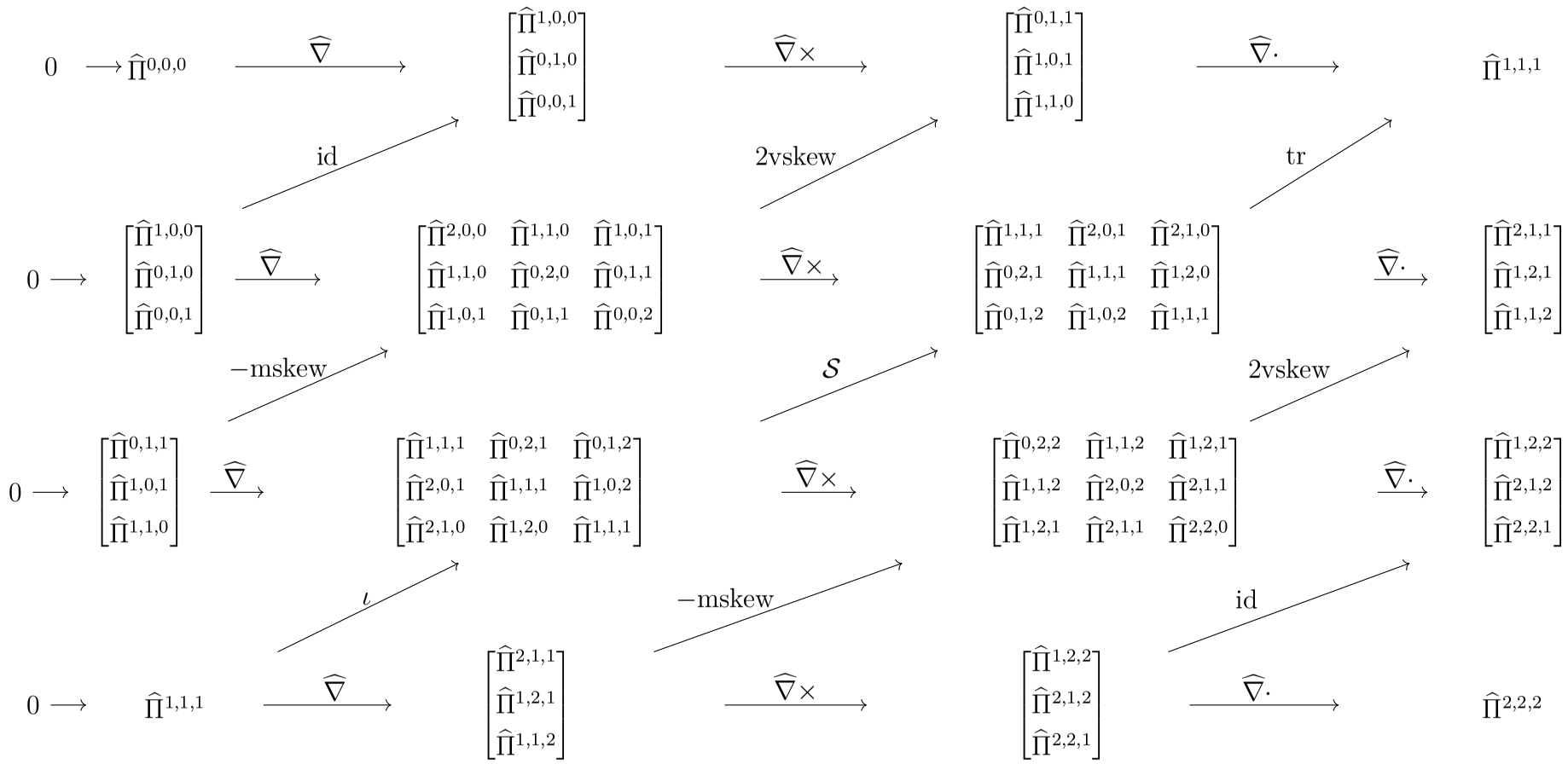

Figure 15: Here we collect the corresponding projections onto the spaces from Figure 14. They already give us the bounded cochain projections onto the output spline spaces. Note, $\widehat{\Pi}^{l_1,l_2,l_3} := \widehat{\Pi}^{\mathbf{l}}_{\mathbf{p},\mathbf{r}},\ \mathbf{l} = (l_i)_i$.

At the end of this section, we would like to make a not particularly surprising but still noteworthy remark that we will use later.

Remark 7.2. Firstly, the entire definition of spline spaces, or rather the splines, was based on the specification that the smallest and largest knot values are 0 and 1, in every coordinate direction; compare Assumption 6.1. Hence, we focused on the situation of the parametric domain $\widehat{\Omega} = (0,1)^n$. However, it is obvious that all these definitions can also be established if we replace 0 and 1 with two other real numbers $a < b$. This means that we can consider a different cube $(a,b)^n$ as the parameter domain and adjust the introduced spaces $\widehat{V}_{h,n}^{k,J}$, $\mathscr{Q}_{\mathbf{p}}^{\mathbf{r}}\Lambda^{k,l}$ etc. and related projections accordingly. The various estimates and approximation properties remain valid in this context. Only the involved constants might need to be adjusted as necessary.

We have explained now with the help of references [19] and [27] how to discretize the second-order complexes $(\mathscr{V}_n^{\circ,J}, \mathscr{D}_n^{\circ,J})$ from Section 4.2.3 in the reference domain $\widehat{\Omega}$ while preserving the structure. This allows us to leverage the results of FEEC and approximate various Hodge–Laplace problems, albeit initially in the rather restrictive case of cubical domains. As illustrated by the numerical tests in the Examples 7.1 and 7.2, we have clarified this for two specific problems. However, our plan remains to investigate mixed formulations for Hodge–Laplace problems in curved geometries as well. Before we finally delve into the central chapter of this work, where the main results are to be found, namely the application of spline complexes for isogeometric discretizations of a class of saddle-point problems, we need to introduce the isogeometric discrete differential forms mentioned at various points and later relevant. We aim to do this briefly in the next section.

7.3 Isogeometric discrete differential forms

Until now the discrete complexes were explained and defined on the reference cube $\widehat{\Omega} = (0,1)^n$. Unfortunately, the definitions cannot be easily extended to other domains due to the central role played by the tensor product structure of B- splines. However, for the specific case of the Rham sequence, a generalization can indeed be made, as demonstrated extensively, for instance, in 3D in [27]. The idea is to reuse the previously introduced spline differential forms and projections, meaning the outcomes of Section 7.1, provided a C^1-diffeomorphic parametrization $\mathbf{F}\colon \widehat{\Omega} \to \Omega,\ \Omega \subset \mathbb{R}^n$ of the actual computational domain. More precisely, the approach made in the framework of isogeometric (discrete) differential forms in [27] is the use of the pullback operation related to $\mathbf{F}^{-1}$; see Definition 3.9. Because this operation commutes with the exterior derivative (i.e. it holds (3.3.4)), we automatically obtain, with the spaces

$$\mathcal{Q}_{\mathbf{p}}^{\mathbf{r}}\Lambda^k := \left\{\mathcal{Y}_{\mathbf{F}^{-1}}^k \omega \mid \omega \in Q_{\mathbf{p}}^{\mathbf{r}}\Lambda^k\right\},$$

a discrete version of the de Rham complex on Ω. The mentioned commutativity and the L^2-boundedness also imply that we are dealing with a structure-preserving discretization, where suitable bounded cochain projections are given by

$$\Pi_{h,n}^{k,\Lambda}\colon L^2\Lambda^k(\Omega) \to \mathcal{Q}_{\mathbf{p}}^{\mathbf{r}}\Lambda^k\ ,\ \Pi_{h,n}^{k,\Lambda} := \mathcal{Y}_{\mathbf{F}^{-1}}^k \circ \widehat{\Pi}_{h,n}^{k,\Lambda} \circ \mathcal{Y}_{\mathbf{F}}^k.$$

For details regarding the mentioned spaces $Q_{\mathbf{p}}^{\mathbf{r}}\Lambda^k$ and the projections $\widehat{\Pi}_{h,n}^{k,\Lambda}$ we refer to Section 7.1.

Due to Lemma 3.8 we see the existence of constants $0 < c_1 < c_2$ such that

$$c_1 \left\|\mathcal{Y}_{\mathbf{F}^{-1}}^k \omega\right\|_{L^2(\Omega)} \leq \|\omega\|_{L^2(\widehat{\Omega})} \leq c_2 \left\|\mathcal{Y}_{\mathbf{F}^{-1}}^k \omega\right\|_{L^2(\Omega)}, \quad \forall \omega \in L^2\Lambda^k(\widehat{\Omega}).$$

Hence, in view of (3.3.4), we get from Lemma 7.2 the next corollary.

Corollary 7.10 (**Isogeometric discrete differential forms**). *Let the assumptions of Lemma 7.2 be fulfilled and let further let the parametrization* $\mathbf{F}\colon \widehat{\Omega} \to \Omega$ *be a* C^1*-diffeomorphism. Besides, we require* $\mathbf{F}$ *and* $\mathbf{F}^{-1}$ *as well as their first derivatives to be continuously extendable to the closures* $\overline{\widehat{\Omega}}$, $\overline{\Omega}$, *respectively.*
Then the above defined spaces $\mathcal{Q}^{\mathbf{r}}_{\mathbf{p}}\Lambda^\circ$ *determine a structure-preserving discretization of the de Rham complex* $(H\Lambda^\circ(\Omega), \mathrm{d}^\circ)$ *in* Ω. *Further, we have for some constant* C_Π *the inequalities*

$$\begin{aligned} \left\|\omega - \Pi^{k,\Lambda}_{h,n}\omega\right\|_{H\Lambda^k} &\leq C_\Pi h^l \left\|\omega\right\|_{H^l(\mathrm{d}^k)}, \quad && \forall \omega \in H^l(\Omega, \mathrm{d}^k, \mathrm{Alt}^k), && 0 \leq l \leq p, \\ \left\|\omega - \Pi^{k,\Lambda}_{h,n}\omega\right\|_{L^2} &\leq C_\Pi h^l \left\|\omega\right\|_{H^l}, && \forall \omega \in H^l\Lambda^k(\Omega), && 0 \leq l \leq \tilde{p}. \end{aligned}$$

Note, $\tilde{p} = p$ *for* $k > 0$ *and* $\tilde{p} = p + 1$ *for* $k = 0$.
We refer to the $\mathcal{Q}^{\mathbf{r}}_{\mathbf{p}}\Lambda^\circ$ *as* isogeometric discrete differential forms.

Sometimes it is more convenient to leave behind the abstract notation with differential forms and work with a proxy complex in the sense of Section 3.3.2. Now, if we define proxy maps $\mathcal{J}_k\colon L^2\Lambda^k(U) \to L^2(U) \otimes \mathbb{R}^{n|k}$ as in the mentioned section, we can introduce discrete spaces for the proxy complex on Ω once again using the pullback. More precisely, we define

$$\widehat{V}^k_{h,n} \coloneqq \mathcal{J}_k\Big(Q^{\mathbf{r}}_{\mathbf{p}}\Lambda^k\Big)$$

and simply set

$$V^k_{h,n} \coloneqq \Big\{\mathcal{J}_k\mathcal{Y}^k_{\mathbf{F}^{-1}}\mathcal{J}_k^{-1}v \;\Big|\; v \in \widehat{V}^k_{h,n}\Big\} = \Big\{\mathcal{J}_k\omega \;\Big|\; \omega \in \mathcal{Q}^{\mathbf{r}}_{\mathbf{p}}\Lambda^k\Big\}. \tag{7.3.1}$$

By our construction of the spaces we get that $V^k_{h,n} \subset H(\Omega, \mathcal{D}^k, \mathbb{R}^{n|k})$, where the latter is the proxy de Rham complex on Ω associated to the proxy maps $\mathcal{J}_k$, i.e. $\mathcal{D}^k = \mathcal{J}_{k+1} \circ \mathrm{d}^k \circ \mathcal{J}_k^{-1}$. This time, we obtain with

$$\Pi^k_{h,n}\colon L^2(\Omega) \otimes \mathbb{R}^{n|k} \to V^k_{h,n}\ ,\ \Pi^k_{h,n} \coloneqq \mathcal{J}_k \circ \Pi^{k,\Lambda}_{h,n} \circ \mathcal{J}_k^{-1} = \mathcal{J}_k \circ \mathcal{Y}^k_{\mathbf{F}^{-1}} \circ \widehat{\Pi}^{k,\Lambda}_{h,n} \circ \mathcal{Y}^k_{\mathbf{F}} \circ \mathcal{J}_k^{-1} \tag{7.3.2}$$

bounded cochain projections, which satisfy analogous estimates as in the last corollary.

Corollary 7.11. *Let the assumptions of Lemma 7.2 and Corollary 7.10 hold and let* $\mathcal{J}_k\colon L^2\Lambda^k(U) \to L^2(U) \otimes \mathbb{R}^{n|k}$ *denote proxy maps in the sense of Definition 3.10. In this situation the spaces* $V^\circ_{h,n}$ *define a structure-preserving discretizaton of the proxy de Rham complex* $(H(\Omega, \mathcal{D}^\circ, \mathbb{R}^{n|\circ}), \mathcal{D}^\circ)$ *with bounded cochain projections* $\Pi^\circ_{h,n}$. *One has the estimates*

$$\begin{aligned} \left\|v - \Pi^k_{h,n}v\right\|_{H(\mathcal{D}^k)} &\leq C_\Pi h^l \left\|v\right\|_{H^l(\mathcal{D}^k)}, \quad && \forall v \in H^l(\Omega, \mathcal{D}^k, \mathbb{R}^{n|k}), && 0 \leq l \leq p, \\ \left\|v - \Pi^k_{h,n}v\right\|_{L^2} &\leq C_\Pi h^l \left\|v\right\|_{H^l}, && \forall v \in H^l(\Omega) \otimes \mathbb{R}^{n|k}, && 0 \leq l \leq \tilde{p}, \end{aligned}$$

for a suitable constant C_Π.

At the end of the section let us further illustrate these isogeometric discrete differential forms in the context of the classical proxy sequences in $2D$ and $3D$; cf. Examples 3.1 and 3.2. This might make the above abstract definitions somewhat more comprehensible.

Example 7.3 (Discrete proxy de Rham sequences). *In principle, the procedure is relatively straightforward. Firstly, we naturally utilize the abstract definition* (7.1.1) *involving differential forms and select the appropriate proxy spline complex by employing the identifications from*

Examples 3.1 and 3.2. This leads us in 3D for $\mathbf{p} = (p_1, p_2, p_3)$, $\mathbf{r} = (r_1, r_2, r_3)$ *with* $0 \leq r_i \leq p_i - 1$ *to the spaces*

$$\begin{aligned}
\widehat{V}^0_{h,3} &\coloneqq S^{r_1,r_2,r_3}_{p_1,p_2,p_3},\\
\widehat{V}^1_{h,3} &\coloneqq \begin{bmatrix} S^{r_1-1,r_2,r_3}_{p_1-1,p_2,p_3} & S^{r_1,r_2-1,r_3}_{p_1,p_2-1,p_3} & S^{r_1,r_2,r_3-1}_{p_1,p_2,p_3-1} \end{bmatrix}^{\mathrm{T}},\\
\widehat{V}^2_{h,3} &\coloneqq \begin{bmatrix} S^{r_1,r_2-1,r_3-1}_{p_1,p_2-1,p_3-1} & S^{r_1-1,r_2,r_3-1}_{p_1-1,p_2,p_3-1} & S^{r_1-1,r_2-1,r_3}_{p_1-1,p_2-1,p_3} \end{bmatrix}^{\mathrm{T}},\\
\widehat{V}^3_{h,3} &\coloneqq S^{r_1-1,r_2-1,r_3-1}_{p_1-1,p_2-1,p_3-1},
\end{aligned}$$

if the associated Bézier mesh $\widehat{M}_h$ *is regular and has mesh size* h*. Besides in 2D let us set similarly*

$$\begin{aligned}
\widehat{V}^0_{h,2} &\coloneqq S^{r_1,r_2}_{p_1,p_2},\\
\widehat{V}^1_{h,2} &\coloneqq \begin{bmatrix} S^{r_1,r_2-1}_{p_1,p_2-1} & S^{r_1-1,r_2}_{p_1-1,p_2} \end{bmatrix}^{\mathrm{T}},\\
\widehat{V}^2_{h,2} &\coloneqq S^{r_1-1,r_2-1}_{p_1-1,p_2-1}.
\end{aligned}$$

The spaces $\widehat{V}^\circ_{h,2}$, $\widehat{V}^\circ_{h,3}$ *discretize the proxy de Rham sequences* (3.3.8) *and* (3.3.9) *on the parametric domain. This is a direct consequence of the remarks in Section 7.1. To extend the last spaces to* Ω*, where the latter is parametrized by some smooth parametrization* $\mathbf{F}\colon (0,1)^n \to \Omega$*, the important thing are the pullbacks. But in Example 4.1 we introduced mappings* $\mathcal{Y}^i_n$ *that define compatible pullbacks, i.e. they commute with the respective differential operators in the de Rham complex. Choosing*

$$V^i_{h,n} \coloneqq \left(\mathcal{Y}^i_n\right)^{-1}\left(\widehat{V}^i_{h,n}\right), \qquad 0 \leq i \leq n,\ n = 2, 3\ ,$$

hence indeed provides structure-preserving discretizations of the de proxy Rham complexes (3.3.8) *and* (3.3.9) *on* Ω*.*

Remark 7.3 (Structure-preserving discretization of the extended de Rham complex)*.* We saw how we can discretize the (proxy) de Rham complex in structure-preserving manner using the isogeometric discrete differential forms. But we considered in Section 4.2.3 also the extended de Rham sequence $(H\Lambda^{\circ,l}, \mathrm{d}^\circ)$. As already explained in the mentioned section we can interpret $(H\Lambda^{\circ,l}, \mathrm{d}^\circ)$ as an $\binom{n}{l}$-fold copy of the classical de Rham sequence $(H\Lambda^\circ, \mathrm{d}^\circ)$. So there is no doubt, that the spaces $\mathcal{Q}^{\mathbf{r}}_{\mathbf{p}}\Lambda^k$ yield also a structure-preserving discretization of $(H\Lambda^{\circ,l}, \mathrm{d}^\circ)$ just by copying the discrete complexes. Certainly, this is also true, if we use proxy maps and go to the extended proxy de Rham complex $\left(H(\Omega, \mathcal{D}^\circ, \mathbb{R}^{(n|l)\times(n|\circ)}), \mathcal{D}^\circ\right)$; see Remark 4.3. We clarified in Section 4.2.3 further that we can assume the differential operators $\mathcal{D}^\circ$ in the extended complex to act row-wise which means

$$\tilde{V}^k_{h,n} \coloneqq \left\{\tau \in L^2(\Omega) \otimes \mathbb{R}^{(n|l)\times(n|k)} \;\middle|\; \text{each row of } \tau \text{ is element of } V^k_{h,n}\right\}$$

give a structure-preserving discretization of $\left(H(\Omega, \mathcal{D}^\circ, \mathbb{R}^{(n|l)\times(n|\circ)}), \mathcal{D}^\circ\right)$. The row-wise application of the projections $\Pi^k_{h,n}$ defined in (7.3.2) yield then L^2-bounded cochain projections, which trivially fulfill the estimates from Corollary 7.11.

Now, finally, comes the chapter where we bring together the various statements and auxiliary results from the previous chapters to discretize a class of saddle-point problems. This pertains to the mixed formulation for the level n Hodge–Laplace problem induced by the complex $(\mathscr{V}^{\circ,J}_n, \mathscr{D}^{\circ,J}_n)$. In this process, we will even acquaint ourselves with two different discretization methods, demonstrating their convergence and stability.

8 Discretization of Mixed Formulations from Alt^l-valued Forms

In the following, we want to focus on the discretization of the mixed formulation of the Hodge-Laplace problem (see Definition 3.5) exploiting spline spaces, IG spaces, respectively. We will restrict ourselves to formulations that are derived from the output complexes $(\mathscr{V}_n^{\circ,J}, \mathscr{D}_n^{\circ,J})$, which we introduced and explained in Section 4.2.3 (compare Lemma 4.9), using a certain class of BGG construction. In principle, it is now a matter of applying the observations and preparatory results from Section 5 to the specific complexes $(\mathscr{V}_n^{\circ,J}, \mathscr{D}_n^{\circ,J})$, whereby this time we want to specify concrete Finite Element spaces (FE spaces). And for the definition of the discrete spaces, we in turn use what we have learned about IGA in Section 6. Therefore, we start analogously to Section 5.1 (see (5.1.1)-(5.1.2)) with the following mixed formulation:

Definition 8.1 (**Continuous problem**). *Let $k \in \{1,\dots,n\}$, $J \in \{1,\dots,n\}$ and $\Omega \subset \mathbb{R}^n$ be a Lipschitz domain and set $\mathscr{D}^i \coloneqq \mathscr{D}_n^{i,J}$, $\forall i$. Given $f \in L^2(\Omega) \otimes \mathbb{A}_n^{k,J}$ we seek for $(\sigma, u) \in \mathscr{V}_n^{k-1,J} \times \mathscr{V}_n^{k,J}$ s.t.*

$$\langle \sigma, \tau \rangle \qquad - \langle u, \mathscr{D}^{k-1}\tau \rangle \;= 0, \qquad \forall \tau \in \mathscr{V}_n^{k-1,J}, \tag{8.0.1}$$

$$\langle \mathscr{D}^{k-1}\sigma, v \rangle + \langle \mathscr{D}^k u, \mathscr{D}^k v \rangle = \langle f, v \rangle, \quad \forall v \in \mathscr{V}_n^{k,J}. \tag{8.0.2}$$

It is worth noting that we used above and will continue to employ the notation established in Section 4.2.3.
The last definition still requires an assumption to truly represent a meaningful weak version of the Hodge–Laplace problem. Specifically, we require for $(\mathscr{V}_n^{\circ,J}, \mathscr{D}_n^{\circ,J})$ trivial cohomology spaces $\mathfrak{H}^k$ spaces, meaning the exactness of the output complexes at the corresponding level k; cf. Definition 3.5. Because of Corollary 4.4 it is sufficient to assume the following:

Assumption 8.1. *We have $k \in \{1,\dots,n\}$, $J \in \{1,\dots,n\}$ and $\Omega \subset \mathbb{R}^n$ is a Lipschitz domain. In case of $k < n$ we require Ω to be a starlike domain.*

Additionally, we aim to reuse the ideas and tools introduced and discussed regarding IGA in Section 6. Therefore, we need to demand more from the computational domain Ω. The latter must be defined by a regular parametrization, which is at least C^1 smooth. This leads us to the stricter

Assumption 8.2. *There is a regular parametrization $\mathbf{F}\colon (0,1)^n \to \Omega$ in the sense of Definition 6.5 which is at least C^1-diffeomorphic. In particular the $\mathbf{F}$ is piecewise smooth.*

With our setting clarified, we can now turn our attention to the actual discretization, this time in the physical domain Ω. This is not a straightforward extension of the results in the parametric domain $\widehat{\Omega}$. While we could rely on pullbacks for the definition of isogeometric discrete differential forms (see Section 7.3), which commuted with the exterior derivative, it can be easily verified that these pullbacks are not compatible with the operators $\mathscr{D}_n^{\circ,J}$. However, at first glance, it seems that the next steps are still clear. One must now simply define new or modified pullback operations that commute with the operators $\mathscr{D}_n^{\circ,J}$. If we indeed have such compatible pullbacks at hand, we could apply the same procedure used for the transition from de Rham spline complexes to isogeometric differential forms for the second-order output complexes; see Section 7.3. The outcome would be structure-preserving discretizations of $(\mathscr{V}_n^{\circ,J}, \mathscr{D}_n^{\circ,J})$ in Ω, and the results of the FEEC theory imply that we have automatically found suitable spaces for treating the problem from Definition 8.1. However, there is a weakness in this apparent straightforward train of

thought, and that weakness lies in the compatible pullbacks. To this day, neither we nor the literature are aware of pullbacks that are valid for arbitrary (smooth) parameterizations and that are also reasonably easy to compute. We have indeed dealt with modified pullbacks in the context of the elasticity complex in [3], which might be usable for discretization. However, there are several disadvantages that have led us not to delve further into this approach here. First, the obtained pullbacks are complicated and not really suitable for efficient implementation. Second, it is not clear whether this approach can be used to discretize other complexes. And since the definition of various spaces in [3] also involves Hilbert complexes with boundary conditions, which is a separate topic in itself, we will refrain from going into further details here. In summary, it can be said once again that discretizing (8.0.1)-(8.0.2) is quite difficult in general, and it is not entirely clear what suitable spaces should look like. For this reason, we want to start by addressing the simpler question of whether we can always expect at least a unique discrete solution with IG ansatz functions, i.e., clarifying the question of the invertibility for a finite-dimensional version. After that, we will again focus on the case of saddle-point problems, that is, $k = n$. For this latter class of problems, we can present two discretization approaches and demonstrate the existence of well-posed IGA discretizations for them.

8.1 Invertibility of the mixed formulation

But first let us define again some spaces utilizing the notation from Section 4.2.3. For the next definition one notes Assumptions 8.1 and 8.2.

Definition 8.2 (**Choice of spaces**). *Let l_{k-1} and l_k denote the order of the differential operators $\mathscr{D}_n^{k-1,J}$ and $\mathscr{D}_n^{k,J}$ and set $l \coloneqq \max\{1, l_k\}$. Further, let $\mathbf{p} = (p_i)_i$, $\mathbf{r} = (r_i)_i$, $\mathbf{q} = (q_i)_i$, $\mathbf{s} = (s_i)_i$ be vectors in $\mathbb{N}^n$ s.t. $p_i > r_i \geq l_k - 1$, as well as $q_i > s_i \geq l - 1$, $\forall i$. Then we set*

$$\begin{aligned} \widehat{\mathscr{V}}_{h,n}^{k-1,J} &\coloneqq S_{\mathbf{q}}^{\mathbf{s}} \otimes \mathbb{A}_n^{k-1,J} \subset H^{l_{k-1}}(\widehat{\Omega}) \otimes \mathbb{A}_n^{k-1,J}, \\ \widehat{\mathscr{V}}_{\theta,n}^{k,J} &\coloneqq S_{\mathbf{p}}^{\mathbf{r}} \otimes \mathbb{A}_n^{k,J} \quad \subset H^{l}(\widehat{\Omega}) \otimes \mathbb{A}_n^{k,J} \subset H^{1}(\widehat{\Omega}) \otimes \mathbb{A}_n^{k,J}, \end{aligned}$$

where the h and θ denote the mesh sizes of the underyling regular meshes. We again use two indices to emphasize the possibility of different meshes for $\widehat{\mathscr{V}}_{h,n}^{k-1,J}$ and $\widehat{\mathscr{V}}_{\theta,n}^{k,J}$.
The spaces in the physical domain are then just defined through

$$\mathscr{V}_{h,n}^{k-1,J} \coloneqq \widehat{\mathscr{V}}_{h,n}^{k-1,J} \circ \mathbf{F}^{-1} \subset H^{l_{k-1}}(\Omega) \otimes \mathbb{A}_n^{k-1,J}, \tag{8.1.1}$$

$$\mathscr{V}_{\theta,n}^{k,J} \coloneqq \widehat{\mathscr{V}}_{\theta,n}^{k,J} \circ \mathbf{F}^{-1} \quad \subset H^{l}(\Omega) \otimes \mathbb{A}_n^{k,J} \subset H^{1}(\Omega) \otimes \mathbb{A}_n^{k,J}. \tag{8.1.2}$$

One observes, that the above inclusions are a direct consequence, of the conditions $r_i \geq l_k - 1$ and $s_i \geq l - 1$ and Assumption 8.2. In particular we obtain subspaces of $\mathscr{V}_n^{k-1,J}$, $\mathscr{V}_n^{k,J}$, respectively.

Straightforwardly, the projections Π_h^V from Lemma 6.2 induce projections onto the spaces $\mathscr{V}_{h,n}^{k-1,J}$, $\mathscr{V}_{\theta,n}^{k,J}$; see Remark 6.2. For reasons of clarification, we write in the following $\Pi_h^V(\mathbf{p}, \mathbf{r})$ for the respective projection onto the spline space with degree and regularity vectors $\mathbf{p}$ and $\mathbf{r}$. Then, given orthonormal bases $\{e_1, \dots, e_m\} \subset \mathbb{A}_n^{k-1,J}$ and $\{\tilde{e}_1, \dots, \tilde{e}_t\} \subset \mathbb{A}_n^{k,J}$ of $\mathbb{A}_n^{k-1,J}$ and $\mathbb{A}_n^{k,J}$, we just set

$$\begin{aligned} \Pi_h^{k-1} \colon L^2(\Omega) \otimes \mathbb{A}_n^{k-1,J} \to \mathscr{V}_{h,n}^{k-1,J}\ ,\ c_i\, e_i \mapsto \big(\Pi_h^V c_i\big)\, e_i, \quad \text{with } \Pi_h^V = \Pi_h^V(\mathbf{q}, \mathbf{s}), \\ \Pi_\theta^{k} \colon L^2(\Omega) \otimes \mathbb{A}_n^{k,J} \to \mathscr{V}_{\theta,n}^{k,J}\ ,\qquad \tilde{c}_i\, \tilde{e}_i \mapsto \big(\Pi_h^V \tilde{c}_i\big)\, \tilde{e}_i, \quad \text{with } \Pi_h^V = \Pi_h^V(\mathbf{p}, \mathbf{r}), \end{aligned}$$

where $c_i \in L^2(\Omega)$ denotes the coefficient function and the actual mapping is determined through linearity. For theses projections we get by Lemma 6.2 directly

Corollary 8.1. *Writing* $p \coloneqq \min_i\{p_i\},\ q \coloneqq \min_i\{q_i\}$, *we have*

$$\left\|\tau - \Pi_h^{k-1}\tau\right\|_{H^s} \leq C_\Pi h^{l-s}\left\|\tau\right\|_{H^l}, \quad \forall \tau \in H^l\mathbb{A}_n^{k-1,J}, \quad 0 \leq s \leq l \leq q+1,\ s \leq \mathrm{ord}(\mathscr{D}_n^{k-1,J}),$$
$$\left\|v - \Pi_\theta^k v\right\|_{H^s} \leq C_\Pi \theta^{l-s}\left\|v\right\|_{H^l}, \quad \forall v \in H^l\mathbb{A}_n^{k,J}, \quad 0 \leq s \leq l \leq p+1,\ s \leq 1,$$

for some constant C_Π.[14] *Besides, there is no issue to see the validity of the inverse estimates*

$$\left\|\tau_h\right\|_{H^s} \leq C_{inv} h^{l-s}\left\|\tau_h\right\|_{H^l}, \quad \forall \tau_h \in \mathscr{V}_{h,n}^{k,J}, \quad 0 \leq l \leq s \leq \mathrm{ord}(\mathscr{D}_n^{k-1,J}),$$
$$\left\|v_\theta\right\|_{H^s} \leq C_{inv} \theta^{l-s}\left\|v_\theta\right\|_{H^l}, \quad \forall v_\theta \in \mathscr{V}_{\theta,n}^{k,J}, \quad 0 \leq l \leq s \leq 1,$$

because this is true for standard spline spaces; see Lemma 6.3. The positive numbers C_Π, C_{inv} *can be chosen independently of* h *and* θ, *provided a family of regular meshes.*

After defining the discrete spaces, we can now turn our attention to the following finite-dimensional problem:

Definition 8.3 (**Discrete problem**). *In view of the assumptions in Definition 8.1 and the previously introduced spaces we want to find* $(\sigma_h, u_\theta) \in \mathscr{V}_{h,n}^{k-1,J} \times \mathscr{V}_{\theta,n}^{k,J}$ *s.t.*

$$\langle \sigma_h, \tau_h\rangle \qquad -\langle u_\theta, \mathscr{D}^{k-1}\tau_h\rangle \ = 0, \qquad \forall \tau_h \in \mathscr{V}_{h,n}^{k-1,J}, \tag{8.1.3}$$
$$\langle \mathscr{D}^{k-1}\sigma_h, v_\theta\rangle + \langle \mathscr{D}^k u_\theta, \mathscr{D}^k v_\theta\rangle = \langle f, v_\theta\rangle, \quad \forall v_\theta \in \mathscr{V}_{\theta,n}^{k,J}, \tag{8.1.4}$$

for some given $f \in L^2(\Omega) \otimes \mathbb{A}_n^{k,J}$.

In principle, we can always find a unique solution for such a discretization formulation.

Theorem 8.1 (**Discrete invertibility**). *Let the Assumptions 8.1 and 8.2 hold. Assume we have a family of pairs* $(\mathscr{V}_{h,n}^{k-1,J}, \mathscr{V}_{\theta,n}^{k,J})_\theta$ *in the sense of Assumption 5.1 with underlying regular meshes, where the spaces are given by* (8.1.1)-(8.1.2). *Then there is a positive constant* c_R *s.t.* $h = h(\theta) \leq c_R\theta$ *implies a unique discrete solution of* (8.1.3)-(8.1.4) *for each* θ.

Proof. If we combine the approximation and inverse estimates of Corollary 8.1 with the statement of Corollary 4.4 the assertion follows directly from Lemma 5.1. □

So looking at the last theorem, one can see that it might be necessary to use different meshes for σ and u. However, with suitable mesh refinement, one can always compute a unique approximate solution. The apparent issue here is the lack of a statement regarding whether well-posed discretizations can also be obtained. It turns out that in the special case of $k = n$, i.e. saddle-point problems, after a slight modification of the mixed formulation, we can indeed achieve the inf-sup stability or well-posedness for the type of spaces (8.1.1)-(8.1.1). We will explain this in more detail in the next section.

8.2 The case of saddle-point problems

We now move from the problem in Definition 8.1 to the case of $k = n$. Since setting the exterior derivative $\mathrm{d}^n = 0$ also implies $\mathscr{D}_n^{n,J} = 0$, i.e. we get a saddle-point problem. In Section 5.2 we also explained why for (8.0.1)-(8.0.2), in the case of $\mathscr{D}^k = 0$, we may also employ the equivalent modified formulation from Definition 5.1. This modified mixed weak form utilizes the graph inner product associated with $\mathscr{D}^{k-1} = \mathscr{D}_n^{n-1,J}$ and is more suitable for making statements about

[14] As already done, we use the abbreviation $H^l\mathbb{E} \coloneqq H^l(\Omega) \otimes \mathbb{E}$; $\mathbb{E}$ inner product space.

well-posedness. To be more precise, our continuous problem for $k = n$ can be reformulated:
Seek for $(\sigma, u) \in \mathscr{V}_n^{n-1,J} \times \mathscr{V}_n^{n,J}$ s.t.

$$\begin{aligned} \langle \sigma, \tau \rangle_{\mathscr{V}} \quad -\langle u, \mathscr{D}^{n-1}\tau \rangle &= \langle f, \mathscr{D}^{n-1}\tau \rangle, \quad \forall \tau \in \mathscr{V}_n^{n-1,J}, && (8.2.1) \\ \langle \mathscr{D}^{n-1}\sigma, v \rangle \qquad\quad &= \langle f, v \rangle, \qquad\quad \forall v \in \mathscr{V}_n^{n,J}, && (8.2.2) \end{aligned}$$

with $\mathscr{D}^{n-1} = \mathscr{D}_n^{n-1,J}$ and $\langle \sigma, \tau \rangle_{\mathscr{V}} = \langle \sigma, \tau \rangle + \langle \mathscr{D}^{n-1}\sigma, \mathscr{D}^{n-1}\tau \rangle$.

Our goal is to build upon the approach and statements from Section 5.2, which is why consider for discretization

Definition 8.4 (**Discrete modified saddle-point problem**). *Find* $(\sigma, u) \in \mathscr{V}_{h,n}^{n-1,J} \times \mathscr{V}_{\theta,n}^{n,J}$ *s.t.*

$$\begin{aligned} \langle \sigma_h, \tau_h \rangle_{\mathscr{V}} \quad -\langle u_\theta, \mathscr{D}^{n-1}\tau_h \rangle &= \langle f, \mathscr{D}^{n-1}\tau_h \rangle, \quad \forall \tau_h \in \mathscr{V}_{h,n}^{n-1,J}, && (8.2.3) \\ \langle \mathscr{D}^{n-1}\sigma_h, v_\theta \rangle \qquad\quad &= \langle f, v_\theta \rangle, \qquad\quad \forall v_\theta \in \mathscr{V}_{\theta,n}^{n,J}. && (8.2.4) \end{aligned}$$

The question now is whether we obtain with this approach a well-posed discretization for (8.2.1)-(8.2.2), at least under certain conditions. To answer this, we now rely on our knowledge that, for the output complex in a cubical domain, we even have a structure-preserving discretization. The latter was introduced in Section 7.2 and satisfies several properties (see Lemmata 7.3 and 7.4), such as the ability to vary the regularity of the test functions. This proves to be useful for the proof of the next theorem.

Theorem 8.2 (**Discrete well-posedness**). *Let the Assumptions 8.1 and 8.2 with $k = n$ hold. Assume we have a family of pairs $(\mathscr{V}_{h,n}^{n-1,J}, \mathscr{V}_{\theta,n}^{n,J})_\theta$ in the sense of Assumption 5.1 with underlying regular meshes, where the spaces are given by* (8.1.1)-(8.1.2). *Then there is a positive constant c_R s.t. $h = h(\theta) \leq c_R\theta$ implies that* (8.2.3)- (8.2.4) *is a well-posed discretization of* (8.2.1)-(8.2.2).

Proof. The basic idea is to apply Lemma 5.4. For the proof we first consider the special case $\Omega \subset (0,1)^n$. The important point is now that we have through the outcomes of Section 7.2, especially Lemma 7.3, a structure-preserving discretization of the output complex on the unit cube $K \coloneqq (0,1)^n$. We will denote this discretization on the auxiliary domain with $(\widehat{\mathscr{V}}_{\rho,n}^{\circ,J}, \mathscr{D}_n^{\circ,J})$, i.e. here the mesh size parameter is denoted with ρ. For the existing bounded cochain projections onto this chains we write $\mathscr{P}_{\rho,n}^{\circ,J,\Lambda}$ and they are given through (7.2.7). Note, we drop the *hat* on top of the operator $\mathscr{D}_n^{\circ,J}$ since we use the same differential operators for K and Ω, meaning K is the unit cube w.r.t. to the physical coordinate system. By dividing the unit cube into m^n equal sub-cubes we can generate obviously a uniform mesh with mesh size $\rho_m = \sqrt{n}/m$ for every $m \in \mathbb{N}_{>0}$.
Let $l = \operatorname{ord}(\mathscr{D}_n^{n-1,J})$. Then, by choosing in the construction from Section 7.2 degrees $p_i = l+3,\ r_i = p_i - 1 = l+2,\ \forall i$ we have $\widehat{\mathscr{V}}_{\rho,n}^{j,J} \subset H^{l+1}(K) \otimes \mathbb{A}_n^{j,J},\ \forall j$; compare Lemma 7.4. Due to the mentioned lemma and Corollary 7.3 we can assume constants $\tilde{C}_1, \tilde{C}_2$ with

- $\left\| \mathscr{P}_{\rho,n}^{n-1,J,\Lambda} w - w \right\|_{H^s(K)} \leq \tilde{C}_1 \rho^{j-s} \left\| w \right\|_{H^j(K)},\ \forall w \in H^j(K) \otimes \mathbb{A}_n^{n-1,J},\ 0 \leq s \leq j \leq l+1$,
- $\left\| \mathscr{P}_{\rho,n}^{n,J,\Lambda} w - w \right\|_{H^s(K)} \leq \tilde{C}_1 \rho^{j-s} \left\| w \right\|_{H^j(K)},\ \forall w \in H^j(K) \otimes \mathbb{A}_n^{n,J},\ 0 \leq s \leq j \leq 1$,
- $\left\| w_\rho \right\|_{H^{l+1}(K)} \leq \tilde{C}_2 \rho^{-1} \left\| w_\rho \right\|_{H^l(K)},\ \forall w_\rho \in \widehat{\mathscr{V}}_{\rho,n}^{n-1,J}$,
- $\left\| w_\rho \right\|_{H^1(K)} \leq \tilde{C}_2 \rho^{-1} \left\| w_\rho \right\|_{L^2(K)},\ \forall w_\rho \in \widehat{\mathscr{V}}_{\rho,n}^{n,J}$.

One notes that we changed above the mesh size parameter from h to ρ compared to the notation in Section 7.2. In view of Remark 5.2 and Corollary 4.4, the assertion follows then directly by Lemma 5.4 in case of $\Omega \subset (0,1)^n$.
It is clear that after a shift of the coordinate system we find a $R > 0$ s.t $\Omega \subset (0,R)^n$. But then, we obtain with Remark 7.2 and analogous proof steps again the well-posedness. □

If we have a well-posed discretization, we can easily provide an approximation error estimate with the help of the general theory regarding variational problems.

Theorem 8.3 (**Error estimate**). *We assume the family of space pairs* $\left(\mathscr{V}_{h(\theta),n}^{n-1,J}, \mathscr{V}_{\theta,n}^{n,J}\right)_\theta$ *define a well-posed discretization in the sense of the last Theorem 8.2. Further let the exact solution* (σ, u) *to system* (8.2.1)-(8.2.2) *fulfill the regularity assumptions* $\sigma \in H^t(\Omega) \otimes \mathbb{A}_n^{n-1,J}$ *and* $u \in H^m(\Omega) \otimes \mathbb{A}_n^{n,J}$ *for* $l \leq t \leq q+1$, $0 \leq m \leq p+1$, *with* $l := \operatorname{ord}(\mathscr{D}^{n-1})$.
Then the error between exact and approximate solution satisfies

$$\|\sigma - \sigma_h\|_{H(\mathscr{D}^{n-1})} + \|u - u_\theta\| \leq C_{conv}\Big(h^{t-l}\,\|\sigma\|_{H^t} + \theta^m\,\|u\|_{H^m}\Big),$$

for a constant C_{conv} *independent of* θ. *Note,* $\|\tau\|^2_{H(\mathscr{D}^{n-1})} := \|\tau\|^2 + \|\mathscr{D}^{n-1}\tau\|^2$.

Proof. This is an easy consequence of the estimates in Corollary 8.1 and the general result in Lemma 2.12 for variational problems. □

When defining the spaces (8.1.1)-(8.1.2), we deal with Alt^l-valued forms. It is worth noting that a similar approach can be employed when considering proxy maps and the proxy output complex, denoted as $(\mathfrak{V}_n^{\circ,J}, \mathfrak{D}_n^{\circ,J})$; see Section 4.2.3.

Remark 8.1 (**Proxy complex**). If we replace in (8.1.1)-(8.1.2) the spaces $\mathbb{A}_n^{\circ,J}$ by the $\mathbb{V}_n^{\circ,J}$ appearing in the definition of the proxy output complex in (4.2.22), we get analog statements as above also for the proxy output complex. This is clear since for the proxy chains we have similar properties; cf. Corollary 7.4.

It is worthwhile to emphasize the following. With the last two theorems, we have now demonstrated a key result of the work. Specifically, we showed the possibility to discretize saddle point problems of the form (8.2.3)-(8.2.4) using standard isogeometric spaces in a well-posed manner. In particular, we have the ability to incorporate geometries with curved boundaries exactly into the calculations, into the Finite Element spaces, respectively. This is achieved even though the mixed problem involves the differential operators of the second-order complexes $(\mathscr{V}_n^{\circ,J}, \mathscr{D}_n^{\circ,J})$, presenting a non-trivial extension beyond the case of classical differential forms. It is also important to mention that the opportunity to increase the regularity of the underlying B-splines is advantageous. By doing so, at least in the single-patch IGA case, obtaining H^2-smooth Finite Element functions becomes relatively straightforward, which is necessary when dealing with second-order differential operators in the formulation. We will leverage this in the next example.

In Section 4.2.3 we outlined, why the Hessian, elasticity or divdiv complexes ((4.2.26),(4.2.27),(4.2.29)-(4.2.31)) can be interpreted as the (proxy) output complexes of the form $(\mathscr{V}_n^{\circ,J}, \mathscr{D}_n^{\circ,J})$. Hence, we can approximate saddle point problems derived from these chains using isogeometric spaces. We would like to illustrate this through an example, where our objective is to compute approximations to the biharmonic equation. Subsequently, we will revisit this approach based on Definition 8.4, but this time within the framework of linear elasticity theory.

Example 8.1 (Bilaplacian)**.** *We assume $\Omega \subset \mathbb{R}^n,\ n = 2, 3$ to be a bounded Lipschitz domain, then we get for the Hodge–Laplace problem of level $k = n$ for the divdiv complex (see* (4.2.27) *and* (4.2.31)*) the associated mixed weak form:* Find $(\sigma, u) \in H(\Omega, \nabla\cdot\nabla\cdot, \mathbb{S}) \times L^2(\Omega)$ s.t.

$$\begin{aligned} \langle \sigma, \tau\rangle \qquad -\langle u, \nabla\cdot\nabla\cdot\tau\rangle &= 0, \qquad \forall \tau \in H(\Omega, \nabla\cdot\nabla\cdot, \mathbb{S}), && (8.2.5)\\ \langle \nabla\cdot\nabla\cdot\sigma, v\rangle \qquad\qquad\quad &= \langle f, v\rangle, \quad \forall v \in L^2(\Omega), && (8.2.6) \end{aligned}$$

where again $\mathbb{S}$ denotes the space of symmetric $n \times n$-matrices.
We suppose here a regular parametrization $\mathbf{F}\colon (0,1)^n \to \Omega$, which is at least a C^1-diffeomorphism. One notes the exactness of the divdiv complex at this level for each bounded Lipschitz domain. Hence, the theory of FEEC yields the well-posedness of the above system. The associated Hodge–Laplace equation itself (compare (3.2.1)*) reads*

$$\nabla\cdot\nabla\cdot\nabla^2 u = f, \qquad u,\ f \in L^2(\Omega), \tag{8.2.7}$$

as the adjoint operator to $\nabla\cdot\nabla\cdot$ is the Hessian ∇^2. To obtain the mentioned mixed weak form and uniqueness for the continuous problem, additional assumptions have to be required. Namely we want to find the solution $u \in H(\Omega, \nabla^2, \mathbb{R})$ s.t. $\nabla^2 u \in H(\Omega, \nabla\cdot\nabla\cdot, \mathbb{S})$ and s.t. u is in the domain of the adjoint $\big(\nabla\cdot\nabla\cdot, H(\Omega, \nabla\cdot\nabla\cdot, \mathbb{S})\big)^*$.
In order to apply Theorems 8.2 and 8.3 we choose for discretization

$$\begin{aligned} \mathscr{V}_h^{n-1} &:= \widehat{\mathscr{V}}_h^{n-1} \circ \mathbf{F}^{-1} \quad \text{with} \qquad \widehat{\mathscr{V}}_h^{n-1} := S^{s_1,\dots,s_n}_{q_1,\dots,q_n} \otimes \mathbb{S}, && (8.2.8)\\ \mathscr{V}_\theta^{n} &:= \widehat{\mathscr{V}}_\theta^{n} \circ \mathbf{F}^{-1} \quad \text{with} \qquad \widehat{\mathscr{V}}_\theta^{n} := S^{r_1,\dots,r_n}_{p_1,\dots,p_n}, \quad 0 \le r_i < p_i \text{ and } 1 \le s_i < q_i,\ \forall i, && (8.2.9) \end{aligned}$$

and we look at the modified problem to find $(\sigma_h, u_\theta) \in \mathscr{V}_h^{n-1} \times \mathscr{V}_\theta^n$, satisfying

$$\begin{aligned} \langle \sigma_h, \tau_h\rangle_\mathscr{V} \qquad -\langle u_\theta, \nabla\cdot\nabla\cdot\tau_h\rangle &= \langle f, \nabla\cdot\nabla\cdot\tau_h\rangle, \quad \forall \tau_h \in \mathscr{V}_h^{n-1}, && (8.2.10)\\ \langle \nabla\cdot\nabla\cdot\sigma_h, v_\theta\rangle \qquad\qquad\quad &= \langle f, v_\theta\rangle, \qquad\quad \forall v_\theta \in \mathscr{V}_\theta^n. && (8.2.11) \end{aligned}$$

Certainly, here we have the graph inner product $\langle \sigma, \tau\rangle_\mathscr{V} := \langle \sigma, \tau\rangle + \langle \nabla\cdot\nabla\cdot\sigma, \nabla\cdot\nabla\cdot\tau\rangle$.
Then for pairs $\big(\mathscr{V}_{h(\theta)}^{n-1}, \mathscr{V}_\theta^n\big)_\theta$ with $h(\theta) \le c_R\theta$ and c_R small enough but fixed, we obtain a well-posed discretization. This is now demonstrated in the two-dimensional setting using a concrete manufactured test setting.

To be more specific, now the computational domain $\Omega \subset \mathbb{R}^2$, i.e. $n = 2$, is parametrized by the smooth mapping $\mathbf{F}\colon (0,1)^2 \to \Omega\ ,\ (\zeta_1, \zeta_2) \to (\zeta_1, \zeta_2 - \zeta_1^2 + \zeta_1)$; cf. Figure 22. Further, the right-hand side f in (8.2.7) *is chosen such that the exact solution is given by*

$$\boxed{u \circ \mathbf{F} = w, \quad w(\zeta_1, \zeta_2) = \sin(\pi\zeta_1)^2 \sin(\pi\zeta_2)^2}.$$

We compute the errors $\|u - u_\theta\|$ and $\|\sigma - \sigma_h\|_{H(\nabla\cdot\nabla\cdot)}$ between the exact solution of (8.2.5)- (8.2.6) *and approximate solutions obtained from* (8.2.10)-(8.2.11) *together with the spline spaces* (8.2.8)-(8.2.9)*. It is natural to use degrees*

$$\boxed{q_i = p + 2,\ p_i = p,\ s_i = p - 1,\ r_i = p - 1,\ \forall i \quad \text{and} \quad \theta = h},$$

since then Theorem 8.3 suggests up to order $p + 1$ convergence. Moreover, we choose $\theta = h$, meaning we have for the spaces $\mathscr{V}_h^1$, $\mathscr{V}_\theta^2$ the same underlying mesh structure. Admittedly, it is not directly clear if the previous spaces yield well-posedness. In view of Theorem 8.2 a mesh refinement for $\mathscr{V}_h^1$, $h < \theta$, respectively, might be needed. Hence, if we see a stable error decay

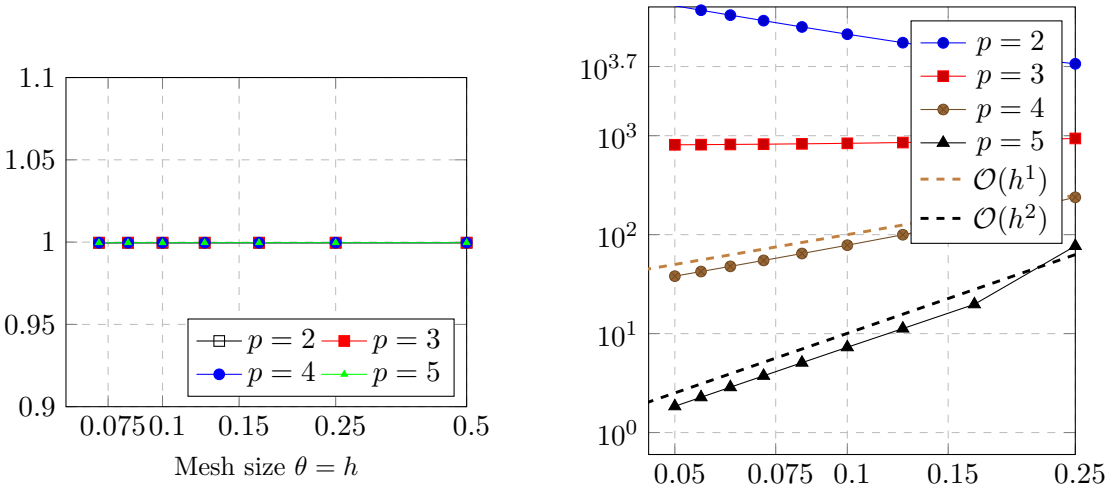

(a) Inf-sup values C_{IS} $(r = s = p - 1)$

(b) $\|\sigma - \sigma_h\|_{H(\nabla\cdot\nabla\cdot)}$

Figure 16: On the left we show the inf-sup constants C_{IS} for the first numerical test with mixed degrees $(q = p + 2)$. On the right we display the errors for the σ variable which we obtain for the manufactured test problem if we use the original saddle-point system (8.2.5)-(8.2.6).

behavior and invertible system matrices associated to the weak form, then this indicates well-posedness. Otherwise, one would e.g. refine the meshes for the σ space and start the computations again. However, to have a more grounded explanation, whether our discrete spaces ensure well-posedness, we preliminary compute numerically the discrete inf-sup constants

$$C_{IS} = C_{IS}(\mathscr{V}_h^1, \mathscr{V}_\theta^2) \coloneqq \inf_{0 \neq v_\theta \in \mathscr{V}_\theta^2} \sup_{0 \neq \tau_h \in \mathscr{V}_h^1} \frac{\langle \nabla \cdot \nabla \cdot \tau_h, v_\theta \rangle}{\|\tau_h\|_{H(\nabla\cdot\nabla\cdot)} \|v_\theta\|},$$

using the MATLAB *([53])* eigs*() function and following the procedure of Bathe et al. ([15, 33]); see Appendix 11.2. Because, if these C_{IS} are bounded from below by a positive constant independent of mesh refinement, we directly see the well-posedness of the discretization. For more details regarding this* inf-sup test *we refer to Appendix 11.2. These values C_{IS} are depicted in the diagram Figure 16 (a) for the degrees $p = 2, \dots, 5$ and regularities $r = s = p - 1$. We observe stable C_{IS} values around 1 for the different spaces and mesh sizes. Thus, we can conclude the appropriateness of $\mathscr{V}_h^1, \mathscr{V}_\theta^2$, at least for the shown degrees and regularities. Consequently, we can move on to the actual convergence test.*
One notes the feasibility of the manufactured solution since it is smooth and $u \in H_0^2(\Omega)$. Looking at the plots in Figure 17 we see a stable error decay fitting to the theoretical statement from Theorem 8.3. Because we indeed see an error decrease of approximately order $p+1$ and thus we can achieve high-order convergence for the approximations of the fourth-order Bilaplace equation (8.2.7).

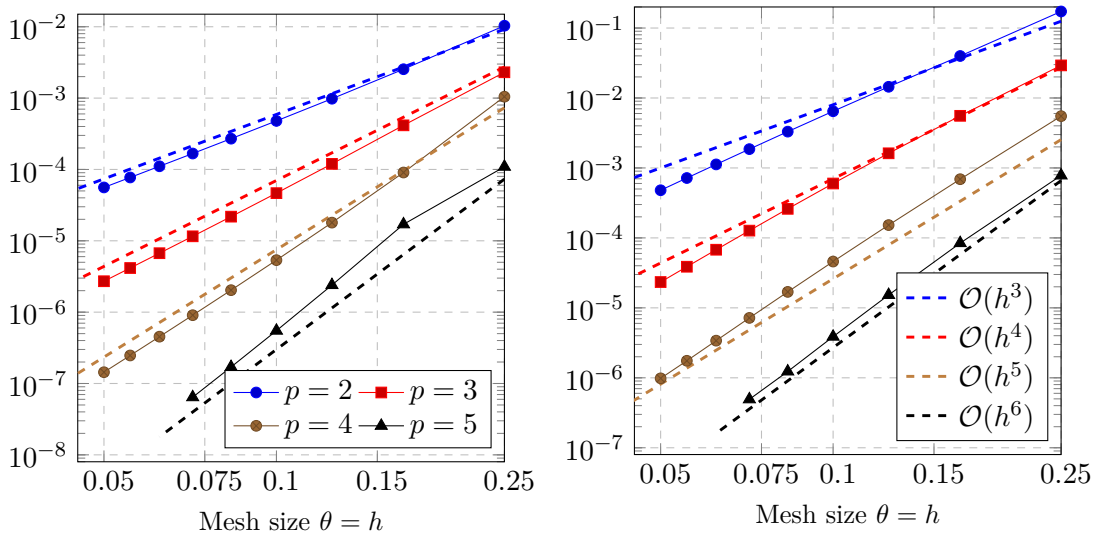

(a) $\|u - u_\theta\|$

(b) $\|\sigma - \sigma_h\|_{H(\nabla\cdot,\nabla\cdot)}$

Figure 17: Errors for the mixed-degree situation meaning $q_i = p + 2,\ p_i = p$. This degree elevation should guarantee a convergence decay of $\mathcal{O}(h^{p+1})$ which is also observed in the plots.

It would also be interesting to see if we can discretize system (8.2.5)-(8.2.6) *directly instead of* (8.2.10)-(8.2.11)*, without the modification involving the inner product. Therefore, we repeated the error calculation using the same spaces but the original formulation. When examining the errors in the σ variable in Figure 16 (b), one can immediately notice a significantly worse convergence behavior compared to Figure 17 (b), and even growing errors despite mesh refinement. This allows us to clearly see that the transition to the modified system not only simplifies making statements regarding well-posedness but also seems to make a distinct difference concerning convergence.*

Remark 8.2. One aspect that should definitely be noted here is the occurrence of large condition numbers for the mixed formulations. This is primarily caused by the presence of second derivatives. High condition numbers for high-order problems are not uncommon, but they should be particularly taken into account during convergence analyses. Therefore, for all calculated errors for the errors in Figure 17, we have also computed the relative and absolute errors when solving the underlying linear system. To be more precise, we checked

$$err_{\text{rel}} := \frac{|Ax - b|}{|b|}, \quad err_{\text{abs}} := |Ax - b|,$$

where $A,\ b$ are the system matrix and righthand-side related to the discrete problem and x is the solution vector obtained by the MATLAB ([53]) *mldivide()* function. In all cases we obtained the absolute errors to be smaller than $1.4 \cdot 10^{-9}$ and the relative errors are always smaller then $1.5 \cdot 10^{-14}$. These observations reinforce our assumption that the plots of the example are meaningful, despite the large condition numbers.

Remark 8.3 (Isoparametric IGA spaces). The well-posedness proofs as well the convergence estimates hold analogously, if we follow the isoparametric paradigm. In other words it is possible to have a non-trivial weight function $W = 1$ for the space definition leading to NURBS spaces; cf. Definition 6.3. Indeed the important approximation properties and inverse estimates are still valid when considering smooth weight functions; see Lemma 6.2 and Lemma 6.3. However, from a computational point of view it is sometimes better to use a non-isoparametric approach, since the evaluation of B-splines an their derivatives can be implemented more efficiently compared to

the situation with weight function. Because then additional evaluations caused by the product rule, chain rule, respectively, are necessary.

So we explained so far, why it is possible to use standard IG spaces to discretize the mixed weak formulation for the Hodge–Laplace problems of the output complex $(\mathscr{V}_n^{\circ,J}, \mathscr{D}_n^{\circ,J})$ at level n. Although we ignored the basic properties coming along with a structure-preserving discretization we still can achieve well-posedness. This is interesting, because we do not need special or adapted implementations for the test spaces, but we can use standard IG spaces pre-implemented in common IGA software; like in the GeoPDEs [37, 73] package we utilize.
However, the important point is that we exploited the existence of such dicretization in cubical domain to show the feasibility of the standard IG spaces. So there is still a connection between the concept of structure-preserving Hilbert complex discretizations and our modified saddle-point problem from Definition 8.4.

In Section 5.3, we introduced an alternative method for discretizing saddle-point problems arising from a BGG construction. Notably, we stipulated a prerequisite for a structure-preserving discretization of an input complex. In the upcoming section, we endeavor to clarify that this approach, outlined in the mentioned section and using Lagrange multipliers, can be employed for complexes $(\mathscr{V}_n^{\circ,J}, \mathscr{D}_n^{\circ,J})$ and the Hodge–Laplace problem of level $k = n$.

8.3 Saddle-point problems with Lagrange multiplier

Again we are in the setting of Section 4.2.3, meaning we deal with Alt^l-valued forms and Hilbert spaces of type $L^2(\Omega)\otimes\mathrm{Alt}^{k,l}$. In particular, we re-use notation and definitions from this mentioned part. Further, here we make

Assumption 8.3. *Let in the whole section $J \in \{1, \dots, n-1\}$. Consequently, the mappings $S^{n-2,J}$, $S^{n-1,J}$ introduced in Section 4.2.3 are surjective and with the notation from Section 4.2.1 it is $S^J = S^{J-1,J}$.*
Further the Assumption 8.2 applies, where we require $\mathbf{F}\colon \widehat{\Omega} \to \Omega$, $\widehat{\Omega} \coloneqq (0,1)^n$ to be C^2-smooth with C^2-smooth inverse.

The objective of this section is to show the feasibility of isogeometric discretizations in the context of the saddle-point problems from the last section, but now for the modified formulation involving a Lagrange multiplier. For this purpose one notes that by the anti-commutativity property (see Lemma 4.9), and the extended de Rham complexes $(H\Lambda^{\circ,J}, \mathrm{d}^\circ)$ we obtain the diagram structure:

$$\begin{array}{ccccccccc} & & & & \cdots & H\Lambda^{n-1,J-1}(\Omega) & \xrightarrow{\mathrm{d}^{n-1}} & H\Lambda^{n,J-1}(\Omega) & \longrightarrow 0 \\ & & & \nearrow^{S^{n-2,J}} & & & \nearrow_{S^{n-1,J}} & & \\ \cdots & & H\Lambda^{n-2,J}(\Omega) & \xrightarrow{\mathrm{d}^{n-2}} & H\Lambda^{n-1,J}(\Omega) & \xrightarrow{\mathrm{d}^{n-1}} & H\Lambda^{n,J}(\Omega) & \longrightarrow 0. & \end{array} \tag{8.3.1}$$

One notes that d^i are the extended exterior derivatives defined in (4.2.17).
This means according to the considerations in Section 4.2.4 we have now instead of the system (8.0.1)-(8.0.2) from Definition 8.1 the next continuous problem underlying:

Definition 8.5 (**Saddle-point problem with Lagrange multiplier**). *Given a $f \in L^2(\Omega) \otimes \mathbb{A}_n^{n,J}$, we seek for $(\sigma, u, \kappa) \in H\Lambda^{n-1,J}(\Omega) \times H\Lambda^{n,J}(\Omega) \times L^2(\Omega) \otimes \mathbb{A}_n^{n,J-1}$, s.t.*

$$\begin{aligned} \langle \sigma, \tau \rangle \qquad - \langle u, \mathrm{d}^{n-1}\tau \rangle + \langle \kappa, S^{n-1,J}\tau \rangle &= 0, \qquad && \forall \tau \in H\Lambda^{n-1,J}(\Omega), \\ \langle \mathrm{d}^{n-1}\sigma, v \rangle &= \langle f, v \rangle, && \forall v \in H\Lambda^{n,J}(\Omega), \\ \langle S^{n-1,J}\sigma, \eta \rangle &= 0, && \forall \eta \in L^2(\Omega) \otimes \mathbb{A}_n^{n,J-1}. \end{aligned} \tag{8.3.2}$$

The system just described corresponds indeed to the mixed weak formulation of the Hodge–Laplace problem for the output complex $(\mathscr{V}_n^{\circ,J}, \mathscr{D}_n^{\circ,J})$ at level $k = n$. It is important to note, under the Assumption 8.3, we have $\mathscr{D}_n^{n-1,J} = \mathrm{d}^{n-1}$ and $\mathscr{D}_n^{n,J} = 0$. Furthermore, following the BGG construction outlined in Section 4.2.3, we demand that $\mathscr{V}_n^{n-1,J} \subset \mathcal{N}(S^{n-1,J})$, and we incorporate this condition by introducing the additional variable $\kappa \in L^2(\Omega) \otimes \mathbb{A}_n^{n,J-1} = \mathcal{R}(S^{n-1,J})$. For details on these formulations with Lagrange multipliers we refer to the discussion in Section 4.2.4. In particular, the exactness of the de Rham complex at level n with the property $\mathcal{R}(\mathrm{d}^{n-1}, H^1(\Omega) \otimes \mathrm{Alt}^{n-1,J}) = L^2(\Omega) \otimes \mathrm{Alt}^{n,J}$ implies the well-posedness of the latter saddle-point problem, due to Lemma 4.14. But this well-posedness property can also be shown with an analogous proof as in the discrete setting; cf. Lemma 5.5. The crucial point is the validity of the auxiliary inf-sup inequality

$$\inf_{0\neq\eta\in H\Lambda^{n,J-1}} \sup_{0\neq\tau\in H\Lambda^{n-2,J}} \frac{\langle \mathrm{d}^{n-1} S^{n-2,J}\tau, \eta\rangle}{\|\tau\|_{H\Lambda}\ \|\eta\|} > 0.^{15}$$

In Section 5.3 we have seen how we can utilize these modified formulations within the context of discretizations. With Lemma 5.5, we have demonstrated conditions under which a well-posed discretization can be achieved. Our goal for the upcoming sections is to show that with the help of isogeometric discrete differential forms (see Section 7.3), we can always satisfy these conditions for C^2-smooth parametrizations of the computational domain.
The basic idea for the proof is to apply the so-called *macroelement technique* in order to show a inf-sup property stability in the discrete case. In doing so, we will follow the steps and reasoning outlined in [22, 23]. To emphasize the parallelism with the approach taken in the mentioned papers and to make our exposition easier and more comprehensible we reduce our problem from Definition 8.5 to a specific setting. However, before delving into the actual proofs and the macroelement technique, we will not only clarify this particular reduction but also explain why it does not impose any limitations compared to the general framework involving differential forms.

8.3.1 Reduction to a special setting

First, according to the definition of the exterior derivative d^k on the spaces $L^2(\Omega) \otimes \mathrm{Alt}^{k,l}$, as mentioned earlier, this simply represents a $\binom{n}{l}$-fold copy of the classical de Rham operator on $L^2\Lambda^k(\Omega)$; see (4.2.17). Additionally, for $\omega \in L^2\Lambda^{n-1,l}$, under sufficient regularity, it is

$$\begin{aligned}
&\mathrm{d}^{n-1}\Bigg(\sum_{\sigma\in\Sigma_<(n-1,n)} c_{\sigma,s}(dx^{\sigma_1}\wedge\cdots\wedge dx^{\sigma_{n-1}})\otimes(dx^{s_1}\wedge\cdots\wedge dx^{s_l})\Bigg)\\
&= \sum_{\sigma\in\Sigma_<(n-1,n)}\sum_{i=1}^{n} \partial_i c_{\sigma,s}(dx^i\wedge dx^{\sigma_1}\wedge\cdots\wedge dx^{\sigma_{n-1}})\otimes(dx^{s_1}\wedge\cdots\wedge dx^{s_l})\\
&= \sum_{j=1}^{n}(-1)^{i_j}\Big(\partial_j c_{\sigma,s}\Big)(dx^1\wedge dx^2\wedge\cdots\wedge dx^n)\otimes(dx^{s_1}\wedge\cdots\wedge dx^{s_l}),
\end{aligned}$$

for suitable $i_j \in \{0,1\}$. The factors $(-1)^{i_j}$ are caused by the re-ordering $(dx^i\wedge dx^{\sigma_1}\wedge\cdots\wedge dx^{\sigma_{n-1}})$ to $(dx^1\wedge dx^2\wedge\cdots\wedge dx^n)$. As explained in Section 4.2.3 we can use proxy maps to identify $L^2(\Omega)\otimes\mathrm{Alt}^{k,l}$ with $L^2(\Omega)\otimes\mathbb{R}^{(n|l)\times(n|k)}$; compare diagram (4.2.24). Let $\sigma \in \Sigma_<(n-1,n)$ and $i \in \mathbb{N}$ s.t. $\{i\}\cup\{\sigma_1,\dots,\sigma_{n-1}\} = \{1,\dots,n\}$. Then we look at the next special identifications

$$\mathcal{J}_{n-1}\Big(c\,dx^{\sigma_1}\wedge\cdots\wedge dx^{\sigma_{n-1}}\Big) \coloneqq \begin{cases} c, & \text{if } dx^1\wedge dx^2\wedge\cdots\wedge dx^n = dx^i\wedge dx^{\sigma_1}\wedge\cdots\wedge dx^{\sigma_{n-1}},\\ -c, & \text{else.}\end{cases}$$

[15] $\|\tau\|_{H\Lambda}$ denotes the graph norm related to d^{n-2}.

and

$$\mathcal{J}_n\Big(c\,dx^1\wedge\cdots\wedge dx^n\Big) \coloneqq c.$$

We directly see that with these proxy maps and the ansatz $\mathcal{D}^{n-1} \coloneqq \mathcal{J}_n \circ \mathrm{d}^{n-1} \circ \mathcal{J}_{n-1}^{-1}$ we obtain the divergence operator $\nabla\cdot$. Thus the exterior derivative d^{n-1} as densely defined operator from $L^2(\Omega)\otimes\mathrm{Alt}^{n-1,l}$ to $L^2(\Omega)\otimes\mathrm{Alt}^{n,l}$, can be interpreted as a $\binom{n}{l}$-fold copy of the classical divergence operator acting on the coefficients. Consequently, in view of diagram (4.2.24) we find proxy maps $\mathcal{J}_k$ such that (8.3.1) can be rewritten equivalently as

$$\begin{array}{ccccccccc} & & & & \cdots & H(\Omega,\nabla\cdot,\mathbb{R}^{(n|J-1)\times n}) & \xrightarrow{\nabla\cdot} & L^2(\Omega)\otimes\mathbb{R}^{n|J-1} & \longrightarrow\ 0 \\ & & & \overset{\tilde{S}^{n-2,J}}{\nearrow} & & & \overset{\tilde{S}^{n-1,J}}{\nearrow} & & \\ \cdots & H(\Omega,\mathcal{D}^{n-2},\mathbb{R}^{(n|J)\times(n|2)}) & \xrightarrow{\mathcal{D}^{n-2}} & H(\Omega,\nabla\cdot,\mathbb{R}^{(n|J)\times n}) & \xrightarrow{\nabla\cdot} & L^2(\Omega)\otimes\mathbb{R}^{n|J} & \longrightarrow & 0, & \end{array} \tag{8.3.3}$$

where $\mathcal{D}^{n-2}$ is a first order differential operator, acting row wise and $\tilde{S}^{m,l}$ are the modified linking maps given through (4.2.21). As we just mentioned, we can assume the divergence acting row-wise, too, and we still have the anti-commutativity property

$$\tilde{S}^{n-1,J}\circ\mathcal{D}^{n-2} = -\nabla\cdot\circ\tilde{S}^{n-2,J}.$$

Considering the previous comments, we can observe that it is justified to simplify system (8.3.2) to a version, where d^{n-1} aligns with the divergence $\nabla\cdot$. Additionally, discussing matrix or vector fields is adequate, eliminating the need for direct usage of differential forms.

Assumption 8.4 (Fixed proxy maps)**.** *We figured out why it is enough to work with diagram* (8.3.3)*. We only need suitable proxy maps $\mathcal{J}_\circ$ in the sense of Definition 3.10. Until Section 9 we require the proxy map to be fixed and to be exactly those which transfer* (8.3.1) *to* (8.3.3)*.*

Consequently, we can rewrite the problem from Definition 8.5 into a more specialized one. More precisely, first we set:

Definition 8.6 (**Auxiliary abbreviations**)**.**

$$\begin{aligned} \tilde{S} &\coloneqq \tilde{S}^{n-1,J}, & \mathbb{E}^{n-2} &\coloneqq \mathbb{R}^{(n|J)\times(n|2)}, & \mathbb{E}^{n-1} &\coloneqq \mathbb{R}^{(n|J)\times n}, \\ \mathbb{E}^{n} &\coloneqq \mathbb{R}^{n|J}, & \bar{\mathbb{E}}^{n-1} &\coloneqq \mathbb{R}^{(n|J-1)\times n}, & \bar{\mathbb{E}}^{n} &\coloneqq \mathbb{R}^{n|J-1}, \end{aligned}$$

And exploiting these abbreviations we consider

Definition 8.7 (**Proxy saddle-point problem with Lagrange multiplier**)**.** *Find $\sigma \in H(\Omega,\nabla\cdot,\mathbb{E}^{n-1})$, $u\in L^2(\Omega)\otimes\mathbb{E}^n$ and $\kappa\in L^2(\Omega)\otimes\bar{\mathbb{E}}^n$, s.t.*

$$\begin{aligned} \langle\sigma,\tau\rangle\ -\ \langle u,\nabla\cdot\tau\rangle\ +\ \langle\kappa,\tilde{S}\tau\rangle &= 0, & \forall\tau&\in H(\Omega,\nabla\cdot,\mathbb{E}^{n-1}), \\ \langle\nabla\cdot\sigma, v\rangle &= \langle f, v\rangle, & \forall v&\in L^2(\Omega)\otimes\mathbb{E}^n, \\ \langle\tilde{S}\sigma,\eta\rangle &= 0, & \forall\eta&\in L^2(\Omega)\otimes\bar{\mathbb{E}}^n. \end{aligned} \tag{8.3.4}$$

Before we address the choice of proper discrete spaces in order to compute approximations in a well-posed manner let us add here some simple but useful observations:

Corollary 8.2 (**Auxiliary right-inverse**)**.**

- *The operators* $\tilde{S}^{n-i,J}$ *have the structure* $\tilde{S}^{n-i,J} = \mathrm{id} \otimes \tilde{s}^{n-i,J}$*, with*

$$\tilde{s}^{n-i,J} \colon \mathbb{R}^{(n|J)\times(n|i)} \to \mathbb{R}^{(n|J-1)\times(n|i-1)}, \quad i \in \{1,2\},$$

being linear and surjective. This is a direct consequence of the $\tilde{S}^{m,l}$ *(see* (4.2.21)*) and Assumption 8.3.*

- *Due to the surjectivity of* $\tilde{s}^{n-2,J}$ *we have a bounded right-inverse* $\tilde{t}^{n-2} \coloneqq (\tilde{s}^{n-2,J})^{\dagger}$*, meaning* $\tilde{s}^{n-2,J}\tilde{t}^{n-2} = \mathrm{id}$ *on* $\bar{\mathbb{E}}^{n-1}$*.*
Clearly, by a tensoring

$$\tilde{T} \coloneqq \mathrm{id} \otimes \tilde{t}^{n-2}$$

we obtain a right-inverse of
$\tilde{S}^{n-2,J} \colon L^2(\Omega) \otimes \mathbb{E}^{n-2} \to L^2(\Omega) \otimes \bar{\mathbb{E}}^{n-1}$*. Then we directly have*

$$\tilde{T}\tau \in H^1_0(\Omega) \otimes \mathbb{E}^{n-2}, \quad \forall \tau \in H^1_0(\Omega) \otimes \bar{\mathbb{E}}^{n-1},$$

and obviously

$$\tilde{T}\left(\left(S^{\mathbf{r}}_{\mathbf{p}} \circ \mathbf{F}^{-1}\right) \otimes \bar{\mathbb{E}}^{n-1}\right) \subset \left(S^{\mathbf{r}}_{\mathbf{p}} \circ \mathbf{F}^{-1}\right) \otimes \mathbb{E}^{n-2},$$

for an arbitrary spline space $S^{\mathbf{r}}_{\mathbf{p}}$*. Furthermore, the boundedness of* $\tilde{t}^{n-2}$ *implies*

$$\left\|\tilde{T}\tau\right\|_{H^l} \leq C \left\|\tau\right\|_{H^l}, \ \forall \tau \in H^l(\Omega) \otimes \bar{\mathbb{E}}^{n-1}, \ l \in \mathbb{N}_0,$$

for some constant C*.*

Next we want to move on to the discretization of (8.3.4) and end this section with an abstract discrete system which we can refer to.

Definition 8.8 (**Discrete proxy saddle-point problem with Lagrange multiplier**)**.**
Let $\Sigma_h \subset H(\Omega, \nabla\cdot, \mathbb{E}^{n-1})$*,* $U_h \subset L^2(\Omega) \otimes \mathbb{E}^n$*,* $\bar{K}_h \subset L^2(\Omega) \otimes \bar{\mathbb{E}}^n$ *be given finite-dimensional spaces.*
Find $(\sigma_h, u_h, \kappa_h) \in (\Sigma_h, U_h, \bar{K}_h)$ *s.t.*

$$\begin{aligned} \langle \sigma_h, \tau_h \rangle \ - \ \langle u_h, \nabla \cdot \tau_h \rangle \ + \ \langle \kappa_h, \tilde{S}\tau_h \rangle &= 0, && \forall \tau_h \in \Sigma_h, \\ \langle \nabla \cdot \sigma_h, v_h \rangle &= \langle f, v_h \rangle, && \forall v_h \in U_h, \\ \langle \tilde{S}\sigma_h, \eta_h \rangle &= 0, && \forall \eta_h \in \bar{K}_h. \end{aligned} \tag{8.3.5}$$

8.3.2 Choice of spaces

It is evident that we cannot choose Σ_h, U_h, $\bar{K}_h$ arbitrarily. However, revisiting Lemma 5.5 and its conditions we can already discern that Σ_h, U_h should be part of a structure-preserving discretization of the bottom complex in (8.3.3). Moreover, in the mentioned lemma an auxiliary space U_h^{n-2} appears, which also needs to align with Σ_h and $\bar{K}_h$. These various aspects, prompted by the Lemma 5.5, inspire the following definitions.

First let us write $V^j_{h,n}(q,s),\ j = 0, \dots, n$ for the isogeometric discrete differential forms from (7.3.1) in Section 7.3 with underlying degree and regularity vector $\mathbf{p} = (q, \dots, q) \in \mathbb{N}_0^n$, $\mathbf{r} = (s, \dots, s) \in \mathbb{N}_0^n$. And as in Remark 7.3 we consider the row-wise extended spaces

$$\tilde{V}^j_{h,n}(q,s) \coloneqq \left\{\tau \in L^2(\Omega) \otimes \mathbb{R}^{(n|J)\times(n|j)} \;\middle|\; \tau_i \in V^j_{h,n}(q,s),\ \forall i\right\}, \tag{8.3.6}$$

writing τ_i for the i-th row of τ. In fact, for the definition of the $V^\circ_{h,n}$ in (7.3.1) we utilized proxy mappings $\mathcal{J}_\circ$, but here we demand that we are precisely using these $\mathcal{J}_\circ$ that we also need to go from (8.3.1) to (8.3.3); see Assumption 8.4. In other words, we proceed with the understanding that the spaces $\tilde{V}^\circ_{h,n}(q,s)$ represent a structure-preserving discretization of the bottom complex in (8.3.3), provided $q > s$. As explained in the Remark 7.3, this last assumption can always be met and does not pose any limitation.

With the underlying requirement

$$p - 1 > r \geq 0$$

we introduce the next abbreviations:

$$R_h \coloneqq \tilde{V}^{n-2}_{h,n}(p+1,r), \quad \Sigma_h \coloneqq \tilde{V}^{n-1}_{h,n}(p+1,r), \quad U_h \coloneqq \tilde{V}^{n}_{h,n}(p+1,r), \tag{8.3.7}$$

as well as

$$\bar{K}_h \coloneqq \Big\{ v = (v_i)_i \in L^2(\Omega) \otimes \bar{\mathbb{E}}^n \;\Big|\; v_i \in V^0_{h,n}(p-1,r) \Big\}. \tag{8.3.8}$$

Besides we introduce two further auxiliary spaces

$$R_{h,0} \coloneqq R_h \cap H^1_0(\Omega) \otimes \mathbb{E}^{n-2}, \quad \bar{K}_{h,0} \coloneqq \bar{K}_h \cap L^2_0(\Omega) \otimes \bar{\mathbb{E}}^n, \tag{8.3.9}$$

with

$$L^2_0(\Omega) \coloneqq L^2(\Omega) \cap \Big\{ v \;\Big|\; \int_\Omega v \, dx = 0 \Big\}.$$

The next helpful points can be easily verified:

Corollary 8.3.

- *Since for a 0-form $\omega \in L^2(\widehat{\Omega})$ the pullback w.r.t. $\mathbf{F}^{-1}$ is just $\omega \circ \mathbf{F}^{-1}$ (see Definition 3.9) we have*
$$\bar{K}_h = \big(S^{r,\dots,r}_{p-1,\dots,p-1} \circ \mathbf{F}^{-1} \big) \otimes \bar{\mathbb{E}}^n \subset H^1(\Omega) \otimes \bar{\mathbb{E}}^n.$$
- *Let us consider Lemma 3.14. With the latter and by the row-wise ansatz in* (8.3.6) *together with C^2-smoothness assumption for $\mathbf{F}^{-1}$ we find a C^1-smooth field $\bar{\mathbf{M}} \colon \Omega \to \mathbb{R}^{(n|2)\times(n|2)}$ of invertible matrices such that*
$$R_h = \Big\{ \big(\tau \circ \mathbf{F}^{-1} \big) \bar{\mathbf{M}}^{-1} \;\Big|\; \tau \colon \Omega \to \mathbb{E}^{n-2} \;,\; \tau_i \in \widehat{V}^{n-2}_{h,n}(p+1,r), \forall i \Big\},$$
where $\widehat{V}^{n-2}_{h,n}(p+1,r)$ is the parametric test space defined in (7.1.5) *with degree and regularity vectors $\mathbf{p} = (p+1,\dots,p+1)$, $\mathbf{r} = (r,\dots,r)$. Hence, because obviously*
$$S^{r,\dots,r}_{p,\dots,p} \otimes \mathbb{R}^{n|2} \subset \widehat{V}^{n-2}_{h,n}(p+1,r),$$
it is also
$$\Big[\big(S^{r,\dots,r}_{p,\dots,p} \otimes \mathbb{E}^{n-2} \big) \circ \mathbf{F}^{-1} \Big] \bar{\mathbf{M}}^{-1} \subset R_h.$$

Since we used spaces from the isogeometric de Rham sequences to define Σ_h, U_h, $\bar{K}_h$, R_h one can introduce L^2-bounded projections onto the mentioned spaces by means of the row-wise application of the $\Pi^j_{h,n}$ from Section 7.3; see (7.3.2). We denote the resulting projections in the following with

$$\begin{aligned} &\Pi^R_h \colon L^2(\Omega) \otimes \mathbb{E}^{n-2} \to R_h, && \Pi^\Sigma_h \colon L^2(\Omega) \otimes \mathbb{E}^{n-1} \to \Sigma_h, \\ &\Pi^U_h \colon L^2(\Omega) \otimes \mathbb{E}^{n} \to U_h, && \Pi^{\bar{K}}_h \colon L^2(\Omega) \otimes \bar{\mathbb{E}}^{n} \to \bar{K}_h. \end{aligned}$$

Consequently, as we have row-wise discrete differential forms with the matching row-wise cochain projections we obtain a commutative diagram

$$\begin{array}{ccccc} H(\Omega,\mathcal{D}^{n-2},\mathbb{E}^{n-2}) & \xrightarrow{\mathcal{D}^{n-2}} & H(\Omega,\nabla\cdot,\mathbb{E}^{n-1}) & \xrightarrow{\nabla\cdot} & L^2(\Omega)\otimes\mathbb{E}^n \\ \Pi_h^R\big\downarrow & & \Pi_h^\Sigma\big\downarrow & & \Pi_h^U\big\downarrow \\ R_h & \xrightarrow{\mathcal{D}^{n-2}} & \Sigma_h & \xrightarrow{\nabla\cdot} & U_h \end{array} \quad . \tag{8.3.10}$$

In view of the above remarks and Corollary 7.11 we can summarize the next approximation properties of latter projections.

Corollary 8.4. *Supposing smooth enough mappings $(\sigma,u,\kappa)\in L^2(\Omega)\otimes\mathbb{E}^{n-1}\times L^2(\Omega)\otimes\mathbb{E}^n\times L^2(\Omega)\otimes\bar{\mathbb{E}}^n$ and $w\in L^2(\Omega)\otimes\mathbb{E}^{n-2}$, it holds for $0\leq r<p-1,\ 0\leq l\leq p$ and proper constants C_R, C_Σ, C_U, C_K:*

$$\begin{aligned} &\left\|w-\Pi_h^R w\right\|\leq C_R h^l\left\|w\right\|_{H^l}\,,\quad \left\|\sigma-\Pi_h^\Sigma\sigma\right\|_{H(\nabla\cdot)}\leq C_\Sigma h^l\left\|\sigma\right\|_{H^l(\nabla\cdot)}\,,\\ &\left\|u-\Pi_h^U u\right\|\leq C_U h^l\left\|u\right\|_{H^l}\,,\quad \left\|\kappa-\Pi_h^{\bar{K}}\kappa\right\|\leq C_K h^l\left\|\kappa\right\|_{H^l}\,. \end{aligned}$$

In the inequalities regarding $\Pi_h^R,\ \Pi_h^\Sigma,\ \Pi_h^U$ we allow for $0\leq l\leq p+1$.

Proof. These estimates follow directly by a row-wise application of the results regarding the isogeometric discrete differential forms; see Section 7.3, Corollary 7.11, respectively. □

For the proof of the inf-sup stability later we also need the space $R_{h,0}$ from (8.3.9) with zero boundary conditions. The next step is to show that for such spaces with boundary conditions we also have proper L^2-bounded projections.
First let us insert an well-known result from IGA theory.

Lemma 8.1 (See (4.6) in [27] or [17, Section 3.4])**.** *Let $\mathbf{q}=(q_i)_i,\ \mathbf{s}=(s_i)_i\in\mathbb{N}_0^n$ s.t. $q_i>s_i\geq 0$ and thus $S_{\mathbf{q}}^{\mathbf{s}}\subset H^1(\widehat{\Omega})$.*
Then there exist L^2-bounded projections $\widehat{\Pi}_{\mathbf{q},\mathbf{s},0}\colon H_0^1(\widehat{\Omega})\to S_{\mathbf{q}}^{\mathbf{s}}\cap H_0^1(\widehat{\Omega})$ s.t.

$$\left\|v-\widehat{\Pi}_{\mathbf{q},\mathbf{s},0}v\right\|_{H^s}\leq C_{P1}h^{l-s}\left\|v\right\|_{H^l}\,,\quad \forall v\in H_0^1(\widehat{\Omega}),\quad 0\leq s\leq l\leq 1, \tag{8.3.11}$$

where h is the mesh size of the underlying spline space and C_{P1} does not depend on h. Here we assume as always regular meshes.

If we have $p>r\geq 0$ and consider the degree and regularity vector $\mathbf{p}=(p+1,\dots,p+1),\ \mathbf{r}=(r+1,\dots,r+1)$ we directly have for the corresponding discrete differential forms $Q_{\mathbf{p}}^{\mathbf{r}}\Lambda^k$ defined through (7.1.1) that $Q_{\mathbf{p}}^{\mathbf{r}}\Lambda^k\subset H^1\Lambda^k(\widehat{\Omega})$. Because then all the spline coefficients are piecewise smooth and globally continuous. Writing $H_0^1\Lambda^k(\widehat{\Omega})$ for the differential forms with coefficients in $H_0^1(\widehat{\Omega})$ we introduce the next mapping

$$\begin{aligned} &\widehat{\Pi}_{h,n,0}^{j,\Lambda}\colon H_0^1\Lambda^j(\widehat{\Omega})\to Q_{\mathbf{p}}^{\mathbf{r}}\Lambda^j\cap H_0^1\Lambda^j(\widehat{\Omega})\ ,\\ &\qquad\qquad \sum_{\sigma\in\Sigma_<(j,n)} c_\sigma\ dx^{\sigma_1}\wedge\cdots\wedge dx^{\sigma_j}\mapsto \sum_{\sigma\in\Sigma_<(j,n)}\left(\widehat{\Pi}_{\mathbf{p}-\mathbf{e}_\sigma,\mathbf{r}-\mathbf{e}_\sigma,0}\,c_\sigma\right)dx^{\sigma_1}\wedge\cdots\wedge dx^{\sigma_j}, \end{aligned}$$

where we exploited the special projections from Lemma 8.1. Further $\mathbf{e}_\sigma\in\{0,1\}^n$ denotes the characteristic vector of $\sigma\in\Sigma_<(j,n)$; see (7.1.2). One observes that our choice of $\mathbf{p}$ and $\mathbf{r}$ ensures $\mathbf{p}-\mathbf{e}_\sigma\geq 1$ and $\mathbf{r}-\mathbf{e}_\sigma\geq 0$. An application of Lemma 8.1 implies

Corollary 8.5. *Assume* $\mathbf{p} = (p+1, \dots, p+1)$, $\mathbf{r} = (r+1, \dots, r+1)$ *with* $p > r \geq 0$. *Then, assuming regular meshes, it is*

$$\left\|\omega - \widehat{\Pi}^{j,\Lambda}_{h,n,0}\omega\right\|_{H^s} \leq C_{P1} h^{l-s} \left\|\omega\right\|_{H^l}, \quad \forall \omega \in H^1_0\Lambda^j(\widehat{\Omega}), \quad 0 \leq s \leq l \leq 1, \tag{8.3.12}$$

for some C_{P1} *independent of mesh size* h.

Let still $p > r \geq 0$ and $\mathbf{p} = (p+1, \dots, p+1)$, $\mathbf{r} = (r+1, \dots, r+1)$. Thus, by the C^2-regularity of the parametrization mapping $\mathbf{F}\colon \widehat{\Omega} \to \Omega$ we can conclude $V^j_{h,n}(p+1, r+1) \subset H^1(\Omega) \otimes \mathbb{R}^{n|j}$. Using the proxy maps $\mathcal{J}_\circ$ and the pullback operation $\mathcal{Y}^j_{\mathbf{F}}$ (see Definition 3.9) we introduce

$$\begin{aligned} \Pi^j_{h,n,0}\colon H^1_0(\Omega) \otimes \mathbb{R}^{n|j} &\to \left(H^1_0(\Omega) \otimes \mathbb{R}^{n|j}\right) \cap V^j_{h,n}(p+1, r+1)\,, \\ \Pi^j_{h,n,0} &\coloneqq \mathcal{J}_j \circ \mathcal{Y}^j_{\mathbf{F}^{-1}} \circ \widehat{\Pi}^{j,\Lambda}_{h,n,0} \circ \mathcal{Y}^j_{\mathbf{F}} \circ \mathcal{J}_j^{-1} \end{aligned} \tag{8.3.13}$$

Let us make clear why the above mapping is well-defined. Since $\mathbf{F}^{-1}$ is C^2-regular we see by Lemma 3.8 that for $u \in H^1_0(\Omega) \otimes \mathbb{R}^{n|j}$ we obtain $v \coloneqq \mathcal{Y}^j_{\mathbf{F}}\mathcal{J}_j^{-1}u \in H^1_0\Lambda^j(\widehat{\Omega})$. This means $w \coloneqq \widehat{\Pi}^{j,\Lambda}_{h,n,0}v$ yields an element in $Q^{\mathbf{r}}_{\mathbf{p}}\Lambda^j \cap H^1_0\Lambda^j(\widehat{\Omega})$. By the definition of the space $V^j_{h,n}(p+1, r+1)$ we have $\mathcal{J}_j\mathcal{Y}^j_{\mathbf{F}^{-1}}w \in V^j_{h,n}(p+1, r+1)$. But additionally, again the smoothness of $\mathbf{F}^{-1}$ and Lemma 3.8 implies also $\mathcal{J}_j\mathcal{Y}^j_{\mathbf{F}^{-1}}w \in H^1_0(\Omega) \otimes \mathbb{R}^{n|j}$. Hence the definition in (8.3.13) is justified.
Note, using Lemma 3.8 we can find constants $c_1 < c_2$ such that

$$c_1 \left\|\mathcal{Y}^j_{\mathbf{F}}\mathcal{J}_j^{-1}v\right\|_{H^s(\widehat{\Omega})} \leq \left\|v\right\|_{H^s(\Omega)} \leq c_2 \left\|\mathcal{Y}^j_{\mathbf{F}}\mathcal{J}_j^{-1}v\right\|_{H^s(\widehat{\Omega})}, \quad \forall v \in H^s(\Omega) \otimes \mathbb{R}^{n|j}, \quad 0 \leq s \leq 1.$$

With this norm equivalence we obtain from Corollary 8.5 directly

Corollary 8.6. *Let* $\mathbf{p} = (p+1, \dots, p+1)$, $\mathbf{r} = (r+1, \dots, r+1)$ *with* $p > r \geq 0$. *Then, assuming regular meshes, it is*

$$\left\|v - \Pi^j_{h,n,0}v\right\|_{H^s} \leq C_{P1} h^{l-s} \left\|v\right\|_{H^l}, \quad \forall v \in H^1_0(\Omega) \otimes \mathbb{R}^{n|j}, \quad 0 \leq s \leq l \leq 1, \tag{8.3.14}$$

for some C_{P1} *independent of mesh size* h.

Now we extend the above projection in the sense

$$\Pi^j_{h,n,0}\colon H^1_0(\Omega) \otimes \mathbb{R}^{(n|J)\times(n|j)} \to H^1_0(\Omega) \otimes \mathbb{R}^{(n|J)\times(n|j)},$$

by a row-wise application of the original projection from (8.3.13). Then we trivially have the same type of estimates as in the previous corollary. Besides, for $v \in H^1_0(\Omega) \otimes \mathbb{E}^{n-2}$ together with (8.3.6) and (8.3.9) we get

$$\Pi^{n-2}_{h,n,0}v \in \tilde{V}^{n-2,J}_{h,n}(p+1, r+1) \cap \left(H^1_0(\Omega) \otimes \mathbb{E}^{n-2}\right) \subset R_{h,0}.$$

In other words, $\Pi^j_{h,n,0}$ is a projection onto a subspace of the auxiliary space $R_{h,0}$ in (8.3.9).
At the end of this section let us introduce here a further abbreviation. Namely, for the following we set

$$\Pi^R_{h,0} \coloneqq \Pi^{n-2}_{h,n,0}. \tag{8.3.15}$$

After we clarified the discrete spaces and introduced proper projections, we should check whether we get with (8.3.5) a reasonable discretization scheme. We focus on this in the subsequent sections.

8.3.3 Well-posedness

Next we check the well-posedness of our finite-dimensional problem (8.3.5), provided the choice (8.3.7) and (8.3.8), where we require $p-1 > r \geq 0$. Then, exploiting Lemma 5.5 we see that the only missing part for a proof of the well-posedness in the discrete setting is the inf-sup condition (5.3.5) related to the diagram (8.3.3). Because, the important point is that the spaces R_h, Σ_h, U_h define a structure-preserving discretization of the bottom chain in (8.3.3). The latter is clear, since we use in (8.3.7) row-wise isogeometric discrete differential.

Theorem 8.4 (**Well-posed discretization**). *Let Assumption 8.3 hold and we require a family of regular meshes $(\mathcal{M}_h)_h$ in the sense of Definition 6.5. Then the choice* (8.3.7) *and* (8.3.8) *of discrete spaces with $p-1 > r \geq 0$ implies the existence of a $h_{\max} > 0$ s.t. we obtain for* (8.3.5) *and for all $h \leq h_{\max}$ a unique solution. Moreover, the discretization is well-posed, meaning we have inf-sup stability independent of h.*

Proof. As just indicated we want to apply Lemma 5.5 to obtain the statement. And in fact we already explained why it is enough to look at the following inf-sup inequality

$$\inf_{0\neq\eta_h\in\bar{K}_h}\ \sup_{0\neq\tau_h\in R_h}\ \frac{\langle \nabla\cdot(\tilde{S}\tau_h),\eta_h\rangle}{\|\tau_h\|_{H(\mathcal{D}^{n-2})}\ \|\eta_h\|} \geq C>0, \quad \tilde{S}\coloneqq\tilde{S}^{n-2,J}, \tag{8.3.16}$$

to prove the global inf-sup stability, where C must not depend on h. Namely, one notes, the last inf-sup relation corresponds to (5.3.5) for our choice of discrete spaces and (8.3.3). Unfortunately, latter condition is not trivial to check and we follow the proof for the Taylor–Hood stability in [22] that is based on the so-called *macroelement technique*. Before we go into detail, we need to adapt the preliminary steps made in the mentioned paper to our setting. Basic idea for preparations is to first reduce the above inf-sup condition to a different one, that is derived utilizing *Verfürth's trick*. Applying this trick, we will consider an even stronger inf-sup condition involving the H^1-norm in the denominator. One observes, by construction the order of $\mathcal{D}^{n-2}$ is 1 and $\|\tau\|_{H(\mathcal{D}^{n-2})} \leq \tilde{C}\,\|\tau\|_{H^1}\,, \forall \tau \in H^1(\Omega)\otimes\mathbb{E}^{n-2}$, for a fixed constant $\tilde{C}$.
The detailed steps for the proof of the inf-sup conditions are outlined in the subsequent sections which result in Lemma 8.3. This lemma finally yields a $h_{\max} > 0$ and a $C > 0$ s.t. (8.3.16) is satisfied $\forall h \leq h_{\max}$. □

Remark 8.4. To increase readability we will write in the following

$$\inf_{\eta\in X}\sup_{\tau\in Y} \quad \text{instead of} \quad \inf_{0\neq\eta\in X}\sup_{0\neq\tau\in Y},$$

although we only consider non-vanishing space elements.

8.3.4 Verfürth's trick

We want to emphasize that the proof structure and steps are inspired by the stability proof of the Taylor–Hood space pair in [22] and [23]. Nevertheless, since the spaces we use differ and since in our setting matrix fields appear, we write down the important steps in a detailed fashion. We begin with a new auxiliary inf-sup condition which involves boundary conditions. Since $\tilde{S}$ defines a H^1-bounded surjection $H^1_0(\Omega)\otimes\mathbb{E}^{n-2} \to H^1_0(\Omega)\otimes\bar{\mathbb{E}}^{n-1}$, $\bar{\mathbb{E}}^{n-1} \coloneqq \mathbb{R}^{(n|J-1)\times n}$,

with bounded right-inverse $\tilde{T}$ (see Corollary 8.2) one has

$$\begin{aligned}
&\inf_{\eta\in L^2_0(\Omega)\otimes\bar{\mathbb{E}}^n}\ \sup_{\tau\in H^1_0(\Omega)\otimes\mathbb{E}^{n-2}}\ \frac{\langle\nabla\cdot(\tilde{S}\tau),\eta\rangle}{\|\tau\|_{H^1}\ \|\eta\|}\\
&\quad\geq \inf_{\eta\in L^2_0(\Omega)\otimes\bar{\mathbb{E}}^n}\ \sup_{w\in H^1_0(\Omega)\otimes\bar{\mathbb{E}}^{n-1}}\ \frac{\langle\nabla\cdot(\tilde{S}\tilde{T}w),\eta\rangle}{\left\|\tilde{T}w\right\|_{H^1}\ \|\eta\|}\\
&\quad\geq \inf_{\eta\in L^2_0(\Omega)\otimes\bar{\mathbb{E}}^n}\ \sup_{w\in H^1_0(\Omega)\otimes\bar{\mathbb{E}}^{n-1}}\ \frac{\langle\nabla\cdot w,\eta\rangle}{C\,\|w\|_{H^1}\ \|\eta\|} > C_{IS1} > 0,
\end{aligned}$$

where the last inequality sign is clear due to the classical result of Girault and Raviart [43].

Now let $\eta\in\bar{K}_{h,0}\backslash\{0\}$ arbitrary, but fixed. Then we find a $\overline{\tau}\in H^1_0(\Omega)\otimes\mathbb{E}^{n-1}$ s.t.

$$\begin{aligned}
\langle\nabla\cdot(\tilde{S}\overline{\tau}),\eta\rangle &\geq C_{IS1}\,\|\eta\|^2\,,\\
\|\overline{\tau}\|_{H^1} &= \|\eta\|\,.
\end{aligned}\tag{8.3.17}$$

Integration by parts and (8.3.17) lead to

$$\begin{aligned}
\langle\nabla\cdot(\tilde{S}\Pi^R_{h,0}\overline{\tau}),\eta\rangle &= \langle\nabla\cdot(\tilde{S}\overline{\tau}),\eta\rangle + \langle\nabla\cdot(\tilde{S}\Pi^R_{h,0}\overline{\tau}-\tilde{S}\overline{\tau}),\eta\rangle\\
&\geq C_{IS1}\,\|\eta\| + \langle(\tilde{S}\Pi^R_{h,0}\overline{\tau}-\tilde{S}\overline{\tau}),\nabla\eta\rangle.
\end{aligned}\tag{8.3.18}$$

The gradient above acts naturally row-wise and we utilized the projection (8.3.15) which preserves zero boundary conditions. And then we see for the last term in (8.3.18):

$$\begin{aligned}
\langle(\tilde{S}\Pi^R_{h,0}\overline{\tau}-\tilde{S}\overline{\tau}),\nabla\eta\rangle &\leq \sum_{\mathcal{K}\in\mathcal{M}_h}|\langle\tilde{S}\Pi^R_{h,0}\overline{\tau}-\tilde{S}\overline{\tau},\nabla\eta\rangle_{L^2(\mathcal{K})}|\\
&\leq \sum_{\mathcal{K}\in\mathcal{M}_h}\left\|\tilde{S}\Pi^R_{h,0}\overline{\tau}-\tilde{S}\overline{\tau}\right\|_{L^2(\mathcal{K})}\|\nabla\eta\|_{L^2(\mathcal{K})}\\
&\leq C_{\tilde{S}}\sum_{\mathcal{K}\in\mathcal{M}_h}h_{\mathcal{K}}^{-1}\left\|\Pi^R_{h,0}\overline{\tau}-\overline{\tau}\right\|_{L^2(\mathcal{K})}h_{\mathcal{K}}\,\|\nabla\eta\|_{L^2(\mathcal{K})}\\
&\leq C_{\tilde{S}}\Big(\sum_{\mathcal{K}\in\mathcal{M}_h}h_{\mathcal{K}}^{-2}\left\|\Pi^R_{h,0}\overline{\tau}-\overline{\tau}\right\|^2_{L^2(\mathcal{K})}\Big)^{1/2}\Big(\sum_{\mathcal{K}\in\mathcal{M}_h}h_{\mathcal{K}}^2\,\|\nabla\eta\|^2_{L^2(\mathcal{K})}\Big)^{1/2},
\end{aligned}$$

with $\mathcal{M}_h$ being the underlying regular mesh. Again we wrote and will write $h_{\mathcal{K}}$ for the element size of the mesh element $\mathcal{K}$.

In view of the regular mesh assumption, Lemma 8.6 and definition (8.3.15), there is a constant $C_{V1}<\infty$ with

$$\begin{aligned}
\langle(\tilde{S}\Pi^R_{h,0}\overline{\tau}-\tilde{S}\overline{\tau}),\nabla\eta\rangle &\leq C_{V1}\,\|\overline{\tau}\|_{H^1(\Omega)}\Big(\sum_{\mathcal{K}\in\mathcal{M}_h}h_{\mathcal{K}}^2\,\|\nabla\eta\|^2_{L^2(\mathcal{K})}\Big)^{1/2}\\
&\leq C_{V1}\,\|\eta\|\,\|\eta\|_{K,h}\,,
\end{aligned}$$

where $\|\eta\|_{K,h}\coloneqq\Big(\sum_{\mathcal{K}\in\mathcal{M}_h}h_{\mathcal{K}}^2\,\|\nabla\eta\|^2_{L^2(\mathcal{K})}\Big)^{1/2}$.

Remark 8.5. Indeed $\|\cdot\|_{K,h}$ defines a norm on $\bar{K}_{h,0}\subset L^2_0(\Omega)\otimes\bar{\mathbb{E}}^{n-1}$.

The above estimate and (8.3.18) yield directly the inequality

$$\langle\nabla\cdot(\tilde{S}\Pi^R_{h,0}\overline{\tau}),\eta\rangle \geq C_{IS1}\,\|\eta\|^2 - C_{V1}\,\|\eta\|\,\|\eta\|_{K,h}\,.\tag{8.3.19}$$

Consequently, setting $C_c \coloneqq 1 + C_{P1}$ it is $\left\|\Pi^R_{h,0}\overline{\tau}\right\|_{H^1} \leq C_c \left\|\overline{\tau}\right\|_{H^1}$ (see Corollary 8.6) and

$$\begin{aligned}\sup_{\tau\in R_{h,0}} \frac{\langle\nabla\cdot(\tilde{S}\tau),\eta\rangle}{\|\tau\|_{H^1}} &\geq \frac{1}{C_c\left\|\overline{\tau}\right\|_{H^1}}\Big(C_{IS1}\|\eta\|^2 - C_{V1}\|\eta\|\,\|\eta\|_{K,h}\Big)\\ &= \frac{C_{IS1}}{C_c}\|\eta\| - \frac{C_{V1}}{C_c}\|\eta\|_{K,h}\,. \end{aligned} \tag{8.3.20}$$

The last relation holds for all $\eta \in \bar{K}_{h,0}$. Now, consider the inf-sup condition

$$\exists C_{IS} > 0 \text{ s.t. } \forall h > 0 : \inf_{\eta\in\bar{K}_{h,0}} \sup_{\tau\in R_{h,0}} \frac{\langle\nabla\cdot(\tilde{S}\tau),\eta\rangle}{\|\tau\|_{H^1}\|\eta\|} \geq C_{IS}. \tag{8.3.21}$$

The Verfürth trick ([74]) can now be used to reduce latter inf-sup condition (8.3.21) to the new condition

$$\exists C_V > 0 \text{ s.t. } \forall h > 0 : \sup_{\tau\in R_{h,0}} \frac{\langle\nabla\cdot(\tilde{S}\tau),\eta\rangle}{\|\tau\|_{H^1}} \geq C_V\|\eta\|_{K,h}\,, \quad \forall\eta\in\bar{K}_{h,0}. \tag{8.3.22}$$

Namely, using (8.3.22) and (8.3.20) we have for $\eta \in \bar{K}_{h,0}$ the estimate

$$\begin{aligned}\sup_{\tau\in R_{h,0}} \frac{\langle\nabla\cdot(\tilde{S}\tau),\eta\rangle}{\|\tau\|_{H^1}} &\geq \frac{C_{IS1}}{C_c}\|\eta\| - \frac{C_{V1}}{C_c}\|\eta\|_{K,h}\\ &\geq \frac{C_{IS1}}{C_c}\|\eta\| - \frac{C_{V1}}{C_cC_V}\sup_{\tau\in R_{h,0}} \frac{\langle\nabla\cdot(\tilde{S}\tau),\eta\rangle}{\|\tau\|_{H^1}}.\end{aligned}$$

Hence

$$\sup_{\tau\in R_{h,0}} \frac{\langle\nabla\cdot(\tilde{S}\tau),\eta\rangle}{\|\tau\|_{H^1}} \geq C_{IS}\|\eta\|\,, \quad \forall\eta\in\bar{K}_{h,0},$$

with $C_{IS} = \frac{C_{IS1}}{C_c}\left(1+\frac{C_{V1}}{C_cC_V}\right)^{-1} = \frac{C_{IS1}}{C_c}\left(\frac{C_cC_V+C_{V1}}{C_cC_V}\right)^{-1} = \frac{C_{IS1}C_V}{C_cC_V+C_{V1}}$.

Applying the well-known Friedrichs's inequality ([20, §1 in Chapter 2]), $\|\tau\|_{H^1} \leq (1+C_{Fr})|\tau|_{H^1}$, $\forall\tau\in H^1_0(\Omega)\otimes\mathbb{E}^{n-2}$, for a suitable C_{Fr}, we can simplify (8.3.22) to

$$\exists C'_V > 0, \text{ s.t. } \forall h > 0 : \sup_{\tau\in R_{h,0}} \frac{\langle\nabla\cdot(\tilde{S}\tau),\eta\rangle}{|\tau|_{H^1}} \geq C'_V\|\eta\|_{K,h}\,, \quad \forall\eta\in\bar{K}_{h,0}. \tag{8.3.23}$$

Above $|\cdot|_{H^1}$ stands for the standard Sobolev seminorm.

Thus it is justified to consider (8.3.23) instead of (8.3.21).

8.3.5 Macroelement technique

Analogously to [22, 23] we use the macroelement technique to prove the condition (8.3.23); compare [22, Section 3.3]. Therefore we first define the set of macroelement domains $\mathfrak{M}^L_h$ corresponding to the triangulation $\mathcal{M}_h$.

Definition 8.9 (Macroelement domains)**.** *For $L \in \mathbb{N}_{>0}$ the set of macroelement domains $\mathfrak{M}^L_h$ in an n-dimensional mesh $\mathcal{M}_h$ is defined as follows: If $L = 1$ we have*

$$\mathfrak{M}^1_h \coloneqq \Big\{\mathfrak{m}^1_{\mathcal{K}} \;\Big|\; \mathcal{K}\in\mathcal{M}_h,\ \#\{U\in\mathcal{M}_h\ |U\subset\mathfrak{m}^1_{\mathcal{K}}\} = 3^n\Big\}, \quad \text{where for} \quad \mathcal{K}\in\mathcal{M}_h \quad \text{it is}$$
$$\mathfrak{m}^1_{\mathcal{K}} \coloneqq \bigcup_{U\in\mathcal{M}_h,\ \overline{U}\cap\overline{\mathcal{K}}\neq\emptyset} \overline{U}.$$

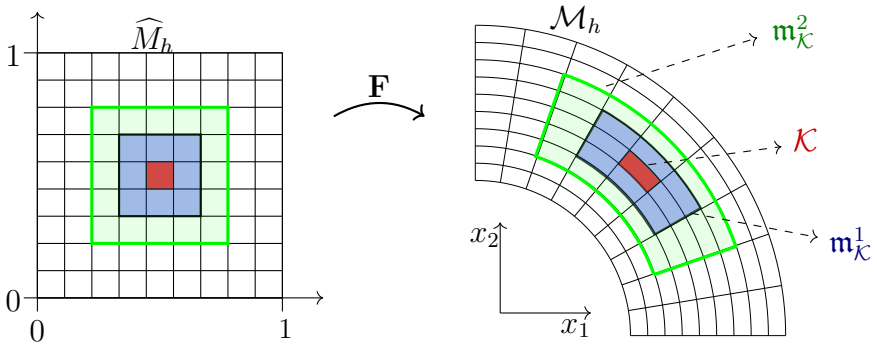

Figure 18: Illustration of the macroelements $\mathfrak{m}^1_{\mathcal{K}}$ and $\mathfrak{m}^2_{\mathcal{K}}$ for the red highlighted mesh element $\mathcal{K} \in \mathcal{M}_h$. For decreasing h the macroelement shapes can be approximated by affine transformed squares. This observation together with the possibility of a covering of Ω by use of the macroelements yields the basic idea for the reduction of a global inf-sup condition to a localized version.

And recursively, for $L > 1$

$$\mathfrak{M}_h^L := \left\{ \mathfrak{m}_{\mathcal{K}}^L \;\middle|\; \mathcal{K} \in \mathcal{M}_h,\ \#\{U \in \mathcal{M}_h \mid U \subset \mathfrak{m}_{\mathcal{K}}^L\} = (2L+1)^n \right\}, \quad \text{where for} \quad \mathcal{K} \in \mathcal{M}_h \quad \text{it is}$$
$$\mathfrak{m}_{\mathcal{K}}^L := \bigcup_{U \in \mathcal{M}_h,\ \overline{U} \cap \overline{\mathfrak{m}_{\mathcal{K}}^{L-1}} \neq \emptyset} \overline{U}.$$

We write $\#Q$ for the cardinality of a set Q.

The $\mathfrak{M}_h^L$ satisfy three obvious but important properties:

- $\forall \mathcal{M}_h,\ \forall \mathcal{K} \in \mathcal{M}_h,\ \exists \mathfrak{m} \in \mathfrak{M}_h^L$ s.t. $\mathcal{K} \subset \mathfrak{m}$.
- $\forall \mathcal{M}_h,\ \forall \mathcal{K} \in \mathcal{M}_h$, there are at most $C_{\text{overlap}} = (2L+1)^n$ many macroelement domains $\mathfrak{m}$ in $\mathfrak{M}_h^L$ s.t. $\mathcal{K} \subset \mathfrak{m}$.
- $\forall \mathcal{M}_h,\ \forall \mathfrak{m} \in \mathfrak{M}_h^L$, there are $C_{\text{elem}} = (2L+1)^n$ different mesh elements in $\mathfrak{m}$.

To see the last properties one notes the tensor-product structure of the parametric meshes in the context of IGA.
An illustration of macroelements as collection of mesh elements is sketched in Figure 18 for $n = 2$. Basic idea of the technique of macroelements is to reduce the global inf-sup condition (8.3.23) to a local alternative on the macroelements. Due to this localization step and a regular mesh assumption one can then prove the new condition more easily by means of considerations on the simple parametric spline spaces and parametric meshes. In the following we assume L to be a fixed natural number and thus drop the index L. Later, we will clarify what L actually is.

Macroelement domains can be defined analogously in the parametric domain and in this case we use the notation $\widehat{\mathfrak{M}}_h$ as well as $\hat{\mathfrak{m}}_K,\ K \in \widehat{M}_h$ for the parametric pendants. For each $\mathfrak{m} \in \mathfrak{M}_h$ we can define the spaces

$$\mathcal{V}_{\mathfrak{m}} := \left\{ \tau_{|\mathfrak{m}} \;\middle|\; \tau \in R_{h,0},\ \operatorname{supp}(\tau) \subseteq \mathfrak{m} \right\}, \tag{8.3.24}$$

$$\mathcal{P}_{\mathfrak{m}} := \left\{ v_{|\mathfrak{m}} \;\middle|\; v \in \bar{K}_h,\ \int_{\mathfrak{m}} v \, dx = 0 \right\} \tag{8.3.25}$$

and interpret mappings in $\mathcal{V}_\mathfrak{m}$ as mappings on Ω through a straight-forward zero extension.[16] We equip $\mathcal{P}_\mathfrak{m}$ with the norm

$$\|\eta\|_{\mathcal{P}_\mathfrak{m}} \coloneqq \left(\sum_{\mathcal{K}\in\mathcal{M}_h,\ \mathcal{K}\subset\mathfrak{m}} h_\mathcal{K}^2 \|\nabla\eta\|_{L^2(\mathcal{K})}^2 \right)^{1/2}$$

and note that

$$\Pi_{\mathcal{P}_\mathfrak{m}}\eta \coloneqq \eta_{|\mathfrak{m}} - \frac{1}{|\mathfrak{m}|}\int_\mathfrak{m} \eta\, dx$$

defines a projection from $\bar{K}_h$ onto $\mathcal{P}_\mathfrak{m}$. The integral is meant in a component-wise manner.

As already mentioned, the idea of the macroelement technique is to reduce the global inf-sup condition (8.3.23) to a local version on macroelements. To be more precise, assume that

$$\exists C_{\text{macro}} > 0, \quad \text{s.t.} \quad \forall h,\ \forall \mathfrak{m}\in\mathfrak{M}_h: \quad \inf_{\eta\in\mathcal{P}_\mathfrak{m}} \sup_{\tau\in\mathcal{V}_\mathfrak{m}} \frac{\langle \tilde{S}\tau, \nabla\eta\rangle}{|\tau|_{H^1}\,\|\eta\|_{\mathcal{P}_\mathfrak{m}}} \geq C_{\text{macro}}. \tag{8.3.26}$$

Then this inf-sup stability on the macroelements leads to stability in the sense of (8.3.23); cf. [22, Section 3.3]. This can be seen as follows. Let $\eta \in \bar{K}_{h,0}$ arbitrary, but fixed. Further let $\tau_\mathfrak{m} \in \mathcal{V}_\mathfrak{m}$ chosen such that

$$\begin{aligned}\langle \tilde{S}\tau_\mathfrak{m}, \nabla\Pi_{\mathcal{P}_\mathfrak{m}}\eta\rangle &\geq C_{\text{macro}}\,\|\Pi_{\mathcal{P}_\mathfrak{m}}\eta\|_{\mathcal{P}_\mathfrak{m}}^2\\ |\tau_\mathfrak{m}|_{H^1(\Omega)} &= \|\Pi_{\mathcal{P}_\mathfrak{m}}\eta\|_{\mathcal{P}_\mathfrak{m}}.\end{aligned}$$

On the one hand, one obtains

$$\begin{aligned}\sup_{\tau\in R_{h,0}} \langle \tilde{S}\tau, \nabla\eta\rangle &\geq \langle \sum_{\mathfrak{m}\in\mathfrak{M}_h} \tilde{S}\tau_\mathfrak{m}, \nabla\eta\rangle = \sum_{\mathfrak{m}\in\mathfrak{M}_h} \langle \tilde{S}\tau_\mathfrak{m}, \nabla\eta\rangle\\ &\geq \sum_{\mathfrak{m}\in\mathfrak{M}_h} C_{\text{macro}}\,\|\Pi_{\mathcal{P}_\mathfrak{m}}\eta\|_{\mathcal{P}_\mathfrak{m}}^2\\ &= \sum_{\mathfrak{m}\in\mathfrak{M}_h} C_{\text{macro}}\Big(\sum_{\mathcal{K}\subset\mathfrak{m}} h_\mathcal{K}^2\,\|\nabla\Pi_{\mathcal{P}_\mathfrak{m}}\eta\|_{L^2(\mathcal{K})}^2 \Big)\\ &\geq C_{\text{macro}} \sum_{\mathcal{K}\in\mathcal{M}_h} \Big(h_\mathcal{K}^2\,\|\nabla\eta\|_{L^2(\mathcal{K})}^2 \Big)\\ &= C_{\text{macro}}\,\|\eta\|_{K,h}^2.\end{aligned}$$

On the other hand, one can estimate

$$\begin{aligned}|\sum_{\mathfrak{m}\in\mathfrak{M}_h} \tau_\mathfrak{m}|_{H^1(\Omega)}^2 &= \sum_{\mathcal{K}\in\mathcal{M}_h} |\sum_{\mathfrak{m}\in\mathfrak{M}_h} \tau_\mathfrak{m}|_{H^1(\mathcal{K})}^2\\ &\leq \sum_{\mathcal{K}\in\mathcal{M}_h} \Big(\sum_{\substack{\mathfrak{m}\in\mathfrak{M}_h\\ \mathcal{K}\subset\mathfrak{m}}} |\tau_\mathfrak{m}|_{H^1(\mathcal{K})} \Big)^2\\ &\leq C_{\text{overlap}} \sum_{\mathcal{K}\in\mathcal{M}_h} \sum_{\substack{\mathfrak{m}\in\mathfrak{M}_h\\ \mathcal{K}\subset\mathfrak{m}}} |\tau_\mathfrak{m}|_{H^1(\mathcal{K})}^2\\ &\leq C_{\text{overlap}} \sum_{\mathfrak{m}\in\mathfrak{M}_h} |\tau_\mathfrak{m}|_{H^1(\Omega)}^2\\ &\leq C_{\text{overlap}} \sum_{\mathfrak{m}\in\mathfrak{M}_h} \|\Pi_{\mathcal{P}_\mathfrak{m}}\eta\|_{\mathcal{P}_\mathfrak{m}}^2\\ &\leq C_{\text{overlap}} \sum_{\mathfrak{m}\in\mathfrak{M}_h} \sum_{\mathcal{K}\subset\mathfrak{m}} h_\mathcal{K}^2\,\|\nabla\eta\|_{L^2(\mathcal{K})}^2\\ &\leq C_{\text{overlap}}^2\,\|\eta\|_{K,h}^2.\end{aligned}$$

[16] $\cdot_{|\mathfrak{m}}$ denotes the restriction to $\mathfrak{m}\subset\Omega$.

Then, it is easy to see that the both inequality chains from above lead to the wanted result (8.3.23). One can set $C_V^{'} = C_{\text{macro}} C_{\text{overlap}}^{-1}$.

Thus, to show the inf-sup stability (8.3.21) it remains to prove (8.3.26).

8.3.6 Proof of the auxiliary inf-sup condition

As mentioned, we face now the inf-sup stability in the sense (8.3.26). For this purpose, we apply a result from [23], where the inf-sup stability of a similar space pair is proven.

Lemma 8.2. *Assume $p-1 > r \geq 0$. Then there is a constant $C_{\text{macro}} > 0$ and a mesh size $h_{\max} > 0$ s.t. for all $\mathcal{M}_h$ and $\forall \mathfrak{m} \in \mathfrak{M}_h$ it holds*

$$\inf_{q \in P_{\mathfrak{m}}} \sup_{v \in V_{\mathfrak{m}}} \frac{\langle v, \nabla q \rangle}{|v|_{H^1} \, \|q\|_{P_{\mathfrak{m}}}} \geq C_{\text{macro}}, \quad \text{if } h \leq h_{\max}, \tag{8.3.27}$$

where

$$V_{\mathfrak{m}} \coloneqq \Big\{ v_{|\mathfrak{m}} \;\Big|\; v \in \left(S^{r,\dots,r}_{p,\dots,p} \circ \mathbf{F}^{-1} \right) \otimes \mathbb{R}^n, \; \operatorname{supp}(v) \subseteq \mathfrak{m}, \; v \in H^1_0(\mathfrak{m}) \Big\}, \tag{8.3.28}$$

$$P_{\mathfrak{m}} \coloneqq \left\{ \eta_{|\mathfrak{m}} \;\middle|\; \eta \in \left(S^{r,\dots,r}_{p-1,\dots,p-1} \circ \mathbf{F}^{-1} \right), \; \int_{\mathfrak{m}} \eta \, dx = 0 \right\} \tag{8.3.29}$$

and $\|\eta\|_{P_{\mathfrak{m}}}$ is analogously defined like $\|\eta\|_{\mathcal{P}_{\mathfrak{m}}}$, i.e. $\|q\|_{P_{\mathfrak{m}}} \coloneqq \left(\sum_{K \subset \mathfrak{m}} h_K^2 \, \|\nabla q\|^2_{L^2(K)} \right)^{1/2}$.

Proof. Since we only consider spline basis functions this follows by Section 4.3 and Theorem 4.1 in [23] with NURBS weight function $\omega = 1$. The mentioned reference shows that the macroelements with $L = p - 1$ are suitable. □

Remark 8.6. Our definition of macroelements depends on L. However, the results in [23, Theorem 4.1] imply that the choice $L = p - 1$ leads to the inf-sup inequality of the last lemma. That is why we assume $\mathfrak{M}_h = \mathfrak{M}_h^{p-1}$ in the rest of the section.

A row-wise application of the last lemma yields the existence of a constant $C_{\text{macro}}^{'} > 0$ s.t. for all macroelements $\mathfrak{m} \in \mathfrak{M}_h$ and $\eta \in \mathcal{P}_{\mathfrak{m}}$ we find a

$$\tau_{\mathfrak{m}} \in \Big\{ \tau \in (S^{r,\dots,r}_{p,\dots,p} \circ \mathbf{F}^{-1}) \otimes \bar{\mathbb{E}}^{n-1} \;\Big|\; \operatorname{supp}(\tau) \subseteq \mathfrak{m} \Big\}$$

with

$$\langle \tau_{\mathfrak{m}}, \nabla \eta \rangle \geq C_{\text{macro}}^{'} |\tau_{\mathfrak{m}}|_{H^1(\mathfrak{m})} \, \|\eta\|_{\mathcal{P}_{\mathfrak{m}}}, \tag{8.3.30}$$

if $h \leq h_{\max}$. One notes that $C_{\text{macro}}^{'}$ is independent from h, η and the macroelement. Next we choose for each macroelement one $x_{\mathfrak{m}} \in \mathfrak{m}$, e.g. the push-forward of the center in the corresponding parametric macroelement $\widehat{\mathfrak{m}}$, meaning $\mathbf{F}(\widehat{\mathfrak{m}}) = \mathfrak{m}$. Then define $\bar{\mathbf{M}}_{x_{\mathfrak{m}}} \coloneqq \bar{\mathbf{M}}(x_{\mathfrak{m}})$ and set

$$\tilde{\tau}_{\mathfrak{m}} \coloneqq \Big[\tilde{T}(\tau_{\mathfrak{m}}) \Big] \bar{\mathbf{M}}_{x_{\mathfrak{m}}} \bar{\mathbf{M}}^{-1} \in \mathcal{V}_{\mathfrak{m}},$$

with $\bar{\mathbf{M}} \colon \Omega \to \mathbb{R}^{(n|2) \times (n|2)}$ denoting the C^1-regular matrix field implied by the pullback operation; see the second point in Corollary 8.3. In particular $\bar{\mathbf{M}}^{-1}$ above means that we consider pointwise the inverses of the matrices $\bar{\mathbf{M}}(\cdot)$.

Indeed, using Corollary 8.2, we have $\overline{\tau}_{\mathfrak{m}} \coloneqq \Big[\tilde{T}(\tau_{\mathfrak{m}}) \Big] \bar{\mathbf{M}}_{x_{\mathfrak{m}}} \in (S^{r,\dots,r}_{p,\dots,p} \circ \mathbf{F}^{-1}) \otimes \mathbb{E}^{n-2}$ and thus

by Corollary 8.3 $\overline{\tau}_{\mathfrak{m}}\bar{\mathbf{M}}^{-1} \in R_h$. One observes that (8.3.28) implies also $\overline{\tau}_{\mathfrak{m}}\bar{\mathbf{M}}^{-1} \in R_{h,0}$ and $\mathrm{supp}(\overline{\tau}_{\mathfrak{m}}\bar{\mathbf{M}}^{-1}) \subseteq \mathfrak{m}$.
Then, one gets

$$\begin{aligned}\langle \tilde{S}\tilde{\tau}_{\mathfrak{m}}, \nabla\eta\rangle &= \Big\langle \tilde{S}\Big[\overline{\tau}_{\mathfrak{m}}\bar{\mathbf{M}}_{x_{\mathfrak{m}}}^{-1}\Big], \nabla\eta\Big\rangle + \Big\langle \tilde{S}\Big[\overline{\tau}_{\mathfrak{m}}\Big(\bar{\mathbf{M}}^{-1} - \bar{\mathbf{M}}_{x_{\mathfrak{m}}}^{-1}\Big)\Big], \nabla\eta\Big\rangle \\ &= \Big\langle \tau_{\mathfrak{m}}, \nabla\eta\Big\rangle + \Big\langle \tilde{S}\Big[\overline{\tau}_{\mathfrak{m}}\Big(\bar{\mathbf{M}}^{-1} - \bar{\mathbf{M}}_{x_{\mathfrak{m}}}^{-1}\Big)\Big], \nabla\eta\Big\rangle. \end{aligned} \tag{8.3.31}$$

The second term in line (8.3.31) can be estimated as follows.

Introduce the auxiliary matrix field $\tilde{\mathbf{M}} \coloneqq \bar{\mathbf{M}}_{x_{\mathfrak{m}}}\Big(\bar{\mathbf{M}}^{-1} - \bar{\mathbf{M}}_{x_{\mathfrak{m}}}^{-1}\Big)$. We set $\sigma_{\mathfrak{m}} \coloneqq \tilde{S}\Big[[\tilde{T}(\tau_{\mathfrak{m}})]\tilde{\mathbf{M}}\Big]$ and by the transformation rule for integrals

$$\langle \sigma_{\mathfrak{m}}, \nabla\eta\rangle_{L^2(\mathfrak{m})} = \langle \widehat{\sigma}_{\mathfrak{m}}|\det(\mathbf{J})|, (\widehat{\nabla}\widehat{\eta})\mathbf{J}^{-1}\rangle_{L^2(\widehat{\mathfrak{m}})},$$

where $\widehat{\sigma}_{\mathfrak{m}} \coloneqq \sigma_{\mathfrak{m}} \circ \mathbf{F}$, $\widehat{\eta} = \eta \circ \mathbf{F}$ and $\mathbf{J}$ denotes the Jacobian of the parametrizaton $\mathbf{F}$. We use the hat notation "$\widehat{\cdot}$" to indicate differentiation w.r.t. the parametric coordinates. With $\widehat{\tau}_{\mathfrak{m}} = \tau_{\mathfrak{m}} \circ \mathbf{F}$ we can find bounded and Lipschitz continuous coefficient functions $c_{ij}^{kl} = c_{ij}^{kl}(\tilde{\mathbf{M}}, \det(\mathbf{J}), \mathbf{J}^{-1}, \tilde{S}, \tilde{T})$ s.t.

$$\begin{aligned}\langle \sigma_{\mathfrak{m}}, \nabla\eta\rangle_{L^2(\mathfrak{m})} &= \int_{\widehat{\mathfrak{m}}} (\widehat{\tau}_{\mathfrak{m}})_{kl}\; c_{ij}^{kl}\; \hat{\partial}_j\widehat{\eta}_i \, d\hat{x} \\ &\le C \left\|c_{ij}^{kl}\right\|_{L^\infty(\widehat{\mathfrak{m}})} \|\widehat{\tau}_{\mathfrak{m}}\|_{L^2(\widehat{\mathfrak{m}})} \left\|\widehat{\nabla}\widehat{\eta}\right\|_{L^2(\widehat{\mathfrak{m}})} \qquad (\text{here } \|v\|_{L^\infty(U)} \coloneqq \sup_{x\in U}|v(x)|\ ) \\ &\le C\tilde{C} \left\|c_{ij}^{kl}\right\|_{L^\infty(\widehat{\mathfrak{m}})} h|\widehat{\tau}_{\mathfrak{m}}|_{H^1(\widehat{\mathfrak{m}})} \left\|\widehat{\nabla}\widehat{\eta}\right\|_{L^2(\widehat{\mathfrak{m}})} \\ &\le \bar{C} \left\|c_{ij}^{kl}\right\|_{L^\infty(\widehat{\mathfrak{m}})} |\widehat{\tau}_{\mathfrak{m}}|_{H^1(\widehat{\mathfrak{m}})} \Big(\sum_{K\subset\widehat{\mathfrak{m}}} h \left\|\widehat{\nabla}\widehat{\eta}\right\|_{L^2(K)} \Big) \\ &\le \bar{C}\sqrt{C_{\mathrm{elem}}} \left\|c_{ij}^{kl}\right\|_{L^\infty(\widehat{\mathfrak{m}})} |\widehat{\tau}_{\mathfrak{m}}|_{H^1(\widehat{\mathfrak{m}})} \Big(\sum_{K\subset\widehat{\mathfrak{m}}} h^2 \left\|\widehat{\nabla}\widehat{\eta}\right\|_{L^2(K)}^2 \Big)^{1/2}, \end{aligned} \tag{8.3.32}$$

where we drop the sum symbol $\sum_{i,j,k,l}$ for better readability. To obtain the second inequality sign above we use the estimate for the Friedrichs's constant $C_{Fr}(D)$ of rectangular domains D:

$$C_{Fr}(D) \le \mathrm{diam}(D) \quad\Rightarrow\quad C_{Fr}(\widehat{\mathfrak{m}}) \le \tilde{C}h, \text{ for a proper } \tilde{C}, \quad \text{see [20, §1, Chapter 2].}$$

Analogously to [22], one introduces the auxiliary mapping $\widehat{\eta}_a \coloneqq \widehat{\eta} - \frac{1}{|\widehat{\mathfrak{m}}|}\int_{\widehat{\mathfrak{m}}} \widehat{\eta}\, d\hat{x}$. Obviously, we have $\widehat{\nabla}\widehat{\eta} = \widehat{\nabla}\widehat{\eta}_a$. Besides, with the norm equivalence statement in line (3.37) of [22] we obtain for some constant C_{H^1} independent of the mesh size

$$|\widehat{\tau}_{\mathfrak{m}}|_{H^1(\widehat{\mathfrak{m}})} \le C_{H^1}|\tau_{\mathfrak{m}}|_{H^1(\mathfrak{m})}. \tag{8.3.33}$$

Further, by the assumed C^2-smoothness of $\mathbf{F}$ and $\mathbf{F}^{-1}$, there is for each $\varepsilon > 0$ a mesh size $h_\varepsilon > 0$ s.t. for all $h \le h_\varepsilon$ we get

$$|\tilde{\mathbf{M}}| = \Big|\bar{\mathbf{M}}_{x_{\mathfrak{m}}}\Big(\bar{\mathbf{M}}^{-1}(\hat{x}) - \bar{\mathbf{M}}_{x_{\mathfrak{m}}}^{-1}\Big)\Big| < \varepsilon, \quad \forall\mathfrak{m} \in \mathfrak{M}_h, \forall\hat{x} \in \widehat{\mathfrak{m}}.$$

Hence, since $\sigma_{\mathfrak{m}} = \tilde{S}\Big[[\tilde{T}(\tau_{\mathfrak{m}})]\tilde{\mathbf{M}}\Big]$, there is a constant $C_{\mathrm{para}} < \infty$ which is independent of h and the macroelement such that

$$|c_{ij}^{kl}| < C_{\mathrm{para}}\varepsilon \;\text{ on } \widehat{\mathfrak{m}}, \tag{8.3.34}$$

for $h \le h_\epsilon$ small enough. Combining (8.3.33) and (8.3.34) we find a constant $C'_{\mathrm{para}} < \infty$ with

$$|\langle \sigma_{\mathfrak{m}}, \nabla\eta\rangle_{L^2(\mathfrak{m})}| \le C'_{\mathrm{para}}\varepsilon|\tau_{\mathfrak{m}}|_{H^1(\mathfrak{m})} \Big(\sum_{K\subset\widehat{\mathfrak{m}}} h^2 \left\|\widehat{\nabla}\widehat{\eta}_a\right\|_{L^2(K)}^2 \Big)^{1/2}. \tag{8.3.35}$$

Applying the inequality chain (3.47) in [22] we obtain a constant C_{est} s.t.

$$\left(\sum_{K \subset \widehat{\mathfrak{m}}} h^2 \left\| \widehat{\nabla} \widehat{\eta}_a \right\|^2_{L^2(K)} \right)^{1/2} \leq C_{\text{est}} \left\| \eta \right\|_{\mathcal{P}_{\mathfrak{m}}} . \tag{8.3.36}$$

In view of (8.3.35) and (8.3.36) it is

$$\langle \tilde{S} \tilde{\tau}_{\mathfrak{m}}, \nabla \eta \rangle \geq C'_{\text{macro}} |\tau_{\mathfrak{m}}|_{H^1(\mathfrak{m})} \left\| \eta \right\|_{\mathcal{P}_{\mathfrak{m}}} - C'_{\text{para}} \varepsilon C_{\text{est}} |\tau_{\mathfrak{m}}|_{H^1(\mathfrak{m})} \left\| \eta \right\|_{\mathcal{P}_{\mathfrak{m}}} . \tag{8.3.37}$$

Hence, if we choose $h \leq h_{\max}$ for some suitable $h_{\max} > 0$ we get $C''_{\text{macro}} = C'_{\text{macro}} - C'_{\text{para}} \varepsilon C_{\text{est}} > 0$. And since $\bar{\mathbf{M}}^{-1}$ is piece-wise smooth and Lipschitz continuous by assumption, we obtain for some $C_{\text{est},1}, C_{\text{est},2}$ and with the Friedrichs's inequality:

$$\begin{aligned} |\tilde{\tau}_{\mathfrak{m}}|_{H^1(\mathfrak{m})} &= \left| \left[\tilde{T}(\tau_{\mathfrak{m}}) \right] \bar{\mathbf{M}}_{x_{\mathfrak{m}}} \bar{\mathbf{M}}^{-1} \right|_{H^1(\mathfrak{m})} \leq C_{\text{est},2} \left\| \tau_{\mathfrak{m}} \right\|_{H^1(\mathfrak{m})} \\ &\leq C_{\text{est},2} (1 + C_{Fr}(\Omega)) |\tau_{\mathfrak{m}}|_{H^1(\mathfrak{m})}. \end{aligned}$$

One notes $\mathfrak{m} \subset \Omega$, i.e. the Friedrichs's constant can be chosen independently from $\mathfrak{m}$. With the last estimate and (8.3.37) we can conclude now

$$\langle \tilde{S} \tilde{\tau}_{\mathfrak{m}}, \nabla \eta \rangle \geq C''_{\text{macro}} |\tau_{\mathfrak{m}}|_{H^1(\mathfrak{m})} \left\| \eta \right\|_{\mathcal{P}_{\mathfrak{m}}} \geq \frac{C''_{\text{macro}}}{C_{\text{est},2}(1 + C_{Fr}(\Omega))} |\tilde{\tau}_{\mathfrak{m}}|_{H^1(\mathfrak{m})} \left\| \eta \right\|_{\mathcal{P}_{\mathfrak{m}}} . \tag{8.3.38}$$

In other words with $C_{\text{macro}} = \frac{C''_{\text{macro}}}{C_{\text{est},2}(1+C_{Fr}(\Omega))} > 0$ and for $h \leq h_{\max}$ we have shown the property (8.3.26).

8.3.7 Inf-sup condition for spaces without boundary conditions

From the last section together with the Verfürth trick we get the validity of (8.3.21) if $h \leq h_{\max}$. However, there we assumed special boundary conditions and the property of vanishing mean value for the variable η. Thus, we want to prove the next lemma.

Lemma 8.3. *There is a mesh size $h_{\max} > 0$ and a constant $C'_{IS} > 0$ s.t.*

$$\forall 0 < h \leq h_{\max} : \inf_{\eta \in K_h} \sup_{\tau \in R_h \cap (H^1(\Omega) \otimes \mathbb{E}^{n-2})} \frac{\langle \nabla \cdot (\tilde{S}\tau), \eta \rangle}{\left\| \tau \right\|_{H^1} \left\| \eta \right\|} \geq C'_{IS}. \tag{8.3.39}$$

Before proving this lemma we first look at a useful auxiliary result.

Lemma 8.4. *It exists a $\tilde{h} > 0$ such that $\forall h \leq \tilde{h}$, we find $M_h^i \in R_h \cap \left(H^1(\Omega) \otimes \mathbb{E}^{n-2} \right)$, $i = 1, \ldots, (n|J-1)$, with*

$$\begin{aligned} \left\| M_h^i \right\|_{H^1} &\leq C_i < \infty, \\ \left\| \nabla \cdot (\tilde{S} M_h^i) - \mathbf{e}_i \right\| &\leq \min \left\{ \frac{C_{IS}}{2\sqrt{C_\Omega}}, \frac{1}{2\sqrt{C_\Omega}(n|J-1)+1} \right\} =: C_{L,1}, \quad \forall i, \quad C_\Omega := 1/|\Omega|. \end{aligned}$$

Above the C_i are independent of h and $\mathbf{e}_i$ denote the canonical basis vectors in $\mathbb{R}^{n|J-1}$.

Proof. In this proof we write $\Pi_h = \Pi_{h,n}^{n-2} \otimes \mathbb{R}^{n|J-1}$, i.e. we have a row-wise application of $\Pi_{h,n}^{n-2}$, where here $\Pi_{h,n}^{n-2} = \Pi_{h,n}^{n-2}(p+1, r+1)$ denotes the projection from (7.3.2) onto the space $V_{h,n}^{n-2}(p+1, r+1)$ with degree $p+1$ and regularity $r+1$. In particular it holds

$$\Pi_h \tau \in R_h \cap \left(H^1(\Omega) \otimes \mathbb{E}^{n-2}\right), \quad \forall \tau \in H^1(\Omega) \otimes \mathbb{E}^{n-2}.$$

Let us define the smooth mappings

$$X_i \colon \Omega \to \mathbb{E}^{n-2} \ , \ x \mapsto X_i(x) = X_i(x_1, \dots, x_n) = x_1 \begin{bmatrix} & 0 & \dots & 0 \\ \mathbf{e}_i & \vdots & 0 & \vdots \\ & 0 & \dots & 0 \end{bmatrix},$$

meaning the first column of the matrix is the i-th basis vector.
Next we introduce the matrices $M_h^i \coloneqq \Pi_h \left[\tilde{T} X_i\right] \in R_h$, where $\tilde{T}$ is the right-inverse of $\tilde{S}$; see Corollary 8.2. Exploiting the approximation properties of the splines, cf. [27, Theorem 5.3 and Remark 5.1], one obtains

$$\begin{aligned} \left\| \nabla \cdot (\tilde{S} M_h^i) - \mathbf{e}_i \right\| &\leq \left\| \tilde{S} M_h^i - \tilde{S} \tilde{T} X_i \right\|_{H^1} \leq C_{\tilde{S}} \left\| M_h^i - \tilde{T} X_i \right\|_{H^1} \\ &\leq C_{\tilde{S}} \left\| \Pi_h \tilde{T} X_i - \tilde{T} X_i \right\|_{H^1} \\ &\leq C_{\tilde{S}} C_R h \left\| \tilde{T} X_i \right\|_{H^2} = C_{\tilde{S}} C_R h \left\| \tilde{T} X_i \right\|_{H^1}, \end{aligned} \tag{8.3.40}$$

for proper constants C_R, $C_{\tilde{S}}$. And by the continuity of the projection operators it is

$$\left\| M_h^i \right\|_{H^1} = \left\| \Pi_h \tilde{T} X_i \right\|_{H^1} \leq \tilde{C}_R \left\| \tilde{T} X_i \right\|_{H^1} =: C_i, \tag{8.3.41}$$

for constants $\tilde{C}_R$, C_i independent of the underlying mesh size h. Hence, combining the estimates (8.3.40) and (8.3.41) finishes the proof. □

Proof of Lemma 8.3. Let $\eta \in K_h$ arbitrary, but fixed. Further we write $\tilde{\eta} \coloneqq \eta - \bar{\eta}$, where

$$\bar{\eta} = (\bar{\eta}_i)_i \quad \text{with} \quad \bar{\eta}_i \coloneqq \frac{1}{|\Omega|} \int_\Omega \eta_i dx = \text{const.}$$

Then we define

$$\overline{M}_h^i \coloneqq \bar{\eta}_i \, M_h^i,$$

with the M_h^i from Lemma 8.4. By the previous section we know that there is a $\tilde{\tau} \in R_h \cap \left(H_0^1(\Omega) \otimes \mathbb{E}^{n-2}\right)$ with

$$\begin{aligned} \langle \nabla \cdot (\tilde{S} \tilde{\tau}), \tilde{\eta} \rangle &\geq C_{IS} \left\| \tilde{\eta} \right\|^2, \\ \left\| \tilde{\tau} \right\|_{H^1} &= \left\| \tilde{\eta} \right\|. \end{aligned}$$

Set

$$\tau \coloneqq \tilde{\tau} + \sum_i \overline{M}_h^i,$$

where here and in the remaining part of the proof all the indices run from 1 to $(n|J-1)$. This means

$$\begin{aligned} \langle \nabla \cdot (\tilde{S} \tau), \eta \rangle = \langle \nabla \cdot (\tilde{S} \tilde{\tau}), \tilde{\eta} \rangle + \underbrace{\sum_i \langle \nabla \cdot (\tilde{S} \overline{M}_h^i), \tilde{\eta} \rangle}_{=:(\star,1)} \\ + \underbrace{\langle \nabla \cdot (\tilde{S} \tilde{\tau}), \bar{\eta} \rangle}_{=:(\star,2)} + \underbrace{\textstyle\sum_i \langle \nabla \cdot (\tilde{S} \overline{M}_h^i), \bar{\eta} \rangle}_{=:(\star,3)}. \end{aligned}$$

Set $N \coloneqq (n|J-1)$. Using Lemma 8.4 the three last terms can be estimated as follows:

$$\begin{aligned}
|(\star,1)| \le \sum_i |\langle \nabla\cdot(\tilde{S}\overline{M}_h^i),\tilde{\eta}\rangle| &\le \sum_i |\langle \nabla\cdot(\tilde{S}\overline{M}_h^i)-\bar{\eta}_i\mathbf{e}_i,\tilde{\eta}\rangle| + |\langle \bar{\eta}_i\mathbf{e}_i,\tilde{\eta}\rangle| \\
&\le \sum_i |\bar{\eta}_i||\langle \nabla\cdot(\tilde{S}M_h^i)-\mathbf{e}_i,\tilde{\eta}\rangle| + 0 \\
&\le \sum_i C_{L,1}|\bar{\eta}_i|\,\|\tilde{\eta}\| \\
&= \sum_i C_{L,1}\sqrt{C_\Omega}\,\|\bar{\eta}_i\|\,\|\tilde{\eta}\| \\
&\le \sqrt{N}C_{L,1}\sqrt{C_\Omega}\,\|\bar{\eta}\|\,\|\tilde{\eta}\| \\
&\le \frac{\sqrt{N}}{2}C_{L,1}\sqrt{C_\Omega}\Big(\|\bar{\eta}\|^2+\|\tilde{\eta}\|^2\Big).
\end{aligned}$$

$$(\star,2) = \langle \tilde{S}\tilde{\tau},\nabla\bar{\eta}\rangle = 0.$$

$$\begin{aligned}
(\star,3) = \sum_i \langle \nabla\cdot(\tilde{S}\overline{M}_h^i),\bar{\eta}\rangle &= \sum_{i,j}\langle \nabla\cdot(\tilde{S}\overline{M}_h^i),\bar{\eta}_j\mathbf{e}_j\rangle \\
&= \sum_{i,j}\langle \nabla\cdot(\tilde{S}\overline{M}_h^i)-\bar{\eta}_i\mathbf{e}_i,\bar{\eta}_j\mathbf{e}_j\rangle + \sum_{i,j}\langle \bar{\eta}_i\mathbf{e}_i,\bar{\eta}_j\mathbf{e}_j\rangle \\
&\ge \sum_i \|\bar{\eta}_i\|^2 - \sum_{i,j}\sqrt{C_\Omega}C_{L,1}\ \|\bar{\eta}_i\|\,\|\bar{\eta}_j\| \\
&\ge \sum_i \|\bar{\eta}_i\|^2 - N\sqrt{C_\Omega}C_{L,1}\ \|\bar{\eta}_i\|^2 \\
&\ge (1-N\sqrt{C_\Omega}C_{L,1})\,\|\bar{\eta}\|^2.
\end{aligned}$$

Consequently, on the one hand we have

$$\begin{aligned}
\langle \nabla\cdot(\tilde{S}\tau),\eta\rangle &\ge C_{IS}\,\|\tilde{\eta}\|^2 + (1-N\sqrt{C_\Omega}C_{L,1})\,\|\bar{\eta}\|^2 - C_{L,1}\sqrt{C_\Omega}\Big(\|\bar{\eta}\|^2+\|\tilde{\eta}\|^2\Big) \\
&= \Big(C_{IS}-C_{L,1}\sqrt{C_\Omega}\Big)\,\|\tilde{\eta}\|^2 + \Big(1-(N+1)C_{L,1}\sqrt{C_\Omega}\Big)\,\|\bar{\eta}\|^2 \\
&\ge C_{IS,2}(\|\tilde{\eta}\|+\|\bar{\eta}\|)^2, \qquad (8.3.42)
\end{aligned}$$

for a suitable $C_{IS,2}>0$ if $C_{L,1}$ is small enough, see Lemma 8.4.
And on the other hand, we can estimate

$$\begin{aligned}
\|\tau\|_{H^1} &\le \|\tilde{\tau}\|_{H^1} + \sum_i \Big\|\overline{M}_h^i\Big\|_{H^1} \\
&\le \|\tilde{\eta}\| + \sum_i |\bar{\eta}_i|\,\Big\|M_h^i\Big\|_{H^1} \\
&\le \|\tilde{\eta}\| + \sum_i \sqrt{C_\Omega}C_i\,\|\bar{\eta}_i\| \\
&\le C_{IS,3}(\|\tilde{\eta}\|+\|\bar{\eta}\|), \qquad (8.3.43)
\end{aligned}$$

where $C_{IS,3} \coloneqq \max_i\{1, N\sqrt{C_\Omega}C_i\}$. Finally, we can combine (8.3.42) and (8.3.43) to see

$$\frac{\langle \nabla\cdot(\tilde{S}\tau),\eta\rangle}{\|\tau\|_{H^1}} \ge \frac{C_{IS,2}}{C_{IS,3}}(\|\tilde{\eta}\|+\|\bar{\eta}\|) \ge \frac{C_{IS,2}}{C_{IS,3}}\,\|\eta\|.$$

The arbitrariness of η finishes the proof.

□

With Lemma 8.3 it follows the well-posedness of the discretization method, we showed Theorem 8.4, respectively . Thereby, we obtain the next error estimate which corresponds to Lemma 2.12 in the abstract setting.

Theorem 8.5 (**Error estimate**). *We consider a well-posed discretization* (8.3.5) *in the sense of Theorem 8.4. Further let the solution* (σ, u, κ) *of the continuous problem* (8.3.4) *fulfill the regularity assumptions* $\sigma \in H^l(\Omega, \nabla\cdot, \mathbb{E}^{n-1}),\ u \in H^l(\Omega)\otimes\mathbb{E}^n,\ \kappa \in H^l(\Omega)\otimes\bar{\mathbb{E}}^n$ *for* $0 \le l \le p$. *Then the error between exact and approximate solution satisfies*

$$\|\sigma-\sigma_h\|_{H(\nabla\cdot)} + \|u-u_h\| + \|\kappa-\kappa_h\| \le C_{conv} h^l \Big(\|\sigma\|_{H^l(\nabla\cdot)} + \|u\|_{H^l} + \|\kappa\|_{H^l} \Big)$$

for a constant C_{conv} *independent of* h.
Additionally we have

$$\|\nabla\cdot\sigma - \nabla\cdot\sigma_h\| \le C_{conv} h^{p+1} \|\nabla\cdot\sigma\|_{H^{p+1}},$$

provided enough regularity for σ.

Proof. By the well-posedness, we have a quasi-optimal estimate like in Lemma 2.12. Thus, due to projection properties in Corollary 8.4 one obtains easily the first estimate. More precisely, setting $\|(\tau,v,\eta)\|_{\mathcal{B}}^2 \coloneqq \|\tau\|_{H(\nabla\cdot)}^2 + \|v\|^2 + \|\eta\|^2$, there is a constant C_{QO} with

$$\begin{aligned}
\|(\sigma-\sigma_h, u-u_h, \kappa-\kappa_h)\|_{\mathcal{B}} &\le C_{QO} \left\|(\sigma-\Pi_h^{\Sigma}\sigma, u-\Pi_h^U u, \kappa-\Pi_h^{\bar{K}}\kappa)\right\|_{\mathcal{B}} \\
&\le C_{QO}\Big(\left\|\sigma-\Pi_h^{\Sigma}\sigma\right\|_{H(\nabla\cdot)} + \left\|u-\Pi_h^U u\right\| + \left\|\kappa-\Pi_h^{\bar{K}}\kappa\right\| \Big) \\
&\le Ch^l \ \Big(\|\sigma\|_{H^l(\nabla\cdot)} + \|u\|_{H^l} + \|\kappa\|_{H^l} \Big).
\end{aligned}$$

The second estimate of the assertion can be obtained by a standard approach. We observe the fact $\langle \nabla\cdot\sigma - \nabla\cdot\sigma_h, w_h\rangle = 0,\ \forall w_h \in U_h$ and that $\nabla\cdot\tau_h \in U_h, \forall \tau_h \in \Sigma_h$. This means we have the equality chain

$$\begin{aligned}
\|\nabla\cdot\sigma - \nabla\cdot\sigma_h\|^2 &= \langle \nabla\cdot\sigma - \nabla\cdot\sigma_h, \nabla\cdot\sigma - \nabla\cdot\sigma_h\rangle \\
&= \langle \nabla\cdot\sigma - \Pi_h^U\nabla\cdot\sigma, \nabla\cdot\sigma - \nabla\cdot\sigma_h\rangle + \langle \Pi_h^U\nabla\cdot\sigma - \nabla\cdot\sigma_h, \nabla\cdot\sigma - \nabla\cdot\sigma_h\rangle \\
&\le \left\|\nabla\cdot\sigma - \Pi_h^U\nabla\cdot\sigma\right\| \ \|\nabla\cdot\sigma - \nabla\cdot\sigma_h\| + 0.
\end{aligned}$$

Thus, again in view of Corollary 8.4, we get
$\|\nabla\cdot\sigma - \nabla\cdot\sigma_h\| \le \left\|\nabla\cdot\sigma - \Pi_h^U\nabla\cdot\sigma\right\| \le Ch^{p+1}\|\nabla\cdot\sigma\|_{H^{p+1}}$. Since we use in (8.3.7) isogeometric discrete differential forms with degree $p+1$ to define $\Sigma_h\text{curl}$ the last estimate is clear. □

With the two Theorems 8.4 and 8.5, we have now encountered a second approach to discretization in the context of the BGG construction from Section 4.2.3 using IGA. The proof of the convergence estimate and well-posedness constitutes a second main result of the thesis. Although we indicated at the beginning of Section 5.3 that analogous types of discretizations with Lagrange multipliers can be found in the literature ([42, 10, 63, 7]), the referenced works focus on FEMs based on classical triangulations with quadrilateral or tetrahedral elements, i.e., elements with straight or flat boundaries. In contrast, we have followed the concept of isogeometric analysis, and therefore, we have not only used completely different test function spaces. It further allows us to incorporate curved geometries in an exact manner but also enables the use of basis functions with high regularity. These last two aspects cannot be readily realized with the methods in above publications. Furthermore, we have indeed investigated the discretization for an entire class of saddle point problems, specifically for the $(\mathscr{V}_n^{\circ,J}, \mathscr{D}_n^{\circ,J})$ complexes in arbitrary dimensions. In a certain sense, one can consider the above as a generalization of the approaches in [42, 10, 63, 7].

Actually, for the second approach with the Lagrange multiplier, we have not yet provided an explicit demonstration example, a numerical test, respectively. However, we plan to address this in the next section in which we will consider a specific application field, namely the theory of linear elasticity. But before we move on to the next chapter, let us briefly recap what we have achieved with this last and central chapter of the thesis. In general terms, we have demonstrated that we can discretize and approximate the Hodge–Laplace problem of level $k = n$ induced by the complex $(\mathscr{V}_n^{\circ,J}, \mathscr{D}_n^{\circ,J})$, or rather its mixed formulations, using isogeometric basis functions. More specifically, we have presented two different discretization approaches in Sections 8.2 and 8.3, and shown that we can obtain a well-posed discretization for each (following possible mesh refinement). In both approaches, we can use arbitrarily high polynomial degrees, and with sufficient regularity of the exact solution, our error estimates theoretically imply arbitrarily high convergence rates. What is noteworthy here is the fact that for both discretization methods, we have indirectly employed the central FEEC concept of structure-preserving for Hilbert complexes. While it is true that we did not explicitly demand such a discretization of the underlying chain in the physical domain, in Section 8.2, we leverage the existence of discretization of the output complexes in cubical domains in the proof of Lemma 8.2. Additionally, in Section 8.3, we utilize isogeometric discrete differential forms to define the Finite Element spaces, which precisely represent a structure-preserving discretization of the de Rham complex.

So far, we have mostly worked in an abstract manner and examined entire classes of problems. Therefore, it is reasonable to consider whether there are relevant application areas for what we have learned. In principle, as we have already seen in Example 8.1, we can use at least the first approach to compute approximate solutions for the biharmonic equation. The latter can, for instance, be used in the context of Kirchhoff plate theory ([54]) to calculate plate deflections, providing us with one potential application. Another area in the field of continuum mechanics suitable for both systems (8.2.1) and (8.3.4) is the deformation of elastic bodies. We aim to illustrate and explore the latter in detail in the upcoming section.

9 Application to Linear Elasticity

This section focuses on our primary application field, the theory of linear elasticity. It revolves around the computation of approximate solutions for mechanical displacements and stresses, following the approximation paradigm of IGA. We aim not only to demonstrate how and why the results from Section 8.2 and Section 8.3 can be applied here, but we will also address generalization directions such as multi-patch IGA geometries and mixed boundary conditions, illustrating our considerations through numerous examples. Additionally, we will show that the numerically challenging case of (nearly) incompressible materials can also be handled. In other words, we want to demonstrate the relevance of the results from Section 8 in an important part of computational mechanics.

Let us begin with some introductory remarks on the physical background and derive the underlying equations. It is essential to mention that we are only examining the stationary case, meaning there is no time dependence in what follows.

9.1 Linear elasticity

The theory of linear elasticity elucidates how a solid undergoes deformation and changes in stress state when subjected to external forces, assuming only infinitesimal deformations. The latter allows to derive a reasonable linear relationship between the stress and strain components. This connection is summarized in the so-called *generalized Hooke's law*. Considering small deformations makes it meaningful for many materials to exhibit elastic behavior, meaning that deformations are reversible, and in the absence of forces, the solid returns to a specific reference configuration. To establish a mathematical description one usually identifies the elastic body with some domain $\Omega \subset \mathbb{R}^n,\ n \in \{2, 3\}$, where we, as always, think of some bounded Lipschitz domain.

In this subsection, we briefly want to address the famous Hooke's law, as it is fundamental for equations of linear elasticity. For the sake of clarity, we start with the definitions of the terms stress tensor and displacement. The derivation should be carried out mainly for the three-dimensional case, but analogous arguments and notions are also valid for the planar situation. All the considerations below can be regarded as basic knowledge in the field of continuum mechanics and are explained in more detail in every standard textbook on this subject. We refer, for example, to Chapter 6 in the book [20].

The application of external forces to a solid induces direction-dependent internal stresses at each point p within the solid. To capture the relation between the stresses and the forces, a tensor relation becomes essential. Since the analysis is conducted within three-dimensional space, rank-2 tensors can be conveniently represented using 3×3 matrices. Now, if we focus on an infinitesimal area element dA containing point P, with its orientation defined by the unit normal vector $\mathbf{n}$, then the force $df_P \in \mathbb{R}^3$ acting on dA satisfies the equation

$$\frac{df_P}{dA} = \sigma \cdot \mathbf{n},$$

where

$$\sigma := \begin{pmatrix} \sigma_{11} & \sigma_{12} & \sigma_{13} \\ \sigma_{21} & \sigma_{22} & \sigma_{23} \\ \sigma_{31} & \sigma_{32} & \sigma_{33} \end{pmatrix}$$

is the *Cauchy stress tensor* from continuum mechanics. The vector $t_P^{\mathbf{n}} := \frac{df_P}{dA}$ is called traction vector which shows us that the unit of the stress tensor entries is force per area. Indeed, a

close look reveals that the traction vector is influenced not only by the point P (indicating its spatial location) but also by the orientation of the associated area element dA. Consequently, we should interpret the traction vectors as constituents of an internal vector field denoted by $t\colon \mathbb{S}^3 \times \Omega \to \mathbb{R}^3\ ,\ (\mathbf{n}, P) \mapsto t_P^{\mathbf{n}} = \sigma(P)\cdot\mathbf{n}$, where $\mathbb{S}^3$ represents the unit sphere in $\mathbb{R}^3$. This vector field determines the internal stress distribution for different points and orientations within the solid.

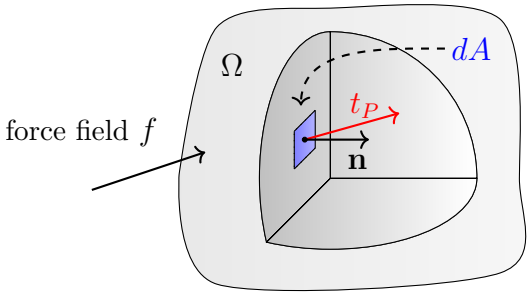

Figure 19: Loading gives rise to internal stresses within a material. The traction vector t_P quantifies the resultant force per infinitesimal area element dA of a cutting plane at point $P \in \Omega$.

Let us further emphasize that within a three-dimensional context, the entire stress state at a given point, and thereby the stress tensor, can be fully characterized by three mutually perpendicular cutting areas. These areas can be thoughtfully chosen with their orientation vectors $\mathbf{n}_1$, $\mathbf{n}_2$, and $\mathbf{n}_3$ aligned parallel to the coordinate axes. As depicted in Figure 20, the corresponding orientations of stress components are illustrated through a conceptual infinitesimal cube. In this configuration, the off-diagonal entries of σ correspond to shear stresses, forces acting tangentially to the cutting areas, respectively, while the diagonal components represent normal stresses, implying forces perpendicular to the different cutting areas. Analogously it is possible to define a stress tensor $\sigma \in \mathbb{R}^{2\times 2}$ for planar elasticity, i.e. $n = 2$. For more details on that we refer to [20, §5 on page 309].
In order to guarantee a conservation of angular momentum one can show in both situations $n = 2$ and $n = 3$ the symmetry of the stress tensor.

Within the context of linear elasticity and under the assumption of deformability, applied forces induce alterations in the solid's shape. Consequently, to quantify and explain this deformation, the concepts of strains and displacements must be introduced.

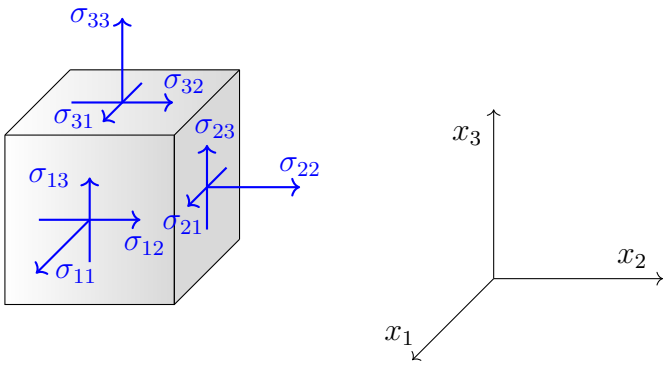

Figure 20: The components of the stress tensor.

Let now the undeformed solid be given as the closure of a Lipschitz domain $\Omega \subset \mathbb{R}^n$. Selecting a fixed coordinate system, a point P within the solid is characterized by its Cartesian coordinates

$P = x_P$. When a force field f is applied, it induces a displacement of point P to a new position $\tilde{P} = \tilde{x}_P$. The displacement experienced by point P is subsequently quantified by the disparity between these positions, expressed as:

$$u(x_P) \coloneqq \tilde{x}_P - x_P.$$

In other words, the shape of the body can be described through the *displacement field* $u\colon \Omega \to \mathbb{R}^n$ that measures the difference between current configuration $\Omega+u$ and initial configuration, namely Ω. The displacement is now used to define the *strain tensor* ε another rank-2 tensor, i.e. a matrix field, which measures the degree of deformation. The linearized version of the strain tensor is symmetric and given by the symmetric gradient

$$\varepsilon(u) \coloneqq \mathrm{sym}\nabla u,$$

which again yields a matrix field; see [20, §1 on page 273].

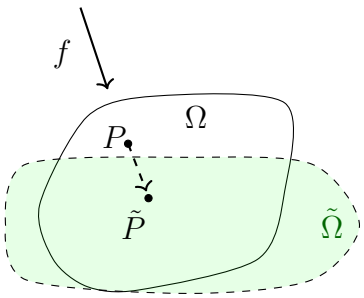

Figure 21: A force field f causes a deformation.

Now we can come to the already mentioned generalized Hooke's law which connects the strain and stress components in a linear manner. More precisely, we assume in linear elasticity the validity of the relation

$$\sigma = C\varepsilon, \quad \text{meaning} \quad \sigma_{ij} = \textstyle\sum_{k,l=1}^{n,n} C_{ijkl}\,\varepsilon_{kl}, \quad \forall i,\, j, \tag{9.1.1}$$

where $C = \big(C_{ijkl}\big)_{i,j,k,l=1}^{n,n,n,n}$ is the rank-4 *elasticity tensor*. An often made assumption in continuum mechanics is that the materials are homogeneous and isotropic. In this case Hooke's law can be expressed by means of the so-called Lamé parameters $0 \le \lambda$, $0 < \mu$. To be more precise one has

$$\sigma = 2\mu\varepsilon + \lambda \mathrm{tr}(\varepsilon)\mathrm{I}, \quad \text{(Here, I denotes the identity tensor.)} \tag{9.1.2}$$

which simplifies calculations significantly.

Next, to derive the governing equations that specify how displacements and stresses change due to a force field, we employ a *balance of momentum* argument. Namely, choosing some local control volume $U \subset \Omega$ then the integral sum

$$\int_{\partial U} \sigma \cdot \mathbf{n}\, ds + \int_U f\, dx \tag{9.1.3}$$

conforms with the total forces acting on the volume U. In this context, the first term corresponds to the contribution arising from internal stresses, and the second term in (9.1.3) represents the contribution provided by a load field $f\colon \Omega \to \mathbb{R}^n$. Since we are working in a static setting, all forces must cancel out according to Newton's laws. In other words, (9.1.3) must vanish for any arbitrary volume U, which yields

$$-\nabla \cdot \sigma = f \quad \text{in } \Omega, \tag{9.1.4}$$

through the use of partial integration.

Both equations (9.1.1) and (9.1.4) can now be exploited to calculate stresses and displacements, given some f. However, we still need to establish boundary conditions to obtain a well-defined problem in the first place. Initially, we want to confine ourselves to the simple scenario of zero displacements on the entire boundary $\partial\Omega$. Later on, we will also address other conditions known as traction boundary conditions and discuss numerical examples for them. Furthermore, it is not difficult to demonstrate that through an appropriate transformation, non-zero displacement boundary conditions can be reduced to the zero case.

One standard approach to solve the problem of linear elasticity in case of homogeneous boundary conditions weakly, is the primal formulation (cf. [20, §3 in Chapter 6]):

$$\text{Find } \; u \in H_0^1(\Omega) \otimes \mathbb{R}^n \;\text{ s.t. }\; \langle C\varepsilon(u), \varepsilon(v)\rangle = \langle f, v\rangle, \quad \forall v \in H_0^1(\Omega) \otimes \mathbb{R}^n. \tag{9.1.5}$$

The latter line is obtained by inserting (9.1.1) into (9.1.4) together with integration by parts. Exploiting the Korn inequality (see [45, Theorem 2]), one can prove the well-posedness of the previous variational problem, at least if the elasticity tensor is bounded and uniformly elliptic; compare [20, 3.4, page 292].[17] However, the formulation (9.1.5) is not optimal, especially when we face discretizations. Even in the isotropic case for large λ stability issues arise, and in the limit as $\lambda \to \infty$, the formulation becomes undefined. This issue becomes evident in numerical examples for nearly incompressible materials ($\lambda >> \mu$), leading to stress oscillations and incorrect displacement values. This phenomenon is sometimes referred to as volumetric *locking*; we refer to [20, §4 in Chapter 6] for detailed information regarding locking.

Furthermore, another aspect that could be considered disadvantageous for the primal formulation is that relying solely on displacements contradicts the fact that stresses are typically the variables of interest in applications. Therefore, a weak formulation that also incorporates stresses as variables would be more appropriate. Another point is the non-locality of stress-strain relations in more general material situations as viscoelasticity. Consequently, the primal weak formulation is not optimal also in view of generalizability. Due to these mentioned points, alternative weak formulations and approximations schemes have been and continue to be investigated in the literature; see e.g. [63, 7, 76, 14, 21] or [25]. One of them is the Hellinger–Reissner method ([44]), which is a stress-displacement mixed formulation we want to address and exploit in the next subsection.

9.2 Mixed weak formulation with strong symmetry

The latter assumes that the elasticity tensor is invertible, allowing the utilization of the compliance tensor $A := C^{-1}$. With the resulting equations

$$A\sigma = \varepsilon(u) \quad \text{and} \quad -\nabla\cdot\sigma = f \text{ in } \Omega, \tag{9.2.1}$$

$$u = 0 \text{ on } \partial\Omega, \tag{9.2.2}$$

establishing the next mixed weak formulation is straightforward:

Definition 9.1 (**Hellinger–Reissner formulation**, cf. [20, (3.22) in Chapter 6])**.** *Find* $\sigma \in H(\Omega, \nabla\cdot, \mathbb{S})$, $u \in L^2(\Omega) \otimes \mathbb{R}^n$ *s.t.*

$$\langle A\sigma, \tau\rangle + \langle u, \nabla\cdot\tau\rangle = 0, \qquad \forall \tau \in H(\Omega, \nabla\cdot, \mathbb{S}), \tag{9.2.3}$$

$$\langle \nabla\cdot\sigma, v\rangle = \langle -f, v\rangle, \quad \forall v \in L^2(\Omega) \otimes \mathbb{R}^n. \tag{9.2.4}$$

[17] C is uniformly elliptic if $\sum_{i,j,k,l} C_{ijkl}\, x_{kl}\, x_{ij} \geq C \sum_{i,j} x_{ij}^2$ for a constant $C > 0$ and all $x = (x_{mn})_{m,n}$.

One notes, the physics-induced symmetry of the stress tensor is directly included, as $\mathbb{S}$ denotes the space of symmetric $n \times n$-matrices. Importantly, a key aspect becomes apparent: The new saddle-point problem aligns well with the abstract theory of Hodge–Laplace problems, as discussed in [5, Chapter 8.7]. Because, if one assumes that $\mathcal{A}(\sigma, \tau) \coloneqq \langle A\sigma, \tau \rangle$ is a bounded and coercive bilinear form on $\Big(L^2(\Omega) \otimes \mathbb{S}\Big)^2$, then $\langle A\cdot, \cdot \rangle$ can be seen as a new weighted inner product. And the "+" in the first line becomes a "−" if we change u to $-u$. Thus, the Hellinger–Reissner system can be interpreted as the mixed weak formulation for the level n Hodge–Laplace problem of the elasticity complexes

$$0 \longrightarrow H^2(\Omega) \xrightarrow{\operatorname{curl}^2} H(\Omega, \nabla\cdot, \mathbb{S}) \xrightarrow{\nabla\cdot} L^2(\Omega) \otimes \mathbb{R}^2 \longrightarrow 0, \tag{9.2.5}$$

and

$$0 \longrightarrow H^1(\Omega) \otimes \mathbb{R}^3 \xrightarrow{\operatorname{sym}\nabla} H(\Omega, \operatorname{inc}, \mathbb{S}) \xrightarrow{\operatorname{inc}} H(\Omega, \nabla\cdot, \mathbb{S}) \xrightarrow{\nabla\cdot} L^2(\Omega) \otimes \mathbb{R}^3 \longrightarrow 0, \tag{9.2.6}$$

from Examples 4.2 and 4.3. In other words, we now have the opportunity to apply knowledge and results from the context of FEEC to compute approximate solutions. Before we move on, we should remark for reason of completeness here similar to (9.1.2) what the compliance tensor looks like for isotropic materials, namely

$$A\sigma = \frac{1}{2\mu}\Big(\sigma - \frac{\lambda}{n\lambda + 2\mu}\operatorname{tr}(\sigma)\mathrm{I}\Big). \tag{9.2.7}$$

In particular, by simple calculations we get that $\lambda \geq 0,\ \mu > 0$ imply a bounded and cercive $\mathcal{A}$. In fact it is

$$2\mu\langle A\tau, \tau\rangle \geq \textstyle\sum_{i\neq j} \|\tau_{ij}\|^2 + \frac{2\mu}{n\lambda+2\mu}\sum_i \|\tau_{ii}\|^2, \quad \forall \tau \in L^2(\Omega) \otimes \mathbb{M}, \tag{9.2.8}$$

where we have an equality if all components τ_{ij} are constant.

From the previous Section 7.2 we know how to construct various structure-preserving B-spline discretizations of the elasticity complexes in the case of cubical domains, i.e. $\Omega = (a, b)^n$. For more details we refer to Corollary 7.5, Corollary 7.8 and Remark 7.2. It was possible to vary not only the polynomial degree but also the regularity of the corresponding splines. And these complex discretizations can be directly utilized to calculate approximations to the Hellinger–Reissner system for $\Omega = (a, b)^n$. However, such a restriction to cubes is not truly what one desires in the IGA context. Therefore we want to follow the approach from Section 8.2 that allows for arbitrary domains with C^1-regular parametrizations $\mathbf{F}\colon (0, 1)^n \to \Omega$. First, analogously to Definition 8.2 let us define and clarify the discrete spaces: We set

$$\mathscr{V}_h^{n-1} \coloneqq \widehat{\mathscr{V}}_h^{n-1} \circ \mathbf{F}^{-1} \quad \text{with} \quad \widehat{\mathscr{V}}_h^{n-1} \coloneqq S^{\mathbf{s}}_{\mathbf{q}} \otimes \mathbb{S}, \tag{9.2.9}$$

$$\mathscr{V}_\theta^{n} \coloneqq \widehat{\mathscr{V}}_\theta^{n} \circ \mathbf{F}^{-1} \quad \text{with} \quad \widehat{\mathscr{V}}_\theta^{n} \coloneqq S^{\mathbf{r}}_{\mathbf{p}} \otimes \mathbb{R}^n. \tag{9.2.10}$$

This means $\mathscr{V}_h^{n-1}$ corresponds to the stresses whereas $\mathscr{V}_\theta^n$ is the discrete displacement space. To fulfill the regularity conditions we require $\mathbf{p} = (p_i)_i$, $\mathbf{r} = (r_i)_i$, $\mathbf{q} = (q_i)_i$, $\mathbf{s} = (s_i)_i$ with

$$0 \leq s_i < q_i,\ 0 \leq r_i < p_i \tag{9.2.11}$$

for all the possible indices, meaning $\mathscr{V}_h^{n-1} \subset H^1(\Omega) \otimes \mathbb{S},\ \mathscr{V}_\theta^n \subset H^1(\Omega) \otimes \mathbb{R}^n$. Secondly, we have to write down the modified discrete system in the sense of Definition 8.4. For this purpose we define with a modified graph inner product $\langle \sigma, \tau \rangle_{\mathscr{A}} \coloneqq \langle A\sigma, \tau\rangle + \langle \nabla\cdot\sigma, \nabla\cdot\tau\rangle$. By doing so, we

aim to pave the way for later applying Theorem 8.2. In other words, we intend to determine $(\sigma_h, u_\theta) \in \mathscr{V}_h^{n-1} \times \mathscr{V}_\theta^n$ that satisfy

$$\begin{aligned} \langle \sigma_h, \tau_h \rangle_{\mathscr{A}} + \langle u_\theta, \nabla \cdot \tau_h \rangle &= \langle -f, \nabla \cdot \tau_h \rangle, \quad \forall \tau_h \in \mathscr{V}_h^{n-1}, && (9.2.12) \\ \langle \nabla \cdot \sigma_h, v_\theta \rangle &= \langle -f, v_\theta \rangle, \quad \forall v_\theta \in \mathscr{V}_\theta^n, && (9.2.13) \end{aligned}$$

The corresponding continuous problem seeks for $(\sigma, u) \in H(\Omega, \nabla\cdot, \mathbb{S}) \times L^2(\Omega) \otimes \mathbb{R}^n$ with

$$\begin{aligned} \langle \sigma, \tau \rangle_{\mathscr{A}} + \langle u, \nabla \cdot \tau \rangle &= \langle -f, \nabla \cdot \tau \rangle, \quad \forall \tau \in H(\Omega, \nabla\cdot, \mathbb{S}), && (9.2.14) \\ \langle \nabla \cdot \sigma, v \rangle &= \langle -f, v \rangle, \quad \forall v \in L^2(\Omega) \otimes \mathbb{R}^n, && (9.2.15) \end{aligned}$$

and is equivalent to the original Hellinger–Reissner formulation (9.2.3)-(9.2.4).

Now we have everything we need to apply Theorems 8.2 and 8.3 to the system (9.2.14)-(9.2.15) and its discrete pendant (9.2.12)-(9.2.13). Both, the spaces in (9.2.9)-(9.2.10) and the made regularity assumptions align with the considerations in Section 8.2. With this in mind, one thing is clear: when we examine the above systems with the canonical graph inner product associated with divergence, i.e. $\langle \sigma, \tau \rangle_{\mathscr{V}} = \langle \sigma, \tau \rangle + \langle \nabla \cdot \sigma, \nabla \cdot \tau \rangle$, instead of the new inner product $\langle \sigma, \tau \rangle_{\mathscr{A}}$, the mentioned theorems provide a statement on well-posedness and also offer an error estimate. Because, using $\langle \sigma, \tau \rangle_{\mathscr{V}}$ instead of $\langle \sigma, \tau \rangle_{\mathscr{A}}$, the system (9.2.14)-(9.2.15) corresponds to the modified saddle-point problem from Definition 8.4, for the above proxy output complexes (9.2.5) ($n = 2$), (9.2.6) ($n = 3$), respectively.

This means, here we just are dealing with a special case of the problem class outlined in Section 8.2. One notes, regarding well-posedness the presence of the inner product $\langle \sigma, \tau \rangle_{\mathscr{A}}$ is, inconsequential as the norms induced by $\langle \sigma, \tau \rangle_{\mathscr{A}}$ and $\langle \sigma, \tau \rangle_{\mathscr{V}}$ are equivalent. Thus, we obtain due to Theorem 8.2 directly

Corollary 9.1 (**Discrete well-posedness for linear elasticity**). *Let the Assumptions 8.1 and 8.2 hold. Assume we have a family of pairs* $\left(\mathscr{V}_{h(\theta)}^{n-1}, \mathscr{V}_\theta^n\right)_\theta$ *with underlying regular meshes, where the spaces are given by* (9.2.9)-(9.2.10). *Then there is a positive constant* c_R *s.t.* $h = h(\theta) \leq c_R\theta$ *implies that* (9.2.12)- (9.2.13) *is a well-posed discretization of* (9.2.14)-(9.2.15).

Besides we can again estimate the discretization error analogous to Theorem 8.3.

Corollary 9.2 (**Error estimate**). *We assume the family of space pairs* $\left(\mathscr{V}_{h(\theta)}^{n-1}, \mathscr{V}_\theta^n\right)_\theta$ *define a well-posed discretization in the sense of the last corollary. Further let the exact solution* (σ, u) *to* (9.2.14)-(9.2.15) *fulfill the regularity properties* $\sigma \in H^t(\Omega) \otimes \mathbb{S},\ 1 \leq t \leq q+1$ *and* $u \in H^m(\Omega) \otimes \mathbb{R}^n,\ 0 \leq m \leq p+1$, *where* $q = \min_i\{q_i\},\ p = \min_i\{p_i\}$ *with* $q_i,\ p_i$ *denoting the entries of the underlying degree vectors* $\mathbf{p},\ \mathbf{q}$.
Then the error between exact and approximate solution satisfies

$$\|\sigma - \sigma_h\|_{H(\nabla\cdot)} + \|u - u_\theta\| \leq C_{conv}\Big(h^{t-1}\,\|\sigma\|_{H^t} + \theta^m\,\|u\|_{H^m}\Big),$$

for a constant C_{conv} *independent of* θ.

Before we come to numerical test examples let us insert two remarks.

Remark 9.1 (Well-posedness in the isoparametric case). As already mentioned and explained in Remark 8.3. there is no problem to incorporate also weight functions and to use NURBS instead of B-spline basis functions.

Remark 9.2 (Non-zero boundary displacement). The first line (9.2.3) corresponds to the weak enforcement of zero displacement boundary conditions. Different boundary values can be handled by a standard argument. To be more precise let us consider the condition $u = u_D$ on $\Gamma \coloneqq \partial\Omega$

with $u_D \in L^2(\partial\Omega) \otimes \mathbb{R}^n$. And let us suppose there is a $\tilde{u} \in H^1(\Omega) \otimes \mathbb{R}^n$ s.t. $\tilde{u} = u_D$ on $\partial\Omega$ in the sense of the trace theorem. Then we solve for the auxiliary displacement $\bar{u} \coloneqq u - \tilde{u}$ with condition $\bar{u} = 0$ on $\partial\Omega$. This reasoning together with integration by parts explains why condition $u = u_D$ on $\partial\Omega$ results in the modified first line (9.2.3):

$$\langle A\sigma, \tau \rangle \; + \; \langle u, \nabla \cdot \tau \rangle \; = \langle \tau \cdot \mathbf{n}, u_D \rangle_\Gamma, \quad \forall \tau \in H(\Omega, \nabla\cdot, \mathbb{S}),$$

where $\langle \tau \cdot \mathbf{n}, u_D \rangle_\Gamma$ denotes the dual pairing between the normal trace operator and u_D; see [5, Theorem 3.12]. If τ is H^1-regular this dual pairing is just the standard integration on the domain boundary. In the same way we get an additional term $\langle \tau_h \cdot \mathbf{n}, u_D \rangle_\Gamma$ on the right-hand side in (9.2.12).

Next, we concentrate in the following on numerical tests for the mixed weak form (9.2.12)-(9.2.13) for planar domains; i.e. $n = 2$. Further we restrict ourselves to the equal degrees and equal regularities in each coordinate direction, meaning we make

Assumption 9.1. *In the next examples and numerical tests we always have*

$$q_i = q, \; p_i = p, \; r_i = r, \; s_i = s, \qquad \forall i,$$

and for different q, p, s, r, where $\mathbf{p} = (p_i)_i$, $\mathbf{r} = (r_i)_i$, $\mathbf{q} = (q_i)_i$, $\mathbf{s} = (s_i)_i$ are the underlying degree and regularity vectors; see (9.2.9)-(9.2.10)*. Besides, below σ and u denote the different exact solutions to the continuous Hellinger–Reissner formulation. For a better understanding of the discretizations, the appearing mesh sizes are meant in the sense of Remark 6.1, i.e. mesh size ρ corresponds to the uniform Bézier mesh consisting of ρ^{-n} squares.*

Example 9.1 (Curved square)**.** *Our first test problem in the planar ($n = 2$) case reads as follows. We have the parametrization mapping $\mathbf{F}\colon (0,1)^2 \to \Omega$, $(\zeta_1, \zeta_2) \mapsto (\zeta_1, \zeta_2 - \zeta_1^2 + \zeta_1)$ leading to the geometry in Figure 22 below.*

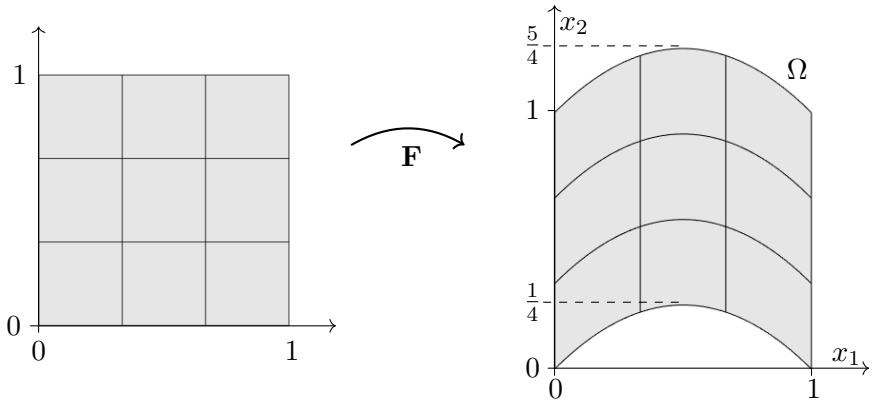

Figure 22: Here we display the computational domain for the first test example which is re-utilized at different places later. In this situation we say the mesh size is $h = 1/3$.

Furthermore, we choose an equal degree ansatz with

$$\boxed{q = p, \; s = p - 1, \; r = p - 1, \quad \text{and} \quad \lambda = 2, \; \mu = 1} \; ,$$

where λ, μ denote the Lamé parameters, i.e. we assume an isotropic material. Then, setting the source function such that the exact solution of the linear elasticity problem is

$$\boxed{u \circ \mathbf{F} = (w, -w)^{\mathrm{T}}, \quad w(\zeta_1, \zeta_2) \coloneqq \sin(\pi\zeta_1)^2 \, \sin(\pi\zeta_2)^2}$$

we might expect a convergence rate

$$\|\sigma - \sigma_h\|_{H(\nabla\cdot)} + \|u - u_\theta\| \in \mathcal{O}(h^q) + \mathcal{O}(\theta^{p+1}) \tag{9.2.16}$$

when we utilize the previously defined spaces $\mathscr{V}_h^1,\ \mathscr{V}_\theta^2$ *(see* (9.2.9)-(9.2.10)*) together with the mixed weak form* (9.2.12)-(9.2.13)*. At least the estimate in Corollary 9.2 suggests such a result. One notes that* $u \in \left(H_0^2(\Omega) \cap C^\infty(\overline{\Omega})\right) \otimes \mathbb{R}^2$ *is indeed an element of the domain of the level* $n = 2$ *Hodge–Laplace operator for the elasticity complex; cf.* (2.2.6)*. But, looking at the statement in Theorem 8.2, the proof of it respectively, we probably have to enlarge the space* $\mathscr{V}_h^1$ *by a mesh refinement step to guarantee inf-sup stability. Indeed, equal meshes i.e.* $h = \theta$ *yield* close to singular *warnings in* MATLAB *([53]) for the system matrices which is a clear indication for the loss of well-posedness and that our spaces are not suitable. This observation, however, is not surprising, as the relevant inf-sup expression for the saddle-point problem* (9.2.12)-(9.2.13) *given in* (9.2.17) *resembles the one obtained for Taylor–Hood IGA elements. And for Taylor–Hood elements it is easy to check that in general a degree elevation is needed to have inf-sup stability; see [23]. Since we also have an additional symmetry condition for the stresses here, we cannot expect equal degrees to directly lead to well-posedness. Thus, we do the calculations with refined* σ*-mesh, namely* $h = \theta/2$*. Besides the obtained errors in Figure 23, we display in Figure 24 (b) also the numerically computed inf-sup constants*

$$C_{IS} = C_{IS}(\mathscr{V}_h^1, \mathscr{V}_\theta^2) := \inf_{0 \neq v_\theta \in \mathscr{V}_\theta^2} \sup_{0 \neq \tau_h \in \mathscr{V}_h^1} \frac{\langle \nabla \cdot \tau_h, v_\theta \rangle}{\|\tau_h\|_{H(\nabla\cdot)} \|v_\theta\|}. \tag{9.2.17}$$

To compute these values numerically we again apply the inf-sup test *approach of Bathe et al. [15, 33]; see Appendix 11.2 for more details. On the one hand, we obtain in Figure 23 an error decay of about* $\mathcal{O}(h^p) = \mathcal{O}(h^p) + \mathcal{O}(\theta^{p+1})$ *that is consistent with the theory. Although the* L^2 *errors of the displacements seem to decrease slightly faster, this can be explained by the choice of equal degrees, which is not the most natural choice when looking at* (9.2.16)*, since there the terms* h^q *and* θ^{p+1} *appear. And on the other hand, the stable behavior of the discrete inf-sup constants in Figure 24 (b) underscores that the choice of the trial spaces is admissible, and that we have a well-posed discretization if* $h = \theta/2$*.*

As we just mentioned, it is not the best choice to use the same polynomial degree for all component functions, as we would then expect a damping of convergence for the displacements since we measure the stress errors w.r.t. the $H(\nabla\cdot)$*-norm and the displacement errors only in the* L^2 *sense. A much more reasonable choice is to select* $q = p + 1$*, which means using mixed degrees. In this situation, we can hope for convergence order* $\mathcal{O}(h^{p+1})$ *if* $\theta \in \mathcal{O}(h)$*. Thus we repeat the above convergence test with change*

$$\boxed{q = p + 1}.$$

This enlargement of the spaces $\mathscr{V}_h^1$ *due to the elevated degrees leads to stable inf-sup constants* C_{IS} *even for* $h = \theta$*, as seen in Figure 24(a). In particular we can expect a well-posed discretization. Therefore, we show in Figure 25 the errors for mixed degrees and the same meshes for* σ *and* u*. The results align well with theoretical convergence estimate.*

For the sake of completeness and illustration, in Figure 26 we show the approximated first displacement component and the stresses $\sigma_{11},\ \sigma_{12}$ *for the mixed degree case. More precisely, we choose* $q = p + 1 = 5,\ r = s = 3$*, and consider the coarse grid consisting of* 9 *elements as shown in Figure 22. Despite the coarse grid, reasonable approximations are obtained. It should also be emphasized here that we use globally* C^3*-regular B-splines to obtain Figure 26. Such smooth test functions are very difficult to define and implement with classical FE approaches.*

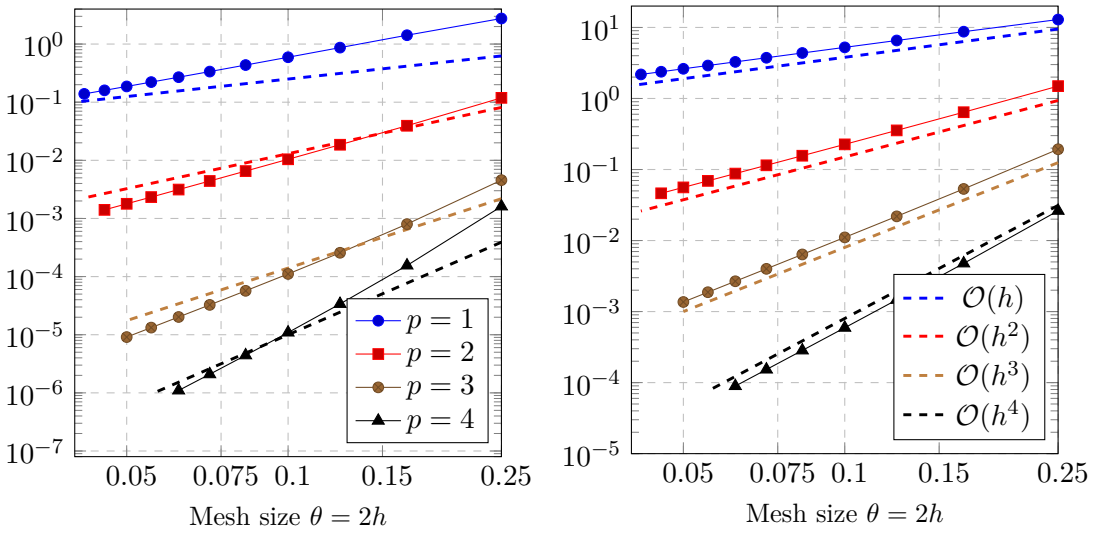

(a) $\|u - u_\theta\|$ (b) $\|\sigma - \sigma_h\|_{H(\nabla\cdot)}$

Figure 23: The errors for the choice $q = p$, $p = 1, \ldots, 4$ with regularities $s = r = p - 1$ and a refined mesh for the stress tensor ($h = \frac{1}{2}\theta$).

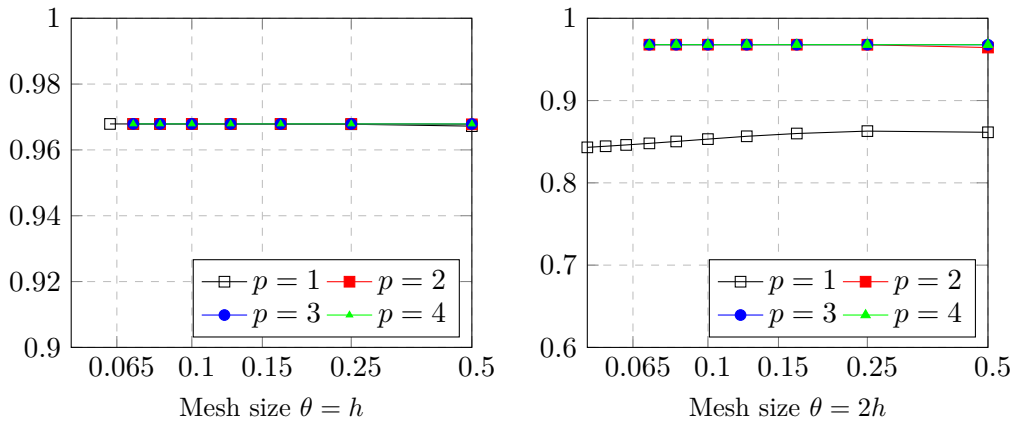

(a) Inf-sup values C_{IS} $(q = p + 1)$ (b) Inf-sup values C_{IS} $(q = p)$

Figure 24: The inf-sup constants C_{IS} for the two numerical tests; see (9.2.17). On the left we show them for mixed degrees $q = p + 1$ and on the right for $q = p$. Further in the former case it is $h = \theta$, whereas for the latter we have $2h = \theta$.

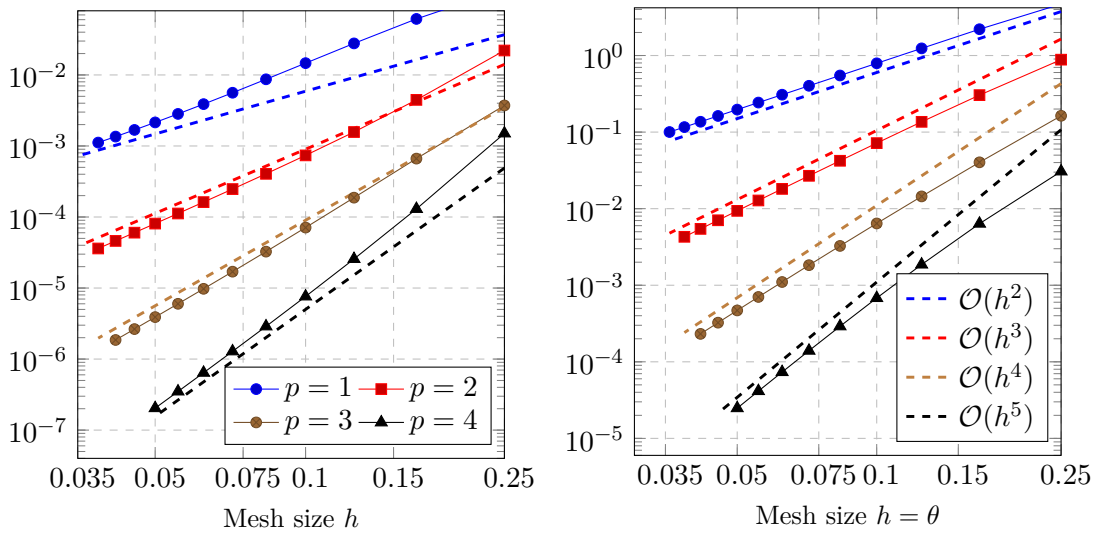

(a) $\|u - u_\theta\|$ (b) $\|\sigma - \sigma_h\|_{H(\nabla\cdot)}$

Figure 25: The errors for mixed degrees, meaning $q = p+1$, $p = 1, \ldots, 4$ with regularities $s = r = p-1$ and equal meshes for stress and displacement, i.e. $h = \theta$.

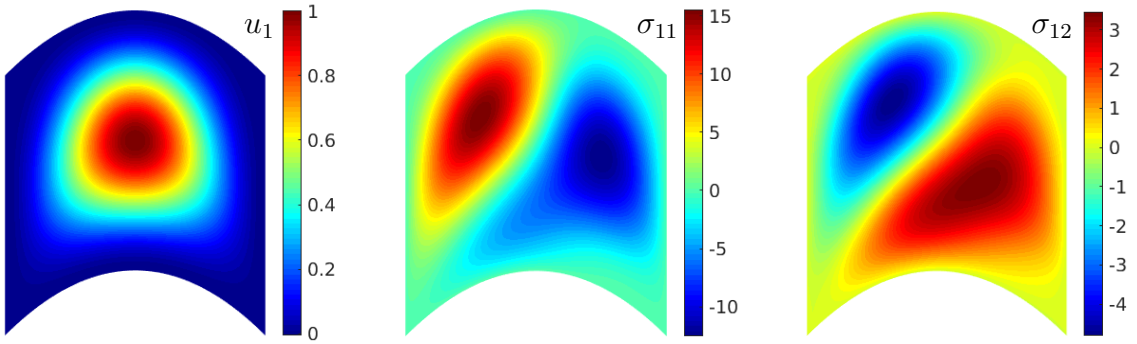

(a) displacement u_1 (b) stress σ_{11} (c) stress σ_{12}

Figure 26: For illustration, we present here results for the case $q = p + 1 = 5$, $r = s = 3$, and the very coarse grid from Figure 3, meaning we have only 9 mesh elements. Nevertheless, satisfactory approximations are obtained.

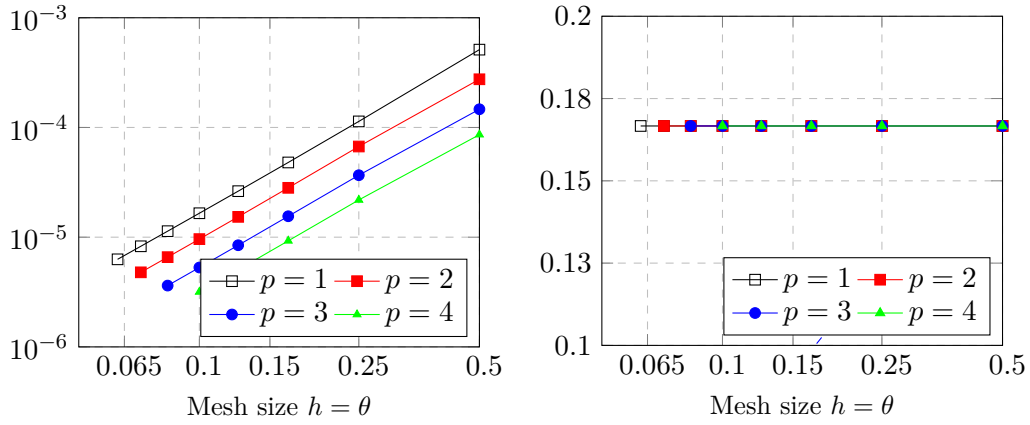

(a) Inf-sup values C_{IS}^u

(b) Inf-sup values C_{IS}^m

Figure 27: The inf-sup constants C_{IS}^m (modified system) and C_{IS}^u (original system) for the mixed degree case, i.e. $q = p + 1$, where the regularities are $r = s = p + 1$. Here we use the same meshes for stresses and displacements, i.e. $h = \theta$.

We want to perform one final test for this example here briefly. Because, up to now, we used the modified weak form (9.2.12)-(9.2.13)*. However, it is reasonable to question whether the discretized original mixed weak form* (9.2.3)-(9.2.4) *suggests well-posedness, too. But now, we aim to demonstrate that replacing* $\langle \cdot, \cdot \rangle_{\mathscr{A}}$ *with* $\langle A\cdot, \cdot \rangle$ *makes a significant difference in terms of inf-sup stability. To achieve this, we numerically compute the inf-sup values*

$$C_{IS}^s = C_{IS}^s(\mathscr{V}_h^1, \mathscr{V}_\theta^2) := \inf_{(0,0)\neq(\tau,v)\in\mathscr{V}_h^1\times\mathscr{V}_\theta^2} \sup_{(0,0)\neq(\sigma,u)\in\mathscr{V}_h^1\times\mathscr{V}_\theta^2} \frac{\mathcal{B}^s\big((\sigma,u),(\tau,v)\big)}{\|(\sigma,u)\|_{\mathcal{B}}\,\|(\tau,v)\|_{\mathcal{B}}}, \quad s \in \{m,u\}, \text{ with} \tag{9.2.18}$$

$$\begin{aligned}
\mathcal{B}^m\big((\sigma,u),(\tau,v)\big) &:= \langle \sigma,\tau\rangle_{\mathscr{A}} - \langle u, \nabla\cdot\tau\rangle - \langle \nabla\cdot\sigma, v\rangle,\\
\mathcal{B}^u\big((\sigma,u),(\tau,v)\big) &:= \langle A\sigma,\tau\rangle - \langle u, \nabla\cdot\tau\rangle - \langle \nabla\cdot\sigma, v\rangle,\\
\|(\tau,v)\|_{\mathcal{B}}^2 &:= \|\tau\|_{H(\nabla\cdot)}^2 + \|v\|^2,
\end{aligned}$$

for the mixed degree case ($q = p + 1,\ h = \theta$)*. Here the bilinear form* $\mathcal{B}^m$ *determines the modified weak formulation (*(9.2.12)-(9.2.13)*), whereas* $\mathcal{B}^u$ *defines the Hellinger–Reissner mixed form (*(9.2.3)-(9.2.4)*). From the theory on variational problems we have a well-posed discretization if* $C_{IS} \geq C > 0$ *and* C *does not depend on the mesh size* θ*.*
The results for different polynomial degrees and mesh sizes are summarized in Figure 27. While in Figure 27 (b), we obtain stable values around 0.167*, Figure 27 (a) shows small, decreasing inf-sup values. This clearly illustrates how the modification leads to enhanced stability. In particular from 27 (a) we can not hope for a well-posed discretization.*

9.2.1 Multi-patch domains

Understandably, in applications with more complex geometries, a single-patch domain is not suitable. Decomposing the computational domain into multiple patches becomes necessary; see Figure 9. We also know that in case of conforming patch couplings (see Assumption 6.3), a continuous coupling of NURBS basis functions can be relatively easily achieved; cf. [32, 31]. Since we require continuous, piecewise smooth test functions for the mixed weak formulation of linear elasticity, we can extend the spaces $\mathscr{V}_h^{n-1}$, $\mathscr{V}_\theta^n$ from above for the multi-patch context without

much effort. More precisely, for the multi-patch framework, i.e. $\overline{\Omega} := \cup_j \overline{\Omega_j} \subset \mathbb{R}^n$, $\mathbf{F}_j \colon (0,1)^n \to \Omega_j$, we use spaces of the form

$$\mathscr{V}_h^{n-1,M} := \left\{ \tau \in C^0(\overline{\Omega}) \otimes \mathbb{S} \;\middle|\; \tau_{|\Omega_j} \in \mathscr{V}_h^{n-1,j} \right\}, \quad \mathscr{V}_\theta^{n,M} := \left\{ v \in C^0(\overline{\Omega}) \otimes \mathbb{R}^n \;\middle|\; v_{|\Omega_j} \in \mathscr{V}_\theta^{n,j} \right\}, \tag{9.2.19}$$

where $\mathscr{V}_h^{n-1,j}$, $\mathscr{V}_\theta^{n,j}$ are the single-patch IGA spaces corresponding to the j-the patch.

To demonstrate the feasibility of the mixed weak form (9.2.12)-(9.2.13) also in the multi-patch context we add in this section two further examples. For reasons of simplification we assume for each coordinate and each patch the same polynomial degree q and regularity s for the space $\mathscr{V}_h^{n-1,M}$. And analogously, we have equal degree p and regularity r for the spaces $\mathscr{V}_\theta^{n,j}$. Further, we have mesh size h for the multi-patch case, if there are $1/h$ subdivisions per coordinate direction in each patch. While this may deviate from the actual mesh size, the smooth parametrization of the patches results in an equivalent mesh size notion. This means that convergence considerations are also meaningful with this type of mesh size and lead to the same convergence rates.

Example 9.2 (Multi-patch curved square)**.** *We are now considering a very similar test case as in Example 9.1. That means we have the same geometry, the same exact solution, and also the same Lamé parameters. However, here we divide Ω into a total of 9 patches, as shown in Figure 28 (b). Note that this also creates curved interfaces. Therefore, for the computations this time, we are using the multi-patch B-spline spaces in the sense of* (9.2.19)*, meaning patch-wise we utilize* (9.2.9)-(9.2.10)*. Below, we will again denote the polynomial degrees and regularities of the underlying spline spaces used patch-wise as q, p and r, s.*

Calculating the errors for mixed degrees $q = p + 1$ with regularities $r = s = p - 1$ between the exact solution and approximations, we obtain the plots in Figure 29. We choose $h = \theta$ for our calculations and observe stable error decreases at approximately order $\mathcal{O}(h^{p+1})$ in the mentioned figure. Although we do not have a well-posedness result for multi-patch geometries available, this is an indication of a well-posed discretization, as we cannot expect faster convergence from classical IGA estimates; compare Lemma 6.2. Furthermore, we have once again computed the inf-sup values C_{IS} (see (9.2.17)*) for this multi-patch case. We observe practically constant values, affirming inf-sup stability.*

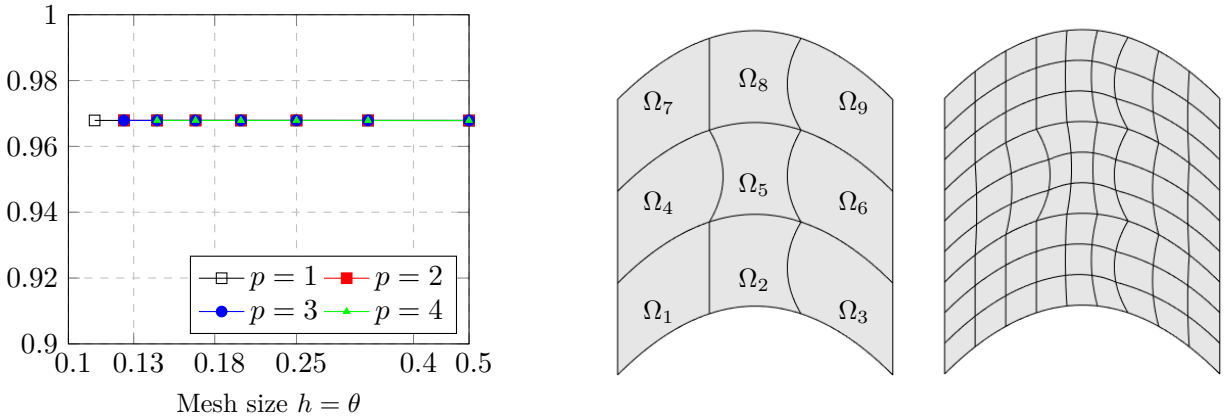

(a) Inf-sup values C_{IS} $(q = p + 1)$

(b) Multi-patch decomposition and mesh $(h = 1/3)$

Figure 28: On the left we have the inf-sup constants C_{IS} for the multi-patch convergence test with $q = p + 1$, $r = s = p - 1$ and equal meshes for both variables σ and u, i.e. $h = \theta$. The underlying multi-patch decomposition and mesh for $h = 1/3$ is depicted on the right.

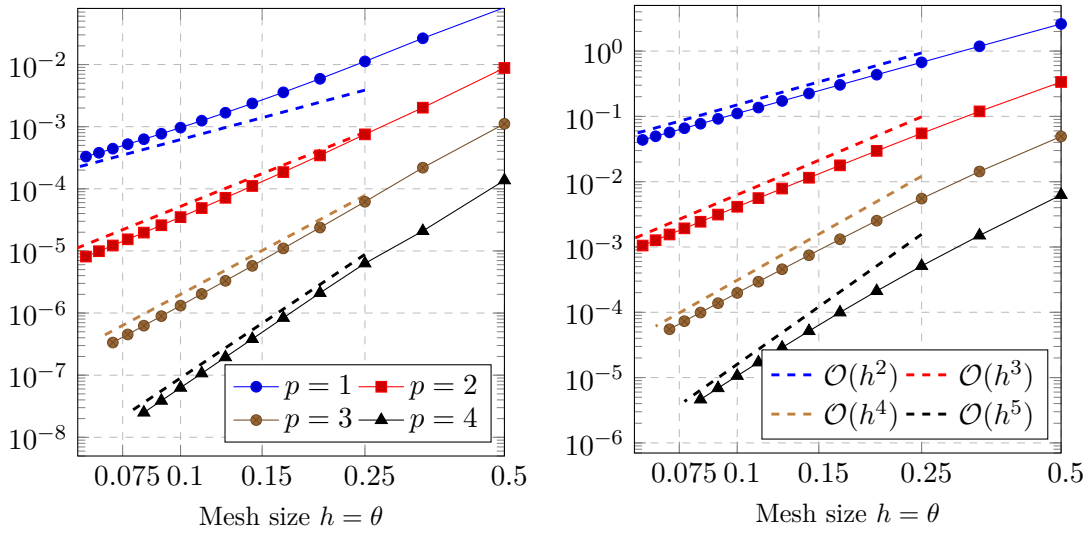

(a) $\|u - u_\theta\|$ (b) $\|\sigma - \sigma_h\|_{H(\nabla\cdot)}$

Figure 29: The error decay for the multi-patch test involving a mixed degree ansatz, namely $q = p+1$, $r = s = p - 1$. We observe convergence rates of approximately $\mathcal{O}(h^{p+1})$, the best rates we can expect from the theoretical approximation estimates for the respective NURBS spaces.

We would like to remark one point regarding multi-patch domains. Namely, to obtain a well-posed discretization in the single-patch case (see Corollary 9.1 and Theorem 8.2) we only need global C^0 smoothness of the test functions. But this is not an issue when we are dealing with conforming patch coupling. Although we cannot provide a strict proof regrading well-posedness, various numerical experiments show that the coupling does not significantly deteriorate stability. For instance, when we examine the inf-sup constants (9.2.17) for the mixed degrees ($q = p + 1$) case and the decomposition in Figure 28 (b), we can observe stable values once again.
We think that an application of the results in [32] might be a good starting point for a closer investigation of the multi-patch situation and maybe helpful to prove a statement similar to Theorem 8.2. Nevertheless, the last simple example shows that an implementation of the modified mixed weak form for multi-patch geometries is manageable, and we do not observe any unexpected stability problems.

Before we address the issue of traction boundary conditions for the mixed formulation with strong symmetry, we want to demonstrate its utility also for complicated geometries in the next second multi-patch example.

Example 9.3 (Fixed violin)**.** *Our multi-patch grid now has a shape of a planar violin, which is assembled from 180 patches. The domain, the multi-patch decomposition and the actual grid for the calculations are given in Figure 30. This computational mesh is obtained by subdividing each patch into* 9 *elements. In this case, a grid was intentionally chosen that also includes very small and thin mesh elements to test whether non-trivial meshes can also be used. For the exact definition of the domain we refer to the repository [64], where the boundary splines are available. Since the natural boundary conditions for the Hellinger–Reissner mixed weak form are zero displacements, we assume the complete boundary to be fixed. Furthermore we set*

$$\boxed{q = 4,\ p = 3,\ s = 2,\ r = 2, \quad \text{and} \quad \lambda = 20,\ \mu = 1}\ ,$$

together with a constant load function $\boxed{f = (0, -1)^{\mathrm{T}}}$.

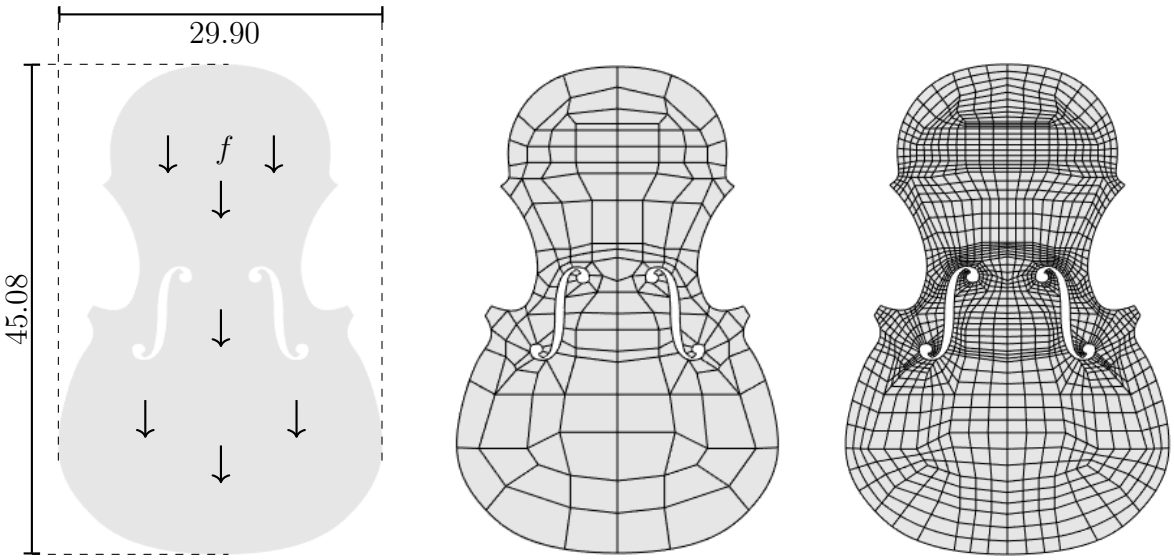

(a) Violin geometry (b) Multi-patch decomp. (c) Multi-patch mesh

Figure 30: The shape of the computational domain for the violin example is given on the left, whereas the used multi-patch decomposition is shown in the middle. For the calculations we utilize the mesh on the right.

Since we do not have an exact solution available for such a setting, we compare in Figure 31 the approximate displacements with those obtained using the primal formulation; see (9.1.5)*. For the latter reference solution, we use the same mesh but with patch-wise* C^0*-continuous B-splines of degree* 4*. The surprisingly good agreement between the two formulations strengthen our assumption that the modified mixed formulation is robust even for intricate meshes.*

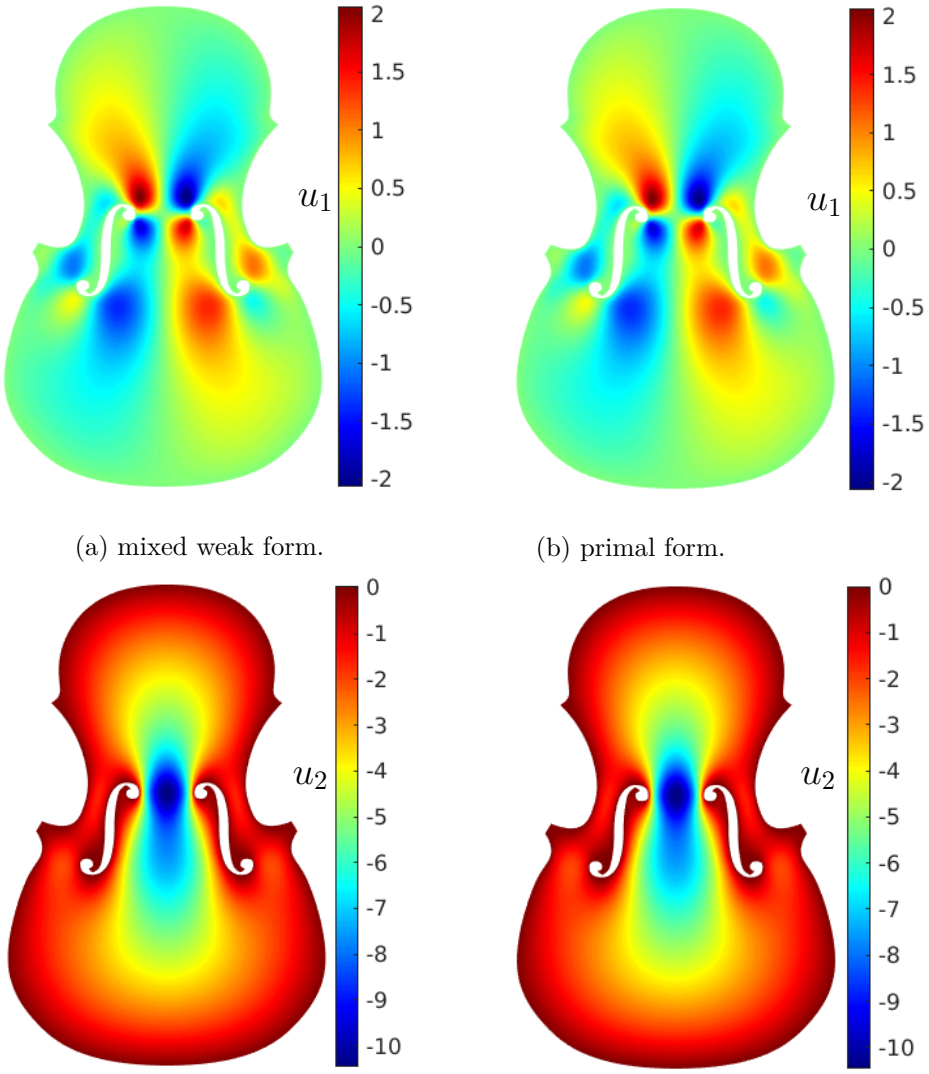

(a) mixed weak form.

(b) primal form.

(c) mixed weak form.

(d) primal form.

Figure 31: Here we see the comparison of the displacements between the classical primal formulation from (9.1.5) (right column) with degree 4 and C^0 B-splines as well as the displacements for the modified mixed weak form (9.2.12)-(9.2.13) (left column). For the latter we use globally C^0-smooth B-splines of degree $q = p + 1 = 4$ and C^2-inner patch regularity. Despite the complicated mesh structure we obtain very similar results.

9.2.2 Traction boundary conditions in 2D

So far, we have only discussed the straightforward scenario involving pure displacement boundary conditions prescribed by some $u_D \in L^2(\partial\Omega) \otimes \mathbb{R}^n$; see Remark 9.2. However, a complexity arises when we delve into the treatment of *traction boundary conditions* within the context of the strong symmetry formulation employing conventional NURBS or B-spline spaces. More precisely, one has a disjoint partition of the boundary $\overline{\Gamma_t} \cup \overline{\Gamma_D} = \partial\Omega$, $\Gamma_t \cap \Gamma_D = \emptyset$ together with a suitable mapping $t_{\mathbf{n}} \in L^2(\partial\Omega) \otimes \mathbb{R}^n$ and the requirement

$$\sigma \cdot \mathbf{n} = t_{\mathbf{n}} \text{ on } \Gamma_t \quad \text{and} \quad u = u_D \text{ on } \Gamma_D.$$

When we encounter situations where traction forces, meaning non-empty Γ_t, are stipulated by a predetermined auxiliary stress mapping $\tilde{\sigma}$, that is $\tilde{\sigma} \cdot \mathbf{n} = t_{\mathbf{n}}$, we can simplify the mixed boundary

conditions to the situation $t_{\mathbf{n}} = 0$. This simplification is achieved by considering the difference between the stress tensors $\sigma - \tilde{\sigma}$. This adjustment effectively brings us to a scenario where $t_{\mathbf{n}}$ is equal to zero.

Below we want to explain an approach in the planar case, how traction forces can be incorporated, i.e. we restrict ourselves to $n = 2$. Nevertheless, we think that the ideas are still applicable for $3D$.

By the above remarks it is justified, for reasons of simplification, to look first at the situation $t_{\mathbf{n}} = 0$ together with $u_D = 0$. Then, in view of the Hellinger–Reissner mixed formulation we shall now consider in the continuous setting the space

$$H_{\Gamma_t}(\Omega, \nabla\cdot, \mathbb{S}) \coloneqq \{\tau \in H(\Omega, \nabla\cdot, \mathbb{S}) \mid \tau \cdot \mathbf{n} = 0 \text{ on } \Gamma_t\}$$

for the stresses.[18] However, in the discrete setting (9.2.12)-(9.2.13) this would lead to test spaces

$$\mathscr{V}^1_{h,\Gamma_t} \coloneqq \mathscr{V}^1_h \cap H_{\Gamma_t}(\Omega, \nabla\cdot, \mathbb{S}).$$

But for curved boundaries with varying normal vector it is apparently non-trivial to find a basis for the latter. Because, the standard push-forward "$\circ\mathbf{F}^{-1}$" as used in (9.2.9)-(9.2.10), does not preserve normal components. Therefore we modify the basis functions relevant for the boundary conditions in order to facilitate the implementation. This approach is explained for a special case to illustrate the underlying idea. Afterwards we comment on generalizations and give several examples.

Let Γ_t correspond to one edge of our single-patch domain as it is shown in the next Figure 32 below, meaning $\Gamma_t = \Gamma_2$. Besides we restrict ourselves for explanations to the situation with equal degree q and regularity $0 \leq s \leq q-1$ for each component and coordinate direction. In particular, we utilize for each stress component the same discrete spaces. This allows to drop in the following indices related to degrees and regularities to improve readability.

Then the normal vector $\mathbf{n}$ along the mentioned edge Γ_t can be expressed as a function depending on ζ_2; compare Figure 32. More precisely, we have

$$\mathbf{n}(\tilde{x}_1, \tilde{x}_2) = \Big[\mathbf{n} \circ \mathbf{F}\Big](1, \zeta_2) = \frac{1}{\sqrt{J_{22}^2(1,\zeta_2) + J_{12}^2(1,\zeta_2)}} \begin{bmatrix} J_{22}(1,\zeta_2) \\ -J_{12}(1,\zeta_2) \end{bmatrix} =: \begin{bmatrix} \hat{a}(\zeta_1,\zeta_2) \\ \hat{b}(\zeta_1,\zeta_2) \end{bmatrix} \quad \text{on } \Gamma_t.$$

Above J_{ij} denote the entries of the parametrization Jacobian $D\mathbf{F} = \mathbf{J}$ and we assume $(\tilde{x}_1, \tilde{x}_2) = \mathbf{F}(1, \zeta_2)$. Then, we obtain for a sufficient regular parametrization $\mathbf{F}$ continuous functions

$$a \coloneqq \hat{a} \circ \mathbf{F}^{-1}, \quad b \coloneqq \hat{b} \circ \mathbf{F}^{-1} \quad \text{on } \Omega. \tag{9.2.20}$$

These auxiliary mappings a and b are utilized to adapt IG basis functions along the traction edge Γ_t. But, before we actually define the modified stress basis functions we need to clarify some notation.

[18] The boundary conditions are meant in the sense of the *normal trace operator*; see [5, Theorem 3.12].

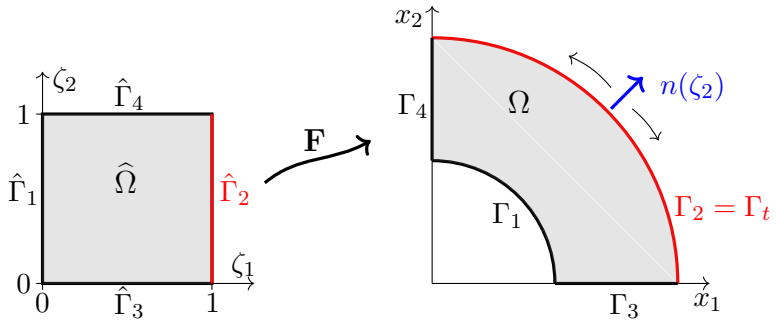

Figure 32: We assume on a part of the computational domain a zero traction force condition. Here $\Gamma_t = \Gamma_2$ is curved which implies a varying normal vector along the mentioned edge. This fact causes an extra effort to enforce the traction boundary conditions since the standard push-forward "$\circ\mathbf{F}^{-1}$" does not preserve normal components.

We suppose the stress component spaces to be spanned by

$$\begin{aligned}&\{N_{1,1},\, N_{2,1}, \ldots, N_{\mathfrak{n}_1,1},\;\; N_{1,2},\, N_{2,2},\, \ldots, N_{\mathfrak{n}_1,2},\;\; N_{1,3}\;\; \ldots, N_{\mathfrak{n}_1,\mathfrak{n}_2}\}\\ &\quad =: \{N_1,\; N_2,\; \ldots N_{\mathfrak{n}_1\mathfrak{n}_2}\},\quad \text{i.e.}\;\; N_{i+(j-1)\mathfrak{n}_1} = N_{i,j} \text{ with } 1 \le i \le \mathfrak{n}_1,\; 1 \le j \le \mathfrak{n}_2,\end{aligned} \tag{9.2.21}$$

where $N_{i,j} := \widehat{N}_{i,j} \circ \mathbf{F}^{-1}$, $\widehat{N}_{i,j}(\zeta_1, \zeta_2) := \widehat{N}_{(i,j),\mathbf{q}}(\zeta_1, \zeta_2)$ are proper scalar basis NURBS functions; cf. Definition 6.1.8. Further, the basis functions $\tau_{h,i}$ for the discrete stress space $\mathscr{V}_h^1$ shall be ordered as follows:

$$\begin{aligned}\tau_{h,i} &= \begin{bmatrix} N_i & 0 \\ 0 & 0 \end{bmatrix}, \;\; i = 1, \ldots, \mathfrak{n}_1\,\mathfrak{n}_2,\\ \tau_{h,i} &= \begin{bmatrix} 0 & N_i \\ N_i & 0 \end{bmatrix}, \;\; i = \mathfrak{n}_1\,\mathfrak{n}_2 + 1, \ldots, 2\,\mathfrak{n}_1\,\mathfrak{n}_2,\\ \tau_{h,i} &= \begin{bmatrix} 0 & 0 \\ 0 & N_i \end{bmatrix}, \;\; i = 2\,\mathfrak{n}_1\,\mathfrak{n}_2 + 1, \ldots, 3\,\mathfrak{n}_1\,\mathfrak{n}_2.\end{aligned}$$

In other words, we assume

$$\mathscr{V}_h^1 = \operatorname{span}\{\tau_{h,i} \mid i = 1, \ldots, 3\,\mathfrak{n}_1\,\mathfrak{n}_2\}.$$

Having the above ordering of the basis mappings in mind we see directly that the only basis functions $\tau_{h,i}$ with indices

$$i \in I := \left\{ k\mathfrak{n}_1\mathfrak{n}_2 + l\mathfrak{n}_1 \mid k \in \{0,1,2\},\; l \in \{1, \ldots, \mathfrak{n}_2\} \right\}$$

do not vanish at Γ_t, i.e. in total $3\,\mathfrak{n}_2$ mappings. The latter will now be changed ($\tau_{h,i} \to \tilde{\tau}_{h,i}$) in the following manner

$$\begin{aligned}\tau_{h,l\mathfrak{n}_1} &= \begin{bmatrix} 1 & 0 \\ 0 & 0 \end{bmatrix} N_{l\mathfrak{n}_1} \quad\longrightarrow\quad \tilde{\tau}_{h,l\mathfrak{n}_1} = \begin{bmatrix} a & b \\ b & -a \end{bmatrix} N_{l\mathfrak{n}_1}, \quad l = 1, \ldots, \mathfrak{n}_2,\\ \tau_{h,l\mathfrak{n}_1+\mathfrak{n}_1\mathfrak{n}_2} &= \begin{bmatrix} 0 & 1 \\ 1 & 0 \end{bmatrix} N_{l\mathfrak{n}_1} \quad\longrightarrow\quad \tilde{\tau}_{h,l\mathfrak{n}_1+\mathfrak{n}_1\mathfrak{n}_2} = \begin{bmatrix} -b & a \\ a & b \end{bmatrix} N_{l\mathfrak{n}_1}, \quad l = 1, \ldots, \mathfrak{n}_2,\\ \tau_{h,l\mathfrak{n}_1+2\mathfrak{n}_1\mathfrak{n}_2} &= \begin{bmatrix} 0 & 0 \\ 0 & 1 \end{bmatrix} N_{l\mathfrak{n}_1} \quad\longrightarrow\quad \tilde{\tau}_{h,l\mathfrak{n}_1+2\mathfrak{n}_1\mathfrak{n}_2} = \begin{bmatrix} b^2 & -ab \\ -ab & a^2 \end{bmatrix} N_{l\mathfrak{n}_1}, \quad l = 1, \ldots, \mathfrak{n}_2,\end{aligned}$$

using (9.2.20) and the numbering (9.2.21). We denote the discrete stress space spanned by the mappings $\tau_{h,i},\ i \notin I$ and new ones $\tilde{\tau}_{h,i},\ i \in I$ by $\tilde{\mathscr{V}}_h^1$, i.e.

$$\tilde{\mathscr{V}}_h^1 \coloneqq \operatorname{span}\Big\{ \{\tau_{h,i} \mid i = 1, \dots, 3\mathfrak{n}_1\mathfrak{n}_2,\ i \notin I\} \cup \{\tilde{\tau}_{h,i} \mid i \in I\} \Big\}. \tag{9.2.22}$$

The question arises whether the modification preserves the linear independence, meaning if the elements on the right-hand side of (9.2.22) form a basis of $\tilde{\mathscr{V}}_h^1$. Therefore assume coefficients $c_{1,l},\ c_{2,l},\ c_{3,l},\ l = 1, \dots, \mathfrak{n}_2$ s.t.

$$\sum_{l=1}^{\mathfrak{n}_2} \left(c_{1,l} \begin{bmatrix} a & b \\ b & -a \end{bmatrix} N_{l\mathfrak{n}_1} + c_{2,l} \begin{bmatrix} -b & a \\ a & b \end{bmatrix} N_{l\mathfrak{n}_1} + c_{3,l} \begin{bmatrix} b^2 & -ab \\ -ab & a^2 \end{bmatrix} N_{l\mathfrak{n}_1} \right) = 0.$$

By the linear independence of the standard NURBS mappings we get the condition

$$\begin{aligned} & c_{1,l} \begin{bmatrix} a & b \\ b & -a \end{bmatrix} + c_{2,l} \begin{bmatrix} -b & a \\ a & b \end{bmatrix} + c_{3,l} \begin{bmatrix} b^2 & -ab \\ -ab & a^2 \end{bmatrix} && = 0, \quad \forall l, \\ \Leftrightarrow \quad & \underbrace{\begin{bmatrix} a & -b & b^2 \\ b & a & -ab \\ -a & b & a^2 \end{bmatrix}}_{=:M} \begin{bmatrix} c_{1,l} \\ c_{2,l} \\ c_{3,l} \end{bmatrix} = 0, \quad \forall l. \end{aligned}$$

A straightforward computation yields for the determinant of M just $\det(M) = (a^2 + b^2)^2 = 1$. In particular all the $c_{i,l}$ have to vanish. Hence, since the unmodified $\tau_{h,i},\ i \notin I$ vanish at Γ_t one obtains indeed with the elements (9.2.22) a basis for $\tilde{\mathscr{V}}_h^1$. The reason to introduce the $\tilde{\tau}_{h,i}$ becomes clear through the next simple calculations: Along Γ_t we have by construction (see (9.2.20)), that the outer unit normal vector $\mathbf{n}$ corresponds to the tuple (a, b), consequently, on Γ_t it is

$$\begin{aligned} \tilde{\tau}_{h,l\mathfrak{n}_1} \cdot \mathbf{n} &= \begin{bmatrix} a & b \\ b & -a \end{bmatrix} \cdot \begin{bmatrix} a \\ b \end{bmatrix} N_{l\mathfrak{n}_1} = \begin{bmatrix} 1 \\ 0 \end{bmatrix} N_{l\mathfrak{n}_1}, \\ \tilde{\tau}_{h,l\mathfrak{n}_1+\mathfrak{n}_1\mathfrak{n}_2} \cdot \mathbf{n} &= \begin{bmatrix} -b & a \\ a & b \end{bmatrix} \cdot \begin{bmatrix} a \\ b \end{bmatrix} N_{l\mathfrak{n}_1} = \begin{bmatrix} 0 \\ 1 \end{bmatrix} N_{l\mathfrak{n}_1}, \\ \tilde{\tau}_{h,l\mathfrak{n}_1+2\mathfrak{n}_1\mathfrak{n}_2} \cdot \mathbf{n} &= \begin{bmatrix} b^2 & -ab \\ -ab & a^2 \end{bmatrix} \cdot \begin{bmatrix} a \\ b \end{bmatrix} N_{l\mathfrak{n}_1} = \begin{bmatrix} 0 \\ 0 \end{bmatrix}. \end{aligned}$$

Thus the basis for space

$$\tilde{\mathscr{V}}_{h,\Gamma_t}^1 \coloneqq \tilde{\mathscr{V}}_h^1 \cap H_{\Gamma_t}(\Omega, \nabla\cdot, \mathbb{S}) \tag{9.2.23}$$

is given by

$$\{\tau_{h,i} \mid i = 1, \dots, 3\mathfrak{n}_1\mathfrak{n}_2,\ i \notin I\} \cup \{\tilde{\tau}_{h,i} \mid i = 2\mathfrak{n}_1\mathfrak{n}_2 + l\mathfrak{n}_1,\ l = 1, \dots, \mathfrak{n}_2\}.$$

In other words, we have now an easy way to construct discrete spaces which can be exploited for the incorporation of the traction boundary condition. In more detail, we use instead of $\mathscr{V}_h^1$ now the spaces $\tilde{\mathscr{V}}_{h,\Gamma_t}^1$ in the mixed weak formulation (9.2.12)-(9.2.13) to enforce the condition $t_{\mathbf{n}} = 0$ on Γ_t in a strong sense.

One point we want to mention here is the following. Due to the local support property of NURBS and in case of regular parametrizations we can approximate $\mathbf{n}(x_1, x_2)$ around a point $P \in \Gamma_t$ by a constant vector $(c_1, c_2)^{\mathrm{T}} \approx \mathbf{n}(x_1, x_2)$. See Figure 33 for an illustration. This means for a basis NURB $N_{l\mathfrak{n}_1}$ non-vanishing at P we get the approximation relations

$$\tau_{h,l\mathfrak{n}_1} \approx \begin{bmatrix} c_1 & c_2 \\ c_2 & -c_1 \end{bmatrix} N_{l\mathfrak{n}_1}, \quad \tau_{h,l\mathfrak{n}_1+\mathfrak{n}_1\mathfrak{n}_2} \approx \begin{bmatrix} -c_2 & c_1 \\ c_1 & c_2 \end{bmatrix} N_{l\mathfrak{n}_1}, \quad \tau_{h,l\mathfrak{n}_1+2\mathfrak{n}_1\mathfrak{n}_2} \approx \begin{bmatrix} c_2^2 & -c_1c_2 \\ -c_1c_2 & c_1^2 \end{bmatrix} N_{l\mathfrak{n}_1}.$$

Hence, the modified basis can be approximated just by a linear combination of the non-modified functions. This suggests the feasibility of the modification approach especially for fine enough meshes to enforce the mentioned traction boundary conditions.

Here we concentrated so far on a very special case with $\Gamma_t = \Gamma_2$ (see Figure 32). However, the next remarks and examples explain, why more general situations can be handled, too. Below we follow the isoparametric paradigm, meaning we use NURBS for the basis function definitions and take into account possible weight functions needed for the parametrizations; see Definition 6.6.

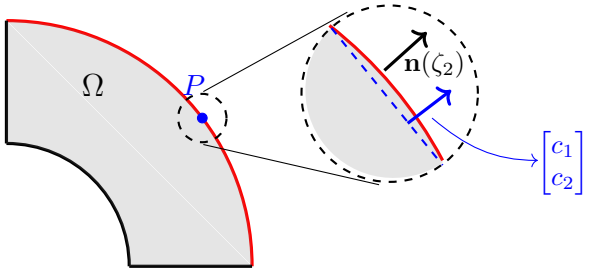

Figure 33: If we have a piece-wise smooth boundary we can approximate small boundary parts using straight lines. By the continuity, the normal vector changes only slightly in a suitable neighborhood of point P away from the corners. In particular it can be approximated around P by a suitable constant vector $(c_1, c_2)^{\mathrm{T}}$. This means for decreasing mesh size the modified local basis functions $\tilde{\tau}_{h,i}$ converge to linear combinations of the unmodified ones.

Yet, we would like to start with a test example that corresponds to the specific case mentioned in the above explanations.

Example 9.4 (Quarter ring with free edge)**.** *As a first numerical test we again consider a quarter ring domain, where the inner and outer radii are* 1 *and* 2*. Further, as in Figure 32 we suppose a zero traction force on* $\boxed{\Gamma_t = \Gamma_2}$*, together with a load mapping* $\boxed{f = (1,0)^{\mathrm{T}}}$ *and material parameters* $\boxed{\lambda = 20, \mu = 1}$*. On the rest of the boundary* $\partial\Omega \backslash \Gamma_t$ *we assume zero displacements and for the discretization we choose*

$$\boxed{q_i = 3,\ p_i = 2,\ s_i = 1,\ r_i = 1,\ \forall i \quad \text{and} \quad \theta = h = 1/9}$$

in the sense of Assumption 9.1. This means we use for the mixed formulation the same mesh for stresses and displacements; see Figure 34 (a). To have a comparative solution we solve this test problem twice. Once with the mixed formulation (9.2.12)-(9.2.13) *with strong symmetry combined with the basis modification approach from above; i.e. we use the FE stress space of the form* (9.2.23)*. And one time with the standard primal formulation which is pre-implemented in the GeoPDEs package [73]. For the latter we utilize a fine tensor Bézier mesh of* 25×25 *subdivisions and for the displacement variable we use continuous NURBS of degree* 4*. The corresponding mesh is shown in Figure 34 (b).*

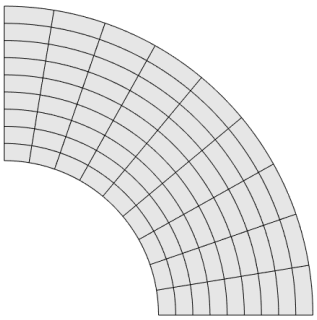

(a) mesh for mixed formulation

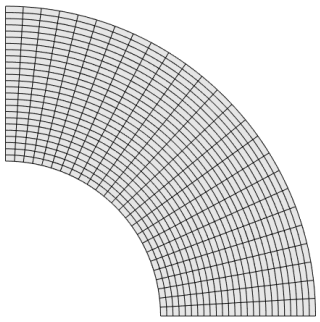

(b) mesh for primal formulation

Figure 34: In Examples 9.4 and 9.5 we utilize for the mixed weak formulation the mesh structure on the left ($h = 1/9$), whereas to generate a comparative solution we use for the primal elasticity formulation the fine mesh on the right ($h = 1/25$).

The results are summarized in Figure 35 in which we compare the primal and mixed formulation. Although we have a relative coarse mesh and low degrees for the mixed ansatz, we obtain very similar displacements. Also the stresses are broadly similar. Only at the vertices one observes a deviation. But this is explicable since in the vertices on the outer radius we expect singular stress values. Therefore, we see for the primal formulation a locally oscillatory behavior of the stresses at the mentioned vertices. Further the zero traction condition is only applied weakly for the primal ansatz. In contrast to that the mixed form seeks for stresses which fulfill the mentioned condition strongly. This leads to a smoothing effect and we do not see a comparable blow up of the stress values at the corners. However, the weakly enforced zero displacement in the mixed formulation leads to non-vanishing u at the vertices. Nevertheless, we think this example demonstrates the possibility of the stress basis modification for the implementation of traction boundary conditions.

After this first test regarding traction boundary conditions we have to address several arising questions, especially respecting generalizations. This shall be done by means of the next remarks and examples.

Remark 9.3 (**Zero traction on several edges**). At first glance there seems to be no problem to transfer the basis modification to a situation with several involved edges by a edge-wise procedure. Though, if there is a vertex P_c adjacent to two zero traction edges in Γ_t we get an additional requirement for the stresses at P_c; see Figure 36. Namely, by regularity of the parametrization the normal vectors $\mathbf{n}^L$, $\mathbf{n}^R$ defined by the two meeting edges are not linearly dependent at the vertex P_c and hence we can conclude:

$$\sigma \cdot \mathbf{n}^L \stackrel{!}{=} 0 \quad \text{and} \quad \sigma \cdot \mathbf{n}^R \stackrel{!}{=} 0 \quad \Longrightarrow \quad \sigma = 0 \text{ at } P_c,$$

if we assume continuous stresses. One notes the piece-wise smoothness of the IGA basis functions. Thus, if we have vertices being part of two edges in Γ_t one drops before the basis modification all stress basis functions which do not vanish at theses vertices. For example, let P_c correspond to the left top corner of the ring domain discussed above and assume $\overline{\Gamma_t} = \overline{\Gamma_1 \cup \Gamma_2 \cup \Gamma_4}$ as shown in Figure 36. Then supposing zero traction on Γ_t implies vanishing stresses at P_c in the discrete setting.

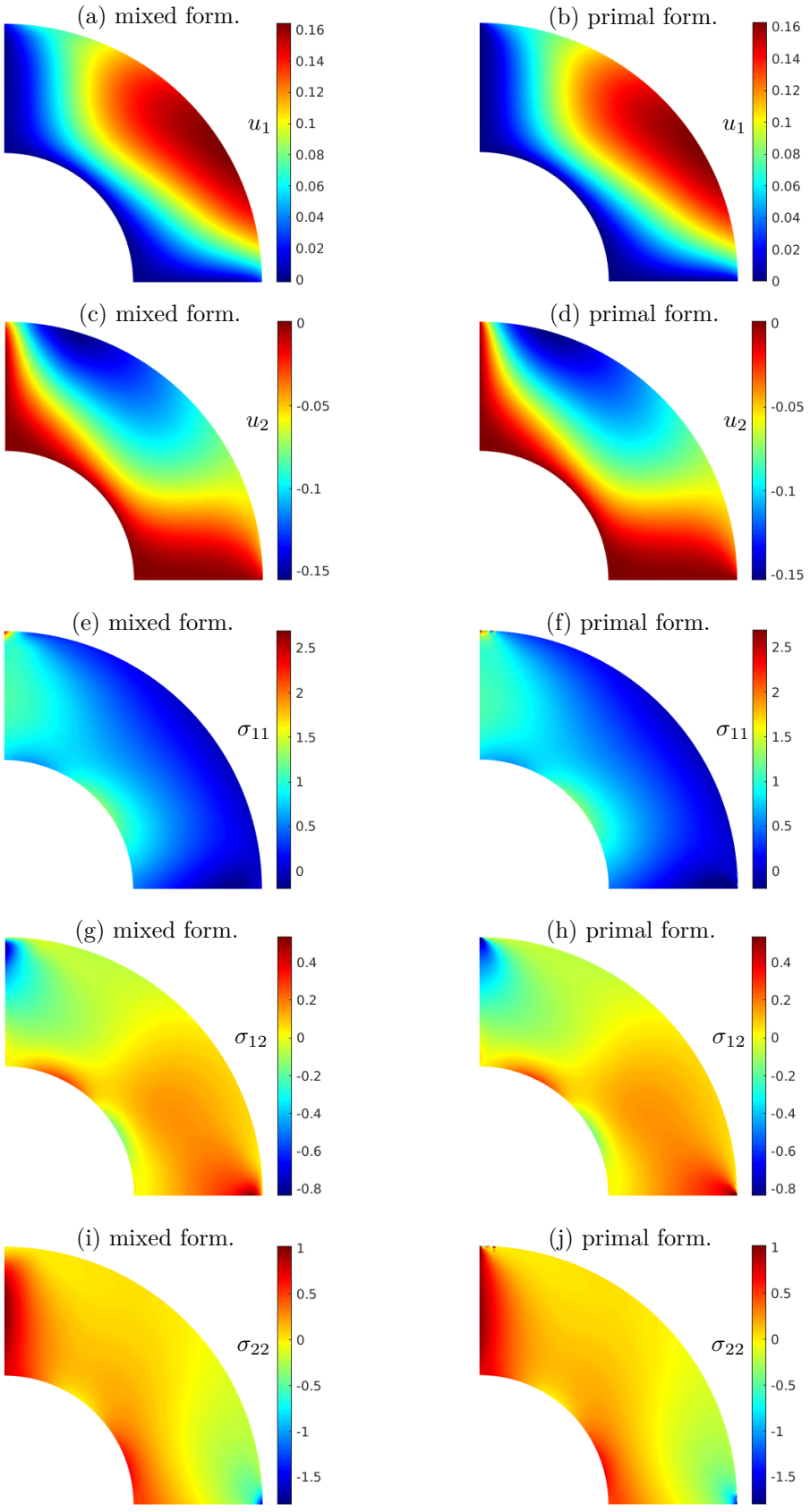

Figure 35: Here we see the comparison between the mixed weak formulation with the basis modification approach (left) and the results of the standard primal formulation implemented in GeoPDEs [73] (right). Up to deviations at the corners, we obtain very similar results.

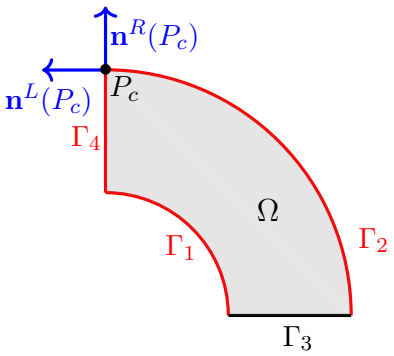

Figure 36: In Example 9.5 we have zero traction condition on three of four edges, namely $\overline{\Gamma_t} = \overline{\Gamma_1 \cup \Gamma_2 \cup \Gamma_4}$. Due to the piece-wise smoothness of the test functions the stresses have to vanish at the left two vertices.

Example 9.5 (Quarter ring with three free edges)**.** *We consider a similar numerical test like in Example 9.4. We only change two things. On the one hand, the traction boundary part is now* $\boxed{\overline{\Gamma_t} = \overline{\Gamma_1 \cup \Gamma_2 \cup \Gamma_4}}$*. And on the other hand, we have here a constant source* $\boxed{f = (0.05, 0.05)^{\mathrm{T}}}$*. Using the mixed and the primal formulation we obtain the deformed rings in Figure 37. For both approaches we obtain similar deformations and away from the bottom vertices also the stress magnitudes fit. So we get reasonable results also if* Γ_t *is composed of multiple edges.*

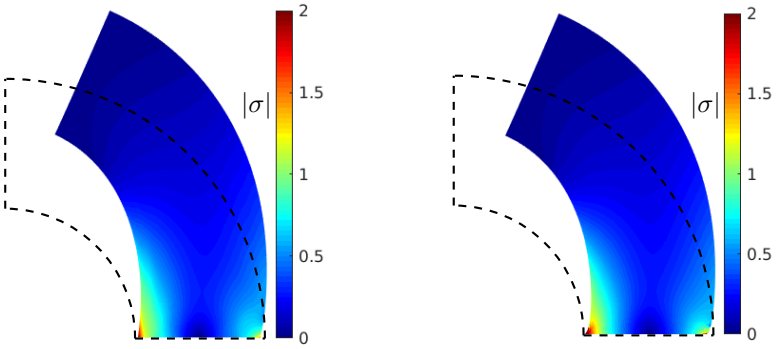

(a) mixed form. (b) primal form.

Figure 37: Here we see the deformed ring domains for the mixed formulation on the left and as a comparative solution the deformation obtained by the primal formulation on the right. The coloring is according to the stress magnitude $|\sigma| = \sqrt{\sigma_{11}^2 + 2\sigma_{12}^2 + \sigma_{22}^2}$.

Remark 9.4 (**Zero traction condition for multi-patch domains**). With no difficulties it is possible to utilize the basis modification approach in the context of a multi-patch domain. The continuous coupling of the patches as we consider for the strong symmetry mixed formulation has to be taken into account. This means, analogous to the previous remark we can set the stress to zero at boundary vertices which are part of two meeting traction edges in Γ_t if the two normal vectors in the vertex determined by the two edges are linearly independent. Whereas if the outer normal vector varies continuously in a whole neighborhood of a vertex point we only adapt the basis functions for the stresses without setting all the stress components to zero. Such a situation of a multi-patch domain with a globally smooth boundary is part of the next example.

Example 9.6 (Ring with free outer boundary)**.** *We have a 4-patch ring domain as shown in Figure 38 (a). Further we suppose the outer boundary to be free endowed with a zero traction*

condition, and the inner boundary circle is fixed with $u = 0$. *For the mesh in Figure 38 (b) and the choices*

$$q_i = 3,\ p_i = 2,\ s_i = 1,\ r_i = 1,\ \forall i, \quad h = \theta \quad \text{and} \quad \lambda = 20,\ \mu = 1,\ f = (0,1)^{\mathrm{T}}$$

we get with the mixed weak formulation the displacements in the left column of Figure 39. In the right column of the latter figure we show the displacements computed by the primal formulation with C^0*-regular degree* 4 *NURBS in a refined mesh. The latter is obtained by a halving of the mesh elements from Figure 38 (b). Both methods lead to nearly the same displacement approximate field.*

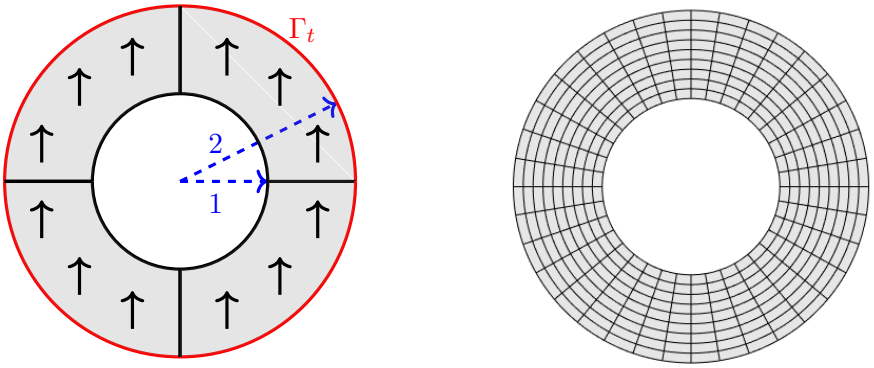

(a) 4-patch geometry

(b) Mesh for σ and u

Figure 38: On the left the 4-patch ring domain with a highlighted boundary part Γ_t is shown. The black arrows indicate the underlying source function $f = (0, 1)$ for Example 9.6. On the right the mesh utilized for the mixed method is displayed.

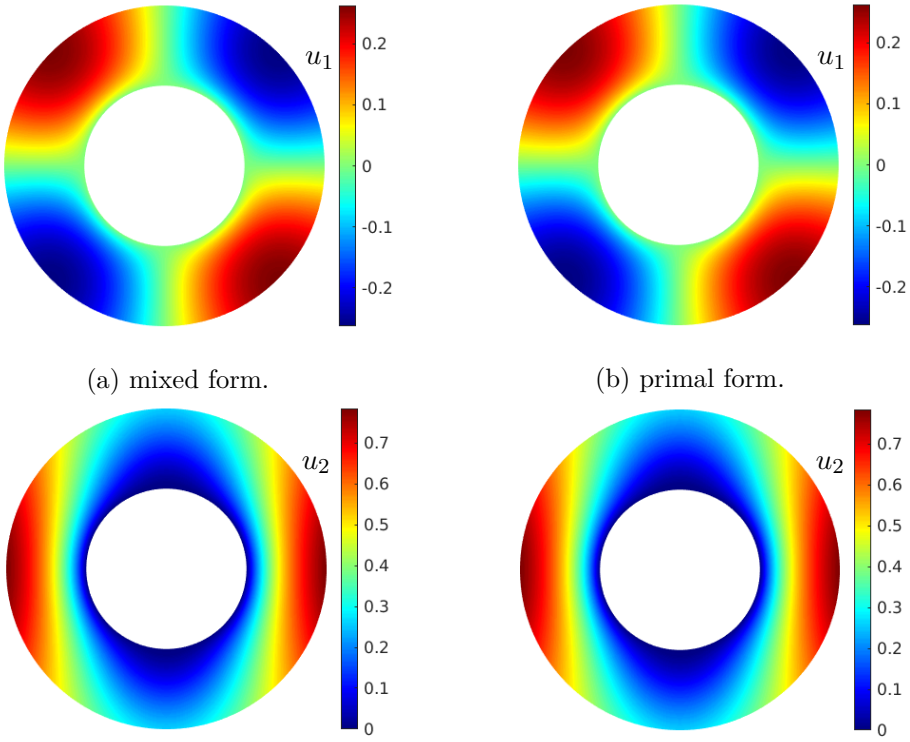

(a) mixed form. (b) primal form.

(c) mixed form. (d) primal form.

Figure 39: Here we see the similarity of the displacements between the mixed method with strong symmetry (combined with the modified basis explained above) and the primal formulation for Example 9.6. To obtain a meaningful comparative solution we halved the mesh size compared to the mesh in Figure 38 and utilized C^0 NURBS of degree 4 to get the results on the right.

Remark 9.5 (**Non-trivial** Γ_t). For simplicity, we only considered the boundary conditions in the case where Γ_t is composed of multiple whole edges. However, it is evident that, in terms of applications, Γ_t can also consist of different sub-sections of the boundary. In principle, it is reasonable to assume, for the sake of implementation simplification, that Γ_t consists of full boundary mesh facets. The latter is a natural assumption in the context of IGA. By doing so, we can proceed in at least two ways. Firstly, the mesh elements themselves can be interpreted and considered as patches, and Γ_t can be easily defined as the union of full mesh edges in a suitable multi-patch geometry. In this case, we already know how to incorporate the corresponding zero traction conditions. Secondly, the modifications for stresses can be performed only for those basis functions that are non-zero on Γ_t. However, even though the latter approach seems reasonable, we have not further investigated it and only mention it here for the sake of completeness.

Remark 9.6 (**Non-zero traction forces**). As already mentioned at the beginning of Section 9.2.2, many traction boundary conditions can be reduced to zero traction. However, it should be noted that in the case of non-smooth traction forces or piecewise defined traction forces, it is often not possible to enforce them exactly. Also due to the symmetry of the stress tensor, non-continuous stress values might implied, which cannot be reproduced by the continuous NURBS we are using. One way to handle this problem would be to approximate and replace $\tilde{\sigma}$ with a smoother version $\tilde{\sigma}_h$ based on the NURBS basis functions. In this case, an L2 projection approach might be used, for example.

A situation with non-zero traction forces arises in the context of the famous *Cook's membrane* (see e.g. [13, Section 5.3]) test case. We address this problem in a further numerical example,

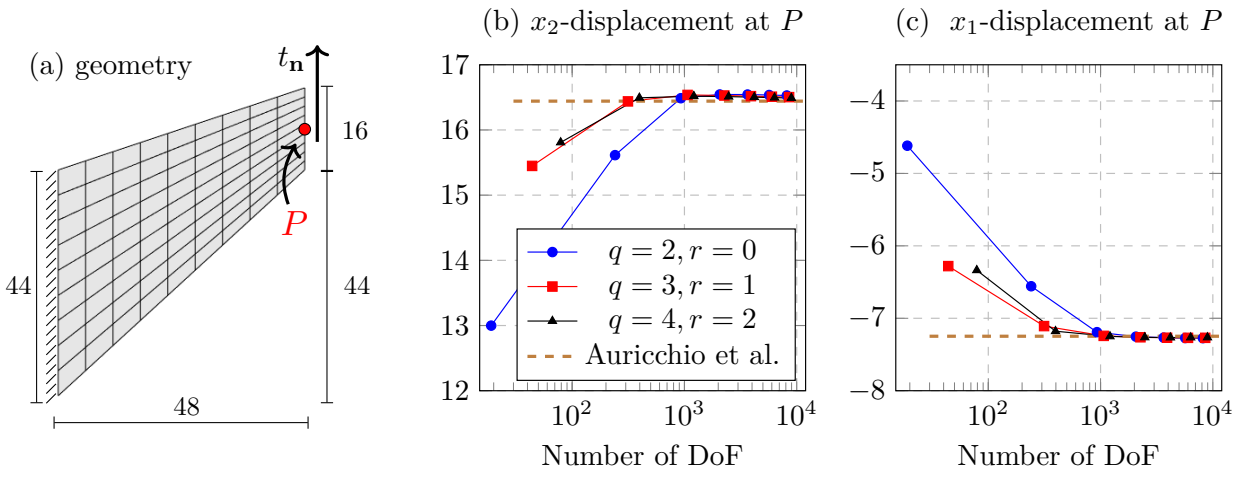

Figure 40: The standard Cook's membrane test case is shown here for the mixed weak form with strong symmetry, where the basis functions are modified according to the procedure at the beginning of this section. We observe a good accordance to the reference values taken from [13].

below.

Example 9.7 (Cook's membrane)**.** *As a final numerical test regarding traction boundary conditions for the mixed formulation with strong symmetry, we would like to consider the classical example of Cook's membrane, for two reasons. Firstly, to demonstrate the possibility of considering non-vanishing and non-smooth traction forces. Secondly, the example showcases the stability of the mixed formulation for the incompressible limit case, where we set* $\boxed{\lambda = +\infty \text{ and } \mu = 0.375}$*. Here, we orient ourselves towards the experiment [13, Section 5.3]. We use a bilinear parametrization to define the membrane in Figure 40 (a) . This means we see in the mentioned figure the mesh for* $h = 1/9$*. Only the left boundary of the domain is fixed and on the top and bottom boundary parts we have zero traction. But on the right edge we apply a tangential traction force* $\boxed{t_{\mathbf{n}} = (0, 1/16)^{\mathrm{T}}}$*. Furthermore, in view of Assumption 9.1, let*

$$\boxed{q_i = q = p + 1,\ p_i = p,\ s_i = p - 1,\ r_i = p - 1,\ \forall i, \quad h = \theta \ \text{ and } \quad f = (0, 0)^{\mathrm{T}}}.$$

Hence, we follow a mixed degrees ansatz and use the same mesh for stress and displacement computations.
Then, we obtain at the highlighted point $P = (48, 52)^{\mathrm{T}}$ *displacements which tend to the reference solution from [13, Section 5.3]. In particular, our ansatz to enforce traction BC does not lead to locking effects here. Additionally, we added in Figure 41 example plots for the stresses* σ_{12}*,* σ_{22} *and illustrated the deformation.*

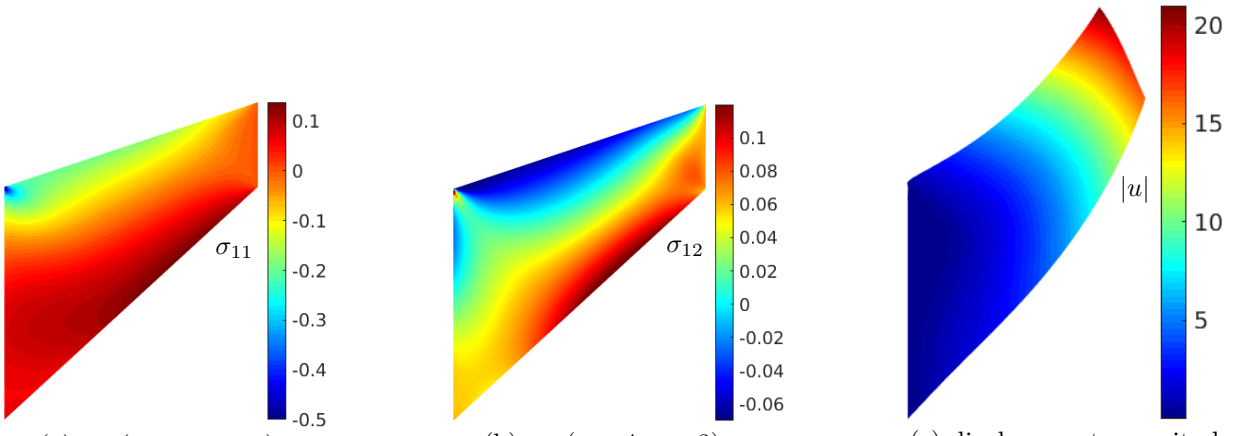

(a) $\sigma_{11}(q = 4, p = 3)$ (b) $\sigma_{12}(q = 4, p = 3)$ (c) displacement magnitude

Figure 41: For the shown stresses and deformation we have the underlying degrees $q = 4$, $p = 3$ and the regularities are $r = s = 2$. The corresponding parametric mesh consists of 24^2 equal square.

9.2.3 Stability in the (nearly) incompressible regime

Within the context of an isotropic elastic material, we have already mentioned the two Lamé parameters λ and μ, which determine the compliance tensor A; see (9.2.7). A special case is represented by (almost) incompressible materials, which correspond to large values of λ. An important motivation for considering mixed formulations is to obtain reasonable approximate solutions even for this regime. Therefore, we aim to demonstrate here that we can achieve stability for $\lambda \to \infty$ with our discretization approach, at least in the case of NURBS parameterizations.

To establish the latter, we follow the reasoning of Arnold et al. in [7] and make use of [20, 66]. Furthermore, we assume the discrete IGA spaces $(\mathscr{V}_h^{n-1}, \mathscr{V}_\theta^n)$ to define a well-posed discretization of the modified mixed weak formulation (9.2.12)-(9.2.13), meaning we obtain a quasi-optimal error estimate

$$\|u - u_\theta\| + \|\sigma - \sigma_h\|_{H(\nabla\cdot)} \leq C_{QO}\Big(\inf_{\tau_h \in \mathscr{V}_h^{n-1},\ v_\theta \in \mathscr{V}_\theta^n} \|u - v_\theta\| + \|\sigma - \tau_h\|_{H(\nabla\cdot)} \Big),$$

similar to Lemma 2.12. But, this means that a certain constant C_{QO} appears. As can be observed in the proof of the mentioned lemma, C_{QO} depends on the global inf-sup condition, cf. (9.2.18), and on the continuity constant of the underlying bilinear form

$$\mathcal{B}^m\Big((\sigma, u), (\tau, v)\Big) \coloneqq \langle \sigma, \tau \rangle_{\mathscr{A}} - \langle u, \nabla \cdot \tau \rangle - \langle \nabla \cdot \sigma, v \rangle.$$

Thus the constant C_{QO} might depend on various quantities, e.g. $\Omega, \mathbf{F}, \mathbf{J}$, etc. However, to ensure stable convergence behavior with respect to λ, we must verify whether we can choose C_{QO} independently of λ.

Due to the estimate

$$\langle \sigma, \tau \rangle_{\mathscr{A}} = \langle A\sigma, \tau \rangle + \langle \nabla \cdot \sigma, \nabla \cdot \tau \rangle \leq \frac{1}{\mu} \|\sigma\| \, \|\tau\| + \|\nabla \cdot \sigma\| \, \|\nabla \cdot \tau\|, \quad \forall \sigma, \tau \in H(\Omega, \nabla\cdot, \mathbb{M}),$$

we see directly that the continuity constant of the bilinear form $\mathcal{B}^m$ does not depend on λ. Hence, it is enough to look at the inf-sup value C_{IS}^m from (9.2.18).

Using [7] we explain briefly why we get stability for the case of homogeneous Dirichlet boundary condition if the identity tensor is part of the discrete space, i.e. $\mathrm{I} \in \mathscr{V}_h^{n-1}$. There is no difficulty to see that we get λ-stability if the coercivity of the bilinear form

$$\mathfrak{a}(\sigma, \tau) \coloneqq \langle \sigma, \tau \rangle_{\mathscr{A}}$$

does not depend on λ. This is clear by the saddle-point structure of (9.2.12)-(9.2.13) and the fact that $\mathfrak{b}(\tau, v) \coloneqq \langle v, \nabla \cdot v\rangle$ is independent of material parameters. On the one hand, the first equation of the mixed system (9.2.12) yields in the discrete setting

$$\langle \sigma_h, \mathrm{I}\rangle_{\mathscr{A}} = \langle A\sigma_h, \mathrm{I}\rangle = \frac{1}{2\mu}\Big(1 - \frac{n\lambda}{n\lambda + 2\mu}\Big)\int_\Omega \mathrm{tr}(\sigma_h)\, dx = 0, \quad \forall \sigma_h \in \mathscr{V}_h^{n-1},$$

if we set $\tau_h = \mathrm{I}$. Hence we have $\int_\Omega \mathrm{tr}(\sigma_h)\mathrm{d}x = 0$ and it is justified to use in the numerical computations the spaces

$$\mathscr{V}_{h,\mathrm{tr}}^{n-1} \coloneqq \mathscr{V}_h^{n-1} \cap \Big\{\tau \;\Big|\; \int_\Omega \mathrm{tr}(\tau)\, dx = 0\Big\}$$

to seek for the solution. Clearly, the trace mean vanishes also in the continuous case.
Let us denote with $\mathrm{dev}(\sigma_h)$ the deviatoric part[19] of σ_h. On the other hand, if we apply now [20, Bemerkung 5.3 and Hilfssatz 5.4 in Chapter VI] one gets a constant $\tilde{C}$ only dependent on the domain Ω s.t.

$$\begin{aligned}\langle \sigma_h, \sigma_h\rangle_{\mathscr{A}} &= \langle A\sigma_h, \sigma_h\rangle + \langle \nabla\cdot\sigma_h, \nabla\cdot\sigma_h\rangle \\ &\geq \frac{1}{2\mu}\left\|\mathrm{dev}(\sigma_h)\right\|^2 + \frac{1}{2}\left\|\nabla\cdot\sigma_h\right\|^2 + \frac{1}{2}\left\|\nabla\cdot\sigma_h\right\|^2 \\ &\geq \tilde{C}\min\Big\{\frac{1}{2\mu}, \frac{1}{2}\Big\}\left\|\sigma_h\right\|^2 + \frac{1}{2}\left\|\nabla\cdot\sigma_h\right\|^2, \quad \text{for all } \ \sigma_h \in \mathscr{V}_{h,\mathrm{tr}}^{n-1}.\end{aligned}$$

Remark 9.7. The proof and derivations in [20, Bemerkung 5.3 and Hilfssatz 5.4 in Chapter VI] are given for the $2D$ case. However, using completely analogous steps lead to the same results in $3D$.

In particular, we can choose a coercivity constant for $\mathfrak{a}$ independent of λ. Consequently, utilizing $\mathscr{V}_{h,\mathrm{tr}}^{n-1}$ and following the isoparametric paradigm, we obtain stability in the (nearly) incompressible regime.

Corollary 9.3. *Let $(\mathscr{V}_h^{n-1}, \mathscr{V}_\theta^n)_\theta$, where $h = h(\theta)$, be a well-posed IGA discretization of* (9.2.12)-(9.2.13) *following the isoparametric paradigm, meaning $\mathrm{I} \in \mathscr{V}_h^{n-1}$. Then, if we use $\mathscr{V}_{h,\mathrm{tr}}^{n-1}$ instead of $\mathscr{V}_h^{n-1}$, we get a well-posed discretization which is stable w.r.t. λ.*

The scenario involving non-zero u_D can be effectively managed by initially solving the original problem within the space $\mathscr{V}_{h,\mathrm{tr}}^{n-1}$. Subsequently, to the obtained solution σ_h we add the term $c\mathrm{I}$, where the constant c is determined by the first equation of the mixed formulation, specifically through the equation:

$$\langle A(\sigma_h + c\mathrm{I}), \mathrm{I}\rangle \overset{!}{=} \langle \mathrm{I}\cdot\mathbf{n}, u_D\rangle_\Gamma, \quad \text{(see Remark 9.2)}.$$

Another point is the incompressibility stability for mixed boundary conditions. Below we follow the steps in [20] and [66] to comment on the case of non-vanishing, open traction part Γ_t. Let us assume discrete spaces $\tilde{\mathscr{V}}_{h,\Gamma_t}^1 \subset H_{\Gamma_t}(\Omega, \nabla\cdot, \mathbb{S})$ and $\sigma_h \in \tilde{\mathscr{V}}_{h,\Gamma_t}^1$. It is well-known (see e.g. [58] or [46, Appendix]) that there exists a

$$w \in H^1_{\Gamma_D}(\Omega)\otimes\mathbb{R}^n \coloneqq \{v \in H^1(\Omega)\otimes\mathbb{R}^n \mid v = 0 \text{ on } \Gamma_D \coloneqq \partial\Omega\backslash\Gamma_t\}^{20}$$

s.t.

$$\nabla\cdot w = \mathrm{tr}(\sigma_h), \quad \text{and} \quad \left\|w\right\|_{H^1} \leq C\left\|\mathrm{tr}(\sigma_h)\right\|,$$

[19] We have the relation $\sigma = \frac{1}{n}\mathrm{tr}(\sigma)\mathrm{I} + \mathrm{dev}(\sigma)$.
[20] The boundary conditions are meant in the sense of the trace theorem.

where C is a constant depending on Ω, Γ_t and Γ_D. Therefore, we can estimate

$$\begin{aligned}\frac{1}{n}\left\|\operatorname{tr}(\sigma_h)\right\|^2 &= \frac{1}{n}\langle \operatorname{tr}(\sigma_h), \nabla\cdot w\rangle = \langle \sigma_h - \operatorname{dev}(\sigma_h), \nabla w\rangle \\ &= \langle \nabla\cdot\sigma_h, w\rangle - \langle \operatorname{dev}(\sigma_h), \nabla w\rangle \\ &\leq \left\|\nabla\cdot\sigma_h\right\| \left\|w\right\| + \left\|\operatorname{dev}(\sigma_h)\right\| \left\|w\right\|_{H^1} \\ &\leq C\Big(\left\|\nabla\cdot\sigma_h\right\| \left\|\operatorname{tr}(\sigma_h)\right\| + \left\|\operatorname{dev}(\sigma_h)\right\| \left\|\operatorname{tr}(\sigma_h)\right\| \Big). \end{aligned} \tag{9.2.24}$$

Hence, it holds

$$\left\|\operatorname{tr}(\sigma_h)\right\|^2 \leq \tilde{C}\Big(\left\|\nabla\cdot\sigma_h\right\|^2 + \left\|\operatorname{dev}(\sigma_h)\right\|^2 \Big), \tag{9.2.25}$$

with a $\tilde{C}$ independent of λ. Set $c \coloneqq \max\{\frac{1}{2\mu}, 1\}$. In view of [20, (5.14) in Chapter VI], which shows us $2\mu\langle A\sigma_h, \sigma_h\rangle \geq \left\|\operatorname{dev}(\sigma_h)\right\|^2$, and using (9.2.25) we obtain

$$\begin{aligned}\langle \sigma_h, \sigma_h\rangle_{\mathscr{A}} = \langle A\sigma_h, \sigma_h\rangle + \left\|\nabla\cdot\sigma_h\right\|^2 &\geq \frac{1}{2\mu}\left\|\operatorname{dev}(\sigma_h)\right\|^2 + \left\|\nabla\cdot\sigma_h\right\|^2 \\ &\geq \frac{1}{4\mu}\left\|\operatorname{dev}(\sigma_h)\right\|^2 + \frac{1}{4\mu c}\left\|\operatorname{dev}(\sigma_h)\right\|^2 + \left\|\nabla\cdot\sigma_h\right\|^2 \\ &\geq \frac{1}{4\mu}\left\|\operatorname{dev}(\sigma_h)\right\|^2 + \frac{1}{4\mu c}\Big(\frac{1}{\tilde{C}}\left\|\operatorname{tr}(\sigma_h)\right\|^2 - \left\|\nabla\cdot\sigma_h\right\|^2\Big) + \left\|\nabla\cdot\sigma_h\right\|^2 \\ &\geq \frac{1}{4\mu}\left\|\operatorname{dev}(\sigma_h)\right\|^2 + \frac{1}{4\mu c\tilde{C}}\left\|\operatorname{tr}(\sigma_h)\right\|^2 + \frac{1}{2}\left\|\nabla\cdot\sigma_h\right\|^2 \\ &\geq C_1\Big(\left\|\operatorname{dev}(\sigma_h)\right\| + \left\|\operatorname{tr}(\sigma_h)\right\|\Big)^2 + \frac{1}{2}\left\|\nabla\cdot\sigma_h\right\|^2 \\ &\geq C_2\left\|\sigma_h\right\|^2_{H(\nabla\cdot)}, \end{aligned}$$

where C_1, C_2 do not depend on λ. So, in the case of mixed boundary conditions, the stability with respect to the parameter λ is ensured. One can recognize that a difficulty arises here. Namely, for mixed boundary conditions, we have not provided proofs of well-posedness. Only various numerical experiments indicate the validity of analogous well-posedness statements as in the case of $\Gamma_t = \emptyset$. Nevertheless, we have mentioned a few words here regarding stability in the incompressible limit, as we intended to emphasize the following. As long as we possess a conforming well-posed discretization of the modified mixed weak form (with or without traction boundary conditions), we automatically achieve stability concerning the Lamé parameter λ. This interesting property is certainly a significant motivation for delving into such a formulation.

Further, we would like to mention that the example of Cook's membrane (Example 9.7) for the limit case $\lambda = \infty$ has already suggested the absence of locking. Since this example involves traction forces, for the sake of completeness, we would like to attach a simple stability test for homogeneous displacement boundary conditions.

Example 9.8 (Stability test)**.** *We do a stability test inspired by [63, Section 7.2] applied to the mixed weak form* (9.2.12)-(9.2.13)*. To be more precise we assume* $\mathbf{F} = \mathrm{id}$*, i.e. we work in the parametric domain and the source function* f *is chosen such that we get the exact displacement* $\boxed{u = (u_1, u_2)^{\mathrm{T}}}$ *with*

$$\boxed{\begin{aligned} u_1(x_1, x_2) &= (\cos(2\pi x_1) - 1)\sin(2\pi x_2) + v(x_1, x_2), \\ u_2(x_1, x_2) &= (1 - \cos(2\pi x_2))\sin(2\pi x_1) + v(x_1, x_2), \\ v(x_1, y_1) &= \sin(\pi x_1)\sin(\pi x_2)/(1+\lambda). \end{aligned}}$$

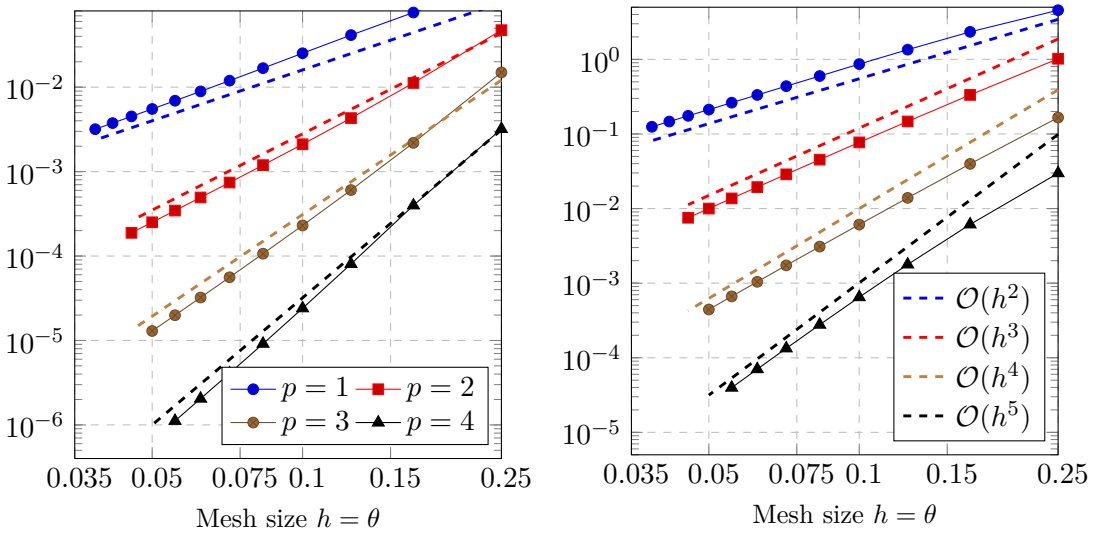

(a) $\|u - u_\theta\|$ $(\lambda = \infty, \mu = 1)$ (b) $\|\sigma - \sigma_h\|_{H(\nabla\cdot)}$ $(\lambda = \infty, \mu = 1)$

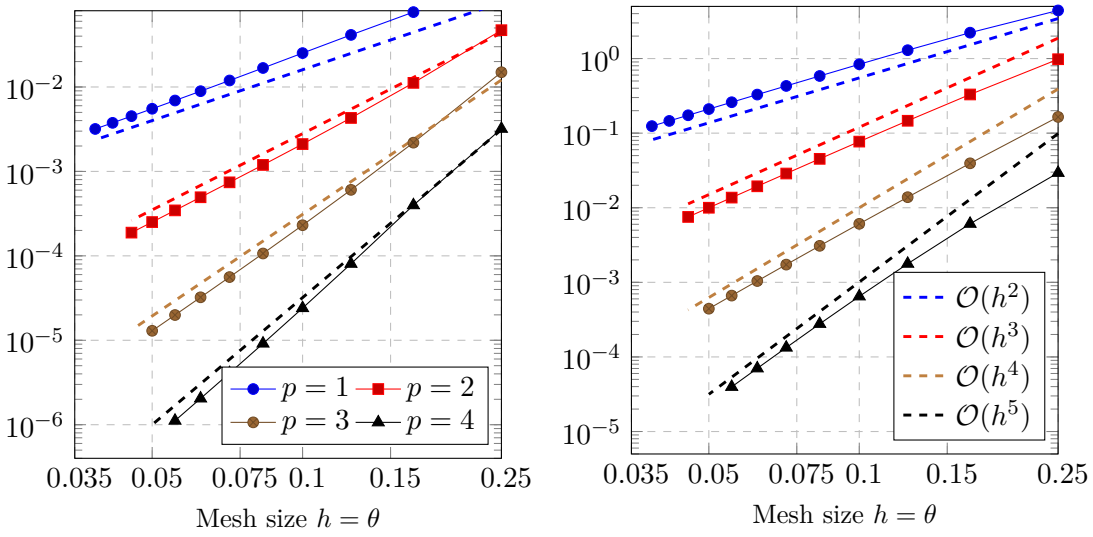

(c) $\|u - u_\theta\|$ $(\lambda = 2, \mu = 1)$ (d) $\|\sigma - \sigma_h\|_{H(\nabla\cdot)}$ $(\lambda = 2, \mu = 1)$

Figure 42: For our simple stability test we compute the errors twice. Once with $\lambda = \infty,\ \mu = 1$ (top row) and a second time setting $\lambda = 2,\ \mu = 1$ (bottom row). The similarity of the obtained errors confirm the theoretically predicted stability w.r.t. λ.

Again we use mixed degrees, meaning we consider (9.2.9)-(9.2.10) *with*

$$\boxed{q_i = p + 1,\ p_i = p,\ s_i = p - 1,\ r_i = p - 1,\ \forall i \quad \text{and} \quad h = \theta,\ \mu = 1}.$$

The results for uniform meshes are shown in Figure 42. In the top row of the mentioned figure we see the errors for the limit case $\boxed{\lambda = \infty}$*, whereas in the bottom row we plotted them for* $\boxed{\lambda = 2}$*. The images effectively demonstrate the stability with respect to* λ*. This is because the errors in Figure 42 (a)-(b) and Figure 42 (c)-(d) are nearly identical, particularly of the same order of magnitude. We also do not observe any blow-up or unstable decay.*

We have now demonstrated with various examples and remarks how we can apply the special setting from Section 8.2 within the framework of linear elasticity theory. Doing so we considered a modified mixed weak formulation equivalent to the well-known Hellinger–Reissner system. It is important to highlight that the underlying Hodge–Laplace problem is derived from the

elasticity complex, a second-order complex. So, the discretization in parametrized domains with curved boundaries is not straightforward. Even more crucial is the fact that we were able to utilize knowledge about the discretization of this complex in cubic geometries to formulate statements regarding well-posedness; see Theorem 8.2. Hence, although for the discretization of the modified saddle-point problem (compare (9.2.12)-(9.2.13)), we did not use structure-preserving discretizations in the sense of Section 3.4, we still exploited FEEC indirectly.

It is noticeable that in the numerical tests, we have always been working in a planar setting. But various aspects, including the stability with respect to the λ parameter, were also addressed for the three-dimensional ($3D$) case. Since the choice of discrete spaces in the three-dimensional space is analogous to the planar case, we do not see any difficulty in conducting similar numerical investigations in $3D$. However, one point requires more careful examination: the treatment of traction boundary conditions for $\Omega \subset \mathbb{R}^3$. In principle, it is conceivable to perform a modification of the basis functions similar to the explanations in Section 9.2.2 to incorporate these conditions more easily. Nevertheless, this modification will likely be different and more involved. However, we intend to explore other discretization approaches and will not delve further into the topic of traction boundary conditions for the strong symmetry formulation (9.2.12)-(9.2.13).

Above in the context of linear elasticity, we have dealt with a system very similar to the classical Hellinger–Reissner formulation, which means we directly incorporated the symmetry condition of the stress tensor into the definition of the discrete spaces. However, we have also become acquainted with another discretization approach in Section 8.3, which involves introducing an additional Lagrange multiplier. This is precisely the direction we are turning our attention to now because we want to demonstrate how we can also apply this second approach to linear elasticity. It is fair to highlight that the resulting *Hellinger–Reissner formulation with weakly imposed symmetry* is not novel and has been addressed, for instance, in [63, 7] and [10, 42]. Especially in the latter two references, the connection between the formulation and the elasticity complex has also been exploited. Whereas the mentioned works are in the tradition of classical Finite Elements, we want to show how the concept of IGA can be integrated. This will allow us to develop methods with smooth test functions and for domains with curved boundaries as well. While the approach and choice of spaces for the strong symmetry approach from above are similar in $2D$ and $3D$, for the weak symmetry approach, we obtain different results for $2D$ compared to $3D$. For this reason, we will provide in the subsequent discussions discretization details and numerical examples for both, the discretization in the $2D$ and $3D$ context.

9.3 Mixed weak formulation with weakly imposed symmetry

Before we exploit the connection between de Rham complexes and linear elasticity as established in [42, 10], we briefly explain the elasticity formulation with weakly imposed symmetry. It is basically a specific case for the Lagrange multiplier formulations for output complexes; see Section 4.2.4. Because, we already know that the Hellinger–Reissner formulation can be interpreted as the mixed weak form of the level n Hodge–Laplace problem corresponding to the elasticity complexes in n dimensions, which in turn are the BGG output complexes of proper de Rham sequences; see Examples 4.2 and 4.3. The new formulation which was e.g. introduced by Arnold et al. in [10] seeks for stresses in $H(\Omega, \nabla\cdot, \mathbb{M})$, $\mathbb{M} = \mathbb{R}^{n\times n}$. That means we have more flexibility in the selection of the FE spaces. Even though we are initially considering only the case of displacement boundary conditions ($u = u_D$ on $\partial\Omega$), it will become relatively straightforward to later address traction boundary conditions as well.

To be more precise, the underlying continuous formulation for this part is as follows:

Definition 9.2 (**Hellinger–Reissner formulation with weak symmetry**)**.** For a given $f \in L^2(\Omega) \otimes \mathbb{R}^n$, find $\sigma \in H(\Omega, \nabla\cdot, \mathbb{M})$, $u \in L^2(\Omega) \otimes \mathbb{R}^n$ *and* $\kappa \in L^2(\Omega) \otimes \mathbb{R}^{s(n)}$, $s(n) \coloneqq 2n-3$, *s.t.*

$$\begin{aligned} \langle A\sigma, \tau\rangle + \langle u, \nabla\cdot\tau\rangle + \langle \kappa, \operatorname{Skew}\tau\rangle &= \langle \tau\cdot\mathbf{n}, u_D\rangle_\Gamma, && \forall \tau \in H(\Omega, \nabla\cdot, \mathbb{M}), \\ \langle \nabla\cdot\sigma, v\rangle &= \langle -f, v\rangle, && \forall v \in L^2(\Omega)\otimes\mathbb{R}^n, \\ \langle \operatorname{Skew}\sigma, \eta\rangle &= 0, && \forall \eta \in L^2(\Omega)\otimes\mathbb{R}^{s(n)}, \end{aligned} \tag{9.3.1}$$

where

$$\operatorname{Skew}\tau \coloneqq \begin{cases} -2\operatorname{sskew}\tau, & \text{if } n=2, \\ 2\operatorname{vskew}\tau, & \text{if } n=3\ . \end{cases}$$

Hence, here we directly include the situation of displacement boundary conditions, meaning the right-hand side of the first line enforces $u = u_D$ on $\partial\Omega$; cf. Remark 9.2. Further, one notes, the system (9.3.1) is obtained by the Hellinger–Reissner formulation by dropping the symmetry condition for the stress tensor and replacing it by a variational statement, namely we assume

$$\langle \operatorname{Skew}\sigma, \eta\rangle = 0,\ \forall \eta \in L^2(\Omega)\otimes\mathbb{R}^{s(n)},$$

which is equivalent to

$$\int_\Omega \eta_i\,(\sigma_{ij} - \sigma_{ji})\,dx = 0, \quad \forall \eta_i \in L^2(\Omega),\ i \neq j.$$

The mentioned constraint is integrated using a Lagrange multiplier, clarifying the presence of the additional variable κ and the final line in (9.3.1). Notably, this novel variational problem fits with the abstract procedure for incorporating constraints from the linking maps, as elucidated in Section 4.2.4. The only difference is that we now have a weighted inner product $\langle A\sigma, \tau\rangle$ and in the first line of the system we have a term $+\langle u, \nabla\cdot\tau\rangle$ instead of $-\langle u, \nabla\cdot\tau\rangle$. As a result, especially by the well-posedness of the original Hellinger–Reissner formulation, one has the well-posedness of (9.3.1) and it yields the solution to (9.2.3)-(9.2.4); cf. [10, Section 1].

Regarding discretizations, we want to utilize next the approach from Section 5.3. To provide a better overview and in view of the mentioned section, we include here two diagrams, before we come to the details and specific FE spaces. On one hand, in Figure 43 and Figure 44 we observe the relevant spaces in the continuous setting analogous to Figure 5. On the other hand, as a kind of preview or outlook, we have incorporated in the mentioned figures the discrete spaces and projections that we aim to introduce in the following. For the definition of the different linking maps we refer to Examples 4.2 and 4.3.

Remark 9.8. Due to the anti-commutativity property of the linking maps from Examples 4.2 and 4.3 the corresponding linking maps in the Figures 43 and 44 are well-defined and ensure the consistency of the diagrams.

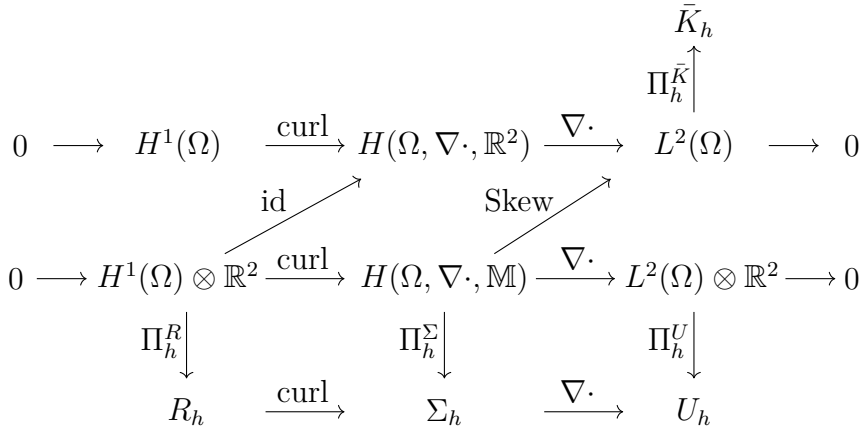

Figure 43: The relevant discrete spaces in $2D$.

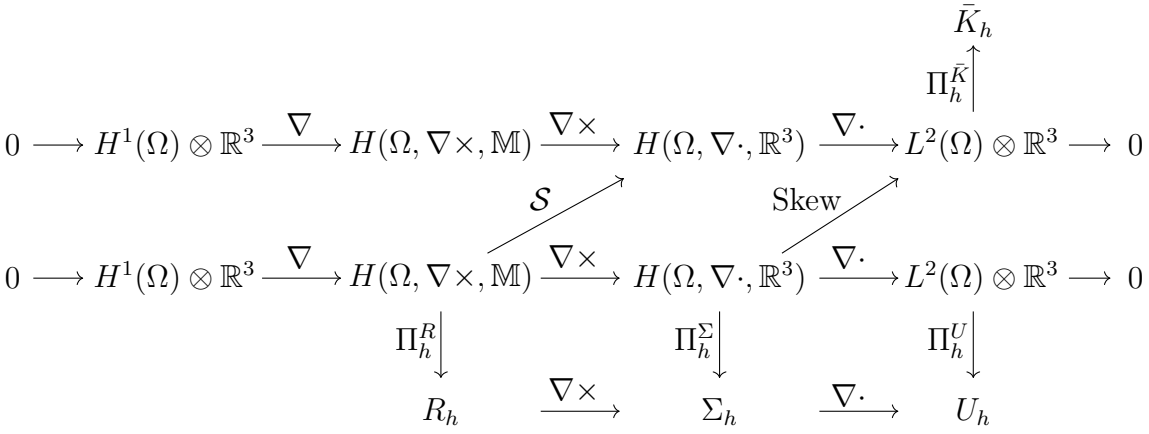

Figure 44: The relevant spaces in $3D$. One notes the special linking map $\mathcal{S}$ which appears in Example 4.3.

Looking back at Lemma 5.5, it becomes evident how the R_h, Σ_h, U_h spaces in the previous diagrams have to be chosen. Namely, we need structure-preserving discretizations of the respective bottom complexes. But since we only have vector-valued de Rham complexes appearing it is clear how to define the discrete spaces. We just use row-wise isogeometric discrete differential forms; see Section 7.3. Even more, it becomes apparent that the diagrams correspond to special cases of the general diagram (8.3.3) in Section 8.3.1. Because, the complex couplings in the above Figures 43 and 44 align with the BGG construction of Alt^k-valued forms in Section 4.2.3. Using special proxy maps (see Examples 3.1 and 3.2) yield then the proxy de Rham sequences in Figure 43 and Figure 44. This is also clear by the diagrams stated in Examples 4.2 and 4.3. So we could follow the elaborations in Sections 8.3 to get suitable R_h, Σ_h, U_h and to get error estimates. In fact, this is what we actually will do for the $3D$ situation. However, we also want to demonstrate that in the planar setting a different and somewhat better choice of spaces is possible. Next we address the precise selection of discrete spaces including the Lagrange multipliers.

We emphasize that we have for the subsequent investigations Assumption 8.2 underlying, i.e. we have a C^1-diffeomorphic parametrization $\mathbf{F}\colon (0,1)^n \to \Omega$ of the computational domain.
As the isogeometric de Rham spaces $V_{h,2}^i$ and $V_{h,3}^i$ introduced in Example 7.3 result in discretizations that preserve the underlying structure of the de Rham sequences in both $2D$ and $3D$, it is natural to opt for the following choices of spaces, U_h, Σ_h, and $\bar{K}_h$, for the discretization of (σ, u, κ) in (9.3.1):

Definition 9.3 (**Choice of spaces**). *For $n \in \{2,3\}$ and $i = 0,\dots,n$ let $V^i_{h,n}(q,s)$ denote the discrete differential forms given in Example 7.3 for the case $p_i = q$ and $r_i = s$, $\forall i$.*
Then for $p-1 > r \geq 0$ together with abbreviations

$$W^1_h \coloneqq V^1_{h,3}(p+1,r), \quad W^2_h \coloneqq V^2_{h,3}(p+1,r), \quad W^3_h \coloneqq V^3_{h,3}(p+1,r), \quad \bar{W}^3_h \coloneqq V^0_{h,3}(p-1,r) \tag{9.3.2}$$

we set in the three-dimensional setting

$$\Sigma_h \coloneqq (W^2_h \times W^2_h \times W^2_h)^{\mathrm{T}}, \quad U_h \coloneqq (W^3_h \times W^3_h \times W^3_h)^{\mathrm{T}}, \quad \bar{K}_h \coloneqq (\bar{W}^3_h \times \bar{W}^3_h \times \bar{W}^3_h)^{\mathrm{T}}, \tag{9.3.3}$$

and

$$R_h \coloneqq (W^1_h \times W^1_h \times W^1_h)^{\mathrm{T}}, \tag{9.3.4}$$

where $(X \times \cdots \times X)^{\mathrm{T}}$ means that we have row-wise spaces X.
In two dimensions we assume $p > r+1 \geq 1$ and choose analogously

$$\Sigma_h \coloneqq \left(V^1_{h,2}(p,r) \times V^1_{h,2}(p,r)\right)^{\mathrm{T}}, \; U_h \coloneqq \left(V^2_{h,2}(p,r) \times V^2_{h,2}(p,r)\right)^{\mathrm{T}}, \; \bar{K}_h \coloneqq V^0_{h,2}(p-1,r), \tag{9.3.5}$$

and define the auxiliary space $R_h \coloneqq \left(V^0_{h,2}(p,r) \times V^0_{h,2}(p,r)\right)^{\mathrm{T}}$.

In contrast to $3D$ we consider in $2D$ maximal degree p, whereas in (9.3.2) there appears a $p+1$. It turns out that this change in $2D$ still leads to convergence and a well-posed scheme. This degree adaption step for the planar situation is inspired by the FE discretization approach in [7]. In other words we can save degrees of freedom (DoF) by omitting the degree elevation step needed in $3D$.
As in Section 8.3 we can define L^2-bounded projections onto the spaces from above by a row-wise exploitation of the de Rham cochain projections $\Pi^k_{h,n}$ defined through (7.3.2). Consequently, there are projections

$$\begin{gathered}\Pi^{\Sigma}_h \colon L^2(\Omega) \otimes \mathbb{M} \to \Sigma_h, \quad \Pi^{U}_h \colon L^2(\Omega) \otimes \mathbb{R}^n \to U_h, \quad \Pi^{\bar{K}}_h \colon L^2(\Omega) \otimes \mathbb{R}^{s(n)} \to \bar{K}_h, \\ \Pi^{R}_h \colon L^2(\Omega) \otimes \mathbb{M} \to R_h \; (3D), \quad \Pi^{R}_h \colon L^2(\Omega) \otimes \mathbb{R}^2 \to R_h \; (2D), \text{ respectively,}\end{gathered}$$

such that the lower two rows in Figure 43 ($2D$) and Figure 44 ($3D$) determine a commutative diagram and such that for $0 \leq l \leq p$ we have

$$\left\| w - \Pi^R_h w \right\| \leq C_R h^l \left\| w \right\|_{H^l}, \quad \left\| \sigma - \Pi^{\Sigma}_h \sigma \right\|_{H(\nabla\cdot)} \leq C_{\Sigma} h^l \left\| \sigma \right\|_{H^l(\nabla\cdot)}, \tag{9.3.6}$$

$$\left\| u - \Pi^U_h u \right\| \leq C_U h^l \left\| u \right\|_{H^l}, \quad \left\| \kappa - \Pi^{\bar{K}}_h \kappa \right\| \leq C_K h^l \left\| \kappa \right\|_{H^l}, \tag{9.3.7}$$

for proper constants C_R, C_{Σ}, C_U, C_K and provided enough regularity. To see the validity of these estimates we refer to Corollary 7.11.

Remark 9.9. Due to the increased degree $p+1$ for the left three spaces in (9.3.2) we can further see the possibility to set $l = p+1$ in the estimates regarding Π^R_h, Π^{Σ}_h, Π^U_h in $3D$.

After we clarified the spaces, it remains to check whether we obtain well-posed discretizations, where the finite-dimensional problem reads: *Find* $(\sigma_h, u_h, \kappa_h) \in (\Sigma_h, U_h, \bar{K}_h)$ s.t.

$$\begin{aligned}
&\langle A\sigma_h, \tau_h \rangle + \langle u_h, \nabla \cdot \tau_h \rangle + \langle \kappa_h, \operatorname{Skew} \tau_h \rangle = \langle \tau_h \cdot \mathbf{n}, u_D \rangle_{\Gamma}, && \forall \tau_h \in \Sigma_h, \\
&\langle \nabla \cdot \sigma_h, v_h \rangle = \langle -f, v_h \rangle, && \forall v_h \in U_h, \\
&\langle \operatorname{Skew} \sigma_h, \eta_h \rangle = 0, && \forall \eta_h \in \bar{K}_h.
\end{aligned} \tag{9.3.8}$$

The matter of achieving a well-posed discretization in the context of three dimensions is relatively straightforward. This simplicity arises from the fact that the choice of function spaces

in Definition 9.3, specifically in (9.3.3) and (9.3.4), aligns precisely with our earlier approach in Section 8.3.2. This alignment is tailored to the specific diagram illustrated in Figure 44. It is worth noting that in equation (9.3.8), we employ a modified inner product, represented as $\langle A\cdot,\cdot\rangle$, as opposed to the standard $\langle\cdot,\cdot\rangle$. This substitution, however, does not pose any issues, as the resulting norms are equivalent. Consequently, in $3D$ we directly obtain similar results as those derived in Theorem 8.4 and Theorem 8.5, signifying stability and convergence.

But in the context of two dimensions, our choice in equation (9.3.5) differs somewhat from the three-dimensional scenario, meaning Theorem 8.4 is not directly applicable. Nevertheless, we can resort to Lemma 5.5, which aligns with the specific setting we are considering. Namely, we have utilize planar row-wise discrete differential forms, as evidenced in (9.3.5), which implies that the spaces R_h, Σ_h, U_h offer a structure-preserving discretization of the lower complex depicted in Figure 43. Hence, to apply Lemma 5.5, the only requirement that remains to be confirmed is the auxiliary inf-sup condition given in (5.3.5). In our case, pertaining to the complex illustrated in Figure 44, this entails verifying the existence of a constant $C_{IS} > 0$ such that

$$\inf_{0\neq v_h\in\bar{K}_h}\ \sup_{0\neq w_h\in R_h}\ \frac{\langle\nabla\cdot w_h, v_h\rangle}{\|w_h\|_{H^1}\ \|v_h\|} \geq C_{IS},$$

independent of h. The existence of such a C_{IS} is actually quickly apparent. Because with the definition of the pullback (Definition 3.9) we have in the two-dimensional setting

$$R_h = \left(S^{r,r}_{p,p}\circ\mathbf{F}^{-1}\right)\otimes\mathbb{R}^2, \quad \bar{K}_h = \left(S^{r,r}_{p-1,p-1}\circ\mathbf{F}^{-1}\right).$$

Hence, $(R_h, \bar{K}_h)$ corresponds to the well-known isogeometric Taylor–Hood space pair; see e.g. [23, Theorem 4.1]. Thus, one indeed has the validity of the above inequality for a suitable C_{IS}, which is independent of h, as long as $h \leq h_{\max}$ for a proper $h_{\max} > 0$. This explains why also in $2D$ we get well-posed discretization. We summarize the last thoughts and remarks in a further

Corollary 9.4 (**Well-posedness**). *Let us assume the parametrization $\mathbf{F}\colon\widehat{\Omega}\to\Omega$, $\widehat{\Omega} \coloneqq (0,1)^n$ to be C^2-smooth with C^2-smooth inverse and we require a family of regular meshes $(\mathcal{M}_h)_h$ in the sense of Definition 6.5. Then the choice of discrete spaces specified through Definition 9.3 implies the existence of a $h_{\max} > 0$ s.t. we obtain for* (9.3.8) *and for all $0 < h \leq h_{\max}$ a unique solution. Moreover, the discretization is well-posed, meaning we have inf-sup stability independent of h.*

With the statement in the last corollary and the estimates (9.3.6)-(9.3.7) we get analogously to Theorem 8.5:

Corollary 9.5 (**Error estimate**). *We consider a well-posed discretization* (9.3.8) *in the sense of Corollary 9.4. Further let the solution (σ, u, κ) of the continuous problem* (9.3.1) *fulfill the regularity assumptions $\sigma \in H^l(\Omega, \nabla\cdot, \mathbb{M})$, $u \in H^l(\Omega)\otimes\mathbb{R}^n$, $\kappa \in H^l(\Omega)\otimes\mathbb{R}^{s(n)}$ for $0 \leq l \leq p$. Then the error between exact and approximate solution satisfies*

$$\|\sigma-\sigma_h\|_{H(\nabla\cdot)} + \|u-u_h\| + \|\kappa-\kappa_h\| \leq C_{conv}h^l\Big(\|\sigma\|_{H^l(\nabla\cdot)} + \|u\|_{H^l} + \|\kappa\|_{H^l}\Big)$$

for a constant C_{conv} independent of h.
Additionally, for $n = 3$ we have due to Theorem 8.5 and our choice (9.3.2) *also*

$$\|\nabla\cdot\sigma - \nabla\cdot\sigma_h\| \leq C_{conv}h^{p+1}\,\|\nabla\cdot\sigma\|_{H^{p+1}}\,, \tag{9.3.9}$$

provided enough regularity for σ.

After the theoretical remarks above, we now want to present different numerical tests that are intended to support the results condensed in the latter two corollaries. In doing so, we utilize the discrete spaces specified in Definition 9.3. We start again with a simple convergence test in 2D.

Example 9.9 (Curved square)**.** *In the first example we consider the convergence behavior for the two-dimensional domain from Figure 22, i.e. with parametrization* $\mathbf{F}(\zeta_1, \zeta_2) = (\zeta_1, \zeta_2 - \zeta_1^2 + \zeta_1)^{\mathrm{T}}$*. We assume homogeneous boundary conditions* $u_D = 0$ *and here we choose the source function* f *in the mixed formulation such that the exact displacement solution is* $u = (u_1, u_2)^{\mathrm{T}} = (w, -w)^{\mathrm{T}}$ *with*

$$\boxed{w \circ \mathbf{F}(\zeta_1, \zeta_2) = \sin(\pi\zeta_1)\sin(\pi\zeta_2), \quad \lambda = 2, \mu = 1}.$$

And again, λ *and* μ *stand for the Lamé parameters. Due to this regular problem and the convergence statement in Corollary 9.5, we can expect for degree* $p \geq 2$ *and regularity* $r = 0$ *that the errors* $\|\sigma - \sigma_h\|_{H(\nabla\cdot)}$, $\|u - u_h\|$, $\|\kappa - \kappa_h\|$ *are of order* $\mathcal{O}(h^p)$*. And indeed, if we look at the errors in Figure 45 one observes the mentioned convergence order and a stable error decrease.*

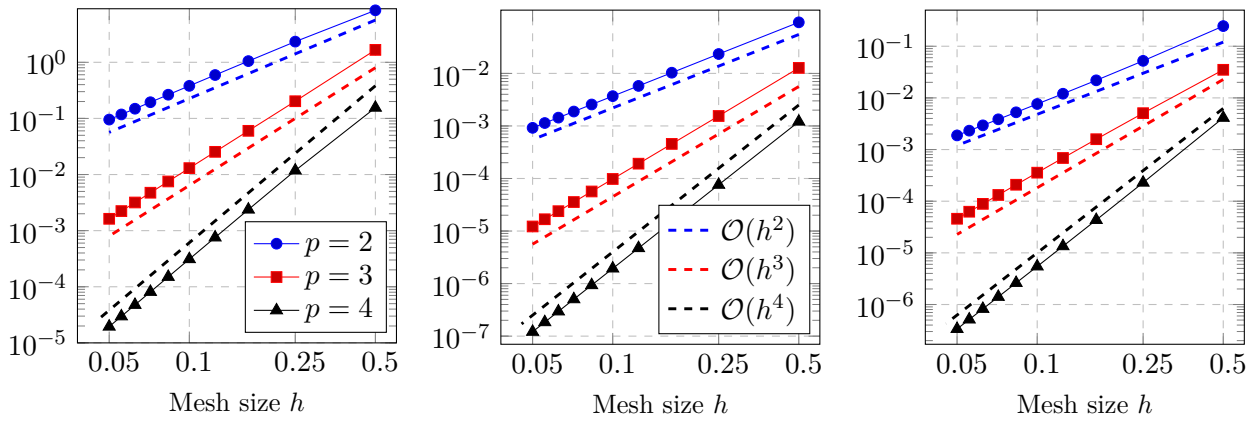

(a) $\|\sigma - \sigma_h\|_{H(\nabla\cdot)}$ (b) $\|u - u_h\|$ (c) $\|\kappa - \kappa_h\|$

Figure 45: Here we plot the different errors w.r.t. h and for the degrees $p = 2, 3, 4$. For all cases we have the regularity parameter $r = 0$; see Definition 9.3. Dashed lines with slopes $2, 3, 4$ are added to verify the convergence rates.

Unlike the approach outlined in Section 9.2, establishing theoretical well-posedness statements for the formulation with weakly imposed symmetry in $3D$ proves to be considerably more challenging. This difficulty arises because, to obtain the statements in Corollaries 9.4 and 9.5 for the three-dimensional setting, we rely on Theorems 8.4 and 8.5 from Section 8.3. The proofs of these mentioned theorems were, in turn, intricate and spanned essentially the entirety of Section 8.3. Furthermore, it is noteworthy that our choice of spaces in $2D$ and $3D$ (see Definition 9.3) differs in the case of weak symmetry. Specifically, in $3D$, splines of degree $p+1$ come into play, whereas in $2D$, B-splines of degree p are sufficient. This discrepancy explains why, in $3D$, with sufficient regularity of the exact solution, we obtain the property $\|\nabla \cdot \sigma - \nabla \cdot \sigma_h\| \in \mathcal{O}(h^{p+1})$; see (9.3.9). For this reason, our next objective is also to present a convergence test in $3D$.

Example 9.10 (Thick ring)**.** *We look at a convergence test example in* $3D$*, where the geometry and the mesh for* $h = 1/6$ *are given in Figure 46 (a). We define the source term* f *such that the exact solution has zero displacement boundary values and the exact solution is* $u = (u_1, u_2, u_3)^{\mathrm{T}}$*, where*

$$\boxed{u_1 = \frac{w}{2}, \; u_2 = w, \; u_3 = -\frac{w}{2}, \quad \text{with} \quad w \circ \mathbf{F}(\zeta_1, \zeta_2, \zeta_3) = \sin(\pi\zeta_1)\sin(\pi\zeta_2)\sin(\pi\zeta_3)}.$$

Above, $\mathbf{F}\colon (0,1)^3 \to \Omega$ *denotes the regular parametrization of* Ω*. The underlying Lamé parameters for this test are* $\boxed{\lambda = 2, \; \mu = 1}$*. The weak formulation with weakly imposed symmetry incorporates besides the displacement also the stresses and the Lagrange multiplier* $\kappa \in L^2(\Omega) \otimes \mathbb{R}^3$*.*

Consequently, if we have finer meshes or higher degrees one runs into trouble due to a large number of degrees of freedom. Especially the solving of the underlying large linear systems causes a lot of computational effort. That is why we applied the iterative solver minres() *to solve the system of equations in the 3D case. The mentioned solver is pre-implemented in* MATLAB *([53]) and as relative tolerance we chose* $5 \cdot 10^{-8}$*, i.e.*

$$\frac{|A\bar{x} - b|}{|b|} \leq 5 \cdot 10^{-8}, \quad ^{2}$$

with A*,* b *denoting the system matrix and right-hand side and* $\bar{x}$ *is the approximate solution obtained by* minres()*. Since the norms of relative and also of the absolute residuals are much less than the errors we computed in the convergence test, we think that the plots remain meaningful. In Figure 47 we see the error decays for* $p = 2, r = 0$ *and* $p = 3, r = 1$ *and the decreasing basically fits to the theoretically predicted order* $\mathcal{O}(h^p)$*. However, the convergence order of the displacement field seems to be ones higher than the order suggested by the theory; see Corollary 9.5. This indicates that the error estimates, especially from Section 8.3, might be too pessimistic. This observation of faster convergence motivates to establish and consider improved error estimates analogous to [5, Theorem 5.6] and to examine the proofs in Section 8.3 for feasible simplifications. We suspect that better estimates might be derived, but we will not delve further into this matter but mention it as a potential starting point for further investigations. Nevertheless, the refined error estimate* $\|\nabla \cdot \sigma - \nabla \cdot \sigma_h\| \in \mathcal{O}(h^{p+1})$ *can be realized well in Figure 46 (b). Furthermore, the approximations for* u_1 *and* σ_{11} *on the middle slice* $x_3 = 0.5$ *through the ring domain are pictured in Figure 48.*

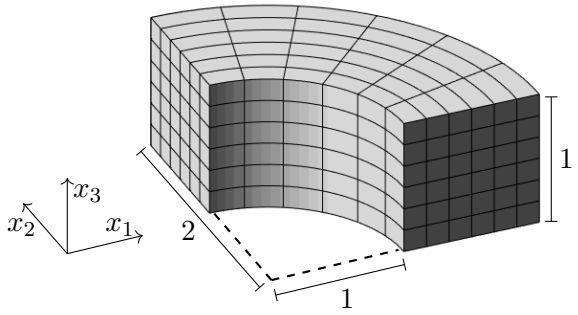

(a) Mesh for $h = 1/6$

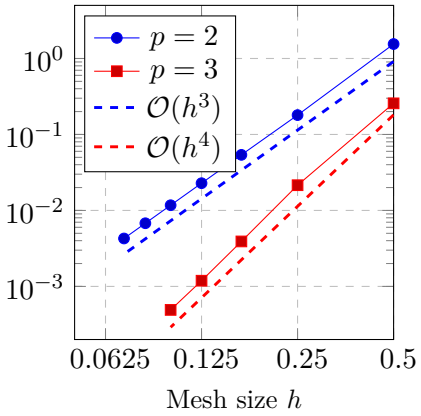

(b) $\|\nabla \cdot \sigma - \nabla \cdot \sigma_h\|$

Figure 46: A mesh for the $3D$ convergence example ($h = 1/6$) is shown on the left, whereas on the right we see the corresponding errors for the stress divergence. For $p = 2$ it is $r = 0$ and for $p = 3$ we set $r = 1$.

[2] $|\cdot|$ stands for the Euclidean norm.

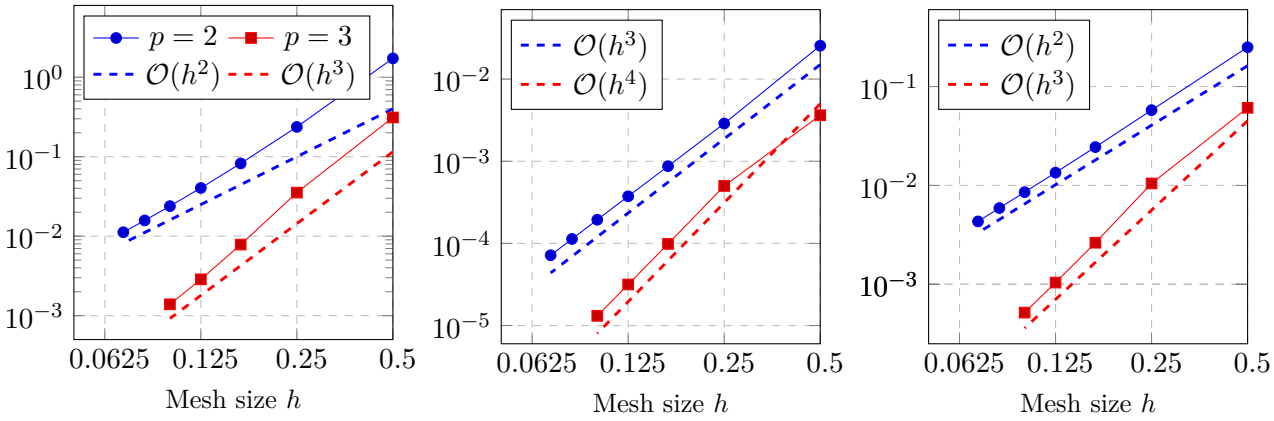

(a) $\|\sigma - \sigma_h\|_{H(\nabla\cdot)}$ (b) $\|u - u_h\|$ (c) $\|\kappa - \kappa_h\|$

Figure 47: Error decay for the $3D$ ring example. We note that we choose the regularity parameter $r = 0$ if $p = 2$, but $r = 1$ for the case $p = 3$.

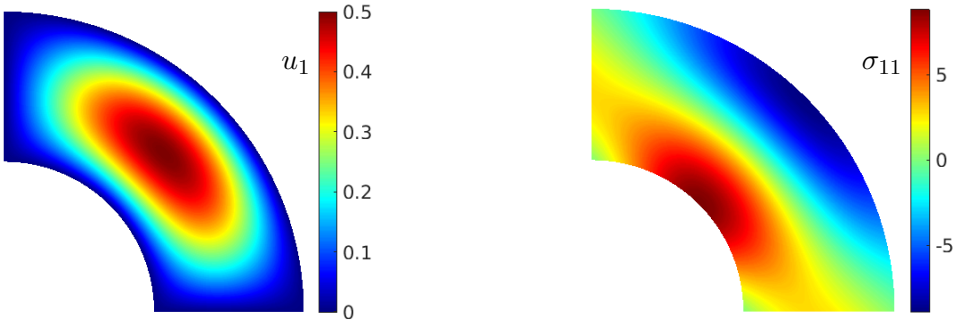

(a) u_1 (b) σ_{11}

Figure 48: View on the approximate solution of the $3D$ ring on the middle slice $x_3 = 1/2$. ($p = 3$, $r = 1$, $h = 1/6$)

In the following we provide similar to Section 9.2 a few remarks regarding extensions and stability for (nearly) incompressible materials.

9.3.1 Multi-patch domains

Supposing that we are in the field of multi-patch IGA, i.e.

$$\overline{\Omega} = \bigcup_{j=1}^{m} \overline{\Omega_j} \quad , \ \mathbf{F}_j \colon (0,1)^n \to \Omega_j \quad ,$$

for a suitable number m. On the j-th patch we can define the discrete spaces $\Sigma_h^{(j)}, U_h^{(j)}$, etc. as described in Definition 9.3. The global spaces are then straightforwardly defined as

$$\Sigma_h := \left\{ \sigma \in H(\Omega, \nabla\cdot, \mathbb{M}) \;\middle|\; \sigma_{|\Omega_j} \in \Sigma_h^{(j)} \right\}, \ U_h = \left\{ u \in L^2(\Omega) \otimes \mathbb{R}^n \;\middle|\; u_{|\Omega_j} \in U_h^{(j)} \right\}, \quad \text{etc.} \quad .$$

Only the stress spaces need a proper coupling between the patches. And the implementation of the coupling conditions for the stresses can then be achieved rather easily by exploiting the well-known divergence preserving property of the pullback mappings $\mathcal{Y}_2^1$, $\mathcal{Y}_3^2$ (see Example 4.1) which are utilized to define the isogeometric differential forms in Example 7.3. Because without difficulties one can show that these two mentioned pullbacks transform boundary normal vectors

again to boundary normals. In other words the $H(\nabla\cdot)$-coupling can effectively be done between the cubical parametric patches. Thus, if the patches are conforming connected there is no problem to find a basis of the multi-patch Σ_h. One further notes the fact that also in the multi-patch setting $\nabla \cdot \Sigma_h \subset U_h$. Numerical tests suggest the well-posedness of the mixed formulation for multi-patch parametrizations.
We show the applicability of the weak symmetry approach for the violin mesh from Example 9.3.

Example 9.11 (Fixed violin)**.** *In fact, we repeat the test from Example 9.3 here. But, instead of using the modified mixed weak form with strong symmetry, we now employ the formulation with weakly imposed symmetry* (9.3.8)*. In particular, we refer to the mentioned example for more details regarding mesh and computational domain.*
By choosing $p = 3$ and $r = 1$ patch-wise, and coupling the stresses between the patches, we obtain the images in the left column of Figure 49. A comparison with the primal formulation as in Example 9.3 demonstrates the feasibility of multi-patch geometries.

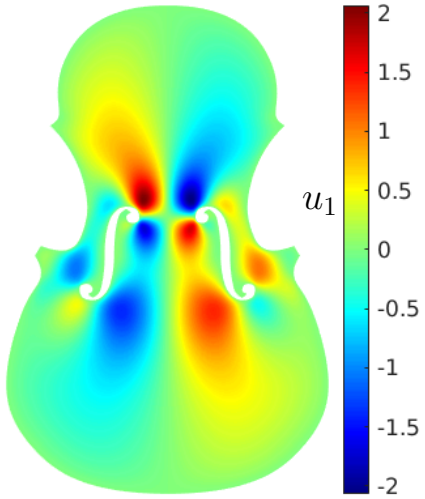

(a) mixed weak form.

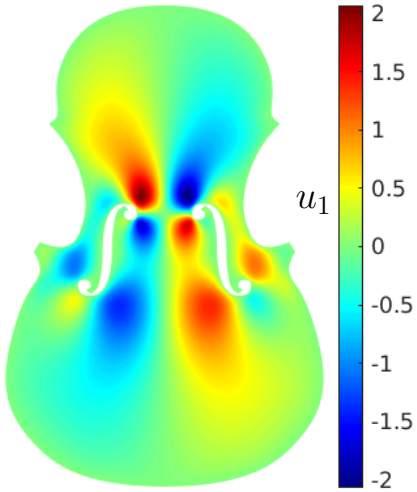

(b) primal form.

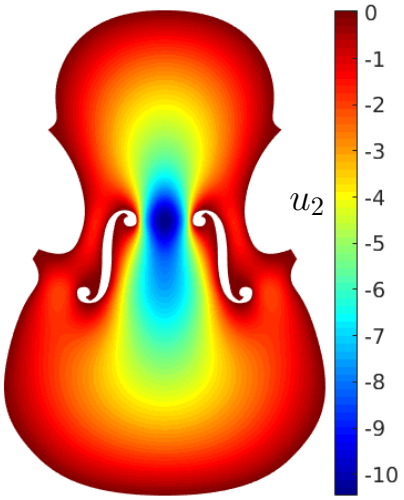

(c) mixed weak form.

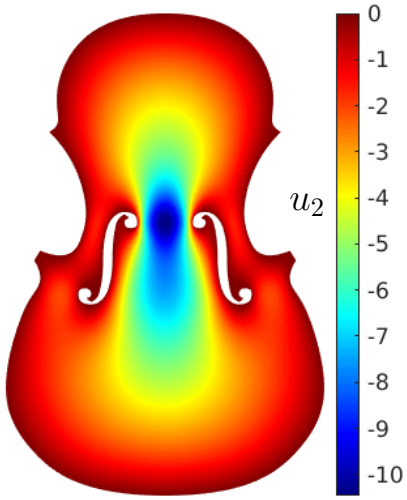

(d) primal form.

Figure 49: Here we see the comparison of the displacements between the classical primal formulation (right column) with degree 4 and C^0 B-splines as well as the displacements for the mixed weak form with weakly imposed symmetry (left column). For the latter we use degree $p = 3$ and inner patch regularity parameter $r = 1$. Between the patches only the normal components $\sigma \cdot \mathbf{n}$ are coupled continuously.

Next we comment on the situation of traction boundary conditions which is easier to handle for the second discretization approach with weakly imposed symmetry.

9.3.2 Traction boundary conditions

Something that is somewhat problematic for the formulation with strong symmetry is the traction boundary conditions. This means $\overline{\Gamma_t} \cup \overline{\Gamma_D} = \partial\Omega$, $\Gamma_t \cap \Gamma_D = \emptyset$ together with a suitable mapping $t_{\mathbf{n}}$ and the requirement

$$\sigma \cdot \mathbf{n} = t_{\mathbf{n}} \text{ on } \Gamma_t \quad \text{and} \quad u = u_D \text{ on } \Gamma_D.$$

However, since we have used structure-preserving discretizations of the bottom complexes in Figure 43 and Figure 44 in this section, finding a basis for the space

$$\Sigma_{h,\Gamma_t} \coloneqq \{\tau \in \Sigma_h \mid \tau \cdot \mathbf{n} = 0 \text{ on } \Gamma_t\}$$

is not an issue. Between the parametric domain and the physical domain, we have the transformations $\mathcal{Y}_{n-1}^n$ (see Example 4.1), which are compatible with the outer unit normals. In particular, traction forces $t_{\mathbf{n}} = 0$ can be implemented in $3D$ and $2D$ without additional modifications. Thus, the discretization approach with weakly imposed symmetry considerably simplifies the treatment of traction boundary conditions.
Clearly, given a proper auxiliary stress mapping $\tilde{\sigma}$, where $\tilde{\sigma} \cdot \mathbf{n} = t_{\mathbf{n}}$, we can reduce again the mixed boundary conditions to the case $t_{\mathbf{n}} = 0$ by considering $\sigma - \tilde{\sigma}$. Finally, we remark that in the discrete setting we shall assume for reasons of simplification that Γ_t and Γ_D are the union of full mesh boundary elements.

For instance, the Cook's membrane (see Example 9.7) test example can be considered without problems.

Example 9.12 (Cook's membrane)**.** *Again we look at the classical benchmark problem of Cook's membrane; cf. Example 9.7. Hence, we apply our discrete scheme with* $\boxed{\lambda = \infty,\ \mu = 0.375}$ *analogous to the example in [13] and utilize the reference displacement values from that paper at the point P as depicted in Figure 50 (a). Our focus lies in analyzing the convergence of our approximations towards these established reference values. As illustrated in Figure 50 (b)-(c), we present the outcomes for the specific cases of $r = p - 2$ and $p = 2, 3, 4$. Notably, as the disparities between the reference and approximate values decrease across all degrees, we can affirm the absence of locking effects in this context.*

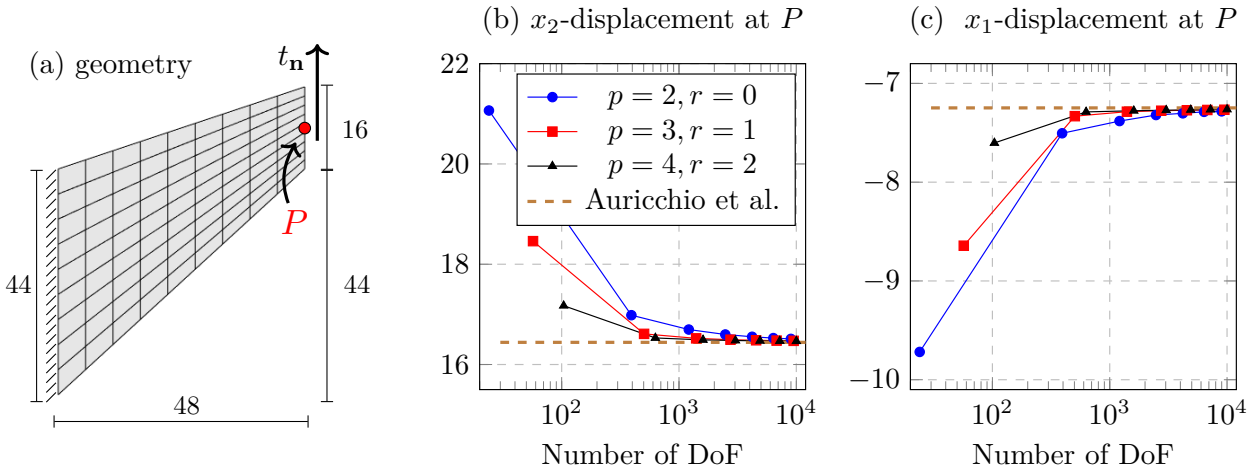

Figure 50: For the Cook membrane we get reasonable displacement values in P although we have set $\lambda = \infty$ as well as $r = p - 2$. The reference values *"Auricchio et al."* are taken from [13].

As a last aspect in the context of the formulation with weakly imposed symmetry let us consider the stability for large λ, meaning (nearly) incompressible materials.

9.3.3 Stability in the (nearly) incompressible regime

A point we still want to address here is the case of (nearly) incompressible materials. The question is whether we can achieve stability w.r.t. λ even when using the approach of weakly imposed symmetry. If we initially consider the scenario of pure zero displacement boundary conditions, we know from [7], for example, that it is sufficient to verify whether $\mathrm{I} \in \Sigma_h$. Because then, with an analogous argumentation as in Section 9.2.3, we can reduce the discrete computations to the spaces

$$\tilde{\Sigma}_h \coloneqq \Sigma_h \cap \left\{ \tau \;\middle|\; \int_\Omega \operatorname{tr}(\tau)\, dx = 0 \right\}. \tag{9.3.10}$$

We want to show here that we can achieve stability for $\lambda \to \infty$ with our discretization ansatz, at least in case of B-spline parametrizations. Below we follow again the considerations in [7, 20] and [66]. However, we restrict ourselves mainly to the three-dimensional case ($n = 3$), since the argumentation for $2D$ is in principle the same.
First we have a look at the three-dimensional situation. In view of the definition of Σ_h (see also Examples 4.1 and 7.3) one has

$$\mathrm{I} \in \Sigma_h \quad \Leftrightarrow \quad \mathrm{adj}(\mathbf{J})^k \in \left(S^{r,r-1,r-1}_{p+1,p,p} \times S^{r-1,r,r-1}_{p,p+1,p} \times S^{r-1,r-1,r}_{p,p,p+1}\right)^{\mathrm{T}}, \forall k,$$

where $\mathrm{adj}(\mathbf{J})^k$ is the k-th column of the adjugate matrix $\mathrm{adj}(\mathbf{J}) \coloneqq \det(\mathbf{J})\mathbf{J}^{-1}$ of $\mathbf{J}$. By the definition of the adjugate matrix as the transpose of the cofactor matrix, it is easy to see that for $\mathbf{F} \in (S^{s,s,s}_{q,q,q})^3$ with $q > s \geq 1$ we obtain

$$\mathrm{adj}(\mathbf{J})^k \in \left(S^{s,s-1,s-1}_{2q,2q-1,2q-1} \times S^{s-1,s,s-1}_{2q-1,2q,2q-1} \times S^{s-1,s-1,s}_{2q-1,2q-1,2q}\right), \quad \mathbf{J} = (J_{ij})_{i,j}.$$

For example, it is

$$\mathrm{adj}(\mathbf{J})_{11} = J_{22}J_{33} - J_{23}J_{32} \in S^{s,s-1,s-1}_{2q,2q-1,2q-1}.$$

Similar thoughts lead to the other entries. Thus $\left(\mathcal{Y}^2_3\right)^{-1}(\mathrm{adj}(\mathbf{J})^k) \in V^2_{h,3}(2q, s)$ for $k = 1, 2, 3$. Consequently, if we choose the discrete spaces such that $2q \leq p + 1$ and $r \leq s$, we have indeed $\mathrm{I} \in \Sigma_h$. In other words, if one wants stability for large λ it might be advisable to apply a p-refinement step.
In the $2D$ case the condition $\mathrm{I} \in \Sigma_h$ is easier to see since then

$$\mathrm{adj}(\mathbf{J}) = \begin{bmatrix} \partial_{\zeta_2} F_2 & -\partial_{\zeta_2} F_1 \\ -\partial_{\zeta_1} F_2 & \partial_{\zeta_1} F_1 \end{bmatrix}.$$

For $\mathbf{F} \in (S^{s,s}_{q,q})^2$ one has $\mathrm{I} \in \Sigma_h$ if $p \geq q,\ s \geq r$. In particular, the isogeometric paradigm fits to the stability condition.

Corollary 9.6. *Suppose a pure displacement boundary condition $u_D = 0$ and let us use the discrete spaces from Definition 9.3 with Σ_h replaced by $\tilde{\Sigma}_h$; see* (9.3.10)*. First, in the three-dimensional case, let $\mathbf{F} \in (S^{s,s,s}_{q,q,q})^3$ with $q > s \geq 1$. Then we achieve stability w.r.t. λ if $2q \leq p+1$ and $r \leq s$. Secondly, let $\mathbf{F} \in (S^{s,s}_{q,q})^2$ with $p \geq q,\ s \geq r$. Then, we also have stability for $\lambda \to \infty$ in $2D$.*

It is natural to ask, whether a generalization to NURBS parametrizations with non-trivial weight functions is possible. Although numerical experiments indicate a generalization possibility, we do not have a proof available.

In the presence of a non-vanishing traction boundary component $\Gamma_t \subset \partial\Omega$, similar to the transformations and steps shown in Section 9.2.3, we can also establish stability w.r.t. λ. However, for the sake of completeness, we still intend to present the main idea here.
Let $\sigma_h \in \Sigma_{h,\Gamma_t}$ arbitrary but fixed with $\emptyset \neq \Gamma_t \subsetneq \partial\Omega$. Let $\Gamma_D \coloneqq \partial\Omega \backslash \Gamma_t$. Then, there exists a $w \in H^1_{\Gamma_D}(\Omega) \otimes \mathbb{R}^n$ s.t.

$$\nabla \cdot w = \mathrm{tr}(\sigma_h), \quad \text{and} \quad \|w\|_{H^1} \leq C \left\|\mathrm{tr}(\sigma_h)\right\|,$$

where C is a constant depending on Ω, Γ_t and Γ_D. In view of Lemma 2.11 and the saddle-point structure of the mixed weak form (9.3.8), to show stability w.r.t. λ we can assume that

$$\sigma_h \in Z \coloneqq \{\tau_h \in \Sigma_h \mid \langle \nabla \cdot \tau_h, v_h \rangle + \langle \mathrm{Skew}\, \tau_h, \eta_h \rangle = 0,\ \forall (v_h, \eta_h) \in U_h \times \bar{K}_h\},$$

which implies $\nabla \cdot \sigma_h = 0$. Hence, using an estimate of the form (9.2.24), we get the inequality

$$\|\mathrm{tr}(\sigma_h)\| \leq C \|\mathrm{dev}(\sigma_h)\|,$$

with a C independent of λ. With [20, Bemerkung 5.3 in Chapter 6] we finally obtain

$$\begin{aligned}\langle A\sigma_h, \sigma_h \rangle &\geq \frac{1}{2\mu} \|\mathrm{dev}(\sigma_h)\|^2 \geq \frac{1}{4\mu} \|\mathrm{dev}(\sigma_h)\|^2 + \frac{1}{4\mu} \|\mathrm{dev}(\sigma_h)\|^2 \\ &\geq \frac{1}{4\mu} \|\mathrm{dev}(\sigma_h)\|^2 + \frac{1}{4C^2\mu} \|\mathrm{tr}(\sigma_h)\|^2 \geq \tilde{C} \Big(\|\mathrm{dev}(\sigma_h)\| + \|\mathrm{tr}(\sigma_h)\| \Big)^2 \geq \tilde{C} \|\sigma_h\|^2 \\ &= \tilde{C} \|\sigma_h\|^2_{H(\nabla\cdot)},\end{aligned}$$

with $\tilde{C} \coloneqq \min\left\{\frac{1}{8\mu}, \frac{1}{8C^2\mu}\right\}$. In particular, there is an estimate for the coercivity condition which does not depend on λ. This guarantees a stable convergence behavior in the incompressible regime also for traction boundary conditions.

The stability for $\lambda \to \infty$ is also evident in the next numerical test, which corresponds to Example 9.8, except this time we utilize the second discretization approach, namely system (9.3.8).

Example 9.13 (Stability test)**.** *As mentioned earlier, we aim to revisit the test from Example 9.8, this time applying the formulation with weakly imposed symmetry* (9.3.8)*. We maintain the same geometry, boundary conditions, and choose the source function to replicate the exact solution from the aforementioned example. Utilizing the discrete formulation with the spaces defined in Definition 9.3, where $p = 2, 3, 4$, and $r = p - 2$, we compute the errors for the two cases:* $\boxed{\lambda = \infty,\ \mu = 1 \text{ and } \lambda = 2,\ \mu = 1}$*. The results are summarized in Figure 51. It is noteworthy that, despite the variation in λ, the errors are almost identical. Additionally, for smaller mesh sizes, the error decrease is stable and aligns with the theoretically derived error estimates.*
In essence, this example illustrates that we have stable convergence, even for (nearly) incompressible materials, using the mixed formulation with weak symmetry.

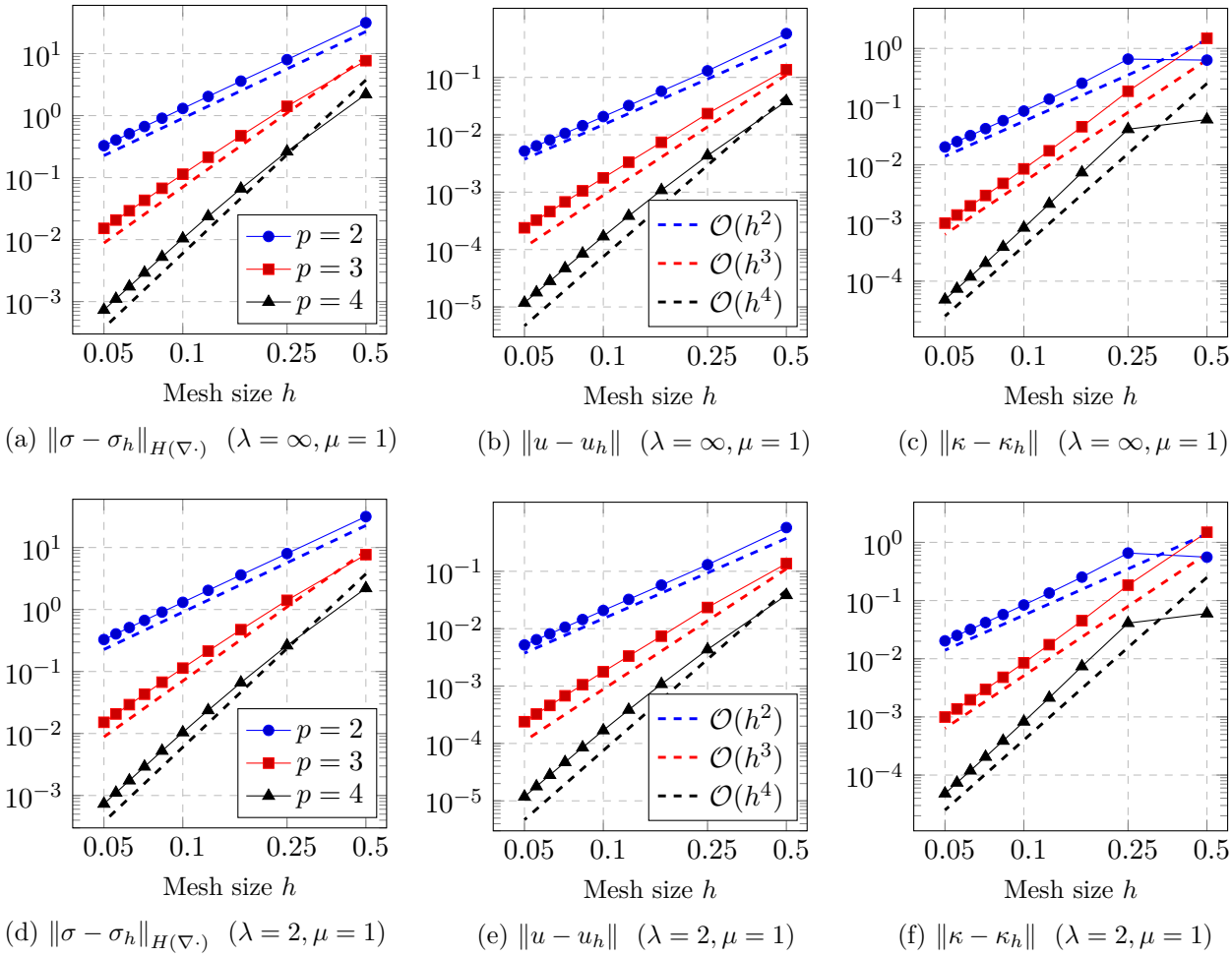

(a) $\|\sigma - \sigma_h\|_{H(\nabla\cdot)}$ $(\lambda = \infty, \mu = 1)$ (b) $\|u - u_h\|$ $(\lambda = \infty, \mu = 1)$ (c) $\|\kappa - \kappa_h\|$ $(\lambda = \infty, \mu = 1)$

(d) $\|\sigma - \sigma_h\|_{H(\nabla\cdot)}$ $(\lambda = 2, \mu = 1)$ (e) $\|u - u_h\|$ $(\lambda = 2, \mu = 1)$ (f) $\|\kappa - \kappa_h\|$ $(\lambda = 2, \mu = 1)$

Figure 51: We display the errors for the stability test in the square domain. In the top row we have the errors for the limit case $\lambda = \infty$, whereas in the bottom row we have $\lambda = 2$. The results confirm to the expected stability w.r.t. λ and thus for (nearly) incompressible materials.

Before delving into potential generalizations and discussing the core findings of our work in the next and final chapter, let us take a moment to recap what we have demonstrated and learned in Section 8. We started the latter with a brief explanation of the key equations and notions within linear elasticity. Then we have illustrated how the discretization methods from Section 8 can be applied in the context of linear elasticity theory. In Sections 9.2 and 9.3, we explored two different mixed formulations, the Hellinger–Reissner formulation as well as its modification with weakly imposed symmetry and clarified the conditions under which a well-posed discretization can be achieved. In both cases, we worked with isogeometric Finite Element spaces, allowing us to incorporate parameterized geometries into the calculations. Following the conventions of Isogeometric Analysis, we not only varied the underlying B-spline degrees but also had the flexibility to alter the regularity of the basis functions. Although our theoretical statements regarding convergence and stability were tailored to single-patch IGA, we suspect that generalization to multi-patch geometries is feasible, a notion supported by the presented numerical examples. Through various tests, including cases involving traction boundary conditions and incompressible materials, we have demonstrated the meaningful application of IGA within the discussed mixed methods framework. In doing so, we have provided evidence that the initially abstract considerations from Section 8 are applicable in the realm of continuum mechanics.

10 Outlook and Conclusion

In the final chapter of this work, we would like to explore some thoughts regarding potential generalizations of the results and provide a concise summary of our achievements.

Concerning generalizations, there are numerous ways to go. Conducting additional numerical tests in complex geometries, particularly in $3D$, and investigating the potential relaxation of assumptions in the various proofs presented in the thesis are considerations that seem plausible. It also appears worthwhile to delve into the realm of multi-patch domains, both theoretically and through numerical examples. However, a pressing question arises: What happens when we move beyond the restriction to saddle-point problems, as we have predominantly done? This would open the door to addressing a broader range of Hodge–Laplace problems. It is clear, and should be addressed directly here, that for the mixed formulation from Definition 8.1 in Section 8 in the case $k < n$, i.e., variational problems that do not fall into saddle-point structure, we lack proofs or concrete statements regarding well-posed IGA discretizations. Nevertheless, below, we will outline why we think the discretization approach using the modified mixed formulation (see Definition 5.1) defined in Section 5.1, might be applicable to further Hodge–Laplace problems. This aims to indicate where we see meaningful directions for further research.

10.1 Outlook

The starting point, basis, respectively, for the discretization considerations in this thesis were the mixed weak formulations of Hodge–Laplace problems induced by second-order Hilbert complexes. Doing so , we focused on the case of Hilbert complexes which arose as an output complex $(\mathscr{V}^\circ, \mathscr{D}^\circ)$ from a BGG construction procedure. This means, as discussed in Section 5, we were faced with the problem to find approximations to the variational formulation: For $f \in \mathscr{W}^k$ calculate an element $(\sigma, u) \in \mathscr{V}^{k-1} \times \mathscr{V}^k$ s.t.

$$\begin{aligned} \langle \sigma, \tau \rangle \qquad - \langle u, \mathscr{D}^{k-1}\tau \rangle \ &= 0, \qquad \forall \tau \in \mathscr{V}^{k-1}, \\ \langle \mathscr{D}^{k-1}\sigma, v \rangle + \langle \mathscr{D}^k u, \mathscr{D}^k v \rangle &= \langle f, v \rangle, \quad \forall v \in \mathscr{V}^k, \end{aligned}$$

where we refer to the mentioned section for the precise definition of the spaces and the underlying assumptions.

Even though we also dealt with mixed weak formulations with additional Lagrange multipliers in Sections 4.2.4, 5.3, and 8.3, all continuous problems appeared could be reduced to a variational problem of the above structure. Then, to capture general observations and formulate auxiliary results, we considered in Section 5 an analogous discrete version ((5.1.1)-(5.1.2)), which seeks $(\sigma_h, u_\theta) \in \mathscr{V}_h^{k-1} \times \mathscr{V}_\theta^k$ with the property:

$$\langle \sigma_h, \tau_h \rangle \qquad - \langle u_\theta, \mathscr{D}^{k-1}\tau_h \rangle \ = 0, \qquad \forall \tau_h \in \mathscr{V}_h^{k-1}, \tag{10.1.1}$$

$$\langle \mathscr{D}^{k-1}\sigma_h, v_\theta \rangle + \langle \mathscr{D}^k u_\theta, \mathscr{D}^k v_\theta \rangle = \langle f, v_\theta \rangle, \quad \forall v_\theta \in \mathscr{V}_\theta^k. \tag{10.1.2}$$

However, as already mentioned throughout the thesis, our primary focus has been on the case where $\mathscr{D}^k = 0$, that is, saddle-point problems. Specifically, all IGA discretizations in the physical domain were conducted within the framework of saddle-point problems. But now let us add some comments regarding the scenario where $\mathscr{D}^k \neq 0$.

First, by modifying the classical mixed formulation in the sense of

$$\langle \sigma, \tau \rangle_\mathscr{V} \qquad - \langle u, \mathscr{D}^{k-1}\tau \rangle \ = \langle f, \mathscr{D}^{k-1}\tau \rangle, \ \forall \tau \in \mathscr{V}^{k-1}, \tag{10.1.3}$$

$$\langle \mathscr{D}^{k-1}\sigma, v \rangle + \langle \mathscr{D}^k u, \mathscr{D}^k v \rangle = \langle f, v \rangle, \qquad \forall v \in \mathscr{V}^k, \tag{10.1.4}$$

(see (5.1.4)-(5.1.5)), we have found in Section 5.1 that the discrete well-posedness can be attributed to the special inf-sup condition

$$\inf_{v_\theta \in \mathscr{V}_\theta^k,\ \mathcal{P}_{\mathcal{N}(\mathscr{D}^k)} v_\theta \neq 0} \ \sup_{0 \neq \tau_h \in \mathscr{V}_h^{k-1}} \frac{\langle \mathscr{D}^{k-1} \tau_h, \mathcal{P}_{\mathcal{N}(\mathscr{D}^k)} v_\theta \rangle}{\|\tau_h\|_{\mathscr{V}} \left\| \mathcal{P}_{\mathcal{N}(\mathscr{D}^k)} v_\theta \right\|} \geq C_{IS} > 0 \ , \tag{10.1.5}$$

(compare (5.1.13)).
For this condition, one considers only the infimum over elements in $\mathcal{P}_{\mathcal{N}(\mathscr{D}^k)} \mathscr{V}_\theta^k$. On the other hand, looking at the general discrete inf-sup condition (5.1.3) of the unmodified system (10.1.1)-(10.1.2), i.e.

$$\inf_{(0,0) \neq (\tau_h, v_\theta) \in \mathscr{V}_h^{k-1} \times \mathscr{V}_\theta^k} \ \sup_{(0,0) \neq (\sigma_h, u_\theta) \in \mathscr{V}_h^{k-1} \times \mathscr{V}_\theta^k} \frac{\mathcal{B}\Big((\sigma_h, u_\theta), (\tau_h, v_\theta)\Big)}{\|(\sigma_h, u_\theta)\|_{\mathcal{B}} \, \|(\tau_h, v_\theta)\|_{\mathcal{B}}} \geq C_{IS} > 0, \tag{10.1.6}$$

with

$$\begin{aligned} \mathcal{B}\Big((\sigma, u), (\tau, v)\Big) &\coloneqq \langle \sigma, \tau \rangle - \langle u, \mathscr{D}^{k-1} \tau \rangle - \langle \mathscr{D}^{k-1} \sigma, v \rangle - \langle \mathscr{D}^k u, \mathscr{D}^k v \rangle, \\ \|(\sigma, u)\|_{\mathcal{B}}^2 &\coloneqq \|\sigma\|_{\mathscr{V}}^2 + \|u\|_{\mathscr{V}}^2 \, , \end{aligned}$$

one takes the infimum over pairs $(\tau_h, v_\theta) \in \mathscr{V}_h^{k-1} \times \mathscr{V}_\theta^k$. Thus, the condition (10.1.5) and the possibility of choosing $v_\theta = -u_\theta$ in the proof of Lemma 5.2 suggest that achieving well-posedness might be easier for the modified version (10.1.3)-(10.1.4). Namely, the naive idea would be to make the spaces $\mathscr{V}_h^{k-1}$ sufficiently large compared to their corresponding $\mathscr{V}_\theta^k$ counterparts since in the limit case where $\mathscr{V}_h^{k-1} \to \mathscr{V}^{k-1}$ well-posedness is guaranteed. In contrast to that, for (10.1.6), one cannot rely on inf-sup stability when performing a refinement or enlargement of the $\mathscr{V}_h^{k-1}$ test spaces, as the infimum is also taken over elements in $\mathscr{V}_h^{k-1}$. Put differently, for the modified system involving the graph inner product $\langle \sigma, \tau \rangle_{\mathscr{V}}$, a clear direction is indicated in terms of what should be done to satisfy the associated inf-sup condition; namely, enlarging $\mathscr{V}_h^{k-1}$. On the other hand, for the original system system without graph inner product ((5.1.1)-(5.1.2)), it is not immediately evident how or what should be refined to achieve its well-posedness. This is, of course, not a precise mathematical argument, just a first intuition. But numerical tests show that without dramatic refinements of the spaces for the σ variable and using classical IGA spaces we can often see inf-sup stability for discretizations of the system (10.1.3)-(10.1.4). We would like to explain and demonstrate this in the following using a further example in the planar case.

More precisely, we are examining an additional Hodge–Laplace problem derived from the $2D$ elasticity complex (4.2.26). Specifically, we are interested in the level $k = 1$ Hodge–Laplacian for this complex. Before specifying the underlying equation, we introduce another test geometry. In the following, we aim to conduct different numerical inf-sup tests. Therefore, it is beneficial to choose a non-trivial domain Ω to increase the significance of the results. Hence, we select a square parametrized with quadratic B-splines and perturb the underlying control points. Figure 52 displays the control points and the resulting geometry, which will be repeatedly used as our computational domain. It is important to note that this deformed square obviously possesses a more complex parameterization function, yet it remains globally smooth.

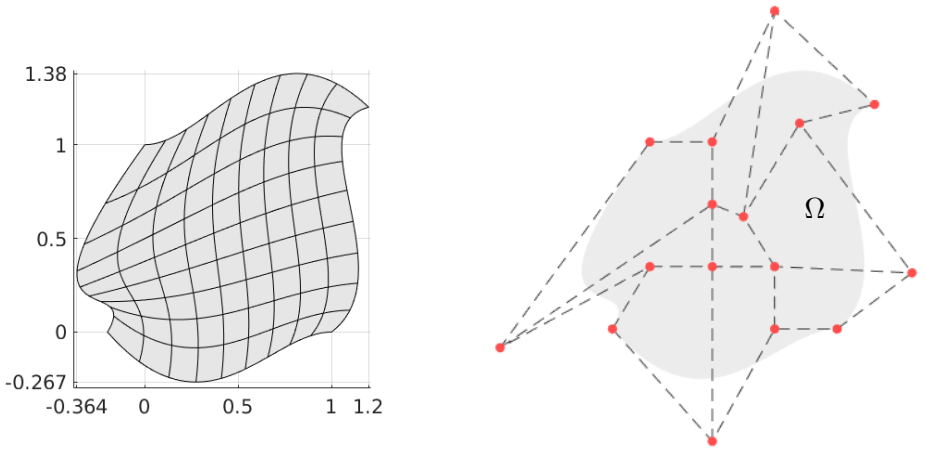

(a) Mesh for $h = 1/9$

(b) Geometry with control points

Figure 52: Here we display the domain utilized for the inf-sup tests below. On the right we highlighted the control points associated to the B-spline parametrization mapping $\mathbf{F}$. On the left we see an example mesh for $h = 1/9$ which illustrates the acting of $\mathbf{F}$.

Example 10.1 (Additional inf-sup test)**.** *There is no problem to see that the level $k = 1$ Hodge–Laplace equation of the planar elasticity complex, meaning*

$$0 \longrightarrow H^2(\Omega) \xrightarrow{\operatorname{curl}^2} H(\Omega, \nabla\cdot, \mathbb{S}) \xrightarrow{\nabla\cdot} L^2(\Omega) \otimes \mathbb{R}^2 \longrightarrow 0, \tag{10.1.7}$$

takes the form

$$\Big(\operatorname{curl}^2(\operatorname{curl}^2)^* - \operatorname{sym}\nabla\nabla\cdot\Big)u = f, \;\; f \in L^2(\Omega) \otimes \mathbb{S}, \;\; u \in H(\Omega, \nabla\cdot, \mathbb{S}),$$

$(\operatorname{curl}^2)^* s = \partial_2^2 s_{11} - 2\partial_1\partial_2 s_{12} + \partial_1^2 s_{22}$. *The continuous mixed weak formulation of the Hodge–Laplace problem seeks $(\sigma, u) \in H^2(\Omega) \times H(\Omega, \nabla\cdot, \mathbb{S})$ with*

$$\langle \sigma, \tau \rangle \qquad - \langle u, \operatorname{curl}^2 \tau \rangle \quad = 0, \qquad \forall \tau \in \mathscr{V}^0 := H^2(\Omega), \tag{10.1.8}$$
$$\langle \operatorname{curl}^2 \sigma, v \rangle + \langle \nabla \cdot u, \nabla \cdot v \rangle = \langle f, v \rangle, \quad \forall v \in \mathscr{V}^1 := H(\Omega, \nabla\cdot, \mathbb{S}). \tag{10.1.9}$$

Moreover, the equivalent modified weak form (10.1.3)-(10.1.4) *formulation in this situation is given by:* Find $(\sigma, u) \in H^2(\Omega) \times H(\Omega, \nabla\cdot, \mathbb{S})$ s.t.

$$\langle \sigma, \tau \rangle_{H(\operatorname{curl}^2)} - \langle u, \operatorname{curl}^2 \tau \rangle \quad = \langle f, \operatorname{curl}^2 \tau \rangle, \quad \forall \tau \in \mathscr{V}^0, \tag{10.1.10}$$
$$\langle \operatorname{curl}^2 \sigma, v \rangle \quad + \langle \nabla \cdot u, \nabla \cdot v \rangle = \langle f, v \rangle, \qquad \forall v \in \mathscr{V}^1, \tag{10.1.11}$$

where $\langle \sigma, \tau \rangle_{H(\operatorname{curl}^2)} := \langle \sigma, \tau \rangle + \langle \operatorname{curl}^2 \sigma, \operatorname{curl}^2 \tau \rangle$. Now, if we want to discretize the latter system using isogeometric FE spaces, we might choose analogously to the definitions in Section 8:

$$\mathscr{V}_h^0 := S_{q,q}^{s,s}, \quad \mathscr{V}_\theta^1 := S_{p,p}^{r,r} \otimes \mathbb{S}, \quad q > s > 0, \; p > r \geq 0, \tag{10.1.12}$$

with h and θ denoting the related mesh sizes. One notes, the necessity of the condition $s \geq 1$ due to the H^2-regularity requirement for σ. In other words our constraints on r and s guarantee $\mathscr{V}_h^0 \subset \mathscr{V}^0$, $\mathscr{V}_\theta^1 \subset \mathscr{V}^1$. Furthermore, since the associated graph norms are $\|\sigma\|_{\mathscr{V}} = \|\sigma\|_{H^2}$ and $\|u\|_{\mathscr{V}} = \|u\|_{H(\nabla\cdot)}$, it is natural to choose a mixed degree approach, specifically setting $q = p+1$. In the case of well-posedness and smooth exact solution, this would result in a convergence of order

$\mathcal{O}(h^p) + \mathcal{O}(\theta^p)$. *However, as we do not have a proof of the validity of the corresponding inf-sup property* (10.1.5)*, we compute for different mesh sizes the inf-sup values* C_{IS}^m *of the underlying variational formulation given by*

$$C_{IS}^m := \inf_{(0,0)\neq(\tau_h,v_\theta)\in\mathcal{V}_h^0\times\mathcal{V}_\theta^1} \sup_{(0,0)\neq(\sigma_h,u_\theta)\in\mathcal{V}_h^0\times\mathcal{V}_\theta^1} \frac{\mathcal{B}^m\Big((\sigma_h,u_\theta),(\tau_h,v_\theta)\Big)}{\|(\sigma_h,u_\theta)\|_{\mathcal{B}}\,\|(\tau_h,v_\theta)\|_{\mathcal{B}}},$$
$$\mathcal{B}^m\Big((\sigma,u),(\tau,v)\Big) := \langle\sigma,\tau\rangle_{H(\mathrm{curl}^2)} - \langle u,\mathrm{curl}^2\tau\rangle - \langle\mathrm{curl}^2\sigma,v\rangle - \langle\nabla\cdot u,\nabla\cdot v\rangle$$

and $\|(\sigma,u)\|_{\mathcal{B}}^2 := \|\sigma\|_{H^2}^2 + \|u\|_{H(\nabla\cdot)}^2$*, using the* MATLAB *([53])* eigs() *function together with the method proposed by Bathe et al. ([15, 33]); see Appendix 11.2. For the regularity of the B-splines we set* $s = r = p-1$ *and for the first test we have* $h = \theta$ *(i.e. equal meshes for* σ *and* u*) with computational domain shown in Figure 52. Then we obtain the values summarized in Figure 53 for* $p = 2,3,4$*. In the latter plot, we not only observe consistently positive values but also a stabilizing behavior of the* C_{IS}^m*. These results lead us to the conjecture that the chosen spaces indeed satisfy the inf-sup condition. In contrast, when we determine the inf-sup values* C_{IS}^u *of the corresponding original system* (10.1.8)-(10.1.9) *analogously, simply by replacing* $\mathcal{B}^m$ *with*

$$\mathcal{B}^u\Big((\sigma,u),(\tau,v)\Big) := \langle\sigma,\tau\rangle - \langle u,\mathrm{curl}^2\tau\rangle - \langle\mathrm{curl}^2\sigma,v\rangle - \langle\nabla\cdot u,\nabla\cdot v\rangle, \tag{10.1.13}$$

we observe in Figure 53 (b) a clear decay behavior and very small C_{IS}^u *values. In fact, in the mentioned figure only very few values appear, since for smaller mesh sizes the* MATLAB *([53])* eigs() *function yields very small and partly imaginary eigenvalues which reveal an issue with inf-sup stability. These observations are a clear hint that we do not have well-posedness for the unmodified mixed weak form. Respectively, it seems that there is no mesh size independent positive bound for the inf-sup value* C_{IS}^u*. Hence, the idea that a modification of the term* $\langle\sigma,\tau\rangle$ *in the mixed formulation to* $\langle\sigma,\tau\rangle_{\mathscr{V}}$ *yields better and more stable inf-sup values is supported by this test.*

We now proceed to the next test, which is very similar to the last one. However, this time, we will assume equal degrees, i.e., $q = p$*,* $s = r = p-1$*. With these changed and smaller spaces* $\mathcal{V}_h^0$*, it is not clear whether we will still obtain acceptable* C_{IS}^m*. However, we observe that by refining* $\mathcal{V}_h^1$ *through the choice* $h = \theta/2$*, one gets values* C_{IS}^m *that suggest again well-posedness; see Figure 54 (a) for the details. But, when calculating the values* C_{IS}^u *for the unmodified system, similar behavior to the first test is observed again; see Figure 54 (b). Thus, the last computations also indicate that achieving inf-sup stability for formulation* (10.1.10)-(10.1.11) *is noticeably easier with classical IG finite element spaces compared to the classical formulation* (10.1.8)-(10.1.9)*.*

As a final point of this example problem (10.1.10)-(10.1.11)*, we would like to present a small convergence test. For this purpose, we use the geometry from Example 9.1 which is given by the parametrization* $\mathbf{F}\colon (0,1)^2 \to \Omega\ ,\ (\zeta_1,\zeta_2) \to (\zeta_1, \zeta_2 - \zeta_1^2 + \zeta_1)$ *and choose the source function* f *such that we obtain*

$$\boxed{u = \begin{bmatrix} 2w & w \\ w & -2w \end{bmatrix}, \quad \text{with} \quad w \circ \mathbf{F}(\zeta_1,\zeta_2) = \sin(\pi\zeta_1)^2 \sin(\pi\zeta_2)^2}$$

as exact solution. As suggested earlier, it makes sense to use the spaces (10.1.12) *with* $q = p+1$*. We then calculate the errors* $\|\sigma - \sigma_h\|_{H^2}$*,* $\|u - u_\theta\|_{H(\nabla\cdot)}$ *for the modified formulation* (10.1.10)-(10.1.11)*. The results can be seen in Figure 55. The convergence behavior is stable and corresponds approximately to the theoretically optimal rates of* $\mathcal{O}(h^p)$*, indicating a well-posed discretization. With the convergence test, we obtain another indication of the appropriateness of the formulation* (10.1.10)-(10.1.11) *for isogeometric discretizations, consistent with the various inf-sup tests we conducted.*

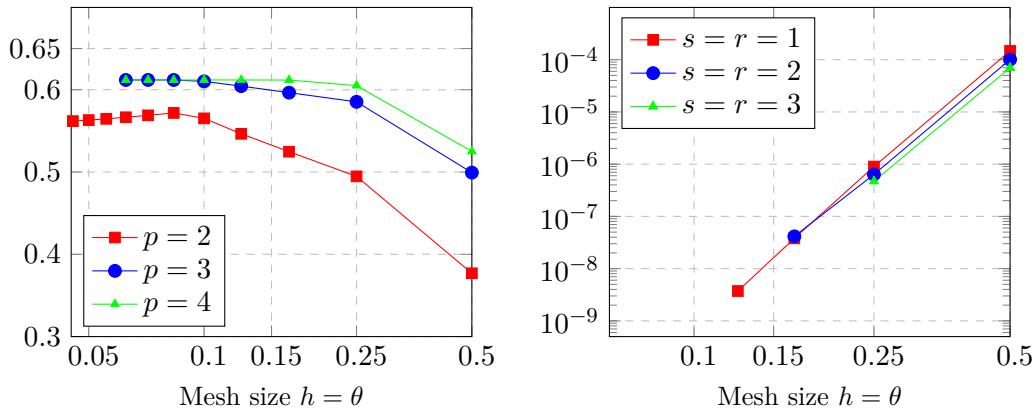

(a) Inf-sup values C_{IS}^m (b) Inf-sup values C_{IS}^u

Figure 53: Here we display the discrete inf-sup values for the planar domain in Figure 52 together with discrete spaces (10.1.12) with $q = p+1$, where we have equal meshes for the σ and u variable, i.e. $h = \theta$. On the left one sees the inf-sup value for the system (10.1.10)-(10.1.11), whereas to get the values on the right we utilized the original mixed weak formulation determined (10.1.8)-(10.1.9).

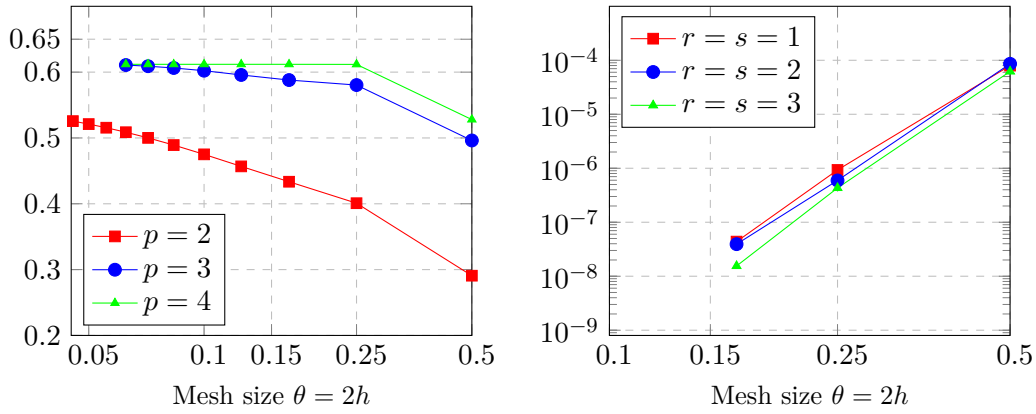

(a) Inf-sup values C_{IS}^m (b) Inf-sup values C_{IS}^u

Figure 54: Analogous to the previous figure, we see the inf-sup values C_{IS}^m (left) and C_{IS}^u (right), but now for the situation $p = q,\ r = s$, where here we have a refined mesh for the σ-variable, namely $2h = \theta$. Again, the C_{IS}^m indicate a well-posed discretization, but the C_{IS}^u not.

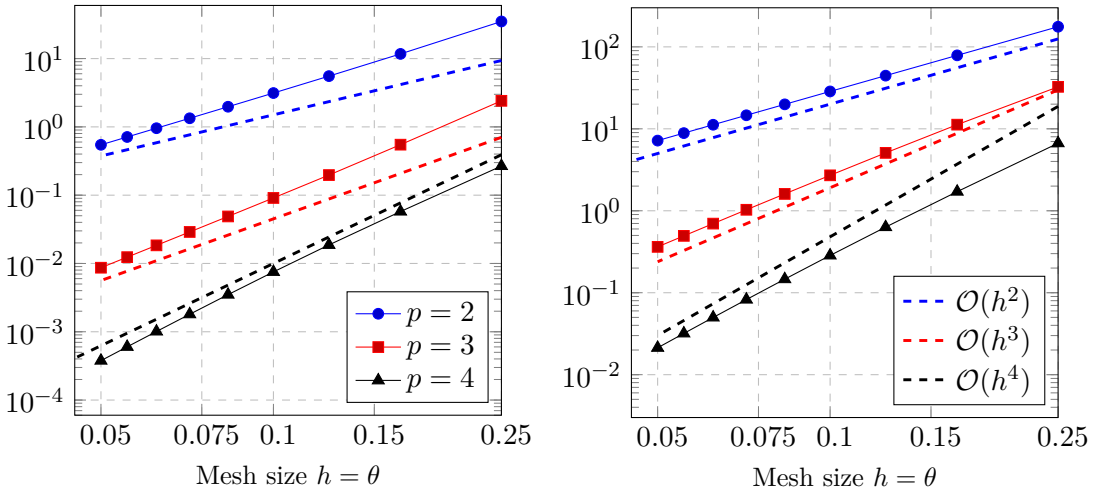

(a) $\|u - u_\theta\|_{H(\nabla\cdot)}$ (b) $\|\sigma - \sigma_h\|_{H^2}$

Figure 55: The discretization errors for the modified mixed weak form (10.1.10)-(10.1.11) and a manufactured test example with smooth exact solution. The underlying degree and regularity parameters are $q = p + 1$, $r = s = p - 1$. Although we do not have a well-posedness proof available, the stable and fast decay behavior hint at the feasibility of the FE spaces (10.1.12).

The observations made in the previous example, as well as in additional numerical tests not shown here, lead us to suspect that classical IG test functions can also be applied to discretize other mixed formulations of Hodge–Laplace problems. By this, we primarily mean variational formulations that do not have a saddle-point structure and are not directly derived from the classical de Rham sequence. For instance, Hodge–Laplace problems arising from second-order complexes, such as the one in above Example 10.1. However, it seems expedient to rely on systems with the graph inner product, namely the modified weak system (10.1.3)-(10.1.3). In our view, a meaningful area for future work would involve a more in-depth and theoretical examination of this modified mixed weak form in connection with higher-order Hilbert complexes.

In addition, in the thesis we considered also a second discretization method within the context of the BGG output complex, which is based on the idea of introducing additional Lagrange multipliers; see Section 5.3. Naturally, the question arises as to whether formulations with Lagrange multipliers, as discussed in Section 4.2.4, can also be employed for the discretization of further Hodge–Laplace problems. This includes systems that do not have a simple structure like the mixed weak formulation with weakly imposed symmetry in the field of linear elasticity, which involves only one Lagrange multiplier and a first-order differential operator; see Section 9.3. Certainly, this question can serve as the starting point for generalization studies. However, we have only conducted numerical tests with Lagrange multipliers in the context of linear elasticity, so we refrain from making definitive statements regarding the feasibility of IGA discretizations for other Lagrange multiplier formulations. Furthermore, we want to highlight a central drawback of introducing additional auxiliary variables, namely the problem of increasing degrees of freedom and the associated challenge of handling large linear systems. Particularly in higher dimensions, including $3D$, the rapid growth of degrees of freedom is a significant aspect. Therefore, we consider it more sensible to initially check generalization possibilities within the framework of mixed formulations without Lagrange multipliers, as these seem to be more suitable for higher dimensions.

Moreover, there are other directions that could be explored. We have focused on second-order complexes, but as shown in [12], it is possible to derive complexes with even higher order through BGG construction by iterating the process. It is therefore, intriguing to investigate whether, for

instance, third-order chains, classical IG test functions can be employed to approximate saddle point problems. Using B-splines or NURBS is particularly advantageous in this context, as it allows the variation of global regularity. At least in the single-patch IGA case combined with smooth parametrization mappings, the design of sufficiently differentiable test functions is not an issue. In the case of multiple IGA patches, the situation becomes more complicated. Therefore, as already hinted at and certainly, there is a need for an in-depth investigation of multi-patch IGA in the realm of higher-order Hilbert complexes. Connecting different patches essentially requires an analogous effort to linking degrees of freedom across individual elements in classical FEM. This aspect deserves further consideration. Indeed, if one aims to develop isogeometric numerical methods that are applicable in more complicated domains, it is inevitable to address multi-patch geometries.

One more point regarding generalizations that we want to address leads in a different direction. In various lemmata and theorems, we have often imposed relatively strict conditions on the parametrization or meshes. We have e.g. consistently referred to regular, meaning quasi-uniform meshes, and frequently mentioned C^2-smooth parametrizations. While these conditions have made it easier to establish statements on well-posedness or error estimates, we suspect, and believe it is worth further investigation, that some of these requirements, such as quasi-uniformity of the meshes, may not be strictly necessary. In other words, we see also potential for generalization by studying and examining the assumptions in the lemmatas and theorems.

10.2 Conclusion

Now, at the end of this work, we want to summarize once again what we have considered, where the difficulties lay, and where they still lie. Further we want to highlight what the main outcomes of this thesis are.

After introducing a few mathematical concepts and explanations, we delved into the framework of Hilbert complexes right from the beginning. The reason for this lies in the Hodge–Laplace problems induced by these complexes, which represent a certain class of PDEs. For these problems, not only solvability statements are known, but the Finite Element Exterior Calculus (FEEC) also provides criteria for approximation methods that lead to stable and quasi-optimal convergence behavior. The key idea is to use so-called structure-preserving discretizations of the underlying Hilbert complexes, along with mixed weak formulations of the Hodge–Laplace problems. With this concept, we initially have everything we need to compute approximate solutions for such Hodge–Laplace PDEs. Indeed, we addressed how to structure-preservingly discretize the important case of the de Rham complexes using B-splines in any dimension. It was essential to use the pullback operation, compatible with the exterior derivative, to obtain discrete de Rham sequences in parametrized geometries. Therefore, FEEC and Isogeometric Analysis (IGA) can be elegantly combined when discussing the de Rham complex. However, when turning to other Hilbert complexes, things become significantly more complicated. By other complexes, we mean those where operators other than the exterior derivative appear or where higher-order derivative operators come into play. Because the idea behind IGA is to introduce ansatz and test spaces in the parametric domain, which typically represents a cubical domain. And then, the discrete spaces in the actual computational domain are defined using the parametrization mapping and parametric test functions. If we have a structure-preserving discretization of the Hilbert complex in the parametric domain, the transition to the physical domain must be compatible with the complex structure to follow the design steps of FEEC. Here lies the problem; for complexes with higher-order differential operators, such as the Hessian or elasticity complex, we lack an analog of the pullback operation used for the de Rham complex. In other words, the structure-preserving transition between the parametric and computational domains appears generally infeasible for

such second-order complexes. Combining FEEC and IGA is thus more challenging for complexes other than the de Rham complex. With our work, we aimed to demonstrate precisely this: IGA can also be applied in the context of Hodge–Laplace problems not originating from de Rham sequences.

We focused on a specific class of complexes, namely those second-order complexes that can be obtained through a BGG construction utilizing two de Rham-type chains, utilizing in fact Alt^l-valued forms. This includes the previously mentioned Hessian and elasticity complexes, as well as various other complexes in arbitrary dimensions. While existing results in the literature show that discretization in cubical domains is possible for these class of sequences and leads to special spline complexes, the question remains of how to proceed with other geometries. To provide statements on well-posedness and error estimates in parametrized domains, we further narrowed our focus, largely examining mixed weak forms with a saddle-point structure. Although we could also prove invertibility for more general mixed weak formulations, ensuring inf-sup stability and well-posed discretization required exploiting the saddle-point property. For the saddle-point systems and leveraging the BGG construction, we introduced two approaches for approximation using IGA. The proof of discrete well-posedness and a priori error estimates for both methods are considered the two main outcomes of our work. Notably, incorporating the Lagrange multiplier required a lengthy and technical proof, which also relied on the macroelement technique. For the other approach, initially considered in the work, we further introduced a modified mixed weak formulation. In doing so, we demonstrated why simple IGA spaces without specific pullback mappings can still be used to define well-posed discretizations. It is worth highlighting that in both discretization approaches, we directly or indirectly utilized the idea of structure-preserving discretization. We used the existence of structure-preserving second-order B-spline complexes in the proof of well-posedness, and for the approach with a Lagrange multiplier, we precisely employed discrete differential forms. Thus, there is indeed a clear connection between IGA and FEEC in our work.

Moreover, to demonstrate the applicability of our results beyond theoretical considerations, we turned our attention to the field of linear elasticity theory in detail. The two discretization approaches, with and without a Lagrange multiplier, provide two different mixed stress-displacement methods. For these, we presented several numerical test examples that support or confirm the theoretical considerations. Additionally, we discussed and illustrated possibilities for generalizations, such as multi-patch geometries.

However, two questions remain at the end: Firstly, what is the motivation and advantage of following the IGA paradigm? Firstly, and most obviously, it allows for the computation of solutions in a wide range of non-polygonal domains. Secondly, the IGA theory enables variations not only in the polynomial degrees but also in the smoothness of the underlying FE basis functions. This allows for a reduction in degrees of freedom without compromising the order of convergence and simplifies the incorporation of second-order differential operators. Furthermore, extending the approach to more complicated and even higher-order complexes seems for us to be more realistic with NURBS compared to classical FE methods with polygonal meshes. On the other hand, what new insights do we gain from our work? We have shown that it is possible to use standard IGA test functions and isogeometric discrete differential forms to obtain well-posed discretizations for Hodge–Laplace PDEs arising from second-order complexes. In essence, we have demonstrated that IGA can meaningfully be utilized within the context of non-de Rham type complexes.

11 Appendix

11.1 Proof for Lemma 3.8

We show only the first three points of this lemma, since, as already mentioned, the last point in the assertion is a well-known result from exterior calculus.
To begin with, we look at an auxiliary statement.

Lemma 11.1. *Let the assumptions of Lemma 3.8 hold.*
Given a $c \in L^2(\Omega)$, a $k \in \{0, \dots, n\}$ and a basis k-form $\omega = c\, dx^{\sigma_1} \wedge \cdots \wedge dx^{\sigma_k}$ there exist $w_s \in C^l(\overline{\widehat{\Omega}})$, $\forall s \in \Sigma_<(k,n)$ s.t.

$$\mathcal{Y}^k_{\mathbf{F}}\omega = \sum_{s\in\Sigma_<(k,n)} (c \circ \mathbf{F})\, w_s\, dx^{s_1} \wedge \cdots \wedge ds^{s_k}, \tag{11.1.1}$$

where the w_s depend only on the first derivatives of $\mathbf{F}$.

Proof. We follow a proof-by-induction argument w.r.t. k.

- Case $k = 0$: By the special definition of $\mathcal{Y}^0_{\mathbf{F}}$ this is trivial; cf. Definition 3.9.
- Case $k = 1$: Below we write $\mathbf{J} = (J_{ij})_{i,j}$ for the Jacobian of $\mathbf{F}$. Then for $\omega = c\, dx^i \in L^2\Lambda^1(\Omega)$ and $v \in \mathbb{R}^n$ it is

  $$\Big[\mathcal{Y}^1_{\mathbf{F}}\omega\Big](v) = (c \circ \mathbf{F})\, dx^i(\mathbf{J}v) = (c \circ \mathbf{F}) \textstyle\sum_j J_{ij} v_j = \sum_j (c \circ \mathbf{F})\, J_{ij}\, dx^j(v).$$

  Consequently,

  $$\mathcal{Y}^1_{\mathbf{F}}\omega = \sum_j (c \circ \mathbf{F})\, J_{ij}\, dx^j \tag{11.1.2}$$

  and we get the wanted representation (11.1.1) for $k = 1$.
- $k \mapsto k+1$: We assume the existence of the wanted w_s for every basis k-form.
  Now let $\omega = c\, dx^{\sigma_1} \wedge \cdots \wedge dx^{\sigma_k} \wedge dx^{\sigma_{k+1}}$. Then set $i \coloneqq \sigma_{k+1}$ and $\eta = c dx^{\sigma_1} \wedge \cdots \wedge dx^{\sigma_k}$. The important point is now the compatibility of the pullback operation with the wedge product. From [51, Lemma 14.16.] we get

  $$\mathcal{Y}^{k+1}_{\mathbf{F}}\omega = \Big[\mathcal{Y}^k_{\mathbf{F}}\eta\Big] \wedge \Big[\mathcal{Y}^1_{\mathbf{F}} dx^i\Big],$$

  with point-wise wedge product. By assumption we have $w_s \in C^l(\overline{\widehat{\Omega}})$, $s \in \Sigma_<(k,n)$ depending on the first derivatives of $\mathbf{F}$ s.t. (11.1.1) holds. Since the wedge-product is bilinear (see [51, Proposition 14.11]) we obtain with (11.1.2) directly

  $$\mathcal{Y}^{k+1}_{\mathbf{F}}\omega = \sum_{s\in\Sigma_<(k,n)} \sum_j w_s\, J_{ij}\, (c \circ \mathbf{F})\, dx^{s_1} \wedge \cdots \wedge ds^{s_k} \wedge dx^j.$$

  Due to the fact $w_s\, J_{ij} \in C^l(\overline{\widehat{\Omega}})$ we get the desired representation also for $k+1$.

□

Hence, we have now a better understanding how the pullback operation changes the coefficients of a k-form. And the first two points in Lemma 3.8 can now be checked easily. Because, if in (11.1.1) we choose $c \in H^l(\Omega)$ we obviously have $w_s\,(c \circ \mathbf{F}) \in H^l(\widehat{\Omega})$. Besides, utilizing the chain and product rule for differentiation we find a constant $\tilde{C}_s$ independent of c such $\|w_s\,(c \circ \mathbf{F})\|_{H^l(\widehat{\Omega})} \leq \tilde{C}_s\,\|c\|_{H^l(\Omega)}$. Thus, for $\omega = c\,dx^{\sigma_1} \wedge \cdots \wedge dx^{\sigma_k}$ with $c \in H^l(\Omega)$ it is $\mathcal{Y}^k_{\mathbf{F}}\omega \in H^l\Lambda^k(\widehat{\Omega})$ and we find another constant $\tilde{C}$ independent of c with

$$\left\|\mathcal{Y}^k_{\mathbf{F}}\omega\right\|_{H^l(\widehat{\Omega})} \leq \tilde{C}_s\,\|\omega\|_{H^l(\Omega)}\,.$$

Exploiting linearity we see the first point in Lemma 3.8.
It remains to face the second point regarding zero boundary conditions. But the latter is also clear, because for $l = 1$ and $c \in H^1_0(\Omega)$ we have in (11.1.1) certainly $w_s\,(c \circ \mathbf{F}) \in H^1_0(\widehat{\Omega})$. Again in view of linearity we see then

$$\mathcal{Y}^k_{\mathbf{F}}\Big(H^1_0\Lambda^k(\Omega)\Big) \subset H^1_0\Lambda^k(\widehat{\Omega}).$$

This finishes our proof. □

11.2 The inf-sup test

At different places in the thesis we display numerically computed inf-sup constants for different inf-sup expressions. The underlying computations follow the inf-sup test from Bathe et al. which leads in the discrete setting to generalized eigenvalue problems. Details and applicability of these tests can be found in [15, 33] . For reasons of completeness we briefly explain here the procedure what type of eigenvalue problem one uses, where we orient ourselves towards the mentioned references.

Let use assume we have a bounded bilinear form $\mathcal{B}\colon V^1 \times V^2 \to \mathbb{R}$ on Hilbert spaces V^i related to some variational formulation. Given conforming discrete spaces $V^i_h \subset V^i,\ i = 1, 2$ an important quantity are the inf-sup constants

$$C_{IS}(h) := \inf_{w_h \in V^1_h}\ \sup_{u_h \in V^2_h} \frac{\mathcal{B}(w_h, u_h)}{\|w_h\|_{V^1}\,\|u_h\|_{V^2}},$$

where for the norms in V^i we write $\|\cdot\|_{V^i}$. The question is now, how $C_{IS}(h)$ is computed for a fixed mesh? This can be done as follows:
First choose bases $\left\{v^{(i)}_1, v^{(i)}_2, \ldots, v^{(i)}_{N_i}\right\} \subset V^i_h$ of the discrete spaces, meaning for $w_h \in V^1_h$ and $u_h \in V^2_h$ it is $w_h = \sum_{j=1}^{N_1} w_j\,v^{(1)}_j,\ u_h = \sum_{j=1}^{N_2} u_j\,v^{(2)}_j$ for suitable $w_j,\ u_j$. The coefficients are stored in column vectors $\underline{w} = (w_1, \ldots, w_{N_1})^{\mathrm{T}},\ \underline{u} = (u_1, \ldots, u_{N_2})^{\mathrm{T}}$. Then let

$$B \in \mathbb{R}^{N_2 \times N_1}, \quad S \in \mathbb{R}^{N_1 \times N_1}, \quad T \in \mathbb{R}^{N_2 \times N_2}$$

be the matrices such that

$$\mathcal{B}(w_h, u_h) = \underline{u}^{\mathrm{T}} B \underline{w}, \qquad \|w_h\|^2_{V^1} = \underline{w}^{\mathrm{T}} S \underline{w}, \qquad \|u_h\|^2_{V^2} = \underline{u}^{\mathrm{T}} T \underline{u}.$$

Consequently, one has for the inf-sup constant

$$C_{IS} = \inf_{\underline{w} \in \mathbb{R}^{N_1}}\ \sup_{\underline{u} \in \mathbb{R}^{N_2}} \frac{\underline{u}^{\mathrm{T}} B \underline{w}}{\sqrt{\underline{w}^{\mathrm{T}} S \underline{w}}\ \sqrt{\underline{u}^{\mathrm{T}} T \underline{u}}}.$$

Then, as shown in [15, Section 2], the computation of the value C_{IS} can be done equivalently through the generalized Rayleigh quotient

$$C_{IS}^2 = \inf_{\underline{w} \in \mathbb{R}^{N_1}} \frac{\underline{w}^{\mathrm{T}} B^{\mathrm{T}} T^{-1} B \underline{w}}{\underline{w}^{\mathrm{T}} S \underline{w}}.$$

One notes that T and $M \coloneqq B^{\mathrm{T}} T^{-1} B$ are symmetric matrices and obviously T is positive definite. Thus M is positive semi-definite and C_{IS} is the square root of the smallest eigenvalue λ_{min} of the generalized eigenvalue problem

$$B^{\mathrm{T}} T^{-1} B \underline{x} = \lambda S \underline{x}, \quad \underline{x} \in \mathbb{R}^{N_1} \qquad \text{(compare (14) in [15])} \ ,$$

i.e. $C_{IS} = \sqrt{\lambda_{min}}$.
After the computation of the different matrices B, T and S we can exploit the MATLAB ([53]) functions *eigs()* and *mrdivide()* to compute the respective smallest eigenvalue, so the inf-sup values C_{IS}. This is done in the different examples through the thesis.

Bibliography

[1] Robert Alexander Adams. *Sobolev spaces*. Academic Press, New York, 1975.

[2] Hans Wilhelm Alt. *Lineare Funktionalanalysis: Eine anwendungsorientierte Einführung*. Springer Berlin Heidelberg, Berlin, Heidelberg, fünfte, überarbeitete auflage edition.

[3] Jeremias Arf and Bernd Simeon. Mixed isogeometric discretizations for planar linear elasticity. *arXiv (2204.08095), https://arxiv.org/abs/2204.08095*, 2022.

[4] Douglas Arnold and Ragnar Winther. Mixed finite elements for elasticity. *Numerische Mathematik*, 92:401–419, 03 2002.

[5] Douglas N. Arnold. Finite element exterior calculus. CBMS-NSF regional conference series in applied mathematics 93, Philadelphia, 2018. SIAM, Society for Industrial and Applied Mathematics.

[6] Douglas N. Arnold and Gerard Awanou. Rectangular mixed finite elements for elasticity. *Mathematical Models and Methods in Applied Sciences*, 15(09):1417–1429, 2005.

[7] Douglas N. Arnold, Gerard Awanou, and Weifeng Qiu. Mixed finite elements for elasticity on quadrilateral meshes. *Advances in Computational Mathematics*, 41:553–572, 2013.

[8] Douglas N. Arnold, Daniele Boffi, and Francesca Bonizzoni. Finite element differential forms on curvilinear cubic meshes and their approximation properties. *Numerische Mathematik*, 129:1–20, 2012.

[9] Douglas N. Arnold, Richard S. Falk, and Ragnar Winther. Finite element exterior calculus, homological techniques, and applications. *Acta Numerica*, 15:1–155, 2006.

[10] Douglas N. Arnold, Richard S. Falk, and Ragnar Winther. Mixed finite element methods for linear elasticity with weakly imposed symmetry. *Mathematics of Computation*, 76(260):1699–1724, October 2007.

[11] Douglas N. Arnold, Richard S. Falk, and Ragnar Winther. Finite element exterior calculus: From Hodge theory to numerical stability. *Bulletin of the American Mathematical Society*, 47:281–354, 2010.

[12] Douglas N. Arnold and Kaibo Hu. Complexes from complexes. *Foundations of Computational Mathematics*, 21(6):1739–1774, March 2021.

[13] F. Auricchio, L. Beirão da Veiga, C. Lovadina, and A. Reali. An analysis of some mixed-enhanced finite element for plane linear elasticity. *Computer Methods in Applied Mechanics and Engineering*, 194(27):2947–2968, 2005.

[14] F. Auricchio, L. Beirão da Veiga, A. Buffa, C. Lovadina, A. Reali, and G. Sangalli. A fully "locking-free" isogeometric approach for plane linear elasticity problems: A stream function formulation. *Computer Methods in Applied Mechanics and Engineering*, 197(1):160–172, 2007.

[15] Klaus-Jürgen Bathe, Dena Hendriana, Franco Brezzi, and Giancarlo Sangalli. Inf–sup testing of upwind methods. *International Journal for Numerical Methods in Engineering*, 48(5):745–760, 2000.

[16] Sebastian Bauer and Dirk Pauly. On korn's first inequality for mixed tangential and normal boundary conditions on bounded Lipschitz domains in $\mathbb{R}^n$. *Annali dell'universita' di ferrara*, 62:173–188, 2015.

[17] Yuri Bazilevs, Lourencurlco Beirão da Veiga, J. Austin Cottrell, Thomas J. R. Hughes, and Giancarlo Sangalli. Isogeometric analysis: Approximation, stability and error estimates for h-refined meshes. *Mathematical Models and Methods in Applied Sciences*, 16:1031–1090, 2006.

[18] Carole Blanc and Christophe Schlick. Accurate parametrization of conics by NURBS. *IEEE Comput. Graph. Appl.*, 16(6):64–71, nov 1996.

[19] Francesca Bonizzoni, Kaibo Hu, Guido Kanschat, and Duygu Sap. Discrete tensor product BGG sequences: splines and finite elements. *arXiv (2302.02434), https://doi.org/10.48550/arXiv.2302.02434*, 2023.

[20] Dietrich Braess. *Finite Elemente: Theorie, schnelle Löser und Anwendungen in der Elastizitätstheorie*. Springer Berlin Heidelberg, Berlin, Heidelberg, vierte, überarbeitete und erweiterte auflage edition.

[21] Jamie Bramwell, Leszek Demkowicz, Jay Gopalakrishnan, and Weifeng Qiu. A locking-free hp DPG method for linear elasticity with symmetric stresses. *Numerische Mathematik*, 122(4):671–707, 2012.

[22] Andrea Bressan. Isogeometric regular discretization for the Stokes problem. *IMA Journal of Numerical Analysis*, 31(4):1334–1356, 11 2010.

[23] Andrea Bressan and Giancarlo Sangalli. *Isogeometric discretizations of the Stokes problem: stability analysis by the macroelement technique, Ima Journal of Numerical Analysis 33 (2013), 629-651.*

[24] F. Brezzi. On the existence, uniqueness and approximation of saddle-point problems arising from Lagrangian multipliers. *Revue fran*curl*caise d'automatique, informatique, recherche opérationnelle. Analyse numérique*, 8(R2):129–151, 1974.

[25] Franco Brezzi and Michel Fortin. *Incompressible Materials and Flow Problems*, pages 200–273. Springer New York, New York, NY, 1991.

[26] Franco Brezzi and Michel Fortin. Mixed and hybrid finite element method. *Springer Series In Computational Mathematics; Vol. 15*, page 350, 01 1991.

[27] A. Buffa, J. Rivas, G. Sangalli, and R. Vázquez. Isogeometric discrete differential forms in three dimensions. *SIAM Journal on Numerical Analysis*, 49(2):818–844, 2011.

[28] A. Buffa, G. Sangalli, and R. Vázquez. Isogeometric analysis in electromagnetics: B-splines approximation. *Computer Methods in Applied Mechanics and Engineering*, 199(17):1143–1152, 2010.

[29] Annalisa Buffa, Carlo de Falco, and Giancarlo Sangalli. Isogeometric analysis: Stable elements for the 2d stokes equation. *International Journal for Numerical Methods in Fluids*, 65, 2011.

[30] Annalisa Buffa, Jürgen Dölz, Stefan Kurz, Sebastian Schöps, Rafael Vázquez Hernández, and Felix Wolf. Multipatch approximation of the de Rham sequence and its traces in isogeometric analysis. *Numerische Mathematik*, 144:201–236, 2018.

[31] Annalisa Buffa and Giancarlo Sangalli. IsoGeometric Analysis: A New Paradigm in the Numerical Approximation of PDEs, Lecture Notes in Mathematics 2161, CIME Foundation Subseries. Springer, Cham, Switzerland, 2016.

[32] Annalisa Buffa, Rafael Hernandez Vázquez, Giancarlo Sangalli, and Lourencurlco Beirão da Veiga. Approximation estimates for isogeometric spaces in multipatch geometries. *Numerical Methods for Partial Differential Equations*, 31(2):422–438, 2015.

[33] Dominique Chapelle and Klaus-Jürgen Bathe. The inf-sup test. *Computers & Structures*, 47(4-5):537–545, 1993.

[34] Long Chen and Xuehai Huang. Finite elements for div- and divdiv-conforming symmetric tensors in arbitrary dimension. *SIAM Journal on Numerical Analysis*, 60(4):1932–1961, 2022.

[35] Long Chen and Xuehai Huang. Finite Element Complexes in Two Dimensions. *arXiv (2206.00851), https://arxiv.org/abs/2206.00851*, 2023.

[36] Martin Costabel and Alan Mcintosh. On bogovskiĭ and regularized poincaré integral operators for de Rham complexes on Lipschitz domains. *Mathematische Zeitschrift*, 265:297–320, 2008.

[37] C. de Falco, A. Reali, and R. Vázquez. GeoPDEs: A research tool for isogeometric analysis of PDEs. *Advances in Engineering Software*, 42(12):1020–1034, 2011.

[38] Eleonora Di Nezza, Giampiero Palatucci, and Enrico Valdinoci. Hitchhikers guide to the fractional Sobolev spaces. *Bulletin des Sciences Mathématiques*, 136(5):521–573, 2012.

[39] Manfredo P. Do Carmo. *Differential Forms and Applications*. Universitext. Springer Berlin Heidelberg, Berlin, Heidelberg, 1st ed. 1994 edition, 1994.

[40] John A Evans, Michael A Scott, Kendrick M Shepherd, Derek C Thomas, and Rafael Vázquez Hernández. Hierarchical B-spline complexes of discrete differential forms. *IMA Journal of Numerical Analysis*, 40(1):422–473, 12 2018.

[41] Lawrence C. Evans. *Partial differential equations*. American Mathematical Society, Providence, R.I., 2010.

[42] Richard S. Falk. Finite element methods for linear elasticity. pages 159–194, 2008.

[43] Vivette Girault and P. A. Raviart. *Finite Element Methods for Navier-Stokes Equations - Theory and Algorithms*. 1986.

[44] E. Hellinger. *Die allgemeinen ansätze der mechanik der kontinua*. Encyklopädie der mathematischen wissenschaften. Vol. 4, (F. Klein and C. Muller, eds.). Leipzig, 1914.

[45] Lie heng Wang. On Korn's inequality. *Journal of Computational Mathematics*, 21(3):321–324, 2003.

[46] Jason Howell and Noel Walkington. Inf–sup conditions for twofold saddle point problems. *Numerische Mathematik*, 118:663–693, 08 2011.

[47] Jun Hu and Yizhou Liang. Conforming discrete gradgrad-complexes in three dimensions. *Math. Comput.*, 90:1637–1662, 2020.

[48] Kaibo Hu. Oberwolfach report: Discretization of Hilbert complexes. *arXiv (2208.03420), https://arxiv.org/abs/2208.03420*, 2023.

[49] Thomas J. R. Hughes, J. Austin Cottrell, and Yuri Bazilevs. Isogeometric analysis : CAD, finite elements, NURBS, exact geometry and mesh refinement. *Computer Methods in Applied Mechanics and Engineering*, 194:4135–4195, 2005.

[50] Ram P. Kanwal. *Generalized Functions : Theory and Applications*. Birkhäuser Boston, Boston, MA, 3rd ed. 2004 edition, 2004.

[51] John M. Lee. *Smooth Manifolds*, pages 1–29. Springer New York, New York, NY, 2003.

[52] R. Glowinski M. Fortin. *Augmented Lagrangian Methods: Applications to the Numerical Solution of Boundary-Value Problems*. Elsevier Science, 2000.

[53] MATLAB. Version 9.9 (R2020b), The MathWorks, Inc., Natick Massachusetts.

[54] Christian Mittelstedt. *Kirchhoff Plate Theory in Cartesian Coordinates*, pages 253–312. Springer Berlin Heidelberg, Berlin, Heidelberg, 2023.

[55] Nečas Jindřich Müller, Manfred. Über die Regularität der schwachen Lösungen von Randwertaufgaben für quasilineare elliptische Differentialgleichungen höherer Ordnung. *Czechoslovak Mathematical Journal*, 25(2):227–239, 1975.

[56] Jindrich Necas. Sur une méthode pour résoudre les équations aux dérivées partielles du type elliptique, voisine de la variationnelle. *Annali della Scuola Normale Superiore di Pisa - Scienze Fisiche e Matematiche*, 3e série, 16(4):305–326, 1962.

[57] Francesco Patrizi. Isogeometric de Rham complex discretization in solid toroidal domains. *CoRR (2106.10470), https://arxiv.org/abs/2106.10470*, abs/2106.10470, 2021.

[58] Dirk Pauly and Michael Schomburg. Hilbert complexes with mixed boundary conditions part 1: de Rham complex. *Mathematical Methods in the Applied Sciences*, 45(5):2465–2507, 2022.

[59] Dirk Pauly and Michael Schomburg. Hilbert complexes with mixed boundary conditions—part 2: Elasticity complex. *Mathematical Methods in the Applied Sciences*, 45(16):8971–9005, 2022.

[60] Dirk Pauly and Walter Zulehner. On closed and exact grad-grad- and div-div-complexes, corresponding compact embeddings for tensor rotations, and a related decomposition result for biharmonic problems in 3d. *arXiv (1609.05873), https://arxiv.org/abs/1609.05873*, 2017.

[61] Les A. Piegl. *The NURBS book*. Springer, Berlin u.a., 2. ed. edition, 1997.

[62] Vincent Quenneville-Bélair. A New Approach to Finite Element Simulations of General Relativity. Ph.D. thesis, Department of Mathematics, University of Minnesota (2015).

[63] Thiago O. Quinelato, Abimael F.D. Loula, Maicon R. Correa, and Todd Arbogast. Full h(div)-approximation of linear elasticity on quadrilateral meshes based on ABF finite elements. *Computer Methods in Applied Mechanics and Engineering*, 347:120–142, 2019.

[64] Mathias Reichle and Jeremias Arf. Mathias1211/violin_boundary: Violin nurbs curve. *Zenodo, https://doi.org/10.5281/zenodo.8168515*, July 2023.

[65] Larry Schumaker. *Spline Functions: Basic Theory*. Cambridge Mathematical Library. Cambridge University Press, 3 edition, 2007.

[66] Joachim Schöberl. Numerische Methoden in der Kontinuumsmechanik. *Lecture notes at TU Wien (winter term 2011/2012), https://www.asc.tuwien.ac.at/ schoeberl/wiki/lva/nummech/nummech.pdf*.

[67] Kendrick Shepherd and Deepesh Toshniwal. Locally-verifiable sufficient conditions for exactness of the hierarchical B-spline discrete de Rham complex in $\mathbb{R}^n$. *arXiv (2209.01504), https://arxiv.org/abs/2209.01504*, 2022.

[68] Elias M. Stein. *Singular integrals and differentiability properties of functions*. Princeton mathematical series 30. Princeton Univ. Press, Princeton, NJ, 1970.

[69] Olaf Steinbach. *Numerical Approximation Methods for Elliptic Boundary Value Problems. Finite and Boundary Elements*. Springer, 2008.

[70] E. Suhubi. *Functional Analysis*. Springer Netherlands, Dordrecht, 1st ed. 2003 edition, 2003.

[71] Deepesh Toshniwal and Thomas J.R. Hughes. Isogeometric discrete differential forms: Non-uniform degrees, bézier extraction, polar splines and flows on surfaces. *Computer Methods in Applied Mechanics and Engineering*, 376:113576, 2021.

[72] Loring W. Tu. *An introduction to manifolds*. Universitext. Springer, New York, 2nd ed. edition, 2011.

[73] R. Vázquez. A new design for the implementation of isogeometric analysis in Octave and Matlab: GeoPDEs 3.0. *Computers and Mathematics with Applications*, 72(3):523–554, 2016. To appear.

[74] R. Verfürth. *Error estimates for a mixed finite element approximation of the Stokes equations, ESAIM: Mathematical Modelling and Numerical Analysis - Modélisation Mathématique et Analyse Numérique*, 18:175–182, 1984.

[75] Joachim Weidmann. *Linear Operators in Hilbert Spaces*. Graduate Texts in Mathematics 68. Springer New York, New York, NY, 1st ed. 1980 edition, 1980.

[76] Liu-Chao Xiao, Yong-Qin Yang, and Shao-Chun Chen. Locking-free nonconforming finite elements for three-dimensional elasticity problem. *Applied Mathematics and Computation*, 217(12):5790–5797, 2011.

Academic Curriculum Vitae

03/2015	**General Qualification for University Entrance** Gymnasium Kusel, Rheinland-Pfalz
03/2018	**Bachelor of Science in Mathematics** Technical University of Kaiserslautern
04/2020	**Master of Science in Mathematics** Technical University of Kaiserslautern
07/2020	**Acceptance as PhD Student of Prof. Dr. Bernd Simeon** Technical University of Kaiserslautern

Wissenschaftlicher Werdegang

03/2015	**Allgemeine Hochschulreife (Abitur)** Gymnasium Kusel, Rheinland-Pfalz
03/2018	**Bachelor of Science in Mathematik** Technische Universität Kaiserslautern
04/2020	**Master of Science in Mathematik** Technische Universität Kaiserslautern
07/2020	**Annahme als Doktorand bei Prof. Dr. Bernd Simeon** Technische Universität Kaiserslautern